

IL  
NUOVO CIMENTO  
ORGANO DELLA SOCIETÀ ITALIANA DI FISICA  
SOTTO GLI AUSPICI DEL CONSIGLIO NAZIONALE DELLE RICERCHE

VOL. IV, N. 6

Serie decima

1° Dicembre 1956

**Bilocal Field Theories and their Experimental Tests. - I.**

J. RAYSKI

*Institute of Theoretical Physics, Nicholas Copernicus University - Toruń, Poland*

(ricevuto il 19 Luglio 1956)

**Summary.** — Two versions of bilocal field theory are presented, one of them assuming the existence of an isospace, the other assuming a particle structure in the usual space. In the first version isospin is a primary concept whereas in the second it is interpreted as a «relative spin». In both formulations we have a very natural systematization of particles into four families: bosons-isobosons, bosons-isofermions, fermions-isobosons, and fermions-isofermions. The difficulty with higher states of charge is avoided. The problem of mechanical mass and field mass is discussed and arguments are given in favour of the opinion that (the main part of) the heavy particle mass is not a field mass. The formalism yields families of particles with increasing masses. The theoretical mass spectra agree remarkably well with experiment. The probability of an accidental coincidence of experimental and theoretical mass values is only 1/900.

**Introduction.**

In the last few years the inadequacy of the traditional field theory became evident for both theoretical and experimental reasons <sup>(1)</sup>. Since in high energy collisions heavy unstable particles are produced copiously, any field theory which ignored their existence is to be regarded as unsatisfactory. If the

<sup>(1)</sup> Compare: W. HEISENBERG: *Naturwiss.*, **42**, 637 (1955).

number of newly discovered particle sorts will increase further, we will be faced unavoidably with the necessity of using new theoretical tools to describe the great variety of particles and their interactions. It would be desirable to find such a formulation where a single field quantity would describe either all particle sorts, or at least a particle family in contradistinction to the traditional theory introducing ad hoc a new field quantity for any new particle sort.

The contemporary efforts to find such tools enabling an automatic inclusion and systematization of all particle sorts tend in various directions. One of them, represented by HEISENBERG <sup>(1)</sup> is characteristic by its departure from linearity, another discussed by several authors, is characteristic by its departure from locality. We shall discuss here only the latter. The aim of the bilocal (or non-local) field theory is to systematize the elementary particles according to representations of certain groups, to determine their spins, isospins, masses, and other attributes. Several proposals of bilocal mass operators have been discussed leading to formulae for mass spectra of elementary particles. These formulae must be regarded only as approximate since they neglect the interaction. HEISENBERG <sup>(1)</sup> has put in doubt whether such an approximation is meaningful: he seems to be of the opinion that every rest mass is a field mass so that any endeavour to determine the masses without taking account of interaction must be a failure. I should like to present here some arguments against this view.

I believe that in the future satisfactory theory of interactions the field masses will be finite (either owing to realistic compensations or owing to form-factors, or some other circumstances which cannot be foreseen yet) and expressible as power series of the renormalized coupling constant. In other words, I assume that finally the point of view of weak interactions will prove to be correct. This opinion is founded on the fact that the traditional field theory is not a complete failure but possesses a practical range of applicability. Therefore, in the lowest approximation, the field masses should be proportional to the second (occasionally to the fourth) powers of the coupling constants. The factors of proportionality may depend upon the particle type but generally these field masses which in the traditional theory are logarithmically divergent (fermions) may be expected to be smaller than those which are more strongly divergent (bosons).

Let us consider the mass values of the best known particles. The electron mass  $1 m_e$  may be regarded surely as a field mass chiefly of electromagnetic origin. The difference between the charged and neutral pion masses  $273 - 265 = 8$  as well as the neutron-proton mass difference 2.5 may be also regarded as electromagnetic field masses. We notice that the electromagnetic masses are of the same order of magnitude for all types of particles. A little larger value 8 for the pion as compared with 1 or 2.5 for electron or nucleon



is easily explicable since these last particles are fermions and their self masses are partly compensated in the sense of WEISSKOPF. Since the order of magnitude of the ratio of the coupling constants  $e^2/f^2$  agrees with  $8/265$ , we believe that also the mass 265 of the pion is a field mass due to the coupling by meso-nuclear forces. It should be expected that the order of magnitude of the nucleon field mass due to meso-nuclear forces will be the same. In consequence of the fact that nucleons (and hyperons) are fermions it seems probable that the ratio of their field masses to that of the pion is similar to the ratio of the respective electromagnetic masses  $2.5/8$ . Thus, it seems reasonable to expect that the nucleon field mass due to meso-nuclear forces will be of the order of magnitude of 80. If it is so, the question arises how to explain the main parts of the nucleon and hyperon masses? To explain them as field masses we should assume the existence of new forces with coupling constants  $g^2$  exceeding  $f^2$  by one or two orders of magnitude. This is not only inconsistent with « the philosophy of weak couplings » but nothing in experiment indicates the existence of such big couplings.

The above considerations make it plausible that the main part of the nucleon and hyperon (may be also of the heavy meson) masses is not a field mass. Thus, it seems reasonable to look for new possible explanations of these masses and to discuss formalisms involving mass operators even in the approximation of free fields.

In order to have a formalism where a single field quantity describes a whole family of particles, we may assume a dependence upon a larger number of degrees of freedom than is the case for the traditional field quantity. Then, the field states will be characterized by a correspondingly larger number of observables specifying not only the state of motion but also the sort of particles. Thus, the variety of particles discovered in the last few years strongly suggests that the field quantities depend upon a larger number of variables

$$\psi = \psi(x, u),$$

where  $x$  symbolizes the coordinates in the Minkowski space and  $u$  means some additional degrees of freedom. At first, neither the number of variables  $u$ , nor their physical meaning are known but some simple possibilities suggest themselves immediately and may be tried successively.

Mathematically, the simplest possibility is to assume that the variables  $u$  have nothing to do with the usual space but form an autonomous space. We may consider the Cartesian product of both spaces. On the other hand, physically the simplest possibility is to assume that  $u$  as well as  $x$  are connected with the usual physical space. In this case the particle could not be a material point but should possess an internal structure described just by the co-ordinates  $u$ . The simplest (except the point) possibility is a bipoint. In

this case the variables  $u$  would mean the relative co-ordinates. Both possibilities have been taken into consideration. The former was suggested by PAIS <sup>(2)</sup>, the latter by YUKAWA <sup>(3)</sup>.

### 1. - A Systematization of elementary Particles Based on the Hypothesis of Isospace.

We shall discuss first a new version of the theory of Pais. Let us assume that the variables  $u$  denote co-ordinates in a metrical, euclidean, three-dimensional space. It is suggestive to consider the following straightforward generalization of the Klein-Gordon equation

$$(1.1) \quad (p_\mu^2 + \mathbf{k}^2)\psi(x, u) = 0,$$

where

$$(1.2) \quad p_\mu = -i \frac{\partial}{\partial x_\mu}, \quad k_j = -i \frac{\partial}{\partial u_j}, \quad \mu = 1, \dots, 4; \quad j = 1, \dots, 3.$$

$\mathbf{k}^2$  is to play the role of the mass operator. In order to have a discrete spectrum of masses it is necessary to introduce either some boundary condition <sup>(4)</sup> or some constraints <sup>(5)</sup>. We shall discuss the latter possibility. The following supplementary condition

$$(1.3) \quad p_\mu^2 + \mathbf{u}^2 = 0$$

means a particularly simple and elegant type of constraints. (1.3) is expressed in natural units  $c = \hbar = l = 1$  where  $l$  denotes a constant with dimension length. More explicitly

$$(1.3') \quad l^4 p_\mu^2 + \mathbf{u}^2 = 0.$$

The supplementary condition (1.3) may be taken into account in two different though equivalent ways. The first way is to regard (1.3) as a condition upon the field quantity

$$(1.4) \quad (p_\mu^2 + \mathbf{u}^2)\psi = 0.$$

<sup>(2)</sup> A. PAIS: *Physica*, **19**, 879 (1953).

<sup>(3)</sup> H. YUKAWA: *Phys. Rev.*, **77**, 219 (1950); **91**, 415 (1953).

<sup>(4)</sup> E. MINARDI: *Nuovo Cimento*, **3**, 968 (1956).

<sup>(5)</sup> J. RAYSKI: *Nuovo Cimento*, **10**, 1729 (1953); **2**, 255 (1955); *Acta Phys. Pol.*, **14**, 107, 337 (1955).



In order to avoid contradiction between (1.1) and (1.4) we have to supplement (1.1) by an additional term  $R$  taking account of the reaction forces brought about by the constraints

$$(1.1') \quad (p_\mu^2 + \mathbf{k}^2)\psi = R\psi.$$

The term  $R$  is to remove those of the derivatives which are inconsistent with the constraints, i.e. the radial part of the Laplace operator. Thus, (1.1') is equivalent to

$$(1.5) \quad \left(p_\mu^2 + \frac{1}{u^2} S^2\right)\psi = 0,$$

with

$$(1.6) \quad S^2 = - \left( \frac{1}{\sin \vartheta} \frac{\partial}{\partial \vartheta} \sin \vartheta \frac{\partial}{\partial \vartheta} + \frac{1}{\sin^2 \vartheta} \frac{\partial^2}{\partial \varphi^2} \right),$$

where  $\varphi, \vartheta$  are spherical angles in the  $u$ -space and  $u^2$  assumes a constant value  $u^2 = -p_\mu^2$ . As the eigenvalues of the operator  $S^2$  are  $n(n+1)$  we get the mass spectrum

$$(1.7) \quad m_n = \frac{1}{l} \sqrt[4]{n(n+1)} \quad n = 0, 1, \dots$$

The general solution of the system of equations (1.4) and (1.5) is

$$(1.8) \quad \psi(x, u) = \sum_{n=0}^{\infty} \sum_{m=-n}^{m=n} \int d^4 p c_{nm} \delta(u^2 - m_n^2) \delta(p_\mu^2 + m_n^2) Y_n^m(\varphi, \vartheta) \exp[ip_\mu x_\mu],$$

where  $Y_n^m$  are spherical harmonics and the coefficients  $c_{nm}$  are still arbitrary functions of  $\mathbf{p}$  and  $\text{sgn } p_0$ . Owing to the appearance of an additional delta-function, the field quantity vanishes for any points in the  $u$ -space except for the points on the surfaces of the spheres with radii  $u^2 = m_n^2$ .

Another (equivalent but simpler) way of taking account of constraints (1.3) consists in the following: instead of regarding (1.3) as a condition upon the field quantity  $\psi$  we consider another field quantity  $\varphi$  independent of  $u^2$ . In other words, we look for solutions of (1.1) which are homogeneous of degree zero in the variables  $u_i$ . Special solutions are again spherical harmonics

$$(1.9) \quad \varphi_{nm} = \delta(p_\mu^2 + m_n^2) Y_n^m(\varphi, \vartheta) \exp[ip^\mu x_\mu],$$

with the same mass eigenvalues as before, and the general solution

$$(1.10) \quad \varphi(x, u) = \sum_{n,m} \int d^4 p c_{nm} \varphi_{nm}$$

differs from (1.8) merely by the absence of a delta-function.  $\varphi$  does not vanish for  $u^2 \neq m_n^2$  but is independent from  $u^2$ .

The elementary particle is represented by a rotator with radius  $u = l^2 m_n$ . The rest mass is quantized together with the angular momentum in the  $u$ -space.

Let us discuss the limit transition  $l \rightarrow 0$ . In this case the particle radius tends to zero while all mass eigenvalues, except  $m_0 = 0$ , tend to infinity. The limiting case is singular. In this limit the supplementary condition degenerates into three conditions

$$(1.11) \quad u_i = 0 \quad i = 1, 2, 3.$$

which may be taken into account by looking for a function  $\varphi$  independent of these variables. Thus (1.1) is equivalent to the conditions

$$(1.12) \quad k_i \varphi(x, u) = 0 \quad i = 1, 2, 3$$

consistent with (1.1). The field quantity satisfying these conditions is nothing else but a local field quantity describing particles with a vanishing rest mass. This establishes a correspondence with the traditional local field theory.

The bilocal field equation (1.1) may be split into a system of two equations

$$(I) \quad (p_\mu^2 + m^2)\varphi = 0, \quad (k^2 - m^2)\varphi = 0,$$

one of them being the usual Klein-Gordon equation, the other an eigenequation for the mass (if the supplementary condition is taken into account). Similarly as in the traditional theory we may linearize these equations. Besides (I) we may consider the system

$$(II) \quad (i\gamma_\mu p_\mu + m)\varphi = 0, \quad (k^2 - m^2)\varphi = 0,$$

but also two further alternatives

$$(III) \quad (i\gamma_\mu p_\mu + m)\varphi = 0, \quad (\tau k + m)\varphi = 0,$$

and

$$(IV) \quad (p_\mu^2 + m^2)\varphi = 0, \quad (\tau k + m)\varphi = 0,$$

where  $\tau$  are Pauli matrices in the  $u$ -space.

The above four alternatives mean respectively: (I)  $\varphi$  is a tensor in both spaces, (II) a spinor in the  $x$ -space but a tensor in the  $u$ -space, (III) a spinor in both spaces, (IV) a tensor in the  $x$ -space but a spinor in the  $u$ -space. When taking account of the supplementary conditions the radial part of the



mass operators drops out and we get the following mass eigenvalues

$$(1.13a) \quad m_n = \left\{ \begin{array}{l} \frac{1}{l} \sqrt{n+1} \\ \frac{1}{l} \sqrt[4]{n(n+1)} \end{array} \right.$$

for the first order and second order mass operators respectively.

## 2. - A Comparison with Experimental Results.

Assuming the proton mass as the basis for (1.13a)

$$m = m_0 = \frac{1}{l},$$

we may compute the remaining masses, and now we witness something like a miracle: the next masses are from (1.13a)

$$m_1 = \sqrt{2} m_p = 2597, \quad m_2 = \sqrt{3} m_p = 3180,$$

whereas the masses from (1.13b) are

$$m_0 = 0, \quad m_1 = \sqrt[4]{2} m_p = 2183.5$$

close to the values of the following hyperons: the cascade hyperon  $\Xi$  (whose mass is  $2586 \pm 6$ ), the hyperon of EISENBERG <sup>(6)</sup> (whose mass is probably close to 3160), and the best known hyperon  $\Lambda^0$  (with mass  $2181 \pm 1$ ). It is striking enough that the mass spectrum (1.13a) applies to particles with half integer isospin while (1.13b) to particles with integer isospin. This agrees with PAIS' supposition that the additional degrees of freedom  $u$  denote coordinates in the isotopic spin space (isospace). The alternatives (I)–(IV) correspond to the cases: (I) boson-isoboson, (II) fermion-isoboson, (III) fermion-isofermion, and (IV) boson-isofermion. Hence, the pion is described by the alternative (I), the electron as well as the hyperons  $\Lambda^0$  and  $\Sigma$  by (II), the nucleon, the cascade hyperon  $\Xi$  and probably also the hyperon of EISENBERG by (III), whereas the K-mesons by (IV).

<sup>(6)</sup> Y. EISENBERG: *Phys. Rev.*, **96**, 541 (1954); *Bull. Research Council Israel*, **4**, 405 (1955).

Since no heavy bosons have been discovered with certainty except those with masses close to 965, it is impossible yet to prove quantitatively the correctness of the mass spectra (1.13) for bosons. However, one feature of the boson spectra is quite satisfactory, namely the fact that bosons-isofermions are much heavier than pion (boson-isoboson). The formula (1.13a) applying to isobosons admits an eigenvalue zero whereas the formula (1.13b) applying to isofermions does not. This means that the lowest member of a boson-isoboson family can possess a vanishing mechanical mass, its whole mass being only a field mass (273 in the case of pion in agreement with the preliminary estimates given in the Introduction). On the other hand, even the lowest member of a boson-isofermion family possesses a mechanical mass and therefore is much heavier than pion. We notice that for the explanation of mechanical masses of the K-meson family we have to assume a new value  $l$  twice as large as that for nucleons and hyperons. We hope that this fact will find a theoretical explanation in the future.

Since the number of data comparable with experiment is scarce, the question arises whether the agreement of our mass spectra with experimental data can be accidental. Let us estimate the probability of an accidental agreement. To avoid a bias let us assume, instead of the proton mass, the arithmetic mean of the proton and neutron masses as the starting point of mass determination. This spoils a little the agreement and gives a value 2598.5 for  $\Xi$  and 2185 for  $\Lambda^0$ . The probability of finding by chance the value 2586 with the accuracy  $\pm 12.5$  for a fermion-isofermion (next to the nucleon) is about 1/30. The probability of finding one of the values for the fermion-isoboson masses (2181 or 2327) by pure chance with the accuracy  $\pm 4$  is also about 1/30. The probability of obtaining both coincidences simultaneously is only 1/900. If the hyperon of Eisenberg will be confirmed and its mass 3160 close to the theoretical 3180 will be ascertained, the probability of an accidental coincidence will become only  $10^{-4}$ .

Since the formulae (1.13) have been published <sup>(5)</sup> before the discovery of the hyperon of Eisenberg, we are enlightened to claim that the theory has predicted its existence. Therefore it seems of particular interest to resume the evidence for its existence. EISENBERG observed an event of the type

$$Y^- \rightarrow K^- + ?^0.$$

The track  $Y^-$  has been several times carefully remeasured and yields for the mass the value  $3220 \pm 700$ . Assuming that the neutral particle ( $?^0$ ) is a neutron, the mass of  $Y^-$  would be 2820 from the  $Q$  value. Assuming alternatively that ( $?^0$ ) is  $\Lambda^0$ , the mass of  $Y^-$  must be 3160. The first alternative seems to be excluded by the following argument: if the process  $Y^- \rightarrow K^- + N$  were possible,  $Y^-$  would possess the same attribute (strangeness) as  $\Xi$  and would



decay into it very rapidly<sup>(7)</sup>. Therefore the attribute of the new hyperon must be larger than that of  $\Xi$  and so the decay  $Y \rightarrow K + \Lambda^0$  preferred in comparison with  $Y \rightarrow K + N$ . Thus, the mass of the new hyperon should be close to 3160. There exists an independent confirmation of the existence of this hyperon. FRY *et al.*<sup>(8)</sup> observed an unusual hyperfragment decaying with the emission of  $K^-$ . Their analysis yields the result that (if the hyperfragment contained a hyperon) its mass must be at least 2900 which agrees with 3160 but not with 2820. Thus, the evidence for the existence of such a hyperon is strong though not yet decisive.

Now, the question may be raised, why the agreement of the theoretical and experimental mass values (for  $\Lambda^0$  and  $\Xi^-$ ) is so good in view of the fact that we have neglected the field masses (estimated to be about 80)? This unexpectedly good agreement may be explained by the remark that to compute the mass ratios we have taken not the mechanical part of the proton mass but its whole mass. In this way the constant  $l$  has been renormalized and the field mass taken automatically into account. If the field mass were strictly proportional to the mechanical mass (independently of the type of particle) we would obtain in this way quite correct results. Of course, the field mass is not strictly proportional but depends on several parameters connected with the type of particle in question. Nevertheless, we may try the approximation consisting in assuming that the field masses of all particles belonging to one family are equal, say  $\kappa$ . With this assumption we get, instead of (1.13a) an improved formula

$$(2.1) \quad m_n = \frac{1}{l} \sqrt{n + 1 + \frac{(\kappa l)^2}{4}} + \frac{\kappa}{2}.$$

Now, we may determine  $\kappa$  by adjusting the ratio  $m_1/m_0$  to the experimental value of the ratio of  $\Xi$  and nucleon masses. The result is  $\kappa \cong 50 m_e$  in excellent agreement with the foregoing estimate of the order of magnitude of nucleon field mass ( $\sim 80 m_e$ ). It is interesting to note that with this value of  $\kappa$  the mass  $m_2$  of the hyperons of Eisenberg is shifted down and becomes exactly 3160.

But in general the field masses do not need to be the same for all types of particles. In particular, the mass 2327 of the hyperon  $\Sigma$  is close enough to the theoretical value  $m_1$  for (1.13b) to regard both  $\Lambda^0$  and  $\Sigma$  as possessing the same mechanical mass  $m_1$ , and to interpret the difference between their masses ( $\sim 140 m_e$ ) as caused by field masses. This mass difference may be

(7) R. SACHS: *Phys. Rev.*, **99**, 1573 (1955).

(8) W. F., J. SCHNEPS and M. S. SWAMI: *Phys. Rev.*, **99**, 1570 (1955).

understood in view of the fact that the two isobosons have different isospins <sup>(9)</sup>.

We notice that the same formula (1.13*b*) which describes the mass of  $\Lambda^0$  allows a mass value zero as well. This mass eigenvalue may correspond to light fermions which probably are isobosons. However, it is difficult to regard  $\Lambda^0$  and light fermions as members of the same family. In view of the law of conservation of the number of heavy fermions, the eigenvalue  $m_0 = 0$  should be excluded from the  $\Lambda^0$ -family. This may be achieved in an elegant way by assuming that the field quantity describing the  $\Lambda^0$ -family is antisymmetric in the  $u$ -variables

$$(2.2) \quad \psi(x, u) = -\psi(x, -u).$$

Consequently, the mass eigenvalues with even  $n$  drop out from the family. The next member of the family is heavier than the hyperon of Eisenberg ( $m_3 = \sqrt[4]{12} m_p = 3400$ ).

Let us discuss in some detail the question of isospin. One of the serious difficulties of Pais' theory turns out to be immaterial in our formulation. PAIS identified the notion of isospin with the total angular momentum in the isospace, which led him to the unpleasant consequence of particles in higher states of charge. In our formulation we distinguish between the isospin and the total angular momentum in the  $u$ -space. Similarly as in the  $x$ -space the index attached to the field quantity determines the isospin whereas the total momentum is determined by vector addition of isospin and orbital angular momentum in  $u$ -space. Particles with higher mass eigenvalues possess higher angular momenta. In contradistinction to Pais formalism particles with different masses may have the same isospin (e.g. nucleon and  $\Xi$ ), and particles with equal (mechanical) masses may possess different isospins (e.g.  $\Lambda^0$  and  $\Sigma$ ). By limiting ourselves to field quantities which belong to the lowest order representation of the group of rotations in the  $u$ -space we may avoid higher charged states.

The above theory is extremely simple from the formal viewpoint. The field equations as well as the supplementary condition are remarkably simple and symmetric and, as it seems, take account satisfactorily of the most conspicuous properties of free elementary particles. In spite of these satisfactory results the above formalism possesses some disquieting features, above all the very fact of assuming a somewhat mystical isospace. This space would possess very ugly properties as the angular momentum in this space is not conserved for electromagnetic (and other weak) interactions. Thus, the isospace could

<sup>(9)</sup> Note added in proof. — An alternative explanation of the mass of the hyperons  $\Sigma$  will be presented in Part II.



not be isotropic. Such complications indicate (similarly as half century ago the complications brought about by the notion of aether) that most probably we have to do here with a fiction and have to dispense with it.

The appearance of the variables  $x$  and  $u$  on equal footing in (1.1) or (1.3) suggests that  $u$  denote some co-ordinates in the usual space. This is understandable provided the elementary particle is not a point but a bipoint in the sense of the bilocal theory proposed by YUKAWA. In the Part II we shall present it in a new version preserving the advantage of the theory described here.

#### RIASSUNTO (\*)

Si presentano due versioni della teoria bilocale dei campi, una delle quali postula l'esistenza di un isospazio, l'altra una struttura a particelle dello spazio ordinario. Nella prima versione l'isospin è un concetto primario, mentre nella seconda è interpretato come « spin relativo ». In ambe le formulazioni abbiamo una sistemazione naturale delle particelle in quattro famiglie: bosoni-isobosoni, bosoni-isofermioni, fermioni-isobosoni, fermioni-isofermioni. La difficoltà data dagli stati superiori di carica risulta evitata. Si discute il problema della massa meccanica e della massa di campo e si danno argomenti a favore dell'opinione che la maggior parte della massa delle particelle pesanti non è una massa di campo. Il formalismo fornisce famiglie di particelle con masse crescenti. Gli spettri di massa teorici si accordano in modo rimarchevole coll'esperienza. La probabilità di una coincidenza accidentale dei valori di massa teorici e sperimentali è solo 1/900.

(\*) Traduzione a cura della Redazione.

# On the Hydrodynamical Model in Multiple Production of Mesons.

M. HAMAGUCHI

*Institute of Theoretical Physics, Kyoto University - Kyoto, Japan*

(ricevuto il 6 Agosto 1956)

**Summary.** — The viscous stress tensors in the relativistic covariant form are introduced in the description of multiple production of the particles in high energy collisions. As the results, the effects of viscosity are calculated in 1-st order approximation and also the qualitative differences from Landau's theory are discussed on the basis of the conception of irreversibility in relativistic thermodynamics.

## 1. — Introduction.

Recently, LANDAU <sup>(1)</sup> proposed a description of the production of new particles in high energy collision processes, using the perfect fluid model. We now investigate the multiple production of mesons by taking the viscous fluid model instead of Landau's one. It is necessary for this model to consider the viscosity of fluid, thermal conductivity and the diffusion of matter in addition to the character of perfect fluid, but we consider here the effects of the ordinary viscous terms in relativistic hydrodynamics.

For the expression of the energy momentum tensors <sup>(2)</sup>, which contain the viscous stress in addition to that of perfect fluid, we have

$$(1) \quad T^{\mu\nu} = T_{(0)}^{\mu\nu} + T_{(\eta)}^{\mu\nu} + T_{(\zeta)}^{\mu\nu},$$

$$= p \cdot g^{\mu\nu} + (\varepsilon + p)v^\mu v^\nu - \delta \cdot \eta \{2v^{\mu\nu} + \delta \cdot (v^\mu v^\nu + v^\nu v^\mu)\} - \delta \cdot \zeta \{g^{\mu\nu} + \delta \cdot v^\mu v^\nu\} \cdot v_\rho^\rho,$$

<sup>(1)</sup> L. D. LANDAU: *Izv. Akad. Nauk SSSR*, **17**, 51 (1953).

<sup>(2)</sup> B. LEAF: *Phys. Rev.*, **84**, 345 (1952); E. C. G. STUECKELBERG and G. WANDERS: *Helv. Phys. Acta*, **26**, 307 (1953); U. ECKART: *Phys. Rev.*, **58**, 919 (1940); G. A. KLUITENBERG: *Relativistic Thermodynamics of Irreversible Processes* (Printed in Leiden).



where

$$v_{\mu\nu} = \frac{1}{2} \left( \frac{\partial v_\nu}{\partial x_\mu} + \frac{\partial v_\mu}{\partial x_\nu} \right), \quad \dot{v} = v^\mu \frac{\partial v}{\partial x_\mu},$$

$$v^\mu v_\mu = g_{\mu\nu} v^\mu v^\nu = -\delta, \quad \delta^2 = +1.$$

In this expression,  $\eta$  and  $\zeta$  are transversal and longitudinal viscosities respectively, and the metric tensor has the components  $g^{\alpha\alpha}$  ( $\alpha=1, 2, 3$ ) = 1,  $g^{00} = -1$  in the case of  $\delta = +1$ ,  $v_\mu$  forms a four velocity, and  $C = 1$ .

Analogously to Landau's method, we use the equation  $p = \varepsilon/3$  as the characteristic equation between the energy  $\varepsilon$  and the pressure  $p$  in the above expressions in order to carry out the hydrodynamical treatments.

In this model, the Lorentz contracted meson cloud will be produced by the collision of two nucleons of high energy. Dividing the above cloud in the assembly of many macroscopic small systems, we can assume that the energy in these divided sub-systems is uniform, although the distribution of the energy in total clouds has initially no uniformity owing to the influence of viscosity. It seems to us that this hypothesis of local uniformity is necessary for the true description of such phenomena. Therefore, some sorts of energies will be exchanged between these sub-systems to realize the uniformity in the total system during the hydrodynamical expanding process of its sub-systems. For this process, we assume that the sum of all kinds of energies in the total system is conserved during the collision process according to the 1st law of thermodynamics. Then, we can expect that the existence of viscous effects results in the increase of the total entropy which is covered by the decrease of internal energy of the system. From the view point of the second law of thermodynamics, such a process corresponds to an adiabatic, irreversible phenomenon which is very different from the model used by LANDAU. However, the relation between the entropy and the particle number in free scattering processes assumed by LANDAU will be still adopted in treating our present problem.

Moreover, we think that the relations similar to that of black body radiation  $s \sim \varepsilon^{\frac{1}{4}}$  ( $K \propto \varepsilon^{\frac{1}{4}}$  ( $K$ : temperature)), are still valid, if we remember that  $d\varepsilon = K ds$  holds between the energy  $\varepsilon$  and the entropy  $s$  per unit volume. As for the way, in which the number of created particles depends on the energy of incident nucleons, the following relations were already given by LANDAU. The meson cloud produced by two nucleon collisions has initially a flat circular form because of the Lorentz contraction. The transverse spread of the cloud is equal to the range of the nuclear force ( $a \sim \hbar/\mu c$ ), and the magnitude of the longitudinal width is contracted by the factor  $\sim Mc^2/E'$  ( $E'$  is the energy of a nucleon in centre of mass system). Since the above volume is given by  $V \sim a^3 \cdot Mc^2/E'$ , the number of produced particles proportional to the entropy is expressed as  $N \propto E'^{\frac{1}{2}}$ . Transforming this relation into the laboratory frame

of reference, from the consideration of the dimensions of physical quantities we have

$$(2) \quad N \approx \left( \frac{E}{2Mc^2} \right)^{\frac{1}{2}};$$

$E$  and  $M$  are the energy and the mass of a nucleon in the laboratory frame of reference, respectively.

## 2. - Equation of Motion.

2'1. *Fundamental equation in relativistic hydrodynamics.* - The fluid motion in hydrodynamical expanding processes is described by the equation

$$(3) \quad \partial T^{\mu\nu} / \partial x^\nu = 0,$$

in which  $T^{\mu\nu}$  is given by eq. (1). The expanding process of the system in centre of mass system develops initially in a direction ( $x$ -axis) parallel to the trajectory of the incident nucleon. We now consider only an one dimensional motion in the direction of the positive  $x$ -axis, though the system is symmetrically expanding to both sides of the  $x$ -axis.

For the equations of motion, we have

$$(4) \quad \left\{ \begin{array}{l} \frac{\partial T^{00}}{\partial t} + \frac{\partial T^{01}}{\partial x} = 0, \quad \frac{\partial T^{10}}{\partial t} + \frac{\partial T^{11}}{\partial x} = 0, \\ T^{00} = \varepsilon(v^0)^2 + p(v^1)^2 - 2\eta \left\{ [1 + (v^0)^2] \cdot \frac{\partial v^0}{\partial t} + v^0 v^1 \frac{\partial v^0}{\partial x} \right\} - \zeta \cdot (v^1)^2 \cdot \left( \frac{\partial v^0}{\partial t} + \frac{\partial v^1}{\partial x} \right), \\ T^{01} = (\varepsilon + p)v^0 v^1 - \eta \left\{ \frac{\partial v^1}{\partial t} + \frac{\partial v^0}{\partial x} + v^0 \cdot \left[ v^0 \frac{\partial v^1}{\partial t} + v^1 \frac{\partial v^1}{\partial x} \right] + \right. \\ \quad \left. + v^1 \cdot \left[ v^0 \frac{\partial v^0}{\partial t} + v^1 \frac{\partial v^0}{\partial x} \right] \right\} - \zeta \cdot (v^0 v^1) \cdot \left( \frac{\partial v^0}{\partial t} + \frac{\partial v^1}{\partial x} \right), \\ T^{11} = \varepsilon(v^1)^2 + p(v^0)^2 - 2\eta \left\{ [1 + (v^1)^2] \cdot \frac{\partial v^1}{\partial x} + v^1 v^0 \cdot \frac{\partial v^1}{\partial t} \right\} - \zeta (v^0)^2 \cdot \left( \frac{\partial v^0}{\partial t} + \frac{\partial v^1}{\partial x} \right), \end{array} \right.$$

where  $v^0$  is connected to  $v^1$  by the relation

$$(5) \quad (v^0)^2 - (v^1)^2 = 1.$$

Analogously to Landau's treatment, we introduce a new coordinate variable

$\xi = t - x$ , then the following two equations are obtained,

$$(6) \quad \begin{cases} \frac{\partial T^{00}}{\partial t} + \frac{\partial(T^{22} - T^{01})}{\partial \xi} = 0, \\ \frac{\partial(T^{00} - T^{01})}{\partial t} + \frac{\partial(T^{00} - 2T^{01} + T^{11})}{\partial \xi} = 0. \end{cases}$$

In the relativistic case, both components of the 4-velocity  $v^0$  and  $v^1$  ( $v^0 = 1/\sqrt{1-u^2}$ ,  $v^1 = u/\sqrt{1-u^2}$ ) have a large value compared with order  $\sim 1$ , and then from eq. (5), we obtain

$$v^0 \approx v^1 = v \gg 1, \quad v^0 - v^1 = \frac{1}{2v},$$

using the same value  $v$  for  $v^0$  and  $v^1$ . If we use the above relations and the characteristic equation,  $T^{\mu\nu}$  is written as follows:

$$(7) \quad \begin{cases} T^{00} \approx \frac{4}{3}(\varepsilon v^2) - 2\eta \left[ (1+v^2) \frac{\partial v}{\partial t} + \frac{\partial v}{\partial \xi} \right] - \zeta \cdot (v)^2 \cdot \frac{\partial v}{\partial t}, \\ T^{00} - T^{01} \approx \frac{\varepsilon}{3} - \frac{\eta}{2} \left[ 3 \frac{\partial v}{\partial t} + 4 \frac{\partial v}{\partial \xi} \right] + \frac{\zeta}{2} \frac{\partial v}{\partial t}, \\ T^{00} - 2T^{01} + T^{11} \approx \frac{\varepsilon}{3v^2} - \frac{\zeta}{4} \cdot \frac{1}{v^2} \frac{\partial v}{\partial t}. \end{cases}$$

Therefore, if we insert (7) into eq. (6), the equations of fluid motion are reduced to the following expressions,

$$(8) \quad \begin{cases} \frac{4}{3} \frac{\partial}{\partial t}(\varepsilon v^2) + \frac{1}{3} \frac{\partial \varepsilon}{\partial \xi} = 2\eta \cdot \frac{\partial}{\partial t} \left\{ (1+v^2) \frac{\partial v}{\partial t} + \frac{\partial v}{\partial \xi} \right\} + \zeta \frac{\partial}{\partial t} \left( v^2 \frac{\partial v}{\partial t} \right) + \\ \quad + \frac{\eta}{2} \frac{\partial}{\partial \xi} \left\{ 3 \frac{\partial v}{\partial t} + 4 \frac{\partial v}{\partial \xi} \right\} - \frac{\zeta}{2} \frac{\partial}{\partial \xi} \left( \frac{\partial v}{\partial t} \right), \\ \frac{1}{3} \frac{\partial \varepsilon}{\partial t} + \frac{1}{3} \frac{\partial}{\partial \xi} \left( \frac{\varepsilon}{v^2} \right) = \frac{\eta}{2} \frac{\partial}{\partial t} \left( 3 \frac{\partial v}{\partial t} + 4 \frac{\partial v}{\partial \xi} \right) - \frac{\zeta}{2} \frac{\partial}{\partial t} \left( \frac{\partial v}{\partial t} \right) + \frac{\zeta}{4} \frac{\partial}{\partial \xi} \left( \frac{1}{v^2} \frac{\partial v}{\partial t} \right). \end{cases}$$

According to eq. (8), we may think that the viscous effect makes a large contribution when the changes of velocity are large, even if the viscosities  $\eta$ ,  $\zeta$  are very small. This condition of large changes of velocity will be satisfied at the extreme point of an one dimensional motion, because the derivatives of the velocity are proportional to inverse powers of the co-ordi-



nate  $\xi$ . Then we can not omit the right hand side of eq. (8) when this equation is solved under the condition  $t \gg \xi \ll 1$ , 1 being the width of the system in Lorentz contraction.

To solve the simultaneous eqs. (8), we use the perturbation method, and expediently expand  $v^2$  and  $\varepsilon$  with respect to the viscosities  $\eta$  and  $\zeta$ ,

$$(9) \quad \begin{cases} v^2 = v_0^2 + \eta v_1^2 - \zeta v_2^2 + f(\eta^2, \zeta^2, \eta\zeta), \\ \varepsilon = \varepsilon_0 + \eta \varepsilon_1 - \zeta \varepsilon_2 + g(\eta^2, \zeta^2, \eta\zeta). \end{cases}$$

$f$  and  $g$  in the above relations contain second and higher order terms with respect to  $\eta$  and  $\zeta$ , and thus these are omitted in our calculation hereafter. Inserting (9) into eqs. (8), we obtain the 0-th order eq. (10) (zero order with respect to  $\eta, \zeta$ ) which is the same as the equation of motion of a perfect fluid,

$$(10) \quad \begin{cases} 4 \frac{\partial}{\partial t} (\varepsilon_0 v_0^2) + \frac{\partial}{\partial \xi} (\varepsilon_0) = 0, \\ \frac{\partial}{\partial t} (\varepsilon_0) + \frac{\partial}{\partial \xi} \left( \frac{\varepsilon_0}{v_0^2} \right) = 0, \end{cases}$$

and also the 1-st order eqs. (11), (12) (first order of  $\eta, \zeta$ ) become as follows:

$$(11) \quad \begin{cases} \frac{4}{3} \frac{\partial}{\partial t} \{ \varepsilon_0 v_1^2 + \varepsilon_1 v_0^2 \} + \frac{1}{3} \frac{\partial \varepsilon_1}{\partial \xi} = 2 \frac{\partial}{\partial t} \left\{ (1 + v_0^2) \frac{\partial v_0}{\partial t} + \frac{\partial v_0}{\partial \xi} \right\} + \frac{1}{2} \frac{\partial}{\partial \xi} \left\{ 3 \frac{\partial v_0}{\partial t} + 4 \frac{\partial v_0}{\partial \xi} \right\}, \\ \frac{1}{3} \frac{\partial \varepsilon_1}{\partial t} + \frac{1}{3} \frac{\partial}{\partial \xi} \left\{ \varepsilon_1 - \varepsilon_0 \cdot \frac{v_1^2}{v_0^2} \right\} = - \frac{1}{2} \frac{\partial}{\partial t} \left\{ 3 \frac{\partial v_0}{\partial t} + 4 \frac{\partial v_0}{\partial \xi} \right\}. \end{cases}$$

$$(12) \quad \begin{cases} \frac{4}{3} \frac{\partial}{\partial t} \{ \varepsilon_0 v_2^2 + \varepsilon_2 v_0^2 \} - \frac{1}{3} \frac{\partial \varepsilon_2}{\partial \xi} = \frac{\partial}{\partial t} \left\{ v_0^2 \frac{\partial v_0}{\partial t} \right\} - \frac{1}{2} \frac{\partial}{\partial \xi} \left( \frac{\partial v_0}{\partial t} \right), \\ \frac{1}{3} \frac{\partial \varepsilon_2}{\partial t} - \frac{1}{3} \frac{\partial}{\partial \xi} \left\{ \varepsilon_2 - \varepsilon_0 \cdot \frac{v_2^2}{v_0^2} \right\} = - \frac{1}{2} \frac{\partial}{\partial t} \left( \frac{\partial v_0}{\partial t} \right) + \frac{1}{4} \frac{\partial}{\partial \xi} \left( \frac{1}{v_0^2} \frac{\partial v_0}{\partial t} \right). \end{cases}$$

2.2. *Solution of the equation of motion of a perfect fluid.* — We first solve the eqs. (10) in this Section, but this solution is already obtained by LANDAU. For the benefit of our following discussions, we may summarize here this results.

LANDAU assumes  $v_0^2 = f_0 \cdot t/\xi$  for the velocity, where  $f_0$  is a function of  $t, \xi$  which decreases logarithmically, and obtains the solution of eqs. (10) under

the condition  $t \gg \xi \gg 1$ . And, he introduces the new variables  $\alpha$ ,  $\beta$  instead of  $t$ ,  $\xi$ ,

$$(13) \quad \alpha = \ln \frac{t}{A}, \quad \beta = \ln \frac{\xi}{A}.$$

Inserting these relations into the eqs. (10), the following two equations are obtained,

$$(14) \quad \begin{cases} f_0 \cdot \left( 1 + \frac{1}{\varepsilon_0} \frac{\partial \varepsilon_0}{\partial \alpha} \right) = -\frac{1}{4} \frac{1}{\varepsilon_0} \frac{\partial \varepsilon_0}{\partial \beta}, \\ f_0 \cdot \frac{1}{\varepsilon_0} \frac{\partial \varepsilon_0}{\partial \alpha} = -\left( 1 + \frac{1}{\varepsilon_0} \frac{\partial \varepsilon_0}{\partial \beta} \right). \end{cases}$$

If we eliminate the function  $f_0$  from the above simultaneous equations, we obtain a partial differential equation

$$(15) \quad 1 + \frac{1}{\varepsilon_0} \frac{\partial \varepsilon_0}{\partial \alpha} + \frac{1}{\varepsilon_0} \frac{\partial \varepsilon_0}{\partial \beta} + \frac{3}{4} \frac{1}{\varepsilon_0^2} \frac{\partial \varepsilon_0}{\partial \alpha} \cdot \frac{\partial \varepsilon_0}{\partial \beta} = 0.$$

Supposing that  $\varepsilon_0$  has an initial value  $\varepsilon_0^*$  at the position satisfying the relations  $\alpha \approx 0$ ,  $\beta \approx 0$ , we can find a solution  $\varepsilon_0$  of the above equation (15).

$$(16) \quad \varepsilon_0 = \varepsilon_0^* \exp \left[ -\frac{4}{3}(\alpha + \beta - \sqrt{\alpha \cdot \beta}) \right].$$

From eqs. (14) and (16), function  $f_0$  is determined as follows:

$$(17) \quad f_0 \approx \frac{1}{2} \sqrt{\frac{\alpha}{\beta}},$$

which has a value of order  $\sim 1$ . Using the above relation, eq. (16) is also written as

$$(18) \quad \varepsilon_0 = \varepsilon_0^* \exp \left[ -\frac{4}{3}(\alpha + \beta \cdot [1 - 2f_0]) \right].$$

**2'3. Solution of the equation of viscous motion in first order approximation.** — We sought for the solution  $\varepsilon_1$  of eqs. (11) of Sect. 2'1 under the condition  $t \gg \xi \gg 1$ , since  $v_0^2$  and  $\varepsilon_0$  were already known. If we insert into eq. (11)  $v_0^2$  and  $\varepsilon_0$  having the expressions  $v_0^2 \approx t/\xi$  and  $\varepsilon_0 \approx \varepsilon_0^* (\xi/t)^{\frac{1}{2}}$  respectively, in which  $f_0$  is assumed as the order  $\sim 1$  in the relation (18), the following two partial differential equations are obtained.

$$(19) \quad \begin{cases} \frac{4}{3} \frac{\partial}{\partial t} \left\{ \varepsilon_0^* \left( \frac{\xi}{t} \right)^{\frac{1}{2}} v_1^2 + \varepsilon_1 \left( \frac{t}{\xi} \right) \right\} - \frac{1}{3} \frac{\partial \varepsilon_1}{\partial \xi} = \frac{3}{2} t^{\frac{1}{2}} \cdot \xi^{-\frac{1}{2}} - \frac{3}{8} t^{-\frac{1}{2}} \cdot \xi^{-\frac{1}{2}} - \frac{1}{2} \xi^{-\frac{1}{2}} \cdot t^{-\frac{3}{2}}, \\ \frac{1}{3} \frac{\partial \varepsilon_1}{\partial t} + \frac{1}{3} \frac{\partial}{\partial \xi} \left\{ \left( \varepsilon_1 - \varepsilon_0^* \left( \frac{\xi}{t} \right)^{\frac{1}{2}} \cdot v_1^2 \right) \cdot \frac{\xi}{t} \right\} = -\frac{1}{2} \xi^{-\frac{1}{2}} \cdot t^{-\frac{1}{2}} - \frac{3}{8} \xi^{-\frac{1}{2}} \cdot t^{-\frac{3}{2}}. \end{cases}$$

We now assume the following form for the velocity  $v_1^2$  in the first approximation of  $v^2$ ,

$$(20) \quad v_1^2 = f_1 \cdot (t/\xi)^N,$$

where the function  $f_1$  is a slow varying function with respect to  $t$ ,  $\xi$ , and substitute this relation (20) into the above eqs. (19) and also omit the derivatives of the function  $f_1$ ,

$$(19') \quad \left\{ \begin{aligned} & 4 \left[ \varepsilon_0^* f_1 \cdot \left( N - \frac{4}{3} \right) \xi^{\frac{1}{2}-N} \cdot t^{N-\frac{3}{2}} + \frac{t}{\xi} \frac{\partial \varepsilon_1}{\partial t} + \frac{\varepsilon_1}{\xi} \right] + \frac{\partial \varepsilon_1}{\partial \xi} = \\ & \quad = \frac{9}{2} t^{\frac{1}{2}} \cdot \xi^{-\frac{3}{2}} - \frac{9}{8} t^{-\frac{1}{2}} \cdot \xi^{-\frac{3}{2}} - \frac{3}{2} t^{-\frac{3}{2}} \cdot \xi^{-\frac{1}{2}}, \\ & \frac{\partial \varepsilon_1}{\partial t} + \frac{\xi}{t} \cdot \frac{\partial \varepsilon_1}{\partial \xi} + \frac{\xi}{t} - \varepsilon_0^* f_1 \cdot \left( \frac{10}{3} - N \right) t^{N-\frac{3}{2}} \cdot \xi^{\frac{1}{2}-N} = -\frac{3}{2} \xi^{-\frac{3}{2}} \cdot t^{-\frac{1}{2}} - \frac{9}{8} \xi^{-\frac{1}{2}} \cdot t^{-\frac{3}{2}}. \end{aligned} \right.$$

Analogously to the method followed in Sect. 2'2, we eliminate the function  $f_1$  from eqs. (19') and using the relations (13), we have the following differential equation:

$$(21) \quad 8 \frac{\partial \varepsilon_1}{\partial \alpha} + (3N-2) \frac{\partial \varepsilon_1}{\partial \beta} - 8\varepsilon_1 + \binom{46-21N}{2} \frac{1}{A} \exp \left[ \frac{\alpha}{2} - \frac{3}{2} \beta \right] + \\ - \binom{18-27N}{8} \frac{1}{A} \exp \left[ -\frac{\alpha}{2} - \frac{\beta}{2} \right] + \left( \frac{3N-10}{2} \right) \frac{1}{A} \exp \left[ -\frac{3}{2} \alpha + \frac{2}{2} \beta \right] =$$

We can easily find the general solution <sup>(3)</sup> of eq. (21) as follows:

$$(22) \quad \alpha + \ln \left\{ \varepsilon_1 + \frac{(21N-46)}{3(10-3N)} \frac{1}{A} \exp \left[ \frac{\alpha}{2} - \frac{3}{2} \beta \right] + \right. \\ \left. + \frac{(27N-18)}{4(10-3N)} \frac{1}{A} \exp \left[ -\frac{\alpha}{2} - \frac{\beta}{2} \right] - \frac{1}{A} \exp \left[ -\frac{3}{2} \alpha + \frac{\beta}{2} \right] \right\} = \psi \left( \alpha - \frac{8}{3N-2} \beta \right),$$

$\psi$  being an arbitrary function. Deforming the above equation, we have

$$(22') \quad \varepsilon_1 = \exp \left[ \psi \left( \alpha - \frac{8}{3N-2} \beta \right) - \alpha \right] - \frac{(21N-46)}{3(10-3N)} \frac{1}{A} \exp \left[ \frac{\alpha}{2} - \frac{3}{2} \beta \right] - \\ - \frac{(27N-18)}{4(10-3N)} \frac{1}{A} \exp \left[ -\frac{\alpha}{2} - \frac{\beta}{2} \right] + \frac{1}{A} \exp \left[ -\frac{3}{2} \alpha + \frac{\beta}{2} \right].$$

<sup>(3)</sup> A. R. FORSYTH: *Differential Equations*, p. 404.



If we now take  $\varepsilon_1 = \varepsilon_1^* \exp[(8/(3N-10)) \cdot \alpha]$  ( $\varepsilon_1^* < 0$ ) for the value  $\varepsilon_1$  at the position  $\beta \approx 0$  ( $\xi \approx 1$ ) of the fluid motion in expanding process, an arbitrary function  $\psi$  can be determined,

$$\exp[\psi(\alpha)] = \left\{ \varepsilon_1^* \exp \left[ \frac{8}{3N-10} \cdot \alpha \right] + \frac{(21N-46)}{3(10-3N)} \frac{1}{A} \exp \left[ \frac{\alpha}{2} \right] + \frac{(27N-18)}{4(10-3N)} \frac{1}{A} \exp \left[ \frac{\alpha}{2} \right] - \frac{1}{A} \exp \left[ \frac{3}{2} \alpha \right] \right\} \cdot \exp[\alpha].$$

Performing the variable transformation,  $\alpha = \alpha + (8/(3N-2)) \cdot \beta$  in the above relation, and inserting the results into eq. (22'), we obtain the solution  $\varepsilon_1$  as follows:

$$(23) \quad \varepsilon_1 = \varepsilon_1^* \exp \left[ \frac{8}{3N-10} (\alpha - \beta) \right] + \frac{(21N-46)}{3(10-3N)} \frac{1}{A} \exp \left[ \frac{\alpha}{2} - \frac{12}{(3N-2)} \cdot \beta \right] + \frac{(27N-18)}{4(10-3N)} \frac{1}{A} \exp \left[ -\frac{\alpha}{2} - \frac{4}{(3N-2)} \cdot \beta \right] - \frac{(21N-46)}{3(10-3N)} \frac{1}{A} \exp \left[ \frac{\alpha}{2} - \frac{3}{2} \beta \right] - \frac{(27N-18)}{4(10-3N)} \frac{1}{A} \exp \left[ -\frac{\alpha}{2} - \frac{\beta}{2} \right] - \frac{1}{A} \exp \left[ -\frac{3}{2} \alpha + \frac{\beta}{2} \right].$$

Moreover, eq. (23) is written again in the following form with the variables  $t, \xi$ ,

$$(23') \quad \varepsilon_1 = \varepsilon_1^* \cdot \left( \frac{t}{\xi} \right)^{8/(3N-10)} - \frac{(21N-46)}{3(10-3N)} \frac{1}{A} \left\{ \left( \frac{t}{1} \right)^{\frac{1}{2}} \cdot \left( \frac{1}{\xi} \right)^{12/(3N-2)} - \left( \frac{t}{1} \right)^{\frac{1}{2}} \cdot \left( \frac{1}{\xi} \right)^{\frac{1}{2}} \right\} - \frac{(27N-18)}{4(10-3N)} \frac{1}{A} \left\{ \left( \frac{t}{1} \right)^{\frac{1}{2}} \cdot \left( \frac{1}{\xi} \right)^{4/(3N-2)} - \left( \frac{t}{1} \right)^{\frac{1}{2}} \cdot \left( \frac{1}{\xi} \right)^{\frac{1}{2}} \right\} - \frac{1}{A} \left\{ \left( \frac{t}{1} \right)^{\frac{1}{2}} \cdot \left( \frac{\xi}{1} \right)^{4/(3N-2)} - \left( \frac{t}{1} \right)^{\frac{1}{2}} \cdot \left( \frac{\xi}{1} \right)^{\frac{1}{2}} \right\}.$$

Using the above expression (23') and one of the eq. (19'), the functional form of  $f_1$  is decided as

$$(24) \quad f_1 = \frac{3}{(10-3N)\varepsilon_0^*} \left[ \varepsilon_1^* \left( \frac{t}{\xi} \right)^{\frac{8}{3}-N+8/(3N-10)} + \frac{(21N-46)}{3(10-3N)} A^{(12/(3N-2))-\frac{3}{2}} \cdot \left( \frac{3}{2} - \frac{12}{3N-2} \right) \frac{t^{\frac{10}{3}-N-\frac{1}{2}}}{\xi^{\frac{7}{3}-N+12/(3N-2)}} + \frac{(27N-18)}{4(10-3N)} A^{(4/(3N-2))-\frac{1}{2}} \cdot \left( \frac{1}{2} - \frac{4}{3N-2} \right) \frac{t^{\frac{10}{3}-N-\frac{3}{2}}}{\xi^{\frac{7}{3}-N+4/(3N-2)}} - A^{\frac{1}{2}-4/(3N-2)} \left( \frac{1}{2} + \frac{4}{3N-2} \right) \frac{t^{\frac{10}{3}-N-\frac{1}{2}}}{\xi^{\frac{7}{3}-N-4/(3N-2)}} + \frac{3}{2} \frac{t^{\frac{10}{3}-N-\frac{1}{2}}}{\xi^{\frac{7}{3}-N+\frac{3}{2}}} + \frac{9}{8} \frac{t^{\frac{10}{3}-N-\frac{3}{2}}}{\xi^{\frac{7}{3}-N+\frac{1}{2}}} \right].$$

For the expression of  $f_1$ , we ask that  $f_1$  be a slow varying function with respect to  $t$ ,  $\xi$ . If we now impose the condition  $\frac{7}{3} - N + 8/(3N - 10) = 0$  for the above relation (24), the expression of the function  $f_1$  reads approximately as follows:

$$(24') \quad f_1 \approx \frac{-0.83}{\varepsilon_0^*} \left\{ \varepsilon_1^* - 2.12 \cdot \frac{1}{\Delta^{0.47}} \frac{\xi^{1.13}}{t^{1.66}} - 1.124 \frac{1}{\Delta^{0.16}} \frac{\xi^{1.82}}{t^{2.66}} + \right. \\ \left. + 0.156 \Delta^{0.15} \frac{\xi^{2.50}}{t^{3.65}} + \frac{3}{2} \frac{\xi^{0.66}}{t^{1.66}} + \frac{9}{8} \frac{\xi^{1.66}}{t^{2.66}} \right\},$$

where we selected  $N = (51 + \sqrt{945})/18 \approx 4.541$  in the values of  $N$  satisfying the above condition. Then, if we select, for instance  $\varepsilon_1^* \approx -\varepsilon_0^*$ , although the method of the determination of  $\varepsilon_i^*$  does not exist, it should be permitted to take for practical use the value  $f_1 \sim 0.83$  and also to omit the derivatives of  $f_1$ , under the condition  $t \gg \xi \gg \Delta$ .

Next, we shall seek for the solution of eq. (12) under the same condition as that of eq. (11).

Analogously to the method followed in eq. (19), we substitute  $v_0^2 \approx t/\xi$ ,  $\varepsilon_n \approx \varepsilon_0^*(\xi/t)^{\frac{1}{2}}$  into the eq. (12) and so obtain the following two equations,

$$(25) \quad \begin{cases} \frac{1}{3} \frac{\partial}{\partial t} \{ \varepsilon_0 v_2^2 + \varepsilon_2 v_0^2 \} + \frac{1}{3} \frac{\partial \varepsilon_2}{\partial \xi} = -\frac{3}{8} \xi^{-\frac{1}{2}} \cdot t^{-1}, \\ \frac{1}{3} \frac{\partial \varepsilon_2}{\partial t} + \frac{1}{3} \frac{\partial}{\partial \xi} \left\{ \frac{\varepsilon_2 - \varepsilon_0 \cdot v_2^2/v_0^2}{v_0^2} \right\} = -\frac{3}{16} \cdot \xi^{-\frac{1}{2}} \cdot t^{-\frac{3}{2}}. \end{cases}$$

We also took for the velocity in 1-st order approximation the relation <sup>(4)</sup>

$$(26) \quad v_2^2 = f_2 \cdot (t/\xi)^M,$$

in which the function  $f_2$  is considered as about constant with respect to  $t$ ,  $\xi$ , and inserted this relation into eq. (25). In this case, omitting the derivatives of the function  $f_2$ ,

$$(25') \quad \begin{cases} 4 \left[ \varepsilon_0^* f_2 \left( M - \frac{4}{3} \right) \xi^{\frac{1}{2}-M} \cdot t^{M-\frac{7}{2}} + \frac{t}{\xi} \frac{\partial \varepsilon_2}{\partial t} + \frac{\varepsilon_2}{\xi} \right] + \frac{\partial \varepsilon_2}{\partial \xi} = -\frac{9}{8} \cdot \xi^{-\frac{1}{2}} \cdot t^{-\frac{1}{2}}, \\ \frac{\partial \varepsilon_2}{\partial t} + \frac{\xi}{t} \frac{\partial \varepsilon_2}{\partial \xi} + \frac{\varepsilon_2}{t} - \varepsilon_0^* f_2 \left( \frac{10}{3} - M \right) t^{M-\frac{10}{2}} \cdot \xi^{\frac{3}{2}-M} = -\frac{9}{16} \cdot \xi^{-\frac{1}{2}} \cdot t^{-\frac{3}{2}}. \end{cases}$$

<sup>(4)</sup> We choose the value  $M = (51 + \sqrt{945})/18 \approx 4.541$  so that the first term in the brackets of the relation (30) has the constant value  $\varepsilon_2^*$ .

If we eliminate the function  $f_2$  from the above equation and use the variable transformation (13), we obtain the following partial differential equation

$$(27) \quad 8 \frac{\partial \varepsilon_2}{\partial \alpha} - (3M - 2) \frac{\partial \varepsilon_2}{\partial \beta} = -8\varepsilon_2 - \frac{(9M + 6)}{8} \frac{1}{A} \exp \left[ -\frac{\alpha}{2} - \frac{\beta}{2} \right].$$

The general solution of the above eq. (27) is obtained by the use of an arbitrary function  $\varphi$  after easy calculation,

$$(28) \quad \varepsilon_2 = \exp \left[ \varphi \left( \alpha - \frac{8}{3M - 2} \beta \right) - \alpha \right] - \frac{(9M + 6)}{4(10 - 3M)} \frac{1}{A} \exp \left[ -\frac{\alpha}{2} - \frac{\beta}{2} \right].$$

In order to decide the form of the arbitrary function  $\varphi$ , we also adopted  $\varepsilon_2 = \varepsilon_2^* \exp [(8/(3M - 10)) \cdot \alpha]$  ( $\varepsilon_2^* < 0$ ) for  $\varepsilon_2$  at the position  $\beta \approx 0$  ( $\xi \approx A$ ). As result, we obtain the following expression according to the same procedure as that of eq. (11),

$$(29) \quad \varepsilon_2 = \varepsilon_2^* \exp \left[ \frac{8}{3M - 10} (\alpha - \beta) \right] - \frac{(9M + 6)}{4(10 - 3M)} \frac{1}{A} \exp \left[ -\frac{\alpha}{2} - \frac{4}{(3M - 2)} \beta \right] - \frac{(9M + 6)}{4(10 - 3M)} \frac{1}{A} \exp \left[ -\frac{\alpha}{2} - \frac{\beta}{2} \right].$$

If we transform the variables  $\alpha, \beta$  into  $t, \xi$  and use  $M \approx 4.541$ , we have the expression

$$(29) \quad \varepsilon_2 \approx \varepsilon_2^* \left( \frac{t}{\xi} \right)^{2.208} + 3.23 \left\{ \frac{1}{A^{0.155} \cdot t^{0.5} \cdot \xi^{0.345}} - \frac{1}{t^{0.5} \cdot \xi^{0.5}} \right\},$$

and the function

$$(30) \quad f_2 \approx -\frac{0.83}{\varepsilon_0^*} \left\{ \varepsilon_2^* - 0.504 \cdot \frac{1}{A^{0.155} \cdot t^{2.69} \cdot \xi^{1.845}} + \frac{9}{16} \frac{\xi^{1.7}}{t^{2.7}} \right\}.$$

Supposing that  $\varepsilon_2^*$  is nearly equal to  $-\varepsilon_0^*$ , the relation (30) may be written over as  $f_2 \sim 0.83$  approximately, because the 1-st term in the brackets of the above expression gives the greatest contribution to  $f_2$  under the condition  $t \gg \xi \gg 1$ . Therefore, the omission of the derivatives of  $f_2$  with respect to  $t, \xi$  in eq. (25') should be permitted.

Here, we must summarize the results obtained in Sections 2.2, 2.3 of this paragraph to calculate the energy and the entropy distributions.

For the velocity  $v^2$  in eq. (8), we assumed as follows:

$$(31) \quad v^2 \approx \frac{t}{\xi} + (\eta - \zeta) \cdot \left( \frac{t}{\xi} \right)^{1.541}.$$



In this case, we considered that all the functions  $f_0$ ,  $f_1$  and  $f_2$  have nearly values of the order  $\sim 1$ . And, from the eqs. (16), (23) and (29) we obtained the expression,

$$(32) \quad \varepsilon \approx \varepsilon_0^* \left\{ \exp \left[ -\frac{4}{3}(\alpha + \beta - \sqrt{\alpha \cdot \beta}) \right] - (\eta - \zeta) \cdot \exp [2.208(\alpha - \beta)] \right\}.$$

The terms omitted in the expression (32) give a small contribution compared with the 2-nd term of the above expression. Hereafter, for brevity of calculation, we shall use the relation (32) for  $\varepsilon$ . Physically the relations (31) and (32) signify that the velocity given by (31) shows a decrease compared with the velocity of a perfect fluid at the extreme point of the fluid's motion, owing to the influence of the viscosity, and that, on the contrary, the energy density increases at the same point as above ( $\eta < 0$ ,  $\zeta > 0$ ).

### 3. Physical Quantities in Hydrodynamical Treatment.

3.1. *The energy and the entropy distributions.* — From the expression (1),  $T^{00}$  describing the energy density is given by

$$T^{00} \approx \frac{4\varepsilon v^2}{3} - 2\eta \left[ (1 + v^2) \frac{\partial v}{\partial t} + \frac{\partial v}{\partial \xi} \right] - \zeta(v^2) \frac{\partial v}{\partial t}.$$

Using the above component of the energy momentum tensor, the energy distribution along the direction of the  $x$ -axis is written as

$$dE \sim a^2 T^{00} d\xi.$$

If we apply the relations (31), (32) of the previous paragraph for the above expression, we obtain

$$(33) \quad dE \propto \left\{ \frac{4}{3} \varepsilon_0^* A \cdot \left( \exp \left[ -\frac{1}{3} (\sqrt{\alpha} - 2\sqrt{\beta})^2 \right] - (\eta - \zeta) \cdot \right. \right. \\ \cdot \left( \exp [3.208\alpha - 2.208\beta] - \exp \left[ 4.541\alpha - 3.541\beta - \frac{4}{3}(\alpha + \beta - \sqrt{\alpha \cdot \beta}) \right] \right) \\ \left. \left. - \eta \exp \left[ -\frac{\alpha}{2} + \frac{\beta}{2} \right] - \frac{\zeta}{2} \exp \left[ \frac{\alpha}{2} - \frac{\beta}{2} \right] \right) \right\} d\beta.$$

The contribution of the 2nd term in the brackets of the above expression is very small, and yet the last term of the brackets of the relation (33) has a large negative contribution ( $\zeta > 0$ ), so that the energy distribution of (33) shows a slight decrease compared with the results obtained by LANDAU.

For the entropy distribution, we also obtain the following relation in using the entropy density  $s_0 \approx sv$  ( $s \propto \varepsilon^{\frac{3}{2}}$ ) and the relations (31), (32),

$$(34) \quad dS \propto \exp \left[ -\frac{1}{2} (\sqrt{\alpha} - \sqrt{\beta})^2 \right] \cdot \left\{ 1 - \frac{3}{4} (\eta - \zeta) \cdot \right. \\ \left. \cdot \exp \left[ \frac{4}{3} (\alpha + \beta - \sqrt{\alpha} \cdot \beta) + 2.208(\alpha - \beta) \right] + \frac{1}{2} (\eta - \zeta) \exp [3.541 \cdot (\alpha - \beta)] \right\} d\beta.$$

Since the contribution of the 2-nd and 3-rd terms of the above expression is roughly estimated as  $\sim \frac{1}{4}(\eta - \zeta) \exp [3.041(\alpha - \beta)]$  ( $\eta < 0, \zeta > 0$ ), we see that the viscous effects result in the increase of the entropy distribution. And, the maximum point of this distribution is formally given by the relation.

$$\xi = \left[ t \cdot \Delta^{8-0.12(\eta-\zeta)} \left( \frac{t}{\xi} \right)^{3.541} \right]^{1/(9-0.12(\eta-\zeta)(t/\xi)^{3.541})}$$

but this expression is not suitable for practical use.

3.2. *Conical scattering process.* — For the limitation that the expanding process of the system forms the one dimensional fluid motion, we impose the condition

$$(35) \quad t \cdot \theta \ll a.$$

In order to estimate the small angle  $\theta$ , we shall use the equation of motion of the system in transverse direction. Now that it is necessary to estimate only the order of magnitude, we can use, according to Landau's method, the relation  $T^{02}/t \sim T^{22}/a$  instead of the equation of motion in the transverse direction  $\partial T^{02}/\partial t \sim \partial T^{22}/\partial y$ .

If we omit the 2-nd order terms of the viscosity and  $\theta$ , the components of  $T^{\mu\nu}$  in the above expression are respectively given by

$$(36) \quad \begin{cases} T^{02} \sim \varepsilon r^2 \theta \left[ \frac{v\theta}{t} + \frac{v}{a} + 2 \frac{v^3 \theta}{t} \right] \approx \left[ \frac{v^3 \theta}{t} \right], \\ T^{22} \sim \varepsilon \cdot 2\eta \left[ \frac{r\theta}{a} \right] \approx \left[ \frac{r}{t} - \frac{v\theta}{a} \right]. \end{cases}$$

From the above expression (36), we obtain

$$\frac{t}{a} = v^2 \theta - \frac{\eta}{\varepsilon} \left[ \frac{v\theta}{t} + 2 \frac{v^3 \theta}{t} + \frac{v}{a} \right],$$

where  $\zeta$ -terms do not appear in 1st order approximation.

We rewrite the above equation as follows:

$$\theta = \frac{t}{a} - \frac{\eta}{a} \left( \frac{r}{\xi} \right) + \frac{\eta}{r^2} \left[ \frac{r}{\xi} - 2 \frac{r^3}{\xi} \right],$$

and substitute eqs. (31), (32) into this relation, and then obtain

$$(37) \quad \theta \approx \frac{\xi}{a} \left\{ 1 - (\eta - \zeta) \left( \frac{t}{\xi} \right)^{3.541} - \frac{\eta}{\varepsilon_0} \left[ (\xi/t^3)^{\frac{1}{2}} - 3 \cdot (1/t \cdot \xi)^{\frac{1}{2}} \right] \right\},$$

where  $\varepsilon_0$  is already given by eq. (16). We can consider that the 3-rd term in the brackets of eq. (37) is very small compared with the other viscous term owing to the condition  $t \gg \xi \gg 1$ . Therefore, we can expect from eq. (37) that the existence of the viscosity results in a large scattering angle compared with the angle obtained by LANDAU.

Moreover, we introduce the limitation of applicability of the one dimensional solution, using the relation (35). Namely, we have the relation

$$(38) \quad t \cdot \xi \ll a^2 \cdot \left\{ 1 + (\eta - \zeta) \left( \frac{t}{\xi} \right)^{3.541} \right\}.$$

If we now suppose  $t \sim t_1$  for this limitation, we obtain

$$(38') \quad t_1 = \frac{a^2}{\xi} \left\{ 1 - (\eta - \zeta) \left( \frac{t_1}{\xi} \right)^{3.541} \right\}.$$

but, by the method of successively substitution, this relation is written over again as

$$(39) \quad t_1 \approx \frac{a^2}{\xi} \left[ 1 + (\eta - \zeta) \left( \frac{a}{\xi} \right)^{7.082} \right],$$

where the second order terms of the viscosity are omitted.

The fluid motion tends to conical scattering at the moment  $t_1$  given by the relation (39) which is smaller than that of LANDAU.

In this conical scattering process, the differentiation of the co-ordinate  $\xi$  of the macroscopic element of the fluid in the expanding system with respect to  $t$  has the following form,

$$\frac{d\xi}{dt} = -1 - u_x = (v^0 - v^1) \cdot \sqrt{1 - u^2} \approx \frac{1}{2v^2},$$



As is shown in the following discussions, the velocity of the fluid in conical scattering is proportional to the time, so that  $\xi$  approaches rapidly a constant value and consequently the velocity of this process reaches rapidly the velocity of light. From the above basis of our argument, we can omit the derivative of hydrodynamical quantity with respect to  $\xi$ . Remembering the thermodynamical assumption described in Sect. 1, we have respectively to admit the relations that the total sum of the energy  $T^{00}$  and the heat flow  $K \cdot r^{1,1} \cdot r$  ( $K$  is the temperature) in a given cone are constantly conserved, and that the changes of these quantities with the development of time cancel each other. From the above two conditional formulas, we can also find the relations

$$(40) \quad \varepsilon \propto \frac{1}{t^3}, \quad r \propto t.$$

**3.3. The number of created particles and angular distribution.** — For the benefit of the calculation, we also introduce the variables  $\lambda$  and  $L$  by the relations

$$(41) \quad \frac{\xi}{a} = \exp[-\lambda], \quad \frac{A}{a} = \exp[-L].$$

$\beta$ , given by eq. (13), is written as

$$\beta = \ln \frac{\xi}{A} = L - \lambda.$$

And, the variable  $z$  at the moment  $t_1$  given by the relation (39) has the form,

$$\begin{aligned} \alpha_1 = \ln \frac{t_1}{A} &= \ln \frac{a^2}{\xi \cdot A} \left[ 1 + (\eta - \zeta) \left( \frac{a}{\xi} \right)^{7.082} \right] \\ &= L + \lambda + \ln [1 + (\eta - \zeta) \exp[7.082\lambda]]. \end{aligned}$$

If we substitute these relations into the entropy distribution (34) and omit the 2-nd order terms of the viscosity, we have the entropy distribution with respect to the variable  $\lambda$ . Moreover, if we remember the relation between the entropy and the number of created particles discussed in Sect. 1, we obtain a distribution rule of the created particle number,

$$(42) \quad dN = C \exp[\sqrt{L^2 - \lambda^2}] \left\{ 1 + \frac{(\eta - \zeta)}{2} \frac{(L - \lambda)}{\sqrt{L^2 - \lambda^2}} \exp[7.082\lambda] - \right. \\ \left. \frac{3}{4} (\eta - \zeta) \exp \left[ \frac{4}{3} (2L - \sqrt{L^2 - \lambda^2}) + 4.416\lambda \right] \right\} d\lambda.$$

$C$  is a normalization constant. And, we have the following form for the scattering angle, using the relation (41),

$$(43) \quad \theta \sim \exp[-\lambda] \cdot (1 - (\eta - \zeta) \exp[7.082\lambda]) .$$

From the particle distribution given by the relation (42), we asked for the scattering angle of the greater part of created particles in the centre of mass system. Since the variable  $\lambda$  satisfying the above consideration is subjected to the condition

$$(44) \quad \lambda \approx \frac{L}{\sqrt{2}} \left\{ 1 + \frac{(\eta - \zeta)}{4} \left( -0.829 \frac{\exp[5.008L]}{L} + 2.933 \exp[5.008L] - 8.624 \exp[4.847L] \right) \right\} ,$$

the scattering angle of the greater part of created particles is expressed as

$$(45) \quad \theta \sim \exp \left[ -\frac{L}{\sqrt{2}} \right] \cdot \left\{ 1 - \frac{(\eta - \zeta)}{4\sqrt{2}} \exp[4.847L] \cdot (4.828 - 2.933L) \exp[0.161L] - 8.624L \right\} .$$

If we apply the relation  $MAC^2/E' = \sqrt{2}MAC^2/E$  ( $MA$  is a mass of particle) used by LANDAU which expresses the order of Lorentz contraction, the following relation is given,

$$(46) \quad L = \ln E'/MA \quad (C=1).$$

Investigating the value of the second term in the brackets of (45) in using the above relation, we see that the viscosity produces a negative effect on the angle  $\theta$  in (45) since by a rough estimate the brackets of (45) have a negative contribution.

Also, we see, by the same rough estimate, that the viscous effects for the distribution of the produced particles given by (42) bring on an increase of the multiplicity of produced particles <sup>(5)</sup>.

Now, we shall decide the normalization const. of eq. (42). From eqs. (2) and (46), the total number of the produced particles  $N$  is roughly given by the order of magnitude  $\sim \exp[L/2]$ . Therefore, from the following relation,

$$\int_{\lambda=0}^{\lambda=L} dN \sim C \cdot \exp[L] \left\{ 1 - \frac{(\eta - \zeta)}{2} \left( 1 - \frac{3}{2} \exp[6.082L] \right) \right\} \sim \exp[L/2] ,$$

<sup>(5)</sup> W. HEISENBERG: *Zeits. f. Phys.*, **126**, 569 (1949).

$U$  is expressed as

$$U \approx \exp \left[ \frac{-L}{2} \right] \left\{ 1 - \frac{(\eta - \zeta)}{2} \left( 1 - \frac{3}{2} \exp [6.082L] \right) \right\}.$$

In this connection, we have for the maximum value of  $\lambda$

$$\lambda_{\text{Max}} = \frac{\sqrt{3}}{2} L \left\{ 1 - \frac{(\eta - \zeta)}{6L} (2 - 0.536 \exp [6.133L] - 3 \exp [5.824L] - 3 \exp [6.082L]) \right\},$$

according to the condition  $\int_{\lambda=\lambda_{\text{Max}}}^{\lambda=L} dN \sim 1$  used by LANDAU.

3.4. *The energy distribution of the particle in free scattering.* — In this Section, we investigate the correlation between the energy and the time component of the 4-velocity of the particle. The velocity given by eq. (31) reaches the velocity expressed with  $v_1 \approx (t_1/\xi)^{\frac{1}{2}} (\eta - \zeta) 2 \cdot (t_1/\xi)^{4.041}$  at the time  $t_1$  which gives the limit of the one dimensional fluid motion.

Now that the time dependence of the velocity in the conical scattering process is given by relation (40), we have the following relation for the velocity in this process, using the above velocity  $v_1$ ,

$$(47) \quad v \sim \left[ \left( \frac{t_1}{\xi} \right)^{\frac{1}{2}} + \frac{(\eta - \zeta)}{2} \left( \frac{t_1}{\xi} \right)^{4.041} \right] \frac{t}{t_1} \sim \frac{t}{a}.$$

We obtained the above expression in terms of the relation (38'). It is interesting to notice that the expression (47) is obtained in spite of the existence of viscous effects.

Analogously to the above method, the energy density at the time  $t \sim t_1$  is expressed by

$$\varepsilon = \varepsilon_0^* \left\{ \exp \left[ -\frac{4}{3} (2L - \sqrt{L^2 - \lambda^2}) \right] \left( 1 - \frac{4}{3} (\eta - \zeta) \exp [7.082\lambda] + \right. \right. \\ \left. \left. + \frac{2}{3} (\eta - \zeta) \left[ \frac{L}{L - \lambda} \exp [7.082\lambda] \right] - (\eta - \zeta) \exp [4.416\lambda] \right) \right\},$$

where the 2-nd order terms of the viscosity are omitted. Using the relation (40) for the time dependence of the energy density, we obtain

$$(48) \quad \varepsilon = \varepsilon_0^* \left( \frac{t_1}{t} \right)^4 \left\{ \exp \left[ -\frac{4}{3} (2L - \sqrt{L^2 - \lambda^2}) \right] \left( 1 - \frac{4}{3} (\eta - \zeta) \exp [7.082\lambda] + \right. \right. \\ \left. \left. + \frac{2}{3} (\eta - \zeta) \left[ \frac{L - \lambda}{L + \lambda} \exp [7.082\lambda] \right] - (\eta - \zeta) \exp [4.416\lambda] \right) \right\}.$$



From the above relation, we can find the critical moment  $t_k$  of the transition from fluid motion to free scattering of the particles:

$$t_k \approx t_1 \left( \frac{\varepsilon_0^*}{\varepsilon_k} \right)^{\frac{1}{2}} \exp \left[ -\frac{1}{3} (2L - \sqrt{L^2 - \lambda^2}) \right] \left\{ 1 - \frac{1}{3} (\eta - \zeta) \exp [7.082\lambda] + \right. \\ \left. + \frac{(\eta - \zeta)}{6} \right\} \frac{L - \lambda}{L + \lambda} \exp [7.082\lambda] - \frac{(\eta - \zeta)}{4} \exp \left[ 4.416\lambda + \frac{4}{3} (2L - \sqrt{L^2 - \lambda^2}) \right] \Bigg\};$$

$\varepsilon_k$  is the energy density corresponding to the time  $t_k$ .

Inserting the above expression into (47), we have an expression for the energy of the particle at the moment of the free scattering,

$$m v_k \sim m \frac{t_k}{a} = \text{const} \cdot \exp \left[ \lambda + \frac{1}{3} \sqrt{L^2 - \lambda^2} \right] \left\{ 1 + \frac{2}{3} (\eta - \zeta) \exp [7.082\lambda] + \right. \\ \left. + \frac{1}{6} (\eta - \zeta) \right\} \frac{L - \lambda}{L + \lambda} \exp [7.082\lambda] - \frac{(\eta - \zeta)}{4} \exp \left[ 4.416\lambda + \frac{4}{3} (2L - \sqrt{L^2 - \lambda^2}) \right] \Bigg\}.$$

The constant value in this expression is given by the use of particle distribution (42) and the relation,  $\int m v dN = E' \sim M A e^L$ .

$$\text{const} \approx M A \exp \left[ -\frac{L}{6} \right] \left\{ 1 + \frac{1}{2} (\eta - \zeta) \left( 1 - \frac{3}{2} \exp [6.082L] \right) - \right. \\ \left. \frac{2}{3} (\eta - \zeta) \exp [7.082L] + (\eta - \zeta) \exp \left[ 4.416L + \frac{8}{3} L \right] \right\}.$$

As final expression, we have for the energy distribution of the produced particles (center of mass system)

$$(49) \quad m v_k \sim M \exp \left[ -\frac{L}{6} - \lambda + \frac{1}{3} \sqrt{L^2 - \lambda^2} \right] \left\{ 1 + \frac{1}{2} (\eta - \zeta) \left( 1 - \frac{3}{2} \exp [6.082L] \right) \right. \\ \left. \frac{2}{3} (\eta - \zeta) \exp [7.082L] + (\eta - \zeta) \exp \left[ \frac{8}{3} L + 4.416L \right] \right\} \cdot \\ \cdot \left\{ 1 + \frac{2}{3} (\eta - \zeta) \exp [7.082\lambda] + \frac{1}{6} (\eta - \zeta) \sqrt{\frac{L - \lambda}{L + \lambda}} \exp [7.082\lambda] - \right. \\ \left. - \frac{1}{4} (\eta - \zeta) \exp \left[ 4.416\lambda + \frac{4}{3} (2L - \sqrt{L^2 - \lambda^2}) \right] \right\}.$$

And also, if we apply the condition (44) to the above expression, the greater

part of free scattering particles has the energy given by

$$(50) \quad m v_i \sim M \exp \left[ \frac{8 - \sqrt{2}}{6\sqrt{2}} \cdot L \right] \left\{ 1 + (\eta - \zeta) [0.638 + 0.346 \cdot L] \exp [5.008 L] \right. \\ \left. - (\eta - \zeta) \cdot [0.25 + 1.016 L] \exp [4.847 L] + \right. \\ \left. + \frac{(\eta - \zeta)}{2} - \frac{3}{4} (\eta - \zeta) \exp [6.082 L] + \frac{1}{3} (\eta - \zeta) \exp [7.802 L] \right\}.$$

Moreover, if we use the relation (46), the above expression may be written again as

$$m v_i \sim M \left( \frac{E'}{MA} \right)^{(8 - \sqrt{2})/6\sqrt{2}} \left\{ 1 + (\eta - \zeta) \left[ 0.638 + 0.346 \cdot \ln \left( \frac{E'}{MA} \right) \right] \cdot \left( \frac{E'}{MA} \right)^{5.008} \right. \\ \left. - (\eta - \zeta) \cdot \left[ 0.25 + 1.016 \cdot \ln \left( \frac{E'}{MA} \right) \right] \cdot \left( \frac{E'}{MA} \right)^{4.847} + \right. \\ \left. \frac{(\eta - \zeta)}{2} - \frac{3}{4} (\eta - \zeta) \cdot \left( \frac{E'}{MA} \right)^{6.082} + \frac{1}{3} (\eta - \zeta) \cdot \left( \frac{E'}{MA} \right)^{7.802} \right\}.$$

Now that the last viscous term in the brackets of the above expression has a larger contribution than other viscous terms, we see, by a rough estimate, that the energy of the particles produced in centre of mass system shows a slight decrease compared with that of a perfect fluid, due to the existence of the viscosity.

#### 4. - Discussions.

From the last expression of Sect. 3, we can roughly investigate the appropriateness of our perturbation method with respect to viscosity. The most effective term perturbed by the viscosity in this expression for the energy of the particle may satisfy the following relation in order to assure the utility of the method of the expansion series supposed for the solution of the equation of motion,

$$(51) \quad \frac{1}{2} (\eta - \zeta) \left( \frac{E'}{MA} \right)^{7.052} < 1.$$

If we now apply the relation,  $T_{(\eta)}^{\alpha\alpha} + T_{(\zeta)}^{\alpha\alpha} = 0$  ( $\mu = \nu = \alpha$ ), in eq. (1), we know that  $\zeta$  is related to  $\eta$  by the relation  $\zeta = -2\eta$  ( $\zeta > 0$ ,  $\eta < 0$ ). Therefore, the above relation (51) is written as follows in the laboratory frame of reference,

$$(52) \quad \eta_0 c \left( \frac{E}{2MAc^2} \right)^{3.541} < 1,$$

where  $\eta_0$  is the viscosity expressed in C.G.S. units and  $C$  is the velocity of light. Considering the case that the incident nucleon in the laboratory system has, say, the energy  $E \sim 30000$  GeV <sup>(\*)</sup>, from the above relation we have roughly the relation  $\eta_0 < 10^{-23}$ .

But, we know that the expressions of the 2-nd viscous terms of eqs. (31) and (32) depend on the arbitrary selection for the values of  $\varepsilon_1^*$  and  $\varepsilon_2^*$  of eqs. (24) and (30). (In eqs. (31), (32), we supposed the relation  $\varepsilon_1^* = \varepsilon_2^* = \varepsilon_0^*$ .)

If we suppose, for instance  $\varepsilon_1^* = \varepsilon_2^* = -\gamma\varepsilon_0^*$ , we shall obtain the relation  $f_1 \approx f_2 \sim 0.83\gamma$  ( $\gamma = |\varepsilon_1^*/\varepsilon_0^*|$  or  $|\varepsilon_2^*/\varepsilon_0^*|$ ), where  $\gamma$  has a small positive value. Moreover,  $\gamma$  may be restricted by the condition that, from eqs. (24), (30),  $\varepsilon_1^* 10^{0.5}l^{0.5}$  and  $\varepsilon_2^* 10^{0.5}l^{0.5}$  have to possess order of magnitude  $\sim 1$  respectively, in order to permit the omission of the derivatives of  $f_1$  and  $f_2$ . In this case, all the expressions obtained by us still can be used if we replace the viscosities  $\eta$ ,  $\zeta$  of our expression by  $\eta\gamma$ ,  $\zeta\gamma$ , respectively. Then, the former condition is written over as  $\eta_0\gamma < 10^{-23}$  (\*). This means that we can not avoid by any means the arbitrary selection of the boundary condition in the solution of the 1-st order approximation.

Now, if we permit that the viscosity  $\eta_0$  should be estimated in using the conception of the usual gas theory, we obtain

$$\eta_0 \sim n \cdot m \cdot \bar{u} \cdot l,$$

where  $n$ ,  $m$  are the density of the meson gas and the mass of meson (Bose gas), respectively.

Since the velocity in conical flight is nearly equal to the velocity of light, if we regard  $\bar{u} \approx c$ , we shall see that the above conditional relation is satisfied when we have a suitable selection for the mean free path  $\bar{l}$  of the constituent particles.

In his famous work, LANDAU stressed the fact that the mean free path of the particles of a strongly compressed Bose gas is very small compared with the linear dimension of the system during the expanding process and, in conical scattering process, this length is comparable to the linear dimensions of the system.

But, in our model, the mean free path may be merely smaller than the linear dimension of the system, say  $h/\mu c \sim 10^{-13}$  cm, even in the conical scattering process, due to the viscous effects.

Our calculation was done continually in the 1-st order approximation with respect to the viscosities  $\eta$  and  $\zeta$ . For the benefit of the quantitative

(\*) E. FERMI: *Phys. Rev.*, **81**, 683 (1950).

(\*) On the other hand,  $\eta_0\gamma$  in our expression may be determined by the agreement of the experimental data with the results obtained by us.



discussion to follow, we also computed the numerical values of the three places of decimals.

The quantitative discussions of the results of our calculation will be published in a forthcoming paper. And, the transformation from the expression in the centre of mass system to that of laboratory frame of reference will be also done in the quantitative discussions.

\* \* \*

In conclusion, we should like to express our gratitude to Professor H. YUKAWA for his kind interest and to Professors T. IVOUE and C. HAYASHI for their helpful discussions and encouragements.

#### RIASSUNTO (\*)

Nella descrizione della produzione multipla delle particelle nelle collisioni ad alta energia si introducono in forma relativistica covariante i tensori degli sforzi viscosi. Come risultato si calcolano in prima approssimazione gli effetti della viscosità e, sulla base del concetto di irreversibilità in termodinamica relativistica, si discutono anche le differenze qualitative dalla teoria di Landau.

(\*) Traduzione a cura della Redazione.

## Vacuum Expectation Values as Sums Over Histories.

P. W. HIGGS

*Tait Institute of Mathematical Physics, University of Edinburgh, Scotland*

(ricevuto l'8 Agosto 1956)

**Summary.** — The way in which vacuum expectation values may be calculated as sums over histories, according to Feynman's formulation of quantum mechanics, is discussed. It is shown that the evaluation of the functional integrals for the matrix elements of chronologically ordered operator products does not automatically lead to the propagators of quantized fields, as seemed to be so in a paper by MATTHEWS and SALAM; their work is criticized for its vagueness about boundary conditions. A limiting procedure for obtaining vacuum expectation values is defined: it involves the device of introducing an infinitesimal imaginary term into the Lagrangian and letting the epoch in which the matrix element is specified tend to infinity. It is demonstrated that the device commonly used in field theory for defining Feynman Green's functions is of this type, but that it does not necessarily lead to vacuum expectation values when the Lagrangian is not quadratic. An alternative trick which is more generally applicable is suggested: this involves the use of a complex time parameter, which selects out the ground state in the limit of infinite epoch in a manner similar to the freezing into the ground state which occurs in thermal equilibrium at the absolute zero of temperature.

### 1. — Introduction.

MATTHEWS and SALAM<sup>(1)</sup> have shown how to calculate the propagators of quantized fields directly as «sums over histories»<sup>(2)</sup> by using the parametric method introduced by DAVISON<sup>(3)</sup> and EDWARDS<sup>(4)</sup> to evaluate the

<sup>(1)</sup> P. T. MATTHEWS and A. SALAM: *Nuovo Cimento*, **2**, 120 (1955). This paper will be referred to henceforth as M.S.

<sup>(2)</sup> R. P. FEYNMAN: *Rev. Mod. Phys.*, **20**, 367 (1948).

<sup>(3)</sup> B. DAVISON: *Proc. Roy. Soc., A* **225**, 252 (1954).

<sup>(4)</sup> S. F. EDWARDS: *Phil. Mag.*, **45**, 758 (1954).

functional integrals involved. In the case of free fields, they arrive in this way at the usual Feynman functions,  $\Delta_F$  and  $S_F$ , for Bose and Fermi fields respectively.

It is, however, not clear why this should be so, for the quantities which are directly expressible as sums over histories are not in fact vacuum expectation values of the type  $T^*A(1) \dots Z(n)_{\text{vac}}$ , which one wants, but ratios such as  $\langle \varphi', \sigma' | T^*A(1) \dots Z(n) | \varphi'', \sigma'' \rangle / \langle \varphi', \sigma' | \varphi'', \sigma'' \rangle$ . (Here, as in M.S.,  $\varphi(x)$  is the field operator,  $\sigma'$  and  $\sigma''$  are space-like surfaces ( $\sigma'$  later than  $\sigma''$ ), and  $q', \sigma'$  and  $q'', \sigma''$  are eigenstates of  $q$  corresponding to eigenvalues  $q'$  on  $\sigma'$  and  $q''$  on  $\sigma''$ , respectively.  $A(1), \dots, Z(n)$  are field operators or their derivatives at points lying between  $\sigma'$  and  $\sigma''$  and  $T^*$  is NISHIJIMA's <sup>(5)</sup> time ordering operator with sign changes as appropriate for Fermi fields <sup>(6)</sup>).

Moreover, MATTHEWS and SALAM do not specify the boundary conditions which define the complete orthonormal set of functions used for the parametrization. Thus, strictly, neither is the Green's function which they obtain adequately defined, and it appears rather to be a fortunate accident that the infinitesimal imaginary term in the Lagrangian, which is introduced in order to make the functional integrals converge, also selects out the Feynman boundary conditions which specify  $\Delta_F$  and  $S_F$ . Similar criticisms of M.S. have been made also by SUNAKAWA *et al.* <sup>(7)</sup>.

The purpose of this paper is to clarify the way in which vacuum expectation values may be calculated as sums over histories. For the most part, the dynamical system discussed is the harmonic oscillator, since this example exhibits the essential features of the problem and the generalization to a free Bose field is trivial. In Sect. 2 it is shown by calculating

$$\langle q', t' | Tq(t_1)q(t_2) | q'', t'' \rangle / \langle q', t' | q'', t'' \rangle,$$

where  $q$  is the oscillator co-ordinate, that the additional term  $\frac{1}{2}i\epsilon q^2$  in the Lagrangian, which is required to make the functional integrals converge, does not automatically give rise to the Feynman Green's function. In Sect. 3 it is shown how vacuum expectation values are reached by a limiting process in which the epoch ( $t' - t''$ ) is made to approach infinity before  $\epsilon$  is allowed to tend to zero. The procedure is demonstrated in detail for the oscillator problem in order to show how the Green's function defined by the Feynman contour in the frequency plane is obtained.

The question posed in Sect. 4 is whether the trick using  $\frac{1}{2}i\epsilon q^2$  and the double

<sup>(5)</sup> K. NISHIJIMA: *Prog. Theor. Phys.*, **5**, 405 (1950).

<sup>(6)</sup> G. C. WICK: *Phys. Rev.*, **80**, 268 (1950).

<sup>(7)</sup> K. KAKI, K. MURATA and S. SUNAKAWA: *Soryusiron-kenkyu* (in Japanese), **11**, No. 3 (1956); quoted by K. YAMAZAKI: *Nuovo Cimento*, **4**, 141 (1956).

limit works for a Lagrangian more general than the quadratic type; a « double box » potential is advanced as a counter example to prove that the trick does not always lead to ground state expectation values. An alternative trick of more general applicability, employing a complex time parameter, is suggested and its relation to the low temperature limit in problems of thermal equilibrium is noted.

The Appendix contains an alternative, and more direct derivation of the explicit expression for  $\langle q', t' | Tq(t_1)q(t_2) | q'', t'' \rangle / \langle q', t' | q'', t'' \rangle$ .

## 2. - Harmonic Oscillator Green's Functions.

Applied to a dynamical system having a single degree of freedom  $q(t)$ , Feynman's <sup>(2)</sup> formulation of quantum mechanics gives as the matrix element of a chronologically ordered product of dynamic variables the expression <sup>(1,8)</sup>

$$(1) \quad \langle q', t' | T^* A(1) \dots Z(n) | q'', t'' \rangle = N^{-1} \int \delta q A(1) \dots Z(n) \exp \left[ i \int_{t''}^{t'} dt L(q, \dot{q}) \right].$$

Here  $L$  is the Lagrangian (we set  $\hbar = 1$ ),  $N$  is a normalizing factor and the functional integration is over all paths  $q(t)$  such that  $q(t') = q'$ ,  $q(t'') = q''$ . All the quantities on the right hand side of (1) are  $c$ -numbers. Evaluation of  $N$  may be avoided if we consider only ratios of expressions of the type (1); in particular, we shall be interested in the quantity

$$(2) \quad \frac{\langle q', t' | Tq(1)q(2) | q'', t'' \rangle}{\langle q', t' | q'', t'' \rangle} = \frac{\int \delta q q(1)q(2) \exp [i \int L dt]}{\int \delta q \exp [i \int L dt]}.$$

The parametrization of the functional integrals is performed by expanding the general path  $q(t)$  in terms of a complete set of functions:

$$(3) \quad q(t) = \tilde{q}(t) + \sum_n a_n q_n(t).$$

In (3)  $\tilde{q}(t)$  is a particular single-valued piecewise continuous function such that  $\tilde{q}(t') = q'$ ,  $\tilde{q}(t'') = q''$ , and  $q_n$  is an infinite set of linearly independent functions, satisfying the boundary conditions  $q_n(t') = q_n(t'') = 0$  (all  $n$ ) and spanning the space of all single-valued piecewise continuous functions which

<sup>(8)</sup> J. C. POLKINGHORNE: *Proc. Roy. Soc., A* **230**, 272 (1955).



satisfy the same conditions. Then (2) becomes

$$(4) \quad \frac{\langle q', t' | Tq(1)q(2) | q'', t'' \rangle}{\langle q', t' | q'', t'' \rangle} = \frac{\prod_n \int_{-\infty}^{+\infty} da_n q(1)q(2) \exp[i \int L dt]}{\prod_n \int_{-\infty}^{+\infty} da_n \exp[i \int L dt]}.$$

That the right hand side of (4) is independent of the particular choice of  $\tilde{q}$  and the set  $q_n$  is easily seen: changing  $\tilde{q}$  merely adds constant amounts to the  $a_n$ ; a different choice of the  $q_n$  leads to a new set  $a_n$  which is a linear combination of the old set and the resulting Jacobian cancels out between the numerator and the denominator. However, if one wishes to avoid numerators and denominators which are simultaneously infinite or zero, one has to choose the normalization of the set  $q_n$  with care<sup>(9)</sup>.

The action integral for the harmonic oscillator may be written (after a partial integration and the dropping of the boundary terms) in the form

$$(5) \quad I = \int_{t''}^{t'} L dt = -\frac{1}{2} \iint_{t''}^{t'} dt_1 dt_2 q(t_1) \mathcal{R}(t_1, t_2) q(t_2),$$

where  $\mathcal{R}(t_1, t_2) = \delta(t_1 - t_2)(d^2/dt^2 - \omega^2)$ . The most convenient parametrization is achieved by choosing for  $\tilde{q}$  the classical path

$$(6) \quad q_c(t) = \frac{q' \sin \omega(t - t'') + q'' \sin \omega(t' - t)}{\sin \omega(t' - t'')},$$

which satisfies the condition

$$(7) \quad \mathcal{R}q_c = 0,$$

and for  $q_n$  the orthonormal set of eigenfunctions of  $\mathcal{R}$ , subject to the stated boundary conditions:

$$(8) \quad q_n(t) = \left( \frac{2}{t' - t''} \right)^{\frac{1}{2}} \sin n\pi \left( \frac{t - t''}{t' - t''} \right), \quad n = 1, 2, \dots, \infty.$$

Then the action (5) takes on the simple form

$$(9) \quad I = -\frac{1}{2} \sum_{n=1}^{\infty} a_n^2 \left( \omega^2 - \frac{n^2 \pi^2}{T^2} \right),$$

where  $T = t' - t''$ .

<sup>(9)</sup> See, for example, DAVISON<sup>(3)</sup>.

Equation (4) now becomes

$$\frac{q^+, t^- Tq(1)q(2) q^-, t^+}{q^+, t^- q^-, t^+} = \frac{\prod_n \int_{-\infty}^{+\infty} da_n [q_-(1) + \sum_l a_l q_l(1)] [q_-(2) + \sum_s a_s q_s(2)] \exp[-(i/2)a_n^2(\omega^2 - (n^2\pi^2/T^2))]}{\prod_n \int_{-\infty}^{+\infty} da_n \exp[-(i/2)a_n^2(\omega^2 - (n^2\pi^2/T^2))]}.$$

If we modify the Lagrangian by substituting  $(\omega^2 - i\varepsilon)$  for  $\omega^2$ , the integrals converge and we obtain finally on passing to the limit  $\varepsilon \rightarrow +0$

$$(10) \quad \frac{q^+, t^- Tq(1)q(2) q^-, t^+}{q^+, t^- q^-, t^+} = q_-(1)q_-(2) - iG_0(1, 2),$$

in which

$$G_0(1, 2) = \sum_{n=1}^{\infty} \left( \omega^2 - \frac{n^2\pi^2}{T^2} \right)^{-1} q_-(1)q_n(2).$$

Using (8) we may write this last expression more explicitly:

$$(11) \quad G_0(t_1, t_2) = \sum_{n=1}^{\infty} \frac{2}{T} \left( \omega^2 - \frac{n^2\pi^2}{T^2} \right)^{-1} \sin \frac{n\pi}{T} (t_1 - t'') \sin \frac{n\pi}{T} (t_2 - t').$$

The evaluation of the sum may be avoided by noticing that  $G_0$  is that Green's function of the operator  $\mathcal{K}$  which corresponds to the boundary conditions imposed on  $q_n$ . Thus it may be found by solving the equation

$$(12) \quad \left( \frac{d^2}{dt_1^2} + \omega^2 \right) G_0(t_1, t_2) = \delta(t_1 - t_2),$$

with these boundary conditions. The explicit solution is

$$(13) \quad G_0(t_1, t_2) = \begin{cases} \frac{\sin \omega(t' - t_1) \sin \omega(t_2 - t'')}{\omega \sin \omega(t' - t'')}, & t_1 > t_2, \\ \frac{\sin \omega(t' - t_2) \sin \omega(t_1 - t'')}{\omega \sin \omega(t' - t'')}, & t_1 < t_2. \end{cases}$$

An alternative derivation of equation (10), which does not involve the evaluation of functional integrals, is described in the Appendix.

We observe at this point that the functional integral method does not automatically lead to the Feynman Green's function, which would indeed be incorrect here. How then is the derivation of this Green's function by MAT-

THEWS and SALAM to be explained? We note first that their parametrization differs from that used here in two important respects: they omit the term  $\tilde{q}$  without justification and fail to specify the boundary conditions which enter into the definition of the set  $q_n$ . Then they write their Green's function as  $\mathcal{K}^{-1}$ , an expression which must be given meaning by reference to the boundary conditions on  $q_n$ ; this they do implicitly by writing  $q$  as a Fourier integral, an expansion which implies that the epoch  $T$  is infinite ( $t' \rightarrow +\infty, t'' \rightarrow -\infty$ ).

We note next that the Fourier integral definition of the Feynman Green's function is very similar in form to (11):

$$(14) \quad G_F(t_1, t_2) = \lim_{\varepsilon \rightarrow +0} \frac{1}{2\pi} \int_{-\infty}^{+\infty} \frac{\exp[ikt_1] \exp[-ikt_2]}{\omega^2 - i\varepsilon - k^2} dk.$$

The significant change is the replacement of the sum by an integral along the Feynman contour in the frequency plane, achieved by making  $T$  tend to infinity *before*  $\varepsilon$  is allowed to tend to zero. We shall now examine the significance of such a limiting process in general <sup>(10)</sup>.

### 3. - Vacuum Expectation Values as Limits.

We consider a general dynamical system having energy levels  $E_n$ ,  $n = 0, 1, 2, \dots$ , such that  $E_0$  is the non-degenerate ground state (« vacuum »). We add to the Lagrangian an infinitesimal imaginary term  $i\varepsilon A(q)$  so as to induce level shifts  $[-i\varepsilon\lambda_n \rightarrow 0(\varepsilon^2)]$ , where by elementary perturbation theory

$$(15) \quad \lambda_n = \langle A \rangle_n,$$

the expectation value of  $A$  in the eigenstate  $|n\rangle$  of the Hamiltonian.

Let  $Q$  be any dynamic variable. Its matrix element between the states  $|q', t'\rangle$  and  $|q'', t''\rangle$  may be expanded as a double series in the states  $|n\rangle$ :

$$(16) \quad \frac{\langle q', t' | Q | q'', t'' \rangle}{\langle q', t' | q'', t'' \rangle} = \frac{\sum_{m,n} \langle q', t' | m \rangle \langle m | Q | n \rangle \langle n | q'', t'' \rangle}{\sum_n \langle q', t' | n \rangle \langle n | q'', t'' \rangle} =$$

$$\frac{\sum_{m,n} \langle q', 0 | m \rangle \langle m | Q | n \rangle \langle n | q'', 0 \rangle \exp[-t'(iE_m - \varepsilon\lambda_m) - t''(iE_n - \varepsilon\lambda_n)]}{\sum_n \langle q', 0 | n \rangle \langle n | q'', 0 \rangle \exp[-(t' - t'')(iE_n + \varepsilon\lambda_n)]}.$$

<sup>(10)</sup> I am grateful to Professor R. E. PEIERLS for pointing out to me the importance of taking the limit  $T \rightarrow \infty$  before letting  $\varepsilon \rightarrow 0$ .

We now choose such a  $\lambda$  that  $\lambda_n > \lambda_0$  ( $n > 0$ ) and let first  $t' \rightarrow +\infty$ ,  $t'' \rightarrow -\infty$ , then  $\varepsilon \rightarrow +0$ : we get

$$(17) \quad \lim_{\varepsilon \rightarrow +0} \left\{ \lim_{\substack{t' \rightarrow +\infty \\ t'' \rightarrow -\infty}} \frac{\langle q', t' | Q | q'', t'' \rangle}{\langle q', t' | q'', t'' \rangle} \right\} = \langle Q \rangle_0.$$

That is, in a field theoretical problem we arrive at vacuum expectation values.

In the oscillator problem, the trick used to make the functional integral converge amounts to choosing

$$\lambda(q) = \frac{1}{2}q^2.$$

It has the effect of changing  $\omega$  to  $\tilde{\omega}$ , defined by

$$\tilde{\omega}^2 = \omega^2 - i\varepsilon.$$

The modified energy levels are

$$\tilde{E}_n = (n + \frac{1}{2})\tilde{\omega}.$$

Thus we find

$$\lambda_n = (n + \frac{1}{2})/2\omega.$$

The condition  $\lambda_n > \lambda_0$  is obviously satisfied.

We may verify by direct calculation that the limiting process (17), applied to (10), leads to  $Tq(1)q(2)_0$ . We replace  $\omega$  everywhere by  $\tilde{\omega}$  and, performing the triple limit <sup>(11)</sup>, find from (6) that

$$(18) \quad \lim q_c(t) = 0$$

and from (13) that

$$\lim G_0(t_1, t_2) = \frac{i}{2\omega} \exp[-i\omega|t_1 - t_2|].$$

This is just the Green's function  $G_F$ , since it contains only positive frequencies. Thus we obtain finally

$$(19) \quad \langle Tq(t_1)q(t_2) \rangle_0 = (2\omega)^{-1} \exp[-i\omega|t_1 - t_2|] = -iG_F(t_1, t_2).$$

---

<sup>(11)</sup> This process will be denoted briefly by « lim ».



Although  $G_0$  has a limit, the orthonormal set (8) to which it is related has none. Nevertheless, in the limit  $t' \rightarrow -\infty$ ,  $t'' \rightarrow +\infty$ , functions which are zero on the boundaries may be expressed as Fourier integrals:

$$(20) \quad q(t)_k = (2\pi)^{-\frac{1}{2}} \int_{-\infty}^{+\infty} dk a(k) \exp [ikt] .$$

However, this parametrization is inconvenient for the purpose of performing the functional integrations, since the label  $k$  is continuous. It is better to employ, as do MATTHEWS and SALAM, a discretely labelled set  $q_n(t)$  satisfying the boundary conditions  $q_n(-\infty) = q_n(+\infty) = 0$  and such that the action is diagonal in  $n$ . That is, we write

$$(21) \quad q(t) = \sum_n a_n q_n(t) ,$$

where

$$(22) \quad \int_{-\infty}^{+\infty} dt_1 \int_{-\infty}^{+\infty} dt_2 q_m(t_1) \mathcal{R} q_n(t_2) = \delta_{mn} .$$

Then the integrations in (4) lead directly to the expression (14) for  $G_F$ .

The principal results of this section provide a justification in detail of the procedure used by MATTHEWS and SALAM. On the one hand, the general theorem (17) shows how vacuum expectation values may be obtained as limits of matrix elements of the type which the Feynman principle yields directly. On the other hand, equation (18) provides the justification for omitting  $q(t)$  from the parametrization (3) in the limit  $T \rightarrow \infty$ ,  $\varepsilon \neq 0$ .

#### 4. - An Alternative Device: Complex Time Parameter.

It is of interest to enquire whether the trick of adding  $\frac{1}{2}i\varepsilon q^2$  to the Lagrangian serves in general to select out the ground state in the limit (17). With the choice  $A = \frac{1}{2}q^2$ , the condition which must be satisfied,  $\dot{\lambda}_n \rightarrow \dot{\lambda}_0$ , becomes

$$(23) \quad \langle q^2 \rangle_n > \langle q^2 \rangle_0 .$$

It is a simple matter to construct a Lagrangian for which (23) is not sa-

tified. For example one may take the double box potential,

$$\begin{aligned} V(q) &= V', & a' < q < b'; \\ V(q) &= V'', & a'' < q < b''; \\ V(q) &= +\infty, & q < a', \quad b' < q < a'', \quad b'' < q. \end{aligned}$$

Then the energy levels form a double sequence,

$$\begin{aligned} E'_n &= V' + \frac{n^2\pi^2}{2(b' - a')^2}, \\ E''_n &= V'' + \frac{n^2\pi^2}{2(b'' - a'')^2}, \end{aligned} \quad n = 1, 2, \dots, \infty.$$

One finds for the expectation values of  $q^2$  the expressions

$$\begin{aligned} \langle q^2 \rangle'_n &= a'b' + (b' - a')^2 \frac{(2\pi^2 n^2 - 3)}{6\pi^2 n^2}, \\ \langle q^2 \rangle''_n &= a''b'' + (b'' - a'')^2 \frac{(2\pi^2 n^2 - 3)}{6\pi^2 n^2}. \end{aligned}$$

The parameters may easily be adjusted so that the ground state does not have the lowest value of  $q^2$ . Thus the device of introducing  $\frac{1}{2}i\epsilon q^2$  into the Lagrangian does not in general lead to vacuum expectation values in the limit (17).

An alternative trick, which can be shown to work quite generally, is to introduce a phase factor into the time parameter. We replace  $t$  everywhere by  $\tau$ , defined by

$$(24) \quad \tau = t \exp[-i\alpha], \quad 0 < \alpha < \pi.$$

Considering the expression (16), we see that now

$$\frac{\langle q', \tau' | Q | q'', \tau'' \rangle}{\langle q', \tau' | q'', \tau'' \rangle} = \frac{\sum_{m,n} \langle q', 0 | m \rangle \langle m | Q | n \rangle \langle n | q'', 0 \rangle \exp[-i(E_m \tau' - E_n \tau'')]}{\sum_n \langle q', 0 | n \rangle \langle n | q'', 0 \rangle \exp[-iE_n(\tau' - \tau'')]}.$$

In the limit  $t' \rightarrow +\infty$ ,  $t'' \rightarrow -\infty$ , the phase factor ensures that the contribution from the ground state predominates:

$$(25) \quad \lim_{t' \rightarrow +\infty, t'' \rightarrow -\infty} \frac{\langle q', \tau' | Q | q'', \tau'' \rangle}{\langle q', \tau' | q'', \tau'' \rangle} = \langle Q \rangle_0.$$

All that remains is to verify that the same device makes the functional integrals converge. This will be done only for the harmonic oscillator. Re-

calling equation (9), we find that the modified argument of the exponential in (2) is

$$\begin{aligned} iI &= \frac{i}{2} \sum_{n=1}^{\infty} a_n^2 \left( \omega^2 - \frac{n^2 \pi^2}{T^2} \exp[2iz] \right), \\ &= -\frac{1}{2} \sum_{n=1}^{\infty} a_n^2 \left[ i \left( \omega^2 - \frac{n^2 \pi^2}{T^2} \cos 2\alpha \right) - \frac{n^2 \pi^2}{T^2} \sin 2\alpha \right]. \end{aligned}$$

Provided that  $0 < \alpha < \frac{1}{2}\pi$ , the convergence of the integrals is ensured.

Finally, we may remark that the part played here by the parameter  $\tau$  is very similar to that played by the parameter  $\beta$  ( $= (k\theta)^{-1}$ , where  $\theta$  is the absolute temperature and  $k$  is Boltzmann's constant) in the behaviour of systems in thermal equilibrium. Indeed it is well known that the density matrix describing thermal equilibrium is related to the transformation function by the equation <sup>(12)</sup>

$$(26) \quad \varrho(q', q''; \beta) = \langle q', -i\beta | q'', 0 \rangle.$$

Thus the picking out of the ground state in the limit  $\tau' \rightarrow +\infty \exp[-i\alpha]$ ,  $\tau'' \rightarrow -\infty \exp[-i\alpha]$  is closely analogous to the freezing into the ground state which occurs as  $\beta \rightarrow \infty$  ( $\theta \rightarrow 0$ ).

\* \* \*

It is a pleasure to thank Professor N. KEMMER for his continued interest and encouragement, Professor R. E. PEIERLS for an illuminating discussion and Dr. D. L. PURSEY for many helpful comments and suggestions during the course of this work.

#### APPENDIX

A simple alternative proof of equation (10) runs as follows. It is well known <sup>(13)</sup> that the chronological product  $Tq(t_1)q(t_2)$  satisfies the inhomogeneous equation

$$\mathcal{R}Tq(t_1)q(t_2) = -i\delta(t_1 - t_2).$$

Therefore the matrix element (2) satisfies the same equation:

$$(A.1) \quad \mathcal{R} \frac{\langle q', t' | Tq(t_1)q(t_2) | q'', t'' \rangle}{\langle q', t' | q'', t'' \rangle} = -i\delta(t_1 - t_2).$$

---

<sup>(12)</sup> F. BLOCH: *Zeits. f. Phys.*, **74**, 295 (1932).

Now since  $|q', t'\rangle$ ,  $|q'', t''\rangle$  are eigenvectors of  $q$  at  $t'$ ,  $t''$  respectively, we have as boundary conditions

$$(A.2) \quad \begin{cases} \frac{\langle q', t' | Tq(t')q(t_2) | q'', t'' \rangle}{\langle q', t' | q'', t'' \rangle} = q' \frac{\langle q', t' | q(t_2) | q'', t'' \rangle}{\langle q', t' | q'', t'' \rangle}, \\ \frac{\langle q', t' | Tq(t'')q(t_2) | q'', t'' \rangle}{\langle q', t' | q'', t'' \rangle} = q'' \frac{\langle q', t' | q(t_2) | q'', t'' \rangle}{\langle q', t' | q'', t'' \rangle}. \end{cases}$$

Moreover, the matrix element on the right hand side of these last equations satisfies the homogeneous equation

$$(A.3) \quad \mathcal{R} \frac{\langle q', t' | q(t) | q'', t'' \rangle}{\langle q', t' | q'', t'' \rangle} = 0,$$

with the boundary conditions

$$(A.4) \quad \begin{cases} \frac{\langle q', t' | q(t') | q'', t'' \rangle}{\langle q', t' | q'', t'' \rangle} = q', \\ \frac{\langle q', t' | q(t'') | q'', t'' \rangle}{\langle q', t' | q'', t'' \rangle} = q''. \end{cases}$$

From (A.3) and (A.4) we obtain

$$(A.5) \quad \frac{\langle q', t' | q(t) | q'', t'' \rangle}{\langle q', t' | q'', t'' \rangle} = q_c(t).$$

Using (A.5), we rewrite the boundary conditions (A.2) in the form

$$(A.6) \quad \begin{cases} \frac{\langle q', t' | Tq(t')q(t_2) | q'', t'' \rangle}{\langle q', t' | q'', t'' \rangle} = q' q_c(t_2), \\ \frac{\langle q', t' | Tq(t'')q(t_2) | q'', t'' \rangle}{\langle q', t' | q'', t'' \rangle} = q'' q_c(t_2). \end{cases}$$

The solution of (A.1), subject to the conditions (A.6), is

$$(A.7) \quad \frac{\langle q', t' | Tq(t_1)q(t_2) | q'', t'' \rangle}{\langle q', t' | q'', t'' \rangle} = q_c(t_1)q_c(t_2) - iG_0(t_1, t_2),$$

where  $G_0$  is that Green's function of  $\mathcal{R}$  which is zero on the boundaries.

<sup>(13)</sup> See, for example, P. T. MATTHEWS and A. SALAM: *Proc. Roy. Soc., A* **221**, 128 (1953).



## RIASSUNTO (\*)

Si discute il modo di calcolare i valori prevedibili per il vuoto secondo la formulazione di Feynman della meccanica quantistica. Si dimostra che il calcolo degli integrali funzionali degli elementi di matrice di prodotti di operatori ordinati cronologicamente non conduce automaticamente ai propagatori dei campi quantizzati, come sembrava essere secondo un lavoro di MATTHEWS e SALAM; si critica tale lavoro per la sua mancanza di precisazioni sulle condizioni al contorno. Si definisce un procedimento di passaggio al limite per ricavare i valori prevedibili del vuoto: consiste nell'introdurre nel lagrangiano un termine infinitesimo immaginario lasciando tendere all'infinito l'epoca in cui si specifica l'elemento di matrice. Si dimostra che l'artificio comunemente usato in teoria dei campi per definire le funzioni di Green di Feynman è dello stesso tipo ma che non conduce necessariamente ai valori prevedibili del vuoto se il lagrangiano non è quadratico. Si suggerisce un accorgimento, più generalmente applicabile, da usare in alternativa: è basato sull'uso di un parametro temporale complesso che sceglie lo stato fondamentale al limite di tempo infinito in modo analogo al congelamento nello stato fondamentale che si ha nello stato di equilibrio termico allo zero assoluto delle temperature.

(\*) Traduzione a cura della Redazione.

## Coherence Effects in the Lee-Yang Parity Doublet Theory of Strange Particles.

R. GATTO

*Istituto di Fisica e Scuola di Perfezionamento in Fisica Nucleare dell'Università - Roma*  
*Istituto Nazionale di Fisica Nucleare - Sezione di Roma*

(ricevuto il 9 Agosto 1956)

**Summary.** — It is shown that certain coherence effects occur in the parity doublet theory of strange particles which may give rise to peculiar time and angular dependences in angular correlations. The possibility of observing such effects is closely related to the values of the mass differences in the parity doublets, and it would in fact permit measurement of the mass differences. A condition for the observability of the coherence effects is that the electromagnetic interaction be minimal. Other physical aspects of the theory, such as the time dependence of the decay rates, the lifetimes of hyperons, and the parity doublet structure of hyperfragments, are discussed.

### Introduction.

In this paper we show that certain coherence effects occur in the parity doublet theory <sup>(1)</sup> of strange particles which give rise to peculiar phenomena, such as time dependent angular correlations with a damped oscillating part consisting of terms of odd parity (\*). The frequency of the oscillations will in general be of the order of the mass difference in a parity doublet (we use units  $\hbar = 1$ ,  $c = 1$ ). If such mass difference is large compared to the inverse decay lifetime the very rapid oscillations would not be observable. If the mass difference

---

<sup>(1)</sup> T. D. LEE and C. N. YANG: *Phys. Rev.*, **102**, 290 (1956).

(\*) *Note added in proof.* - A parallel investigation has been carried out by G. MORPURGO (*Nuovo Cimento*: to be published). Similar results have been obtained by T. D. LEE and C. N. YANG (*Phys. Rev.*: to be published).

is comparable to the inverse decay lifetime the effects could be observed and provide a very accurate measurement of the mass difference itself. The problem of the mass differences in a parity doublet is related to the question of the minimal electromagnetic interaction. If the electromagnetic interaction is minimal only the weak interactions can originate a mass difference between the two members of a parity doublet. In this case the mass differences may be expected to be of the order of the inverse decay lifetimes, and the coherence effects discussed here could result observable. Effects due to the superposition of amplitudes corresponding to the two components of a parity doublet will be most apparent if the two components have nearly equal lifetimes. This possibility is however not implied by the Lee-Yang theory.

We show that, except for cascade decays, no odd parity terms are expected to occur in the case of parity nonconservation in weak interactions. The detection of such terms would be a stringent argument in favor of the parity doublet theory. Other physical consequences of the parity doublet theory, such as the time dependence of the decay rates, the question of the relative frequencies of the various kinds of events in associated production and their relation to the hyperon lifetimes, and the parity doublet structure of hyperfragments are discussed.

## 1. — The Lee-Yang Parity Doublet Theory.

It has been shown by DALITZ <sup>(2)</sup> from an analysis of the data on  $K_{3\pi}^+$  decays that the particle responsible for these events cannot decay according to the  $K_{\pi^-}$  mode — if angular momentum and parity are conserved in the transition. It must be stressed that this result entirely rests on the present rather limited statistics and also on a number of theoretical assumptions which could be not valid if the  $\tau$  had a very complicated structure. (One could argue, for instance, that to reconcile with a unique  $K^+$ -meson the observed ratio between the  $K_{3\pi}^+$  and the  $K_{2\pi}^+$  frequencies, a comparison of the two available phase spaces leads to postulate an interaction radius for the decay much larger than the  $K$ -meson Compton wavelength.) Experimentally all  $K$ -mesons exhibit same mass, same lifetime, and same cross-sections in strong interactions. Assuming the existence of two different  $K$ -mesons,  $\tau$  and  $\theta$ , with same spin but opposite parity, LEE and YANG <sup>(1)</sup> consider the assumption that the approximate equality of masses follows from some invariance property. This assumption leads to postulate that the strong hamiltonian (that part of the total hamiltonian which conserves total isotopic spin) commutes with a parity

---

<sup>(2)</sup> R. H. DALITZ: *Phys. Rev.*, **94**, 1046 (1954); *Proceedings of the Rochester Conference, 1956* (to be published).

conjugation operator. It follows that all particles with odd strangeness exist in parity doublets, and that for each strong reaction there is a parity conjugate reaction of equal cross section (this last result would explain the equality of the excitation functions). If the electromagnetic interaction does not commute with the parity conjugation operator the mass differences between the two members of a parity doublet could be of the order of magnitude of the mass difference between charged and neutral pions. If the electromagnetic interaction commutes with the parity conjugation operator the mass differences may only originate from the weak interactions and be of the order of the inverse decay lifetime, about  $10^{-6} - 10^{-5}$  eV. Of the two possibilities only the latter would be consistent with the principle of minimal electromagnetic interaction<sup>(3)</sup>. It must explicitly be remarked that this scheme does not seem to offer any simple explanation of the equality of the  $K^+$  lifetimes. It has been shown that the existence of a parity conjugation quantum number for strong (and possibly also for electromagnetic) interactions leads in some cases to new selection rules<sup>(4)</sup>.

## 2. - Angular Correlations in the Parity Doublet Theory.

2.1. - The effects considered here may occur quite generally for a coherent superposition of amplitudes relative to the two components of the same parity doublet. We shall examine two particular angular correlation experiments which have already been proposed as possible methods for determining the spins. The first deals with the angular correlation in the cascade decay  $\Xi^- \rightarrow \Lambda^0 + \pi^-$ ,  $\Lambda^0 \rightarrow p + \pi^-$ <sup>(5)</sup>. The distribution considered is that of the angle  $\theta$  between the direction of flight of the  $\Lambda^0$  and the direction of emission in the  $\Lambda^0$  center of mass system of the pion emitted in the  $\Lambda^0$  decay. The second experiment deals with the angular correlation in the cascades  $K^- \rightarrow p \rightarrow Y + \pi$ ,  $Y \rightarrow N + \pi$ <sup>(6)</sup>. Here again the distribution considered is that of the angle between the direction of flight of the hyperon and the direction of emission in the hyperon center of mass system of the pion created in the hyperon decay. The formal angular correlation problem is exactly the same

<sup>(3)</sup> M. GELL-MANN: *Proceedings of the Rochester Conference*, 1956 (to be published).

<sup>(4)</sup> R. GATTO: *Nuovo Cimento*: **4**, 526 (1956). In Tables I and II of this work the indications of the final states were inadvertently not reported. Columns 2 and 3 of each table refer to « final state of the first group » and « final state of the second group » respectively.

<sup>(5)</sup> R. GATTO: *Proceedings of the International Pisa Conference*, 1955 (to be published in *Suppl. al Nuovo Cimento*).

<sup>(6)</sup> S. B. TREIMAN: *Phys. Rev.*, **101**, 1216 (1956); R. GATTO: *Nuovo Cimento*, **2**, 1142 (1956).



as for the case of the  $\Xi^-$  cascade decay. The  $\Xi^-$  having even strangeness has a definite parity. The incident  $K^-$  can be a coherent mixture of  $\theta^-$  and  $\tau^-$ . However it is easy to show that the interference terms between  $\theta^-$  and  $\tau^-$  do not appear in the final result because of the summation over the polarizations of the intermediate hyperon. We call  $S$  the spin of the initial system ( $\Xi^-$  or bound  $K^-p$  system),  $s$  the  $\Lambda^0$  spin, while the proton spin is  $\frac{1}{2}$ . Moreover we call  $\lambda_+$  and respectively  $\lambda_-$  the inverse lifetimes of the two members of the  $\Lambda^0$  parity doublet and  $r_+$  and respectively  $r_-$  their masses. If we take the line of flight of the  $\Lambda^0$  as polarization axis the sum over the polarizations of the intermediate  $\Lambda^0$  can be done incoherently. The angular correlation will be given by

$$(1) \quad F(\cos \theta) = \sum_{m_S} \sum_{m_{\frac{1}{2}} m_s} |\langle f | T_2 | j_+ \rangle \exp[-\frac{1}{2}\lambda_+ t - i\nu_+ t] \langle j_+ | T_1 | i \rangle + \\ + \langle f | T_2 | j_- \rangle \exp[-\frac{1}{2}\lambda_- t - i\nu_- t] \langle j_- | T_1 | i \rangle|^2,$$

where  $i$  refers to the initial state of the  $\Xi^-$ , or  $K^- + p$ , at rest,  $j_+$  and  $j_-$  refer to the intermediate state corresponding to a given parity of the  $\Lambda^0$ , and  $f$  refers to the final state. The transition matrix of the first reaction of the cascade is called  $T_1$ , that of the second reaction  $T_2$ . Quite generally we can write for  $F(\cos \theta)$

$$(2) \quad F(\cos \theta) = \exp[-\lambda_+ t] F_+(\cos \theta) + \exp[-\lambda_- t] F_-(\cos \theta) + \\ + \exp[-\frac{1}{2}(\lambda_+ + \lambda_-)t] \frac{1}{2} (\exp[-i(\nu_+ - \nu_-)t] F'(\cos \theta) + \exp[i(\nu_+ - \nu_-)t] F'^*(\cos \theta)),$$

where  $F_+(\cos \theta)$  ( $F_-(\cos \theta)$ ) is the angular correlation for the case that only the  $+$  ( $-$ ) member of the  $\Lambda^0$  parity doublet exists, and  $F'(\cos \theta)$  is given by

$$(3) \quad \frac{1}{2} F'(\cos \theta) = \sum_{m_S m_s m_{\frac{1}{2}}} \langle f | T_2 | j_+ \rangle \langle j_+ | T_1 | i \rangle \langle f | T_2 | j_- \rangle^* \langle j_- | T_1 | i \rangle^*.$$

Note that  $F_-$  is formally given by the same expression for  $\frac{1}{2} F'$  where all  $-$  indices are changed into  $+$  indices, and similarly  $F'$  is given by the same expression where all  $+$  indices are changed into  $-$  indices.

2.2. *The time dependence of the correlation.* — The summation over the magnetic quantum numbers can be carried out with the technique developed by RACAH (<sup>7</sup>). We call  $T_1(l)$  the reduced matrix element of the first step of the cascade leading to  $\Lambda^0$  with parity  $+$  and  $\pi_+$  in a state of relative angular momentum  $l$ , and similarly we define  $T_1^-(l)$ , and, for the second step of the

(<sup>7</sup>) G. RACAH: *Phys. Rev.*, **84**, 910 (1951).

cascade,  $T_2^+(l)$  and  $T_2^-(l)$ . The relative phases of the reduced matrix elements are always 0 or  $\pi$  if the interaction hamiltonian commutes with the time reversal operator<sup>(8)</sup>. This result is certainly true if perturbation theory is applicable. Perturbation theory may be assumed to hold for the weak decay interactions leading to  $\Xi^-$  decay and to  $\Lambda^0$  decay but its applicability to the case of the fast  $K^-$  absorption can be questioned. If the reduced matrix elements can all be chosen real we can write for the angular correlation

$$(4) \quad F(\cos \theta) = \exp[-\lambda_+ t] F_+(\cos \theta) + \exp[-\lambda_- t] F_-(\cos \theta) + \\ + \exp[-\tfrac{1}{2}(\lambda_+ + \lambda_-)t] \cos[(v_+ - v_-)t] F'(\cos \theta),$$

where  $F'(\cos \theta)$  is given by

$$(5) \quad \tfrac{1}{2} F'(\cos \theta) = \sum_{l_1 l'_1 l_2 l'_2} T_1^-(l_1) T_1^+(l'_1) T_2^-(l_2) T_2^+(l'_2) (l_1 l'_1 00 \nu 0) \cdot \\ \cdot W(s l_1 s l'_1 S \nu) (l_2 l'_2 00 \nu 0) W(s l_2 s l'_2 \tfrac{1}{2} \nu) P_\nu(\cos \theta),$$

and  $F_+$  and  $F_-$  are formally obtained by changing all  $-$  indices into  $+$  indices and respectively all  $+$  indices into  $-$  indices in the expression (5) of  $\tfrac{1}{2} F'$ . In (5)  $W(s l s l' S \nu)$  are particular Racah coefficients and  $(l l' 00 \nu 0)$  are particular Clebsch-Gordon coefficients. If the reduced matrix elements cannot be chosen all real the time dependence of the interference term would be modified by the appearance of an additive constant phase in the argument of the cosine. Other general conclusions remain unaltered.

### 2.3. The asymmetry around $90^\circ$ . — The general limitations

$$(6) \quad 0 \leq \nu \leq 2s, 2(l_1)_{\max}, 2(l_2)_{\max},$$

for the possible order  $\nu$  of Legendre polynomials appearing in the angular correlation still hold in our case — these limitations are contained in the two Racah coefficients of (5). In the expressions for  $F_+$  and for  $F_-$  only even values of  $\nu$  will appear since  $l_1$  and  $l'_1$  must always have the same parity and similarly  $l_2$  and  $l'_2$  — we recall the property of  $(l l' 00 \nu 0)$  of being zero for  $l + l' + \nu$  odd. In the expression for  $F'$  only odd values of  $\nu$  appear since  $l_1$  and  $l'_1$  must have opposite parities, and, similarly,  $l_2$  and  $l'_2$ . Geometrically this means that the distribution is not symmetrical around  $\theta = 90^\circ$  and  $\theta = 270^\circ$ . The appearance of odd values of  $\nu$  in the interference term is a typical feature of the parity doublet model. It is in fact known that only even values of  $\nu$  intervene in the usual angular correlation theory in a double correlation if parity is conserved and if no distinction is introduced between left- and right-handed

(8) S. P. LLOYD: *Phys. Rev.*, **81**, 161 (1951).

systems (as would be for instance in a measurement of the circular polarization of photons).

**2.4. Digression on the case of parity non-conservation.** — We can illustrate the case of parity non-conservation, assuming, of course, in this case that only one kind of  $\Lambda^0$  exists, having a definite parity. The angular correlation will be given by <sup>(5)</sup>

$$(7) \quad F(\cos \theta) = \sum_{\nu, l_1 l_1' l_2} T_1^*(l_1) T_1(l_1') T_2^*(l_2) T_2(l_2') (l_1 l_1' 00 | \nu 0) \cdot \\ \cdot W(ss l_1 l_1' \nu S) (l_2 l_2' 00 | \nu 0) W(ss l_2 l_2' \nu \frac{1}{2}) P_\nu(\cos \theta),$$

with a similar meaning of the symbols as explained before. We know that parity must be conserved in strong and electromagnetic interactions as suggested by present experimental evidence with pions, nucleons, and  $\gamma$ -rays, which requires that also in strong virtual processes involving new particles parity must be conserved. Suppose parity is not conserved in weak interactions <sup>(6)</sup>. In the case of  $\Xi^-$  cascade decay, both steps of the cascade being due to weak interactions,  $l_1$  and  $l_1'$  are not restricted to have the same parities, and similarly  $l_2$  and  $l_2'$ . Therefore odd values of  $\nu$  can occur giving a distribution not symmetrical around  $90^\circ$  and  $270^\circ$ . On the other hand, in the cascade initiated by  $K^-$  absorption the strong parity-conserving absorption interaction requires  $l_1$  and  $l_1'$  to have the same parities. Therefore only even values of  $\nu$  can occur as required by the coefficient  $(l_1 l_1' 00, \nu 0)$ . In conclusion an asymmetry around  $90^\circ$  only appears if parity is not conserved in both steps of the cascade.

**2.5. Derivation of particular cases.** — From (4) and (5) we can derive the angular correlations for the particular cases of interest by specializing the values of the spin  $S$  and parity  $P$  of the initial  $\Xi^-$  or  $K^- - p$  bound system, and of  $s$ . The possible values of  $l_1$  and of  $l_2$  are then determined by conservation of angular momentum (see Table I).

TABLE I.

$S$	$P$	$s$	$l_1$		$l_2$	
			if $\Lambda_+^0$	if $\Lambda_-^0$	if $\Lambda_+^0$	if $\Lambda_-^0$
$\frac{1}{2}$	+	$\frac{1}{2}$	1	0	1	0
$\frac{1}{2}$	—	$\frac{1}{2}$	0	1	1	0
$\frac{1}{2}$	+	$\frac{3}{2}$	1	2	1	2
$\frac{1}{2}$	—	$\frac{3}{2}$	2	1	1	2
.....		.....	.....	.....	.....	.....

<sup>(6)</sup> The implications of parity non-conservation on time reversal are discussed in a forthcoming paper.

The angular correlations for the particular cases considered in Table 1 are found to be ( $\xi$  is a real unknown parameter)

$$(8) \quad \left\{ \begin{array}{l} (S = \frac{1}{2}, P = +, s = \frac{1}{2}), (S = \frac{1}{2}, P = -, s = \frac{1}{2}), \\ F(\cos \theta) = \exp[-\lambda_+ t] + \xi^2 \exp[-\lambda_- t] + \\ + 2\xi \cos \theta \exp[-\frac{1}{2}(\lambda_+ + \lambda_-)t] \cos[(\nu_+ - \nu_-)t], \end{array} \right.$$

$$(9) \quad \left\{ \begin{array}{l} (S = \frac{1}{2}, P = +, s = \frac{3}{2}), (S = \frac{1}{2}, P = -, s = \frac{3}{2}), \\ F(\cos \theta) = (\exp[-\lambda_+ t] + \xi^2 \exp[-\lambda_- t])(1 + 3 \cos^2 \theta) + \\ + \xi(-10 \cos \theta + 18 \cos^3 \theta) \exp[-\frac{1}{2}(\lambda_+ + \lambda_-)t] \cos[(\nu_+ - \nu_-)t]. \end{array} \right.$$

The  $\Xi^-$  having even strangeness will have a definite parity. The  $K^-$  may be of positive or of negative parity. However, if the absorption occurs from an  $S$  state, the resulting correlations are formally the same in the two cases.

### 3 - Discussion.

3.1. - The angular correlation (4) is a sum of a term varying with time as  $\exp[-\lambda_+ t]$ , one varying as  $\exp[-\lambda_- t]$  and one varying as  $\exp[-\frac{1}{2}(\lambda_+ + \lambda_-)t] \cdot \cos[(\nu_+ - \nu_-)t]$ . The first two terms only contain even powers of  $\cos \theta$  and therefore remain unchanged if  $\theta \rightarrow \pi - \theta$ . The third term only contains odd powers of  $\cos \theta$  and therefore it changes sign if  $\theta \rightarrow \pi - \theta$ . This last term comes from the interference between amplitudes corresponding to the two components of the  $\Lambda^0$  parity doublet.

We distinguish two cases:

i) the two lifetimes  $\lambda_+^{-1}$  and  $\lambda_-^{-1}$  are very different, so that one practically observes only one of the two components of the coherent superposition in the experiment. In this case the measured correlation will be that for the component observed;

ii) the two lifetimes are comparable in magnitude. In this case one observes different correlations at different times (i.e. at different distances from the point where the first interaction occurs). The dependence on time will be given by the sum of the two exponentials and, if the mass difference  $\nu_+ - \nu_-$  is comparable in magnitude to the decay rates, also the oscillating interference term will appear. The mass difference equivalent to a lifetime  $\sim 4 \cdot 10^{-10}$  s is  $\nu_+ - \nu_- \sim 0.5 \cdot 10^{-5}$  eV. If the mass difference is much larger the oscillations will average to zero and the coherence effect will not be observable.

3.2. *The mass differences in the parity doublets. The principle of minimal electromagnetic interaction.* — It remains to discuss the meaning of such small mass differences. One has in principle two different possibilities in the Lee-Yang parity doublet theory as to the behaviour of the electromagnetic interaction with respect to parity conjugation:

1) the electromagnetic interaction is not invariant with respect to parity conjugation;

2) the electromagnetic interaction is invariant with respect to parity conjugation.

In the first case the mass differences can be produced by the electromagnetic interaction and can be of the order of the  $\pi^\pm - \pi^0$  mass difference. This case would correspond to complete undetectability of the coherence effects discussed. In the second case only the weak interactions can produce the mass differences between members of the same parity doublet. These mass differences would then very roughly be expected to be of the order of  $10^{-6} - 10^{-5}$  eV, and therefore the coherence effects could result observable.

Of the two possibilities, 1) and 2), only 2) is consistent with the principle of minimal electromagnetic interaction. This principle, formulated by Gell-Mann, states that the photons only interact with the charges and the currents. The non-validity of the principle could lead to the possibility of strangeness non-conserving processes occurring electromagnetically, a possibility which seems excluded by present experimental evidence. It may be useful to note that experiments of photoproduction of K-mesons will provide a direct way of choosing between 1) and 2). If the electromagnetic interaction is minimal the photoproduction processes permitted must conserve the third component of total isotopic spin. Moreover, in the Lee-Yang theory, the branching ratios of K<sup>-</sup>-meson decays must be identical to those observed for K<sup>+</sup>-mesons produced in strong interactions.

It is apparent from the expressions reported that the measurements of the angular correlations considered here may provide a method for determining the mass differences, if these are of such a magnitude to give rise to an observable effect. Such measurements would still provide informations on the spins and parities, and on the lifetimes.

#### 4. — Other Physical Consequences of the Parity Doublet Theory.

4.1. *The time dependence of the decay rates.* — Coherence effects of the kind discussed here can also arise in other experiments. Consider, for instance, the production of a  $\Lambda^0 K^+$  pair by ordinary particles and the subsequent decay of



the  $K^-$ . The two particles are produced in a coherent superposition of the general form

$$(10) \quad a(\Lambda_+^0 K_+^+) + b(\Lambda_+^0 K_-^+) + b(\Lambda_-^0 K_+^+) + a(\Lambda_-^0 K_-^+),$$

( $K_+^+ \rightarrow \theta^+, K_-^+ \rightarrow \tau^+$ ) where  $a$  and  $b$  are complex coefficients (in general energy and momentum dependent). We have made use in (10) of the parity conjugation invariance of the strong interaction responsible for the production. Now, let us assume that both  $K_+^+$  and  $K_-^+$  have some common decay modes, for instance that into  $\mu^+ + \nu$  (and/or that into  $\mu^+ + \nu + \pi^0$ , and/or that into  $e^+ + \nu + \pi^0$ ). The decay rates into one such common decay mode will in general be given by the sum of a term varying with time as  $\exp[-\lambda_+ t]$ , where  $\lambda_+$  is the inverse lifetime of  $\theta^+$ , one varying as  $\exp[-\lambda_- t]$ , where  $\lambda_-$  is the inverse lifetime of  $\tau^+$ , and an interference term varying as  $\exp[-\frac{1}{2}(\lambda_+ + \lambda_-)t] \cos((m_+ - m_-)t)$ ,  $m_+$ ,  $m_-$  being the masses. Not in all experiments however will this interference term be revealed. Suppose the  $K$ -meson has spin zero. In the most simple experiments one would consider the  $K^+$ -mesons emitted with a given momentum, summing over the states of all other particles that are produced. This summation eliminates the interference term. The reason is that such term must behave as a pseudoscalar and no pseudoscalar can be constructed from the incident momentum and from the momentum of the emitted  $K^+$ , which are the only vectors observed in such conditions.

We note that these coherence effects may also occur for the possible common leptonic decay modes of the hyperon doublets. We also note that they are similar in some respects to those considered by TREIMAN and SACHS<sup>(10)</sup>, but may be more difficult to detect in our case because of the energy and momentum dependence of the coefficients in the superposition (10).

4.2. *The relative frequencies of the various kinds of events in associated production. The lifetimes of the hyperons.* — In associated production from ordinary particles the final state must be an eigenstate of the parity conjugation operator with eigenvalue  $-1$ . This means a restriction for the coefficients of the produced amplitude, and, by combining with assumptions concerning the branching ratios at decay, one can derive predictions about the relative frequencies of the various kinds of events. To illustrate the procedure in a physical interesting case let us consider the production of a  $\Lambda^0$  and a  $K^0$  from ordinary particles. We recall that the produced  $K^0$  must be considered as a mixture of two particles,  $K_1^0$  and  $K_2^0$ <sup>(11)</sup>. Conservation of the parity conjugation

<sup>(10)</sup> S. B. TREIMAN and R. G. SACHS: *Phys. Rev.* (in the press).

<sup>(11)</sup> M. GELL-MANN and A. PAIS: *Phys. Rev.*, **97**, 1387 (1955).

number requires that the final amplitude be of the form

$$(11) \quad A(\Lambda_1\theta_1) + iA(\Lambda_1\theta_2) + B(\Lambda_1\tau_1) + iB(\Lambda_1\theta_2) + B(\Lambda_1\theta_1) + \\ + iB(\Lambda_1\theta_2) + A(\Lambda_1\tau_1) + iA(\Lambda_1\tau_2),$$

where  $A$  and  $B$  are complex coefficients which satisfy  $4|A|^2 + |B|^2 = 1$ . Let us call  $f_\Lambda$  the fraction of the total number of production events in which a  $\Lambda^0 \rightarrow p + \pi^-$  decay is observed not accompanied by a  $\theta^0 \rightarrow \pi^+ + \pi^-$  decay,  $f_\theta$  the fraction showing a  $\theta^0 \rightarrow \pi^+ + \pi^-$  not accompanied by a  $\Lambda^0 \rightarrow p + \pi^-$ , and  $f_{\Lambda\theta}$  the fraction showing a  $\Lambda^0 \rightarrow p + \pi^-$  accompanied by a  $\theta^0 \rightarrow \pi^+ + \pi^-$ . We assume that the decay interactions satisfy the  $\Delta I = \frac{1}{2}$  rule<sup>(12-14)</sup> and we neglect decay modes of  $\Lambda^0$  different from  $\Lambda^0 \rightarrow N + \pi$ , and possible decay modes of  $\theta_1^0$  (the component of the  $\theta^0$  mixture which decays in two pions) different from  $\theta_1^0 \rightarrow \pi^+ + \pi^-$ . We also assume that the K-meson has even spin. The reader can easily derive from (11) and from the branching ratios derived in reference<sup>(12)</sup> the following conclusions. If the lifetimes of  $\Lambda_1^0$  and of  $\Lambda^0$  are very similar so that both particles decay in the observing apparatus.

$$f_\Lambda = \frac{10}{18}, \quad f_\theta = \frac{1}{18}, \quad f_{\Lambda\theta} = \frac{2}{18}.$$

If the two lifetimes are very different so that only one of the two components of the  $\Lambda^0$  parity doublet decays in the observing apparatus

$$\frac{4}{18} \leq f_\Lambda \leq \frac{6}{18}, \quad \frac{1}{18} \leq f_\theta \leq \frac{3}{18}, \quad 0 \leq f_{\Lambda\theta} \leq \frac{2}{18}, \quad \text{and} \quad f_\Lambda = \frac{1}{3} - f_{\Lambda\theta}, \quad f_\theta = \frac{1}{6} - f_{\Lambda\theta}.$$

Note that in the first case one sees four  $\Lambda^0 \rightarrow p + \pi^-$  against one  $\theta^0 \rightarrow \pi^+ + \pi^-$ , in the second case two  $\Lambda^0 \rightarrow p + \pi^-$  against one  $\theta^0 \rightarrow \pi^+ + \pi^-$ . In this way one can hope to discriminate between two possibilities for the  $\Lambda^0$  lifetimes.

4.3. *The parity doublet structure of hyperfragments.* — The  $\Lambda^0$  hyperfragments being systems of odd strangeness will exist in parity doublets. Since weak interactions are not invariant under parity conjugation the two components of a same parity doublet will have different lifetimes, decay with different branching ratios, and also possibly have different decay modes. For instance, of the two components of the  ${}^4\text{H}_\Lambda$  parity doublet only that with parity  $(-)^{s+1}$ ,  $S$  being the spin, can decay into  ${}^4\text{He} + \pi$  (the same conclusion holds for  ${}^4\text{He}_\Lambda$

<sup>(12)</sup> R. GATTO: *Nuovo Cimento*, **3**, 318 (1956).

<sup>(13)</sup> G. WENTZEL: *Phys. Rev.*, **101**, 1215 (1956).

<sup>(14)</sup> B. D'ESPAGNAT and J. PRENTKI: *Nuovo Cimento*, **3**, 1044 (1956).

which belongs to the same isotopic spin doublet). It must be remarked that in each of the two components of the hyperfragment parity doublet a superposition of both  $\Lambda^0_+$  and  $\Lambda^0_-$  will be contained, what is fixed being only the total parity of the hyperfragment. Therefore the hyperfragment lifetime may result widely different from the lifetimes of  $\Lambda^0_+$  and of  $\Lambda^0_-$ . However, in the case that the two  $\Lambda^0$  lifetimes are different in order of magnitude, we expect that the lifetimes of relatively heavy hyperfragments will be of the order of the shorter of the two  $\Lambda^0$  lifetimes.

\* \* \*

The author wishes to thank Professors N. KROLL and L. MEZZETTI for the stimulating discussions.

#### RIASSUNTO

Si mostra come nella teoria dei doppietti di parità delle particelle strane si hanno certi effetti di coerenza che possono dare particolari dipendenze dal tempo e dagli angoli nelle correlazioni angolari e particolari dipendenze dal tempo nelle curve di decadimento. La possibilità di misurare questi effetti di coerenza è strettamente collegata al valore della differenza di massa in un doppietto di parità, e fornirebbe la possibilità di misurare queste differenze di massa. Una condizione per la osservabilità degli effetti di coerenza è che la interazione elettromagnetica sia minima. Altri aspetti fisici della teoria, come la dipendenza dal tempo delle curve di decadimento, le vite medie degli iperoni, e la struttura a doppietti di parità degli iperframmenti, vengono pure discussi.

## New Determination of the Intensities of Primary Cosmic Ray Alpha Particles and Li, Be, B Nuclei at $\lambda = 41.5^\circ$ Using a Čerenkov Detector (\*).

W. R. WEBBER

*Department of Physics, State University of Iowa - Iowa City, Iowa*

(ricevuto il 17 Agosto 1956)

**Summary.** — Measurements of the intensities of the  $\alpha$ -particles and Li, Be, B nuclei in the primary cosmic radiation have been made at an average atmospheric depth of  $18.5 \text{ g/cm}^2$  in two «Skyhook» balloon flights at  $\lambda = 41.5^\circ$ . The measuring instrument consisted of a thin ( $3.0 \text{ g/cm}^2$ ) Čerenkov detector placed within the solid angle of a Geiger counter telescope. This detector yielded unusually good resolution of the  $\alpha$ -particle and Li, Be, B components. This fact and the slow rate of rise of the two balloons made possible a detailed determination of the dependence of  $\alpha$ -particle intensity on atmospheric depth. The quality of the data justified a new approach to the problem of extrapolating the  $\alpha$ -particle intensity to the top of the atmosphere. This extrapolation was carried out by applying a «diffusion» equation of the type previously used for nuclei with  $Z > 2$  to the observed pressure-altitude dependence of  $\alpha$ -particle intensity. The resulting estimate of the  $\alpha$ -particle intensity at the top of the atmosphere is significantly lower than previous estimates. At  $18.5 \text{ g/cm}^2$  the sum of the vertical intensities of the Li, Be, B components was found to be  $(3.11 \pm 0.31) (\text{m}^2 \cdot \text{sr} \cdot \text{s})^{-1}$  and the intensities  $J_{\text{Li}}/J_{\text{Be}}/J_{\text{B}}$  were found to be as  $3/4/2$ . The (light nuclei/medium nuclei) intensity ratio at the top of the atmosphere as determined by this experiment was  $0.35 \pm 0.09$ . The vertical intensities at the top of the atmosphere of the various components of the primary radiation as obtained in this experiment at  $\lambda = 41.5^\circ$  were:

Component	$J^{\text{v}} (\text{m}^2 \cdot \text{sr} \cdot \text{s})^{-1}$
Protons . . . . .	$< 526$
$\alpha$ -Particles . . . . .	$74 \pm 5$
Li, Be, B . . . . .	$2.28 \pm 0.55$
$Z > 6$ . . . . .	$9.2 \pm 1.2$

(\*) Assisted by a joint program of the Office of Naval Research and the Atomic Energy Commission.

## 1. — Introduction.

Due to its unique properties, the Čerenkov detector is being used increasingly in experiments requiring charge determination of the cosmic radiation in the upper atmosphere <sup>(1)</sup>. Most important of these properties is the fact that the output from a Čerenkov detector, in the form of visible electromagnetic radiation, is proportional to  $Z^2(1 - (1/\beta^2 n^2))$ , where  $Z$  is the charge of the incident particle,  $\beta c$  is its velocity and  $n$  is the index of refraction of the medium. Thus in a Čerenkov detector one has the advantage of a  $Z^2$  charge dependence similar to ionization detectors; but the Čerenkov output decreases with decreasing  $\beta$ , in distinct contrast to the  $Z^2/\beta^2$  output of ionization detectors. As a result, low energy singly charged particles, which are indeed plentiful in the upper atmosphere, do not contribute to the background in the range of outputs characterizing high energy  $\alpha$ -particles and Li, Be, B nuclei in a Čerenkov detector. Hence, one can obtain much more certain identification of these components than by any method depending upon ionization alone.

A second important property of a Čerenkov detector is the fact that the optical radiation is emitted in the forward direction in a cone of half angle  $\alpha$  given by  $\cos \alpha = 1/\beta n$ . This means that the Čerenkov detector can function as a directional device and thus can be used to provide discrimination against upward moving albedo particles.

A main disadvantage of Čerenkov detectors as used for cosmic ray research in the upper atmosphere has been their somewhat poor charge resolution in the low  $Z$  region. This is due partly to the necessity for using thin radiating materials (to minimize nuclear interactions) and partly to the inherently low light output from the Čerenkov effect—both effects tending to introduce wide statistical fluctuations in the photomultiplier tube output for particles of the same  $\beta$ .

By careful choice of the photomultiplier tube and by control of the various parameters affecting this statistical fluctuation it has been possible to create a unit with unusually good charge resolution. Using a one inch thick Lucite radiator, pulse height distributions with half widths (width at half height divided by the magnitude of the pulse height at the maximum of the distribution) of 35% were consistently obtained using sea level  $\mu$ -mesons as a beam of high energy particles. Since the half widths of the individual charge distributions may be expected to be roughly proportional to  $1/Z$  (due to  $Z^2$  increase in light output and consequent improvement in photomultiplier statistics)

---

<sup>(1)</sup> See W. R. WEBBER and F. B. McDONALD: *Phys. Rev.*, **100**, 1460 (1955) for a discussion of the Iowa work leading up to the present experiment and for a summary of the work of other experimenters using Čerenkov detectors to measure the primary radiation in the upper atmosphere.



this indicated that very satisfactory resolution could be expected for the individual charge components in the  $\alpha$ -particle and Li, Be, B pulse height regions.

## 2. - Description of Apparatus.

The core of the apparatus, consisting of a Čerenkov detector (an aluminized Lucite block in optical contact with a photomultiplier tube), was placed within the solid angle of a Geiger counter telescope (Fig. 1). The geometrical factor of the telescope was calculated to be  $9.2 \pm 0.3 \text{ sr cm}^2$  based on measurements of the effective lengths of the individual counters.

An extensive guard and shower system surrounded the telescope and was used to detect showers originating outside the telescope and nuclear interactions occurring in the local material of the telescope. In addition to the guard

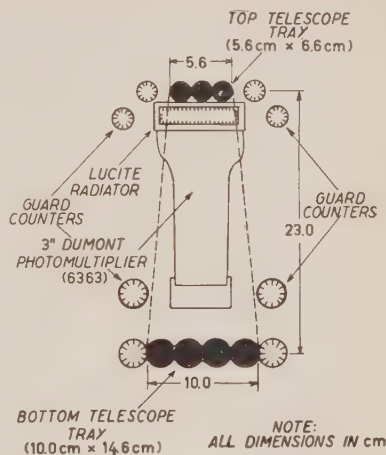


Fig. 1. Outline drawing of Geiger counter telescope and Čerenkov detector showing arrangement of guard counters.

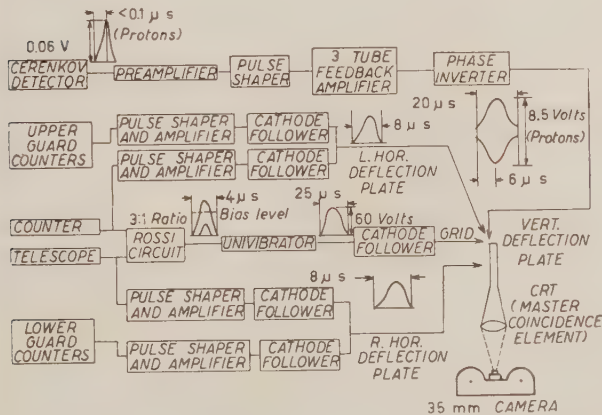


Fig. 2. - Block diagram of the electronic circuitry.

Fig. 2. A highly stable amplifier consisting of three 6AK5 tubes arranged in a feedback loop provided the necessary gain for the photomultiplier tube outputs. At flight settings the amplifier had a dynamic range of 15 times

counters surrounding the top and bottom telescope trays, the counters in the telescope were used as shower counters in such a manner that if two or more counters in either tray were triggered simultaneously with a telescope count, a shower count was recorded.

A block diagram of the electronic circuitry is shown in

the mean pulse for singly charged particles ( $h_0$ ). Thus in order to get unsaturated pulses from relativistic Boron nuclei ( $\sim 25h_0$ ) it was necessary to make the amplifier somewhat non-linear in the upper 50% of its gain curve.

The pulses from the amplifier were placed on one set of deflection plates of a cathode ray tube (CRT). The amplitude of the traces on the CRT, provided by the deflections of the spot (the spot was intensified only when a telescope coincidence was recorded), provided a quantitative measure of the amount of Čerenkov light emitted by the particles as they passed through the Lucite block. Maximum deflection, corresponding to saturation of the amplifier, gave a 6.3 cm trace on the CRT and corresponded to a particle with  $Z \geq 6$ .

The passage of a particle through the telescope accompanied by a simultaneous guard or shower pulse caused the ensuing trace on the CRT to be marked in such a manner that one could tell which group of guard or shower counters («top» or «bottom») had been triggered. Such a count was called a « $J$ » count after the shape of the trace. Traces unaccompanied by « $J$ » marking were called regular counts.

### 3. Discussion of the Effect of Nuclear Interactions and Knock-On Electrons Occurring in the Local Material of the Telescope.

3.1. *Nuclear Interactions.* — The average telescope particle passed through 5.5 g/cm<sup>2</sup> between the 2.5 g/cm<sup>2</sup> «identification» level in the Lucite block and the lower telescope tray. A correction for the nuclear interactions of the various particles must be made since we are interested in the number of regular counts at the «identification» level—not at the level of the lower telescope tray. These interacting particles should appear as « $J$ » counts principally in the bottom « $J$ » pulse height distribution. Since these particles have passed through the Lucite block in a normal manner they should as a group give a pulse height distribution similar to that from regular counts. This so-called «structure» should appear superimposed on the general background of counts in the bottom « $J$ » pulse height distribution. Indeed, this «structure» will help identify these particles, as will be seen later on.

No regular count would be expected from a particle passing through either the bottom or top tray at large angles and having nuclear interactions in the local material since at least one of the guard or shower counters should be triggered by the secondaries from such an event—thus giving a « $J$ » count. If some of these particles happen to pass through Lucite block, some of these « $J$ » counts should also show «structure» however.

Table I gives a summary of the effects of nuclear interactions in the telescope.

TABLE I. — *Corrections due to nuclear interactions occurring in the Counter telescope.*

	Amount of material	$Z$	MFP (g/cm <sup>2</sup> )	Correction to regular counts (% of $J^{18.5}$ )	Structure counts (% of $J^{18.5}$ )
Telescope events	5.5 g/cm <sup>2</sup>	1	80	+ 6.6	6.6
		2	50	+ 10.6	10.4
		3, 4, 5	36	+ 14.2	14.2
		6	24	+ 20.5	20.5
Non-telescope events (Large angles)	3.0 g/cm <sup>2</sup>	—	—	No	Yes (some)

3.2. *Knock-on Electrons.* — The problem presented by knock-on electrons produced in the material of the telescope by the incident particles is two-fold. In one case the knock-ons can cause a bottom guard or shower counter to be triggered simultaneously with the passage of the primary particle through the telescope—thus causing a « $J$ » count to occur in place of a regular count. In the other case particles passing through the top tray and Lucite block at large angles such that their trajectories miss the bottom tray may produce knock-ons in the telescope. These knock-ons may in turn pass through the bottom tray thus causing regular counts. This effect, which tends to enlarge the geometric factor of the Geiger counter telescope, has recently been discussed by LINSLEY in connection with the measurement of the intensities of heavy primaries by Geiger counter telescopes (2). The bottom guard counters will tend to minimize this effect somewhat by recording as « $J$ » counts many of these particles. It should be noted that the above two knock-on effects tend to cancel one another. All the « $J$ » counts caused by these knock-ons should show «structure» since presumably the primary particles have passed through the Lucite block in nearly normal manner, even though in some cases they may have missed the lower telescope tray.

An effect analogous to the above effects may occur in the top tray and surrounding guard counters due to back scattered electrons produced in the telescope. The evidence, both theoretical and experimental, indicates this effect is small, however.

A theoretical analysis of the effect of knock-on electrons has been carried out using a modified Rutherford formula (3) to find the probability per unit

(2) J. LINSLEY: *Phys. Rev.*, **97**, 1292 (1955).

(3) B. ROSSI: *High Energy Particles* (New York, 1952), p. 14-23.

path length in the telescope that a knock-on of a given energy is produced. If one folds in the energy spectrum of the primary radiation and the range-energy relation for the knock-on electrons (<sup>4</sup>), the probability that a knock-on electron with energy great enough to penetrate the bottom counters will emerge from the local material can be calculated as a function of the  $Z$  of the incident particle. This relation is found to be  $P(Z) = 1 - e^{-0.0137Z^2}$ . The work of BROWN *et al.* (<sup>5</sup>) on the angular distribution of knock-on electrons from penetrating particles (mesons) indicates a distribution of  $\cos^{2.5} \theta$  for the emerging knock-on electrons where  $\theta$  is the angle between the knock-on and its primary. Integrating over all possible trajectories of the primary particles passing through the top tray and Lucite block one can then obtain the total probability that upon the passage of a particle of a given  $Z$  through the Lucite block a regular or a « $J$ » count will be obtained.

A summary of the effects of knock-on electrons is given in Table II.

TABLE II. — Corrections due to knock-on electrons occurring in the counter telescope.

$Z$		1	2	3, 4, 5	$\geq 6$
Correction to regular counts (% of $J^{18,5}$ )	Telescope events	+ 1.1	+ 2.6	+ 10.0	+ 48.2
	Non-telescope events (Large angles)	— 0.4	— 0.9	— 3.7	— 20.8
Total		+ 0.7	+ 1.7	+ 6.5	+ 34.5
Structure counts (% of $J^{18,5}$ )	Telescope events	+ 1.1	+ 2.6	+ 10.0	+ 48.0
	Non-telescope events	+ 0.4	+ 0.9	+ 3.7	+ 20.8
Total		+ 1.5	+ 3.5	+ 13.3	+ 59.0

An experimental check on the above calculations for knock-on electrons can be obtained in the case of sea level  $\mu$ -mesons. Table II predicts that 1.5% of these singly charged particles should be accompanied by «structure» type « $J$ » counts due to knock-on electrons (no nuclear interactions present). Experimentally it is found that  $1.7\% \pm 0.3\%$  of the  $\mu$ -mesons are indeed accompanied by «structure» type bottom « $J$ » counts.

In later sections, as a check on the preceding calculations, the experimentally observed « $J$ » «structure» for each charge component will be compared with that expected due to knock-on electrons and nuclear interactions.

(<sup>4</sup>) L. R. GLENDENIN: *Nucleonics*, **2**, No. 1, 12 (1948).

(<sup>5</sup>) W. W. BROWN, A. S. MCKAY and R. S. PALMATIER: *Phys. Rev.*, **76**, 507 (1949).

#### 4. - Balloon Flights.

The apparatus, enclosed in an airtight aluminum cylinder, was flown by balloon from San Angelo, Texas ( $\lambda = 41.5^\circ$ ) on January 12th and 19th, 1955. A feature of both flights was the very slow rise of the balloons to altitude, thus enabling good statistics to be obtained on the variation of the various cosmic ray charge components with atmospheric depth. Both flights reached maximum altitude at approximately 10 A.M. local time and remained nearly level at this altitude for 5 hours before the apparatus was released and parachuted to earth. Flight I maintained an average altitude of 90200 ft ( $17.5 \text{ g/cm}^2$ ) during this 5 hour period while Flight II averaged 94300 ft ( $14.5 \text{ g/cm}^2$ ). The atmospheric pressure as a function of time was determined by photographing a Wallace and Tiernan pressure gauge and a watch at 2 minute intervals. The pressure determined in this manner agreed to within  $\pm 1.0 \text{ g/cm}^2$  at maximum altitude on both flights with independent measurements supplied by Winzen Research, Inc.

#### 5. - Experimental Results.

Data from the two flights were first analyzed separately, but since the separate results were consistent in every way, the data have been combined in this paper.

A breakdown of the results obtained at maximum altitude for Flights I and II ( $18.5 \text{ g/cm}^2$  average depth-including  $16.0 \text{ g/cm}^2$  of air  $\mp 2.5 \text{ g/cm}^2$  correction due to local material and finite opening angle of telescope) according to apparent  $Z$  and type of count is shown in Table III.

TABLE III. - *Raw data obtained at maximum altitude (Flights I and II) grouped according to apparent  $Z$ .*

Pulse Height	C o u n t s					
	Flight I			Flight II		
	Regular	Top «J»	Bott. «J»	Regular	Top «J»	Bott. «J»
0	2940	572	504	2576	612	352
$0.2h_0^* \leq h < 2.6h_0$ ( $Z=1$ )	15243	1017	1777	14259	1196	1901
$2.6h_0 \leq h < 6.0h_0$ ( $Z=2$ )	739	169	304	788	224	370
$7.0h_0 \leq h < 15h_0$ ( $Z=3, 4, 5$ )	44	45	60	52	48	62
$h \geq 15h_0$ ( $Z \geq 6$ )	46	86	97	47	93	110
Totals	19012	1889	2722	17732	2173	2795

Time intervals are identical for Flights I and II.



5.1. *Alpha Particles.* — The pulse height distributions in the range  $2h_0 \leq h \leq 6h_0$  are shown in Fig. 3. The peak due to  $\alpha$ -particles at  $\sim 4h_0$  is clearly

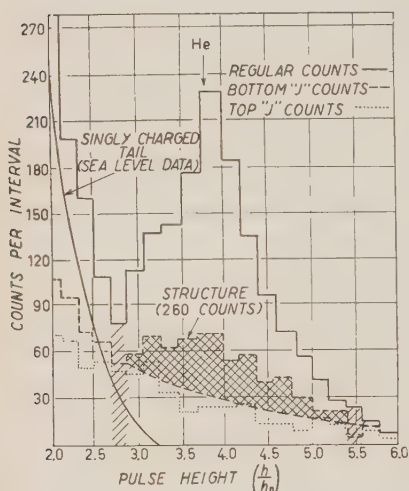


Fig. 3. — Differential pulse height distributions of regular and «J» counts in  $\alpha$ -particle region at  $18.5 \text{ g/cm}^2$  (Flights I and II combined).

II, a total of 1527 regular counts were obtained. To this value we must make the following corrections:

(1) Interpolation between singly and doubly charged distributions. This interpolation is facilitated by the fact that, on theoretical grounds, the singly charged «tail» at high altitude should be very similar to the «tail» observed on the  $\mu$ -meson distribution at sea level. One has only to normalize the two distributions and subtract out the  $\mu$ -meson tail. Data obtained as the balloons rose to altitude corroborate this method of correction: viz., in the region below  $150 \text{ g/cm}^2$ , where protons would be expected to be quite abundant and the composition of the singly charged group would be more nearly like that at maximum altitude, the normal sea level  $\mu$ -meson «tail» was observed. Above this depth, as the  $\alpha$ -particles became more plentiful the pulse height region above  $2h_0$  steadily filled out and the structure of the  $\alpha$ -peak became more and more apparent with increasing altitude. (See Fig. 4).

The correction for the singly charged tail adds  $155 \pm 50$  counts lying between  $h = 2h_0$  and  $h = 2.6h_0$  to the regular  $\alpha$ -particle distribution.

(2) Correction due to knock-on electrons and nuclear interactions oc-

evident in the distribution of regular counts. Note that even if all «J» and regular counts in this region are grouped into a single pulse height distribution a partially resolved  $\alpha$  peak is still obtained, the only discrimination involved being the inherent discrimination of a Čerenkov counter against slow particles. An improvement in resolution by a factor of 2 is obtained, however, when only regular counts are considered. This indicates that the guard and shower counters are successfully identifying many non- $\alpha$  events in this pulse height region.

As a first step in the determination of the number of counts that can actually be attributed to  $\alpha$ -particles we arbitrarily consider the pulse height region  $2.6h_0 \leq h \leq 5.6h_0$  as the  $\alpha$ -particle region. Within this region, combining the results of Flights I and

curing in the telescope. The correction due to these effects has been discussed in a previous section and amounts to  $\pm 12.1\%$  of the total number of  $\alpha$ -particle counts or an addition of  $230 \pm 40$  counts to the regular  $\alpha$ -particle distribution.

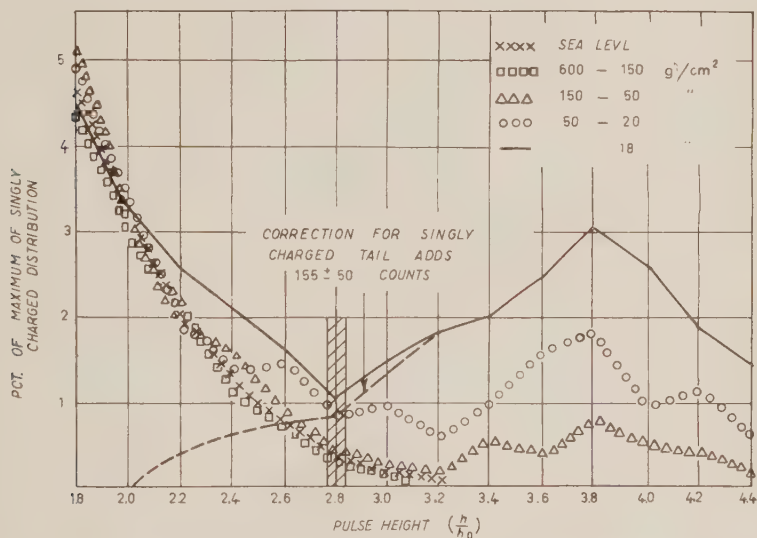


Fig. 4. Differential pulse height distribution of regular counts as a function of altitude in the region  $1.8h_0 \leq h \leq 4.4h_0$  showing the development of the  $\alpha$ -particle peak and extrapolation of the singly charged tail.

We are now in a position to compare our theoretical estimates on the effect of nuclear interactions and knock-on electrons occurring in the telescope with the experimental results. In the previous section it was calculated that at least  $12.8\%$  of the total number of  $\alpha$ -particle counts should appear as «structure» in the lower « $J$ » pulse height distribution. Reference to Fig. 3 shows that this «structure» is indeed present and contains approximately 260 counts of  $13.7\%$  of the total number of  $\alpha$ -particle counts—a result in close agreement with the predicted value. Note that the « $J$ » distribution from the top guard and shower counters shows no «structure». This would be expected since the products of the events showing a pulse height «structure» generally would not be expected to reach these counters.

(3) Background in the regular  $\alpha$ -particle distribution due to inefficiency of guard and shower devices. Any such inefficiency would allow events that

are not due to true  $\alpha$ -particles to appear as background in this region of the regular distribution.

Since at sea level (no interactions) and in the atmosphere below  $150 \text{ g/cm}^2$  (where proton interactions occur but  $\alpha$ -particles are absent) all counts in the region  $2.0h_0 < h \leq 6.0h_0$  should be « $J$ » counts, (save the well defined singly charged tail) a measure of the efficiency of the detection system for « $J$ » type events can be gained by comparing the number of regular and « $J$ » counts obtained in this pulse height region at these altitudes. The results—2 regular counts and 31 « $J$ » counts—indicate that the guard and shower system is  $93 \pm 4\%$  efficient in detecting background events lying in the  $\alpha$ -particle pulse height region. This value for the efficiency is corroborated by the number of background events lying in the regular distribution from  $7h_0 \leq h \leq 15h_0$ . In this pulse height region it is found that the guard and shower system is  $\sim 97\%$  efficient in detecting « $J$ » type events. This slightly higher efficiency can be accounted for by the fact that the guard and shower system tends to become more efficient the larger the background event being considered.

At altitude approximately 1000 « $J$ » events occurred in the  $\alpha$ -particle pulse height region. Thus  $70 \pm 40$  undetected « $J$ » events must lie in the  $\alpha$ -particle region as background. These counts must be subtracted from the regular  $\alpha$ -particle distribution.

(4) Alpha particle tail above  $5.6h_0$ . This accounts for an additional  $45 \pm 10$  counts.

Thus we have a grand total of  $1527 + 360 = 1887 \pm 110$  (statistical and experimental errors included)  $\alpha$ -particle counts at a depth of  $18.5 \text{ g/cm}^2$ . To extrapolate this value to the top of the atmosphere we must take cognizance of the fact that an appreciable fraction of these alphas may be fast fragments from collisions of the heavier components in the atmosphere above the apparatus. A straight exponential extrapolation is not appropriate and one should consider the diffusion equation for the  $\alpha$ -particles. Neglecting ionization loss and assuming energy independence for the parameters  $\lambda_I$ ,  $P_{I'I}$  this is, (after notation of NOON and KAPLON <sup>(6)</sup>).

$$\frac{dJ_I(x)}{dx} = -\frac{J_I(x)}{\lambda_I} + \sum_{I' \geq I} \frac{P_{I'I} J_{I'}(x)}{\lambda_{I'}},$$

where  $I = H, M, L, \alpha$  and  $x$  is the vertical depth below the top of the atmosphere. The definition and values of the parameters used in these equations may be found in the appendix.

<sup>(6)</sup> J. H. NOON and M. F. KAPLON: *Phys. Rev.*, **97**, 769 (1955).

The solution of this equation for  $\alpha$ -particles is:

$$J_{\alpha}(x) = J_{\alpha}^0 \exp\left[-x/\lambda'_{\alpha}\right] + \left\{ \frac{\lambda'_L \lambda'_{\alpha} P_{L\alpha}}{(\lambda'_{\alpha} - \lambda'_L)\lambda'_L} \right\} \left[ J_L^0 + \frac{\lambda'_M \lambda'_L P_{ML}}{(\lambda'_L - \lambda'_M)\lambda'_M} J_M^0 + \frac{\lambda'_H \lambda'_L}{(\lambda'_L - \lambda'_H)\lambda'_H} J_H^0 \right. \\ \cdot \left( P_{HL} + \frac{\lambda'_M \lambda'_L P_{HM} P_{ML}}{(\lambda'_L - \lambda'_M)\lambda'_M} \right) \left( \exp\left[-\frac{x}{\lambda'_L}\right] - \exp\left[-\frac{x}{\lambda'_L}\right] \right) + \\ \left. + \left\{ \frac{\lambda'_M \lambda'_{\alpha}}{(\lambda'_{\alpha} - \lambda'_M)\lambda'_M} \left( P_{M\alpha} - \frac{\lambda'_M \lambda'_L P_{ML} P_{L\alpha}}{(\lambda'_L - \lambda'_M)\lambda'_L} \right) \right\} \left[ J_M^0 + \frac{\lambda'_M \lambda'_M P_{HM} P_H^0}{(\lambda'_M - \lambda'_H)\lambda'_H} \right] \right. \\ \cdot \left( \exp\left[-\frac{x}{\lambda'_{\alpha}}\right] - \exp\left[-\frac{x}{\lambda'_M}\right] \right) + \left\{ \frac{\lambda'_H \lambda'_{\alpha}}{(\lambda'_{\alpha} - \lambda'_H)\lambda'_H} J_H^0 \right\} \left[ P_{H\alpha} - P_{HM} P_{M\alpha} \frac{\lambda'_H \lambda'_M}{(\lambda'_M - \lambda'_H)\lambda'_M} - \right. \\ \left. - P_{HL} P_{L\alpha} \frac{\lambda'_H \lambda'_L}{(\lambda'_L - \lambda'_H)\lambda'_L} + \frac{P_{HM} P_{ML} P_{L\alpha}}{\lambda'_M \lambda'_L} \left( \frac{\lambda'_H \lambda'_M}{(\lambda'_M - \lambda'_H)} \frac{\lambda'_M \lambda'_L}{(\lambda'_L - \lambda'_M)} \right. \right. \\ \left. \left. - \frac{\lambda'_H \lambda'_L}{(\lambda'_L - \lambda'_H)} \frac{\lambda'_M \lambda'_L}{(\lambda'_L - \lambda'_M)} \right) \right] \left( \exp\left[-\frac{x}{\lambda'_{\alpha}}\right] - \exp\left[-\frac{x}{\lambda'_M}\right] \right).$$

In the above expression the first term on the right hand side represents the absorption of the incident  $\alpha$ -particle flux whereas the other terms represent contributions to this flux at a depth  $x$  due to interactions of the heavier nuclei.

Using the parameters listed in the appendix we still have two undetermined quantities,  $J_{\alpha}^0$  and  $\lambda'_{\alpha}$ . Due to the aforementioned slow rise of the balloons, satisfactory statistics were obtained on the intensity of  $\alpha$ -particles as a function of depth above 120 g/cm<sup>2</sup> (Fig. 4 and 5). If we choose  $J_{\alpha}^0$  and  $\lambda'_{\alpha}$  to give

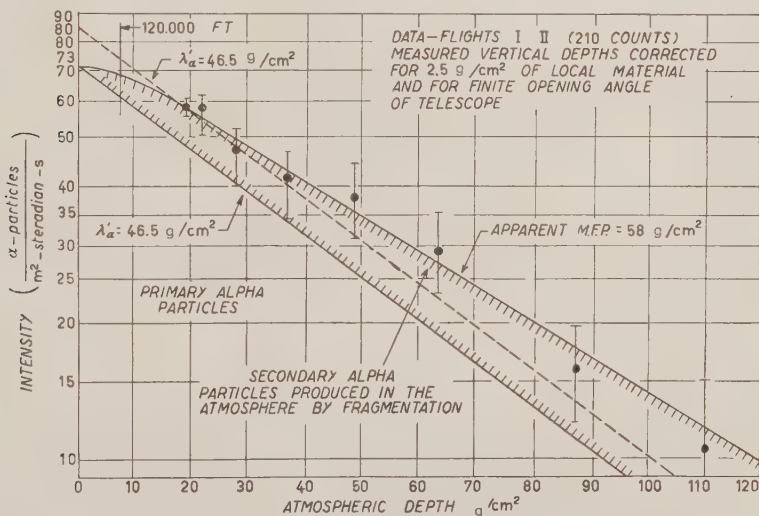


Fig. 5. —  $\alpha$ -particle intensity vs. atmospheric depth; showing extrapolation to the top of the atmosphere using the  $\alpha$ -particle diffusion equation.

agreement with the experimental data at 18.5 g/cm<sup>2</sup> and with the best least squares fit to the data as a function of atmospheric depth we find,

$$J_{\alpha}^0 = 74 \pm 5 \frac{\alpha\text{-particles}}{\text{m}^2 \cdot \text{sr} \cdot \text{s}},$$

$$\lambda_{\alpha} = 46.5 \pm 3.0 \text{ g/cm}^2.$$

To directly compare the results of this experiment with those obtained previously by other experimenters at this latitude it is necessary to extrapolate the known intensity at 18.5 g/cm<sup>2</sup> to the top of the atmosphere (M.F.P. = 45 g/cm) without benefit of the fragmentation correction. This extrapolation gives  $J_{\alpha}^0 = 86 \pm 5$   $\alpha$ -particles/m<sup>2</sup>-sr-s. The correction due to the fragmentation of the heavier nuclei thus reduces the  $\alpha$ -particle intensity at the top of the atmosphere by  $14 \pm 4\%$  for experiments made at this altitude. Corresponding

TABLE IV. - Comparison of primary  $\alpha$ -particle intensities obtained at the top of the atmosphere by different observers ( $\lambda=41^{\circ}$  N) (uncorrected for fragmentation).

Author	References	Method	Lat.	$\alpha$ -particle intensity (particles/m <sup>2</sup> ·sr·s)	
WEBBER and McDONALD	(1)	Čerenkov detector	41.5°	82 ± 9	
WEBBER	—	Čerenkov detector	41.5°	86 ± 5	Weighted
BOHL	(7)	Double scintillator	41.5°	90 ± 10	Average
LINSLEY	(8)	Čerenkov det. + cloud cham.	41.5°	88 ± 8	90.0 ± 3.0
McDONALD	(9)	Čerenkov det. + scintillator	41.5°	96 ± 9	
HOROWITZ	(10)	Čerenkov detector	41.5°	99 ± 15	
PERLOW <i>et al.</i>	(11)	Proportional counters	40.0°	110 ± 20	
BRADT and PETERS	(12)	Photographic emulsions	41.7°	138 ± 20	

(7) L. BOHL: *Ph. Doct. Thesis*, University of Minnesota (1954).

(8) J. LINSLEY: *Phys. Rev.*, **101**, 826 (1956).

(9) F. B. McDONALD: Private communication (1956).

(10) N. HOROWITZ: *Phys. Rev.*, **98**, 165 (1955).

(11) G. J. PERLOW *et al.*: *Phys. Rev.*, **88**, 321 (1953).

(12) H. BRADT and B. PETERS: *Phys. Rev.*, **77**, 54 (1950).



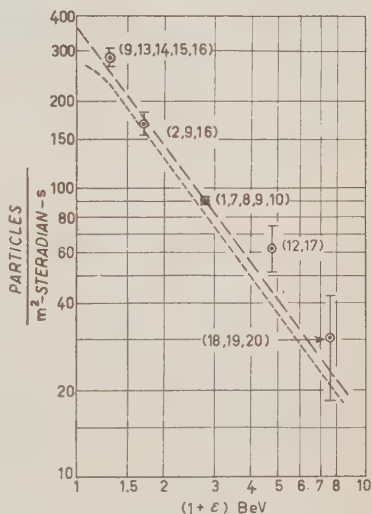
reductions are necessary at other altitudes and latitudes. The error on the fragmentation correction listed above comes about by considering the errors on the individual parameters in the diffusion equation for  $\alpha$ -particles. See Sect. 5.2 and the Appendix). This propagation of errors analysis indicates that such a fragmentation correction is justified by the accuracy of the present data.

Note that, as a consequence of the production of secondary alphas, the absorption of  $\alpha$ -particles deviates considerably from an exponential in the uppermost region of the atmosphere, although below  $18.5 \text{ g/cm}^2$  the absorptoin is approximately exponential with an apparent M.F.P. of  $58 \text{ g/cm}^2$ . A balloon flight at 120000 feet ( $7.5 \text{ g/cm}^2$  including material) should be decisive in confirming this non-exponential absorption in the extreme upper region of the atmosphere.

Table IV summarizes the work to date of various observers on the  $\alpha$ -particle component of the primary radiation at  $\lambda = 41^\circ$ . A weighted average, based on the experimental values quoted by these observers gives a value of  $90.0 \pm 3.0 \text{ } \alpha\text{-particles/m}^2\text{-sr-s}$  at this latitude, (uncorrected for fragmentation).

A review of the situation with regard to the integral intensity-energy spectrum for  $\alpha$ -particles in the latitude sensitive region ( $13^\circ$ - $20^\circ$ ) is shown in Fig. 6.

Fig. 6. Integral intensity-energy spectrum for  $\alpha$ -particles in the latitude sensitive region. The dashed line refers to spectrum  $N(>\epsilon) = 360/(1+\epsilon)^{1.4}$ . The dotted line indicates the corrected spectrum obtained when fragmentation of the heavier components is considered. The numbers in the figure next to the experimental points give the reference numbers in the text of the experimental data used in calculating the weighted averages of the intensity for each latitude.



- (13) E. P. NEY and D. M. THON: *Phys. Rev.*, **81**, 1068 (1951).
- (14) L. R. DAVIS, H. M. CAULK and C. Y. JOHNSON: *Phys. Rev.*, **101**, 801 (1956).
- (15) F. B. McDONALD: Private communication to E. P. NEY (1953).
- (16) C. J. WADDINGTON: *Phil. Mag.*, **45**, 1312 (1954).
- (17) B. PETERS: *Proc. Ind. Acad. Sci.*, **40**, 231 (1954).
- (18) M. A. POMERANTZ: *Journ. Franklin Inst.*, **258**, 443 (1954).
- (19) G. W. MCCLURE: *Phys. Rev.*, **96**, 1391 (1954).
- (20) S. F. SINGER: *Phys. Rev.*, **80**, 47 (1950).

As in the case of the  $\lambda = 41^\circ$  intensity a weighted average of the experimental data is made to determine the intensity at each latitude where more than one observation has been made. The errors on these average intensities have been assigned in accordance with the reliability of the experimental data at each latitude. Notice that the situation at  $\lambda = 55^\circ$  and  $\lambda = 41^\circ$  is much better than at the other latitudes, particularly near the equator. A spectrum of the form  $N(\varepsilon) = K/(1 + \varepsilon)^\alpha$  where  $\varepsilon$  is the kinetic energy per nucleon is used to fit the data. The value of  $\alpha$  is chosen to be 1.4 in accordance with the value deduced by KAPLON <sup>(21)</sup> for particles with  $Z \geq 6$ . The points at  $\lambda = 55^\circ$  and  $\lambda = 41^\circ$  are in good agreement with such a value for  $\alpha$  and do not permit a variation of much more than  $\pm 0.15$  in the value chosen for this exponent.

The necessity for accurate intensity measurements on  $\alpha$ -particles near the equator in order to clarify the form of the intensity-energy spectrum for these particles is emphasized by Fig. 6.

If one corrects the  $\alpha$ -particle data to a constant altitude of 90 000 ft (18 g/cm<sup>2</sup>) using an absorption M.F.P. of 58 g/cm<sup>2</sup>, and to a constant geomagnetic latitude of  $41.5^\circ$  using geomagnetic theory in conjunction with the energy spectrum given in Fig. 6, the resulting hourly counting rates indicate that the  $\alpha$ -particle intensity was constant to within  $\pm 9\%$  during both flights from 10 A.M. to 3 P.M. local time. In addition, the average hourly counting rates of  $\alpha$ -particles for the two flights agreed to within  $\pm 2\%$  during this time interval.

**5.2. Li, Be, B Nuclei.** — Before we consider the observations on nuclei heavier than  $\alpha$ -particles, the pulse height calibration will be discussed, since the impending results depend more on pulse size information than those presented so far. Due to the non-linearities in the system it was also necessary to know that the gain had remained constant throughout the flights. This could be verified by measuring the amplitude of the saturation pulses on the CRT. It was found that this level varied less than  $\pm 2\%$  for the duration of both flights, indicating a negligible change in  $B^+$  voltage and a consequent minimal change in gain characteristics of the system.

The method of system calibration was as follows: carefully calibrated pulses measured as 4 times the average sea level  $\mu$ -meson pulse were passed through the system. These pulses were compared with and adjusted slightly so as to coincide with the peak of  $\alpha$ -particle distribution obtained at altitude. Then a gain curve over the entire range was made using these adjusted pulses as a base and giving special emphasis to pulses 9, 16, and 25 times those for the singly charged particles. Various runs were made exploring the effect of slight errors in the adjusted  $\alpha$ -particle pulse height. A final calibration

(<sup>21</sup>) M. F. KAPLON *et al.*: *Phys. Rev.*, **85**, 295 (1952).

curve was then made by comparing photographs of the traces produced by the calibrated pulse with those obtained at maximum altitude during the two balloon flights. The arrows in Fig. 7 give the pulse height expected for relativistic Li, Be, B as determined by this system calibration.

It can be seen from the differential pulse height distribution of all counts in Fig. 7 that, while there is some indication of Li, Be, and B peaks, the resolution is quite poor. If one examines the differential pulse height distribution of the regular counts, however, the peaks due to Li, Be, and B are now clearly resolved. If we correct for the  $\alpha$ -particle tail in the Li region and consider that 6 of the counts in the Li, Be, B region are background for undetected «J» events (detection efficiency for «J» events determined to be  $\sim 97\%$  in this pulse height region) we obtain 28 Li, 36 Be and 19 B counts or a total of 83 counts that can reasonably be attributed to light (L) nuclei. The above breakdown gives a ratio of intensities  $J_{Li}/J_{Be}/J_B$  of approximately  $3/4/2$ .

The above value for the number of light nuclei observed must be corrected for knock-on electrons and nuclear interactions occurring in the local material of the telescope. The corrections due to these effects have already been discussed in a previous section and amount to  $19.7\%$  of the total number of light particle counts or an addition of  $20 \pm 5$  counts to the 83 regular Li, Be, and B counts.

The observed «structure» in the bottom «J» distribution amounted to 7 Li, 14 Be and 8 B counts for a total of 29 counts or  $27.7\%$  of the total number of light particle counts obtained. This result compares favorably with the predicted value of at least  $25.6\%$  for the fraction of light particles that should appear as «structure» counts in the bottom «J» distribution. As before the top «J» pulse height distribution showed no «structure» in this region.

The total number of counts that can finally be attributed to light nuclei is thus  $83 + 20 = 103 \pm 11$ . This gives an intensity  $3.11 \pm 0.33$  light

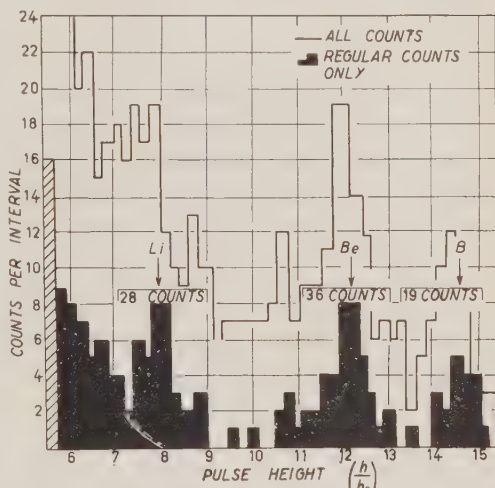


Fig. 7. — Differential pulse height distribution of all counts and of regular counts in Li, Be, B region at  $18.5 \text{ g/cm}^2$ .

nuclei/m<sup>2</sup>-sr-s at 18.5 g/cm<sup>2</sup>. Extrapolating this value to the top of atmosphere using the parameters that are given in the appendix in the diffusion equation for the light component given by NOON and KAPLON <sup>(6)</sup>, gives an intensity of

$$2.28 \pm 0.55 \frac{\text{light nuclei}}{\text{m}^2 \cdot \text{sr} \cdot \text{s}}.$$

Note that the intensity of light nuclei at the top of the atmosphere is less than that at 18.5 g/cm<sup>2</sup> due to fragmentation of the heavier components.

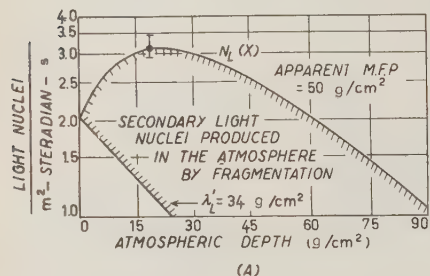


Fig. 8-1. Intensity of light nuclei in the upper atmosphere at  $\lambda = 41^\circ$  as predicted by the diffusion equation for light nuclei using the value of  $J_L^{18.5}$  obtained in this experiment.

Fig. 8-A shows the intensity of light nuclei in the upper atmosphere at  $\lambda = 41^\circ$  as predicted by the diffusion equation using the value of  $J_L$  at 18.5 g/cm<sup>2</sup> obtained in this experiment. This behavior seems to be supported quantitatively by the work of the Bristol group <sup>(22)</sup>.

Using the values for the intensity of medium nuclei obtained in this experiment and reported in the next section ( $H/M$  ratio of 0.33 assumed at the top of the atmosphere) and the values for the intensity of light nuclei reported above gives  $L/M$  ratios of  $0.80 \pm 0.09$  and  $0.35 \pm 0.09$

at 18.5 g/cm<sup>2</sup> and at the top of the atmosphere, respectively. If, in calculating the medium intensity, an  $H/M$  ratio of 0.5 is assumed at the top of the atmosphere the  $L/M$  ratios become  $0.88 \pm 0.10$  and  $0.38 \pm 0.10$ , respectively. The  $L/M$  ratio at the top of the atmosphere as deduced from this experiment is thus only slightly dependent on the value of  $H/M$  assumed at the top of the atmosphere.

If, as a comparison, we take the latest emulsion values for the intensity of medium nuclei at this latitude <sup>(23)</sup> along with the values for the intensity of light nuclei obtained in this experiment the corresponding  $L/M$  ratios become  $0.73 \pm 0.11$  at 18.5 g/cm<sup>2</sup> and  $0.29 \pm 0.11$  at the top of the atmosphere.

One might ask whether the above experimental results represent a positive indication of a finite intensity of light nuclei at the top of the atmosphere or whether the uncertainties in the fragmentation parameters are such that the

<sup>(22)</sup> D. H. PERKINS, Report on work of DANTON, FOWLER and KENT: *Proceedings of the Duke Conference on Cosmic Radiation* (1953) (unpublished).

<sup>(23)</sup> M. F. KAPLON J. H. NOON and G. W. RACETTE: *Phys. Rev.*, **96**, 1408 (1954).

data are inconclusive. To examine this question further a propagation of errors analysis was made on the diffusion equation for the light nuclei. The errors in the 9 independent parameters in this equation were estimated from the work of NOON and KAPLON<sup>(6)</sup> and are given in the appendix. The results of this errors analysis showed that the fraction of light nuclei at 18.5 g/cm<sup>2</sup> produced by the fragmentation of heavier components in the atmosphere above can be considered uncertain by  $\pm 25\%$ . As a consequence, the intensity of light nuclei at the top of the atmosphere becomes  $2.28 \pm 0.87$  (m<sup>2</sup>·sr·s)<sup>-1</sup> when both fragmentation and statistical errors are included compared with  $2.28 \pm 0.55$  (m<sup>2</sup>·sr·s)<sup>-1</sup> when only statistical errors are considered, and the  $L/M$  ratio at the top of the atmosphere as deduced from this experiment ( $H/M$  ratio of 0.33 assumed at top of atmosphere) becomes  $0.35 \pm 0.13$  compared with the value of  $0.35 \pm 0.09$  quoted above when only statistical errors are considered. As a result of the above analysis we can conclude that the results obtained in this experiment provide the first positive non-emulsion indication that a finite intensity of Li, Be, B nuclei is present at the top of the atmosphere.

Fig. 8-B gives a summary of  $L/M$  ratios at the top of the atmosphere as deduced from measurements of various observers<sup>(24-28)</sup> in the upper atmosphere. Only the most recent available results from each group working on this problem are shown. The ratios given in the figure may differ somewhat from those reported in the literature since an attempt was made to standar-

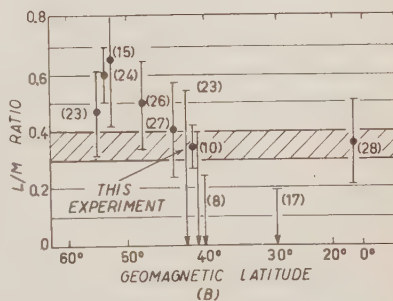


Fig. 8-B. — Summary of  $L/M$  ratios deduced at the top of the atmosphere from the work of various experimenters. All extrapolations to the top of the atmosphere are standardized using the fragmentation parameters given by NOON and KAPLON<sup>(6)</sup> and therefore may differ slightly from those reported in the literature. The numbers in figure next to the experimental points refer to the reference numbers in the text.

(<sup>24</sup>) A. D. DANTON, P. A. FOWLER and D. W. KENT: *Phil. Mag.*, **93**, 729 (1952) (est.).

(<sup>25</sup>) K. GOTTSTEIN: *Phil. Mag.*, **95**, 347 (1954) (est.).

(<sup>26</sup>) H. FOWLER: *Results reported at International Congress on Cosmic Radiation, Guanajuato, Mexico* (1955) (est.).

(<sup>27</sup>) K. GOTTSTEIN: *Results reported at International Congress on Cosmic Radiation, Guanajuato, Mexico* (1955) (est.).

(<sup>28</sup>) R. F. HOURD, J. R. FLEMING and J. J. LORD: *Phys. Rev.*, **95**, 641 (1954) revised by J. J. LORD, Private communication (1956).



dize the various extrapolation procedures by using the fragmentation parameters given by NOON and KAPLON <sup>(6)</sup> throughout, in the extrapolation of the data to the top of the atmosphere by the diffusion equations. The net effect of such a standardization procedure was to reduce certain of the  $L/M$  ratios deduced at the top of the atmosphere. The results that were so affected are indicated by (est.) in the references.

It is apparent from Fig. 8-B that, despite a continuing disagreement in the ratios reported by emulsion observers, all the standardized data are reasonably consistent with a  $L/M$  ratio of between 0.3 and 0.4. Furthermore, within the statistical accuracy of the observations, this ratio does not appear to be latitude dependent although there appears to be a slight tendency for higher  $L/M$  ratios at the higher geomagnetic latitudes.

5.3. *Nuclei with  $Z \geq 6$ .* — Despite the fact that the pulses from particles with  $Z \geq 6$  generally were « off scale », valuable information could be obtained about the total intensity of these particles.

A total of 93 « off scale » regular counts were obtained. It is assumed that all these counts are caused by legitimate particles with  $Z \geq 6$  since the detection efficiency for « J » events is approaching 100% in this large pulse height region.

The correction for knock-on electrons and nuclear interactions occurring in the local material of the telescope amounts to 46.5% of the total number of  $Z \geq 6$  counts. This necessitates adding  $77 \pm 15$  counts to the 93 regular counts to take into account the above effects, giving a total of  $93 + 77 = 170 \pm 20$  counts at 18.5 g/cm<sup>2</sup> due to nuclei having  $Z \geq 6$ . The corresponding intensity is  $5.12 \pm 0.60$   $Z \geq 6$  nuclei/m<sup>2</sup>·sr·s. Using the parameters in the appendix in the diffusion equations for the medium and heavy components as given by NOON and KAPLON <sup>(6)</sup> ( $H/M = 0.33$  assumed at the top of the atmosphere) gives an intensity of

$$9.2 \pm 1.2 \frac{Z \geq 6 \text{ nuclei}}{\text{m}^2 \cdot \text{sr} \cdot \text{s}},$$

at the top of the atmosphere. Assuming  $H/M = 0.5$  at the top of the atmosphere gives an intensity of  $9.1 \pm 1.2$   $Z \geq 6$  nuclei/m<sup>2</sup>·sr·s. Thus the intensity of  $Z \geq 6$  nuclei at the top of the atmosphere is not sensitive to the value of  $H/M$  assumed at the top of the atmosphere. The above intensity is to be regarded as less certain than those reported for the other charge components, due to the various assumptions necessitated by the fact that these pulses were « off scale ». It may be compared with the intensity of  $9.7 \pm 1.5$   $Z \geq 6$  nuclei/m<sup>2</sup>·sr·s obtained at  $\lambda = 41^\circ$  using the latest emulsion techniques <sup>(23)</sup>.

5.4. *Singly Charged Particles.* — To find the maximum number of counts attributable to primary protons at 18.5 g/cm<sup>2</sup> let us compare the singly charged

pulse height distribution at this altitude with the sea-level  $\mu$ -meson distribution. If the singly charged pulse height distribution at altitude were due entirely to primary protons it should have an almost identical shape to that obtained from  $\mu$ -mesons at sea level. This is so because all of the factors that are believed to contribute to the half-widths of the respective pulse height distributions are equal except for that due to the variation in  $\beta$  of the incoming particles. This introduces a 15% half width contribution to the sea level  $\mu$ -meson pulse height distribution but only a 2% half width contribution to the pulse height distribution for primary protons near the top of the atmosphere at  $\lambda = 41^\circ$ . The net effect is that the primary proton distribution should be expected to have a half width only 2% less than for  $\mu$ -mesons at sea level; or for the present purposes the two pulse height distributions may be considered identical in shape.

Fig. 9 shows the two pulse height distributions normalized in the region  $1.2h_0 \leq h \leq 2.0h_0$  and superimposed. This region is chosen for normalization

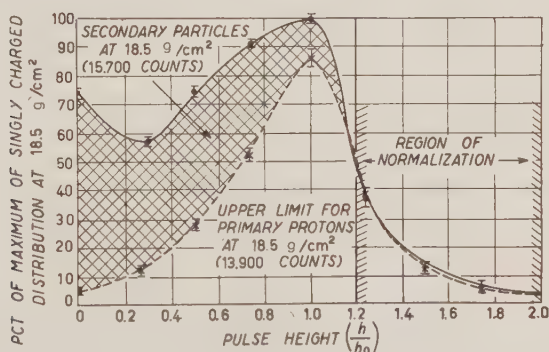


Fig. 9. — Determination of an upper limit on primary proton intensity at 18.5 g/cm<sup>2</sup> by superimposing the sea level  $\mu$ -meson distribution on the singly charged distribution obtained at 18.5 g/cm<sup>2</sup> (Flights I and II combined. Distributions normalized in  $1.2h_0 \leq h \leq 2.0h_0$  pulse height region).

because few of the low energy particles at high altitude would be expected to statistically scatter into this region. All or most of the counts in this region then, should be due to the normal statistical scatter of the more energetic particles (presumably mostly primary protons) similar to the scatter of pulses from  $\mu$ -mesons at sea level. Therefore normalization in this region should most nearly give an indication of the number of counts that can be attributed to primary protons at this altitude. It is evident from the figure that, using this normalization procedure, there is a considerable excess of counts in the

low and medium pulse height regions of the singly charged distribution at  $18.5 \text{ g/cm}^2$ . It seems reasonable to attribute these counts to: (1) secondary protons with  $0.5 \leq \beta \leq 0.9$ , (2) mesons with  $0.7 \leq \beta \leq 0.9$  and (3) upward moving albedo particles (downward to upward ratio of detector sensitivity is 2.5).

Fig. 9 indicates that only about  $\frac{1}{2}$  (13900 counts) of the singly charged counts at  $18.5 \text{ g/cm}^2$  lie under the normalized  $\mu$ -meson curve and can therefore be reasonably attributed to downward moving primary protons or very energetic mesons and electrons, all of which will give pulses identical to those from  $\mu$ -mesons at sea level. The percentage of energetic mesons and electrons at this depth in the atmosphere is not well known; therefore this method should serve only to set some sort of an upper limit on the primary proton intensity at this altitude. To arrive at a flux value for primary protons one must take into account, as in the case of the other charge components, those primary protons having nuclear interactions in the local material of the telescope or producing knock-on electrons capable of giving «*J*» counts. The correction for these effects amounts to 7.3% of the total number of proton counts or an addition of 1100 counts to the regular proton distribution.

The observed «structure» in the singly charged pulse height region of the bottom «*J*» distribution amounts to 1500 counts compared with a predicted «structure» of 1200 counts due to primary protons alone. This excess of observed «structure» counts is presumably due to those «*J*» counts produced by secondary particles passing through the telescope.

A maximum of  $13900 + 1100 = 15000$  counts can reasonably be attributed to primary protons at this altitude. The corresponding intensity is  $\leq 452$  primary protons/ $\text{m}^2 \cdot \text{sr} \cdot \text{s}$  at  $18.5 \text{ g/cm}^2$ .

To extrapolate this value to the top of the atmosphere one should take into account the production of very energetic protons by the interactions of the heavier components in the atmosphere above. This effect may be appreciable, as in the case of the  $\alpha$ -particle calculations, and could similarly be handled by a proton diffusion equation. Many of the important parameters involved in this equation are still relatively unknown however, and, in addition, the present data hardly warrant such a careful extrapolation.

Instead, to allow for this effect to some extent, we shall take a generous attenuation M.F.P. for protons in air of  $120 \text{ g/cm}^2$ . This extrapolation gives an estimated intensity of

$$\leq 526 \frac{\text{primary protons}}{\text{m}^2 \cdot \text{sr} \cdot \text{s}},$$

at the top of the atmosphere.

This result is in quantitative agreement with the recent results of VERNOV

and CHARAKHCHYAN <sup>(29)</sup> and WINCKLER and ANDERSON <sup>(30)</sup> which indicate a lower primary proton intensity than was originally supposed.

A tabular summary of the results of the present work is given in Table V.

TABLE V. - Summary of experimental results ( $\lambda = 41.5^\circ$ ).

Component	Vertical intensity Particles/m <sup>2</sup> ·sr·s		Pct. of Total Primary Radiation
	Observed at 18.5 g/cm <sup>2</sup>	Estimated top of atmosphere (Primaries)	
Protons	$\leq 452$	$\leq 526$	$\leq 86.1$
$\alpha$ -Particles	$57 \pm 3.5$	$74 \pm 5$	12.1
Li, Be, B	$3.11 \pm 0.33$	$2.28 \pm 0.55$	0.4
$Z \geq 6$	$5.12 \pm 0.60$	$9.2 \pm 1.2$	1.4
Total	$\leq 517$	$\leq 611$	100

## APPENDIX

### Parameters Used in Diffusion Equation Extrapolations <sup>(31)</sup>.

Intensities Particles/m<sup>2</sup>·sr·s

M.F.P.

$$\begin{array}{ll}
 J_H^0 = 2.6 \pm 0.9^{(23)} & \lambda_H = 18.0 \text{ g/cm}^2 \quad \lambda'_H = 24.0 \pm 2.7 \text{ g/cm}^2 \\
 J_M^0 = 7.1 \pm 1.3^{(23)} & \lambda_M = 26.5 \text{ g/cm}^2 \quad \lambda'_M = 30.5 \pm 3.6 \text{ g/cm}^2 \\
 J_L^0 = 2.28 \pm 0.25 \quad \left. \begin{array}{l} \text{as determined by} \\ \text{this experiment} \end{array} \right\} & \lambda_L = 31.5 \text{ g/cm}^2 \quad \lambda'_L = 34.0 \pm 4.2 \text{ g/cm}^2 \\
 J_\alpha^0 = 74 \pm 5 \quad \left. \begin{array}{l} \text{as determined by} \\ \text{this experiment} \end{array} \right\} & \lambda_\alpha = 45.5 \text{ g/cm}^2 \quad \lambda'_\alpha = 46.5 \pm 5.0 \text{ g/cm}^2
 \end{array}$$

$$\text{where } \lambda'_x = \frac{\lambda_x}{1 - P_{xx}}.$$

<sup>(29)</sup> S. N. VERNOV and A. N. CHARAKHCHYAN: *Dokl. Akad. Nauk SSSR*, **91**, 487 (1953).

<sup>(30)</sup> Work of J. R. WINCKLER and K. ANDERSON reported by E. P. NEY at *International Congress on Cosmic Radiation, Guanajuato, Mexico* (1955).

<sup>(31)</sup> All values and errors from NOON and KAPLON, loc. cit., unless otherwise noted. The M.F.P. are considered to be accurate within  $\pm 10\%$ .

**Fragmentation Probabilities.**

$$\begin{array}{lll}
 P_{HH} = 0.25 \pm 0.05 & P_{MM} = 0.13 \pm 0.05 & P_{LL} = 0.07 \pm 0.07 \text{ (}^{24}\text{)} \\
 P_{HM} = 0.27 \pm 0.05 & P_{ML} = 0.42 \pm 0.09 & P_{L\alpha} = 0.5 \pm 0.3 \text{ (}^{32}\text{)} \\
 P_{HL} = 0.48 \pm 0.07 & P_{M\alpha} = 1.42 \pm 0.15 & P_{\alpha\alpha} = 0.02 \text{ (est.)} \\
 P_{H\alpha} = 2.07 \pm 0.15 & & 
 \end{array}$$

\* \* \*

I wish to express my deepest appreciation to Professor J. A. VAN ALLEN for his continued encouragement and interest in this work; to Dr. F. B. McDONALD for his helpful advice throughout the course of this project; to R. F. MISSERT for his many stimulating discussions; to the members of the shop for their continued co-operation; to Winzen Research, Inc. for two very fine balloon flights; and to the Office of Naval Research and the Atomic Energy Commission for their assistance of the Iowa Cosmic Ray program.

(<sup>32</sup>) M. F. KAPLON: Private communication (1955) (est.).

**RIASSUNTO (\*)**

Mediante due voli di palloni tipo « Skyhook » si sono eseguite ad un'altezza atmosferica media di 18.5 g/cm<sup>2</sup> misure d'intensità delle particelle  $\alpha$  e dei nuclei di Li, Be, e B presenti nella radiazione cosmica primaria a  $\lambda = 41.5^\circ$ . Lo strumento di misura era un sottile (3.0 g/cm<sup>2</sup>) detettore Čerenkov posto nell'angolo solido di un telescopio di contatori Geiger. Questo detettore dette una risoluzione straordinariamente buona delle componenti  $\alpha$  e Li, Be, B. Questa circostanza e la lentezza d'ascesa dei due palloni hanno reso possibile una determinazione dettagliata della dipendenza dell'intensità delle  $\alpha$  dalla profondità atmosferica. La qualità dei dati raccolti giustifica un nuovo esame del problema dell'estrapolazione dell'intensità delle particelle  $\alpha$  alla sommità dell'atmosfera. Tale estrapolazione fu eseguita applicando alla dipendenza dell'intensità delle  $\alpha$  dalla relazione pressione-altitudine osservata un'equazione di « diffusione » del tipo precedentemente usato per nuclei con  $Z > 2$ . Il valore risultante per l'intensità delle particelle  $\alpha$  alla sommità dell'atmosfera è in misura significativa più basso dei valori precedentemente ammessi. A 18.5 g/cm<sup>2</sup> la somma delle intensità verticali delle componenti Li, Be, B fu trovata essere  $(3.11 \pm 0.31) \text{ (m}^2 \cdot \text{sr} \cdot \text{s)}^{-1}$  ed il rapporto fra le intensità  $J_{\text{Li}}/J_{\text{Be}}/J_{\text{B}}$  risultò 3/4/2. Il rapporto d'intensità (nuclei leggeri/nuclei medi) alla sommità dell'atmosfera determinato con questa esperienza fu  $0.35 \pm 0.09$ . Le intensità verticali alla sommità dell'atmosfera delle varie componenti della radiazione primaria ottenute nella presente esperienza a  $\lambda = 41.5^\circ$  sono:

Componente . . . . .	$J^0 \text{ (m}^2 \cdot \text{sr} \cdot \text{s)}^{-1}$
Protoni . . . . .	$< 526$
Particelle $\alpha$ . . . . .	$74 \pm 5$
Li, Be, B . . . . .	$2.28 \pm 0.55$
$Z \geq 6$ . . . . .	$9.2 \pm 1.2$

(\*) Traduzione a cura della Redazione.



## Rotational States of Spheroidal Nuclei (\*).

F. COESTER

*Department of Physics, State University of Iowa - Iowa City, Iowa*

(ricevuto il 18 Agosto 1956)

**Summary.** — A new method of introducing collective co-ordinates as dynamical variables is proposed. A hamiltonian for rotating spheroidal nuclei is constructed by this method. The resulting moments of inertia are discussed. They depend on a parameter  $\xi$  which is determined if the intrinsic particle wave function of the nucleus is known. If  $\xi$  is treated as an empirical parameter the observed moments of inertia can be fitted. In order to illustrate the theoretical determination of  $\xi$  calculations have been carried out for independent particles in a harmonic oscillator well without spin-orbit coupling.

### 1. — Introduction.

Strongly deformed nuclei in the rare earth region exhibit symmetric top rotational spectra <sup>(1,2)</sup>. The moments of inertia defined by the observed level spacings are roughly a third to one half times the moment of inertia of a rigid nucleus. They are several times larger than the moment of inertia obtained for irrotational motion of a liquid drop <sup>(1,2)</sup>. Several attempts have been made to account for the existence of such rotational spectra as well as for the size of the moment of inertia. The former can be done in many ways, the latter proved to be much harder.

The unified model of Bohr and Mottelson <sup>(3,4)</sup> which assumes a liquid drop

---

(\*) Supported in part by the U. S. Atomic Energy Commission.

(1) See for instance A. BOHR and B. R. MOTTELSON: *Beta and Gamma Spectroscopy*, Chapter XVII, Edit by K. SIEGBAHN (New York, 1955) and references quoted there.

(2) A. BOHR and B. R. MOTTELSON: *Dan. Mat. Fys. Medd.*, **30**, No. 1 (1955).

(3) A. BOHR: *Dan. Mat. Fys. Medd.*, **26**, No. 14 (1952).

(4) A. BOHR and B. R. MOTTELSON: *Dan. Mat. Fys. Medd.*, **27**, No. 16 (1953).

core in strong interaction with one or several extra core particles predicts rotational levels. But the moment of inertia in this model is that of the liquid drop core which is too small by a factor 3 to 5. The same result has been obtained by many authors who start from a quantum mechanical many particle description and introduce collective coordinates by appropriate canonical transformations<sup>(5-10)</sup>. The unified model is subject to the obvious criticism that the wave function of the nucleus cannot be antisymmetrical in intra core and extra core nucleons. Moreover calculations by S. G. NILSON<sup>(11)</sup> and K. GOTTFRIED<sup>(12)</sup> show that for the large deformations prevailing in the rare earth region the single particle energy levels exhibit no gap which would separate the neutrons in a «magic core» from the extra core neutrons.

An approach which is not subject to these objections has been proposed by INGLIS<sup>(13,14)</sup>. The independent particle model for the nucleus is used with a spheroidal oscillator potential. The rotation of the nucleus is described classically as a uniform rotation of the deformed potential. The rotational energy of a single nucleon in such a rotating potential is calculated in the adiabatic approximation<sup>(15)</sup>. The total rotational energy and hence the moment of inertia is then obtained by summing over all nucleons in the nucleus. The resultant moment of inertia is that of a rigid nucleus<sup>(2,15)</sup>. BOHR and MOTTELSON have shown that the pairing interaction of two nucleons will decrease their effective moment of inertia as calculated in the Inglis model<sup>(2,14)</sup>. By adjusting the strength of the pairing interaction the observed values of the moments of inertia can be fitted.

If we wish to treat all nucleons in a symmetrical fashion by shell model methods and still introduce collective co-ordinates as dynamical variables we must formally augment the number of degrees of freedom of the system. In general this increase is compensated by appropriate subsidiary conditions on the wave functions. LIPKIN, DE SHALIT and TALMI<sup>(8)</sup> have shown how certain results can be derived without the use of subsidiary conditions. In any case one usually attempts a complete description of the system in terms of collective and intrinsic co-ordinates while such a description has an empirical

<sup>(3)</sup> H. A. TOLHOEK: *Physica*, **21**, 1 (1955).

<sup>(6)</sup> F. COESTER: *Phys. Rev.*, **99**, 170 (1955).

<sup>(7)</sup> T. MARUMORI, J. YUKAWA and R. TANAKA: *Prog. Theor. Phys.*, **13**, 442 (1955);  
T. MARUMORI and E. YAMADA: *Prog. Theor. Phys.*, **13**, 557 (1955).

<sup>(8)</sup> H. J. LIPKIN, A. DE SHALIT and I. TALMI: *Nuovo Cimento*, **2**, 773 (1955).

<sup>(9)</sup> T. TAMURA: *Nuovo Cimento* (to be published).

<sup>(10)</sup> F. VILLARS: (1955), unpublished

<sup>(11)</sup> S. G. NILSON: *Dan. Mat. Fys. Medd.*, **29**, No. 16 (1955).

<sup>(12)</sup> K. GOTTFRIED: *Phys. Rev.* **103**, 1017 (1956).

<sup>(13)</sup> D. R. INGLIS: *Phys. Rev.*, **96**, 1059 (1954); **97**, 701 (1955).

<sup>(14)</sup> S. A. MOSZKOWSKI: *Phys. Rev.*, **103**, 1328 (1956).

<sup>(15)</sup> A rigorous calculation has been done by J. G. VALATIN (to be published).

basis only for a few low lying energy levels. If we want to arrive at an approximate description of only a few states the collective co-ordinates need not be introduced by a canonical transformation. In this sense I want to propose here a new method of introducing collective dynamical variables and show that it can account for the rotational levels of spheroidal nuclei. The description is well defined by conditions which must be imposed for physical or symmetry reasons. Only one parameter remains which is determined by minimizing the ground state energy.

## 2. - The Collective Hamiltonian.

Since the spheroidal shell model seems to account well for many features of deformed nuclei we assume that the rotational states of such nuclei can be represented by wave functions of the form

$$(1) \quad \Psi = \Psi^0(\mathbf{y}^{(1)} \dots \mathbf{y}^{(A)})\Phi(\mathfrak{R}),$$

where  $\Phi$  is a symmetric top eigenfunction and  $\Psi^0$  is a spheroidal shell model wave function suitably modified by pairing effects if necessary.  $\mathbf{y}^{(1)} \dots \mathbf{y}^{(A)}$  are nucleon co-ordinates referred to the principal axes of the spheroidal nucleus.  $\Psi^0$  depends also on  $A$  spin variables, specifically the components of the nucleon spins in the direction of the symmetry axis of the spheroidal nucleus. These variables are suppressed from the notation merely for the sake of convenience.  $\mathfrak{R}$  stands for three Euler angles  $q, \vartheta, \chi$  which specify the orientation of the nucleus with respect to space fixed axes. The  $y$ 's and the Euler angles are treated as independent variables. By the same token it is assumed that the nucleon spins commute with  $\mathfrak{R}$ . The nucleon co-ordinates  $\mathbf{x}^{(s)}$  ( $s = 1 \dots A$ ) referred to space fixed axes are given by

$$(2) \quad x_i^{(s)} = \sum_{\nu} R_{i\nu}(\mathfrak{R}) y_{\nu}^{(s)},$$

$R_{i\nu}(\mathfrak{R})$  is an orthogonal matrix.

We must find the Hamiltonian which operates on the wave function (1). The potential energy does not depend on the orientation of the nucleus: It depends on the  $y$ 's but not on the collective angles. The kinetic energy is  $(m/2) \sum_{\mathbf{x}} \dot{\mathbf{x}}^{(s)2}$ . Our problem is therefore to find  $\dot{\mathbf{x}}^{(s)}$  as an operator operating on  $\mathfrak{R}$  and the  $y$ 's. These operators are subject to the following requirements:

1) The momenta  $m\dot{\mathbf{x}}^{(s)}$  and the co-ordinates  $\mathbf{x}^{(s)}$  must satisfy the canonical commutation rules.

$$(3) \quad m[\dot{x}_j^{(s)}, x_k^{(t)}] = -i\delta_{jk}\delta_{ts}$$

$$(4) \quad [\dot{x}_j^{(s)}, \dot{x}_k^{(t)}] = 0.$$

This requirement must be modified if velocity dependent nuclear forces are assumed. If we adopt a model which leads to an « effective nucleon mass »<sup>(16,17)</sup> then  $m$  in eq. (3) and in the following is this effective mass and not the mass of the free nucleon.

## 2) The total angular momentum

$$(5) \quad J = m \sum_{s \neq l} \varepsilon_{khl} x_h^{(s)} \dot{x}_l^{(s)} + S_k$$

is the generator of the infinitesimal rotations of the co-ordinate system and must therefore satisfy the relations

$$(6) \quad [J_k, R_{lv}] = -i \sum_h \varepsilon_{khl} R_{hv}.$$

$S_k$  in (5) is the sum of all nucleon spins. As a consequence  $\mathbf{J}$  commutes with  $y_v^{(s)}$ ,  $\partial/\partial y_v^{(s)}$ , and the projections of the nucleon spins on the principal axis of the nucleus. The same is true for the projections of  $\mathbf{J}$  on the principal axes,

$$(7) \quad Q_\sigma \equiv \sum_k R_{k\sigma} J_k.$$

There follows from (6)

$$(8) \quad [Q_\sigma, R_{kv}] = -i \sum_\mu \varepsilon_{\sigma v \mu} R_{k\mu}.$$

$Q_\sigma$  operates only on  $\Phi(\mathfrak{R})$  and does not affect  $\Psi^0$ .

In order to arrive at an expression for the collective velocities we consider the infinitesimal deformations of a continuum  $\mathbf{y} \rightarrow \mathbf{x}$ :

$$(9) \quad x_i = y_i + \sum_k w_{ik} y_k.$$

The symmetrical and antisymmetrical parts of  $w_{ik}$  describe dilational and rotational deformations respectively. The corresponding collective velocity  $\mathbf{v}^c$  is

$$(10) \quad v_i^c = \sum_k \dot{w}_{ik} y_k.$$

Assuming that the velocities are linear in the  $Q_\sigma$  we conclude that the collective part of the particle velocities  $\dot{x}_i^{(s)}$  should be of the form

$$(11) \quad \frac{1}{2m} \sum_\sigma \varepsilon_{\sigma v \mu} X_{\mu v} y_\mu^{(s)} \{ R_{iv}, Q \},$$

<sup>(16)</sup> K. A. BRUECKNER: *Phys. Rev.*, **97**, 1353 (1955).

<sup>(17)</sup> M. H. JOHNSON and E. TELLER: *Phys. Rev.*, **98**, 783 (1955). See also H. P. DUERR: *Phys. Rev.*, **103**, 469 (1956).

where the  $X_{\mu\nu}$  are functions of the  $y$ 's which are still to be determined. They are independent of  $s$ . ( $\{a, b\} = ab + ba$ ). The commutation rules (3) are then satisfied if we put

$$(12) \quad m\dot{x}_i^{(s)} = \sum_{\nu} R_{i\nu} p_{\nu}^{(s)} + \frac{1}{2} \sum_{\sigma\mu\nu} \{ (Q_{\sigma} - G_{\sigma}), \varepsilon_{\sigma\mu\nu} y_{\mu}^{(s)} R_{i\nu} X_{\mu\nu} \},$$

where  $p_{\nu}^{(s)} = -i(\partial/y_{\nu}^{(s)})$  and

$$(13) \quad G_{\sigma} \equiv \sum_s \sum_{\mu\nu} \varepsilon_{\sigma\mu\nu} y_{\mu}^{(s)} p_{\nu}^{(s)} + S_{\sigma}.$$

The equations (5), (7) and (12) are consistent only if

$$(14) \quad \sum_s \sum_{\mu\nu\varrho} y_{\mu}^{(s)} y_{\varrho}^{(s)} X_{\mu\nu} \varepsilon_{\tau\mu\nu} \varepsilon_{\sigma\varrho\nu} = \delta_{\tau\sigma}.$$

We shall replace here and in the following  $\sum_s y_{\mu}^{(s)} y_{\nu}^{(s)}$  by its expectation value

$$(15) \quad \langle \sum_s y_{\mu}^{(s)} y_{\varrho}^{(s)} \rangle = \delta_{\mu\varrho} q_{\mu}.$$

For any quantity  $F$  this is a good approximation if the relative width of its probability distribution is small

$$(16) \quad \frac{\Delta F}{\langle F \rangle} \equiv \sqrt{\frac{\langle F^2 \rangle}{\langle F \rangle^2}} - 1 \ll 1.$$

In our case this relative width is of order  $A^{-\frac{1}{2}}$  (18). It is instructive to consider first the almost trivial case of a spherically symmetrical nucleus  $q_1 = q_2 = q_3 = q$ . From (14) and the condition of spherical symmetry follows

$$(17) \quad X_{\mu\nu} = \frac{1}{2q}.$$

The commutation rules (4) are satisfied approximately if terms of order  $A^{-1}$  are negligible. The kinetic energy then takes the form

$$(18) \quad \frac{m}{2} \sum_s |\dot{x}^{(s)}|^2 = \frac{1}{2m} \left[ \sum_s \sum_{\nu} p_{\nu}^{(s)2} + \frac{1}{2q} (Q^2 - G^2) \right].$$

The stationary states are eigenstates of  $Q^2$ ,  $Q_3$ ,  $G^2$ ,  $G_3$ . Since there is no physically distinguished set of body fixed axes  $\mathcal{P}$  must be subject to the con-

(18) For a proof see S. TOMONAGA: *Prog. Theor. Phys.*, **13**, 467 (1955). Appendix I.



ditions

$$(19) \quad (Q^2 - G^2)\Psi = 0$$

and

$$(20) \quad (Q_3 - G_3)\Psi = 0.$$

There are no rotational states in this case. Our model reduces to the ordinary shell model.

In the case of spheroidal symmetry  $q_1 = q_2 \neq q_3$   $X_{12}$  and  $X_{21}$  are determined by (14) and the symmetry:

$$(21) \quad X_{12} = X_{21} = \frac{1}{q_1 + q_2},$$

while  $X_{23}$  etc., satisfy (14) if they are of the form

$$(22) \quad X_{13} = X_{23} = \frac{1 - \xi}{q_2 + q_3} + \frac{\xi}{q_2 - q_3},$$

$$(23) \quad X_{31} = X_{32} = \frac{1 - \xi}{q_2 + q_3} + \frac{\xi}{q_3 - q_2}.$$

For symmetry reasons the stationary states are now eigenstates of  $Q^2 = J^2$ ,  $Q_3$  and  $G_3$  but not  $G^2$ . Only the subsidiary condition (20) survives.

The Hamiltonian can now be written in the form

$$(24) \quad H = H_{\text{part}} + H_{\text{rot}} + H',$$

$H_{\text{part}}$  operates only on  $\Psi^0$ ,  $H_{\text{rot}}$  is the Hamiltonian of the collective rotation and  $H'$  is a coupling term which must be small if our initial assumption (1) is to be consistent.

$$(25) \quad H_{\text{part}} = \frac{1}{2m} \sum_{s\nu} p_{\nu}^{(s)2} + V + \frac{\xi^2 q_2 + q_3}{m(q_3 - q_2)^2} + \\ + \frac{1}{2m} \sum_{\kappa=1}^2 \left\{ G_{\kappa}, \left[ \frac{\xi}{q_3 - q_2} D_{\kappa} + \frac{1}{2} \left( \frac{\xi^2(q_2 + q_3)}{(q_3 - q_2)^2} - \frac{(1 - \xi)^2}{(q_3 + q_2)} \right) G_{\kappa} \right] \right\},$$

where

$$(26) \quad D_{\kappa} = -i \sum_{\mu\nu} \sum_s |\epsilon_{\kappa\mu\nu}| y_{\mu}^{(s)} \frac{\partial}{\partial y_{\nu}^{(s)}}.$$

$$(27) \quad H_{\text{rot}} = \frac{1}{2m(q_3 + q_2)} \left( 1 - \xi^2 + \xi^2 \left( \frac{q_2 + q_3}{q_3 - q_2} \right)^2 \right) (Q^2 - Q_3^2),$$

and

$$(28) \quad H' = -\frac{1}{m} \sum_{\kappa=1}^2 Q_{\kappa} \left[ \frac{\xi}{q_3 - q_2} D_{\kappa} + \left( \frac{\xi^2(q_2 + q_3)}{(q_3 - q_2)^2} + \frac{\xi(1 - \xi)}{q_2 + q_3} \right) G_{\kappa} \right],$$

$H'$  vanishes if either  $\xi = 0$  or if  $\Psi^0$  satisfies the conditions

$$(29) \quad \left( \frac{1}{q_3 - q_2} D_{\kappa} + \left( \frac{\xi(q_2 + q_3)}{(q_3 - q_2)^2} + \frac{1 - \xi}{q_2 + q_3} \right) G_{\kappa} \right) \Psi^0 = 0, \quad \kappa = 1, 2.$$

The meaning of this condition becomes clearer if we carry out a scale transformation

$$(30) \quad y_{\kappa}^{(s)} = \tau_{\kappa} y_{\kappa}^{(s)'}$$

If

$$(31) \quad \left( \frac{\tau_2}{\tau_3} + \frac{\tau_3}{\tau_2} \right) \frac{1}{q_3 - q_2} + \left( \frac{\tau_2}{\tau_3} - \frac{\tau_3}{\tau_2} \right) \left( \frac{\xi(q_2 + q_3)}{(q_3 - q_2)^2} + \frac{1 - \xi}{q_3 + q_2} \right) = 0,$$

then (29) becomes

$$(32) \quad G'_{\kappa} \Psi^0 = 0.$$

That means  $\Psi^0$  can be reduced to a spherically symmetrical function by the distortion (30). There follows that  $\tau_{\kappa}^{-2} q_{\kappa}$  must be independent of  $\kappa$  since

$$(33) \quad \tau_{\kappa}^{-2} q_{\kappa} = \left\langle \sum_s y'^{(s)2} \right\rangle,$$

(31) and (33) are compatible only for  $\xi = 1$ . We conclude that  $H'$  can vanish only for the two special cases  $\xi = 0$  when we have a rigid moment of inertia and  $\xi = 1$  when we have the irrotational moment of inertia. The observed moments of inertia require  $\frac{1}{3} < \xi < \frac{1}{2}$ . Strict vanishing of  $H'$  is not a requirement, but we must verify that it is small enough to be treated as a perturbation. It then effectively increases the moment of inertia. Theoretically the parameter  $\xi$  is determined by minimizing the ground state energy. For even-even nuclei  $G_3 = 0$  and  $Q^2 = 0$  for the ground state. Only  $H_{\text{part}}$  contributes to the ground state energy in this case. A theoretical value of  $\xi$  in agreement with experiment should only be expected from a detailed discussion of sufficiently realistic wave functions  $\Psi^0$ . The case of independent nucleons

in oscillator potential without spin dependent forces <sup>(19)</sup>, has the advantage that all calculations can be carried out easily without further approximations. This case provides a convenient illustration of the qualitative aspects of our model.

Let the potential  $V$  be

$$(34) \quad V = \frac{m}{2} \omega_0^2 [\gamma^2 (y_1^2 + y_2^2) + \gamma^{-4} y_3^2].$$

For 112 neutrons the equilibrium value of  $\gamma$  is  $\gamma = 1.13$ ,  $q_3/q_2 = \gamma^6 = 2.10$ . The deformation parameter  $A \equiv (q_3 - q_2)/\frac{2}{3}(q_1 + q_2 + q_3) = 0.4$ .  $\xi = 0.26$  minimizes the ground state energy. The admixture of excited oscillator levels due the last term in (25) is negligible.

The resultant moment of inertia is about 0.7 times the value for a rigid nucleus and about one and one half times typical observed values <sup>(20)</sup>. One can easily verify by direct computation that  $H'$  is indeed a very small perturbation.

A sizable reduction of the moment of inertia would be achieved if  $m$  were the effective nucleon mass which has been introduced elsewhere <sup>(16,17)</sup>. If one wants to adopt such a model the dependence of the effective mass on the deformation would have to be investigated.

We have constructed a model for rotating spheroidal nuclei based on the idea that the number and the kind of independent variables in the wave functions can be chosen by empirical considerations provided we are interested only in an approximate description of a limited number of states. Consistence and symmetry requirements have led to a well defined model which yields definite predictions. The qualitative features of the model are satisfactory and encouraging. Whether the model is quantitatively successful remains to be determined by a detailed investigation of the intrinsic wave functions  $\Psi^0$  and their effect on the moments of inertia. We have restricted our discussion to collective rotations because both the theoretical problem and the empirical information are most clear cut in this case. It is hoped, however, that the ideas developed here may also prove useful for the description of other collective modes.

<sup>(19)</sup> This case has been considered by INGLIS (ref. <sup>(13)</sup>) and *Phys. Rev.*, **103**, 1786 (1956)) and BOHR and MOTTELSON (ref. <sup>(2)</sup>). See also ref. <sup>(15)</sup>.

<sup>(20)</sup> A previous statement (*Bull. Amer. Phys. Soc.*, **1**, 194, MA 3 (1956)) that our model agrees with the Inglis model was based on a numerical error in the computation of  $\xi$ . The Inglis model, which gives the rigid moment of inertia in this case, is plausible in the limit of extremely heavy nuclei. It has not been demonstrated that actual nuclei are heavy enough for this model to be applicable.

\* \* \*

I wish to thank the Institute for Nuclear Studies at the University of Chicago and Argonne National Laboratory for their kind hospitality during the summer 1955 when part of this work was performed.

---

## RIASSUNTO (\*)

Si propone un nuovo metodo per introdurre coordinate collettive come variabili dinamiche. Con questo metodo si costruisce un'hamiltoniana per nuclei sferoidali rotanti. Si discutono i momenti d'inerzia risultanti. Questi dipendono da un parametro  $\xi$  determinato qualora sia nota la funzione d'onda delle particelle intrinseche del nucleo. Trattando  $\xi$  come un parametro empirico si possono adattare i momenti d'inerzia osservati. Per illustrare la determinazione teorica di  $\xi$  si sono eseguiti calcoli per particelle indipendenti nella buca di un oscillatore armonico senza accoppiamento spin-orbita.

---

(\*) *Traduzione a cura della Redazione.*

## Causality and Dispersion Relations for the Scattering of Mesons by Fixed Nucleons (\*).

R. OEHME (+)

*Enrico Fermi Institute for Nuclear Studies  
University of Chicago - Chicago, Illinois*

(ricevuto il 20 Agosto 1956)

**Summary.** — The derivation of dispersion relations for meson-nucleon scattering is reexamined. So far, all proofs given require the assumption that the Fourier representation of the scattering amplitude exists in the unphysical energy region. In this note it is shown that in the limit of fixed nucleons the causality condition and the properties of the spectrum are already sufficient to derive dispersion formulae for the forward scattering amplitudes. With the same assumptions one can also derive dispersion relations for the derivative amplitudes. The complete relativistic case is discussed briefly in the appendix.

### 1. — Introduction.

Dispersion relations for the forward scattering amplitude of photons by Fermions or Bosons can be derived from the covariant field theory using only general principles which are inherent to this theory (<sup>1</sup>). The essential assumption in this derivation is the principle of microscopic causality. In a similar way it is possible to obtain physical dispersion formulae for the derivatives of finite order of the photon scattering amplitude with respect to the momentum transfer  $\Delta$ , taken at  $\Delta = 0$ . However, if one tries to derive corresponding relations for the scattering of relativistic particles with finite rest

(\*) Supported by a grant from the U.S. Atomic Energy Commission.

(+) Present Address: Institute for Advanced Study, Princeton, New Jersey.

(<sup>1</sup>) M. GELL-MANN, M. L. GOLDBERGER and W. THIRRING: *Phys. Rev.*, **95**, 1612 (1954); M. L. GOLDBERGER: *Phys. Rev.*, **97**, 508 (1955).



mass  $(^{2-6})$ , the causality condition alone does not seem to be sufficient. Some additional assumptions about the interaction are necessary, which, at a glance, seem to be even more restrictive if one tries to justify dispersion formulae for amplitudes with fixed, finite momentum transfer  $(^7)$ . To illustrate the problem, let us consider the non-spin-flip amplitude for the scattering of neutral mesons by nucleons. This Feynman amplitude may be represented in the Breit System by the Fourier integral  $(^8)$

$$M(K_0, A^2) = i \int d^4x \exp[-i\mathbf{K} \cdot \mathbf{x}] \eta(x_0) \cdot \left\langle \frac{\Delta}{2}, \left( M^2 + \frac{A^2}{4} \right)^{\frac{1}{2}} \left| \left[ j\left(\frac{x}{2}\right), j\left(-\frac{x}{2}\right) \right] - \frac{\Delta}{2}, \left( M^2 + \frac{A^2}{4} \right)^{\frac{1}{2}} \right\rangle ,\right.$$

where  $K_0 \geq (\mu^2 + A^2/4)^{\frac{1}{2}}$  is the energy of the incident meson,  $|\mathbf{K}| = (K_0^2 - \mu^2 - A^2/4)^{\frac{1}{2}}$  and  $\mathbf{K} \cdot \Delta = 0$ . If we invoke the causality condition, this is an improper integral over the region inside and on the future light cone, and for  $K_0$  in the physical range we can safely assume that the integral exists as an Abel limit. Singularities of the matrix element on the light cone affect only the high frequency behavior of the amplitude. But in order to derive dispersion relations using the Titchmarsh theorems only, we need a representation of the function  $M(K_0, A^2)$  for all real values of  $K_0$ . More specifically we have to show that, with a suitable definition of the amplitude for  $K_0 < (\mu^2 + A^2/4)^{\frac{1}{2}}$ , the function  $M(K_0, A^2)$  (or possibly  $M(K_0, A^2)/(K_0 - a_1)(K_0 - a_2)$  with  $\text{Im } a_i < 0$ ) is the limit  $\text{Im } K_0 \rightarrow 0_+$  of a complex function which is regular and sufficiently bounded in the entire upper half  $K_0$  plane. In order to obtain physical dispersion relations, we must be able in addition to express the amplitude in the unphysical region  $K_0 < (\mu^2 + A^2/4)^{\frac{1}{2}}$  by physical quantities.

(2) M. L. GOLDBERGER: *Phys. Rev.*, **99**, 979 (1955).

(3) M. L. GOLDBERGER, H. MIYAZAWA and R. OEHME: *Phys. Rev.*, **99**, 986 (1955).

(4) R. KARPLUS and M. A. RUDERMAN: *Phys. Rev.*, **98**, 771 (1955).

(5) R. OEHME: *Phys. Rev.*, **100**, 1503 (1955).

(6) R. OEHME: *Phys. Rev.*, **102**, 1174 (1956); (hereafter referred to as II).

(7) R. H. CAPPS and G. TAKEDA: *UCRL* - 3397; the author wishes to thank Dr. CAPPS and Dr. TAKEDA for sending him preprints of this paper; M. GELL-MANN and J. C. POLKINGHORNE: unpublished; M. L. GOLDBERGER, Y. NAMBU and R. OEHME: unpublished, see M. L. GOLDBERGER: *Proc. Rochester Conference*, 1956; A. SALAM: *Nuovo Cimento*, **111**, 424 (1956); A. SALAM and W. GILBERT: *Nuovo Cimento*, **3**, 607 (1956); K. SYMANZIK: unpublished.

(8) If the current operator contains the meson field explicitly, then there appear additional terms in Eq. (1) which contain equal time commutators. These terms do not alter the causal structure of the expression for  $M(K_0, A^2)$ . They are unimportant for the considerations in this note and will be neglected. Furthermore, we have omitted a factor depending only on  $A^2$ .

For the definition of  $M(K_0, \Delta^2)$  in the region  $K_0 \leq -(\mu^2 + \Delta^2/4)^{1/2}$  we may choose to use the representation given in Eq. (1) without difficulties. But in the range  $|K_0| < (\mu^2 + \Delta^2/4)^{1/2}$  the factor  $\exp[-iK \cdot x]$  in Eq. (1) contains the exponentially increasing part  $\exp[|\mathbf{x}|(\Delta^2/4 + \mu^2 - K_0^2)^{1/2}]$ . Here the damping factor  $\exp[-\varepsilon|\mathbf{x}|]$  (with  $\varepsilon > 0$  and the understanding that  $\varepsilon \rightarrow 0$  after the integration is performed), which is supplied by the asymptotic condition, is no more sufficient to guarantee the existence of the integral. Clearly this difficulty prevails also in the case of forward scattering for the region  $|K_0| < \mu$ . Consequently we need even in this case some other condition in addition to the causality principle in order to derive dispersion relations. A sufficient, but not necessary condition would be the assumption that the matrix element of the commutator in Eq. (1) has an asymptotic behavior in the future light cone which assures the existence of the integral for  $|K_0| < (\mu^2 + \Delta^2/4)^{1/2}$  at least for a given order of integration. However, this condition may be too restrictive and it would be desirable to have a proof of the dispersion formulae which uses, in addition to the causality principle, only general properties of the interacting system as, for instance, certain features of the energy-momentum spectrum of the meson nucleon system. It is the purpose of this note to give such a proof for the case of the forward scattering of pions by fixed nucleons. By use of the same methods, we can also derive dispersion relations for the corresponding derivative amplitudes. In the appendix we give a short discussion of the relativistic problem and show that for forward scattering it is only the existence of the single nucleon intermediate state which introduces the difficulties mentioned above.

## 2. - Derivation for Forward Scattering.

In the limit of fixed nucleons we can represent the non-spin-flip amplitude for meson nucleon scattering by the Fourier integral

$$(2) \quad M(\omega, \cos \vartheta) = \int d^3x \int d^3y \exp[-i\mathbf{q} \cdot \mathbf{x}] \exp[i\mathbf{k} \cdot \mathbf{y}] \cdot \\ \cdot i \int_{-\infty}^{\infty} dx_0 \exp[i\omega x_0] \eta(x_0)^{1/2} \text{Tr} \langle P | [j^\dagger(\mathbf{x}, x_0), j(\mathbf{y}, 0)] | P \rangle,$$

where we have used the same notation as in II<sup>(8)</sup>. We recall that for  $\omega \geq \mu$  the function  $M(\omega, \cos \vartheta)$  describes the scattering of  $\pi^\pm$ -mesons if we insert for  $j$  the corresponding currents  $j_\pm$ ; furthermore we have  $M_{\pi^0} = \frac{1}{2}(M_{\pi^+} + M_{\pi^-})$ . For our present purpose it will be convenient to write Eq. (2) for the limit of

forward scattering in the form

$$(3) \quad M_{\pm}(\omega) = \int d^3x \exp[-i\mathbf{q} \cdot \mathbf{x}] F_{\pm}(\omega, x^2),$$

with

$$(3a) \quad F_{\pm}(\omega, x^2) = i \int_{-\infty}^{+\infty} dx_0 \exp[i\omega x_0] \eta(x_0) K_{\pm}(x_0, x^2).$$

Here and in the following we write  $x$  for the magnitude of the vector  $\mathbf{x}$ . The space-time functions  $K_{\pm}$  are defined by

$$(3b) \quad K_{\pm} = \frac{1}{2} \{ K_{\pi^+} \pm K_{\pi^-} \},$$

where

$$(3c) \quad K_{\pi^{\pm}}(x_0, x^2) = \lim_{A \rightarrow 0} \int d^3y \exp[i\mathbf{A} \cdot \mathbf{y}] \cdot \frac{1}{2} \text{Tr} \left\langle P \left[ j_{\pm}^{\dagger} \left( \mathbf{y} + \frac{\mathbf{x}}{2}, \frac{x_0}{2} \right), j_{\pm} \left( \mathbf{y} - \frac{\mathbf{x}}{2}, -\frac{x_0}{2} \right) \right] \right| P \right\rangle.$$

We will always perform the  $x_0$  integral before the  $x$  integration.

Let us first explore the properties of the functions  $K_{\pm}(x_0, x^2)$ . The requirement of invariance with respect to space inversion leads to the symmetry relations

$$(4) \quad K_{\pm}^{*}(x_0, x^2) = K_{\pm}(-x_0, x^2) = \mp K_{\pm}(x_0, x^2).$$

The causality condition demands that the commutator of the current operators vanishes for space-like regions. This implies that

$$(5) \quad K_{\pm}(x_0, x^2) \equiv 0 \quad \text{for } x_0^2 < x^2.$$

In order to exhibit the  $x_0$  dependence of  $K_{\pm}$ , we decompose the matrix elements in Eq. (3c) with respect to a complete set of intermediate states  $|n\rangle$  of the pion nucleon system. The operator  $P_0$  describing the total energy of this system will be normalized such that for single nucleon states

$$(6) \quad P_0 |P\rangle = P_0 |N\rangle = 0.$$

Then we have

$$K_{\pm}(x_0, x^2) = \int_{0-\infty}^{\infty} d\lambda \mathfrak{K}_{\pm}(\lambda, x^2) \frac{1}{2} \{ \exp[-i\lambda x_0] \mp \exp[+i\lambda x_0] \},$$

where

$$\begin{aligned} \langle 7a) \quad \mathfrak{R}_{\pm}(\lambda, x^2) = & \frac{1}{2} \text{Tr} \int d^3y \sum_{|n\rangle}^{\lambda=E_n} \left\{ \left\langle P \left| j_{\mp}^{\dagger} \left( \mathbf{y} + \frac{\mathbf{x}}{2}, 0 \right) \right| n \right\rangle \left\langle n \left| j_{\mp} \left( \mathbf{y} - \frac{\mathbf{x}}{2}, 0 \right) \right| P \right\rangle \right. \\ & \left. \pm \left\langle P \left| j_{\mp}^{\dagger} \left( \mathbf{y} - \frac{\mathbf{x}}{2}, 0 \right) \right| n \right\rangle \left\langle n \left| j_{\mp} \left( \mathbf{y} + \frac{\mathbf{x}}{2}, 0 \right) \right| P \right\rangle \right\}. \end{aligned}$$

Here  $E_n$  denotes the energy eigenvalue of the state  $|n\rangle$ . We notice that with the normalization (6) of the nucleon energy we have  $E_n = 0$  for the single nucleon states and  $E_n \gg \mu$  for all other intermediate states. Thus the real weight functions  $\mathfrak{R}_{\pm}$  must be of the form

$$(8) \quad \mathfrak{R}_{\pm}(\lambda, x^2) = \delta(\lambda) \mathfrak{B}_{\pm}(x^2) + \mathfrak{G}_{\pm}(\lambda, x^2),$$

where  $\mathfrak{G}_{\pm}(\lambda, x^2) \equiv 0$  for  $\lambda < \mu$ .

Consider now the function  $F_{\pm}(\omega, x^2)$ , which is defined in Eq. (3a), for fixed values of the parameter  $x$  in the region  $0 \leq x < \infty$ . Because of the causality condition (Eq. (5)) and the factor  $\eta(x_0)$  it is the Fourier transform of a function which vanishes for  $x_0 < x$ . Furthermore, if we define  $s(\omega, x^2)$  by

$$(9) \quad s(\omega, x^2) \equiv 4\pi x \frac{\sin x(\omega^2 - \mu^2)^{\frac{1}{2}}}{(\omega^2 - \mu^2)^{\frac{1}{2}}},$$

we find easily that the product

$$(10) \quad m_{\pm}(\omega, x^2) = s(\omega, x^2) F_{\pm}(\omega, x^2)$$

is the Fourier transform of a function which vanishes for all negative values of its argument. Let us suppose for the moment that  $m_{\pm}(\omega, x^2)$  is  $L^2(-\infty, +\infty)$  with respect to  $\omega$ <sup>(9)</sup>. Then the property mentioned above is necessary and sufficient that  $m_{\pm}(\omega, x^2)$  should be the limit as  $\nu \rightarrow 0_+$  of a function  $m_{\pm}(\omega + i\nu, x^2)$  which is analytic for  $\nu > 0$  and for which the integral

$$\int_{-\infty}^{+\infty} d\omega |m_{\pm}(\omega + i\nu, x^2)|^2,$$

is bounded if  $\nu > 0$ <sup>(10)</sup>. But if these conditions are fulfilled, it follows that the real part  $d_{\pm}(\omega, x^2)$  and the imaginary part  $a_{\pm}(\omega, x^2)$  of  $m_{\pm}(\omega, x^2)$  are Hilbert transforms of each other.

<sup>(9)</sup> We consider here the positive constant  $\varepsilon$  as small but finite.

<sup>(10)</sup> E. C. TITCHMARCH: *Fourier Integrals* (Oxford, 1937), p. 119.

From Eq. (4) and the definitions (3a), (9), and (10), we find the symmetry properties

$$(11) \quad \begin{cases} d_+(\omega, x^2) = d_-(\omega, x^2), \\ a_+(\omega, x^2) = -a_-(\omega, x^2). \end{cases}$$

Furthermore, we have for the imaginary part of  $F_{\pm}$ :

$$(12) \quad F_{a\pm}(\omega, x^2) = \frac{1}{2} \int_{-\infty}^{\infty} dx_0 \exp[i\omega x_0] K_{\pm}(x_0, x^2),$$

and by use of Eq. (7) this gives

$$(13) \quad F_{a\pm}(\omega, x^2) = \frac{1}{2} \int_0^{\omega} d\lambda \mathfrak{F}_{\pm}(\lambda, x^2) \pi \{ \delta(\lambda - \omega) \mp \delta(\lambda + \omega) \}.$$

Hence, recalling the properties of the spectrum which we expressed in Eq. (8), we find that

$$(14) \quad \begin{cases} F_{a+}(\omega, x^2) = 0 & \text{for } |\omega| < \mu \\ \text{and} \\ F_{a-}(\omega, x^2) = \pi \delta(\omega) \mathfrak{B}_-(x^2) & \text{for } |\omega| < \mu. \end{cases}$$

Evidently the functions  $a_{\pm}(\omega, x^2)$  have corresponding properties for  $|\omega| < \mu$ .

Because  $d_{\pm}$  and  $a_{\pm}$  are Hilbert transforms, we find the relations

$$(15a) \quad d_+(\omega, x^2) = \frac{2}{\pi} P \int_{\mu}^{\omega} d\omega' \frac{\omega' a_{\pm}(\omega', x^2)}{\omega'^2 - \omega^2},$$

$$(15b) \quad d_-(\omega, x^2) = \frac{2\omega}{\pi} P \int_{\mu}^{\omega} d\omega' \frac{a_-(\omega', x^2)}{\omega'^2 - \omega^2} - \frac{2s(0, x^2)}{\omega} \mathfrak{B}_-(x^2),$$

where we have made use of Eqs. (11) and (14). In order to derive Eqs. (15), we have assumed that  $m_{\pm}(\omega, x^2)$  is  $L^2(-\infty, +\infty)$ . We must expect, however, that  $K_{\pm}(x_0, x^2)$  has singularities on the light cone which are of the form  $\delta(x_0^2 - x^2)$  or even derivatives thereof. Under these conditions  $m_{\pm}(\omega, x^2)$  is no more a function of integrable square and we must supply some powers of  $\omega$  in the denominator. Very probably it is safe to assume that the function



$m_{\pm}(\omega, x^2)/[(\omega + i\alpha)^2 - \mu^2]$  with  $\alpha > 0$  is  $L^2(-\infty, +\infty)$  <sup>(9)</sup>. Then we obtain, by the same arguments which led to Eqs. (15), the more bounded relations

$$(16) \quad \begin{cases} d_{+}(\omega, x^2) - d_{+}(\mu, x^2) = \frac{2(\omega^2 - \mu^2)}{\pi} P \int_{\mu}^{\infty} d\omega' \frac{\omega' a_{+}(\omega', x^2)}{(\omega'^2 - \omega^2)(\omega'^2 - \mu^2)}, \\ d_{-}(\omega, x^2) - \frac{\omega}{\mu} d_{-}(\mu, x^2) = \frac{2\omega(\omega^2 - \mu^2)}{\pi} P \int_{\mu}^{\infty} d\omega' \frac{a_{-}(\omega', x^2)}{(\omega'^2 - \omega^2)(\omega'^2 - \mu^2)} + \\ \quad + \frac{\omega^2 - \mu^2}{\omega\mu^2} 2s(0, x^2) \mathfrak{B}_{-}(x^2), \end{cases}$$

where we have performed the limit  $\alpha \rightarrow 0$ . For reasons of simplicity, we will continue to assume that  $m_{\pm}(\omega, x^2)$  is a function of integrable square, or that it is at least sufficiently bounded to guarantee the validity of Eqs. (15). This may even be physically reasonable for the difference  $m_{-}(\omega, x^2)$ . But in any case, the following considerations can be easily generalized.

So far we have considered  $m_{\pm}(\omega, x^2)$  for  $0 \leq x < \infty$ . We recall now that for  $\omega \geq \mu$  the integral

$$(17) \quad \int_0^{\infty} dx m_{\pm}(\omega, x^2) = M_{\pm}(\omega)$$

represents the sum or difference of the physical amplitudes  $M_{\pi^{+}}$  and  $M_{\pi^{-}}$ . Because of the symmetry properties given in Eq. (11), the same is true for  $\omega < -\mu$ . By virtue of the factor  $\exp[-\varepsilon x]$ , which is supplied by the asymptotic condition, we can assume that in the physical region the integral (17) converges uniformly to a bounded function  $M_{\pm}(\omega)$ . This assumption does not impose unreasonable restrictions on the behavior of the matrix element  $K_{\pm}(x_0, x^2)$ . For the same reason we will imply that the integral

$$(18) \quad \int_0^{\infty} dx \frac{\partial m_{\pm}(\omega, x^2)}{\partial \omega}$$

converges uniformly for  $|\omega| \geq \mu$ , and that the integral

$$\int_{-\infty}^{+\infty} d\omega' \frac{\partial m_{\pm}(\omega', x^2)}{\partial \omega'} \log \left| 1 - \frac{\omega'}{\omega} \right|$$

represents a bounded function in this energy region. This condition will enable us to perform the  $x$  integration in Eqs. (15) inside the principal value integrals.

With these precautions we may integrate both sides of Eq. (15a) over  $x$  for  $|\omega| \geq \mu$ . We find

$$(19) \quad D_+(\omega) = \frac{2}{\pi} P \int_{\mu}^{\infty} d\omega' \frac{\omega' A_+(\omega')}{\omega'^2 - \omega^2},$$

which is already the desired dispersion relation for the physical amplitude  $M_-(\omega)$ . For  $|\omega| < \mu$  the Eq. (15a) expresses  $d_+(\omega, x^2)$  by an absolutely convergent integral over  $\omega'$  which involves  $a_+(\omega', x^2)$  only in the physical range  $\omega' \geq \mu$ . Therefore, also in the questionable region  $|\omega| < \mu$ , the integral

$$\int_0^{\infty} dx \bar{d}_+(\omega, x^2) = D_+(\omega),$$

must converge uniformly to a bounded function  $D_+(\omega)$ .

Consider now Eq. (15b) for  $|\omega| \geq \mu$ . We can perform the  $x$  integration over  $d_-(\omega, x^2)$  and, because of  $\omega' \geq \mu$ , also over  $a_-(\omega', x^2)$  inside the principal value integral. Due to the uniform convergence we have assumed, the resulting functions of  $\omega$  are bounded in the region considered. We conclude that also the integral

$$(20) \quad \int_0^{\infty} dx s(0, x^2) \mathfrak{B}_-(x^2) = \Gamma,$$

must be finite, which implies that for large  $x$  the exponential factor  $\exp[\mu x]$  in  $s(0, x^2)$  will be cancelled by a corresponding damping factor in  $\mathfrak{B}_-(x^2)$  (see Eq. (8)). Thus we have for  $|\omega| \geq \mu$  the dispersion relation

$$(21) \quad D_-(\omega) = \frac{2\omega}{\pi} P \int_{\mu}^{\infty} d\omega' \frac{A_-(\omega')}{\omega'^2 - \omega^2} - \frac{2\Gamma}{\omega}.$$

Having established the convergence of the integral (20) to a finite constant, we may use Eq. (15b) for  $|\omega| < \mu$  in order to show that in this region the improper  $x$  integration over  $d_-(\omega, x^2)$  converges uniformly to a function which has a simple pole at  $\omega = 0$  and which is bounded for all other values  $|\omega| < \mu$ .

If we now take all pieces together, then we find that for all real  $\omega$  the integral

$$(22) \quad \int_0^{\infty} dx m_{\pm}(\omega, x^2) = M_{\pm}(\omega)$$

converges uniformly to a bounded function  $M_{\pm}(\omega)$  <sup>(9)</sup>. Because all functions of the continuous sequence  $m_{\pm}(\omega, x^2)$  are analytic in the upper half  $\omega$ -plane, the integral (22) must also converge uniformly for  $\text{Im } \omega > 0$ . It represents there an analytic and bounded function. These properties are expressed by the dispersion relations (19) and (21).

### 3. - Discussion and Extension.

In the preceding section we have seen that for fixed nucleons it is possible to derive dispersion relations for the forward scattering amplitude without making very restrictive assumptions about the behavior of the matrix element of the commutator. Due to the properties of the spectrum, the dispersion formulae are essentially a consequence of the causality condition. Only for reasons of simplicity we have assumed that  $m_{\pm}(\omega, x^2)$  is square integrable. We can go through the same arguments on the basis of Eqs. (16), which then lead to the familiar dispersion formulae <sup>(5)</sup>

$$(23) \quad \left\{ \begin{aligned} D_+(\omega) - D_+(\mu) &= \frac{2(\omega^2 - \mu^2)}{\pi} P \int_{\mu}^{\infty} d\omega' \frac{\omega' A_+(\omega')}{(\omega'^2 - \omega^2)(\omega'^2 - \mu^2)}, \\ D_-(\omega) - \frac{\omega}{\mu} D_-(\mu) &= \\ &= \frac{2\omega(\omega^2 - \mu^2)}{\pi} P \int_{\mu}^{\infty} d\omega' \frac{A_-(\omega')}{(\omega'^2 - \omega^2)(\omega'^2 - \mu^2)} + 2\Gamma \frac{\omega^2 - \mu^2}{\omega\mu^2}. \end{aligned} \right.$$

Note that so far we have made no assumption about the parity of the mesons. In Eq. (23) we can express the absorptive parts by the total cross-sections for positive and negative mesons:

$$\frac{4\pi}{q} A_{\pm}(\omega) = \frac{1}{2} \{ \sigma_{\pi^+(\omega)} \pm \sigma(\omega) \}.$$

Then Eqs. (23) are formally identical with the relativistic dispersion formulae given in Ref. <sup>(3)</sup>, Eq. (2.13), provided we keep in these relations only the terms of zero order in  $\mu/2M$  in the contributions from the single nucleon state; furthermore we must identify  $\Gamma$  with  $f^2$ . We will come back to the relativistic problem in the appendix of this note.

In a preceding paper <sup>(6)</sup> we have given dispersion relations for the derivatives of the non-spin-flip amplitude  $M_{\pm}(\omega, \cos \theta)$  with respect to  $\cos \theta$  (or the momentum transfer  $t$ ), evaluated at  $\theta = 0$ . These formulae have been derived in the limit of fixed nucleons and under the assumption that the

Fourier representation of the derivative amplitudes exists for all real  $\omega$ . But by use of the same methods which we have employed in Sect. 2, one can show that also in these cases the causality condition and the properties of the spectrum are sufficient to derive the dispersion formulae given in Eqs. (24) or (25) of II. For the derivative of first order these relations appear in the form

$$(24) \quad \begin{cases} D_+^{(1)}(\omega) = \frac{2(\omega^2 - \mu^2)}{\pi} P \int_{\mu}^{\infty} d\omega' \frac{\omega' A_+^{(1)}(\omega')}{(\omega'^2 - \omega^2)(\omega'^2 - \mu^2)}, \\ D_-^{(1)}(\omega) = \frac{2\omega(\omega^2 - \mu^2)}{\pi} P \int_{\mu}^{\infty} d\omega' \frac{A_-^{(1)}(\omega')}{(\omega'^2 - \omega^2)(\omega'^2 - \mu^2)} + 2\Gamma^{(1)} \frac{\omega^2 - \mu^2}{\omega\mu^2}. \end{cases}$$

Here we have used the definitions  $M_{\pm}^{(1)} = D_{\pm}^{(1)} + iA_{\pm}^{(1)}$  and <sup>(11)</sup>

$$(25) \quad M_{\pm}^{(1)}(\omega) = \left\{ \frac{\partial M_{\pm}(\omega', \cos \vartheta)}{\partial \cos \vartheta} \right\}_{\vartheta=0}.$$

For pseudoscalar mesons one can show that the constants  $\Gamma$  and  $\Gamma^{(1)}$  must be positive and equal:  $\Gamma = \Gamma^{(1)} = f^2$ . This has been discussed in II.

It is interesting to compare the dispersion formulae obtained here with similar relations derived by CHEW and LOW <sup>(12)</sup>. These authors use the static model with extended source, where the condition of microscopic causality is certainly not valid. If  $G_{\pm}(\omega) = \frac{1}{2}\{G_{\pi^+}(\omega) \pm G_{\pi^-}(\omega)\}$  describes the forward scattering amplitude in this theory, one finds the relations

$$(26) \quad \begin{cases} v^{-2}(\omega) \operatorname{Re} G_+(\omega) = -\frac{2(\omega^2 - \mu^2)}{\pi} P \int_{\mu}^{\infty} d\omega' \frac{\omega' v^{-2}(\omega') \operatorname{Im} G_+(\omega')}{(\omega'^2 - \omega^2)(\omega'^2 - \mu^2)}, \\ v^{-2}(\omega) \operatorname{Re} G_-(\omega) = \frac{2\omega(\omega^2 - \mu^2)}{\pi} P \int_{\mu}^{\infty} d\omega' \frac{v^{-2}(\omega') \operatorname{Im} G_-(\omega')}{(\omega'^2 - \omega^2)(\omega'^2 - \mu^2)} + 2f^2 \frac{\omega^2 - \mu^2}{\omega\mu^2}. \end{cases}$$

Here  $v(\omega) = \varrho(q^2)$  is the Fourier transform of the extended source distribution of the nucleon, which acts as a cut-off factor in this theory;  $f$  is the renormalized, unrationalized coupling constant. Eqs. (26) are essentially a consequence of the simple energy dependence of the Fourier transform of the current operator, which is given by

$$j_{\pm}(\mathbf{q}) = f/\mu \tau_{\pm} \boldsymbol{\sigma} \cdot \mathbf{q} \varrho(q^2).$$

<sup>(11)</sup> Note that in II we have used derivatives with respect to  $1 - \cos \vartheta$ .

<sup>(12)</sup> G. F. CHEW and F. E. LOW: *Phys. Rev.*, **101**, 1570 (1956); G. C. WICK: *Rev. Mod. Phys.*, **27**, 339 (1955); F. E. LOW: *Phys. Rev.*, **97**, 1392 (1955).

We see that in the Chew-Low theory, instead of the amplitude itself, the product  $v^{-2}(\omega)G(\omega)$  is analytic in the upper half  $\omega$ -plane. This seems reasonable because the factor  $v^{-2}(\omega)$  in Eqs. (26) is cancelled by another factor  $v^2(\omega)$  which is contained in  $G(\omega)$  (see e.g. Eqs. (26) and (4) in Ref. (12)). However, the amplitude  $G(\omega)$  depends in addition also implicitly on the source distribution.

Concluding this section we might mention that the methods of this note are also applicable to the spin-flip amplitude (5). We can derive the dispersion relations for the «forward» spin-flip amplitudes  $S_{\pi\pi}(\omega)$  (see Ref. (5), Eqs. (32) or (38)) in the limit  $M \rightarrow \infty$  without restrictive assumptions about the asymptotic behavior of the matrix element of the commutator.

\* \* \*

The author would like to thank Professor M. L. GOLDBERGER, Professor Y. NAMBU, and Dr. K. SYMANZIK for helpful discussions.

## APPENDIX

Here we will give a short discussion of the difficulties in the relativistic case. We consider the forward scattering amplitude for neutral mesons in the rest system of the nucleon. This function is given by Eq. (1) for  $\Delta = 0$ . We write it in a form corresponding to Eqs. (2) and (3), where now the expectation value  $K(x_0, x^2)$  is defined by

$$(A.1) \quad K(x_0, x^2) = \frac{1}{2} \text{Tr} \left\langle 0, M \left| \left[ j\left(\frac{\mathbf{x}}{2}, \frac{x_0}{2}\right), j\left(-\frac{\mathbf{x}}{2}, -\frac{x_0}{2}\right) \right] \right| 0, M \right\rangle.$$

Proceeding as in Sect. 2, we assume that  $m(\omega, x^2) = s(\omega, x^2)F(\omega, x^2)$  is square integrable (9). Then the causality condition implies that this function is analytic and bounded in the upper half plane for  $0 \leq x < \infty$ . Furthermore, the real and the imaginary parts of  $m(\omega, x^2)$  are Hilbert transforms of each other; i.e. we have

$$(A.2) \quad d(\omega, x^2) = \frac{2}{\pi} P \int_0^\infty d\omega' \frac{\omega' a(\omega', x^2)}{\omega'^2 - \omega^2},$$

and the conjugate relation. For the same reasons as in the case of fixed nucleons we take it for granted that in the region  $|\omega| > \mu$  the function  $m(\omega, x^2)$  is sufficiently bounded for  $x > \infty$  to secure the uniform convergence of the improper  $x$  integrals over  $m(\omega, x^2)$  and  $\partial m(\omega, x^2)/\partial \omega$ . Then we obtain from



Eq. (A.2) for  $|\omega| \geq \mu$ :

$$(A.3) \quad D(\omega) - \frac{2}{\pi} P \int_{\mu}^{\infty} d\omega' \frac{\omega' A(\omega')}{\omega'^2 - \omega^2} = \int_0^{\infty} dx \frac{2}{\pi} \int_0^{\mu} d\omega' \frac{\omega' a(\omega', x^2)}{\omega'^2 - \omega^2}.$$

By virtue of the uniform convergence we have implied, the two terms on the left hand side of Eq. (A.3) are bounded functions of  $\omega$  in the region  $|\omega| \geq \mu$ . Therefore also the double integral must represent a bounded function in this range, provided the integrals are performed in the order indicated <sup>(13)</sup>. This double integral vanishes in the limit of fixed nucleons [ $M \rightarrow \infty$ ], as can be seen by comparison of Eq. (A.3) with Eq. (19) of Sect. 2. We cannot simply interchange the order of integration at the right hand side of Eq. (A.3), because a priori this interchange would imply more restrictive assumptions about the behavior of  $F_a(\omega, x^2)$  for  $|\omega| < \mu$  and  $x \rightarrow \infty$ .

Let us now decompose the matrix element  $K$  with respect to a complete set of intermediate states. Then we find for the imaginary part of  $F$  a representation of the form

$$(A.4) \quad F_a(\omega, x^2) = \frac{1}{4\pi} \int_M^{\infty} d\mathcal{M} \int_{\mathcal{M}}^{\infty} dE \Re(\mathcal{M}^2, E) \frac{\sin[x(E^2 - \mathcal{M}^2)^{\frac{1}{2}}]}{x} \cdot \{\delta(\omega - E + M) - \delta(\omega + E - M)\},$$

where  $\Re(\mathcal{M}^2, E)$  is a real weight function, which is non-zero only for  $\mathcal{M} = M$ ,  $E \geq M$  and  $\mathcal{M} \geq M + \mu$ ,  $E \geq M + \mu$ . From Eq. (A.4) we learn that for  $|\omega| < \mu$  only single nucleon states with  $\mathcal{M} = M$ ,  $M \leq E < M + \mu$  contribute to  $a(\omega, x^2) = s(\omega, x^2) F_a(\omega, x^2)$ . In contrast to the fixed nucleon case, we obtain a continuous function for  $|\omega| < \mu$ .

The intermediate states with  $\mathcal{M} = M$ ,  $E \geq M + \mu$  contribute to  $a(\omega, x^2)$  in the region  $|\omega| \geq \mu$ . But, if we perform the  $x$ -integration using Eq. (A.4), these contributions drop out because of momentum conservation. We see that the double integral in Eq. (A.4) describes just that part of  $D(\omega)$  which comes from the single nucleon intermediate state. We have already proven that it must be a bounded function for  $|\omega| \geq \mu$ . It remains to be shown rigorously that this function reduces to the familiar single nucleon term

$$-2f^2 \frac{\mu^2}{2M} \frac{1}{\omega^2 - (\mu^2/2M)^2}.$$

Such a proof is certainly possible on the basis of the causality condition and the properties of the spectrum. If we imagine a system where  $\Re(\mathcal{M}^2, E)$

<sup>(13)</sup> We may also write

$$\lim_{\xi \rightarrow \infty} \frac{2}{\pi} \int_0^{\mu} d\omega' \frac{\omega'}{\omega'^2 - \omega^2} \int_0^{\xi} dx a(\omega', x^2).$$

is zero for  $M < M - \mu$ , then Eq. (A.3) reduces to the relativistic dispersion relation for the corresponding physical amplitude <sup>(14)</sup>.

Finally, we would like to mention that a relation similar to Eq. (A.3) can be obtained if the  $x$ -integration is performed before the  $x_0$ -integration. We find the formula

$$(A.5) \quad D(\omega) = \frac{2}{\pi} P \int_{\mu}^{\infty} d\omega' \frac{\omega' A(\omega')}{\omega'^2 - \omega^2} + \int_0^{\infty} dx_0 \frac{2}{\pi} \int_0^{\mu} d\omega' \frac{\omega' g(\omega', x_0)}{\omega'^2 - \omega^2},$$

where

$$g(\omega, x_0) = \eta(x_0) \exp \left[ i\omega x_0 \right] \int_0^{x_0} dx s(\omega, x^2) K(x_0, x^2).$$

Also in this case we cannot simply interchange the order of integration in the last term of Eq. (A.5).

### Note added in proof.

Meanwhile it has been shown rigorously that the right hand side of Eq. (A.3) reduces to the familiar single nucleon term (N. N. BOGOLIUBOV, R. JOST, H. LEHMANN and K. SYMANZIK: *Reports at the International Conference on Theoretical Physics*, Seattle, Sept. 17-22, 1956). The proof given by K. SYMANZIK (*Phys. Rev.*: to be published) makes use of the method developed in the present paper. The mathematical methods of N. N. BOGOLIUBOV make it possible to derive also the dispersion relations for amplitudes with fixed, finite momentum transfer.

<sup>(14)</sup> A proof for this case has been obtained independently by R. JOST and H. LEHMANN, who use a somewhat different approach; private communication from K. SYMANZIK.

### RIASSUNTO (\*)

Si riesamina la derivazione delle relazioni di dispersione per lo scattering mesone-nucleone. Finora, tutte le prove fornite richiedono l'ipotesi che la rappresentazione di Fourier dell'ampiezza di scattering esista nella regione non fisica. In questa nota si mostra come al limite dei nucleoni fissi la condizione di causalità e le proprietà dello spettro sono già sufficienti per derivare delle formule di dispersione per le ampiezze di scattering in avanti. Con la stessa ipotesi si possono anche ottenere relazioni di dispersione per le ampiezze di derivazione. Il caso relativistico completo si discute brevemente in appendice.

(\*) Traduzione a cura della Redazione.

## Binding Energies of the Light Hyperfragments.

J. T. JONES, jr. (\*) and J. M. KELLER

*Institute for Atomic Research and Department of Physics (+)  
Iowa State College - Ames Iowa*

(ricevuto il 29 Agosto 1956)

**Summary.** — The purpose of the present paper is to determine the constants of a phenomenological potential assumed for the  $\Lambda^0$ -nucleon interaction by fitting them to the observed binding energies of the mass 3 and 4 hyperfragments. Variational calculations have been carried out for these hyperfragments and hyperhelium-5. The calculations indicate that the  $\Lambda^0$ -nucleon force is strongly spin dependent, and also that the hypertrineutron and hyperhelium-3 are not bound. The chief assumptions that have made are: (a) the spin of the  $\Lambda^0$  is  $\frac{1}{2}$ ; (b) the hyperdeuteron is not bound; (c) the  $\Lambda^0$ -nucleon interaction arising from the virtual exchange of heavy mesons may be represented by the assumed phenomenological potential (any possible pion admixture resulting from the virtual exchange of at least two pions between the  $\Lambda^0$  and nucleon being neglected); (d) all but the principal  $S$ -states of the hyperfragments with mass numbers less than or equal to five may be neglected; (e) the nucleon-nucleon interaction is represented by the central Yukawa interaction. The last three assumptions are rather severe and imply that the present calculations are to be considered as preliminary to a more complete investigation, in which the tensor interaction between nucleons and also the pion admixture of the  $\Lambda^0$ -nucleon force are included.

### 1. — Introduction.

In the present paper, we consider only  $\Lambda^0$ -hyperfragments, i.e., bound systems, consisting of a  $\Lambda^0$  together with a number of nucleons, that are stable for times of the order of lifetime of the free  $\Lambda^0$ . There is tentative evidence <sup>(1,2)</sup>

(\*) Present address: Department of Physics, North Texas State College, Denton, Texas.

(+) Work performed in the Ames Laboratory of the U. S. Atomic Energy Commission.

(1) W. F. FRY, J. SCHNEPS and M. S. SWAMI: *Phys. Rev.*, **99**, 1561 (1956).

(2) C. CASTAGNOLI, G. CORTINI and C. FRANZINETTI: *Nuovo Cimento*, **2**, 550 (1959).

that « strange » particles other than the  $\Lambda^0$  may also form bound systems with nucleons; however, such systems will not be discussed here.

Theoretical considerations concerning the  $\Lambda^0$ -nucleon force have been given by many authors<sup>(3-13)</sup>. In most of the semi-quantitative descriptions presented so far, the  $\Lambda^0$ -nucleon interaction is assumed to arise predominantly from the virtual exchange of heavy mesons. There is, *a priori*, no reason why this mode of interaction should be the dominant one among some of the other<sup>(10)</sup> possible interactions. However, in this preliminary investigation, any possible pion admixture resulting from the virtual exchange of at least two pions between a nucleon and the  $\Lambda^0$  is neglected.

Although the spin of the  $\Lambda^0$  has not yet been definitely determined<sup>(\*)</sup>, we assume that it is  $\frac{1}{2}$ . Furthermore, on the basis of present indications<sup>(14)</sup>, we believe that the hyperdeuteron ( $\Lambda^0 + p$ ) has no bound states<sup>(+)</sup>.

The phenomenological interaction potential for two nucleons in light hyperfragments is assumed to be the same as that for two nucleons in light nuclei. For simplicity, all interactions other than the central interaction are neglected.

<sup>(3)</sup> S. IWAO: *Prog. Theor. Phys.*, **13**, 111 (1955).

<sup>(4)</sup> K. NISHIJIMA: *Prog. Theor. Phys.*, **13**, 285 (1955); **14**, 527 (1955).

<sup>(5)</sup> F. DUIMIO: *Nuovo Cimento*, **1**, 688 (1955); F. DIANA and F. DUIMIO: *Nuovo Cimento*, **2**, 370 (1955).

<sup>(6)</sup> R. H. DALITZ: *Phys. Rev.*, **99**, 1475 (1955).

<sup>(7)</sup> R. H. DALITZ: *Nucl. Phys.*, **1**, 372 (1956), as quoted from a lecture given at the opening of the Tait Institute.

<sup>(8)</sup> J. T. JONES JR. and J. K. KNIPP: *Nuovo Cimento*, **2**, 857 (1955).

<sup>(9)</sup> R. GATTO: *Nuovo Cimento*, **2**, 373 (1955).

<sup>(10)</sup> R. GATTO: *Nuovo Cimento*, **3**, 499 (1956).

<sup>(11)</sup> G. WENTZEL: *Phys. Rev.*, **101**, 835 (1956).

<sup>(12)</sup> J. M. BLATT and S. T. BUTLER: *Nuovo Cimento*, **3**, 409 (1956).

<sup>(13)</sup> T. TATI and H. TATI: *Nuovo Cimento*, **3**, 1136 (1956).

<sup>(\*)</sup> As recent work on the spin of the  $\Lambda^0$  see, e.g., references<sup>(15-17)</sup>.

<sup>(14)</sup> W. F. FRY, J. SCHNEPS and M. S. SWAMI: *Phys. Rev.*, **101**, 1526 (1956).

<sup>(15)</sup> M. RUDERMAN and R. KARPLUS: *Phys. Rev.*, **102**, 247 (1956).

<sup>(16)</sup> R. BUDDE, M. CHRETIEN, J. LEITNER, N. P. SAMIOS, M. SCHWARTZ and J. STEINBERGER: *Properties of Heavy Unstable Particles Produced by 1.3 BeV  $\pi^-$  Mesons* (Nevis Cyclotron Laboratory, Columbia Univ., preprint, May, 1956).

<sup>(17)</sup> H. PRIMAKOFF: *Nuovo Cimento*, **3**, 1394 (1956).

<sup>(+)</sup> The event discovered by G. ALEXANDER *et al.*<sup>(18)</sup> which could have been interpreted<sup>(9)</sup> as a hyperdeuteron, may possibly have been the disintegration in flight of a hypertriton, similar to that reported by SKJEGGESTAD and SØRENSEN<sup>(19)</sup>. See also L. LEPRINCE-RINGUET *et al.*<sup>(20)</sup>.

<sup>(18)</sup> G. ALEXANDER, C. BALLARIO, R. BIZZARRI, B. BRUNELLI, A. DEMARCO, A. MICHELINI, G. MONETI, E. ZAVATTINI, A. ZICHICHI and J. ASTBURY: *Nuovo Cimento*, **2**, 365 (1955).

<sup>(19)</sup> O. SKJEGGESTAD and S. O. SØRENSEN: *Nuovo Cimento*, **3**, 652 (1956).

<sup>(20)</sup> L. LEPRINCE-RINGUET, J. CRUSSARD, V. FOUCHÉ, J. HENNESSEY, G. KAYAS, D. MORELLET and F. RENARD: *Compt. Rend. Acad. Sci. (Paris)*, **242**, 1554 (1956).

From comparable calculations on light nuclei, it is known that tensor forces are in fact important. Their neglect here implies that the present calculations are to be considered as preliminary to a more complete investigation, in which the nuclear tensor interaction and also the pion admixture of the  $\Lambda^0$ -nucleon force are included.

The interaction between nucleons is represented by the potential <sup>(21)</sup>

$$(1.1) \quad V_{km} = \boldsymbol{\tau}_k \cdot \boldsymbol{\tau}_m [(1/4)(1 - q) + (1/12)(1 + 3q)\boldsymbol{\sigma}_k \cdot \boldsymbol{\sigma}_m] J(r_{km}),$$

where  $r_{km}$  is the distance between nucleons  $k$  and  $m$ ;  $J(r_{km})$  is the absolute value of the effective triplet potential;  $\boldsymbol{\tau}$  and  $\boldsymbol{\sigma}$  are the i-spin and Pauli spin vectors, respectively;  $q$  is the ratio of the strength of the singlet interaction to that of the triplet interaction. We will assume that  $J(r_{km})$  is a Yukawa potential,

$$(1.2) \quad J(r_{km}) = V_0(\beta_c r_{km})^{-1} \exp[-\beta_c r_{km}], \quad (V_0 < 0)$$

where  $V_0$  is the strength of the triplet interaction and  $\beta_c$  is the inverse of the range of the central interaction. For this type of interaction, constants which fit the binding energy of the deuteron and low energy scattering data are (11)

$$(1.3) \quad \beta_c^{-1} = 1.17 \cdot 10^{-13} \text{ cm}, \quad V_0 = 67.3 \text{ MeV}, \quad q = 0.69.$$

The  $\Lambda^0$ -nucleon interaction is represented by the potential,

$$(1.4) \quad W_{0j} = \{b_0 + c_0 \boldsymbol{\sigma}_0 \cdot \boldsymbol{\sigma}_j + P_{0j}[(1 - b_0) + (a_0 - c_0)\boldsymbol{\sigma}_0 \cdot \boldsymbol{\sigma}_j]\} K(r_{0j}),$$

where  $P_{0j}$  is a space exchange operator which interchanges the positions of particles 0 and  $j$ ;  $r_{0j}$  is the distance between the  $\Lambda^0$  (particle 0) and  $j$ -th nucleon;  $a_0$ ,  $b_0$  and  $c_0$  are numerical constants. As will be pointed out in Sect. 3, the existence of a bound state for hyperhelium-5 requires that  $K(r_{0j})$  be attractive. The space part of the interaction is assumed to have a Yukawa radial dependence,

$$(1.5) \quad K(r_{0j}) = -K_0(\beta_0 r_{0j})^{-1} \exp[-\beta_0 r_{0j}], \quad (K_0 > 0)$$

where  $K_0$  is the strength and  $\beta_0$  is the inverse of the range of the  $\Lambda^0$ -nucleon interaction. Because the interaction is assumed to arise from the virtual exchange of heavy mesons,  $\beta_0$  should be approximately equal to the inverse of the heavy meson Compton wave length.

(<sup>21</sup>) L. ROSENFELD: *Nuclear Forces* (New York, 1949).



Since the virtual exchange of heavy mesons between a nucleon and the  $\Lambda$  reverses the nature of the two particles, the lowest order interaction of this type must lead to a space exchange force. This suggests that the first two terms of Eq. (1.4) are small in comparison with the other terms containing the operator  $P_{0j}$ . In the present calculations, we ignore the space exchange nature of the interaction by choosing spatially symmetric wave functions. For these functions,  $W_{0j}$  of Eq. (1.4) may be written as

$$(1.6) \quad W_{0j} = (1 + a_0 \boldsymbol{\sigma}_0 \cdot \boldsymbol{\sigma}_j) K(r_{0j}) .$$

The purpose of the present paper is to determine the constants  $a_0$  and  $K_0$ , for given values of  $\beta_0$ . Using the potential of Eq. (1.6), we obtain in Sect. 2 conditions which determine whether the hyperdeuteron is bound for various values of  $a_0$  and  $K_0$ . The variational calculations for the hypertriton, the four-particle hyperfragments ( ${}^4\text{H}_\Lambda$  and  ${}^4\text{He}_\Lambda$ ) (\*) and hyperhelium-5 are presented in Sect. 3. The conclusions implied by the calculations are discussed in Sect. 4.

## 2. - The Hyperdeuteron.

For this two-particle system, the variational calculation outlined by SACHS (22) for the deuteron may be applied here with only slight modifications. The amplitude,  $-(1 + a_0 \boldsymbol{\sigma}_0 \cdot \boldsymbol{\sigma}_j) K_0$ , of the Yukawa potential takes on the values  $-(1 - 3a_0)K_0$  if the  $\Lambda^0$  and proton spins are antiparallel, and  $-(1 + a_0)K_0$  if the spins are parallel for the ground state of  ${}^2\text{H}_\Lambda$ . From the results of Sachs' calculations, as contained in his Eqs. (3.35) and (3.36), one finds that the hyperdeuteron is bound if

$$(2.1) \quad kK_0 > 6.444 \cdot 10^{-25} \beta_0^2 \text{ MeV} \cdot \text{cm}^2 ,$$

where  $k$  is either  $(1 - 3a_0)$  or  $(1 + a_0)$ , and a mass of the  $\Lambda^0$  equal to 2181 electron masses (23) has been used. For two values of  $\beta_0$ , the conditions on the effective strength,  $kK_0$ , in order for the hyperdeuteron to be bound are

$$(2.2) \quad \begin{cases} kK_0 > 589.3 \text{ MeV} , & (\beta_0^{-1} = 3.31 \cdot 10^{-14} \text{ cm}) , \\ kK_0 > 423.7 \text{ MeV} , & (\beta_0^{-1} = 3.90 \cdot 10^{-14} \text{ cm}) . \end{cases}$$

(\*) The notation used is the same as that of reference (8).

(22) R. G. SACHS: *Nuclear Theory* (Baltimore, 1953), pp. 34-38.

(23) M. W. FRIEDLANDER, D. KEEFE, M. G. K. MENON and M. MERLIN: *Phil. Mag.*, **45**, 533 (1954).

The latter value of  $\lambda_0^{-1}$  is approximately the Compton wave length of a heavy meson with a mass equal to 966 electron masses.

### 3. - Hyperfragments of Masses 3, 4 and 5.

The space parts of the trial wave functions for the three, four and five particle hyperfragments were all assumed to be of the form

$$(3.1) \quad \psi = N \exp \left[ -\lambda \left( \sum r_{ij}^2 \right)^{\frac{1}{2}} \right],$$

where  $\lambda$  is a variational parameter, and the sum is over all pairs of particles. The normalization constant  $N$  is given by

$$(3.2) \quad N^{-2} = (1/\sqrt{\pi})(\pi/\lambda^2 A)^{3(A-1)/2} \Gamma((3A-2)/2),$$

for the case of a hyperfragment with mass number  $A$ . The wave function (3.1) is symmetric to interchange of the positions of any pair of particles. A better approximation would undoubtedly be obtained by allowing different parameters to describe the hyperon-nucleon and nucleon-nucleon ranges. But the extra complexity in evaluating matrix elements of the interaction potential of Eq. (1.4) does not seem justified in a preliminary calculation of the type reported here. Trial wave functions of the form of Eq. (3.1) have been used rather successfully in recent calculations of the properties of ordinary light nuclei (<sup>21-27</sup>). They permit all the matrix elements of interest to be expressed in terms of elementary integrals.

The expectation value for the kinetic energy corresponding to the wave function (3.1) can be shown to be equal to

$$(3.3) \quad \langle \text{K. E.} \rangle = \hbar^2 \lambda^2 [(A-1)M_0 + M]/2MM_0,$$

where  $M$  is the nucleon mass, and  $M_0$  is the mass of the  $\Lambda^0$ .

The total angular momentum of each hyperfragment is of course a constant; because of the assumed spin-coupling to the hyperon, the spin of the nucleons alone is not strictly constant. However, within the limitation of a nuclear space-symmetric wave function, a given value of i-spin determines a unique value of nuclear spin for the hyperfragments under consideration here. Ac-

(<sup>24</sup>) J. IRVING: *Phil. Mag.*, **42**, 338 (1951).

(<sup>25</sup>) J. IRVING: *Proc. Phys. Soc. (London)*, A **66**, 17 (1953).

(<sup>26</sup>) G. ABRAHAM, L. COHEN and A. S. ROBERTS: *Proc. Phys. Soc. (London)*, A **68**, 265 (1955).

(<sup>27</sup>) M. MORITA and T. TAMURA: *Prog. Theor. Phys.*, **12**, 653 (1954).

cordingly, the spin configuration for a hyperfragment state can be represented in a parenthesis notation as  $(S, S')$ , where  $S$  is the total spin of the hyperfragment and  $S'$  is the spin of the nucleons in it.

The interaction potential for the hyperfragments is assumed to be

$$(3.4) \quad U = \sum_{j=1}^{A-1} W_{0j} + \sum_{k>m=1}^{A-1} V_{km},$$

where  $W_{0j}$  and  $V_{km}$  are given by Eqs. (1.6) and (1.1), respectively. Expectation values for the interaction energy  $U$  are summarized for the several cases calculated:

$A$	Spin Configuration	$\langle U \rangle$
3	$(\frac{3}{2}, 1)$	$2(1 + a_0)\langle K \rangle_3 - \langle J \rangle_3$
	$(\frac{1}{2}, 1)$	$2(1 - 2a_0)\langle K \rangle_3 - \langle J \rangle_3$
	$(\frac{1}{2}, 0)$	$2\langle K \rangle_3 - q\langle J \rangle_3$
4	$(1, \frac{1}{2})$	$(3 + a_0)\langle K \rangle_4 - (\frac{3}{2})(1 + q)\langle J \rangle_4$
	$(0, \frac{1}{2})$	$3(1 - a_0)\langle K \rangle_4 - (\frac{3}{2})(1 + q)\langle J \rangle_4$
5	$(\frac{1}{2}, 0)$	$4\langle K \rangle_5 - 3(1 + q)\langle J \rangle_5.$

The symbols  $J_A$  and  $K_A$  stand for expectation values of  $J(r_{12})$  and  $K(r_{01})$ , respectively. The value of  $\langle J \rangle_A$  is

$$(3.5) \quad \langle J \rangle_A = V_0[3(A-2)/\sqrt{\pi}] [ \Gamma(3(A-1)/2) / \Gamma((3A-2)/2) ] C_A^{3(A-1)} I_A,$$

where

$$(3.6) \quad C_A = \lambda\sqrt{2A}/\beta_c,$$

$$(3.7) \quad I_A = \int_0^{\pi/2} (C_A + \sin \theta)^{4-2A} (\cos \theta)^{3A-7} \sin \theta \, d\theta;$$

$\langle K \rangle_A$  is obtained from  $\langle J \rangle_A$  upon replacing  $V_0$  and  $\beta_c$  by  $(-K_0)$  and  $\beta_0$ , respectively. Expressions for  $I_A$  in terms of elementary functions have been given by J. IRVING<sup>(24)</sup> for  $A=3$  and 4 (\*). Although  $I_5$  can be similarly expressed, it is more expedient to integrate it numerically for each value of  $C_5$ .

Note that  $\langle U \rangle$  for  $A=5$  does not depend upon the constant  $a_0$ . Up to this point,  $K(r_{01})$  has been assumed to be attractive (i.e.,  $K_0 > 0$ ). It is apparent that if  $K(r_{01})$  were repulsive hyperhelium-5 would not be bound.

(\*) For  $A=3$ , Irving states  $I_3$  only for  $C_3^2 > 1$ ; the results for  $I_3$  with  $C_3^2 \leq 1$  are listed in the Appendix.

For the helium hyperfragments, there is also an energy of Coulomb repulsion between the protons. The expectation value for Coulomb repulsion per pair of protons in a hyperfragment of mass  $A$  is

$$(3.8) \quad \langle E_{\text{Coul}} \rangle = (2A/\pi)^{1/2} \lambda e^2 F[(3A-3)/2] F[(3A-2)/2] .$$

#### 4. - Discussion.

Since the  $\Lambda^0$  is not restricted by the Pauli principle in nuclear matter, the ground state of the hypertriton can, *a priori*, have one of three possible spin orientations:  $(\frac{3}{2}, 1)$ ,  $(\frac{1}{2}, 1)$  and  $(\frac{1}{2}, 0)$ . The spin configuration  $(\frac{1}{2}, 0)$  is important for the case of  ${}^3\text{H}_\Lambda$  or  ${}^3\text{He}_\Lambda$ . But this configuration (which is a spin doublet in an i-spin triplet state) cannot be the ground state of  ${}^3\text{H}_\Lambda$  for the following reasons. Since the ground state of the deuteron is a spin triplet, so far as nucleon-nucleon forces are concerned a parallel alignment of nucleon spins gives a lower energy. Parallel spin alignment of nucleons must also be favored by the  $\Lambda$ -nucleon forces represented by the potential of Eq. (1.6). For whether the  $\Lambda$ -nucleon interaction tends to align the spin of one nucleon parallel or antiparallel to the  $\Lambda$ , it will tend to align the spin of another nucleon in the same way.

Observed total binding energies of the mass 3, 4, and 5 hyperfragments are listed in Table I.

TABLE I. - Total binding energies of light hyperfragments.

Hyperfragment	$B_\Lambda$ (a) (MeV)	$ E $ (b) (MeV)
${}^3\text{H}_\Lambda$	$0.5 \pm 0.3$ (c)	$2.73 \pm 0.3$
${}^4\text{H}_\Lambda$	$2.0 \pm 0.4$ (d)	$10.48 \pm 0.4$
${}^4\text{He}_\Lambda$	$1.8 \pm 0.4$ (d)	$9.52 \pm 0.4$
${}^5\text{He}_\Lambda$	$2.0 \pm 0.6$ (e)	$30.6 \pm 0.6$

(a) The binding energy of the  $\Lambda^0$  is denoted by  $B_\Lambda$ .

(b) In determining the total binding energies,  $|E|$ , data on light nuclei reported by C. W. LI<sup>(28)</sup> were used.

(c) D. M. HASKIN *et al.*<sup>(29)</sup>.

(d) W. F. FRY<sup>(30)</sup>.

(e) W. F. FRY *et al.*<sup>(14)</sup>.

(28) C. W. LI, W. WHALING, W. A. FOWLER and C. C. LAURITSEN: *Phys. Rev.* **83**, 512 (1951).

(29) D. M. HASKIN, T. BOWEN, R. G. GLASSER and M. SCHEIN: *Phys. Rev.* **102**, 244 (1956).

(30) W. F. FRY: private communication (April, 1956).

For a particular value of the range constant  $\beta_0^{-1}$ , the potential constants  $a_0$  and  $K_0$  of Eqs. (1.5) and (1.6) were determined as follows. If  $a_0 > 0$  (favoring parallel spins of hyperon and nucleon), the stable spin configurations for  ${}^3\text{H}_\Lambda$  and mass 4 hyperfragments are respectively  $(\frac{3}{2}, 1)$  and  $(1, \frac{1}{2})$ . By a trial procedure, values of  $(1 + a_0)K_0$  were found for which the calculated total binding energy of  ${}^3\text{H}_\Lambda$  in the  $(\frac{3}{2}, 1)$  spin configuration was a maximum and equal (within limits of errors) to the observed total binding energy of  ${}^3\text{H}_\Lambda$ . A value of  $(3 - a_0)K_0$  was similarly obtained from mass 4 hyperfragments in an assumed spin configuration  $(1, \frac{1}{2})$ . These two relations involving  $a_0$  and  $K_0$  were then solved for values of the separate parameters. The entire procedure was repeated for a negative value of  $a_0$ , using the  $(\frac{1}{2}, 1)$  and  $(0, \frac{1}{2})$  spin configurations for  ${}^3\text{H}_\Lambda$  and the mass 4 hyperfragments, respectively. The results for two values of  $\beta_0^{-1}$  are presented in Table II, where the constant  $k_0$  is defined by  $k_0 = K_0/V_0$ , with  $V_0 = 67.3$  MeV.

TABLE II. — Values of  $a_0$  and  $k_0$  determined from variational calculations.

Spin configuration (a)		$a_0$ (b)	$k_0 = K_0/V_0$	
${}^3\text{H}_\Lambda$	${}^4\text{H}_\Lambda$ and ${}^4\text{He}_\Lambda$			
$(\frac{3}{2}, 1)$	$(1, \frac{1}{2})$	$0.840 \pm 0.020$	$4.359 \pm 0.044$	$\beta_0^{-1} = 3.31 \cdot 10^{-14}$ cm
$(\frac{1}{2}, 1)$	$(0, \frac{1}{2})$	$-0.779 \pm 0.020$	$3.133 \pm 0.060$	
$(\frac{3}{2}, 1)$	$(1, \frac{1}{2})$	$0.907 \pm 0.019$	$2.926 \pm 0.033$	$\beta_0^{-1} = 3.90 \cdot 10^{-14}$ cm
$(\frac{1}{2}, 1)$	$(0, \frac{1}{2})$	$-0.866 \pm 0.027$	$2.042 \pm 0.049$	

(a) The results for  ${}^4\text{H}_\Lambda$  and  ${}^4\text{He}_\Lambda$  with the same spin configuration were averaged before the individual values of  $a_0$  and  $k_0$  were determined.

(b) The uncertainties in  $a_0$  and  $k_0$  arise only from uncertainties in the observed binding energies of the mass 3 and 4 hyperfragments and do not include any estimate of the inaccuracies of the variational calculations.

For both values of  $\beta_0^{-1}$ , we can show from the conditions (2.2) and the values of  $a_0$  and  $k_0$  given in Table II that the hyperdeuteron will *not* be bound if the parallel alignment of the  $\Lambda^0$  and nucleon spins is assumed to be favored. This conclusion is relatively insensitive to the inaccuracies of the variational calculations (\*). On the other hand, if the antiparallel  $\Lambda^0$ -nucleon spin orientation is assumed to be favored, then the hyperdeuteron will be bound, for either value of  $\beta_0^{-1}$ . The latter conclusion, however, might be invalidated by an error of five per cent or more. On the basis of previous <sup>(21)</sup> experience with similar trial functions, and also from our results for  ${}^3\text{He}_\Lambda$ , we cannot exclude

(\*) Note that for this case the potential energies of  ${}^2\text{H}_\Lambda$  and  ${}^3\text{H}_\Lambda$  contain the same factor,  $(1 + a_0)K_0$ , which is not too sensitive to changes in the total energy of  ${}^3\text{H}_\Lambda$ .



an error of this amount due principally to neglect of nuclear tensor forces, and we are forced to admit the possibility that an antiparallel spin alignment of the  $\Lambda^0$  and nucleon may be favored and still be consistent with no bound states for  ${}^2\text{H}_\Lambda$ .

For the two values of  $k_0$  given in Table II corresponding to a parallel alignment of the  $\Lambda^0$  and nucleon spins, the calculated binding energies of  ${}^3\text{He}_\Lambda$  are found to be very large:

$$E' = 71.0 \pm 1.5 \text{ MeV}, \quad (\beta_0^{-1} = 3.31 \cdot 10^{-14} \text{ cm}),$$

$$E = 64.8 \pm 0.9 \text{ MeV}, \quad (\beta_0^{-1} = 3.90 \cdot 10^{-14} \text{ cm}).$$

We expect that a large fraction of this excess binding energy arises from neglecting the nucleon-nucleon tensor interaction.

We have concluded that the ground state of the hypertriton must be an i-spin singlet. The question arises whether an i-spin triplet state for  $A = 3$  is also stable, and hence whether  ${}^3\text{H}_\Lambda$  or  ${}^3\text{He}_\Lambda$  can be bound. It follows from the previous calculations that for this case the energy does not depend on the constant  $a_0$  and also that the effective strength of the nucleon-nucleon interaction has been reduced from that of the other spin configuration for  ${}^3\text{H}_\Lambda$  by about 30 per cent (since  $q = 0.69$ ). For  $\beta_0^{-1} = 3.31 \cdot 10^{-14} \text{ cm}$ , one can show by detailed calculations that even for  $k_0 = 8.5$  no bound level corresponding to the  $(\frac{1}{2}, 0)$  spin configuration of  ${}^3\text{H}_\Lambda$  exists. (See Table II). For this reason, we conclude that the hypertrineutron, which is an i-spin triplet, would also not be bound; and, considering the additional Coulomb energy, hyperhelium-3 would also have no bound states. These conclusions are not sensitive either to the value of  $\beta_0$  or to the inaccuracies in the variational calculations. We believe that the conclusions will be unaltered when nuclear tensor forces are considered.

\* \* \*

We gratefully acknowledge an interesting and valuable discussion with Professor J. K. KNIPP.

## APPENDIX

A useful technique of evaluating the integrals for a general value of  $A$  involves making a unitary transformation from the coordinate vectors  $\mathbf{r}_i$  to a new set of vectors, one of which equals  $(1/\sqrt{A}) \sum \mathbf{r}_i$ ,  $({}^{21})$ . The normalization and kinetic energy integrands are then observed to depend only on the distance from the origin in a  $3(A-1)$  dimensional space. The integrals are reduced at once to simple integrals over the radius by use of the expression for volume

of a hypersphere of radius  $R$  in  $n$  dimensions:

$$V_n = (\pi R^2)^{n/2} [I(n/2 + 1)]^{-1}.$$

The potential energy integrals similarly involve only the distance from the origin of a  $3(1-2)$  dimensional space, and the distance between the two interacting particles.

Irving <sup>(24)</sup> has evaluated the integral  $I_3$  for the case  $C_3 > 1$ . Values of  $I_3$  with  $0 < C_3 < 1$  were required in the present work. For this range of values,

$$\begin{aligned} I_3 &= 1/21, & (b = 1), \\ &= -(1/24)(b^2 - 1)^{-3} [f(b) + 15b(b^2 - 1)^{-\frac{1}{2}}g(b)], & (b^2 > 1), \end{aligned}$$

where  $b = C_3^{-1}$ , and

$$\begin{aligned} f(b) &= (8 - 9b^2 - 2b^4), \\ g(b) &= \ln |b - (b^2 - 1)^{\frac{1}{2}}|. \end{aligned}$$

# RIASSUNTO (\*)

Scopo del presente lavoro è di determinare le costanti di un potenziale fenomenologico assunto per l'interazione  $\Lambda^0$ -nucleone adattandole alle energie di legame osservate della massa 3 e degli iperframmenti 4. Si sono eseguiti calcoli variazionali per questi iperframmenti e per l'iperelio 5. I calcoli indicano che la forza  $\Lambda^0$ -nucleone dipende fortemente dallo spin e anche che l'iperneutrone e l'iperelio 3 non sono legati. Le principali ipotesi che si sono fatte sono: (a) lo spin del  $\Lambda^0$  è  $\frac{1}{2}$ ; (b) l'iperdeutrone non è legato; (c) l'interazione  $\Lambda^0$ -nucleone prodotta dallo scambio virtuale di mesoni pesanti può essere rappresentata dal potenziale fenomenologico assunto (trascuando qualunque possibile aggiunta di pioni risultante dallo scambio virtuale di almeno due pioni tra il  $\Lambda^0$  e il nucleone); (d) si possono trascurare tutti gli stati degli iperframmenti con numero di massa inferiore o uguale a cinque, all'infuori degli stati  $S$  principali; (e) l'interazione nucleone-nucleone è rappresentata dall'interazione centrale di Yukawa. Le ultime tre ipotesi sono alquanto restrittive e implicano che i calcoli attuali sono da considerare come preliminari di un esame più completo in cui siano inclusi l'interazione tensoriale tra nucleoni, come pure l'aggiunta di pioni nella forza  $\Lambda^0$ -nucleone.

(\*) Traduzione a cura della Redazione.

# On the Solutions of the Fluctuation Problem in Cascade Showers.

H. MESSEL

*The F. B. S. Falkner Nuclear Research and Adolph Basser Computing Laboratories,  
School of Physics (\*) The University of Sydney - Sydney, N. S. W.*

(ricevuto il 30 Agosto 1956)

**Summary.** — A practical method of obtaining numerical results in special cases for the number distribution function in shower theory is considered. It is also shown that Lopuszanski's and Moyal's recent solutions of the number distribution function equations are only formal expansions of these functions in terms of their factorial moments.

## 1. — Introduction.

Ever since BHABHA and HEITLER <sup>(1)</sup> suggested that the formation of an electron-photon cascade is an important factor in the penetration of electrons through matter, much theoretical work has been done on cascades. This work has been roughly divided into two branches: one dealing with the angular and radial spread of a cascade shower as it penetrates matter, the other with the longitudinal development which considers the number development of shower particles.

The purpose of the present work, which deals only with the longitudinal development, is to consider a practical method of obtaining numerical results in special cases for the number distribution function and to discuss recent work by ŁOPUSZAŃSKI <sup>(2)</sup> and MOYAL <sup>(3)</sup> on the same topic. It will be shown that their direct solutions for the distribution function are only formal expansions

---

(\*) Also supported by the Nuclear Research Foundation within the University of Sydney.

<sup>(1)</sup> H. BHABHA and W. HEITLER: *Proc. Roy. Soc.*, A **159**, 432 (1937).

<sup>(2)</sup> J. ŁOPUSZAŃSKI: *Acta Phys. Pol.*, **14**, 191, 251 (1955).

<sup>(3)</sup> J. E. MOYAL: *Journ. of Nuclear Phys.*, **1**, 180 (1956).

of the function in terms of its moments and hence of little value for obtaining information about the distribution itself. The analysis of their work also gives a lead to obtaining practical numerical information on the fluctuation problem.

## 2. Number Distribution Functions in Shower Theory.

In this section we shall define and discuss a number of the important distribution functions arising in cascade theory. To simplify notation, we shall whenever possible, consider a one type particle cascade; the extension to more than one type of particle being trivial.

The distribution function which describes completely the longitudinal development of a shower, and from which one can in principle obtain all other distribution functions of interest is given by  $p_n(E_0; E_1, \dots, E_n; z) dE_1 \dots dE_n$ . It defines the probability of finding exactly  $n$  particles, in any order, at an absorber depth  $z$ , with energies in the specified intervals  $E_k, E_k + dE_k, k = 1, \dots, n$ ; due to a primary particle with energy  $E_0$ .

The product density function

$$q_n(E_0; E_1, \dots, E_n; z) dE_1 \dots dE_n,$$

defining the probability of finding  $n$  particles, in any order, at an absorber depth  $z$ , with energies in the specified intervals  $E_k, E_k + dE_k, k = 1, \dots, n$ ; due to a primary particle with energy  $E_0$ , and any number of particles with arbitrary energies is given by:

$$(1.1) \quad q_n(E_0; E_1, \dots, E_n; z) = \sum_{a=0}^{\infty} \frac{1}{a!} \int_0^{\infty} dE_{n+1} \dots \int_0^{\infty} dE_{n+a} p_{n+a}(E_0; E_1, \dots, E_{n+a}; z).$$

If one requires the probability  $\varphi(E_0; E, n_1, n_2; z)$  of finding exactly  $n_1$  particles with energy greater than  $E$  ( $E < E_0$ ) and  $n_2$  particles with energies less than  $E$  ( $n_1 + n_2 = n$ ), then this likewise can be obtained from  $p_n$ ;

$$(1.2) \quad \varphi(E_0; E, n_1, n_2; z) = \frac{1}{n_1! n_2!} \int_E^{\infty} n_1 \int_E^{\infty} n_2 \int_0^E p_n(E_0; E_1, \dots, E_n; z) dE_1 \dots dE_n.$$

However the distribution function of most direct interest to experimentalists is that which gives the probability of finding  $n$  particles with energies greater than  $E$  and any number particles with energies less than  $E$ . Thus

$$(1.3) \quad \Phi(E_0; E, n; z) = \sum_{a=0}^{\infty} \varphi(E_0; E, n, a; z).$$

The moments of  $\Phi$  are also of interest to the experimentalists since they can provide, in some instances, useful information about the distribution itself. As will be seen below, factorial moments arise naturally in cascade theory and hence it has become customary to deal with these. The  $n$ -th factorial moment  $T_n$  is given by:

$$(1.4) \quad T_n(E_0; E, z) = \sum_{a=0}^{\infty} \frac{(n+a)!}{a!} \Phi(E_0; E, n+a; z),$$

with  $T_0 = 1$  when  $\Phi$  is normalized to 1.  $T_1(E_0; E, z)$  is simply the average number of particles with energies greater than  $E$  at an absorber depth  $z$ , due to a primary particle of energy  $E_0$ .

It has been shown by MESSEL and POTTS<sup>(4)</sup> that an interesting and important relation exists between the product density function  $q_n$  and the factorial moments  $T_n$ :

$$(1.5) \quad T_n(E_0; E, z) = \int_E^{\infty} dE_1 \dots \int_E^{\infty} dE_n q_n(E_0; E_1, \dots, E_n; z),$$

thus the factorial moments are easily obtained from the  $q_n$ .

The inverse relations corresponding to the above are given by:

$$(1.6) \quad p_n(E_0; E_1, \dots, E_n; z) = \sum_{a=0}^{\infty} \frac{(-1)^a}{a!} \int_0^{\infty} dE_{n+1} \dots \int_0^{\infty} dE_{n+a} q_{n+a}(E_0; E_1, \dots, E_{n+a}; z),$$

and

$$(1.7) \quad \Phi(E_0; E, n; z) = \sum_{a=0}^{\infty} \frac{(-1)^a}{a! n!} T_{n+a}(E_0; E, z).$$

It is thus obvious that if either  $p_n$  or  $q_n$ , or both, are known then the fluctuation problem is *in principle* solved; for one can then obtain any of the other distributions of interest by integration and summation. However, it is here that one of the great difficulties arise, for the summations and integrations over the functions  $p_n$  and  $q_n$  are usually of such a nature that to date it has been impossible to carry them out: the one exception is given by (1.5); once the product density function  $q_n$  is known then it is a very simple matter to obtain the factorial moments  $T_n$ .

The above fact, in conjunction with the most forbidding looking nature of the diffusion equations for  $p_n$  and  $q_n$ , led most workers to make a direct

(4) H. MESSEL and R. B. POTTS: *Proc. Phys. Soc.*, A **65**, 854 (1952).



attack upon the distribution function  $\Phi$  itself. Furthermore as will be seen below the diffusion equation for  $\Phi$  appears at first sight disarmingly simple. JÁNOSY (5) was the first to derive equations for it. Using what is now known as the « first collision equation » method (see MESSEL and POTTS (4) or MESSEL and POTTS (6)) he derived the following equation for  $\Phi$  in the case of a nucleon cascade developing in homogeneous nuclear matter (similar equations are easily derived for an electron-photon cascade):

$$(1.8) \quad \left\{ \frac{\partial}{\partial z} + 1 \right\} \Phi(\varepsilon, n, z) = \sum_{n_1+n_2=n} \int_0^1 \int_0^1 d\varepsilon_1 d\varepsilon_2 w(\varepsilon_1, \varepsilon_2) \Phi\left(\frac{\varepsilon}{\varepsilon_1}, n_1, z\right) \Phi\left(\frac{\varepsilon}{\varepsilon_2}, n_2, z\right),$$

with

$$(1.8a) \quad \Phi(\varepsilon, n, z=0) = \begin{cases} \delta_{n,1} & \varepsilon < 1, \\ \delta_n & \varepsilon > 1. \end{cases}$$

where we have written  $(E_i/E_0) = \varepsilon_i \cdot w(\varepsilon_1, \varepsilon_2) d\varepsilon_1 d\varepsilon_2$  is the probability that when a primary nucleon suffers a collision, it gives rise to two nucleons with energies  $\varepsilon_1, \varepsilon_1 + d\varepsilon_1$ ;  $\varepsilon_2, \varepsilon_2 + d\varepsilon_2$ ; and the remainder of the energy  $1 - \varepsilon_1 - \varepsilon_2$  is carried away by a meson or mesons. It is assumed that  $w(\varepsilon_1, \varepsilon_2)$  is a homogeneous function of the primary and secondary energies only, that is, it is a function of the ratios  $E_i/E_0$  and not of  $E_i$  and  $E_0$  separately. It should be noted that in the important physical case of an electron-photon cascade, the cross sections for pair production and bremsstrahlung are homogeneous functions at high energies.

Unable to do anything with the non-linear equations for  $\Phi$  directly, JÁNOSY introduced the generating function  $G(\varepsilon, u, z)$ ;

$$(1.9) \quad G(\varepsilon, u, z) = \sum_{n=0}^{\infty} u^n \Phi(\varepsilon, n, z),$$

thus throwing (1.8) into the form

$$(1.10) \quad \left\{ \frac{\partial}{\partial z} + 1 \right\} G(\varepsilon, u, z) = \int_0^1 \int_0^1 d\varepsilon_1 d\varepsilon_2 w(\varepsilon_1, \varepsilon_2) G\left(\frac{\varepsilon}{\varepsilon_1}, u, z\right) G\left(\frac{\varepsilon}{\varepsilon_2}, u, z\right),$$

(5) L. JÁNOSY: *Proc. Phys. Soc.*, A **63**, 241 (1950).

(6) H. MESSEL and R. B. POTTS: *Phys. Rev.*, **86**, 847 (1952).

with

$$(1.10a) \quad G(\varepsilon, u, z = 0) = \begin{cases} u & \text{for } \varepsilon < 1, \\ 1 & \text{for } \varepsilon > 1. \end{cases}$$

These equations though at first sight appearing simpler than those for  $\Phi$ , are again non-linear and in fact just as intractable. They were of value although, for by noting that

$$(1.11) \quad \left( \frac{\partial G^n}{\partial u^n} \right)_{u=1} = T_n(\varepsilon, z),$$

one could immediately obtain a recursion relation for the factorial moments  $T_n$ , from which practical values of  $T_1$ ,  $T_2$  and  $T_3$  could be obtained with some effort (see for instance JÁNOSSY and MESSEL<sup>(7)</sup>, MESSEL<sup>(8)</sup>).

Noting the above non-linearity difficulties, MESSEL and his collaborators (see MESSEL<sup>(9)</sup> and MESSEL and POTTS<sup>(6)</sup> for references) were successful in setting up a series of linear equations for the electron-photon and nucleon cascade and solving them completely for the functions  $p_n$ ,  $q_n$  and  $T_n$ ; thus the formal solution of the cascade fluctuation problem was complete. However, due to the difficulty of performing the summations and integrations over these functions necessary to obtain  $\Phi$ , the obtaining of practical, useful results was as far away as ever.

It should be noted that it is impossible to set up linear equations for  $\Phi$  as was done in the case of  $p_n$  and  $q_n$ . The linearity of these equations arises from the fact that they are derived by considering all possible «last collisions» giving rise to the final cascade. In the case of  $p_n$  and  $q_n$  the distribution in energy of the particles before this collision are known. For  $\Phi$ , the distribution in energy among the particles at this last stage is not known, since one is considering only particles with energies above a given limit.

### 3. - Direct Solutions for $\Phi$ and $G$ .

Recently a new approach has been suggested by ŁOPUSZAŃSKI<sup>(2)</sup> and MOYAL<sup>(3)</sup>. ŁOPUSZAŃSKI considered the  $G$ -equations for the nucleon and electron-photon cascade and MOYAL the characteristic functional and  $G$ -function of a knock-on electron cascade. They use the fact that conservation of energy

(7) L. JÁNOSSY and H. MESSEL: *Proc. Phys. Soc.*, A **63**, 1101 (1950).

(8) H. MESSEL: *Commun. Dublin Inst. for Adv. Studies*, Series A, No. 7.

(9) H. MESSEL, in: J. G. WILSON: *Progress in Cosmic Ray Physics* (Amsterdam, 1954), **2**, 135.

limits the number of particles of energies above  $E$  in a shower started by a particle of energy  $E_0$ . Using  $\varepsilon = E/E_0$ , it is clear that the number of particles cannot be larger than  $[1/\varepsilon]$ , the largest integer contained in  $1/\varepsilon$ , and thus the probability  $\Phi(n)$  vanishes identically for all  $n > [1/\varepsilon]$ .

Both authors make use of this fact and carry out a stepwise iteration procedure on the energy variable  $E$  or  $\varepsilon$ . The authors claim to have obtained a complete solution for the characteristic functional and the  $G$  and hence  $\Phi$  distribution, in terms of finite sums for any finite value of  $1/\varepsilon$ . Upon examination of Moyal's and Lopuszański's results it will be found that their iteration procedure does in fact lead to a formal series solution. However, it will also be seen that it is nothing more or less than a formal expansion of the distribution function in terms of its factorial moments. In fact in both cases one can compare the coefficients in their series expansion with the already known<sup>(9-6)</sup>  $T_n$  and see that they are identical term by term. Thus their solutions for  $\Phi$  and  $G$  are of no direct value for obtaining numerical values of  $\Phi$ .

It is in fact easy to see that any procedure wherein an iteration upon the energy variable is used will merely lead to a formal expansion of  $\Phi$  or  $G$  in terms of the factorial moments. We now show how this comes about.

Consider relation (1.4) for  $T_n(\varepsilon, z)$ . Since you can only have from 0 to  $n-1$  particles for  $\varepsilon > 1/n$ ,

$$(3.1) \quad \Phi\left(\varepsilon > \frac{1}{n}, k > n; z\right) = 0,$$

and hence

$$(3.2) \quad \begin{cases} T_{k > n}\left(\varepsilon > \frac{1}{n}, z\right) = 0, \\ T_n\left(\varepsilon > \frac{1}{n+1}, z\right) = n! \Phi\left(\varepsilon > \frac{1}{n+1}, n, z\right). \end{cases}$$

Thus it is seen that generally,

$$(3.3) \quad T_n\left(\varepsilon > \frac{1}{n+J}, J, z\right) = \sum_{k=0}^{J-1} \frac{(n+k)!}{k!} \Phi\left(\varepsilon > \frac{1}{n+J}, k = n, z\right); \quad J = \left\lfloor \frac{1}{\varepsilon} \right\rfloor - n + 1,$$

and that the series is finite.

Likewise consider the inverse relation (1.7) given for  $\Phi$ , which has usually been considered of little value for obtaining  $\Phi$  from  $T_n$  because of its infinite series and slowly converging character. Using the same considerations as above, one finds that

$$(3.4) \quad \Phi\left(\varepsilon > \frac{1}{n+J}, n, z\right) = \sum_{k=0}^{J-1} \frac{(-1)^k}{k!n!} T_{n+k}\left(\varepsilon > \frac{1}{n+J}, z\right),$$

and

$$\begin{aligned}
 (3.5) \quad G\left(\varepsilon > \frac{1}{n}, u, z\right) &= \sum_{k=0}^{n-1} u^k \Phi\left(\varepsilon > \frac{1}{n}, k, z\right) \\
 &= \sum_{k=0}^{n-1} \frac{(u-1)^k}{k!} \left(\frac{\partial^k G}{\partial u^k}\right)_{u=1} \\
 &= \sum_{k=0}^{n-1} \frac{(u-1)^k}{k!} T_k\left(\varepsilon > \frac{1}{n}, z\right),
 \end{aligned}$$

which shows that in carrying out a stepwise iteration on  $\varepsilon$  for either  $\Phi$  or  $G$ , you simply generate one further factorial moment at each iteration.

#### 4. - Practical Considerations for Obtaining $\Phi$ .

The impossibility so far, of obtaining a practical solution for  $\Phi$  from which numerical results may be obtained has led several authors <sup>(10-14)</sup> to consider methods of reconstructing this function from its moments.

ARLEY <sup>(10)</sup> in his work on the electron-photon distribution assumed that it was a Polya distribution, used the calculated first moment and a « guessed » value of the second moment to fit the two Polya parameters.

MESSEL <sup>(11)</sup> likewise assumed that the electron-photon distribution was a Polya distribution, but used the calculated values of both the first and second moments ( $T_1, T_2$ ) to fit the two parameters.

GARDNER *et al.* <sup>(12)</sup> carried the above methods a step further in the case of a nucleon cascade. They calculated  $T_1$ ,  $T_2$  and  $T_3$  and then using the Polya distribution as a weight function proceeded to reconstruct  $\Phi$  by a polynomial method <sup>(15)</sup>. The results of this long calculation were disappointing and pointed to the need for accurate numerical values of the moments  $T_n$ , especially when one was considering  $\Phi(n)$  for large  $n$  ( $n \sim 10$  to  $20$ ).

The work of the previous section suggests a practical method for obtaining  $\Phi$  for small values of  $n$  (the most important case as far as the experimentalist is concerned); and large values of the depth  $z$ , that is for small dying showers.

Equation (3.4) shows that the series expansion of  $\Phi$  in terms of its moments  $T_n$ , is a finite series for any finite value of  $1/\varepsilon$ . For instance consider  $\Phi(\varepsilon > 1/10, 0, z)$ : the probability of finding no particles with energy greater

<sup>(10)</sup> N. ARLEY: *On the Theory of Stochastic Processes* (New York, 1943).

<sup>(11)</sup> H. MESSEL: *Proc. Phys. Soc.*, A **64**, 809 (1951).

<sup>(12)</sup> J. W. GARDNER, H. GELLMAN and H. MESSEL: *Nuovo Cimento*, **2**, 58 (1955).

<sup>(13)</sup> J. ŁOPUSZAŃSKI: *Acta Phys. Pol.*, **14**, 265, 269 (1955).

<sup>(14)</sup> J. ŁOPUSZAŃSKI: *Suppl. Nuovo Cimento*, **2**, 1150 (1955).

<sup>(15)</sup> H. S. GREEN and H. MESSEL: *Quarterly of Applied Maths.*, **11**, 403 (1954).

than one tenth of the primary and any number of particles below that energy, at a depth  $z$ . The series

$$(4.1) \quad \Phi(\varepsilon > \frac{1}{10}, 0, z) = 1 - T_1 + \frac{1}{2}T_2 - \frac{1}{6}T_3 + \dots,$$

contains nine terms and requires knowledge of the nine factorial moments  $T_1$  to  $T_9$ . Due to the fact that in shower theory the numerical evaluation of the  $n$ -th factorial moment requires the evaluation of an  $n$ -fold complex integral, there is little hope of ever obtaining numerical results of  $T_n$  for  $n$  greater than 3 or 4. Thus the usefulness of the above series is limited to that range of  $z$  and  $\varepsilon$  where the values of the terms containing  $T_n$ ,  $n > 3$  are negligible. Similar considerations apply when one considers  $\Phi$  for higher values of  $n$ .

To obtain  $\Phi(n)$  one requires the factorial moments  $T_a$ ,  $a \leq n$ , thus if  $\Phi(5)$  is wanted then the fifth and higher factorial moments must be known. Though this limits the value of the present method to small values of  $n$ , it should be noted that from a practical point of view usually only small values of  $n$  are of interest; in fact  $\Phi(0)$  is one of the most important distributions for the experimentalist.

TABLE I. —  $\Phi(0) = 1 - T_1 + \frac{1}{2}T_2 - \frac{1}{6}T_3$ .

$z$	$T_1$	$\frac{1}{2}T_2$	$\frac{1}{6}T_3$	$1 - \Phi(\varepsilon > \frac{1}{10}, 0, z)$	$1 - \Phi$ (Gardner <i>et al.</i> )
5	0.3100	0.065	0.0053	$0.25 \pm 0.01$	0.25
10	$1.063 \cdot 10^{-2}$	$0.075 \cdot 10^{-2}$	$0.0035 \cdot 10^{-2}$	$(9.9 \pm 0.1) \cdot 10^{-3}$	$9.9 \cdot 10^{-3}$
15	$2.186 \cdot 10^{-4}$	$0.090 \cdot 10^{-4}$	$0.0033 \cdot 10^{-4}$	$(2.099 \pm 0.003) \cdot 10^{-4}$	$2.1 \cdot 10^{-4}$
20	$3.507 \cdot 10^{-6}$	$0.085 \cdot 10^{-6}$	$0.003 \cdot 10^{-6}$	$(3.425 \pm 0.003) \cdot 10^{-6}$	$3.4 \cdot 10^{-6}$
30	$6.05 \cdot 10^{-10}$	—	—	$(6.05 \pm 0.005) \cdot 10^{-10}$	—

$z$	$T_1$	$\frac{1}{2}T_2$	$\frac{1}{6}T_3$	$1 - \Phi(\varepsilon > \frac{1}{100}, 0, z)$	$1 - \Phi$ (Gardner <i>et al.</i> )
5	3.079	5.25	5.3	—	0.94
10	$3.807 \cdot 10^{-1}$	$2.3 \cdot 10^{-1}$	$1.0 \cdot 10^{-1}$	$0.25 \pm 0.03$	—
15	$1.884 \cdot 10^{-2}$	$0.475 \cdot 10^{-2}$	$0.18 \cdot 10^{-2}$	$(1.59 \pm 0.03) \cdot 10^{-2}$	$1.52 \cdot 10^{-2}$
20	$5.974 \cdot 10^{-4}$	$0.80 \cdot 10^{-4}$	$0.20 \cdot 10^{-4}$	$(5.37 \pm 0.01) \cdot 10^{-4}$	$5.28 \cdot 10^{-4}$
30	$2.924 \cdot 10^{-7}$	$0.175 \cdot 10^{-7}$	$0.017 \cdot 10^{-7}$	$(2.77 \pm 0.02) \cdot 10^{-7}$	$2.76 \cdot 10^{-7}$

$z$	$T_1$	$\frac{1}{2}T_2$	$\frac{1}{6}T_3$	$1 - \Phi(\varepsilon > \frac{1}{1000}, 0, z)$	$1 - \Phi$ (Gardner <i>et al.</i> )
5	12.96	90	530	—	—
10	4.909	18.5	95	—	—
15	$5.3 \cdot 10^{-1}$	$6.5 \cdot 10^{-1}$	1.3	—	—
20	$3.093 \cdot 10^{-2}$	$1.8 \cdot 10^{-2}$	$1.2 \cdot 10^{-2}$	$(3 \pm 1) \cdot 10^{-2}$	$2.1 \cdot 10^{-2}$
30	$3.85 \cdot 10^{-5}$	$0.7 \cdot 10^{-5}$	$0.2 \cdot 10^{-5}$	$(3.1 \pm 0.1) \cdot 10^{-5}$	$3.3 \cdot 10^{-5}$

Recently ŁOPUSZAŃSKI<sup>(13,14)</sup> considered the problem of determining the range of  $z$  for which  $\Phi(n)$  could be obtained using (1.7). However, an examination of numerical results for  $T_1$ ,  $T_2$ ,  $T_3$ , etc. immediately shows one the values of  $\varepsilon$ ,  $n$  and  $z$  for which  $\Phi$  can be computed (see Table I). Furthermore since (3.4) is an alternating finite series and only of value when we use it for the case when the values of the last available moments are decreasing, one can also determine the error involved by neglecting the higher factorial moments.

As a test of the method we have taken the calculations of GARDNER *et al.*<sup>(12)</sup> for  $T_1$ ,  $T_2$  and  $T_3$  in the case of a nucleon cascade developing in homogeneous nuclear matter. Calculation of  $\Phi$  using (3.4) was then made for various cases and compared with the calculations of GARDNER *et al.*<sup>(12)</sup> for  $\Phi$  wherein they used a tedious polynomial method with the Polya distribution as a weight function.

TABLE II.

$z$	$\Phi(\varepsilon > \frac{1}{10}, 1, z)$	$\Phi(\varepsilon > \frac{1}{10}, 2, z)$	$\Phi(\varepsilon > \frac{1}{100}, 1, z)$	$\Phi(\varepsilon > \frac{1}{100}, 2, z)$
5	0.2	0.05	—	—
10	$9.2 \cdot 10^{-3}$	$0.06 \cdot 10^{-2}$	—	—
15	$2.1 \cdot 10^{-4}$	$0.08 \cdot 10^{-4}$	—	—
20	$3.3 \cdot 10^{-6}$	$0.08 \cdot 10^{-6}$	$5 \cdot 10^{-4}$	$0.4 \cdot 10^{-4}$
30	$6.1 \cdot 10^{-10}$	—	$2.6 \cdot 10^{-7}$	$0.2 \cdot 10^{-7}$

The results are presented in Tables I and II; the number of significant figures should not be treated seriously as the calculation of  $T_1$  and  $T_2$  and  $T_3$  is not extremely accurate. It will be seen immediately that for energies close to that of the primary (large  $\varepsilon$ ) and small  $n$ , the series (3.4) gives accurate results for most of the range of  $z$  and that as  $\varepsilon$  decreases or  $n$  increases the values of  $z$  for which results can be obtained increases. The theory furthermore gives results in a much more direct manner than those by which GARDNER *et al.*<sup>(12)</sup> obtained theirs.

## 5. — Conclusions.

It is obvious that though the present method is still of limited value; it can, in many instances, provide answers which simply could not be obtained in any other manner — allowing at the same time an estimation to be made of the errors involved through the use of the method. It is therefore now possible to proceed to the important case of an electron-photon cascade and to obtain meaningful results for certain important ranges of the variables  $\varepsilon$ ,  $n$



and  $n$ ; accurate numerical evaluation of  $T_1$ ,  $T_2$  and  $T_3$  will have to be performed both with and without ionization loss being taken into account.

The work of ŁOPUSZAŃSKI and MOYAL shows one how difficult it is to obtain a direct solution for  $\Phi$  which could then be treated numerically. Any iteration procedure on the energy variable merely leads to an expansion of the distribution in terms of its factorial moments. It is a strange fact in shower theory that the distribution function  $p_n$  which contains the most information is of little value to the experimentalist, but can be obtained simply by the theoretician. On the other hand the distribution function  $\Phi$  which contains much less information about the shower but is of importance to the experimentalist, still presents a major challenge to the theoretician. Perhaps this difficulty could be overcome partially by the introduction of a shower distribution function intermediate to  $p_n$  and  $\Phi$ . This point is being examined at present and will in the near future be the subject of a separate paper.

\* \* \*

The author wishes to thank Dr. J. M. BLATT and Mr. J. E. MOYAL for a number of stimulating discussions, and Mr. P. J. GROUSE for performing the calculations of the distribution function.

---

#### RIASSUNTO ( \*)

Si esamina un metodo pratico per ottenere in casi speciali risultati numerici per la funzione di distribuzione nella teoria degli sciame. Si dimostra anche che le recenti soluzioni di Łopuszański e di Moyal delle equazioni della funzione di distribuzione sono solo sviluppi formali di tali funzioni in termini dei loro momenti fattoriali.

(\*) Traduzione a cura della Redazione.

## Investigation of the States of an Electron in a Proposed Electromagnetic Field.

E. VAN DER SPUY

*Departement of Physics - University of Stellenbosch, South Africa*

(ricevuto il 31 Agosto 1956)

**Summary.** — This investigation discusses, in terms of quantum mechanics, the polarization of a beam of electrons in a proposed experiment which is a modification of the Rabi type of radio-frequency spectroscopy experiment. The level structure of the electron in the uniform field and its discrimination in the inhomogeneous fields, as well as the stimulated transitions in the uniform field, is discussed essentially in quantal terms.

N. BOHR first suggested that the classical STERN and GERLACH experiment is impossible for the electron. The quantitative statement of this, as an experimental problem is difficult in view of the inevitable complication of inhomogeneous magnetic fields and the velocity spread of any practical beam, and the available discussions are simplified <sup>(1)</sup>, and depend too definitely on certain Lorentz force deflections that may be eliminated. Nevertheless it has come to be recognized that the above mentioned restriction may be more accurately put as: « It is impossible to make a classically describable experiment of the STERN and GERLACH type to determine the essentially quantal feature of the spin moment of the electron ». This then does not really preclude a STERN and GERLACH experiment for the electron, but rather demands that the dynamics shall be described essentially in proper wavemechanical terms. In view of the fundamental importance of such an experiment, if possible, in itself and to determine the higher order spin moment correction, it is of interest

<sup>(1)</sup> N. F. MOTT and H. S. W. MASSEY: *The Theory of Atomic Collisions* (Oxford, 1933), pp. 45-48.

to consider this more closely. The present author investigated aspects of a proposal to do such an experiment in an unpublished report (1952). The proposal essentially consisted of the Rabi type of radio-frequency spectroscopy experiment to determine the intervals between the magnetic levels of a dipolar particle, modified for electrons in the way mentioned below. In consideration of the Rabi type of experiment this paper shall use the following symbols: The inhomogeneous magnetic field regions A, B are separated by the uniform magnetic field region C. In field A the required level may be separated out, a radio-frequency field stimulates transitions from the latter level in the C region, and the residual population of this level may then be detected, after discrimination against transitions in the B field. Slits are used to select particles of the appropriate level. To fix the co-ordinate system, the axis of the system, or the line of centres of the slits for selecting the zero-moment level right through, shall be the  $X$  axis. The direction of the C field, and the direction of deflection, gives the  $Z$  axis. The magnetic field lines are all ideally speaking in  $YZ$  planes. Now the proposal envisaged the following modification in the Rabi type of experiment for the case of electrons:

(a) Consider all the magnetic fields,  $\mathbf{H}$ , crossed orthogonally by electric fields,  $\mathbf{E}$ , such that at one particular  $\mathbf{V}_m$  (in the  $X$  direction) for the whole beam length

$$(1) \quad \mathbf{E} + \frac{[\mathbf{V}_m \wedge \mathbf{H}]}{c} = 0.$$

Then consider the Lorentz transformation to the reference frame going at a velocity  $\mathbf{V}_m$  relative to the laboratory frame. The field in the moving reference frame is  $\mathbf{H}$ , only. In this frame consider only the differences,  $\mathbf{V}$ , of the electron velocity from the mean velocity  $\mathbf{V}_m$  in the laboratory frame. Only these  $\mathbf{V}$  would lead to Lorentz force deflections in the moving frame, and lead to orbital precession of  $\mathbf{V}$  round  $\mathbf{H}$ , in fact.

(b) Consider that  $\mathbf{V}$  can be limited by some method to a sufficiently small range to make the experiment possible.

In principle (a) should be possible. In the uniform field region (C) a parallel plate condenser could provide  $\mathbf{E}$ . In the inhomogeneous field regions (A, B) the following artifice is suggested:

Consider the inhomogeneous field generated by 2 parallel (parallel to the  $X$  axis) round conductors carrying a go-and-return current. Consider a thin uniform insulation sheath round each wire with a thin uniform metal foil sheath on top. A potential applied between the foils of the 2 conductors should provide  $\mathbf{E}$  everywhere orthogonal to  $\mathbf{H}$  and can be arranged to satisfy (1) everywhere.

A semi-classical theoretical discussion attempted to estimate the required limitation of  $V$  to make the experiment possible. The discussion was essentially based on general wavemechanical considerations formulated by PAULI<sup>(2)</sup>, who indicated that the mechanics of such an experiment can be expressed in terms of a power expansion in  $h$ , Planck's constant. The term  $h^0$  essentially gives the classical electron ray path in the electromagnetic field. Term  $h^1$  corresponds to a first order wave diffraction and spin moment beam splitting. The discussion then assumed that these 2 terms are the main ones, and that the  $h^1$  term may be estimated by taking the diffraction fringe due to an electron wave of wavelength  $\lambda = h/mV_m$  (in the above  $V_m \gg V$ ), and a beam split as due to the electron spin moment, used in a classical calculation.

To fix the magnitudes of the various parameters, consider the following values, which are not meant to be the optimum, but may be used to scale from:

$l_1$ , the length of the A or B regions, = 15 cm,

$l_2$ , the length of the C region, = 15 cm.

Effective slit cross-section 0.005  $\times$  0.005 cm, the dimension in the  $Z$  direction being  $d$ .

Corresponding to a kinetic energy of 0.28 eV (the most probable at 3300  $^\circ$ K),  $V_m = 3.2 \cdot 10^7$  cm/s.

The electron wavelength, in the laboratory frame,

$$\lambda = \frac{h}{mV_m} = 2.3 \cdot 10^{-7} \text{ cm}.$$

The wavepacket diffraction fringe in the  $Z$  direction, after a length  $l_1$ ,

$$\frac{\lambda l_1}{2d} = 0.35 \cdot 10^{-3} \text{ cm}$$

$H_z = 500$  G and  $\partial H_z / \partial z = 2000$  G/cm, (at  $\frac{1}{4}$  cm above the mean plane of 2 conductors  $\frac{1}{2}$  cm apart, carrying 625 A).

Split of spin moment levels =  $0.47 \cdot 10^{-2}$  cm over a length  $l_1$ .

Spin resonance frequency = 1400 MHz (an energy interval of  $0.58 \cdot 10^{-5}$  eV).

Change of  $H_z$  over slit height = change of  $H_y$  over slit width = 10 G.

$E$  on the beam axis, or in the C field = 158 V/cm. This means a change of potential over the slit width,  $b$ , of 0.79 V.

The number of precession cycles in  $l_1$  or  $l_2$ , namely  $N$ , = 665.

Although, by the above separation of terms, and wave and particle aspects,

(2) W. PAULI: *Helv. Phys. Acta*, 5, 179 (1932).

each term is in fact calculated classically, the overall effect is not classically describable and the discussion gives effect to the requirements of quantum mechanics, as far as it goes. In the discussion it appears that the main deflection spreads and other interference to the observation of the magnetic levels under high resolution, arises from the  $\hbar^0$  terms due to the velocity spread  $V$  of the beam and not from the wave diffraction. In this discussion the wave-mechanical uncertainty of the electron wavepacket velocity  $\ll V$ . In fact, the discussion requires  $V$  to be limited to so low a value that the angular momentum of the electron orbits in the moving frame is below one unit of  $\hbar$  ( $\approx \hbar/10$  in fact). But then one requires in effect that the orbital motion in the moving frame should be quantized. This requirement completely changes the problem and requires a reconsideration in such terms. To a complete range of orbits in the above now correspond stationary states associated with discrete level energies. The classical change of position and velocity over the orbit no longer concerns one for a stationary orbit, and neither does the classical spread of orbital energies, if one considers the lower levels. Thus discrete deflections and stationary fields replace certain troublesome classical effects, but in their stead certain other effects arise from the completely quantized theory. Below, some aspects of the above proposal shall be considered in this light, namely completely in quantum mechanical terms.

As under (a) above, transform to the Lorentz frame moving at  $V_m$  relative to the Laboratory frame. In this frame the only applied field is  $\mathbf{H}$ , and the electron wave equation is the Dirac equation. Since the present interest is in low energy phenomena, the following discussion shall take the low energy Hamiltonian indicated by DIRAC<sup>(3)</sup>. RABI<sup>(4)</sup> considered the general Dirac equations for a uniform magnetic field, and arrived at the same levels as will be given below. The wavefunction below, corresponds essentially to one of his four. The radiative correction to the spin moment can always be readily applied to the analysis, and will remove the twofold degeneracy of all the levels found below (except the lowest).

## 1. — The Electron Levels in a Uniform Magnetic Field $H_z$ .

Consider  $H_z$  generated by a cylindrically symmetric current system, with axis through the origin.

Then  $A_x = -\frac{1}{2}H_z y$ ,  $A_y = \frac{1}{2}H_z x$ ,  $A_z = 0$ , give the components of the vector potential.

<sup>(3)</sup> P. A. M. DIRAC: *The Principles of Quantum Mechanics* (Oxford, 1949), p. 265.

<sup>(4)</sup> I. I. RABI: *Zeits. f. Phys.*, **49**, 507 (1928).

Therefore the low energy Hamiltonian:

$$\mathcal{H} = \frac{1}{2m} (p_x^2 + p_y^2 + p_z^2) + \frac{\omega^2 r^2}{2m} + \frac{\hbar\omega}{m} (L_z + \sigma_z),$$

where  $\omega = eH_z/2c$ ,  $r^2 = x^2 + y^2$ , and  $\hbar L_z$  is the  $z$  component of the electron orbital angular momentum.

Clearly  $p_z$ ,  $\sigma_z$ , and  $L_z$  are constants of motion. Consider therefore the wavefunction:

$$\psi = \theta \exp \left[ i \left( lq + \frac{p_z z}{\hbar} - \frac{Et}{\hbar} \right) \right] e^{\lambda p} \left| -\frac{\omega}{2\hbar} r^2 \right| r^l f(r),$$

where  $\theta$  is the spin eigenfunction:

$$\theta = (1) \quad \text{for} \quad + \text{ spin},$$

$$\theta = (-1) \quad \text{for} \quad - \text{ spin},$$

and  $E$  is an energy eigenvalue, and  $l$  must be a whole number for single-valuedness. Consider  $l$  positive first of all.

Therefore,

$$\begin{aligned} \mathcal{H}\psi - E\psi &= \left[ \frac{\hbar^2}{2m} \left\{ \frac{\partial^2}{\partial z^2} + \frac{\partial^2}{\partial r^2} + \frac{1}{r} \frac{\partial}{\partial r} + \frac{1}{r^2} \frac{\partial^2}{\partial \phi^2} \right\} + \frac{\omega^2 r^2}{2m} + \frac{\hbar\omega}{m} \left( \frac{1}{i} \frac{\partial}{\partial \phi} + \sigma \right) \right] \psi \\ &= \left[ \frac{p_z^2}{2m} - \frac{\hbar^2}{2m} \left\{ \frac{\partial^2}{\partial r^2} + \frac{1}{r} \frac{\partial}{\partial r} \right\} + \frac{\hbar^2 l^2}{2mr^2} + \frac{\omega^2 r^2}{2m} + \frac{\hbar\omega}{m} (l + \langle \sigma_z \rangle) \right] \psi, \end{aligned}$$

where  $\langle \sigma_z \rangle$ , the expectation value of  $\sigma_z$ ,  $= \pm 1$  respectively for  $\theta(1)$  and  $\theta(-1)$  states.

Thus,

$$Ef(r) = \left[ \frac{p_z^2}{2m} + (2l + 1 + \langle \sigma_z \rangle) \frac{\hbar\omega}{m} - \frac{\hbar^2}{2m} \left\{ \frac{\partial^2}{\partial r^2} + \left( \frac{2l + 1}{r} - \frac{2\omega}{\hbar} r \right) \frac{\partial}{\partial r} \right\} \right] f(r).$$

Put  $x = \omega r^2/\hbar$ , and  $f(r) = F(x)$ , then the previous equation reads

$$\left[ x \frac{\partial^2}{\partial x^2} + (l + 1 - x) \frac{\partial}{\partial x} + \left\{ \left( E - \frac{p_z^2}{2m} \right) \frac{m}{2\hbar\omega} - \left( l + \frac{1 + \langle \sigma_z \rangle}{2} \right) \right\} \right] F(x) = 0.$$

For  $F(x)$  not to diverge exponentially as  $x$  tends to  $\infty$ , it must be a closed polynomial, and for this

$$(2a) \quad \left( E - \frac{p_z^2}{2m} \right) \frac{m}{2\hbar\omega} - \left( \frac{1 + \langle \sigma_z \rangle}{2} \right) = k \quad \text{a whole number} \geq 0.$$



Then  $F(x) = L_k^l(x)$ , the Laguerre polynomial, for which non-zero functions arise for  $k \geq l$ .

Thus,

$$E = \left( k + \frac{1 + \langle \sigma_z \rangle}{2} \right) \frac{2\hbar\omega}{m} + \frac{p_z^2}{2m},$$

and

$$\psi = \theta \exp \left[ i \left( l\varphi + \frac{p_z z}{\hbar} - \frac{Et}{\hbar} \right) \right] \exp \left[ -\frac{\omega r^2}{2\hbar} \right] r^l L_k^l \left( \frac{\omega r^2}{\hbar} \right).$$

When  $l$  is negative, or we consider states of negative orbital angular momentum,  $E$  is specified in the same way but

$$\psi = \theta \exp \left[ i \left( l\varphi + \frac{p_z z}{\hbar} - \frac{Et}{\hbar} \right) \right] \exp \left[ -\frac{\omega r^2}{2\hbar} \right] r^{|l|} L_{k+|l|}^{|l|} \left( \frac{\omega r^2}{\hbar} \right).$$

Thus the energy levels are infinitely degenerate, since  $l$  does not affect  $E$  and is only restricted by  $k \geq l$ . The cases for which  $l \neq k$  correspond classically to orbits which have centres off the origin. Since  $p_z$  is a constant of motion, it can be considered fixed at a selected value. Below, the value,  $p_z = 0$  shall be considered (unless otherwise stated).

Then

$$(2) \quad E = \left( k + \frac{1 + \langle \sigma_z \rangle}{2} \right) \frac{2\hbar\omega}{m}.$$

The levels are clearly discrete and have an additional doubling of the degeneracy on account of the spin, that is for all levels except the lowest. This particular degeneracy is removed when the spin moment radiative correction is taken into account. This can be done by associating a factor  $g_s/2$  (taken = 1, in the above) with  $\langle \sigma_z \rangle$  in the expression for  $E$ , where  $g_s$  is the correct spin moment Landé factor. Except for this very small correction, the level intervals given by (2) are the same as for the two spin levels in the semi-classical treatment referred to above.

The wavefunctions show no directed propagation in the  $xy$  plane, but just a circulation round the origin. For short, these states, which are selfpropagating in the laboratory frame with a unique velocity  $V_m$ , may be given a name, say zeron. This name must be used with great care. This is not a new particle (such as an electron bound to an atomic centre of force is), distinct from just an electron in just such a state, and especially motion of the zeron, rather than the electron, in the  $xy$  plane must be carefully dealt with. Collisions in the  $xy$  plane more properly are collisions of the electron, and would not

permanently change the  $x$  velocity of the zeron but rather generate new zeron with  $x$  velocity  $= V_m$ . Since, however, the  $Z$  momentum may be selected at will and the relevant mass in (2a) is  $m$ , it is clear that one has a diffraction at the slits equal to that calculated for the electron, of  $x$  velocity  $= V_m$ , in the semi-classical treatment above.

Limit integrations for expectation values to the  $xy$  plane. It can then easily be shown that the wavefunctions with distinct sets of  $(\langle\sigma_z\rangle, l, k)$  are orthogonal. For the integrals over  $r$ , involving Laguerre polynomials, reference may be made to a formula due to Schrödinger <sup>(5)</sup> (\*). These wavefunctions complete the description of the stationary states in the field in a typically wave-mechanical form.

The expectation value of the square of the radius =

$$\overline{r^2} = \frac{l, k | r^2 | l, k \rangle}{\langle l, k | l, k \rangle} = \frac{\hbar}{\omega} (2k - l + 1), \quad \text{for all } l.$$

Therefore  $(\overline{r^2})^{\frac{1}{2}} =$  root mean square radius  $= \sqrt{(\hbar/\omega)} \{k + (k - l) + 1\}^{\frac{1}{2}}$ , which goes up with  $k$  and  $(k - l)$ , as may be expected.

On classical lines the orbital radius,  $r_0$ , for an electron with an orbital angular momentum  $\hbar$ , is given by  $2r_0^2 = \hbar/\omega$  or  $r_0 = \sqrt{\frac{1}{2}(\hbar/\omega)}$ .

Therefore  $(\hbar/\omega)^{\frac{1}{2}}$  ( $1.62 \cdot 10^{-5}$  cm in a field of 500 G), is the unit of orbital radius. Since  $b/2(\hbar/\omega)^{\frac{1}{2}}$  is large, (150 in the above example), the wavefunctions are well down within a very small portion of the slit width.

The energy,  $E$ , depends only on  $H_z$  and not explicitly on its mode of generation. The calculation started with the origin of co-ordinates on the axis of the current system. For an origin off the axis, one obtains of course, the same system of energy levels, because the two situations are in fact related by a unitary transformation—a gauge transformation, and the theory is gauge invariant. The corresponding change in wavefunctions is obtained by applying the appropriate unitary phase factor to the above wavefunctions. The new wavefunctions are not eigenfunctions of  $L_z$  as above, since the problem is no longer rotation invariant round the  $Z$  axis, but the new wavefunction corresponding in the above way to the wavefunction for a given  $l$  in the above system leaves  $(\overline{r^2})^{\frac{1}{2}}$ , for example, unchanged. The new wavefunctions correspond to mixtures of different  $l$  values. Thus the motion of the origin of the moving frame across the uniform field, region C, corresponds to half a cycle of changes in the vector potentials and should unfold as a continuously

<sup>(5)</sup> N. F. MOTT and I. N. SNEDDON: *Wave Mechanics and its Applications* (Oxford, 1948), p. 380.

(\*) This formula has to be amended by another factor  $(p - n')!$  (which has obviously slipped out as may be seen by symmetry in  $n, n'$ ).

changing gauge transformation of the wavefunctions only, if the change occurs adiabatically. Especially since there is no corresponding change in level energies, it should be relatively easy to ensure that  $\frac{1}{2}$  a cycle of  $\mathcal{A}$  changes in  $N$  orbital cycles corresponds to an adiabatic transit. In any case one can avoid this problem, and other similar problems at the change between the field regions, in principle by generating the fields by longitudinal current elements only (in the  $x$  direction). This problem of a time changing gauge comes in with bound electrons, etc., too, but it is presumably more severe for an unbound electron. Similarly, an electron in a uniform field  $H_z$ , generated by a parallel current system, will have the same energy levels, with wavefunctions differing from the above by the phase factors of the corresponding gauge transformation, which mix the angular momenta, but do not change the corresponding  $(\bar{p}^2)^{\frac{1}{2}}$ .

## 2. — Inhomogeneous Field.

To the first approximation this field is a uniform field which can be arranged  $= H_z$  on the central axis of the slits. This field is generated by a parallel current system and the last remark in the previous section applies here specifically. In transit from this uniform field to the C field generated by a circular current system there is necessarily a change in vector potential, even though  $H_z$  is held constant. For the same reasons as above it shall be assumed an adiabatic change—here again one should consider the number of orbital cycles occupied by the transition between the regions. Off the slit axis as in all Rabi-type experiments, although the field will still be sensibly equal to  $H_z$  in magnitude, the direction will be different. Hence as usual in transit from A to C, or C to B, off axis particles in the Rabi type experiments experience a small rotation of the magnetic field vector. This can cause inter-level transitions, if the change is not effected slowly and adiabatically. The changing fields seem likely to be chiefly such as cause transitions rather than motion of the zeron along  $\mathbf{H}$ . Although the relevant quantities are the number of orbital cycles occupied by the transition from one region to the other, and  $H_z$  ( $\leq 5$  G in the example), it is difficult to be specific about this aspect of adiabatic transit. In practice one could to some extent hope to estimate this, as regards spin transitions at least, by comparison with the experience on bound electron experiments. In principle, however there seems in any case to be no reason why  $N$  (by  $V_m$  and  $H_z$ ) may not be selected so large as to render this and other troublesome perturbations adiabatic.

The approximation of regarding the field uniform, for the lowest energy state, and with  $k = l$ , may be seen by noting the magnetic field variation over a distance twice its root mean square radius,  $2(\hbar/\omega)^{\frac{1}{2}} \cdot \partial H_y / \partial y$ . This will

be a small fraction of  $H_z$  in general, (0.065 G compared with 500 G in the example taken).

To a second approximation one must realize  $H_z$  as being a function of  $z$ , or  $E$ , (2), as a potential function of  $z$ . Then (2a) indicates the possibility of adiabatic exchange between the magnetic field energy and the kinetic energy in the  $z$  direction  $= p_z^2/2m$ , with the zeron moving to the weak field region. Since the split is  $\approx d$  and  $H_z$  only varies  $(\partial H_z/\partial z)d$  (say, 10 G) in this distance, over  $N$  (say, 665) orbital cycles, the condition for adiabatic deflection may in principle be satisfied, at least for the lower levels. Thus these levels will be split practically as given in numerical terms for two spin levels in the semi-classical treatment. In fact, the split is as usual

$$(3) \quad = -\frac{\partial I}{\partial z} \cdot \frac{1}{2m} \cdot \left( \frac{l_1}{V_m} \right)^2 = -\frac{I}{a'} \cdot \frac{l_1^2}{4K_z},$$

where  $I$  is the level interval  $= 2\hbar\omega/m$  (which  $\approx$  the interval between the spin levels, used in the above semi-classical calculation of numerical values);  $a'$  is the inhomogeneity parameter in  $\partial H_z/\partial z = H_z/a'$ ;  $K_z = \frac{1}{2}mV_m^2$  is the kinetic energy of the electron due to the zeron velocity in the laboratory frame. Since split easily preponderates over diffraction one can in principle prepare a fairly clean state in the A field, and discriminate transitions, effected in region C, in the B field.

One must mention a few additional points in connection with the inhomogeneity of the field, or of  $H_y$  (chiefly) changing over the orbit.

The effect will be largest for orbits with large  $\bar{r}^2$ , or  $k$  and  $(k-l)$  large, and there are 2 aspects of this effect:

(1) In contradistinction with the classical orbit, where the particle precession in the orbit in an inhomogeneous field causes an oscillating field in the electron rest system nearly in resonance with the spin toppling frequency, the expectation value of the field for a stationary state is time-independent. Consequently the first effect of the inhomogeneity is only to tend to lift the degeneracy of the levels. The small field variation over the diameter of the lowest orbit, suggests that the effect may be small, except for the rather larger values of  $k$  and  $(k-l)$ .

(2) One only has an oscillating field in transition, and then it acts directly for transition, but at radio-frequency. As a stimulation of transitions it is thus inversely proportional to the number of cycles in the A field region, say. Thus, and because the actual change of field over the orbit is small, it will be assumed that the effect is small at least for the lower values of  $k$  and  $(k-l)$ .

Both (1) and (2) collaborate for large  $k$  and  $(k-l)$  towards interlevel

transitions, and in fact these orbits will furthermore tend to exhibit classical behaviour anyway. This discrimination against these orbits will also tend to occur at all transitions between regions.

It is now suggested that the zero energy level (according to (2)) is selected for study—in other words the other levels are split off. This level has  $k=0$  and  $\langle\sigma_z\rangle=-1$ . Except for a small spin moment correction this state will suffer no deflection in the A and B regions, will be the most stable (other things being equal), and a proper quantum stationary state.

The present discussion is not concerned with proving the feasibility of the experiment. In the consideration of an actual experiment one shall have to consider tolerances for the field balance and disturbing potentials and other perturbations. The criterion will always be whether a change can be negotiated adiabatically. Other things being equal, it may be best to use a very small  $V_m$ , and a rather large magnetic field or transition frequency, that is a large  $N$ . Now note:

The total energy of any level,  $T(y_m) = K_x + \varphi_0 + y_m f_e + E$ , where  $y_m$  is the  $y$  co-ordinate of the origin of a zeron of energy  $E$ ;  $\varphi_0$  is the potential at  $y=0$ ;  $f_e$  is the balancing electric field. For the useful levels  $E$  is a relatively very small term in the above expression. Provided that the changes are slow, a zeron may conserve its  $T(y_m)$  and  $E$  by complementary changes among the first 3 quantities. Changes in  $f_e$ ,  $y_m$  and  $K_x$ ; and  $\varphi_0$ ,  $y_m$  may be naturally associated. Note  $K_x \propto V_m^2$  and  $f_e \propto V_m$ . Slowness of change here means a small effective change in energy, relative to the level interval, in the time of one cycle (or the corresponding distance of zeron's travel).

Now for  $y_m$  ranging over  $b$ , the effective slit width,  $T(y_m)$  changes by  $b \cdot f_e$  (0.79 eV, in the example). Qualitative consideration seems to indicate that in principle there seems to be no reason why the system cannot collect its beam from a beam of thermal velocity spread, with collimation in the  $Z$  direction and permitting a very wide angle of entry in the  $xy$  plane.

### 3. — Transition Theory.

It has already been suggested that the zero energy state shall be separated for consideration. Neglecting errors in collimation and diffraction, this means that in the C field one is concerned with transitions from the prepared zero energy level to other levels ( $k \neq 0$ , or  $\langle\sigma_z\rangle \neq -1$  or both) because such transitions can be discriminated in the B field. In line with the discussion of the uniform field case above, it shall be taken for simplicity that the transition theory can be established for a zeron having its origin on the axis of the circular current system generating the uniform field. For simplicity, in the face of the infinite degeneracy of the levels, the calculation shall assume weak



stimulation fields, for which in any case one will have the narrowest lines. The time of traverse of the zeron across the C field is definite, and this will undoubtedly simplify the calculation of the line shape, which will in itself increase the accuracy of the measurement of the transition frequency.

In general, one sets up a wavefunction for the state during transition:  $\Psi = \sum_{s,l,k} C(s, l, k; t) \psi(s, l, k)$ , where  $\psi(s, l, k)$  are the eigenfunctions for the uniform field case, given above, for spin, orbital and energy quantum numbers  $s, l, k$ , respectively.  $\psi(s, l, k)$  are now normalized in the  $xy$  plane.  $C(s, l, k; t)^2$  determines the probability of occupation of the corresponding state. If the perturbing Hamiltonian is a function of  $z$  then one will have changes in the  $Z$  motion or momentum  $p_z$  (and the corresponding kinetic energy, since  $p_z$  is no longer a constant of motion), and the  $C$ 's will have to be functions of  $z$  as well. The calculations below will not consider this possibility quantitatively.

The weak stimulation means that the  $C$ 's, but not necessarily their time derivatives, are all small, except the  $C(s', l', k'; t)$  which correspond to the prepared states  $s' = -\frac{1}{2}$ ,  $k' = 0$  and general  $l' \leq k'$ .

Since  $g_s$  is so near 2, one can anticipate it to be difficult to separate spin and orbital transitions. To effect the latter one attempts to separate their stimulation and to reduce the line width (or increase  $N$ ). The requirement of separate stimulation involves the separation of the electric and magnetic field vectors of the stimulating radio-frequency field, by using, say, the standing wave conditions in transmission lines, such that:

(a) To stimulate the spin transition, one prefers a magnetic field  $h_x \sin \nu t$  with no attendant electric field and generated by  $A_z = y h_x \sin \nu t$  (or radio-frequency conduction currents in the  $Z$  direction only). Amongst others  $A_y$ , for example, would increase the relative effect of orbital transitions and leads to undesirable resonant changes in  $p_z$ .

(b) To stimulate the orbital transitions, one prefers a pure electric field  $\epsilon_y \sin \nu t$ . These fields are both assumed independent of  $Z$  (that is, cause no changes of  $Z$  motion). This is true to the first order and one may get a field with such properties if one considers it generated in a parallel strip line (with  $x$  width  $= l_2$ ), with very small  $y$  separation and with strips as  $ZX$  planes, excited in the principal mode, and appropriately terminated for cases (a) and (b), respectively.

CASE (a): *Spin transitions.* — The Hamiltonian

$$\mathcal{H} = \mathcal{H}_0 + p_z y \cdot \frac{e h_x}{mc} \sin \nu t + \frac{e \hbar}{2mc} \cdot \sigma_x h_x \sin \nu t,$$

if one neglects terms in  $\hbar^2$ , since  $h_x$  is small, and where  $\mathcal{H}_0$  is now used for the



Hamiltonian in the uniform field  $H_z$  as used above. Since  $p_z$  is still a constant of motion, and may hence be chosen  $= 0$ , as above,

$$\mathcal{H} = \mathcal{H}_0 + \frac{e\hbar}{2mc} \cdot \sigma_x h_x \sin \nu t.$$

Using the general wavefunction  $\Psi$ , and the orthogonality and weak stimulation conditions, one can obtain  $(\partial/\partial t) C(s, l, k; t)$  from the time-dependent Schrödinger equation. One finds:

(1)  $C(s', l', k'; t)$  which starts off as a prepared state probability amplitude is effectively constant with time—even when the above  $p_z$  term is not neglected, the time dependence is a rapid oscillation and inversely proportional to the number of cycles in the  $C$  field, and may thus be arranged to be small. This constancy depends of course on the weak stimulation assumption, and is true in the first approximation.

(2) One has the selection rule:  $\Delta s = +1$ ,  $\Delta l = 0 = \Delta k$ ; and

$$\frac{\hbar}{i} \cdot C \frac{\partial}{\partial t} \left( \frac{1}{2}, l', 0; t \right) = \frac{\hbar e h_x}{2mc} \exp \left[ i \frac{g_s \omega t}{m} \right] C \left( -\frac{1}{2}, l', 0; 0 \right) \sin \nu t.$$

Therefore neglecting small rapidly oscillating (non-resonant) terms:

$$C \left( \frac{1}{2}, l', 0; t \right) = \frac{e h_x}{2mc} \cdot \frac{t}{2} \cdot \frac{\sin \theta}{\theta} \cdot C \left( -\frac{1}{2}, l', 0; 0 \right),$$

where

$$\theta = \frac{t}{2} \left( \frac{g_s \omega}{m} - \nu \right).$$

Thus one has a resonance at  $\nu = g_s \omega / m = g_s e H_z / 2mc$ , as expected; with a half probability width,  $\Delta \nu$ , given by  $\sin \theta / \theta = 1/\sqrt{2}$ . Taking  $t = l_2 / V_m$ ,

$$1\nu = 4 \cdot 1.39 \cdot \frac{V_m}{l_2}, \quad \text{or} \quad \Delta f = \frac{2}{\pi} \cdot 1.39 \cdot \frac{V_m}{l_2} = \frac{0.885 V_m}{l_2}.$$

At resonance,

$$(4) \quad p_a^{\frac{1}{2}} = \left| \frac{C \left( \frac{1}{2}, l', 0; t \right)}{C \left( -\frac{1}{2}, l', 0; 0 \right)} \right| = \frac{e h_x}{2mc} \cdot \frac{t}{2},$$

where  $p_a$  is the transition probability at spin resonance. Note, the only adjustable quantities in this expression are  $h_x$  and  $t$ . It is interesting that (4) does not involve  $\hbar$ , Planck's constant, or show an  $l'$  dependence. For example,

consider

$$p_a = \left| \frac{C(\frac{1}{2}, l', 0; t)}{C(-\frac{1}{2}, l', 0; 0)} \right|^2 = \frac{1}{10},$$

say. With  $V_m$  and  $l_2$  as in the numerical example above,  $h_w = 0.15$  G. This is quite a small field.

CASE (b): *Purely orbital transitions.* — Now

$$\mathcal{H} = \mathcal{H}_0 + e\mathcal{E}_y \cdot y \sin vt = \mathcal{H}_0 + e\mathcal{E}_y r \sin \varphi \sin vt.$$

Therefore  $l_s = 0$ . The time derivatives of the probability amplitudes are obtained as before, and are affected by the product of two factors which determine the selection rules:

$$\int_0^{2\pi} \exp[i(l' - l)\varphi] \sin \varphi \frac{d\varphi}{i} = \pi \{ -\delta_{l', l-1} + \delta_{l', l+1} \},$$

or  $\Delta l = \pm 1$ ; and

$$I_1 = \int_0^\infty \exp \left[ -\frac{\omega r^2}{\hbar} \right] r^{l+|l|+2} L_k^l \left( \frac{\omega r^2}{\hbar} \right) L_{|l'|}^{|l'|} dr,$$

where  $r^2 L_k^l$  is replaced by  $r^{2|l|} L_{k+|l|}^{|l|}$  when  $l$  is negative.  $I_1$  may be evaluated by reference to MOTT and SNEDDON<sup>(5)</sup> (pag. 380). The effect of  $I$ , is that  $\Delta l = +1$  and  $\Delta k = 0$  and  $+1$ ; but  $\Delta l = -1$ ,  $\Delta k = 0$ .

Again  $C(s', l', k'; t)$  is constant with time except for a small rapidly oscillating term.

$$\frac{\hbar}{i} \cdot \frac{\partial}{\partial t} C(-\frac{1}{2}, l, 1; t) = \frac{e\mathcal{E}_y}{2i} \cdot \left( \frac{\hbar}{\omega} \right)^{\frac{1}{2}} \exp \left[ i \frac{2\omega t}{m} \right] \sin vt \cdot \{ + C(-\frac{1}{2}, l-1, 0; 0) \},$$

where the  $(-)$  obtains for  $l = 1$  and the  $(+)$  for all other values of  $l < 1$ . Note  $l-1 = l'$  here ( $\Delta l = +1$ ).

The main resonance term yields:

$$\left| \frac{C(-\frac{1}{2}, l, 1; t)}{C(-\frac{1}{2}, l-1, 0; 0)} \right| = \frac{e\mathcal{E}_y}{2(\hbar\omega)^{\frac{1}{2}}} \cdot \frac{t}{2} \cdot \frac{\sin \theta}{\theta},$$

where  $\theta = (2\omega/m - v)t/2$ ; again showing a resonance, at  $v = 2\omega/m$ , and with the same line width as above.

At resonance,

$$(5) \quad p_b^{\frac{1}{2}} = \left| \frac{C(\frac{1}{2}, l, 1; t)}{C(-\frac{1}{2}, l-1, 0; 0)} \right| = \frac{e\epsilon_n}{2(\hbar\omega)^{\frac{1}{2}}} \cdot \frac{l}{2},$$

where  $p_b$  is clearly the transition probability at orbital resonance, and shows no  $l$  dependence. The  $\hbar$  in the denominator of  $p_b$  indicates that one must take the orbital quantization into account.

In terms of the above numerical parameters  $p_b \approx 10^{-1}$ , when  $\epsilon_n = 1.07 \cdot 10^{-1}$  V/cm, a small field. Realize now that  $h_x = 0.15$  G, as above, would correspond, in a plane travelling wave, to an electric field  $\epsilon_h$ , say,  $= 0.45 \cdot 10^2$  V/cm. Thus  $\epsilon_h \gg \epsilon_n$  and this means that when studying spin transitions it is difficult to separate the attendant  $\epsilon_h$ , say, sufficiently from the beam. This is a difficulty which would attend any method attempting to discriminate orbital and spin transitions of the unbound electron. In principle there seems to be no reason, however, why a large frequency separation of the two lines (or a large  $H_z$ ) together with a large  $N$  (or a narrow line), and the maximum separation of  $\epsilon_h$ , should not allow this discrimination. It is interesting to put the above findings which clearly shows the greater ease with which orbital transitions are effected, in the following form:

$$\left( \frac{p_b}{p_a} \right)^{\frac{1}{2}} = \frac{\epsilon_y}{\hbar_x} \cdot \left( \frac{mc^2}{\hbar\omega/m} \right)^{\frac{1}{2}} = \frac{\epsilon_y}{\epsilon_h} \cdot \left( \frac{2mc^2}{I} \right)^{\frac{1}{2}}.$$

$I$  is the interval between adjacent levels in the field  $H_z$ , and is naturally  $\ll mc^2$  for the usual  $H_z$ .

The discussion shows, in general, a demand for high  $H_z$  and  $N$ . Note therefore the formula for

$$N = \frac{l_2}{V_m} \cdot \frac{1}{2\pi} \cdot \frac{2\omega}{m} = \frac{l_2}{V_m} \cdot \frac{eH_z}{2\pi mc}.$$

Thus the demand is for large  $H_z$  and low  $V_m$ .

#### 4. - Conclusion.

The present discussion gives a description, essentially in terms of quantum mechanics, of an experiment which can detect the spin polarization of the electron in principle. It is clear that not only the wavepacket diffraction and the spin moment, but also the orbital motion and the full level structure requires a description in quantal terms.

It is necessary to mention again that the zeronos do not exist independently of the electromagnetic fields. Although the zeronos have definite energies and

a definite traverse velocity in the  $x$  direction, this does not mean that the fields act as a super-refrigerator, because the velocity of emergence of the electron, now, from the fields, will show a complete range of values. This corresponds to the indeterminacy of the  $x$ ,  $y$  velocities in the stationary states and the range of mean potentials of the zeron.

\* \* \*

The author wishes to acknowledge gratefully the advice of and discussions with Prof. L. ROSENFELD in connection with this paper.

#### RIASSUNTO (\*)

Nel presente lavoro si discute in termini di meccanica quantistica la polarizzazione di un fascio di elettroni in un'ipotetica esperienza, modificazione dell'esperimento di spettroscopia a radiofrequenza tipo Rabi. La struttura dei livelli dell'elettrone nel campo uniforme, e la sua discriminazione nei campi non omogenei, come pure le transizioni provocate nel campo uniforme, si discutono essenzialmente in termini quantici.

## Electronic Spectra of Mono-, Di- and Tri-Azines of the Naphtalene Series.

### I. Benzotriazine and its Derivatives.

M. SIMONETTA, G. FAVINI, S. CARRÀ and V. PIERPAOLI

*Istituto di Chimica Industriale  
Laboratorio di Chimica Fisica dell'Università - Milano*

(ricevuto il 3 Settembre 1956)

**Summary.** — The visible and near ultraviolet spectra of 1,2,4-benzotriazine and some of its derivatives have been obtained in cyclohexane and in methanol. Bands are assigned to  $n \rightarrow \pi^*$  and  $\pi \rightarrow \pi^*$  electron transitions and for  $\pi \rightarrow \pi^*$  bands in benzotriazine and pyridazine a theoretical treatment is given by the standard L.C.A.O. molecular orbital method and by Pariser and Parr's semiempirical method.

— —

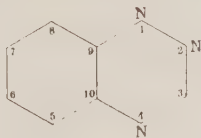
The ultraviolet spectra of the azines of the benzene series have been extensively studied in recent years both from experimental <sup>(1,2)</sup> and theo-

<sup>(1)</sup> F. M. UBER: *Journ. Chem. Phys.*, **9**, 777 (1941); F. M. UBER and R. WINTERS: *Journ. Am. Chem. Soc.*, **63**, 137 (1941); R. C. EVANS and F. Y. WISELOGLE: *Journ. Am. Chem. Soc.*, **67**, 60 (1945); H. SPONER and H. STÜCKLEN: *Journ. Chem. Phys.*, **14**, 101 (1946); H. SCHULL: *Journ. Chem. Phys.*, **17**, 295 (1949); H. SPONER and J. H. PRUSH: *Journ. Chem. Phys.*, **17**, 587 (1949); F. HALVERSON and R. HIRT: *Journ. Chem. Phys.*, **17**, 1165 (1949); C. LIN, E. LIEBER and J. P. HORWITZ: *Journ. Am. Chem. Soc.*, **76**, 427 (1954); H. C. BARANY, E. A. BRAUDE and M. PIANKA: *Journ. Chem. Soc.*, 1898 (1949); E. HERINGTON: *Disc. Faraday Soc.*, **9**, 26 (1950); J. RUSH and H. SPONER: *Journ. Chem. Phys.*, **20**, 1847 (1952); R. HIRT and D. SALLEY: *Journ. Chem. Phys.*, **21**, 1181 (1953); R. HIRT, F. HALVERSON and R. SCHMITT: *Journ. Chem. Phys.*, **22**, 1148 (1954); H. STEPHENSON: *Journ. Chem. Phys.*, **22**, 1077 (1954); R. HIRT and R. SCHMITT: *Journ. Chem. Phys.*, **23**, 600 (1955).

<sup>(2)</sup> F. HALVERSON and R. HIRT: *Journ. Chem. Phys.*, **19**, 711 (1951).

retical<sup>(2,3)</sup> viewpoint. As a result the bands present in these spectra were assigned to  $n \rightarrow \pi^*$  or  $\pi \rightarrow \pi^*$  electronic transitions (as defined by KASHA<sup>(4)</sup>), and the positions of maxima and the intensities of  $\pi \rightarrow \pi^*$  transitions correctly calculated.

We extended these investigations to the azines of the naphthalene series and in the present paper results are reported for 1,2,4-benzotriazine (I), 6-chloro- 6-methyl-, 6-methoxy-benzotriazine and the corresponding 3-carb-ethoxy derivatives.



(I)

(numbering used in the text is indicated).

## 1. - Experimental Procedure and Results.

All compounds were furnished by Prof. R. FUSCO<sup>(5)</sup>, whom we deeply thank, and were recrystallized or resublimed to a high degree of purity. Eastman Kodak Spectrograde cyclohexane and methanol were used as solvent. The spectra were obtained using a Beckmann quartz Spectrophotometer, model D.U., with a Tungsten lamp in the region 6000 to 3500 Å and with a Hydrogen lamp in the region 3500 to 2200 Å. Corex glass cells were

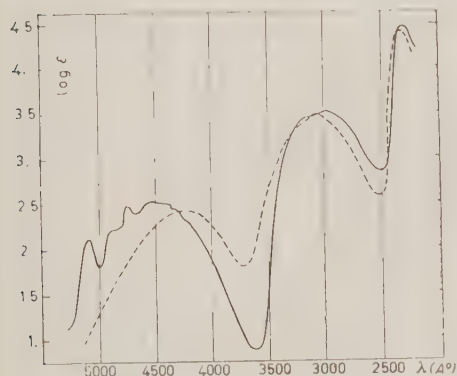


Fig. 1. - 1,2,4-benzotriazine in; cyclohexane —, methanol - - -.

<sup>(3)</sup> A. MACCOLL: *Journ. Chem. Soc.*, 670 (1946); G. NORDHEIM and H. SPONER: *Journ. Chem. Phys.*, **20**, 285 (1952); R. PARISER and R. PARR: *Journ. Chem. Phys.*, **21**, 767 (1953); D. DAVIES: *Trans. Faraday Soc.*, **51**, 449 (1955); M. DEWAR and L. PAOLONI: in the press.

<sup>(4)</sup> M. KASHA: *Disc. Faraday Soc.*, **9**, 14 (1950); see also J. PLATT: *Journ. Chem. Phys.*, **19**, 101 (1951).

<sup>(5)</sup> R. FUSCO and S. ROSSI: *Gazz. Chim. Ital.*, **86**, 484 (1956).



used in the visible region and quartz cells in the ultraviolet region, all of 1 cm light path length.

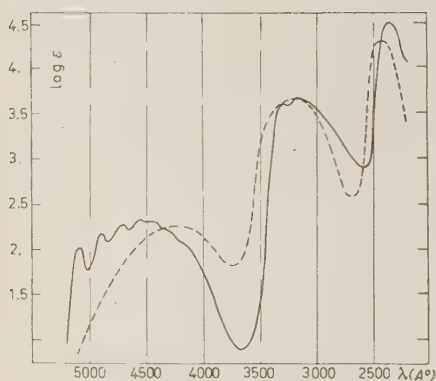


Fig. 2. — 6-chloro-1,2,4-benzotriazine in; cyclohexane —, methanol - - - -.

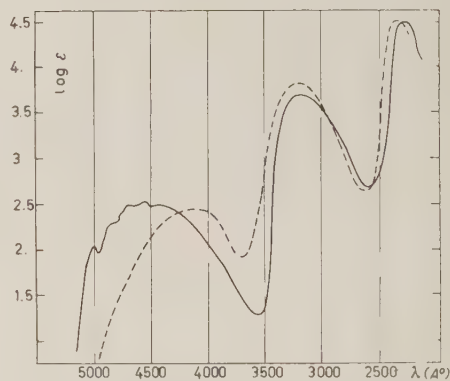


Fig. 3. — 6-methyl-1,2,4-benzotriazine in; cyclohexane —, methanol - - - -.

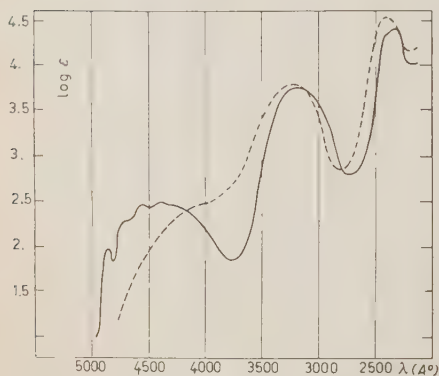


Fig. 4. — 6-methoxy-1,2,4-benzotriazine in; cyclohexane —, methanol - - - -.

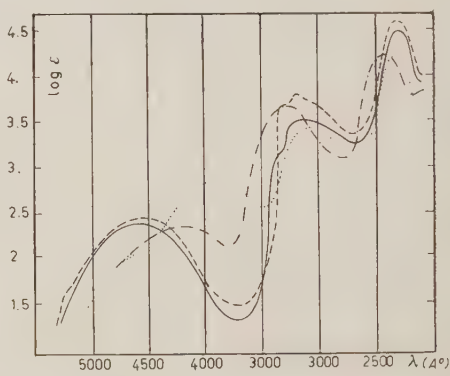


Fig. 5. — 3-carbethoxy-benzotriazine —; 6-chloro-3-carbethoxy-benzotriazine ····; 6-methyl-3-carbethoxy-benzotriazine - - -; 6-methoxy-3-carbethoxy-benzotriazine: in cyclohexane - · - ·.

The data are plotted in Figs. 1 to 5, as the log of the molar extinction versus wave length (in Å). Beer's law was used in the form  $\log_{10} I_0/I = C \cdot l \cdot \epsilon$  where  $I_0$  and  $I$  are the intensities of the incident and transmitted light,  $\epsilon$  is

the molar extinction,  $l$  is the cell path length in cm, and  $C$  is the concentration in moles per liter.

Also wave lengths and molar extinctions of the observed bands are collected in Tables I and II.

TABLE I. - Observed bands of benzotriazine and its derivatives.

Compounds	Solvent	Band origin					
		1 <sup>1</sup> $\pi \cdot \pi^*$		1 <sup>1</sup> $\pi \cdot \pi^*$		2 <sup>1</sup> $\pi \cdot \pi^*$	
		$\lambda_{\max}$ (Å)	$\log \epsilon$	$\lambda_{\max}$ (Å)	$\log \epsilon$	$\lambda_{\max}$ (Å)	$\log \epsilon$
1, 2, 4-benzotriazine	C	5 060	2,146	2 970	3,588	2 290	4,533
		4 930	2,325				
		4 740	2,500				
		4 580 (*)	2,532				
		4 460	2,505				
	M	4 380	2,446	3 050	3,435	2 310	4,455
6-chloro-1, 2, 4-benzotriazine	C	5 100	2,088	3 260	3,741	2 335	4,545
		4 930	2,280	3 155	3,779		
		4 760	2,468	3 115 (*)	3,787		
		4 610 (*)	2,538				
		4 500	2,518				
	M	4 350	2,465	3 180	3,765	2 355	4,337
6-methyl-1, 2, 4-benzotriazine	C	5 010	2,050	3 060	3,731	2 320	4,498
		4 800 (*)	2,321				
		4 690	2,514				
		4 530 (*)	2,568				
		4 420	2,531				
	M	4 240	2,528	3 150	3,775	2 350	4,525
6-methoxy-1,2,4-benzotriazine	C	4 840	1,954	3 240	3,832	2 400	4,439
		4 670 (*)	2,247				
		4 550	2,444				
		4 400 (*)	2,506				
		4 300	2,502				
	M	4 000 (*)	2,605	3 310	3,836	2 445	4,537

C = cyclohexane      M = methanol

(\*) Maximum with the highest absorption coefficient.

(+) Shoulder.

TABLE II. — Observed bands of 3-carbethoxy-benzotriazine and its derivatives.

Compounds	Sol-vent	Band origin					
		n- $\pi^*$		1 $^\circ$ $\pi$ - $\pi^*$		2 $^\circ$ $\pi$ - $\pi^*$	
		$\lambda_{\max}$ (Å)	log $\epsilon$	$\lambda_{\max}$ (Å)	log $\epsilon$	$\lambda_{\max}$ (Å)	log $\epsilon$
3-carbethoxy-1, 2, 4-benzotriazine	C	4600	2,481	3120	3,550	2380	4,543
6-chloro-3-carbethoxy-1, 2, 4-benzotriazine	C	4600	2,474	3325 3206 (*)	3,708 3,765	2420	4,613
6-methyl-3-carbethoxy-1, 2, 4-benzotriazine	C	3975	2,806	3140	3,490	2410	4,209
6-methoxy-3-carbethoxy-1, 2, 4-benzotriazine	C	4350	2,413	3350	3,685	2480	4,365

C= cyclohexane

(\*) Maximum with the highest absorption coefficient.

## 2. — Discussion.

All the spectra show three bands and have the same general character. The highest wave length band shows a marked blue shift from cyclohexane to methanol and can be classified as a « blue-shift » band (<sup>6</sup>).

Intensity considerations and the rapid loss of vibrational structure from cyclohexane to alcohol permit to assign this band to an n- $\pi^*$  electronic transition.

The second and third bands show high intensities and slight red shifts in the solvent sequence and are assigned to the first and second  $\pi$ - $\pi^*$  allowed transitions, analogous to similar bands in the diazines, *s*-triazines and *as*-triazines of the benzene series. The spectrum of *as*-triazine is unknown but from the spectra of diazines, benzodiazines and benzotriazines it may be predicted the existence of a n- $\pi^*$  band with maximum not far from 4000 Å and a  $\pi$ - $\pi^*$  band at about 2600-2700 Å. These positions of maxima are consistent with observations from the *s*-triazine, 2-amino-*s*-triazine and 3-amino-*as*-triazine spectra.

In 6-chloro-benzotriazine the two  $\pi$ - $\pi^*$  bands are shifted toward the red as usual for chlorination: however in all examined 6-substituted benzotriazines the  $\pi$ - $\pi^*$  bands are shifted to the red and a tentative explanation for this will

(<sup>6</sup>) H. McCONNELL: *Journ. Chem. Phys.*, **20**, 700 (1952).

be given later. Red shift is produced in all cases by the introduction of the carbethoxyl group in position 3.

Values from the spectra in methanol are used in this paper for comparison with theoretical results.

### 3. - Standard L.C.A.O. Molecular Orbital Treatment.

The simple LCAO molecular orbital calculations can be used to predict the frequency of the two longest wave-length  $\pi$ - $\pi^*$  transitions in spectra of conjugated molecules (<sup>7</sup>).

Standard LCAO M.O. calculations excluding overlap were performed for the benzotriazine molecule with the following values for coulomb integrals ( $\alpha$ ) and exchange integrals ( $\beta$ ):

$$\alpha_C = 0, \quad \alpha_N = -\beta, \quad \beta_{CN} = \beta_{CN} = \beta_{NN} = \beta.$$

The energy differences between the orbitals interested in the two transitions are:

$$\Delta E_1 = -0.893\beta \quad \text{and} \quad \Delta E_2 = -1.686\beta$$

and the related experimental values are 4.06 eV and 5.37 eV.

In Table III theoretical and experimental results are compared for some of the usually adopted  $\beta$  values.

TABLE III.

$\Delta E_1$ (eV)	$\Delta E_2$ (eV)	$-\beta$ (eV)	Reference
2.286	4.316	2.56	R. S. MULLIKEN ( <sup>8</sup> )
2.411	4.552	2.70	D. DAVIES ( <sup>3</sup> )
2.545	4.804	2.85	J. R. PLATT ( <sup>7</sup> )
2.590	4.889	2.90	present paper ( <sup>9</sup> )

Inclusion of overlap correction, according to PLATT (<sup>7</sup>), whose technique was shown by DAVIES (<sup>3</sup>) to give reliable results even for heterocyclic mole-

(<sup>7</sup>) J. R. PLATT: *Journ. Chem. Phys.*, **18**, 1168 (1950). For inclusion of overlap correction see also G. W. WHELAND: *Journ. Am. Chem. Soc.*, **63**, 2025 (1941).

(<sup>8</sup>) R. S. MULLIKEN: *Journ. Chim. Phys.*, **46**, 675 (1943).

(<sup>9</sup>) A M.O. calculation was performed, following identical prescriptions, for the pyridine molecule and  $\beta$  was calculated from  $\Delta E = -1.705\beta$  and the experimental value 4.95 eV.

cules, as far as orbital energies are concerned, seems to give no better agreement:  $\Delta E_1 = -0.743\beta$  and  $\Delta E_2 = -1.753\beta$ . It is clear, that no value of  $\beta$  can be found that gives agreement for both the transitions, since  $(\Delta E_2/\Delta E_1)_{\text{theor}}$

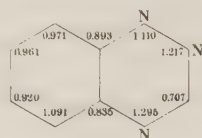
1.89 or 2.36 and  $(\Delta E_2/\Delta E_1)_{\text{exp.}} = 1.32$ .

The intensities of the two transitions were calculated by the method described by MULLIKEN and RIECKE<sup>(10)</sup>: the experimental and the semitheoretical values for the oscillator strength  $f$  are:

$$f_1 (\text{teor.}) = 0.23, \quad f_1 (\text{exp.}) = 0.10,$$

$$f_2 (\text{teor.}) = 0.56, \quad f_2 (\text{exp.}) = 0.43.$$

The  $\pi$ -electron charge distribution is as shown:



Unfortunately no direct substitution reactions are known, at present, to compare the reactivity at the different positions in the rings. We have seen that the introduction of a Cl, CH<sub>3</sub>, or OCH<sub>3</sub> group in position 6 produces a red shift of the two  $\pi$ - $\pi^*$  bands in benzotriazine spectra. The results of preliminary calculations are presented here, in which the influence on the spectra of the substituent was roughly taken care of, using different values for the Coulomb integrals of the carbon atom in position 6. Results are shown in Fig. 6 and 7. It is seen that both  $\Delta E_1$  and  $\Delta E_2$  versus  $\alpha$  curves show a maximum at  $\alpha = 0$  or very close to  $\alpha = 0$ ; electron-releasing or electron-attracting substituents always produce a red shift of the bands.

Calculations without overlap on 6-vinyl-benzotriazine may suggest that covalent resonance also produces red shifts: the calculated energy differences are  $\Delta E_1 = -0.746\beta$  and  $\Delta E_2 = -1.418\beta$ .

Perturbation theory calculations are on the way, to attack this problem and the 3-carbethoxy substitution red-shift problem: both seem to be interesting at present, since a new series of 6-substituted benzotriazines, and the corresponding carbethoxy derivatives, has been prepared<sup>(11)</sup>.

<sup>(10)</sup> R. S. MULLIKEN and C. A. RIECKE: *Repts. Prog. Phys.*, **8**, 231 (1941). See also PARISER and PARR<sup>(3)</sup>.

<sup>(11)</sup> R. FUSCO: Private communication.

Fig. 6.  $-x_i$  is the coefficient of  $\beta$  in the energy expression of the  $i$ -th molecular orbital:  $E_i = \alpha_c + x_i\beta$ ;  $\alpha$  = Coulomb integral of the carbon atom in position 6; both  $x_i$  and  $\alpha$  in  $\beta$  units.

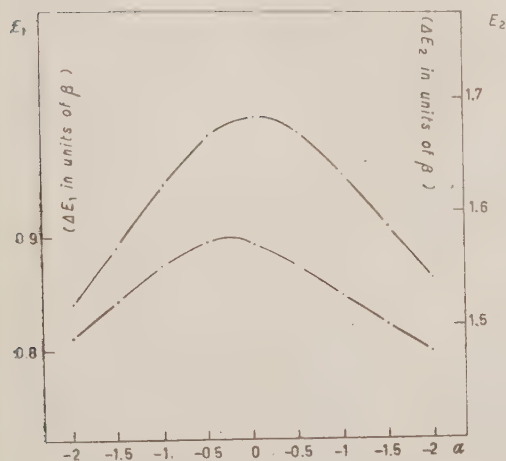
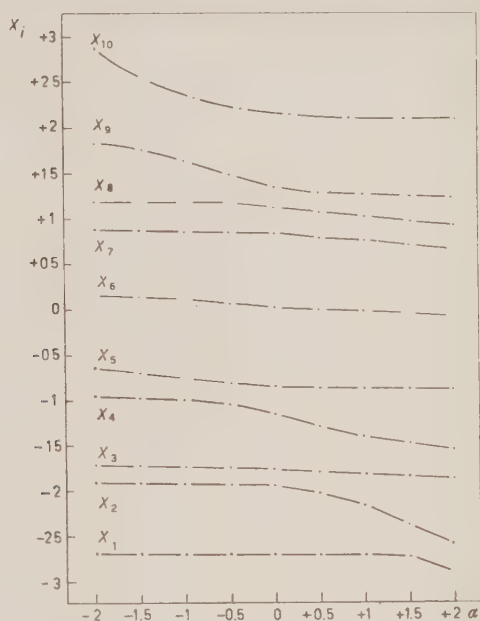


Fig. 7.  $-\Delta E_1 = x_6 - x_5$ ;  $\Delta E_2 = x_7 - x_5$ ;  $\alpha$  as in Fig. 6.



#### 4. - The Pariser and Parr Semiempirical Treatment.

In recent years a semiempirical theory for the correlation and prediction of the lower electronic absorption bands of complex unsaturated molecules has been developed <sup>(12)</sup>, which has been successfully tested on pyridine and di- and triazines of the benzene series <sup>(13)</sup>. We expected that this theory might offer the best method of attack to the analogous problems in the azines of the naphthalene series and that it might be worthwhile to take the risk and perform the rather lengthy and cumbersome calculations for the benzotriazine molecule. Calculations were performed following the lines given by PARISER and PARR <sup>(12,14)</sup>, with neglect of all penetration integrals as suggested for the more complex molecules <sup>(14)</sup> and with the usual values for ionization potentials: ( $W_N = -14.63$  eV and  $W_C = -11.22$  eV) and electron affinities ( $A_N = 2.36$  eV and  $A_C = 0.69$  eV) and for bond resonance integrals ( $\beta_{CC} = -2.39$  eV and  $\beta_{NC} = -2.576$  eV).

Integrals over atomic orbitals (Coulomb repulsion integrals:

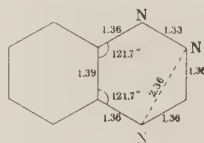
$$(pp|qq) = \int \varphi_p^*(1) \varphi_q^*(2) \frac{e^2}{r_{12}} \varphi_p(1) \varphi_q(2) dv_1 dv_2,$$

were evaluated graphically, from energy-distance curves drawn from the semiempirical values reported in Table II of the paper by PARISER and PARR <sup>(12)</sup> or by extrapolation. The Coulomb integrals are given by the formula:

$$\alpha_p = W_p - \sum_{q \neq p} (pp|qq).$$

The integrals ( $pp|pp$ ) were taken as: ( $pp|pp$ ) =  $-W_p - A_p$ .

The assumed geometry for the benzotriazine molecule was as follows <sup>(15)</sup>:



<sup>(12)</sup> R. PARISER and R. PARR: *Journ. Chem. Phys.*, **21**, 466 (1953).

<sup>(13)</sup> See R. PARISER and R. PARR <sup>(3)</sup>.

<sup>(14)</sup> For a brief outline of the method see R. PARISER: *Journ. Chem. Phys.*, **24**: 250 (1956).

<sup>(15)</sup> The benzene ring was assumed as a regular hexagon with C—C bond length 1.39 Å; the  $\widehat{CNC}$  angle value was taken from the value for phenazine, as determined by F. H. HERBSTEIN and G. M. J. SCHMIDT (*Acta Cryst.*, **8**, 406 (1955)); the N—N distance was estimated from the C—C value in benzene and the C—N value given by PARISER and PARR <sup>(13)</sup>.

Some choices are rather arbitrary, but it is easily seen that variations up to five per cent, or perhaps more, of the assumed bond distances and angles do not sensibly affect the final values.

One new basic quantity of the theory appears, the bond resonance integral for the two nitrogen atoms:  $\beta_{\text{NN}}$ . This quantity was evaluated empirically by us assuming, as usual in standard M.O. theory <sup>(16)</sup>, a rough proportionality to the overlap integral <sup>(17)</sup>; this assumption gives at the estimated N-N distance  $\beta$  equal to  $-1.67$  eV.

We checked, however, that  $\beta_{\text{NN}}$  values in the range  $-1$  to  $-3$  eV lead to satisfactory agreement between calculated quantities and experiment.

As starting molecular orbital we used naphthalene molecular orbitals, as given by PULLMAN and PULLMAN <sup>(18)</sup>:

$$\psi_0 = 0.3005 (\varphi_1 + \varphi_4 + \varphi_5 + \varphi_8) + 0.2307 (\varphi_2 + \varphi_3 + \varphi_6 + \varphi_7) + 0.4614 (\varphi_9 + \varphi_{10})$$

$$\psi_1 = 0.2628 (\varphi_1 + \varphi_4 - \varphi_5 - \varphi_8) + 0.4253 (\varphi_2 + \varphi_3 - \varphi_6 - \varphi_7)$$

$$\psi_2 = 0.3996 (\varphi_1 - \varphi_4 - \varphi_5 + \varphi_8) + 0.1735 (\varphi_2 - \varphi_3 - \varphi_6 + \varphi_7) + 0.3470 (\varphi_9 - \varphi_{10})$$

$$\psi_3 = 0.4083 (\varphi_2 + \varphi_3 + \varphi_6 + \varphi_7) - 0.4083 (\varphi_9 + \varphi_{10})$$

$$\psi_4 = 0.4253 (\varphi_1 - \varphi_4 + \varphi_5 - \varphi_8) - 0.2628 (\varphi_2 - \varphi_3 + \varphi_6 - \varphi_7)$$

$$\psi_5 = 0.4253 (\varphi_1 + \varphi_4 - \varphi_5 - \varphi_8) - 0.2628 (\varphi_2 + \varphi_3 - \varphi_6 - \varphi_7)$$

$$\psi_6 = -0.4083 (\varphi_2 - \varphi_3 - \varphi_6 + \varphi_7) + 0.4083 (\varphi_9 - \varphi_{10})$$

$$\psi_7 = 0.3996 (\varphi_1 + \varphi_4 + \varphi_5 + \varphi_8) - 0.1735 (\varphi_2 + \varphi_3 + \varphi_6 + \varphi_7) - 0.3470 (\varphi_9 + \varphi_{10})$$

$$\psi_8 = 0.2628 (\varphi_1 - \varphi_4 + \varphi_5 - \varphi_8) - 0.4253 (\varphi_2 - \varphi_3 + \varphi_6 - \varphi_7)$$

$$\psi_9 = 0.3005 (\varphi_1 - \varphi_4 - \varphi_5 + \varphi_8) - 0.2307 (\varphi_2 - \varphi_3 - \varphi_6 + \varphi_7) - 0.4614 (\varphi_9 - \varphi_{10})$$

It is usually assumed that any molecular orbitals of the proper form may be employed as starting orbitals, since configuration interaction will compensate deviations from the best molecular orbitals.

We wish to point out that, in practice, interaction is limited to a few con-

<sup>(16)</sup> See, for example, G. W. WHELAND and P. S. K. CHEN: *Journ. Chem. Phys.*, **24**, 67 (1956).

<sup>(17)</sup> Values for overlap integrals were taken from R. S. MULLIKEN, C. A. RIEKE, D. ORLOFF and H. ORLOFF: *Journ. Chem. Phys.*, **17**, 1248 (1949).

<sup>(18)</sup> B. PULLMAN and A. PULLMAN: *Les théories électroniques de la chimie organique* (Paris, 1952).

figurations, so that care must be taken that the choice of the starting orbitals will lead to the right choice of configurations. This condition seems to be satisfied in our case. The included configurations were: ground state configuration (with two electrons in each of the orbitals  $\psi_0, \psi_1, \psi_2, \psi_3, \psi_4$ ), singlets and triplets arising through the promotion of one electron from  $\psi_3$  or  $\psi_4$  to  $\psi_5$  or  $\psi_6$ . Configurations were labelled according to PARISER and PARR'S symbolism:  $V_0, V_{35}, V_{36}, V_{45}, V_{46}, T_{35}, T_{36}, T_{45}, T_{46}$ . Interaction leads to a secular equation of the fifth order and one of the fourth; the matrix elements are given in appendix. The equations were numerically solved <sup>(19)</sup> and the obtained energy values (in eV) are:

$$E_0 = -0.1595, \quad E_1 = 3.7040, \quad E_2 = 5.4463, \quad E_3 = 6.6849, \quad E_4 = 7.3863,$$

for the singlets and

$$E'_1 = 2.7853, \quad E'_2 = 3.2790, \quad E'_3 = 4.2342, \quad E'_4 = 5.0592 \text{ for the triplet states}$$

which give for the two lower allowed  $\pi$ - $\pi^*$  transitions:

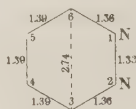
$$\Delta E_1 = 3.86 \text{ eV} \quad \text{and} \quad \Delta E_2 = 5.61 \text{ eV},$$

in good agreement with experiment ( $\Delta E_1 = 4.06, \Delta E_2 = 5.37$ ).

For all states the corresponding wave functions were calculated (see Appendix) and the theoretical oscillator strengths for the first and second transitions are:

$$f_1 = 0.14, \quad f_2 = 0.09 \quad (20).$$

We wanted to test the assumed value for  $\beta_{NN}$  and the approximations on a different molecule, and our choice was the pyridazine molecule. The numbering and the assumed geometry were:



<sup>(19)</sup> H. MARGENAU and G. M. MURPHY: *The Mathematics of Physics and Chemistry* (New York, 1949).

<sup>(20)</sup> Some of the final results with different values of  $\beta_{NN}$  were:

$$\text{for } \beta_{NN} = -2.2, \quad \Delta E_1 = 3.90, \quad \Delta E_2 = 5.74, \quad f_1 = 0.15, \quad f_2 = 0.03,$$

$$\text{for } \beta_{NN} = -3.0, \quad \Delta E_1 = 4.03, \quad \Delta E_2 = 5.82, \quad f_1 = 0.18, \quad f_2 = 0.11.$$

TABLE IV. — *Energy formulas for pyridazine (\*)*.

Quantity (**)	(11/11)	(33/33)	(11/22)	(11/33)	(11/44)	(11/55)	(11/66)	(33/44)	(33/55)	(33/66)
	72	72	72	72	72	72	72	72	72	72
$E_{V_{14}} - E_{V_0} - \Delta I_{14}$	15	- 9	35	- 36	46	30	- 20	15	- 36	- 40
$E_{V_{33}} - E_{V_0} - \Delta I_{33}$	- 9	15	- 13	12	- 50	- 66	28	15	12	56
$E_{V_{13}} - E_{V_0} - \Delta I_{13}$	1	17	- 11	8	2	2	8	- 3	8	- 32
$E_{V_{24}} - E_{V_0} - \Delta I_{24}$	9	9	- 3	0	- 30	18	0	- 3	0	0
$\frac{3}{2}(V_3/V_{14}) - 3I_{14}$	18	- 18	48	36	0	0	12	- 60	- 36	0
$\frac{3}{2}(V_0/V_{23}) - 3I_{23}$	18	- 18	24	36	0	0	60	- 84	- 36	0
$(V_{14}/V_{23})$	3	3	9	0	- 18	- 6	0	9	0	0
$(V_{13}/V_{24})$	3	3	- 3	24	- 18	18	- 24	- 27	24	0
$E_{T_{14}} - E_{V_0} - \Delta I_{14}$	9	- 15	29	- 36	58	42	- 20	9	- 36	- 40
$E_{T_{33}} - E_{V_0} - \Delta I_{33}$	- 15	9	- 19	12	- 38	- 54	28	9	12	56
$E_{T_{13}} - E_{V_0} - \Delta I_{13}$	- 1	17	- 9	- 8	6	- 2	24	15	- 8	0
$E_{T_{24}} - E_{V_0} - \Delta I_{24}$	- 9	- 9	15	0	6	- 18	0	15	0	0
$(T_{14}/T_{23})$	- 3	- 3	3	0	- 6	6	0	3	0	0
$(T_{13}/T_{24})$	- 3	- 3	3	0	- 6	6	0	3	0	0

(\*) Numbers in each row are the coefficients of the atomic orbital integrals at the top of columns in the formula for the energy quantity given in the first column.

(\*\*) Here:

$$\Delta I_{14} = I_{44} - I_{11} = \frac{1}{3}(\alpha_1 + \alpha_4 - 2\alpha_3 - \beta_{NN} - 2\beta_{NO} - 3\beta_{CO})$$

$$\Delta I_{33} = I_{33} - I_{33} = -\frac{1}{3}(\alpha_1 + \alpha_4 - 2\alpha_3 + \beta_{NN} + 2\beta_{NO} + 3\beta_{CO})$$

$$\Delta I_{13} = I_{33} - I_{11} = \frac{1}{3}(\beta_{NN} - 4\beta_{NO} - 3\beta_{CO})$$

$$\Delta I_{24} = I_{44} - I_{33} = -\beta_{NN} - \beta_{CO}$$

$$I_{14} = \frac{1}{2\sqrt{3}}(\alpha_1 - \alpha_4 - \beta_{NN} + 2\beta_{NO} - \beta_{CO})$$

$$I_{33} = \frac{1}{2\sqrt{3}}(\alpha_1 - \alpha_4 + \beta_{NN} - 2\beta_{NO} + \beta_{CO})$$

$$\alpha_1 + \alpha_4 - 2\alpha_3 = W_N - W_O - (11/22) + (11/33) + (11/66) + (33/55) + 2[(33/66) - (11/44) - (11/55)]$$

$$\alpha_1 - \alpha_4 = W_N - W_O - (11/22) - (11/33) - (11/66) + (33/55) + 2(33/44).$$

The starting molecular orbitals were benzene orbitals <sup>(21)</sup>:

$$\psi_0 = \frac{1}{\sqrt{6}} (\varphi_1 + \varphi_2 + \varphi_3 + \varphi_4 + \varphi_5 + \varphi_6),$$

$$\psi_1 = \frac{1}{\sqrt{12}} (\varphi_1 - \varphi_2 - 2\varphi_3 - \varphi_4 + \varphi_5 + 2\varphi_6),$$

$$\psi_2 = \frac{1}{\sqrt{4}} (\varphi_1 + \varphi_2 - \varphi_4 - \varphi_5),$$

$$\psi_3 = \frac{1}{\sqrt{12}} (\varphi_1 + \varphi_2 - 2\varphi_3 + \varphi_4 + \varphi_5 - 2\varphi_6),$$

$$\psi_4 = \frac{1}{\sqrt{4}} (\varphi_1 - \varphi_2 - \varphi_4 - \varphi_5),$$

$$\psi_5 = \frac{1}{\sqrt{6}} (\varphi_1 - \varphi_2 + \varphi_3 - \varphi_4 + \varphi_5 - \varphi_6),$$

and the interacting configurations were:  $V_0, V_{13}, V_{14}, V_{23}, V_{21}, T_{13}, T_{14}, T_{23}, T_{21}$ . The singlets give one third order and one second order equations, the triplets two second order; matrix elements are given in Table IV.

By numerical solution we obtained the following energy values (in eV):

$$E_{0(S)} = -0.4076, \quad E_{1(S)} = 4.7411,$$

$$E_{2(A)} = 5.0836, \quad E_{2(A)} = 7.0472,$$

$$E_{4(S)} = 7.5806$$

$$E'_{1(A)} = 3.3871, \quad E'_{2(S)} = 3.6623,$$

$$E'_{3(A)} = 4.7626, \quad E'_{4(S)} = 5.4341,$$

where the subscripts (S) and (A) refer to symmetry properties of the corresponding wave functions; expressions for these are:

$$\psi_0 = 0.96725\psi_{V_0} + 0.25061\psi_{V_{14}} + 0.04020\psi_{V_{23}}$$

$$\psi_1 = 0.19418\psi_{V_0} - 0.83261\psi_{V_{14}} + 0.51870\psi_{V_{23}}$$

$$\psi_2 = 0.49471\psi_{V_{13}} + 0.86906\psi_{V_{21}}$$

<sup>(21)</sup> H. EYRING, J. WALTER and G. KIMBALL: *Quantum Chemistry* (New York, 1949).

$$\psi_3 = 0.86906\psi_{v_{13}} - 0.49471\psi_{v_{24}}$$

$$\psi_4 = 0.16348\psi_{v_0} - 0.49392\psi_{v_{14}} - 0.85403\psi_{v_{23}}$$

$$\psi'_1 = 0.19457\psi_{x_{13}} + 0.98088\psi_{x_{24}}$$

$$\psi'_2 = 0.98872\psi_{x_{14}} + 0.14975\psi_{x_{23}}$$

$$\psi'_3 = 0.98088\psi_{x_{13}} - 0.19457\psi_{x_{24}}$$

$$\psi'_4 = 0.14975\psi_{x_{14}} - 0.98872\psi_{x_{23}}.$$

For the first  $\pi$ - $\pi^*$  electronic transition  $\Delta E$  is equal to 5.15 eV and  $f$  to 0.027. As experimental values (2) are  $\Delta E = 5.00$  eV and  $f = 0.019$ ; the agreement is quite satisfactory.

The value  $\beta_{\text{NC}} = -2.576$  eV at 1.36 Å N—C distance adopted here was evaluated by PARISER and PARR (12) on the assumption that the lowest singlet  $\pi$ - $\pi^*$  transition in the (at that time unknown) absorption spectra of *s*-triazine had a maximum at 2340 Å. Later HIRT, HALVERSON and SCHMITT (1) obtained the spectra for *s*-triazine and the maximum was found at 2220 Å: the authors pointed out that this new values yields  $\beta_{\text{NC}} = -2.74$  eV: however the general results of PARISER and PARR's calculations do not seem to be seriously affected by the change. We introduced the new  $\beta_{\text{NC}}$  value in our calculations for pyridazine and benzotriazine, and the principal results are:

$$\text{pyridazine:} \quad \Delta E_1 = 5.38, \quad f = 0.022,$$

$$\text{benzotriazine:} \quad \Delta E_1 = 3.97, \quad f_1 = 0.13,$$

$$\Delta E_2 = 5.66, \quad f_2 = 0.13.$$

Agreement with experiment is more or less unchanged and we suggest that the old value is retained on the basis of the general agreement with experiment for the whole set of azine molecules.

\* \* \*

We are indebted to the Italian Consiglio Nazionale delle Ricerche for a grant.



## APPENDIX

TABLE I-A. - *Energy form*

	$\frac{E_{V_{45}} - E_N}{- \Delta I_{45}}$	$\frac{E_{V_{46}} - E_N}{- \Delta I_{46}}$	$\frac{E_{V_{55}} - E_N}{- \Delta I_{55}}$	$\frac{E_{V_{56}} - E_N}{- \Delta I_{56}}$	$\frac{1}{\sqrt{2}} \left( \frac{V_0}{V_{45}} \right) - I_{45}$	$\frac{1}{\sqrt{2}} \left( \frac{V_0}{V_{46}} \right) - I_{46}$	$\frac{1}{\sqrt{2}} \left( \frac{V_0}{V_{55}} \right) - I_{55}$
(11/11)	0.07021	-0.12052	0.13203	0.02779	-0.03453	-0.05365	0.05
(33/33)	0.07975	0.16669	-0.13215	0.13896	0.03453	-0.05365	0.05
(11/22)	0.08698	-0.03243	0.13405	0.=	0.11182	-0.04439	-0.17
(11/33)	0.02498	-0.11339	0.05309	0.=	0.24992	-0.10728	-0.17
(11/44)	-0.06521	-0.29616	0.42726	0.=	0.=	0.=	0.=
(11/55)	-0.33120	-0.69271	0.75411	0.=	0.=	0.=	0.=
(11/66)	0.04966	-0.22679	0.10618	0.=	0.=	0.21458	0.21
(11/77)	-0.07402	-0.18884	0.14412	0.=	0.=	0.18510	0.24
(11/88)	0.13088	-0.72344	0.72344	0.=	0.=	0.=	0.=
(11/99)	0.07577	0.15608	-0.03423	0.03440	-0.11182	-0.42004	-0.22
(11/1010)	0.=	-0.08871	-0.03191	0.=	0.=	0.=	0.=
(22/44)	0.02498	-0.11339	0.05309	0.=	-0.24992	-0.10728	-0.10
(22/55)	0.02498	-0.11340	0.05309	0.=	-0.24992	-0.10729	-0.10
(22/66)	-0.00707	0.16299	-0.20455	-0.11473	0.=	0.=	0.=
(22/77)	0.00954	0.12616	-0.24129	0.05558	-0.13813	0.=	0.=
(22/88)	-0.03701	-0.09442	0.07206	0.=	0.11182	-0.09255	-0.12
(22/99)	0.=	0.25265	-0.27567	0.05558	-0.06907	-0.10730	-0.10
(22/1010)	0.=	0.29283	-0.23553	-0.08642	-0.06907	0.12023	0.09
(33/55)	-0.03701	-0.09442	0.07206	0.=	-0.11182	-0.09255	-0.12
(33/66)	0.00954	0.12616	-0.24129	0.0558	+0.13813	0.=	0.=
(33/77)	-0.00707	0.16299	-0.20455	-0.11473	0.=	0.=	0.=
(33/88)	0.02498	-0.11340	0.05309	0.=	0.24993	-0.10729	-0.10
(33/99)	0.=	0.29283	-0.23553	-0.08642	0.06907	-0.12023	-0.09
(33/1010)	0.=	0.25265	-0.27567	0.05558	0.06907	-0.10730	-0.10
(55/66)	0.15410	0.54332	-0.14668	0.04082	0.=	0.46443	0.39
(55/77)	0.04996	0.18980	-0.47708	0.11116	0.=	0.42916	0.42
(55/88)	-0.06521	0.28951	-0.04380	-0.17284	0.=	0.24046	0.18

(\*) Numbers in columns 2 to 15 are the coefficients of the integrals indicated in the first column in

benzotriazine (singlets) (\*)

$\begin{matrix} V_{01} V_{36} \\ - I_{36} \end{matrix}$	$(V_{45}, V_{46}) - I_{56}$	$(V_{35}, V_{33}) + I_{34}$	$(V_{45}, V_{36})$	$(V_{46}, V_{35})$	$(V_{16}, V_{36}) - I_{34}$	$(V_{35}, V_{36}) - I_{56}$
0.08335	0.06106	-0.04624	0.01151	0.01151	-0.03576	0.07154
0.08335	-0.06106	0.04624	0.03454	0.03454	0.03576	-0.07154
0.16668	0.11195	-0.10262	-0.06031	0.=	-0.04439	0.17018
0.16668	-0.12669	0.08788	0.06031	0.=	0.10728	-0.10728
0.=	0.=	0.=	0.=	0.=	0.=	0.=
0.=	0.=	0.=	0.=	0.=	0.=	0.=
0.=	0.=	0.=	0.12062	0.=	0.=	0.=
0.=	0.=	0.=	-0.12062	0.=	0.=	0.=
0.=	0.=	0.=	0.=	0.=	0.=	0.=
0.16668	-0.11195	0.10262	-0.20395	0.06908	0.04439	-0.17018
0.=	0.=	0.=	0.12062	0.=	0.=	0.=
0.16668	0.12669	-0.08788	0.06031	0.=	-0.10728	0.10728
0.16668	0.12669	-0.08788	0.06031	0.=	-0.10729	0.10729
0.=	0.18687	-0.24231	-0.06908	-0.06908	-0.30518	0.12401
0.33337	0.=	0.=	0.06908	-0.02303	0.=	0.=
0.16668	0.06380	-0.15077	-0.06031	0.=	-0.09255	0.12202
0.33322	0.10730	-0.10730	0.02303	0.=	-0.08941	0.12518
0.00016	0.12023	-0.09438	-0.02303	0.=	-0.14804	0.06657
0.16668	-0.06380	0.15077	-0.06031	0.=	0.09255	-0.12202
0.33337	0.=	0.=	0.06908	-0.02303	0.=	0.=
0.=	-0.18687	0.24231	-0.06908	-0.06908	0.30518	-0.12401
0.16668	-0.12669	0.08788	0.06031	0.=	0.10729	-0.10729
0.00016	-0.12023	0.09438	-0.02303	0.=	0.14804	-0.06657
0.33322	-0.10730	0.10730	0.02303	0.=	0.08941	-0.12519
0.=	0.=	0.=	-0.26426	0.06908	0.=	0.=
0.=	0.=	0.=	0.28728	0.=	0.=	0.=
0.=	0.=	0.=	-0.04605	0.=	0.=	0.=

\* Values for the energy quantity given at the top of each column.

TABLE II-A. — *Energy form*

	$E_{T_{15}} - E_N - A_{I_{45}}$	$E_{T_{44}} - E_N - A_{I_{44}}$	$E_{T_{35}} - E_N - A_{I_{35}}$	$E_{T_{38}} - E_N - A_{I_{38}}$
(11/11)	— 0.07021	0.14355	0.10901	— 0.02779
(33/33)	— 0.07974	0.09761	— 0.20123	— 0.13896
(11/22)	0.13694	0.03243	0.13405	0.
(11/33)	— 0.02498	0.11339	0.05309	0.
(11/44)	0.06566	— 0.29616	0.42726	0. —
(11/55)	0.06946	0.69271	0.75411	0. —
(11/66)	— 0.04997	0.22679	0.10618	0.
(11/77)	0.02593	— 0.18884	0.14412	0.
(11/88)	0.13087	0.72344	0.72344	0.
(11/99)	0.04407	0.11002	— 0.08029	0.14556
(11/1010)	0. —	— 0.08871	0.03191	0.
(22/44)	— 0.02498	— 0.11339	0.05309	0.
(22/55)	— 0.02498	— 0.11340	0.05309	0.
(22/66)	0.01201	0.20904	— 0.15849	— 0.00356
(22/77)	— 0.00954	0.17221	0.19524	— 0.05558
(22/88)	0.01296	0.09442	0.07206	0. =
(22/99)	0. =	0.25265	0.27567	— 0.05558
(22/1010)	0. —	0.29283	0.23553	— 0.02475
(33/55)	0.01296	0.09442	0.07206	0.
(33/66)	— 0.00954	0.17221	0.19524	0.05558
(33/77)	0.01201	0.20904	— 0.15849	— 0.00356
(33/88)	0.02498	— 0.11340	0.05309	0. =
(33/99)	0. —	0.29283	0.23553	— 0.02475
(33/1010)	0. =	0.25265	0.27567	— 0.05558
(55/66)	0.27312	0.49727	— 0.19273	0.26315
(55/77)	— 0.04997	0.18980	— 0.47708	— 0.11117
(55/88)	0.06566	0.28951	— 0.04380	— 0.04950

(\*) Numbers in columns 2 to 15 are the coefficients of the integrals indicated in the first column 1

*benzotriazine (triplets) (\*)*

$(T_{46}) - I_{56}$	$(T_{45}/T_{35}) + I_{34}$	$(T_{45}/T_{36})$	$(T_{46}/T_{35})$	$(T_{46}/T_{36}) + I_{34}$	$(T_{35}/T_{36}) - I_{56}$
0.04624	-0.06106	-0.01151	-0.01151	-0.07154	0.03576
0.04624	0.06106	-0.03454	-0.03454	0.07154	-0.03576
0.15077	-0.06380	0. =	0. =	-0.04439	0.17018
0.08788	0.12669	0. =	0. =	0.10728	-0.10728
0. =	0. =	0. =	0. =	0. =	0. =
0. =	0. =	0. =	0. =	0. =	0. =
0. =	0. =	0. =	0. =	0. =	0. =
0. =	0. =	0. =	0. =	0. =	0. =
0. =	0. =	0. =	0. =	0. =	0. =
0.15077	0.06380	0.02303	0.02303	0.04439	0.17018
0. =	0. =	0. =	0. =	0. =	0. =
0.08788	-0.12669	0. =	0. =	0.10728	0.10728
0.08788	0.12669	0. =	0. =	-0.10729	0.10729
-0.21651	0.21267	-0.02303	-0.02303	0.23363	0.19556
0. =	0. =	0.02303	0.02303	0. =	0. =
0.10262	0.11195	0. =	0. =	0.09255	0.12202
0.10730	-0.10730	0. =	0. =	0.12518	0.08941
0.12023	-0.09438	0. =	0. =	0.11226	0.10234
-0.10262	0.11195	0. =	0. =	0.09255	0.12202
0. =	0. =	0.02303	0.02303	0. =	0. =
-0.21651	0.21267	-0.02303	-0.02303	0.23366	-0.19556
-0.08788	0.12669	0. =	0. =	0.10729	0.10729
-0.12023	0.09438	0. =	0. =	0.11226	0.10234
-0.10730	0.10730	0. =	0. =	0.12518	0.08941
0. =	0. =	0.02303	0.02303	0. =	0. =
0. =	0. =	0. =	0. =	0. =	0. =
0. =	0. =	0. =	0. =	0. =	0. =

= for the energy quantity given at the top of each column.

TABLE III-A. — *Benzotriazine: core integrals and Coulomb integrals.*

$$\begin{aligned}
I_{I_{45}} &= -0.447075\beta_{NN} - 0.17082\beta_{NC} - 0.617895\beta_{CC} . \\
I_{I_{46}} &= -0.18088(\alpha_1 + \alpha_4 + \alpha_5 + \alpha_8) + 0.097645(\alpha_2 + \alpha_3 + \alpha_6 + \alpha_7) - 0.166709(\alpha_9 + \alpha_{10}) - \\
&\quad - 0.223538\beta_{NN} - 0.418828\beta_{NC} - 0.975783\beta_{CC} . \\
I_{I_{35}} &= 0.18088(\alpha_1 + \alpha_4 + \alpha_5 + \alpha_8) - 0.097645(\alpha_2 + \alpha_3 + \alpha_6 + \alpha_7) - 0.166709(\alpha_9 + \alpha_{10}) - \\
&\quad - 0.223538\beta_{NN} - 0.418828\beta_{NC} - 0.975783\beta_{CC} . \\
I_{I_{36}} &= -0.666836\beta_{NC} - 1.333671\beta_{CC} . \\
I_{45} &= 0.18088(\alpha_1 - \alpha_4 - \alpha_5 + \alpha_8) - 0.069064(\alpha_2 - \alpha_3 - \alpha_6 + \alpha_7) . \\
I_{46} &= -0.107301(\alpha_2 + \alpha_3 - \alpha_6 - \alpha_7) - 0.17365\beta_{NN} + 0.388252\beta_{NC} - 0.214602\beta_{CC} . \\
I_{35} &= -0.107301(\alpha_2 + \alpha_3 - \alpha_6 - \alpha_7) + 0.17365\beta_{NN} - 0.214602\beta_{NC} + 0.040952\beta_{CC} . \\
I_{36} &= -0.166709(\alpha_2 - \alpha_3 - \alpha_6 + \alpha_7 + \alpha_9 - \alpha_{10}) . \\
I_{56} &= 0.107301(\alpha_2 - \alpha_3 + \alpha_6 - \alpha_7) - 0.17365\beta_{NN} + 0.17365\beta_{NC} . \\
I_{34} &= 0.107301(\alpha_2 - \alpha_3 + \alpha_6 - \alpha_7) + 0.17365\beta_{NN} - 0.17365\beta_{NC} .
\end{aligned}$$

$$\alpha_1 = W_N - 47.32 \text{ eV} \qquad \alpha_6 = W_C - 41.11 \text{ eV}$$

$$\alpha_2 = W_N - 43.01 \text{ »} \qquad \alpha_7 = W_C - 41.18 \text{ »}$$

$$\alpha_3 = W_C - 43.93 \text{ »} \qquad \alpha_8 = W_C - 46.56 \text{ »}$$

$$\alpha_4 = W_N - 47.08 \text{ »} \qquad \alpha_9 = W_C - 54.61 \text{ »}$$

$$\alpha_5 = W_C - 46.54 \text{ »} \qquad \alpha_{10} = W_C - 54.54 \text{ »}$$

TABLE IV-A. — *Benzotriazine: wave functions and state energies (\*)*.

	$\psi_{V_0}$	$\psi_{V_{45}}$	$\psi_{V_{46}}$	$\psi_{V_{35}}$	$\psi_{V_{36}}$	Energy (eV)
$\psi_0$	0.98351	− 0.04926	0.00687	− 0.14175	− 0.10072	− 0.1595
$\psi_1$	0.13061	− 0.11981	− 0.43841	0.87850	0.06808	3.7040
$\psi_2$	0.11112	0.80446	0.08479	0.09011	0.57024	5.4463
$\psi_3$	0.02745	0.12713	0.80943	0.44939	− 0.35490	6.6849
$\psi_4$	0.05009	− 0.57070	0.36774	0.04029	0.73139	7.3863

		$\psi_{T_{45}}$	$\psi_{T_{46}}$	$\psi_{T_{35}}$	$\psi_{T_{36}}$	Energy (eV)
$\psi_1'$	—	0.09717	− 0.03120	− 0.95076	− 0.29263	2.7853
$\psi_2'$	—	0.95665	0.24263	0.04233	0.15542	3.2790
$\psi_3'$	—	0.07090	0.26532	0.28123	− 0.91950	4.2342
$\psi_4'$	—	0.26524	− 0.93278	0.12264	− 0.21103	5.0592

(\*) Energies are with reference to zero energy for  $V_0$ . Each row gives the coefficients of the configurational functions on the top of columns in the final wave functions listed in the first column.

## RIASSUNTO

Sono stati esaminati gli spettri di assorbimento nel visibile e nell'ultravioletto in cicloesano e in metanolo dei seguenti composti: 1,2,4-benzotriazina; 6-cloro-, 6-metil-, 6-metossi-1,2,4-benzotriazina; 3-carbetossi-benzotriazina; 6-cloro-, 6-metil-, 6-metossi-3-carbetossi-benzotriazina. In ciascun spettro sono state messe in evidenza tre bande, che sono state assegnate ad una transizione elettronica  $n \rightarrow \pi^*$  e a due transizioni  $\pi \rightarrow \pi^*$ . Per le transizioni  $\pi \rightarrow \pi^*$  della benzotriazina e della piridazina la posizione dei massimi e l'intensità sono state calcolate sia con il metodo degli orbitali molecolari standard, che con il metodo semiempirico di Pariser e Parr. Si è indagato sull'influenza dei sostituenti in posizione 6 sullo spostamento dei massimi  $\pi \rightarrow \pi^*$ .



## Dispersion Relations for Photoproduction of Mesons.

E. CORINALDESI

*Department of Natural Philosophy, The University of Glasgow*

(ricevuto il 6 Settembre 1956)

**Summary.** — The Feynman amplitude for the reaction  $\gamma + \text{nucleon} \rightarrow \pi + \text{nucleon}$  is simply related to a causal amplitude which satisfies dispersion relations. These are derived in the «natural» frame. The connection with the amplitudes in the centre of mass frame is discussed in detail.

### 1. — Introduction.

During the last two years a copious amount of work has been done on the use of dispersion relations in scattering problems. This seems to be a very promising line of investigation, which may have far-reaching consequences.

While at the outset the construction of dispersion relations appeared to be possible only for the forward scattering amplitude <sup>(1)</sup>, generalized dispersion relations were later discovered <sup>(2,3)</sup> for pion-nucleon scattering at any angle.

The purpose of the present paper is to establish generalized dispersion relations for photoproduction of mesons (i.e. the reaction:  $\gamma + \text{nucleon} \rightarrow \text{meson} + \text{nucleon}$ ), which is but a trivial extension of the work quoted in references <sup>(2)</sup> and <sup>(3)</sup>.

<sup>(1)</sup> Cf., e.g., M. L. GOLDBERGER: *Phys. Rev.*, **99**, 979 (1955) and M. L. GOLDBERGER, H. MIYAZAWA and R. OEHME: *Phys. Rev.*, **99**, 986 (1956).

<sup>(2)</sup> R. OEHME: *Phys. Rev.*, **100**, 1503 (1955); **102**, 1174 (1956); A. SALAM: *Nuovo Cimento*, **3**, 424 (1956); A. SALAM and W. GILBERT: *Nuovo Cimento*, **3**, 607 (1956).

<sup>(3)</sup> M. L. GOLDBERGER: *Talk at Midwest Conference of Theoretical Physics*, Iowa City, March 1956. It is stated in the report (kindly lent to us by the Birmingham group) that Profs. NAMBU, CHEW, LOW and GOLDBERGER are also studying dispersion relations for photoproduction.

We shall go as far as discussing fully the connection between the photo-production amplitude in the «natural» frame <sup>(4)</sup>, for which the dispersion relations are particularly simple, and that in the centre of mass frame. Numerical calculations and a discussion of the experimental data will be the object of a subsequent paper.

## 2. — Notation and Invariant Parameters.

We shall denote by  $k$ ,  $l$ ,  $p$  and  $q$  the 4-momenta of the photon, the meson, and of the initial and final nucleons, respectively. Thus <sup>(5)</sup>

$$(1) \quad k^2 = 0, \quad l^2 = -\mu^2, \quad p^2 = q^2 = -M^2,$$

where  $\mu$  and  $M$  are the meson and nucleon masses. In analogy with the corresponding case of pion-nucleon scattering, the use of the 4-vectors

$$(2) \quad P = \frac{p + q}{2}, \quad K = \frac{k + l}{2},$$

is particularly advantageous at some stages of the calculations, while the final results are best expressed in terms of the two invariant parameters

$$(3) \quad A^2 = (k - l)^2, \quad v = -\frac{(P \cdot K)}{M}.$$

By a straightforward calculation (and employing the energy-momentum conservation) it is easy to establish the relationship between these two invariants and quantities having a more direct physical meaning. Thus we find

$$(4) \quad v = k_L \frac{1^2 + \mu^2}{4M^2},$$

where  $k_L$  is the energy of the photon in the laboratory system, and

$$(5) \quad A^2 = -\mu^2 + \frac{(\omega^c + E^c)^2 - M^2}{\omega^c + E^c} (\omega^c - |l^c| \cos \theta^c),$$

$$(6) \quad v = \frac{1}{4M} [4E^c(\omega^c + E^c) - A^2 + \mu^2 - 4M^2],$$

<sup>(4)</sup> In which the momenta of the initial and final nucleon are equal and opposite.

<sup>(5)</sup> Hereafter, for any 4-vectors  $a \equiv (\mathbf{a}, a_4 = ia_0)$  and  $b$ ,  $(a \cdot b) = (\mathbf{a} \cdot \mathbf{b}) - a_0 b_0$  and  $a^2 = \mathbf{a}^2 - a_0^2$ .

where  $\omega^c = \sqrt{(l^c)^2 + \mu^2}$ ,  $E^c = \sqrt{(l^c)^2 + M^2}$  are the energies of the meson and of the final nucleon and  $\vartheta^c$  is the angle between the photon and meson momenta in the centre of mass frame.

The dispersion relations will connect the amplitudes for processes characterized by the same  $A^2$ , but different  $\nu$ . It is worth noticing that  $A^2 = 0$  for forward meson production at infinite energy, and  $A^2 = M\mu^2/(\mu \mp M)$  at the threshold <sup>(6)</sup>. On the other hand, for a given  $A^2$  the minimum value of  $\nu$  is

$$(7) \quad \nu_{\min} = \mu + \frac{\mu^2 - A^2}{4M},$$

corresponding to threshold production <sup>(6)</sup>. We must, however, bear in mind that, for a given  $A^2$ ,  $\nu > \nu_{\min}$  does not necessarily correspond to a physically realizable process. This is the case only if, substituting into (5)  $|l^c|$  expressed in terms of  $\nu$  and  $A^2$  by means of (6), and solving with respect to  $\cos \vartheta^c$ , the result is  $|\cos \vartheta^c| \leq 1$ . We shall come back to this point in Sect. 7.

For want of a better place, we shall record here two pairs of identities which will be of use in Sect. 6. The first pair is

$$(8) \quad (P \pm K)^2 + M^2 = \mp 2M(\nu \pm \nu_B),$$

with

$$(9) \quad \nu_B = \frac{A^2 + \mu^2}{4M}.$$

The second,

$$(10) \quad (q \cdot k) = -M(\nu - \nu_B), \quad (p \cdot k) = -M(\nu + \nu_B),$$

though not quoted anywhere in this paper, comes in useful in deriving eq. (60).

### g. — Frames of Reference.

3'1. *The « natural » frame.* — The « natural » or « Breit » frame has been used extensively in deriving the generalized dispersion relations for pion-nucleon scattering <sup>(2,3)</sup>. It is characterized by the fact that the momenta of

<sup>(6)</sup> I.e.,  $l^c = 0$  so that the meson is produced at rest in the centre of mass frame.

the initial and final nucleons are equal and opposite,  $\mathbf{p} = -\Delta/2$  and  $\mathbf{q} = \Delta/2$  (<sup>7</sup>), while the photon and meson momenta are  $\mathbf{k} = \boldsymbol{\pi} + \Delta/2$  and  $\mathbf{l} = \boldsymbol{\pi} - \Delta/2$ . The common value of the initial and final nucleon energies is  $E = \sqrt{M^2 + \Delta^2/4}$ . Since the energies of the photon and of the meson must be equal, we have  $(\boldsymbol{\pi} \cdot \Delta) = \mu^2/2$  (<sup>8</sup>) and  $k_0 = l_0 = \omega$ ,  $\omega = \sqrt{\boldsymbol{\pi}^2 + (\mu^2/2) + (\Delta^2/4)}$ . It is useful to introduce a system of axes as shown in Fig. 1.

Then  $\mathbf{p} \equiv (0, 0, \Delta/2)$ ,  $\mathbf{q} \equiv (0, 0, -\Delta/2)$ ,  $\mathbf{k} \equiv (\pi_x, 0, \pi_z + \Delta/2)$ ,  $\mathbf{l} \equiv (\pi_x, 0, \pi_z - \Delta/2)$  with  $\pi_x = \sqrt{\omega^2 - ((\mu^2 + \Delta^2)/2\Delta)^2}$ ,  $\pi_z = -\mu^2/2\Delta$ . In the natural frame  $P$  and  $K$  defined by eqs. (2) have components  $P = (0, E)$ ,  $K = (\boldsymbol{\pi}, \omega)$  while for the invariant parameters we find  $A^2 = \Delta^2$ ,  $\nu = \omega E/M$ .

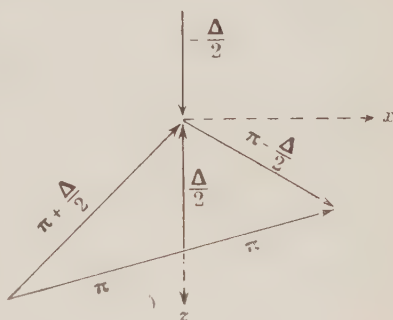


Fig. 1. — Momenta of the nucleons ( $\pm \Delta/2$ ), of the photon ( $\boldsymbol{\pi} + \Delta/2$ ) and of the meson ( $\boldsymbol{\pi} - \Delta/2$ ) in the «natural» frame.

3.2. *The centre of mass frame.* — The coefficients  $a_{\mu\nu}$  of the transformation  $u_\mu^c = a_{\mu\nu} u_\nu^r$  from the centre of mass frame where  $\mathbf{p}^c + \mathbf{k}^c = \mathbf{q}^c + \mathbf{l}^c = 0$ , are

$$(11) \quad \left\{ \begin{array}{l} a_{11} = 1 + \sin^2 \varphi (\cosh \chi - 1), \quad a_{12} = 0, \\ \quad \quad \quad a_{13} = \sin \varphi \cos \varphi (\cosh \chi - 1), \quad a_{14} = i \sin \varphi \sinh \chi, \\ a_{21} = 0, \quad a_{22} = 1, \quad a_{23} = a_{24} = 0, \\ a_{31} = a_{13}, \quad a_{32} = 0, \quad a_{33} = 1 + \cos^2 \varphi (\cosh \chi - 1), \quad a_{34} = i \cos \varphi \sinh \chi, \\ a_{41} = -a_{14}, \quad a_{42} = 0, \quad a_{43} = -a_{34}, \quad a_{44} = \cosh \chi, \end{array} \right.$$

with

$$(12) \quad \sin \varphi = \frac{\pi_y}{|\boldsymbol{\pi}|}, \quad \cos \varphi = \frac{\pi_z}{|\boldsymbol{\pi}|}, \quad \tanh \chi = \frac{|\boldsymbol{\pi}| E}{\nu M + E^2}.$$

The relative velocity of the two frames is manifestly in the direction of the vector  $\boldsymbol{\pi}$ .

(<sup>7</sup>) In the following, quantities referring to the natural frame will not be distinguished by a special sign, while those in the centre of mass frame will bear an index, e.g.  $p^\sigma$ ,  $k^\sigma$  etc.

(<sup>8</sup>) While for pion-nucleon scattering the analogous vectors  $\boldsymbol{\pi}$  and  $\Delta$  would be at right angles.

3.3. *The photon polarization vector.* — The polarization 4-vector  $e \equiv (e, e_0)$  must satisfy the twofold condition  $(e \cdot k) = 0$ ,  $e^2 = 1$ . We shall study separately the two cases:  $\alpha$ )  $e$  in the direction of the  $y$  axis;  $\beta$ )  $e$  in the  $(xz)$  plane.

In the case  $\alpha$ ), the four vector  $e \equiv (0, 1, 0, 0)$  is transformed into  $e^c \equiv (0, 1, 0, 0)$  when we go over to the centre of mass system. In the case  $\beta$ ), the fourth components  $e_0$  and  $e_0^c$  cannot vanish simultaneously. We find it preferable to have  $e_0^c = 0$ , for which the components in the natural frame are

$$(13) \quad \begin{cases} e_1 = \frac{2[\nu M \Delta^2 + (\mu^2 + \Delta^2)E^2]}{E \Delta (4M\nu + \mu^2 + \Delta^2)}, & e_2 = 0, & e_3 = \frac{4E\pi_\nu}{4M\nu + \mu^2 + \Delta^2}, \\ e_0 = \frac{2\Delta\pi}{4M\nu + \mu^2 + \Delta^2}. \end{cases}$$

It is easy to verify that this 4-vector satisfies  $(e \cdot k) = 0$ ,  $e^2 = 1$  and transforms into one with  $e_0^c = e_2^c = 0$  in the centre of mass frame. Note the useful formula

$$(14) \quad (e \cdot l) = (e^c \cdot l^c) = - (e \cdot \Delta).$$

#### 4. — Positive Energy Solutions of the Dirac Equation.

The nucleons in the initial and final states will be described by positive energy solutions of the equations <sup>(9)</sup>

$$(15) \quad [i(\gamma \cdot p) + M]u^\lambda(p) = 0, \quad [i(\gamma \cdot q) + M]u^\lambda(q) = 0, \quad (\lambda = 1, 2),$$

with the normalization

$$(16) \quad \bar{u}^{\lambda'}(p)u^\lambda(p) = \bar{u}^{\lambda'}(q)u^\lambda(q) = \delta_{\lambda'\lambda}.$$

4.1. — In the natural frame we have

$$(17a) \quad u^1(p) = \frac{1}{\sqrt{2M(M+E)}} \begin{vmatrix} M+E & 0 \\ \Delta/2 & 0 \\ 0 & -\Delta/2 \end{vmatrix}, \quad u^2(p) = \frac{1}{\sqrt{2M(M+E)}} \begin{vmatrix} 0 & M+E \\ 0 & \Delta/2 \end{vmatrix},$$

<sup>(9)</sup> We choose  $\gamma = \begin{pmatrix} 0 & -i\sigma \\ i\sigma & 0 \end{pmatrix}$ ,  $\gamma_4 = \begin{pmatrix} I & 0 \\ 0 & -I \end{pmatrix}$ ;  $\gamma_5 = \gamma_1\gamma_2\gamma_3\gamma_4 = -\begin{pmatrix} 0 & I \\ I & 0 \end{pmatrix}$ , and define  $\bar{u} = u^\dagger \gamma_4$ .

$$(17b) \quad u^1(q) = \frac{M+E}{\sqrt{2}M(M+E)} \begin{vmatrix} 1 & 0 \\ 0 & -A/2 \end{vmatrix}, \quad u^2(q) = \frac{1}{\sqrt{2}M(M+E)} \begin{vmatrix} M+E & 0 \\ 0 & A/2 \end{vmatrix}.$$

The following formulae will be of use later:

$$(18a) \quad \bar{n}^{\lambda'}(q)\gamma_5 u^{\lambda}(p) = \frac{1}{2M} (\boldsymbol{\sigma} \cdot \boldsymbol{\Delta})_{\lambda'\lambda},$$

$$(18b) \quad i\bar{u}^{\lambda'}(q)\gamma_5(\boldsymbol{\gamma} \cdot \boldsymbol{k})u^{\lambda}(p) = \frac{E}{M} (\boldsymbol{\sigma} \cdot \boldsymbol{\pi})_{\lambda'\lambda} + \frac{4M(M+E) - \mu^2}{8M(M+E)} (\boldsymbol{\sigma} \cdot \boldsymbol{\Delta})_{\lambda'\lambda},$$

$$(18c) \quad \bar{u}^{\lambda'}(q)\gamma_5(\boldsymbol{\gamma} \cdot \boldsymbol{e})(\boldsymbol{\gamma} \cdot \boldsymbol{k})u^{\lambda}(p) = \frac{i}{2M} [(\boldsymbol{e} \times \boldsymbol{\pi}) \cdot \boldsymbol{\Delta}] \delta_{\lambda'\lambda} + \omega(\boldsymbol{\sigma} \cdot \boldsymbol{e})_{\lambda'\lambda} \\ - e_0(\boldsymbol{\sigma} \cdot \boldsymbol{\pi})_{\lambda'\lambda} + \frac{[2\omega(\boldsymbol{e} \cdot \boldsymbol{\Delta}) - e_0(\mu^2 + 4E(M+E))]}{8M(M+E)} (\boldsymbol{\sigma} \cdot \boldsymbol{\Delta})_{\lambda'\lambda}.$$

$$(18d) \quad i\bar{u}^{\lambda'}(q)\gamma_5(\boldsymbol{\gamma} \cdot \boldsymbol{e})u^{\lambda}(p) = \frac{E}{M} (\boldsymbol{\sigma} \cdot \boldsymbol{e})_{\lambda'\lambda} - \frac{1}{4M(M+E)} (\boldsymbol{e} \cdot \boldsymbol{\Delta})(\boldsymbol{\sigma} \cdot \boldsymbol{\Delta})_{\lambda'\lambda},$$

$$(18e) \quad \bar{u}^{\lambda'}(q)\gamma_5(\boldsymbol{\gamma} \cdot \boldsymbol{l})(\boldsymbol{\gamma} \cdot \boldsymbol{e})u^{\lambda}(p) = \frac{i}{2M} [\boldsymbol{\Delta} \cdot (\boldsymbol{\pi} \times \boldsymbol{e})] \delta_{\lambda'\lambda} - \omega(\boldsymbol{\sigma} \cdot \boldsymbol{e})_{\lambda'\lambda} + \\ + e_0(\boldsymbol{\sigma} \cdot \boldsymbol{\pi})_{\lambda'\lambda} + \frac{[e_0(\mu^2 - 4E(M+E)) - 2(\boldsymbol{e} \cdot \boldsymbol{\Delta})(\omega + 2(M+E))]}{8M(M+E)} (\boldsymbol{\sigma} \cdot \boldsymbol{\Delta})_{\lambda'\lambda}.$$

If  $\boldsymbol{e}$  lies in the  $(xz)$  plane, and for any combination of the indices  $\lambda = 1, 2$  and  $\lambda' = 1, 2$ , the quantities (18a, ... e) are all real. On the other hand, if  $\boldsymbol{e}$  is in the direction of the  $y$  axis and  $e_0 = 0$ , only the last three, (18c, d, e), are of interest, and are all purely imaginary.

4.2. — In the centre of mass frame we have the positive energy solutions

$$(19a) \quad u^1(p^c) = \frac{M+p_0^c}{\sqrt{2}M(M+p_0^c)} \begin{vmatrix} M+p_0^c & 0 \\ p_3^c & p_1^c \end{vmatrix}, \quad u^2(p^c) = \frac{1}{\sqrt{2}M(M+p_0^c)} \begin{vmatrix} 0 & M+p_0^c \\ p_1^c & -p_3^c \end{vmatrix}.$$

$$(19b) \quad u^1(q^c) = \frac{1}{\sqrt{2}M(M+q_0^c)} \begin{vmatrix} M+q_0^c & 0 \\ q_3^c & q_1^c \end{vmatrix}, \quad u^2(q^c) = \frac{1}{\sqrt{2}M(M+q_0^c)} \begin{vmatrix} 0 & M+q_0^c \\ q_1^c & q_3^c \end{vmatrix}.$$



Here

$$(20) \quad \begin{cases} p_1^c = \frac{1}{2} \sin \varphi \cos \varphi (\cosh \chi - 1) \Delta - \sin \varphi \sinh \chi E, \\ p_2^c = 0, \\ p_3^c = \frac{1}{2} [1 + \cos^2 \varphi (\cosh \chi - 1)] \Delta - \cos \varphi \sinh \chi E, \\ p_0^c = -\frac{1}{2} \cos \varphi \sinh \chi \Delta + \cosh \chi E, \end{cases}$$

and the components  $q_\mu^c$  are obtained from the  $p_\mu^c$  by changing the sign of  $\Delta$ . Consequently  $p_0^c \neq q_0^c = E^c$ .

### 4.3. - The transformation

$$(21) \quad S \gamma_\nu S^{-1} = a_{\mu\nu} \gamma_\mu,$$

of the  $\gamma$  matrices is generated by the matrix

$$(22) \quad S = \cosh \frac{\chi}{2} + i \gamma_1 \gamma_4 \sin \varphi \sinh \frac{\chi}{2} + i \gamma_3 \gamma_4 \cos \varphi \sinh \frac{\chi}{2}.$$

The result of applying  $S$  to the positive energy solutions (17a) is a linear combination of the centre of mass solutions (19a),

$$(23) \quad \begin{cases} Su^1(p) = \frac{1}{2\sqrt{M+E}\sqrt{M+p_0^c}} \left\{ \left[ 2(M+E) \cosh \frac{\chi}{2} - \Delta \cos \varphi \sinh \frac{\chi}{2} \right] u^1(p^c) - \right. \\ \left. - \Delta \sin \varphi \sinh \frac{\chi}{2} u^2(p^c) \right\}, \\ Su^2(p) = \frac{1}{2\sqrt{M+E}\sqrt{M+p_0^c}} \left\{ \Delta \sin \varphi \sinh \frac{\chi}{2} u^1(p^c) + \right. \\ \left. + \left[ 2(M+E) \cosh \frac{\chi}{2} - \Delta \cos \varphi \sinh \frac{\chi}{2} \right] u^2(p^c) \right\}. \end{cases}$$

Similarly

$$(24) \quad \begin{cases} \bar{u}^1(q) S^{-1} = \frac{1}{2\sqrt{M+E}\sqrt{M+q_0^c}} \left\{ \left[ 2(M+E) \cosh \frac{\chi}{2} + \Delta \cos \varphi \sinh \frac{\chi}{2} \right] \bar{u}^1(q^c) + \right. \\ \left. + \Delta \sin \varphi \sinh \frac{\chi}{2} \bar{u}^2(q^c) \right\}, \\ \bar{u}^2(q) S^{-1} = \frac{1}{2\sqrt{M+E}\sqrt{M+q_0^c}} \left\{ -\Delta \sin \varphi \sinh \frac{\chi}{2} \bar{u}^1(q^c) + \right. \\ \left. + \left[ 2(M+E) \cosh \frac{\chi}{2} + \Delta \cos \varphi \sinh \frac{\chi}{2} \right] \bar{u}^2(q^c) \right\}. \end{cases}$$

Employing these formulae, it is easy to write the relation between a  $2 \times 2$  matrix of the type <sup>(10)</sup>

$$(25) \quad M(\lambda' \lambda) = \bar{u}^{\lambda'}(q) A u^{\lambda}(p),$$

and the corresponding matrix <sup>(11)</sup>

$$(26) \quad M^c(\lambda' \lambda) = \bar{u}^{\lambda'}(q^c) A^c u^{\lambda}(p^c),$$

in the centre of mass frame. In fact, since  $SAS^{-1} = A$ ,  $M(\lambda' \lambda)$  is a linear combination of  $M^c(\lambda'' \lambda'')$ . In order to be able to write this explicitly, we must distinguish two cases:

$$(27) \quad a) \quad \begin{cases} M(11) = M(22), & M(12) = -M(21), \\ M^c(11) = M^c(22), & M^c(12) = -M^c(21), \end{cases}$$

as is the case for any of the  $A$  and  $A^c$  given in <sup>(10-11)</sup> as long as  $e$  is in the  $y$  direction and  $e_0 = e_0^c = 0$ . Then

$$(28) \quad \begin{cases} M(11) = \alpha M^c(11) + \beta M^c(21), \\ M(21) = -\beta M^c(11) + \alpha M^c(21), \end{cases}$$

with

$$(29) \quad \begin{cases} \alpha = \frac{E + M \cosh \chi}{\sqrt{(M + p_0^c)(M + q_0^c)}}, \\ \beta = \frac{\Delta \sin \varphi \sinh \chi}{2\sqrt{(M + p_0^c)(M + q_0^c)}}. \end{cases} \quad (\chi^2 = p^2 - 1).$$

$$(30) \quad b) \quad \begin{cases} M(11) = -M(22), & M(12) = M(21), \\ M^c(11) = -M^c(22), & M^c(12) = M^c(21), \end{cases}$$

as is the case when  $e$  lies in the  $(xz)$  plane. Then

$$(31) \quad \begin{cases} M(11) = \alpha M^c(11) + \beta M^c(21), \\ M(21) = \beta M^c(11) - \alpha M^c(21), \end{cases}$$

<sup>(10)</sup>  $A$  being one of the operators  $\gamma_5$ ,  $i\gamma_5(\gamma \cdot k)$ ,  $\gamma_5(\gamma \cdot e)(\gamma \cdot k)$ ,  $i\gamma_5(\gamma \cdot e)$ ,  $\gamma_5(\gamma \cdot l)(\gamma \cdot e)$  as in eqs. (18a, ..., e).

<sup>(11)</sup>  $A^c$  being the operator that corresponds to  $A$  among  $\gamma_5$ ,  $i\gamma_5(\gamma \cdot k^c)$  etc.

with

$$(32) \quad \begin{cases} \alpha = \frac{(M + E) \cosh^2 \chi/2 + (M - E) \cos 2\varphi \sinh^2 \chi/2}{\sqrt{(M + p_0^c)(M + q_0^c)}}, \\ \beta = \frac{(E - M) \sin 2\varphi \sinh^2 \chi/2}{\sqrt{(M + p_0^c)(M + q_0^c)}}. \end{cases} \quad (\alpha^2 + \beta^2 = 1),$$

## 5. - Feynman and Causal Photoproduction Amplitudes.

The meson field and the electromagnetic field are described by the operators  $\Phi_\alpha(x)$  ( $\alpha = 1, 2, 3$ ) and  $A_\mu(x)$  ( $\mu = 1, 2, 3, 4$ ) obeying the equations

$$(33) \quad \begin{cases} (\mu^2 - \square^2)\Phi_\alpha(x) = j_\alpha(x), \\ \square^2 A_\mu(x) = J_\mu(x). \end{cases}$$

where  $j_\alpha(x)$  and  $J_\mu(x)$  denote the sources of the two fields.

The Feynman amplitude responsible for photoproduction is

$$(34) \quad \mathcal{F}_{\alpha\mu}(l, k) = i \int d^4x \int d^4y \exp[-i(l \cdot x) + i(k \cdot y)] \cdot \\ \cdot (\square_x^2 - \mu^2) \square_y^2 \langle q | (\Phi_\alpha(x), A_\mu(y))_+ | p$$

with

$$(35) \quad (\Phi_\alpha(x), A_\mu(y))_+ = \frac{1}{2} \{ \Phi_\alpha(x), A_\mu(y) \} + \frac{1}{2} \varepsilon(x - y) [\Phi_\alpha(x), A_\mu(y)].$$

Performing the differentiations, and taking into account the fact that the commutator  $[j_\alpha(x), A_\mu(y)]$  vanishes for  $x_0 = y_0$ , we find

$$(36) \quad \mathcal{F}_{\alpha\mu}(l, k) = i \int d^4x \int d^4y \exp[-i(l \cdot x) + i(k \cdot y)] \cdot q \cdot (j_\alpha(x), J_\mu(y)) \cdot p,$$

which, by the change of variables  $x = u + z/2$ ,  $y = u - z/2$  reduces to

$$(37) \quad \mathcal{F} = (2\pi)^4 \delta(p + k - q - l) F,$$

with  $(K = (k + l)/2)$

$$(38) \quad F_{\alpha\mu}(l, k) = i \int d^4x \exp[-i(K \cdot x)] \left\langle q \left| \left( j_\alpha \left( \frac{x}{2} \right), J_\mu \left( -\frac{x}{2} \right) \right) \right| p \right\rangle.$$

The corresponding causal amplitude is  $\langle \eta(x_0) = (1 + \varepsilon(x_0))/2 \rangle$

$$(39) \quad M_{\alpha\mu}(l, k) = i \int d^4x \exp[-i(K \cdot x)] \eta(x_0) \left\langle q \left\| j_\mu \left( \frac{x}{2} \right), J_\mu \left( -\frac{x}{2} \right) \right\| p \right\rangle.$$

In the natural frame

$$(40) \quad (K \cdot x) = (\boldsymbol{\pi} \cdot \mathbf{x}) - \omega x_0,$$

from which it is easy to see that, if the momentum transfer  $\Delta^2$  is held fixed,  $M_{\alpha\mu}$  may be regarded as a function of the photon energy  $\omega$ . For this purpose  $\pi(\omega)$  must be defined as follows:

$$(41) \quad \pi(\omega) = \begin{cases} +\sqrt{\omega^2 - \frac{\mu^2}{2} - \frac{\Delta^2}{4}} & \text{for } \omega > \sqrt{\frac{\mu^2}{2} + \frac{\Delta^2}{4}} \\ -\sqrt{\omega^2 - \frac{\mu^2}{2} - \frac{\Delta^2}{4}} & \text{for } \omega < -\sqrt{\frac{\mu^2}{2} + \frac{\Delta^2}{4}} \\ i\sqrt{\frac{\mu^2}{2} + \frac{\Delta^2}{4} - \omega^2} & \text{for } |\omega| < \sqrt{\frac{\mu^2}{2} + \frac{\Delta^2}{4}}. \end{cases}$$

Since the sign of  $\pi$  changes with that of  $\omega$  provided that  $|\omega| > \sqrt{(\mu^2/2) + (\Delta^2/4)}$ , we find for

$$(42) \quad M_{\alpha\mu}(l, k) = M_{\alpha\mu}(\omega, \Delta^2; q, p),$$

the important relation

$$(43) \quad M_{\alpha\mu}(\omega, \Delta^2; q, p) = [M_{\alpha\mu}(-\omega, \Delta^2; p, q)]^*,$$

(\* denotes the complex conjugate).

Hereafter it is more convenient to work with

$$(44) \quad M_\alpha(\omega, \Delta; \lambda' l', \lambda l) = e_\mu M_{\alpha\mu}(\omega, \Delta^2; q, p),$$

where  $e_\mu$  is the photon polarization vector, while  $(\lambda, \lambda')$  and  $(l, l')$  denote the spin and isospin nucleon variables. Thus our basic relation (43) now reads

$$(45) \quad M_\alpha(\omega, \Delta; \lambda' l', \lambda l) = [M_\alpha(-\omega, -\Delta; \lambda l, \lambda' l')]^*.$$

The derivation of dispersion relations now runs along familiar lines. We split  $M_\alpha$  into a dispersive and an absorptive part,

$$(46) \quad M_\alpha = \mathcal{D}_\alpha + i\mathcal{A}_\alpha,$$

with

$$(47) \quad \begin{cases} \mathcal{D}_\alpha = \frac{i}{2} \int d^4x \exp[-i(\boldsymbol{\pi} \cdot \mathbf{x}) + i\omega x_0] \varepsilon(x_0) \left\langle q \left[ \left| j_\alpha \left( \frac{x}{2} \right), e_\mu J_\mu \left( -\frac{x}{2} \right) \right| \right] p \right\rangle, \\ \mathcal{A}_\alpha = \frac{1}{2} \int d^4x \exp[-i(\boldsymbol{\pi} \cdot \mathbf{x}) + i\omega x_0] \left\langle q \left[ \left| j_\alpha \left( \frac{x}{2} \right), e_\mu J_\mu \left( -\frac{x}{2} \right) \right| \right] p \right\rangle, \end{cases}$$

and remark that, if  $F_\alpha$  is also written in the form  $F_\alpha = \mathcal{D}_\alpha + iA_\alpha$  ( $A_\alpha$  differing from  $\mathcal{A}_\alpha$  in that the commutator is replaced by the anticommutator), then  $\mathcal{A}_\alpha = \varepsilon(\omega)A_\alpha$ .

Before proceeding further, we must resolve  $M_\alpha$  into a sum of terms which are either odd or even against a change of the sign of  $\omega$ . For this it is convenient to write

$$(48) \quad M_\alpha = \delta_{\alpha 3} M^{(1)} + \tau_\alpha M^{(2)} + \frac{1}{2}[\tau_\alpha, \tau_3] M^{(3)}.$$

According to (45),  $M^{(i)}$  ( $i = 1, 2, 3$ ) has the property

$$(49) \quad M^{(i)}(\omega, \boldsymbol{\Delta}; \lambda', \lambda) = (1 - 2\delta_{i3})[M^{(i)}(-\omega, -\boldsymbol{\Delta}; \lambda, \lambda')]^*.$$

$M^{(i)}$  can now be expressed in the form

$$(50) \quad M^{(i)} = \frac{M}{iE} \bar{u}(q) \left\{ (e \cdot l) \gamma_3 M^{(j,1)} + (e \cdot l) i \gamma_5 (\gamma \cdot k) M^{(j,2)} + (e \cdot p + q) i \gamma_3 (\gamma \cdot k) M^{(j,3)} + \right. \\ \left. + i \gamma_5 (\gamma \cdot e) M^{(j,4)} + \gamma_3 (\gamma \cdot e) (\gamma \cdot k) M^{(j,5)} + \frac{1}{2} \gamma_3 [(\gamma \cdot e), (\gamma \cdot l)] M^{(j,6)} \right\} u(p),$$

where the  $M^{(j,l)}$  are functions of  $\nu$  and  $\Delta^2$ . They are multiplied by matrix elements of the type  $(M/iE) \bar{u}(q) A u(p)$ , which (cfr. Sect. 4) are all imaginary for  $e$  lying in the  $(xz)$  plane, and either zero or real for  $e$  in the  $y$  direction. Remembering that  $\omega = \nu M/E$ , and that  $l_0, \mathbf{l}$  (but not  $E$ ) change sign if  $\omega$  and  $\boldsymbol{\Delta}$  do so, we find

$$(51) \quad M^{(j,l)}(\nu, \Delta^2) = \zeta_{jl} M^{(j,l)*}(-\nu, \Delta^2),$$

(no summation with respect to  $j$  and  $l$ ), where  $\zeta_{jl}$  is the matrix

$$(52) \quad \|\zeta_{jl}\| = \begin{vmatrix} -1 & -1 & -1 & -1 & +1 & +1 \\ -1 & -1 & -1 & -1 & +1 & +1 \\ +1 & +1 & +1 & +1 & -1 & -1 \end{vmatrix}.$$

The dispersion relations then are

$$(53) \quad \operatorname{Re} M^{(j,l)}(\nu, \Delta^2) = \frac{2}{\pi} \int_0^{\infty} \frac{\eta_{jl}}{\nu'^2 - \nu^2} \operatorname{Im} M^{(j,l)}(\nu', \Delta^2) d\nu',$$

with

$$(54) \quad \|\eta_{jl}\| = \begin{vmatrix} \nu & \nu & \nu & \nu & \nu' & \nu' \\ \nu & \nu & \nu & \nu & \nu' & \nu' \\ \nu' & \nu' & \nu' & \nu' & \nu & \nu \end{vmatrix}.$$

## 6. - Non-Physical Part of the Range of Integration.

For  $\nu < \nu_{\min}$ ,  $\operatorname{Im} M^{(j,l)}(\nu, \Delta^2)$  will not be provided by the experimental data, so that a theoretical expression must be found instead. This is done by actually evaluating  $\mathcal{A}_\alpha$  defined by eq. (47). We have

$$(55) \quad \mathcal{A}_\alpha = \pi \sum_n \{ \langle q | j_\alpha | n, \mathbf{p}_n = \boldsymbol{\pi} \rangle \langle n, \mathbf{p}_n = \boldsymbol{\pi} | e_\mu J_\mu | p \rangle \delta(\omega + E - E_n) - \\ - \langle q | e_\mu J_\mu | n, \mathbf{p}_n = -\boldsymbol{\pi} \rangle \langle n, \mathbf{p}_n = -\boldsymbol{\pi} | j_\alpha | p \rangle \delta(-\omega + E - E_n) \}.$$

For  $\nu < \nu_{\min}$  only intermediate states consisting of one single nucleon will be important. Using eqs. (8) and effecting the integrations implied by  $\sum_n$ , we obtain

$$(56) \quad \mathcal{A}_\alpha = 2\pi \sqrt{\boldsymbol{\pi}^2 + M^2} \sum_{\lambda'' \ell''} \{ \langle q | j_\alpha | \lambda'' \ell'', \boldsymbol{\pi}, \sqrt{\boldsymbol{\pi}^2 + M^2} \rangle \cdot \\ \cdot \langle \lambda'' \ell'', \boldsymbol{\pi}, \sqrt{\boldsymbol{\pi}^2 + M^2} | e_\mu J_\mu | p \rangle \delta((P + K)^2 + M^2) - \\ - \langle q | e_\mu J_\mu | \lambda'' \ell'', -\boldsymbol{\pi}, \sqrt{\boldsymbol{\pi}^2 + M^2} \rangle \langle \lambda'' \ell'', -\boldsymbol{\pi}, \sqrt{\boldsymbol{\pi}^2 + M^2} | j_\alpha | p \rangle \cdot \\ \cdot \delta((P - K)^2 + M^2) \}.$$

We now make use of the matrix elements

$$(57) \quad \langle q | j_\alpha | p \rangle = -ig \bar{u}(q) \gamma_\alpha \tau_\alpha u(p) \frac{M}{\sqrt{p_0 q_0}}, \quad (p - q)^2 = -\mu^2,$$

and

$$(58) \quad \langle q | J_\mu | p \rangle = \frac{ie}{2} \frac{M}{\sqrt{p_0 q_0}} \bar{u}(q) [\gamma_\mu (1 + \tau_3) + (a + b\tau_3) \sigma_{\mu\nu} (q_\nu - p_\nu)] u(p), \\ (q - p)^2 = 0,$$



with  $\sigma_{\mu\nu} = (i/2)[\gamma_\mu, \gamma_\nu]$  and  $a = (1/2M)(\mu_p + \mu_n)$ ,  $b = (1/2M)(\mu_p - \mu_n)$  ( $\mu_p = 1.7896$ ,  $\mu_n = -1.9103$  are the anomalous magnetic moments of the proton and the neutron). These matrix elements amount to a definition of the renormalized charge  $e$  and coupling constant  $g$ .

Thus, by a straightforward calculation, we find

$$(59) \quad \mathcal{A}_x = \delta_{\alpha 3} \mathcal{A}^{(1)} + \tau_\alpha \mathcal{A}^{(2)} + \frac{1}{2}[\tau_\alpha, \tau_3] \mathcal{A}^{(3)},$$

with

$$(60) \quad \left\{ \begin{array}{l} \mathcal{A}^{(1)} = \delta(\nu - \nu_B) \frac{eg\pi}{4Ei} \bar{u}(q) \{ (e \cdot l) \gamma_5 + b(e \cdot l) i \gamma_5 (\gamma \cdot k) - \\ \quad - b(e \cdot p + q) i \gamma_5 (\gamma \cdot k) + 2Mb \gamma_5 (\gamma \cdot e) (\gamma \cdot k) + \frac{1}{2} \gamma_5 [(\gamma \cdot e), (\gamma \cdot l)] \} u(p), \\ \mathcal{A}^{(2)} = \delta(\nu - \nu_B) \frac{eg\pi}{4Ei} \bar{u}(q) \{ (e \cdot l) \gamma_5 + a(e \cdot l) i \gamma_5 (\gamma \cdot k) - \\ \quad - a(e \cdot p + q) i \gamma_5 (\gamma \cdot k) + 2Ma \gamma_5 (\gamma \cdot e) (\gamma \cdot k) + \frac{1}{2} \gamma_5 [(\gamma \cdot e), (\gamma \cdot l)] \} u(p), \\ \mathcal{A}^{(3)} = -\mathcal{A}^{(1)}, \end{array} \right.$$

from which terms with  $\delta(\nu - \nu_B)$  have been dropped. With the help of these formulae, putting  $\text{Im } M^{(j,l)} = \mathcal{A}^{(j,l)}$  in the non-physical range  $\nu < \nu_{\min}$ , we finally obtain <sup>(12)</sup>

$$(61) \quad \text{Re } M^{(j,l)}(\nu, \Delta^2) = \frac{eg}{2M} \frac{1}{\nu_B^2 - \nu^2} \varepsilon_{jl} + \frac{2}{\pi} \int_{\nu_{\min}}^{\infty} \frac{\eta_{jl}}{\nu'^2 - \nu^2} \text{Im } M^{(j,l)}(\nu', \Delta^2) d\nu',$$

where

$$(62) \quad \varepsilon_{jl} = \begin{vmatrix} \nu & b\nu & -b\nu & 0 & 2Mb\nu_B & \nu_B \\ \nu & a\nu & -a\nu & 0 & 2Ma\nu_B & \nu_B \\ -\nu_B & -b\nu_B & b\nu_B & 0 & -2Mb\nu & -\nu \end{vmatrix}.$$

## 7. - Dispersion Relations for Centre of Mass Amplitudes.

With a view to actual calculations (to be presented in a subsequent paper) we express the photoproduction amplitude in the centre of mass frame in

<sup>(12)</sup> For  $\nu_B < \nu_{\min}$ , otherwise the first term in the right member of (61) is to be dropped.

the form given by Gell-Mann and Watson in their 1954 review article <sup>(13)</sup>,

$$(63) \quad T^{(j)c} = i\mathcal{E}_1^{(j)}(\boldsymbol{\sigma} \cdot \mathbf{e}^c) - \mathcal{M}_1^{(j)}(\tfrac{1}{2})[\mathbf{k}^c \times \mathbf{e}^c \cdot \mathbf{l}^c - i\boldsymbol{\sigma} \cdot (\mathbf{k}^c \times \mathbf{e}^c) \times \mathbf{l}^c]|\mathbf{k}^c|^{-1}|\mathbf{l}^c|^{-1} - \\ - \mathcal{M}_1^{(j)}(\tfrac{3}{2})[2\mathbf{k}^c \times \mathbf{e}^c \cdot \mathbf{l}^c + i\boldsymbol{\sigma} \cdot (\mathbf{k}^c \times \mathbf{e}^c) \times \mathbf{l}^c]|\mathbf{k}^c|^{-1}|\mathbf{l}^c|^{-1} + \\ + (i/2)\mathcal{E}_2^{(j)}[(\boldsymbol{\sigma} \cdot \mathbf{k}^c)(\mathbf{e}^c \cdot \mathbf{l}^c) + (\boldsymbol{\sigma} \cdot \mathbf{e}^c)(\mathbf{k}^c \cdot \mathbf{l}^c)]|\mathbf{k}^c|^{-1}|\mathbf{l}^c|^{-1},$$

where  $\mathcal{E}_1$ ,  $\mathcal{E}_2$  denote electric dipole and quadrupole matrix elements, while  $\mathcal{M}_1(\tfrac{3}{2})$  and  $\mathcal{M}_1(\tfrac{1}{2})$  are magnetic dipole matrix elements for production of a meson in a  $P$ -state with  $j = \tfrac{3}{2}$  and  $j = \tfrac{1}{2}$  respectively.

For simplicity we shall confine ourselves to the case when  $\mathbf{e}$  is in the  $y$  direction ( $e_2 = e_2^c = 1$ , all other components being zero in both frames).

For the theoretical amplitude we find

$$(64) \quad \begin{cases} M^{(j)}(11) = M^{(j)}(22) = \frac{\pi_x A}{E} (M^{(j,5)} + M^{(j,6)}), \\ M^{(j)}(21) = -M^{(j)}(12) = \frac{2\omega M}{E} (M^{(j,5)} + M^{(j,6)}), \end{cases}$$

while

$$(65) \quad \begin{cases} T^{(j)c}(11) = T^{(j)c}(22) = [\mathcal{M}_1^{(j)}(\tfrac{1}{2}) + 2\mathcal{M}_1^{(j)}(\tfrac{3}{2})] \sin \vartheta^c, \\ T^{(j)c}(21) = -T^{(j)c}(12) = -[\mathcal{E}_1^{(j)} + (\mathcal{M}_1^{(j)}(\tfrac{1}{2}) - \mathcal{M}_1^{(j)}(\tfrac{3}{2}) + \tfrac{1}{2}\mathcal{E}_2^{(j)}) \cos \vartheta^c], \end{cases}$$

( $\vartheta^c$  being the angle of  $\mathbf{k}^c$  and  $\mathbf{l}^c$ ).

Employing the relations

$$(66) \quad \begin{cases} M(11) = \alpha T^c(11) + \beta T^c(21), \\ M(21) = -\beta T^c(11) + \alpha T^c(21), \end{cases}$$

with  $\alpha$  and  $\beta$  given by eqs. (29),  $M^{(j,1)}$  and  $M^{(j,5)} + M^{(j,6)}$  can be expressed in terms of  $[\mathcal{M}_1(\tfrac{1}{2}) + 2\mathcal{M}_1(\tfrac{3}{2})] \sin \vartheta^c$  and  $[\mathcal{E}_1 + (\mathcal{M}_1(\tfrac{1}{2}) - \mathcal{M}_1(\tfrac{3}{2}) + \tfrac{1}{2}\mathcal{E}_2) \cos \vartheta^c]$  so that the dispersion relations (61) with  $l = 4$ , and the sum of those with  $l = 5$  and  $l = 6$ , amount to dispersion relations for certain linear combinations of  $\mathcal{E}_1$ ,  $\mathcal{E}_2$ ,  $\mathcal{M}_1(\tfrac{1}{2})$  and  $\mathcal{M}_1(\tfrac{3}{2})$ .

The same method could be applied to the case when  $\mathbf{e}$  is in the  $(xz)$  plane (the appropriate formulae would then be (30), (31) and (32)).

One last remark will not come amiss. As we pointed out in Sect. 2,  $r > v_{\min}$

<sup>(13)</sup> M. GELL-MANN and K. M. WATSON: *Annual Review of Nuclear Science*, **4**, 219 (1954).

corresponds to a physical process only if  $\cos \vartheta^c$ , expressed in terms of  $\nu$  and  $\Delta^2$  by means of eqs. (5) and (6), is comprised between  $-1$  and  $+1$ . Even if this is not the case, however, the method just outlined will work if we assume that (63) may be used also when  $|\cos \vartheta^c| > 1$ . GOLDBERGER <sup>(3)</sup> has expressed doubts about the legitimacy of this procedure.

\* \* \*

To Prof. J. C. GUNN, who suggested this investigation, and to his collaborators working on the photoproduction projects, the author is indebted for interest and encouragement.

#### RIASSUNTO

L'ampiezza di transizione di Feynman per la reazione  $\gamma + \text{nucleone} \rightarrow \pi + \text{nucleone}$  è esprimibile in termini di un'ampiezza causale che soddisfa relazioni di dispersione. Queste vengono derivate nel sistema di riferimento «naturale». La connessione con le ampiezze nel sistema del baricentro viene discussa in dettaglio.

## Nucleon Recoil in the Pion-Nucleon Scattering.

L. FONDA and I. REINA

*Istituto di Fisica dell'Università - Trieste*

(ricevuto il 6 Settembre 1956)

**Summary.** — The effect of nucleon recoil has been taken into account in the extended source theory of pion-nucleon scattering with PS-PV interaction Hamiltonian. We have compared the results on  $P$ -waves with experimental data and with the results of the Chew's cut-off theory and discussed the influence of nucleon recoil in the determination of the renormalized coupling constant. In order to discuss, on the same theoretical line, the influence of nucleon recoil on  $S$ -phases, we have added to the PS-PV interaction Hamiltonian two terms, which are bilinear in the meson field, as can be obtained from a Dyson-Foldy transformation applied to the PS-PS coupling. The effect of nucleon recoil is found to be remarkable.

### 1. — Introduction.

Recently CHEW <sup>(1)</sup> has developed a method of calculation based on the application of the Tamm-Dancoff formalism to the pion-nucleon scattering, using PS-PV interaction Hamiltonian with cut-off. The results he obtained at low energy are in substantial agreement with the experimental results on  $P$ -wave scattering.

In the work of CHEW, as well in those he wrote in collaboration with Low <sup>(2)</sup>, the nucleon is considered as a fixed source of mesons and therefore not subjected to any recoil in a scattering process with mesons.

In this paper we want to look upon the effect of nucleon recoil and to show in which direction CHEW's results are to be modified. In the first sections

---

<sup>(1)</sup> G. F. CHEW: *Phys. Rev.*, **95**, 1669 (1954).

<sup>(2)</sup> G. F. CHEW and F. E. Low: *Phys. Rev.*, **101**, 1570, 1579 (1956).

we shall treat the  $P$ -wave scattering and point out how the value of the renormalized coupling constant is to be increased, compared with that of the fixed source, in order to fit the experimental data. Taken into consideration two terms, bilinear in the meson field, we shall discuss in the Sect. 4 the interference of these ones with nucleon recoil terms of the PS-PV Hamiltonian in the  $S$ -wave scattering. It will be seen how nucleon recoil acts on the behaviour of the  $S$ -phases contributing a large amount to them. It is to be thought that the qualitative aspects of these corrections will be kept also in a more refined theory of pion-nucleon scattering.

## 2. - The Extended Source Theory.

We start with the Hamiltonian (3):

$$(1) \quad H(t) = H_{\text{Nucleons}}^0 + H_{\text{Pions}}^0 + \\ - \frac{i f}{\mu} \sqrt{4\pi} \iint d^4x_1 d^4x_2 \delta(t_1 - t_2) \delta(t_1 - t_2) f(\mathbf{x}_1 - \mathbf{x}_2) \bar{\psi}(x_1) \gamma_{\mu} \tau \frac{\partial \varphi(x_2)}{\partial x_{2\mu}} \psi(x_1),$$

with

$$(2) \quad f(\mathbf{x}_1 - \mathbf{x}_2) = \frac{1}{(2\pi)^3} \int v(k) \exp[i\mathbf{k} \cdot (\mathbf{x}_1 - \mathbf{x}_2)] d^3k,$$

where  $v(k)$  is a function of the modulus of  $\mathbf{k}$  going to zero for high momenta, whose value is 1 for  $\mathbf{k} = 0$ .

Using the free-particle expansions for the field operators and eliminating the small components of the Dirac fields in favour of the large ones, in the non relativistic limit we obtain for the Hamiltonian the following form (\*):

$$(3) \quad H = H_{\text{Nucleons}}^0 + H_{\text{Pions}}^0 + \frac{-i f}{\mu} \frac{\sqrt{4\pi}}{(2\pi)^{\frac{3}{2}}} \iint \frac{d^3k' d^3p'}{\sqrt{2\omega'}} v(k') \cdot \\ \cdot [\psi^+(p' - k') F(p', k') (\boldsymbol{\tau} \cdot \boldsymbol{\sigma}_k^+) \psi(p') - \psi^+(p') F(p', k') (\boldsymbol{\tau} \cdot \boldsymbol{\sigma}_k^-) \psi(p' - k')],$$

with  $F(p', k')$ , given by:

$$(4) \quad F(p', k') = (\boldsymbol{\sigma} \cdot \mathbf{k}') - \frac{\omega'}{2} \left( \boldsymbol{\sigma} \cdot \left[ \frac{\mathbf{p}'}{E_{p'}} + \frac{\mathbf{p}' - \mathbf{k}'}{E_{p' - k'}} \right] \right),$$

where the second term is referred to as « galileian » and the first is the only one retained in the fixed source theory.

(\*) We have omitted the exponential dependence from the Hamiltonian (3), since in the application of the Tamm-Dancoff formalism these terms disappear.

(3) P. BUDINI: *Nuovo Cimento*, **3**, 835 (1956).

### 3. - Pion-Nucleon Scattering in the $P$ -State.

We have to resolve the Schrödinger equation for scattering processes of pions on nucleons at low energy:

$$(5) \quad (H - E) P = 0,$$

where  $E$ , eigenvalue of the total Hamiltonian, is calculated at energy shell:

$$(6) \quad E = E_k + \omega_k.$$

We develop now the state vector  $P$  in eigenstates for the unperturbed Hamiltonian  $H^0$  and retain the terms in one nucleon, neglecting those in three or more mesons. With the usual procedure <sup>(4)</sup> we obtain, in the center-of-mass system, the following equation for the scattering amplitude  $a_i(k) = a_i(-k, k)$ :

$$(7) \quad (E_k + \omega - S - E)a_i(k) = \frac{f^2}{4\pi^2\mu^2} \int \frac{d^3k}{\omega\omega'} \tau(k)\tau(k') \cdot \\ \cdot \left[ \tau_1\tau_2 \frac{F(0, k)F(0, k')}{M - E} - \tau_1\tau_2 \frac{F(-k, k)F(-k', k')}{E_{k-k'} - \omega - \omega' - E} \right] a_i(k'),$$

where the term  $S$  arises as a result of a self-energy process and has the form:

$$(8) \quad S = -\frac{3f^2}{4\pi^2\mu^2} \int \frac{d^3k'}{\omega'} \tau^2(k') \frac{F(-k, k')F(-k, k')}{E_{k-k'} - \omega - \omega' - E}.$$

We keep still a term now; it will be taken properly into account in the normalization of the equation.

The separation of the equation (7) for eigenstates of isospin can be done directly: one obtains:

$$(9) \quad \begin{cases} (E_k + \omega - E)\tau_1(k) = \frac{f^2}{4\pi^2\mu^2} \int \frac{d^3k'}{\omega\omega'} \delta(k)\delta(k') \cdot \\ \cdot \left[ \frac{3F(0, k)F(0, k')}{M - E} - \frac{F(-k, k')F(-k', k)}{E_{k-k'} - \omega - \omega' - E} \right] \sigma_1(k'), \\ (E_k + \omega - E)\sigma_1(k) = \frac{f^2}{4\pi^2\mu^2} \int \frac{d^3k'}{\omega\omega'} \delta(k)\delta(k') \frac{F(-k, k')F(-k', k)}{E_{k-k'} - \omega - \omega' - E} \sigma_1(k'). \end{cases}$$

<sup>(4)</sup> See for instance: F. J. DYSON, M. ROSS, E. E. SALPETER, S. S. SCHWEBER, M. K. SUGARMAN, W. M. YSSINGER and H. A. BETHE, *Phys. Rev.* **95** (1954) 1654.



We shall consider now only the second of these equations and resolve it for  $P$ -state and for the value  $j = \frac{3}{2}$  of the total angular momentum.

Inserting the explicit expressions of  $F(-k, k')$  and  $F(-k', k)$ , the second of the equations (9) becomes:

$$(10) \quad (E_k + \omega - E) a_{\frac{3}{2}}(\mathbf{k}) - \frac{f^2}{2\pi^2 \mu^2} \int_{\mu}^{\infty} \frac{d\omega'}{\sqrt{\omega\omega'}} k' \omega' \delta(k) \delta(k') \cdot \\ \cdot [I_1(\omega|\omega') + I_2(\omega|\omega') + I_3(\omega|\omega') + I_4(\omega|\omega')],$$

with

$$(11) \quad \left\{ \begin{aligned} I_1(\omega|\omega') &= \int_{4\pi} d\Omega_{k'} \frac{(\boldsymbol{\sigma} \cdot \mathbf{k}')(\boldsymbol{\sigma} \cdot \mathbf{k})}{E_{\mathbf{k}+\mathbf{k}'} + C} a_{\frac{3}{2}}(\mathbf{k}'), \\ I_2(\omega|\omega') &= \int_{4\pi} d\Omega_{k'} \left[ \frac{\omega k'^2}{2} \left( \frac{1}{E_{k'}} + \frac{1}{E_{\mathbf{k}+\mathbf{k}'}} \right) + \frac{\omega' k^2}{2} \left( \frac{1}{E_k} + \frac{1}{E_{\mathbf{k}+\mathbf{k}'}} \right) \right] \frac{a_{\frac{3}{2}}(\mathbf{k}')}{E_{\mathbf{k}+\mathbf{k}'} + C}, \\ I_3(\omega|\omega') &= \int_{4\pi} d\Omega_{k'} \frac{\omega + \omega'}{2E_{\mathbf{k}+\mathbf{k}'}} \cdot \frac{(\boldsymbol{\sigma} \cdot \mathbf{k}')(\boldsymbol{\sigma} \cdot \mathbf{k})}{E_{\mathbf{k}+\mathbf{k}'} + C} a_{\frac{3}{2}}(\mathbf{k}'), \\ I_4(\omega|\omega') &= \int_{4\pi} d\Omega_{k'} \frac{\omega\omega'}{4} \left[ \frac{(\boldsymbol{\sigma} \cdot \mathbf{k})}{E_k} + \frac{(\boldsymbol{\sigma} \cdot \mathbf{k})}{E_{\mathbf{k}+\mathbf{k}'}} + \frac{(\boldsymbol{\sigma} \cdot \mathbf{k}')}{E_{\mathbf{k}+\mathbf{k}'}} \right] \cdot \\ &\quad \cdot \left[ \frac{(\boldsymbol{\sigma} \cdot \mathbf{k}')}{E_{k'}} + \frac{(\boldsymbol{\sigma} \cdot \mathbf{k}')}{E_{\mathbf{k}+\mathbf{k}'}} + \frac{(\boldsymbol{\sigma} \cdot \mathbf{k})}{E_{\mathbf{k}+\mathbf{k}'}} \right] \frac{a_{\frac{3}{2}}(\mathbf{k}')}{E_{\mathbf{k}+\mathbf{k}'} + C}, \end{aligned} \right.$$

and

$$(12) \quad C = \omega + \omega' - E.$$

We develop  $[E_{\mathbf{k}+\mathbf{k}'} + C]^{-1}$  and  $[E_{\mathbf{k}+\mathbf{k}'}]^{-1}$  in Legendre polynomial series<sup>(5)</sup>:

$$(13) \quad \left\{ \begin{aligned} [E_{\mathbf{k}+\mathbf{k}'} + C]^{-1} &= \sum_{n=0}^{\infty} Z_n(\omega|\omega') P_n(\theta_{k'}) \\ [E_{\mathbf{k}+\mathbf{k}'}]^{-1} &= \sum_{n=0}^{\infty} X_n(\omega|\omega') P_n(\theta_{k'}), \end{aligned} \right.$$

$Z_n$  and  $X_n$  are given by:

$$(14) \quad \left\{ \begin{aligned} Z_n(\omega|\omega') &= (n + \frac{1}{2})(r\bar{E})^{-1} \int_{1-r}^{1+r} dz \left( \frac{z}{c+z} \right) P_n \left( \frac{z^2 - 1 - r^2}{2r} \right), \\ X_n(\omega|\omega') &= Z_n(\omega|\omega') \Big|_{c=0}, \end{aligned} \right.$$

(5) See reference (4).

with

$$\bar{E} = \frac{E_{k+k'} + E_{k-k'}}{2}, \quad r = \frac{kk'}{\bar{E}^2}, \quad c = \frac{C}{\bar{E}}.$$

Let us determine now the first two coefficients and find approximate formulas, more suitable in calculations, for them:

$$(15) \quad \left\{ \begin{aligned} Z_0(\omega|\omega') &\simeq \left[ \frac{E_{k+k'} + E_{k-k'}}{2} + \omega + \omega' - E \right]^{-1}, \\ Z_1(\omega|\omega') &\simeq - \frac{2kk'}{E_{k+k'} + E_{k-k'}} \left[ \frac{E_{k+k'} + E_{k-k'}}{2} + \omega + \omega' - E \right]^{-2}, \\ X_0(\omega|\omega') &\simeq \left[ \frac{E_{k+k'} + E_{k-k'}}{2} \right]^{-1}, \\ X_1(\omega|\omega') &\simeq -kk' \left[ \frac{E_{k+k'} + E_{k-k'}}{2} \right]^{-3}, \end{aligned} \right.$$

all the others being negligible.

We can evaluate now the integrals  $I_1$ ,  $I_2$ ,  $I_3$  and  $I_4$  at the right hand side of the equation (10). Neglecting terms of order higher than  $k^3 Z_0(\mu/M)$ , for the  $P$ -state, writing  $a(|k|, 0) = a(\omega)$ , we obtain:

$$(16) \quad (\omega - \omega_0 + E_k - E_{k_0}) a_{33}(\omega) = \frac{4f^2}{3\pi\mu^2} \int_{\mu}^{\infty} d\omega' \frac{v(k)v(k')k\omega'k'^2}{\sqrt{\omega\omega'}} \cdot \left[ \omega + \omega' - \omega_0 + \frac{E_{k+k'} + E_{k-k'}}{2} - E_{k_0} \right]^{-1} \left( 1 + \frac{\omega + \omega'}{E_{k+k'} + E_{k-k'}} \right) a_{33}(\omega').$$

This equation differs from the corresponding one in Chew's theory, both at the L.H.S. and at the R.H.S. In these members we have in fact respectively the terms  $E_k - E_{k_0}$  and  $\frac{E_{k+k'} + E_{k-k'}}{2} - E_{k_0}$  which are not included in the Chew's equation; moreover at the R.H.S. appears the factor  $\left( 1 + \frac{\omega + \omega'}{E_{k+k'} + E_{k-k'}} \right)$  due to the galileian term.

The equation (16) can be renormalized by using the method proposed by CHEW<sup>(6)</sup>; in the considered approximation we write

$$(17) \quad (\omega - \omega_0 + E_k - E_{k_0}) [1 + \Lambda_r(\omega_0 - \omega)] a_{33}(\omega) = \frac{4f^2}{3\pi\mu^2} \int_{\mu}^{\infty} d\omega' \frac{v(k)v(k')k\omega'k'^2}{\sqrt{\omega\omega'}[1 + \Lambda_r(\omega_0 - \omega - \omega')]} \cdot \left[ \omega + \omega' - \omega_0 + \frac{E_{k+k'} + E_{k-k'}}{2} - E_{k_0} \right]^{-1} \left( 1 + \frac{\omega + \omega'}{E_{k+k'} + E_{k-k'}} \right) a_{33}(\omega'),$$

where  $f$  is hereafter the renormalized coupling constant.

<sup>(6)</sup> G. F. CHEW: *Phys. Rev.*, **94**, 1748, 1755 (1954).

$\Delta_r$  has the following form:

$$(18) \quad \Delta_r(x) = \frac{3f^2}{\pi\mu^2} \int_{\mu}^{\infty} d\omega' \cdot v^2(k') \frac{xk'^3}{(\omega' - x)\omega'^2}.$$

The integral equation for the amplitude  $a_{33}$  is thus:

$$(19) \quad a_{33}(\omega) = \delta(E_k + \omega - E) + \int_{\mu}^{\infty} d\omega' \frac{K(\omega|\omega')}{E_k + \omega - E} a_{33}(\omega'),$$

where the kernel  $K(\omega|\omega')$  is given by:

$$(20) \quad K(\omega|\omega') = \frac{4f^2}{3\pi\mu^2} \cdot \frac{v(k)v(k')k\omega'k'^2}{\sqrt{\omega\omega'}[1 + \Delta_r(\omega_0 - \omega - \omega')][1 + \Delta_r(\omega_0 - \omega)]} \cdot \left[ \frac{E_{k+k'} + E_{k-k'}}{2} + \omega + \omega' - E \right]^{-1} \left( 1 + \frac{\omega + \omega'}{E_{k+k'} + E_{k-k'}} \right).$$

In order to solve the integral equation (19), one takes its Fredholm solution and substitutes it back in (19) (?), then, in the usual way, the  $\delta_{33}$  phase shift turns out to be

$$(21) \quad \text{tg } \delta_{33} = \frac{4f^2}{3\mu^2} k_0^3 \frac{\frac{M}{\omega_0 + M} \left( 1 + \frac{2\omega_0}{E_{2k_0} + M} \right) v^2(k_0)}{\left( \omega_0 + \frac{E_{2k_0} + M}{2} - E_{k_0} \right) [1 + \Delta_r(-\omega_0)]} \frac{1 - \Delta_c(\omega_0) - \Delta_F(\omega_0)}{1 - \Delta_F(\omega_0)},$$

with  $\Delta_c(\omega_0)$  and  $\Delta_F(\omega_0)$  given by

$$(22) \quad \Delta_c(\omega_0) = \frac{4f^2}{3\pi\mu^2} \int_{\mu}^{\infty} d\omega' \left[ 1 + \frac{\omega_0 + \omega'}{E_{k_0+k'} + E_{k_0-k'}} \right]^2 \left[ 1 + \frac{2\omega_0}{E_{2k_0} + M} \right]^{-1} k'^3 v^2(k') \cdot \frac{\left( \omega_0 + \frac{E_{2k_0} + M}{2} - E_{k_0} \right) [1 + \Delta_r(-\omega_0)]}{\left( \omega' + \frac{E_{k_0+k'} + E_{k_0-k'}}{2} - E_{k_0} \right)^2 [1 + \Delta_r(-\omega')]^2 (\omega' + E_{k_0} - E) [1 + \Delta_r(\omega_0 - \omega')]},$$

$$(22') \quad \Delta_F(\omega_0) = \frac{4f^2}{3\pi\mu^2} \int_{\mu}^{\infty} d\omega' \left[ 1 + \frac{2\omega'}{E_{2k'} + M} \right] k'^3 v^2(k').$$

$$(2\omega' - \omega_0 - ((E_{2k_0} + M)/2) - E_{k_0}) [1 - \Delta_r(\omega_0 - 2\omega')] (\omega' - \omega_0 - E_{k_0} - E_{k_0}) [1 - \Delta_r(\omega_0 - \omega')]$$

(?) J. L. GAMMEL: *Phys. Rev.*, **95**, 209 (1954); P. BUDINI: *Nuovo Cimento*, **3**, 1104 (1956).

Table I shows the results calculated choosing for  $r(k)$  the cut-off function of Chew, i.e. its value is one for  $1 < \omega < 5.6$ , zero for  $\omega > 5.6$ .

TABLE I. —  $\delta_{33}$  phase shift ( $\omega_{\max.} = 5.6$ ).

$\omega_1$	$E_{\text{lab}}$ (MeV)	$\delta_{33}$ (Exp)	$f^2 = f_{\text{Chew}}^2 = 0.058$		$f^2 = 0.0632$
			fixed source $\Lambda_{33}$	with recoil $\Lambda_{33}$	with recoil $\Lambda_{33}$
1.3	57	7.6°	8.0°	5.0°	9.2°
1.6	122	32°	39.4°	18.7°	42.9°
1.9	190	84°	85.8°	41.6°	84.6°
2.0	215	105°	94.6°	50.8°	93.8°

The above Table I shows under column fourth the calculated values of  $\delta_{33}$  phase-shift from Chew's theory and under columns fifth and sixth the results when nucleon recoil is taken into account, for the two values of the renormalized coupling constant,  $f^2 = f_{\text{Chew}}^2$  and  $f^2 = 1.09f_{\text{Chew}}^2$ .

We obtain good agreement with experimental data and with Chew's results with the second value of the renormalized coupling constant ( $f^2 = 0.0632$ ). We observe that  $\delta_{33}$ -phase shift is considerably affected by nucleon recoil especially at high energy. The increase of the renormalized coupling constant in order to fit the experimental data, is, however, rather small, lower than 1/10 (\*) in respect of Chew's choice.

#### 4. — Pion-Nucleon Scattering in the S-State.

Introducing two terms bilinear in the meson field in the previous Hamiltonian and neglecting nucleon recoil, DRELL, FRIEDMAN and ZACHARIASEN (7) obtain, with the Chew-Low method, good agreement with experimental data on S-wave scattering of pions on nucleons, as far as the incident meson energy is less than  $\omega_0 = 1.25$ .

We now shall apply the Tamm-Dancoff formalism in order to achieve results similar to those shown by DRELL *et al.* (7) when nucleon recoil is neglected. The correction due to this effect is then evaluated.

\* We point out that keeping  $f^2 = f_{\text{Chew}}^2 = 0.058$ , we must increase the cutoff energy to about  $\omega_{\max} = 6$ , in order to obtain results comparable with Chew's data.

(7) Work reported by WEISSBERG at the Rochester Conference (1956); see also S. FUBINI: *Nuovo Cimento*, **5**, 564 (1953); S. FUBINI, S. GOTTES, S. GURIN and K. SAWADA: *Prog. Theor. Phys.*, **12**, 79 (1954); J. F. DRELL, M. ROSS, E. E. SALPETER, S. S. SCHWARTZ, M. K. SUNDARESAN, W. M. VINCIGUERRA and H. A. BETHE: *Phys. Rev.*, **95**, 1644 (1954); M. M. LEIT and R. E. MARSHALL: *Nuovo Cimento*, **4**, 366 (1954).

We choose therefore for our Hamiltonian the following one:

$$(23) \quad H = H_0 + H_{\text{pv}} + H_1 + H_2,$$

where  $H_{\text{pv}}$  is the usual PS-PV coupling and the form of  $H_1 + H_2$  is suggested from a Dyson-Foldy transformation applied to the PS-PS interaction Hamiltonian<sup>(9)</sup>. In order to obtain a form factor in the PS-PV interaction Hamiltonian, we start from a correspondingly non-local PS-PS coupling, this gives for  $H_1$  and  $H_2$ :

$$(24) \quad \left\{ \begin{aligned} H_1 &= \lambda_0 \iiint d^4x_1 d^4x_2 d^4x_3 f(\mathbf{x}_1 - \mathbf{x}_2) f(\mathbf{x}_1 - \mathbf{x}_3) \delta(t - t_1) \delta(t - t_2) \delta(t - t_3) \cdot \\ &\quad \cdot \bar{\psi}(x_1) (\boldsymbol{\varphi}(x_2) \cdot \boldsymbol{\varphi}(x_3)) \psi(x_1), \\ H_2 &= \lambda \iiint d^4x_1 d^4x_2 d^4x_3 f(\mathbf{x}_1 - \mathbf{x}_2) f(\mathbf{x}_1 - \mathbf{x}_3) \delta(t - t_1) \delta(t - t_2) \delta(t - t_3) \cdot \\ &\quad \cdot \psi^+(x_1) \boldsymbol{\tau} \cdot (\boldsymbol{\varphi}(x_2) \times \boldsymbol{\Pi}(x_3)) \psi(x_1). \end{aligned} \right.$$

The coefficients  $\lambda_0$  and  $\lambda$  are given by:

$$(25) \quad \left\{ \begin{aligned} \lambda_0 &= l_0 \frac{G^2}{2M} = l_0 \cdot 2M \frac{4\pi f^2}{\mu^2}, \\ \lambda &= l \left( \frac{G}{2M} \right)^2 = l \cdot \frac{4\pi f^2}{\mu^2}, \end{aligned} \right.$$

where  $l_0$  and  $l$  are positive parameters whose magnitude is left now open.

We develop the field operators in Fourier series, using eq. (2) we obtain (\*).

$$(26) \quad \left\{ \begin{aligned} H_1 &= \frac{\lambda_0}{2(2\pi)^3} \iiint \frac{d^3p d^3p' d^3k d^3k' v(k) v(k')}{\sqrt{\omega\omega'}} \psi^+(p) \beta \psi(p') \cdot \\ &\quad \cdot [\alpha_i(k) \alpha_i(k') \delta(p' - p + k + k') + \alpha_i^+(k) \alpha_i^+(k') \delta(p' - p - k - k') + \\ &\quad + \alpha_i^+(k) \alpha_i(k') \delta(p' - p - k + k') + \alpha_i(k) \alpha_i^+(k') \delta(p' - p + k - k')], \\ H_2 &= \frac{-i\lambda}{2(2\pi)^3} \sum_{(123)} \iiint \frac{d^3p d^3p' d^3k d^3k' v(k) v(k')}{\sqrt{\omega\omega'}} \psi^+(p) \tau_1 \psi(p') \cdot \\ &\quad \cdot \{ (\omega' - \omega) [\alpha_2(k) \alpha_3(k') \delta(p' - p + k + k') - \alpha_2^+(k) \alpha_3^+(k') \delta(p' - p - k - k')] + \\ &\quad + (\omega' + \omega) [\alpha_2^+(k) \alpha_3(k') \delta(p' - p + k' - k) - \alpha_3^+(k') \alpha_2(k) \delta(p' - p + k - k')] \}. \end{aligned} \right.$$

(9) F. J. DYSON: *Phys. Rev.*, **73**, 929 (1948); L. L. FOLDY: *Phys. Rev.*, **84**, 168 (1951); S. D. DRELL and E. M. HENLEY: *Phys. Rev.*, **88**, 1053 (1952).

(\*) The summation  $\sum_{(123)}$  is referred to cyclic permutation of the suffixes 1, 2, 3: here too we have omitted the exponential time dependence.

Let us resolve now the Schrödinger equation (5) with the new Hamiltonian (23), in the second Tamm-Dancoff approximation, taking into account, however, only terms of order  $f^2/\mu^2$ . We obtain, in the center-of-mass system the following equation for the amplitude  $a_0(\mathbf{k})$ :

$$(27) \quad (E - \omega - E)a_0(\mathbf{k}) = \frac{Z_0}{(2\pi)^3} \int \frac{d^3k'}{\sqrt{\omega\omega'}} v(k)r(k')a_0(\mathbf{k}') - \\ - \frac{i\lambda}{2(2\pi)^3} \int \frac{d^3k'}{\sqrt{\omega\omega'}} v(k)r(k')(\omega + \omega')\boldsymbol{\tau} \cdot \boldsymbol{\alpha}(\mathbf{k}') + \\ + \frac{f^2}{4\pi^2\mu^2} \int \frac{d^3k'}{\sqrt{\omega\omega'}} v(k)r(k') \frac{\mp(0, k) \mp (0, k')}{M - E} \tau_0 \tau_\lambda a_\lambda(\mathbf{k}') + \\ + \frac{f^2}{4\pi^2\mu^2} \int \frac{d^3k'}{\sqrt{\omega\omega'}} v(k)r(k') \frac{\mp(-k, k') \mp (-k', k)}{E_{\mathbf{k}+\mathbf{k}'} + \omega + \omega' - E} \tau_\lambda \tau_0 a_\lambda(\mathbf{k}'),$$

where we have neglected all self-energy terms.

The equation (27) can be easily separated for states of definite isotopic spin and angular momentum, for the  $S$ -state we obtain (\*)

$$(28) \quad \left\{ \begin{aligned} (\omega - \omega_0 + E_k - E_{k_0})a_1(\omega) &= \\ &= \frac{f^2}{\mu^2} \int_{\mu}^{\infty} d\omega' [K_1^r(\omega|\omega') + K_1^{B_1}(\omega|\omega') + K_1^{B_2}(\omega|\omega')]a_1(\omega'), \\ (\omega - \omega_0 + E_k - E_{k_0})a_3(\omega) &= \\ &= \frac{f^2}{\mu^2} \int_{\mu}^{\infty} d\omega' [K_3^r(\omega|\omega') + K_3^{B_1}(\omega|\omega') + K_3^{B_2}(\omega|\omega')]a_3(\omega'), \end{aligned} \right.$$

where the kernels with superscript  $r$  represent the effect of nucleon recoil and their form is

$$(29) \quad \left\{ \begin{aligned} K_1^r(\omega|\omega') &= \frac{-k'\omega'}{\pi\sqrt{\omega\omega'}} v(k)r(k')Z_0(\omega|\omega') \cdot \\ &\cdot \left\{ \left[ \frac{\omega k'^2}{2E_{k'}} + \frac{\omega' k^2}{2E_k} \right] + X_0(\omega|\omega') \frac{\omega k'^2 + \omega' k^2}{2} \right\}, \\ K_3^r(\omega|\omega') &= -2K_1^r(\omega|\omega'), \end{aligned} \right.$$

as can be easily obtained using eqs. (13) and (15) and neglecting terms of order higher than  $k^2 Z_0(\mu/M)$ .

(\*) In this approach the Hamiltonians (24) do not give any contribution to the scattering in the  $P$ -state.



The kernels signed with superscripts  $H_1$  and  $H_2$  are due to the Hamiltonians  $H_1$  and  $H_2$  respectively; their form is:

$$(30) \quad \begin{cases} K_1^{H_1}(\omega|\omega') = K_3^{H_1}(\omega|\omega') = -\frac{2k'\omega'}{\pi\sqrt{\omega\omega'}} v(k)v(k') \cdot 2Ml_0, \\ K_1^{H_2}(\omega|\omega') = \frac{2k'\omega'}{\pi\sqrt{\omega\omega'}} v(k)v(k') \cdot (\omega + \omega')l, \\ K_3^{H_2}(\omega|\omega') = -\frac{1}{2}K_1^{H_2}(\omega|\omega'). \end{cases}$$

We see from (29) and (30) that nucleon recoil will give a contribution to the  $S$ -phases, opposite in sign to the experimental values, while the effect of the Hamiltonian  $H_2$  will have the same sign as the experimental phases. The Hamiltonian  $H_1$  does not depend on isotopic spin, consequently its contribution to the  $S$ -phases is quite the same in both cases, i.e. for  $T=\frac{1}{2}$  and  $T=\frac{3}{2}$ .

We resolve the integral equation first in Born approximation (see Table II)

TABLE II. —  $\delta_1$  and  $\delta_3$  phase shifts ( $f^2 = 0.082$ ,  $l_0 = 0.0288$ ,  $l = 0.3882$ ).

*Born approximation*

$\omega_0$	without recoil	with recoil	without recoil	with recoil	Drell's values (*)	
	$\delta_1$		$\delta_3$		$\delta_1$	$\delta_3$
1.3	4.1°	3.4°	— 5.8°	— 4.5°	7.1°	— 6.0°
1.6	8.0°	6.1°	— 9.5°	— 5.5°	12.2°	— 10.2°
1.921	13.0°	9.0°	— 13.3°	— 5.4°	18.8°	— 15.0°

(\*) These values have been taken from the diagram of WEISSKOPF'S report at the Rochester Conference (1956).

and we obtain, when nucleon recoil is left out, results fairly similar to those given by DRELL, FRIEDMAN and ZACHARIASEN, choosing for  $l_0$  and  $l$  the same values as in Drell's paper and with the value of the coupling constant  $f^2 = 0.082$ . Table III shows the phase shifts calculated more carefully (First Fredholm approximation).

TABLE III. —  $\delta_1$  and  $\delta_3$  phase shifts ( $f^2 = 0.082$ ,  $l_0 = 0.0288$ ,  $l = 0.3882$ ,  $\omega_{\max.} = 5.6$ ).

*First Fredholm approximation.*

$\omega_0$	without recoil	with recoil	without recoil	with recoil	Drell's values (*)	
	$\delta_1$		$\delta_3$		$\delta_1$	$\delta_3$
1.3	10.6°	6.0°	— 3.9°	— 4.1°	7.1°	— 6.0°
1.6	23.4°	11.0°	— 6.3°	— 5.2°	12.2°	— 10.2°
1.921	39.5°	16.6°	— 8.8°	— 5.3°	18.8°	— 15.0°

(\*) These values have been taken from the diagram of WEISSKOPF'S report at the Rochester Conference (1956).

We observe how the effect of nucleon recoil is rather large <sup>(10)</sup> and how it increases with increasing energy. The contribution from nucleon recoil is increasing faster (with  $k^3$ ) than the one due to the Hamiltonian  $H_1$ ,  $H_2$  (with  $k$ ); furthermore it has opposite sign so that, at high energy, the  $S$ -phase shifts could reverse their signs. In our case, with the chosen values for the parameters  $l_0$  and  $l$  the change in sign is obtained at too high energy. Probably, with a proper choice of the parameters  $l_0$  and  $l$  the experimental behaviour of the  $S$ -phase shifts could be better approached, but this would not make much sense if terms of order higher than  $f/\mu^2$  and renormalization effects are not properly taken into account.

We believe however, that any theory which claims to reproduce  $S$ -wave scattering, must look upon the effect of nucleon recoil if it wants to explain some remarkable experimental feature.

\* \* \*

It is a great pleasure to thank Professor P. BUDINI for having suggested this work and for his continuous advice and encouragement.

<sup>(10)</sup> See E. M. HENLEY and M. A. RUDERMAN: *Phys. Rev.*, **90**, 719 (1953).

#### RIASSUNTO (\*)

Nell'estensione della teoria delle sorgenti dello scattering pione-nucleone con hamiltoniana d'interazione PS-PV si è tenuto conto dell'effetto del rinculo dei nucleoni. Abbiamo confrontato i risultati sulle onde  $P$  coi dati sperimentali e coi risultati del taglio di Chew e discusso l'influenza del rinculo dei nucleoni sulla determinazione della costante d'accoppiamento rinormalizzata. Per discutere sulle stesse basi teoriche l'influenza del rinculo dei nucleoni sulle fasi  $S$ , abbiamo aggiunto alla hamiltoniana d'interazione PS-PV due termini, bilineari nel campo mesonico, quali si possono ottenere da una trasformazione di Dyson-Foldy applicata all'accoppiamento PS-PS. L'effetto del rinculo dei nucleoni risulta notevole.

## Anisotropy of Cosmic Rays During the Cosmic-Ray Storms.

S. YOSHIDA

*Physical Institute, Nagoya University - Nagoya*

(ricevuto il 6 Settembre 1956)

**Summary.** — Various phenomena about the cosmic-ray diurnal variations, especially anomalous diurnal variations associated with geomagnetic storms, were studied. A very important part of cosmic-ray diurnal variations was interpreted as the result of the anisotropic flow of cosmic-rays which takes place during the cosmic-ray storms. Through a study of the energy and latitude dependence of the anomalous diurnal variations, it was indicated that this anisotropy is produced by the acceleration of cosmic rays in the solar stream. The variations of this acceleration observed at various positions in a solar stream, the variations in different streams of various ages and the variation in a 11-year period are described.

### 1. — Introduction.

The author <sup>(1)</sup> has reported the anomalous diurnal variation of cosmic-ray intensities associated with a geomagnetic storm or a geomagnetic disturbance (Fig. 1). The characteristic features of this anomaly were the amplitude increase and the phase advancement. The amplitude increment was comparable with the amplitude on usual days. Therefore, it was suggested that the nature of the anomalous diurnal variation should be known before the explanation of the average diurnal variation.

Similar anomalous diurnal variations were observed by several other authors. The characteristic features observed by them are nearly the same, but not exactly. The difference may come from the difference in the method of sta-

---

<sup>(1)</sup> S. YOSHIDA: *Proc. Cosmic-Ray Lab. Nagoya Univ.*, **1**, (No. 4), 18 (1947); Y. SEKIDO and S. YOSHIDA: *Rep. Ionosphere Res. Japan*, **4**, 37 (1950).

tistical analysis and condition of observation. Now, it is desirable to establish the physical state which appears as the cause of these anomalous diurnal variations. For this purpose, the interpretation of each individual event as the

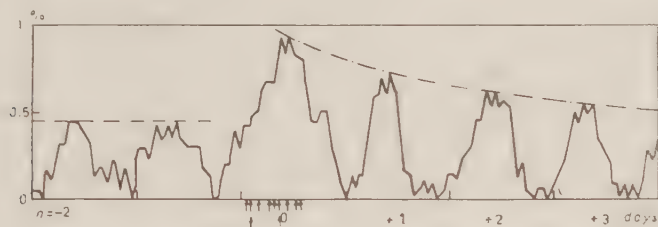


Fig. 1. — Anomalous diurnal variation ( $I$ ).  $\wedge$ : commencement of a magnetic storm.

result of the anisotropic flow of cosmic rays during a cosmic-ray storm is described in Sect. 2, and the comparisons of the results obtained through various statistical methods or observed under various experimental conditions are described in Sect. 3 and 4.

On the other hand, theoretical explanations of total or anomalous diurnal variations were tried by various authors. But no satisfactory explanation was given as yet. If it is difficult to find the complete mechanism at once, it may be a promising way of approach to establish one step of the mechanism which is directly connected with the established physical state. This problem is discussed in Sect. 5, and the anisotropy during the cosmic-ray storm is attributed to acceleration of cosmic-ray particles. The other effects which also contribute to the diurnal variation are discussed in Sect. 6.

## 2. — Individual Events.

The diurnal variation of the cosmic-ray intensities, corrected for the atmospheric effect, is considered to be due to the rotation of the earth in an anisotropic flow of cosmic rays. As the last approximation, this flow consists of a large isotropic flow and a small directional flow of cosmic-ray energy. Let the flux and the direction of this directional flow be  $a$  and  $\varphi$  respectively, then time variations of  $a$  and  $\varphi$  (i.e. additional anisotropy) will produce an anomalous diurnal variation. On the other hand, the flux of the isotropic flow gives the world-wide mean intensity  $I$ , and its rapid variation ( $d^2I/dT^2$ ) may appear as an anomalous diurnal variation (curvature effect) at any station rotating with the earth. It must be remembered that the anomalous diurnal variation is associated with a magnetic storm or a magnetic disturbance, and

it is often associated with a remarkable decrease of  $I$ . Therefore, the time variation of  $(a, q)$ , which is considered as the physical base of the anomalous diurnal variation, can not be known from the observation at a single station. Simultaneous observations done at three widely separated longitudes are necessary to know the variations of  $(a, \varphi)$  and  $I$  at a given instant. This method of analysis is important especially for the study of individual events.

At present, it is difficult to get sufficient accuracy for correcting the temperature effect, therefore barometer corrected intensities have been used throughout. The author <sup>(2)</sup> analyzed several events observed simultaneously at various stations ( $n = 1, 2, 3$ ), to obtain  $(a', \varphi')$  and  $I$  as the functions of the universal time  $T$  at every two hours, by assuming the following formula:

$$K_n \cdot I_n(T) = I(T) + a'(T) \cos(t_n - \varphi'(T)) + A_n(T),$$

where,  $I_n$ : barometer corrected intensity observed at the  $n$ -th station,

$K_n$ : constant near unity,  $t_n$ : the local time, and  $A_n$ : local variation of intensity with periods longer than one day, probably due to atmospheric effect.

$A_n$  was determined through a successive approximation method, and then  $(a', \varphi')$  and  $I$  were obtained as the solution of simultaneous equations at each universal time  $T$ . The vector  $(a', \varphi')$  (see Fig. 2 (a)) includes the effect of the diurnal variation due to the temperature effect, but the time variation i.e. the vector  $(a, \varphi)$  is free from the temperature effect and represents the

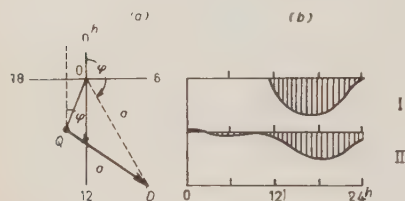


Fig. 2. - (a) Representation of additional anisotropy  $(a, q)$  in a harmonic dial.  $Q$ : quiet period;  $D$ : disturbed period. (b) Apparent higher harmonics.  $I$ : observed by EHMERT *et al.* <sup>(7)</sup>;  $II$ : expected from the time variation of  $(a, \varphi)$  (Fig. 3 (a)).

additional anisotropy, provided the diurnal variation of the temperature is not affected by the storm.

10 events thus analyzed are listed in Table I, and the results are shown in Fig. 3. The decrease of  $I$  and the increase of  $a'$  occur simultaneously within the error of a small number of hours. Thus, the combined variation may be called as a cosmic-ray storm <sup>(3)</sup>, where the decrease of the isotropic intensity  $II$

<sup>(2)</sup> Y. SEKIDO, S. YOSHIDA and Y. KAMIYA: *Rep. Ionosphere Res. Japan*, **6**, 195 (1952).

<sup>(3)</sup> Y. SEKIDO: *Proceedings of International Conference on Theoretical Physics, 1953, Symposium on Cosmic Rays*. Working Association of Primary Cosmic-Ray Research, Japan, Communication to the Meeting of I.A.T.M.E., at Rome (1954).

TABLE I. — *Individual events.*

Cosmic-ray storm commencement $T_0$	Magnetic storm S.C. main	Longitude of stations (*)	Result Fig. 3(c)
6 <sup>h</sup> 17 <sup>th</sup> Jan. 1938	25 <sup>h</sup> 16 <sup>th</sup> 23 <sup>h</sup> 16 <sup>th</sup>	13° E 140° E 75° W	<i>a</i>
6 22 Jan. 1938	3 22 7 22	13 140 75	<i>b</i>
14 25 Jan. 1938	12 25 14.5 25	13 140 75	<i>c</i>
8 1 Mar. 1942	7 1 9.5 1	10 140 77	<i>d</i>
6 27 Jul. 1946	19 26 4 27	0 140 76	<i>e</i>
22 24 Jan. 1949	18 24 23 24	0 140 76	<i>f</i>
14 12 Apr. 1949	15 12 21 12	0 138 76	<i>g</i>
18 20 Feb. 1950	23 19 18 20	8 140 76	<i>h</i>
2 22 Feb. 1950	0 22 1 22	8 140 76	<i>i</i>
14 23 Feb. 1950	11 23 12 23	8 140 76	<i>j</i>

(\*) European stations: Dahlem (13° E), Friedrichshafen (10° E), Freiburg (8° E), Manchester (0°); Oriental stations: Tokyo (140° E), Nagoya (137° E); American stations: Huan-cayo (75° W), Cheltenham (77° W).

is the  $D_s$ -component and the additional anisotropy  $1(a', q')$  or  $(a, q)$  is the  $DN$ -component of the cosmic-ray storm, after the terminology of the magnetic storm. The commencement  $T_0$  was determined by the sudden decrease of  $I$  in each event, and  $T_0$  thus determined was almost the same time as the main phase of the associated magnetic storm as shown in Table I. The cosmic-ray storm, begun with a magnetic storm, attains its maximum a little after the maximum of the magnetic storm and the duration of the cosmic-ray storm is longer than that of the magnetic storm. The time variations of  $I$  and  $(a', q')$  are shown in Fig. 3 (a) and (b) as the functions of the storm time  $T_s = T - T_0$ . During the storm, the additional anisotropy  $(a, q)$  makes an anti-clockwise loop as shown in Fig. 3 (b). This anti-clockwise variation was noticed in each event. The additional anisotropy  $(a, q)$  during a storm may be simply represented

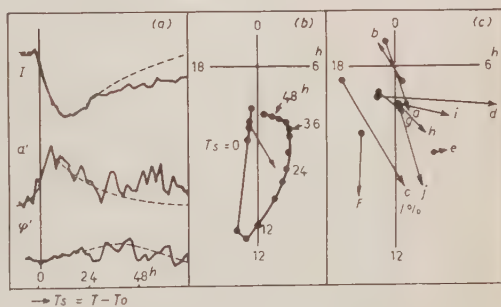


Fig. 3. — Additional anisotropy determined from the simultaneous observations at three different longitudes (see Table I). (a), (b) Storm time variation of the average for 10 cosmic-ray storms.  $T_s$ : storm time;  $T$ : universal time;  $T_0$ : commencement i.e. sudden decrease of the world-wide intensity  $I$ ; Curve in (b):  $(a', q')$  reproduced in a harmonic dial. (c)  $\vec{QD}$  vectors for individual storms.  $Q$ : pre-storm period;  $D$ : storm period;  $a, b, c, \dots$ : see Table I.



by a vector  $\vec{QD}$  as shown in Fig. 3 (b) and (c), where  $Q$  is the quiet period ( $-48$  hours  $\leq T_s \leq 0$ ), and  $D$  is the disturbed period ( $0 \leq T_s \leq +48$  hours). The distribution of  $\varphi$  is shown in Fig. 12 (a), and the average is about 10 h.

Corresponding to the anti-clockwise variation of the additional anisotropy ( $a, q$ ),  $a'$  increases and then  $q'$  decreases in most cases. Through the rotation of the earth, this appears as the amplitude increase and the phase advancement of the diurnal variation observed at a certain station, if the time variations of  $I$ ,  $a$  and  $\varphi$  are not so rapid. In general, the diurnal variation on the day including the commencement of a storm is much deformed, but there are many cases in which the amplitude increase and the phase advancement in the 2-nd and the 3-rd days of a storm are easily seen. ELLIOT and DOLBEAR<sup>(4)</sup> and TRUMPY<sup>(5)</sup> noticed that such anomalous diurnal variations were observed associated with magnetic storms. FIROR *et al.*<sup>(5)</sup> published an example of anomalous diurnal variation of neutron intensity on November 13, 1951. EHMERT and SITTKUS<sup>(6)</sup> noticed some events when the anomalous diurnal variations were observed at two stations. There were magnetic storms on those days respectively, though they did not refer to them.

### 3. - Statistical Results.

Most of the statistical works on the anomalous diurnal variations are based on the observations at a single station. In those cases, the anti-clockwise variation of ( $a, q$ ) produces apparently higher harmonics in the diurnal variation, and they can not be eliminated through averaging on many days. The apparent diurnal variation expected from a typical time variation of ( $a, q$ ) is shown in Fig. 2 (b). EHMERT and SITTKUS<sup>(7)</sup> noticed that the average wave form observed at Freiburg and Weissenau on the days of large diurnal amplitude had a bay shaped decrease in the afternoon (Fig. 2 (b)) superposed on a diurnal sine curve. As most of the days used by them were magnetically disturbed days, this bay may be interpreted as the apparent higher harmonics described above, though this argument does not exclude the existence of higher harmonics of the anisotropy.

Though the diurnal variation observed at a single station includes the curvature effect due to  $d^2I/dT^2$ , this effect can be decreased if a sufficient number of storms are averaged, for the occurrence of a storm is independent of the

(4) H. ELLIOT and D. W. N. DOLBEAR: *Journ. Atmos. Terr. Phys.*, **1**, 205 (1951).

(5) B. TRUMPY: *Physica*, **111**, 645 (1953).

(6) J. W. FIROR, W. H. FONGER and J. A. SIMPSON: *Phys. Rev.*, **94**, 1031 (1954).

(7) A. EHMERT and A. SITTKUS: *Zeits. f. Naturf.*, **6a**, 618 (1951).

local time of a particular station. Various authors have noticed anomalous diurnal variations comparing the diurnal variations observed on disturbed days ( $D$ ) and quiet days ( $Q$ ) at a single station respectively. Their principles of selecting days were not the same. Some of them selected days according to geomagnetic activity, while some of them according to cosmic-ray activity, as shown in Table II. The 1st harmonics on  $D$ -days and  $Q$ -days respectively, published by them or calculated from their results, are shown in Fig. 4. After simplifying each curve in Fig. 4 into a  $\vec{QD}$  vector respectively (\*), the phase  $q$  of the anomaly vector  $\vec{QD}$  distributes between  $2^h$  and  $15^h$  as shown in Fig. 12 ( $a$ ).

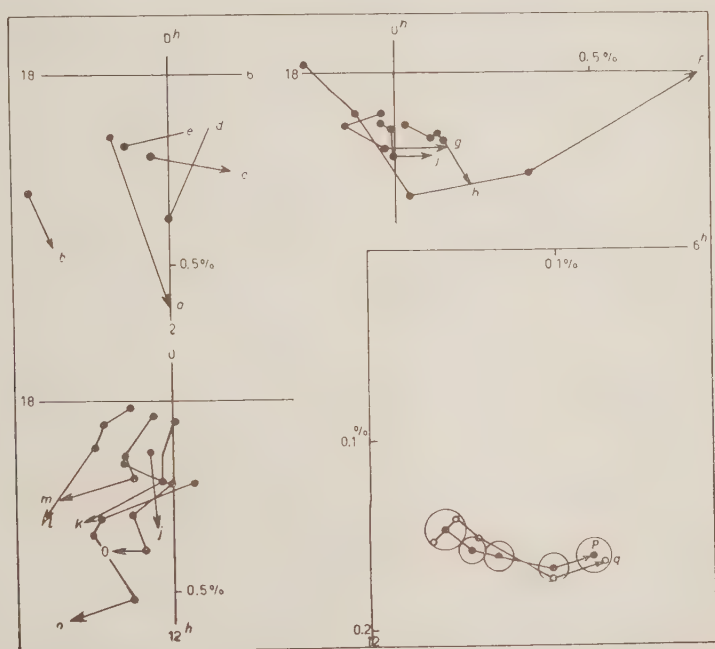


Fig. 4. — Anomalous diurnal variations represented by  $\vec{QD}$  vectors (see Table II).

Among them, the methods of selecting days adopted in the case  $j, k, l, m, n$  and  $o$  are unsuitable for the phase advancement, for  $q'$  does not yet advance when  $a'$  attains its maximum as shown in Fig. 3 ( $a$ ). If these four cases are omitted,  $q$  distributed between  $2^h$  and  $11^h$ . In any case, the average phase

(\*) For example, curves  $f$  and  $g$  in Fig. 4 are simplified into vectors  $L$ , and  $K$  (period  $e$ ) in Fig. 7 respectively.

is nearly the same as that of the additional anisotropies described in Sect. 2. Therefore the anomalous diurnal variations noticed by various authors approximately represent the additional anisotropy, though their statistical method is not perfectly free from the curvature effect. Though the selection of the  $D$ -days in  $j, k, \dots, q$  did not refer to magnetic activity, a large part of the selected  $D$ -days (most of  $D$ -days in  $n, o, p$  and  $q$  at least) were magnetically disturbed days. Therefore, the cosmic-ray activity selected by them may be considered as the cosmic-ray storms associated with magnetic disturbance. Thus, all the additional anisotropies noticed in Table II are associated with

TABLE II. — *Anomalous diurnal variations noticed by various authors.*

	Selection of days		Author	Observation		Result Fig. 4	
	D-days	Q-days		Period	Station		
Geomagnetic activity	2 magnetic storms	Annual mean	ELLIOT and DOLBEAR <sup>(4)</sup>	1946-49	Manchester	<i>a</i>	
	International disturb. day	quiet day	HOGG <sup>(8)</sup>	1935-40	Canberra	<i>b</i>	
			WADA <sup>(9)</sup>	1947-49	Tokyo	<i>c</i>	
			SEKIDO <i>et al.</i> <sup>(10)</sup>	1949-50	Nagoya (*)	<i>d, e</i>	
	Character figure (C)		SEKIDO and KODAMA <sup>(11)</sup>	1949-50	Nagoya (*)	<i>f, g</i>	
	1.4, 0.9, 0.6, 0.3, 0			1947-49	Tokyo	<i>h</i>	
1.75, 1.2, 0.7, 0.2				1937-45	Huancayo	<i>i</i>	
Cosmic-ray activity	Diurnal amplitude (%) large ----- small		SITTKUS <sup>(12)</sup>	1949-51	Freiburg	<i>j</i>	
			MALMFORS <sup>(13)</sup>	1948	Stockholm (+)	<i>k, l, m</i>	
	Day-night difference		FIROR <i>et al.</i> <sup>(6)</sup>	1952	Climax	<i>n</i>	
	1.4, 1.2, 0.7, 0.5, 0.3			neutron	Huancayo	<i>o</i>	
			Daily mean intensity — 0.3, — 0.2, 0.1, 0.3, 0.4	YOSHIDA and KONDO <sup>(14)</sup>	1936-45	Huancayo	<i>p, q</i>

(\*)  $d, f$ :  $Z$  max  $-12^\circ$ , e.g.:  $Z$  max  $-40^\circ$ .

(+)  $k$ : North,  $l$ : South,  $m$ : vertical.

<sup>(4)</sup> A. R. HOGG: *Memoirs Commonwealth Obs.*, No. 10, 67 (1949).

<sup>(9)</sup> M. WADA: *Rep. Cosmic-Ray Lab., Sci. Res. Inst. Tokyo*, **1**, 29 (1952).

<sup>(10)</sup> Y. SEKIDO, M. KODAMA and T. YAGI: *Rep. Ionosphere Res. Japan*, **4**, 207 (1950).

<sup>(11)</sup> Y. SEKIDO and M. KODAMA: *Rep. Ionosphere Res. Japan*, **6**, 111 (1952).

<sup>(12)</sup> A. SITTKUS: private communication.

<sup>(13)</sup> K. G. MALMFORS: *Tellus*, **1**, 55 (1949).

<sup>(14)</sup> S. YOSHIDA and I. KONDO: will be published; S. YOSHIDA and I. KONDO: *Journ. Geomag. Geoelec.*, **6**, 15 (1954).

magnetic disturbances or cosmic-ray storms. The  $D$ -days in  $q$  were selected excluding the days of magnetic storms. Still, the result is nearly the same as  $p$ , which includes magnetic storms. Now, the magnetic storm is not essential for the additional anisotropy. But, the additional anisotropy is one of the features of the cosmic-ray storm, which is associated with more or less magnetic disturbance.

As described above, the cosmic-ray storm is sometimes associated with a typical magnetic storm, and sometimes with a small magnetic disturbance. This relation become a little clearer through a study of 27-day recurrence. YOSHIDA and KONDO (<sup>14</sup>) examined Huancayo data, taking the days of magnetic S.C. storms associated with appreciable cosmic-ray decrease ( $\Delta I = 0.4\%$ ) as the epochs. The result is shown in Fig. 5. The diurnal harmonic is expressed by  $\alpha \cos t - \beta \sin t$ , where  $t$  is the local time. The anomaly in the diurnal variation is most remarkably shown in the time variation of  $\beta$ , just as expected from the phase of  $\vec{QD}$  vectors at Huancayo (see  $p, q$  in Fig. 4). There is day-to-day persistence of  $\beta$  ranging over several days. This duration is longer than that of a magnetic storm, and seems to be a little longer than that of intensity decrease ( $\Delta I$ ). Beside this day-to-day persistence, the 27-day recurrence of  $\beta$  is strongly persistent over 3 or 4 solar rotations, though there is no appreciable recurrence in the number of magnetic storms ( $N$ ). Thus the cosmic-ray storm is associated with a typical magnetic storm at the 1st cycle ( $v = 0$ ), but is associated with a small magnetic disturbance after the next cycle ( $v = 1$ ). The anomaly vectors ( $D-Q$ ) corresponding to each cycle ( $v = -1, 0, +1, \dots, +4$ ) respectively are shown in Fig. 5 (b), where

$$\begin{aligned} D\text{-days: } n &= v \times 27 \pm \varepsilon, & \varepsilon &= 0, 1, 2, 3, \\ Q\text{-days: } n &= v \times 27 \pm 13.5 \pm \varepsilon, & \varepsilon &= 0.5, 1.5, 2.5. \end{aligned}$$

The phase  $\varphi$  of the anomaly distributes between  $5^h$  and  $13^h$  as shown in Fig. 12 (a), and the average phase is nearly the same as that of the additional anisotropy. Through a number of the solar rotations, the absolute value of the additional anisotropy  $a$  diminishes slowly, and the phase  $\varphi$  seems to make a clock-wise variation. SITTKES (<sup>12</sup>) also noticed the day-to-day persistence and the 27-day recurrence of the days of large diurnal amplitude. FIROR *et al.* (<sup>6</sup>) applied the superposed epoch method on the day-night difference of the neutron intensities observed by them, taking the days of large day-night difference as the epochs. They obtained a little day-to-day persistence and 27-day recurrence, but not so remarkable. These small effects may be attributed to their method of analysis, for the «day interval» was a fixed local time interval while the phase of the diurnal variation might be a variable.

It is well known that the magnetic storms or the cosmic-ray storms are

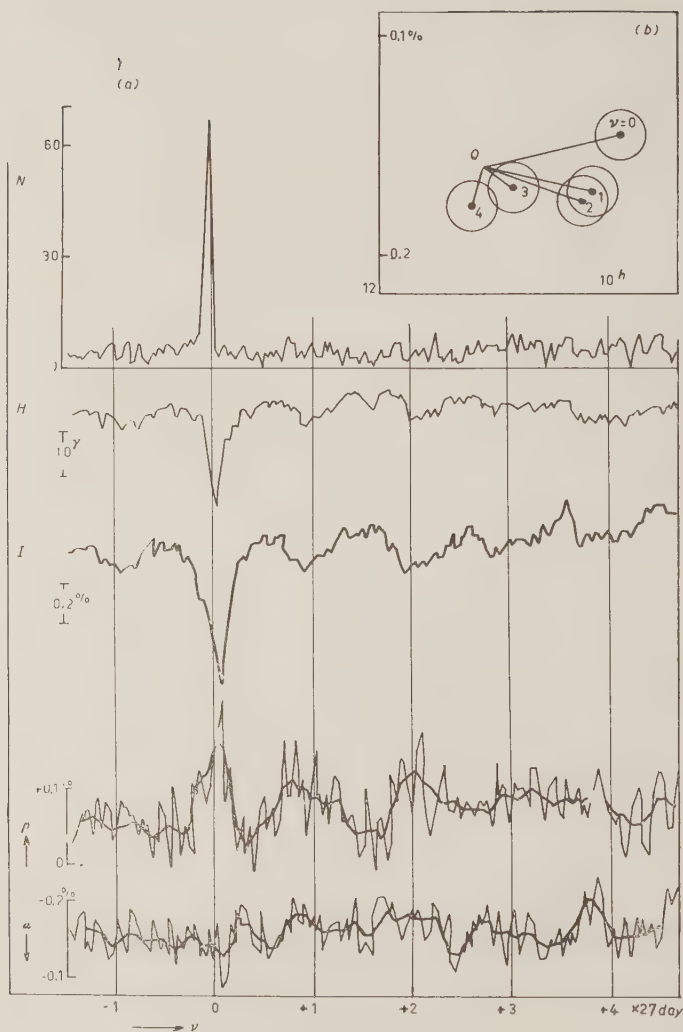


Fig. 5. - 27-day recurrence of diurnal variation.  $n = 0$ : days including a magnetic storm with appreciable cosmic-ray decrease (1936-1946);  $N$ : number of storms;  $H$ : magnetic horizontal force (Kakioka);  $I$ : daily mean intensity (Huancayo);  $\alpha \cos t + \beta \sin t$ : diurnal variation (Huancayo); (b):  $\vec{QD}$  vectors of 27-day cycles.

frequent in the equinox period. SEKIDO and YOSHIDA<sup>(15)</sup> have noticed the « equinox effect » of cosmic-ray diurnal variation. Here, more data were added

(15) Y. SEKIDO and S. YOSHIDA: *Journ. Geomag. Geoelec.*, 2, 66 (1950).

and the result is shown in Fig. 6 (a) and Table III, where  $D$ -days are all the days in the equinox period (Feb.-Apr. and Aug.-Oct.),  $Q$ -days are all the days in the solstice period (May-July and Nov.-Jan.), and the difference vectors  $D - Q$

Fig. 6. — Anomalous diurnal variations represented by  $(D - Q)$  vectors. The origins correspond to  $Q$ -days. (a) Equinox ( $D$ ) minus solstice ( $Q$ ) at various stations (see Table III),  $e$  (neutron): plotted in the scale  $1/3.2$  (see reference <sup>(6)</sup>). (b) Total days diurnal variation, ( $T$ ) minus quiet days ( $Q$ ) in each year (Huancayo); conditions for selecting the quiet days of  $\bullet$  is more strict than that of  $\circ$ .

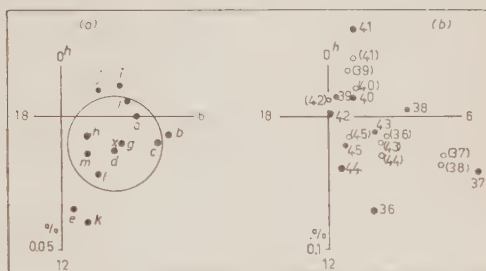


TABLE III. — Half-year variation at various stations.

Station	Detector	Period	Result Fig. 6 (a)
Canberra <sup>(16)</sup>	ion-chamber	1935-40	<i>a</i>
Capetown <sup>(17)</sup>	»	1933-36	<i>b</i>
Cheltenham <sup>(18)</sup>	»	1937-46	<i>c</i>
Christchurch <sup>(18)</sup>	»	1937-46	<i>d</i>
Climax <sup>(19)</sup>	BF3 counter	1951-53	<i>e</i>
Freiburg <sup>(20)</sup>	ion-chamber	1951-52	<i>f</i>
Godhavn <sup>(18)</sup>	»	1939-46	<i>g</i>
Hafelekar <sup>(21)</sup>	»	1936	<i>h</i>
Huancayo <sup>(18)</sup>	»	1937-46	<i>i</i>
London <sup>(22)</sup>	G.M. counter	1941-44	<i>j</i>
Manchester <sup>(23)</sup> (*)	»	1948	<i>k</i>
Nagoya <sup>(11)</sup>	»	1949-50	<i>l</i>
Tokyo <sup>(24)</sup>	»	1947-49	<i>m</i>

(\*) (North + South)/2.

<sup>(16)</sup> A. R. HOGG: *Nature*, **162**, 613 (1948).

<sup>(17)</sup> B. F. J. SCHONLAND: *Terr. Mag.*, **42**, 137 (1937).

<sup>(18)</sup> I. LANGE and S. E. FORBUSH: *Carnegie Inst. Wash. Publ.*, No. 175 (1948).

<sup>(19)</sup> J. FIROR: *Phys. Rev.*, **94**, 1017 (1954).

<sup>(20)</sup> A. SITTKUS: private communication.

<sup>(21)</sup> A. DAUVILLIER: *Les Rayons Cosmiques* (Paris, 1954), p. 455.

<sup>(22)</sup> A. DUPERIER: *Sixième Rapport: Relations entre phenom. Solaires et Terr.*

<sup>(23)</sup> H. ELLIOT and D. W. N. DOLBEAR: *Proc. Phys. Soc.*, **13**, 137 (1950).

<sup>(24)</sup> Y. MIYAZAKI: private communication.



obtained for various stations are shown in Fig. 6 (*a*). The phase  $\varphi$  of the anomaly vectors ( $D-Q$ ) distributes between  $3^h$  and  $11^h$  as shown in Fig. 12 (*a*), and the average phase is nearly the same as that of the additional anisotropy described in Sect. 2. Therefore the equinox effect will be explained as the result of the additional anisotropy.

Not only this half-year periodicity, but also 11-year variation may be expected, for the magnetic storms or the cosmic-ray storms are frequent in the sunspot active period. SARABHAI and KANE<sup>(25)</sup> noticed 11-year variation of the diurnal amplitude ( $a'$ ), while THAMBYAPILLAI and ELLIOT<sup>(26)</sup> found a secular variation of the diurnal phase ( $q'$ ). The year-to-year variation of the annual mean diurnal variation is not simple, and will be discussed in Sect. 6. In order to see the year-to-year variation of the anomaly of the diurnal variation,  $T-Q$  vector is an appropriate measure, where  $T$  is the diurnal variation averaged over total days in a year, while  $Q$  is the average diurnal variation of the magnetically quiet days in the year. Thus,  $T-Q$  vector represents the anomaly in the year, including the frequency of the storms. In Fig. 6 (*b*) the  $T-Q$  vectors (Huancayo<sup>(18)</sup>) calculated for each year are shown, the phase  $q$  of the anomaly distributes between  $2^h$  and  $12^h$  as shown in Fig. 12 (*a*). The year-to-year variation of  $\Phi$  is plotted in Fig. 16 (*g*). It seems to make a 11-year variation.

#### 4. - Energy and Latitude Dependence.

Simultaneous observations of the anomalous diurnal variations at various altitudes or under various thicknesses of absorbing materials are available to

TABLE IV. - Events used for the study of energy and latitude dependence.

Period	$D$ -days (*)	$Q$ -days	Equipment (see Table V)	Result Fig. 7	$\Phi$
5-12th May 1948	0, +1 days	the rest	JNOP	<i>a</i>	$16^h$
Jan. 1949	24-26th Jan.	Annual mean	BHNP	<i>b</i>	15
15-28th Feb. 1950	20-26 th	the rest	KLNP	<i>c</i>	11
Mar.-Apr. 1949	0, +1, +2 days	the rest	KLNP	<i>d</i>	12
Mar. 1949-Sept. 1950	C-index > 2.5/3	$C < 1.0/3$	KL	<i>e</i>	13
10-19th Jan. 1938	0, +0.5 days	-7, -6 days	CGP	<i>f</i>	18
20-25th Jan. 1938	0, +0.5 days	-1, -2 days	CFGP	<i>g</i>	16
26th Feb.-6th Mar. 1942	0, +0.5 days	-1, -2 days	ABDEGMP	<i>h</i>	9
26-31th Jul. 1946	0, +0.5 days	+2.5, +3 days	AEGIP	<i>i</i>	14

(\*) *a*, *d*: 0-day includes the commencement of a magnetic storm. *f*, *g*, *h*, *i*: 0-day corresponds to  $0 < T_s < 24$  h,  $T_s$  being the storm time.

<sup>(25)</sup> V. SARABHAI and R. P. KANE: *Phys. Rev.*, **90**, 204 (1953).

<sup>(26)</sup> T. THAMBYAPILLAI and H. ELLIOT: *Nature*, **171**, 918 (1953).

know the energy and latitude dependence of the additional anisotropy. Some available data are shown in Tables IV, V and Fig. 7. Among them  $f$ ,  $g$ ,  $h$  and  $i$

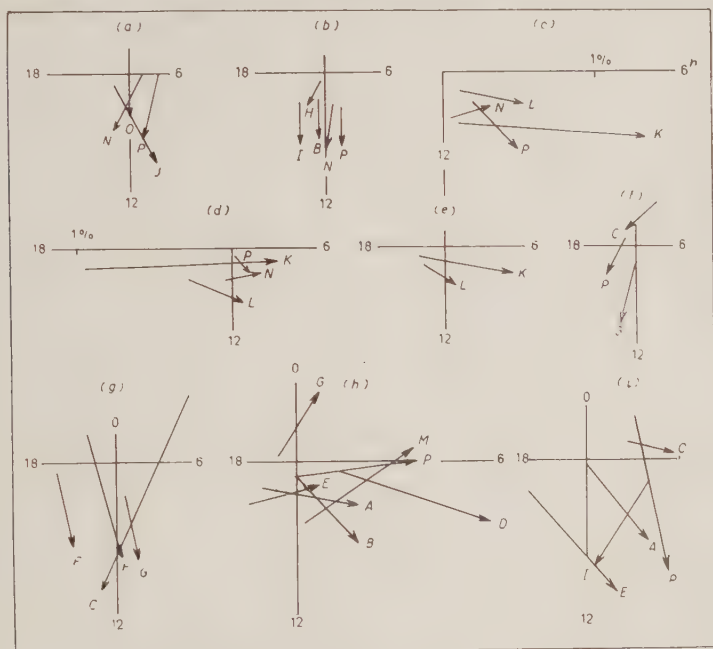
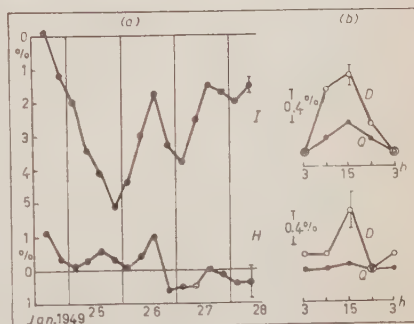


Fig. 7. - Anomalous diurnal variations ( $\vec{QD}$  vectors) observed simultaneously with various equipments or at various latitudes.  $a, b, c, \dots$ : period of observation (see Table IV)  $A, B, C, \dots$ : station and equipment (see Table V).

were calculated by KAMIYA<sup>(27)</sup> carefully eliminating the error due to the curvature effect. It may be worthwhile to note that the additional anisotropy displayed itself even un-

Fig. 8. - Anomalous diurnal variation underground. (a) Time variation reproduced from reference<sup>(31)</sup>.  $H$ : underground (London);  $I$ : sea level (Manchester);  $0\%$ : average for a long period. (b) Diurnal variation.  $D$ : 24-28 th, Jan. 1949;  $Q$ : annual mean.



(<sup>27</sup>) Y. KAMIYA: to be published.

derground. The intensity-time variation observed by MAC ARNUFF is reproduced in Fig. 8 (a). Its diurnal variation is shown in Fig. 8 (b). The anomaly ( $D - Q$ ) observed underground is a little smaller than that at sea level.

As shown in Fig. 7, larger anomalies were observed by the detectors with smaller aperture. This tendency may be attributed to the different thicknesses of the absorbing materials, consequently the different energy of the effective primaries. The mass of materials in the path ( $\text{g cm}^2$ ) is not suitable for the energy parameter, for there is the effect of meson disintegration. The flux  $I$

TABLE V. — Equipments used for the study of energy and latitude dependence.

Station	Equip- ment $Z_{\text{max}}$	$Z$	$I$ $10^{-3}$	$E$ GeV	$\psi E$	$\Delta\Phi$	$s$	Result Fig. 7
Cheltenham ( <sup>28</sup> ) . . .	90° (*)	41°	3.6	39	38°	— 2°	0.83	A
Christchurch ( <sup>28</sup> ) . . .	90 (*)	41	3.6	39	38	— 2	0.83	B
Dahlem ( <sup>29</sup> ) . . . . .	12	7	9.7	19	44	— 2	1.00	C
Friedrichshafen ( <sup>30</sup> ) .	40	22	7.8	23	43	— 1	0.98	D
Godhavn ( <sup>28</sup> ) . . . . .	90 (*)	41	3.6	39	29	+ 1	0.63	E
Hafelekarr ( <sup>31</sup> ) . . . . .	90 (*)	41	7.0	25	40	— 3	0.83	F
Huancayo ( <sup>18, 28</sup> ) . . . .	90 (*)	41	3.4	40	47	+ 36	0.73	G
London ( <sup>31</sup> ) (+) . . . . .	85	40	0.2	220	6	+ 15	0.70	H
Manchester ( <sup>4</sup> ) . . . . .	60	33	7.0	25	36	+ 4	0.92	I
Manchester ( <sup>33</sup> ) (—) . . .	50	30	6.9	25	58	+ 1	0.88	J
Nagoya ( <sup>11, 34, 35</sup> ) . . . .	12	7	9.2	20	78	+ 17	0.87	K
Nagoya ( <sup>17, 34, 35</sup> ) . . . .	40	22	7.4	24	64	+ 13	0.92	L
Teoloyucan ( <sup>28</sup> ) . . . . .	90 (*)	41	4.2	35	46	+ 13	0.83	M
Tokyo ( <sup>23, 35</sup> ) . . . . .	85	40	4.6	33	47	+ 19	0.85	N
Tokyo ( <sup>24</sup> ) (†) . . . . .	50	29	4.8	32	49	+ 15	0.89	O
Tokyo ( <sup>24, 35</sup> ) . . . . .	90 (*)	41	3.4	40	41	+ 23	0.82	P

(\*) ion-chamber.

(—) 60 m.w.e. underground.

(+)  $Z = 30^\circ$  North.

(†) 10 cm Pb absorber.

(<sup>28</sup>) S. E. FORBUSH, T. B. STINCHCOMB and M. SCHEIN: *Phys. Rev.*, **79**, 501 (1950).

(<sup>29</sup>) W. KOLHÖRSTER: *Terr. Mag.*, **43**, 333 (1938).

(<sup>30</sup>) A. EHMERT, *Zeits. f. Naturf.*, **3a**, 264 (1948).

(<sup>31</sup>) V. F. HESS, R. STEINMAURER and A. DIMMELMAIR: *Nature*, **141**, 689 (1938).

(<sup>32</sup>) E. P. GEORGE, in J. G. WILSON: *Prog. Cosmic Ray Phys.* (Amsterdam, 1952), p. 422.

(<sup>33</sup>) H. ELLIOT: private communication.

(<sup>34</sup>) Y. SEKIDO, M. KODAMA and T. YAGI: *Cosmic-Ray Results from Nagoya* (1951).

(<sup>35</sup>) Y. SEKIDO and S. YOSHIDA: *Rep. Ionosphere Res. Japan*, **5**, 43 (1951).

( $\text{cm}^2 \text{ s sr}^{-1}$ ) of the cosmic rays incident into the latitude ( $\lambda$ ) and the depth of the station from the median zenith distance ( $Z$ ) effective to the equipment is a better parameter. Flux  $I$  was calculated from  $Z$  and the vertical flux at the station (see Table V), and then the mean energy  $E$  of the effective primaries corresponding to the flux  $I$  was obtained through the curve shown in Fig. 9 (*a*). In Fig. 9, *a* is the result at Ithaca, where  $I$  is the vertical flux at 1600 m.w.e. underground, and  $E$  was estimated by BARRET *et al.* <sup>(36)</sup> from the frequency of the associated air shower. *b* is the result from the observation with an alt-azimuth counter telescope at Nagoya <sup>(37)</sup> where  $I$  was observed at  $Z = 80^\circ$ , and  $E$  was estimated from the identification of narrow anisotropies fixed on the celestial sphere observed at East and West directions. *c* is the result by FONGER <sup>(38)</sup>, where  $I$  is the flux on the ion-chamber at Cheltenham, and  $E$  was estimated from an empirical yield function generating the latitude

TABLE VI. — *Observations with inclined telescopes.*

Period	Station	$Z$	
1940	Stockholm	30° N	60° S
1940	Berlin	45° N	45° S
1940	»	45° E	45° W
1948	Stockholm	30° N	30° S
1948	Manchester	30° N	30° S
1949	»	40° N	40° S
1949	»	30° E	30° W
1949	»	40° N	40° S 35 cm Pb
1951	»	40° N	40° S
1952	»	40° N	40° S

effect of the intensities. The other points were obtained through Brunberg's method <sup>(39)</sup>, where  $E$  were estimated from the identification of the anisotropy corresponding to the diurnal variations observed at different directions. Brunberg's method was applied on several pairs of observations shown in Table VI, after the correction for the temperature effect using the data published by MAEDA <sup>(41)</sup> (see Sect. 6).  $E$  and  $\Phi$  (direction of anisotropy outside the geo-

<sup>(36)</sup> P. H. BARRETT, L. M. BOLLINGER, G. COCCONI, Y. EISENBERG and K. GREISEN: *Rev. Mod. Phys.*, **24**, 133 (1952).

<sup>(37)</sup> Y. SEKIDO, S. YOSHIDA and Y. KAMIYA: *Journ. Geomag. Geoelec.*, **6**, 22 (1954).

<sup>(38)</sup> W. H. FONGER: *Phys. Rev.*, **91**, 351 (1953).

<sup>(39)</sup> E. A. BRUNBERG and A. DATNER: *Tellus*, **6**, 73 (1954).

<sup>(40)</sup> W. KOLHÖRSTER: *Phys. Zeits.*, **42**, 55 (1941).

<sup>(41)</sup> K. MAEDA: *Journ. Geomag. Geoelec.*, **5**, 105 (1953).

magnetic field) thus obtained seem to make a secular variation as shown in Fig. 16 (b) (c). The secular variation of  $\Phi$  is consistent with Thambyahpillai's secular variation of  $q$ .

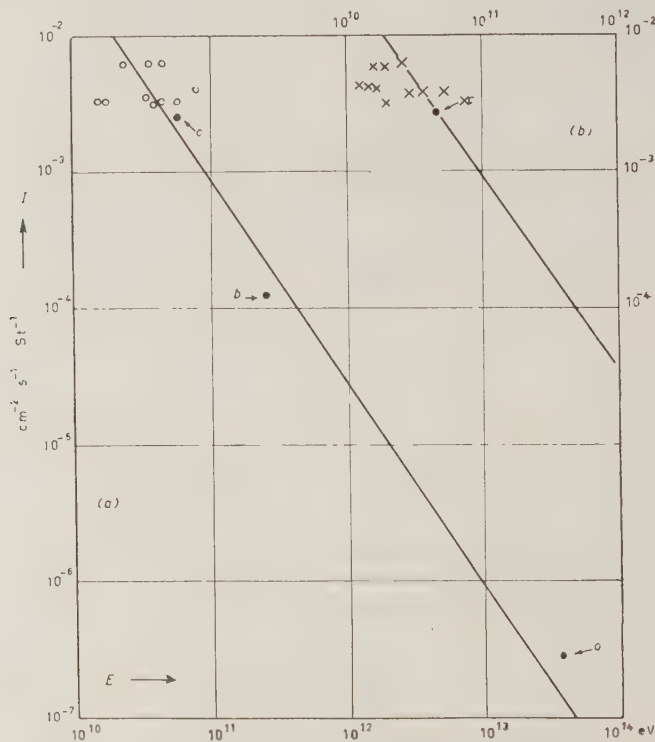
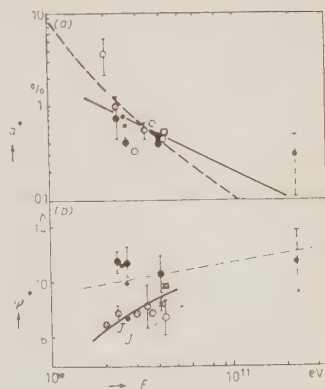


Fig. 9. (a) Relation between the primary energy ( $E$ ) and the secondary flux ( $I$ ).  $a$ : associated air shower (BARRET *et al.* (<sup>36</sup>));  $b$ : narrow anisotropy;  $c$ : latitude effect (FONGER (<sup>38</sup>)); the other points: diurnal variation (Brunberg's method (<sup>39</sup>)). (b) shows the points obtained by Brunberg's method not corrected for the temperature effect (see Chap. VI).

In order to eliminate the inter storm difference, let  $a^* = a \cdot \bar{a}_p/a_p$  and  $q^* = q - q_p + \bar{q}_p$ , where  $(a_p, q_p)$  is the anisotropy observed with the equipment  $P$  (see Table V) and  $(\bar{a}_p, \bar{q}_p)$  is the average of  $(a_p, q_p)$  over all the periods ( $a, b, \dots, i$ ) (\*). After this normalization,  $(a^*, q^*)$  is considered as a function of  $E$ ,  $\lambda$  and  $Z$ . As shown in Fig. 10,  $a^*$  decreases with  $E$ , and  $q^*$  increases with  $E$ , provided  $\lambda$  and  $Z$  remain constant; while  $q^*$  decreases with  $|\lambda|$  and  $Z$ , provided  $E$  remains constant.

(\*)  $a$  was normalized through  $c$  and  $d$ .

Fig. 10. -- Energy and latitude dependence of the additional anisotropy.  $E$ : primary energy;  $\circ$ : equator ( $G$ );  $\odot$ ,  $\boxtimes$ : lower latitude ( $KLMNOP$ );  $\bullet$ : higher latitude ( $ABCDEFGHIJ$ );  $+$ : pole ( $E$ );  $ABC$ ---: see Table V;  $a^*$ ,  $\varphi^*$ : amplitude and phase of the additional anisotropy, interstorm difference being normalized to the equipment  $P$ ; small points: single event; large points: average of more than two events, the dispersion being shown with thick bars; Dotted line for  $a^*$ : calculated by Nagashima's theory (<sup>42</sup>). The other curves: calculated by assuming two empirical values, eq. (4): [Curves for  $\varphi^*$ ] dotted line:  $\lambda = 0^\circ$ ,  $\Delta\varphi = 36^\circ$ ; full line:  $\lambda = 25^\circ$ ,  $\Delta\varphi = 19^\circ$ ; broken line:  $\lambda = 54^\circ$ ,  $\Delta\varphi = 4^\circ$ .



## 5. - Nature of the Storm Anisotropy.

There have been various ideas to explain the anisotropy during the cosmic-ray storm. Possible heating of the upper atmosphere associated with the storm may cause the anomaly. But, such heating is not established at present, and it may be difficult to expect a sudden temperature variation at the night side of lower latitudes. The variation of albedo due to the  $DS$  magnetic field of the associated magnetic storm was suggested (<sup>13</sup>) as a possible cause of the anisotropy. But the energies of the albedo particles are not so much larger than 1 GeV. SINGER (<sup>14</sup>) suggested a possibility that the geomagnetic cut-off energy depends on the local time when the geomagnetic field is modified by the influence of the solar stream. In this case also, the effect is limited at the lowest end of the energy spectrum. Concerning the world-wide intensity decrease of cosmic rays, NAGASHIMA (<sup>45</sup>) examined quantitatively the energy dependence, which was expected from the variation of the cut-off energy. According to his result, the energy dependence of the anisotropy described in Sect. 4 is too insensitive to be explained as the variation of the cut-off energy or albedo. Also, the cosmic-ray emission from the sun will be considered too much energy sensitive. On the other hand, ELLIOT and DOLBEAR (<sup>4</sup>) and NAGASHIMA (<sup>12</sup>) assumed an acceleration of cosmic-ray particles by the solar stream. This idea seems to be successful to explain the energy and latitude dependence.

(<sup>42</sup>) K. NAGASHIMA: *Journ. Geomagn. Geoelec.*, **7**, 81 (1955).

(<sup>43</sup>) M. S. VALLARTA: private communication.

(<sup>44</sup>) S. F. SINGER: private communication to Y. SEKIDO.

(<sup>45</sup>) K. NAGASHIMA: *Journ. Geomagn. Geoelec.*, **5**, 141 (1953).



Let the cosmic ray with energy  $E$  coming from the direction  $\Phi$  get energy  $\Delta E$  before entering into the geomagnetic field, then the following anisotropy ( $a_0, \varphi_0$ ) will be produced:

$$(1) \quad (38) \quad a_0 = q \frac{\Delta E}{10^9 \text{ eV} + E}, \quad q = \frac{2}{1 - 1/(1 + E/10^9 \text{ eV})}^z$$

$$(2) \quad (46) \quad \varphi_0 = \bar{\Phi} - \psi E, \quad \psi E = \psi E(E, \lambda, Z),$$

where  $z$  is the power of the differential energy spectrum <sup>(36)</sup>, and  $\psi E$  is the longitude difference published by BRUNBERG <sup>(46)</sup> (see Table V). If  $(a, \varphi)$  is observed with a finite aperture of the detector around  $Z$  and finite range of energies around  $E$ , then the observed  $(a, \varphi)$  is the vector sum of the anisotropies of directional and monochromatic constituents, hence  $s = a/a_0 < 1$ ,  $\Delta\varphi = \varphi_0 - \varphi \neq 0$ .  $s$  and  $\Delta\varphi$  are the constants characteristic to the detector.

Therefore

$$(3) \quad a^* = s \cdot q \frac{\overline{\Delta E}}{10^9 \text{ eV} + E}, \quad \varphi^* = \bar{\Phi} - (\psi E - 1q),$$

where  $\overline{\Delta E}$  and  $\bar{\Phi}$  are averages of  $\Delta E$  and  $\Phi$  respectively over various storms, and  $(a^*, \varphi^*)$  are given in Fig. 10. Assuming that the anisotropy observed with each equipment consists of 16 directional and monochromatic constituents,  $s$  and  $1q$  were estimated using the results of the model experiments

by BRUNBERG <sup>(46)</sup>, and the values obtained are shown in Table V. Now,  $\overline{\Delta E}$  and  $\bar{\Phi}$  were obtained from the equation (3). ( $\overline{\Delta E}$ ,  $\bar{\Phi}$ ) look like independent of  $E$  and  $\lambda$  as shown in Fig. 11, where the average acceleration is

$$(4) \quad \begin{cases} \langle \overline{\Delta E} \rangle = (0.6^{+0.3}_{-0.2}) \cdot 10^8 \text{ eV}, \\ \langle \bar{\Phi} \rangle = 13.1 \pm 0.6 \text{ h}. \end{cases}$$

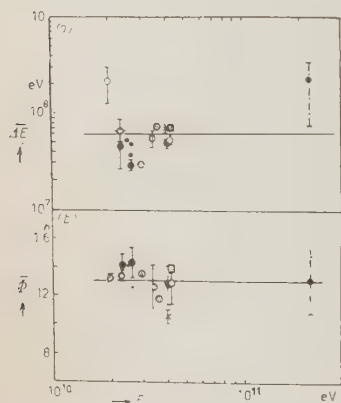


Fig. 11. — Acceleration during the cosmic-ray storm.  $E$ : primary energy;  $\Delta E$ : energy gain during an average storm;  $\Phi$ : direction of accelerated cosmic rays going to enter into geomagnetic field during an average storm.

<sup>(46)</sup> E. A. BRUNBERG: *Tellus*, 5, 135 (1953); E. A. BRUNBERG and A. DATNER: *Tellus*, 5, 269 (1953).

By assuming these two values, the energy dependence curves of  $(a^*, q^*)$  were calculated and are shown in Fig. 10. This result implies that the additional anisotropy during the storm is due to an acceleration  $(\Delta E, \Phi)$  of cosmic rays in the solar stream. As this acceleration is directional ( $\Phi = \text{const}$ ) and energy independent ( $\Delta E = \text{const}$ ), it will be presumably due to an electromagnetic field.

From the result above described, the acceleration  $(\Delta E, \Phi)$  is considered to be independent of  $(E, \lambda)$  but there are considerable inter-storm differences. Fig. 7 will suggest this differences.  $\Phi$  calculated for each storm distributes between  $1^h$  and  $18^h$  as shown in Table IV and Fig. 12 (b). Thus the direction of the acceleration field is one of the characteristics of the solar stream. Fig. 5 (b) seems to show that  $\Phi$  of the fresh stream ( $v = 0$ ) is about  $12^h$ ,  $\Phi$  increases with  $v$  and  $\Phi$  of the old stream is about  $18^h$ . Now the distribution of  $\varphi$  and  $\Phi$  in Fig. 12 may be considered to be chiefly due to the inter-storm difference of the acceleration field and Fig. 3 (c) indicates that the direction of the acceleration in the fresh streams are still not constant.  $\Phi$  in Table IV are plotted in Fig. 16 (g).

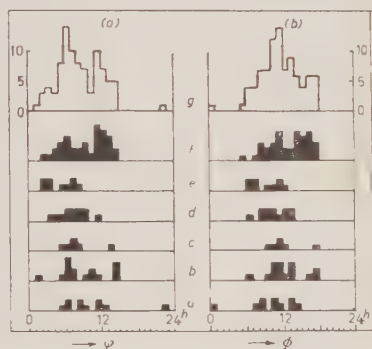


Fig. 12. - Frequency diagrams of the direction of additional anisotropy.  $\varphi$ : phase of anomalous diurnal variation, or the direction inside the geomagnetic field;  $\Phi$ : the direction before entering into the geomagnetic field; a: individual events (Fig. 3); b: anomalous diurnal variations (Figure 4); c: 27-day recurrence (Fig. 5); d: equinox effect (Fig. 6 (a)); e: anomaly in each year (Fig. 6 (b)); f: anomalous diurnal variations (Fig. 7); g: total.

It seems to make a 11-year variation. The acceleration given in the equation (4) is the time average of the acceleration during an average storm, while the anti-clockwise variation shown in Fig. 3 (b) means that the acceleration varies with the storm time  $T_s = T - T_0$ . This storm time variation is shown in Fig. 13, assuming the  $\vec{QD}$  vector in Fig. 3 (b) corresponds to the average acceleration given in the equation (4).

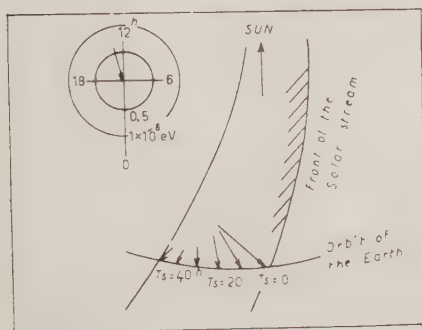


Fig. 13. - Acceleration observed at various positions in a solar stream.  $T_s$ : storm time.

## 6. Components of Diurnal Variation and Their Secular Variations.

The average diurnal variation over all days is considered to consist of various components. The statistical process to pick up one of these components may be affected by the other components.

The atmospheric effect has been considered uncertain to discuss its diurnal variation. However, the following four studies indicate the existence of day-time positive diurnal variation as shown in Fig. 14 (a).

1) MAEDA (<sup>41</sup>) obtained negative and positive temperature coefficients from the seasonal variation, and examined the diurnal variation of the temperature at various altitudes and latitudes. According to his result, the positive temperature effect is more effective on the diurnal variation than the negative temperature effect does. The resultant vectors are shown in Fig. 14 (a).

2) ELLIOT and DOLBEAR (<sup>4</sup>) and KOLHÖRSTER (<sup>40</sup>) observed the average diurnal variations of four different directional intensities (N, S, E, W) under nearly the same atmospheric depth (see Table VI) in the same period respectively. Anisotropies obtained from these observations can be identified through Brunberg's method. But there is a considerable discrepancy between the result from the N-S pair and that from the E-W pair, if the temperature effect is not taken into account. The atmospheric diurnal variation which mini-

mizes this discrepancy is shown in Fig. 14 (a). ( $E$  values thus obtained are  $31.5 \pm 3.5$  GeV and  $36.0 \pm 0.5$  GeV respectively).

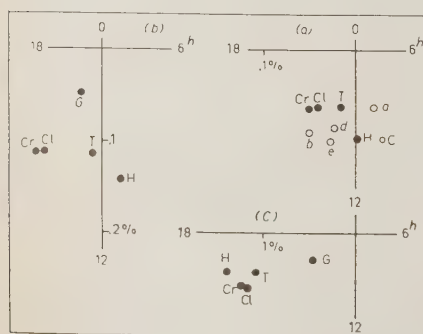


Fig. 14. - Diurnal variation at various stations, averaged for a long period. (a) Atmospheric effect obtained by various methods.  $a, b$ : Maeda's method ( $a$ : equator,  $b$ : middle latitude);  $c, d$ : combined Brunberg's method ( $c$ : Berlin,  $d$ : Stockholm, see Table VI);  $e$ : Brunberg's method (see Fig. 9 (b)) the

other points calculated from Fig. 14 (b, c). (b) Diurnal variation averaged for a long period. (c) Diurnal variation corrected for geomagnetic deflection, without the correction for atmospheric effect.

3) As shown in Fig. 9 (b), there is a considerable difference between the result obtained by FONGER (<sup>38</sup>) and those obtained by Brunberg's method without correction for the temperature effect. This difference may be attributed

to the temperature effect provided the primary energy effective to the latitude effect (FONGER) is equal to that effective to the diurnal variation (BRUNBERG).

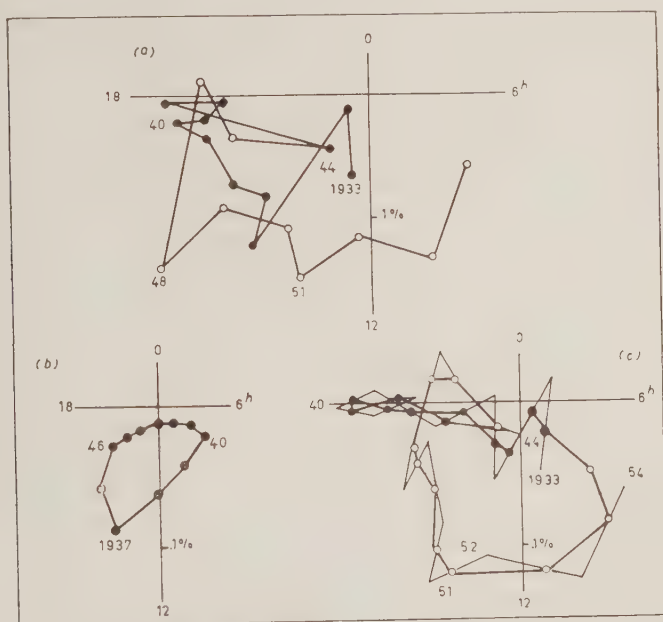


Fig. 15. — Year-to-year variation of the anisotropy before entering into geomagnetic field. (a) Total days. (b) Total days minus quiet days, *DS*. (c) Quiet days, *Sq*.

TABLE VII. — Data used for the study of secular variations.

Station	1933	'36	'39	'42	'45	'48	'51	'54
Capetown	* *							
Cheltenham		**	***	***	***		**	
Christchurch		**	***	***	*		***	*
Godhavn			**	***	**			
Hafelekhar	*	**					*	
Huancayo	*	**	***	***	***		*	
Tokyo		*	*	**		**	***	**

The atmospheric diurnal variation which minimizes this discrepancy is shown in Fig. 14 (a).

1) The diurnal variations observed at various stations averaged for many years are widely different from each other, as shown in Fig. 14 (b). But, after the correction for the deflection by the geomagnetic field, they become near

except Godhavn, as shown in Fig. 14 (e). For there is no appreciable diurnal variation of atmospheric temperature at very high latitude, the result of Godhavn in Fig. 14 (c) will represent the anisotropy of cosmic rays at the outside of

the geomagnetic field, while the differences between Godhavn and the other stations will be due to the atmospheric effect. These differences are plotted in Fig. 14 (a). They are in accordance with the atmospheric effects obtained through the other methods. The results obtained by these four methods are quantitatively consistent, as shown in Fig. 14 (a).

Now we can correct for the atmospheric diurnal variation. The corrected diurnal variation is due to the anisotropy of cosmic rays at the outside of the geomagnetic field, as de-

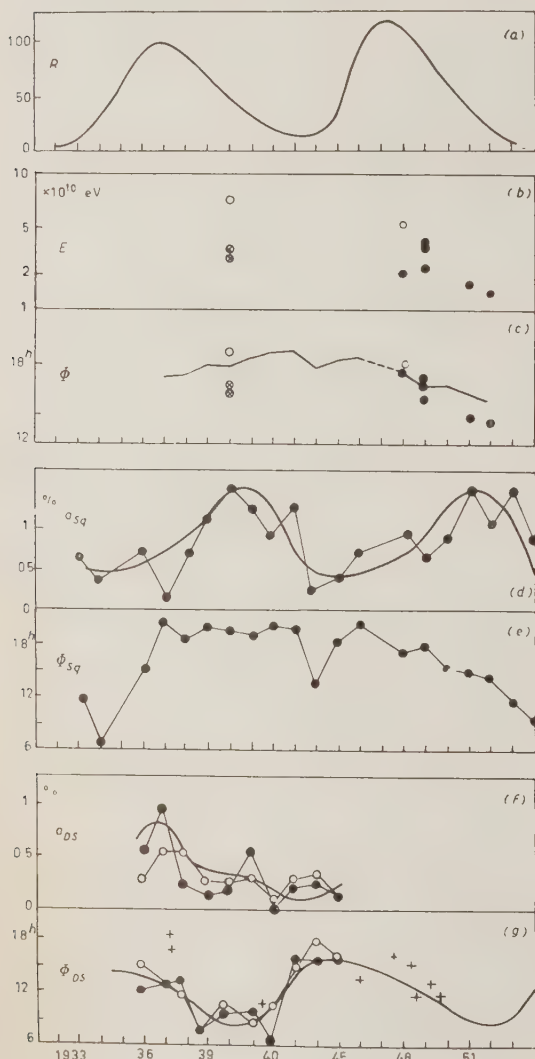


Fig. 16. — Year-to-year variations. (a) Relative sun-spot number. (b, c) Primary energy,  $E$  and the direction before entering into geomagnetic field,  $\Phi$ , obtained from the identification of diurnal variation averaged for total days (see Table VI).  $E$  were normalized so as to correspond to a constant value of  $I$  in Fig. 9 (a).  $\circ$ : Stockholm;  $\otimes$ : Berlin;  $\bullet$ : Manchester; curve: average of the points in Fig. 4 of reference (39).

(d, e) Quiet days anisotropy,  $Sq$ . (f, g) Storm anisotropy,  $DS$ .  $+$ : individual event shown in Table IV;  $\circ$  and  $\bullet$ : total days diurnal variation. (T) minus quiet days diurnal variation. (Q): conditions for selecting the quiet days of  $\bullet$  is more strict than that of  $\circ$ .

scribed above. The year-to-year variation of the anisotropy was obtained with the data of various stations (Table VII), by assuming that the anisotropy does not depend on the latitude. The result is shown in Fig. 15 (a).

The anisotropies shown in Fig. 15 (a) are the averages for total days ( $T$ ) during each year, and include the year-to-year variation of storm anisotropy which was mentioned in Sect. 3 and 5.  $T-Q$  vectors were calculated with the Huancayo data and the materials of Fig. 6 (b) and Table IV, thus obtaining the year-to-year variation of the storm anisotropy which includes also the frequency of the storms. It makes an 11-year variation as shown in Fig. 15 (b) and Fig. 16 (h, g). The variation of the magnitude of this storm anisotropy is similar to that of the sunspot activity. But, the phase is the latest at the beginning of a sunspot cycle, and advance during the cycle.

The year-to-year variation of the anisotropy of quiet days was obtained by subtracting Fig. 15 (b) from Fig. 15 (a). The result makes a secular variation and was shown in Fig. 15 (c) and Fig. 16 (d, e). The magnitude of this quiet days anisotropy relates still to the solar activity. But, the year-to-year variation of the magnitude is not similar as the sunspot number, rather resembling to the phase of the storm anisotropy (Fig. 16 (g)). It must be noticed that the phase of the quiet day's anisotropy is late during the 1-st 11-year cycle, and early during the 2-nd cycle. The secular variation of the diurnal variation, found by ELLIOT *et al.* (26), which has not 11-year periodicity, will be due to this secular variation of the quiet day's anisotropy. The quiet day's anisotropy must include something of different nature from the storm anisotropy, for they display different types of secular variation. But, the contribution of the solar flare effect is considered to be very small, for the above results were obtained from the observations with ion-chambers.

As described above, the diurnal variation of cosmic rays consists of the following four components:

- 1)  $At$ : atmospheric effect;
- 2)  $DS$ : storm anisotropy;
- 3)  $Sq$ : quiet day's anisotropy;
- 4)  $Fl$ : solar flare effect.

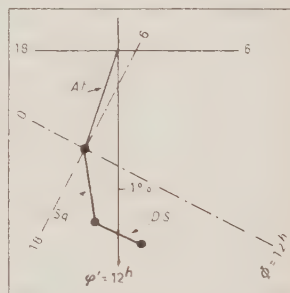


Fig. 17. - Four components of diurnal variation averaged for 22 years.  $At$ : atmospheric effect;  $Sq$ : quiet days anisotropy;  $DS$ : storm anisotropy;  $Fl$ : solar flare effect, not shown for it is negligibly small. Coordinates: full line for  $\varphi'$ , the phase of diurnal variation observed at middle latitude; chain line for  $\varphi$ , the direction of anisotropy before entering into geomagnetic field.



The contributions of these four components to the diurnal variation averaged for about 22 years were estimated as shown in Fig. 17.

## 7. - Conclusion.

As described above, various phenomena about the cosmic-ray diurnal variation could be arranged systematically by introducing the following idea. The anisotropy of cosmic rays during the cosmic-ray storm produces an important part of the cosmic-ray diurnal variation, and this storm anisotropy is produced by the acceleration of cosmic rays in the solar stream. The variation of this acceleration observed at various positions in a solar stream, the variation in different streams of various ages, and the variation in a 11-year period were described, as the first step for making clear the acceleration mechanism and the nature of the solar stream. The acceleration field, presumably an electromagnetic field, in the solar stream must be such that its effect integrated along the path of a cosmic ray gives the resultant acceleration described above.

\* \* \*

In conclusion, the writer wishes to thank Prof. Y. SEKIDO for his kind guidance and encouragement throughout the study. The writer is also indebted to Dr. S. E. FORBUSH, Dr. H. ELLIOT, Dr. A. SITTKUS, Dr. J. W. BEAGLEY, Director of the Christchurch Observatory, Mr. Y. MIYAZAKI of the Scientific Research Institute, and Messrs. T. YAGI and M. KODAMA of the Nagoya University, for their kind arrangement for the copies of cosmic-ray data used here. The writer wishes to express her hearty thanks to Prof. T. NAGATA, Dr. K. NAGASHIMA and Mr. I. KONDO for their useful suggestions and discussions, and to Miss Y. KAMIYA for her help in this work.

## RIASSUNTO (\*)

Si sono studiati vari fenomeni manifestati dalla variazione diurna dei raggi cosmici, specialmente la variazione diurna anomala associata alle tempeste geomagnetiche. Si è interpretata una parte assai importante della variazione diurna dei raggi cosmici come il risultato del flusso anisotropico di raggi cosmici che ha luogo durante le tempeste geomagnetiche. Attraverso uno studio della dipendenza della variazione diurna anomala dall'energia e dalla latitudine si è rilevato che tale anisotropia è prodotta dall'accelerazione dei raggi cosmici nella corrente solare. Si descrivono la variazione di questa accelerazione osservata in varie posizioni di una corrente solare, la variazione in differenti correnti di differenti età e la variazione in un periodo undecennale.

\*) Traduzione a cura della Redazione.

## A Probable Example of the Production and Decay of a Neutral Tau-Meson.

W. A. COOPER, H. FILTHUTH, J. A. NEWTH, G. PETRUCCI,  
R. A. SALMERON and A. ZICHUCCI

*C.E.R.N. - Geneva*

(ricevuto il 9 Settembre 1956)

**Summary.** — A four-pronged event observed in a magnet cloud chamber is described. It is interpreted as the decay in flight of a neutral  $\tau$ -meson according to the scheme  $\tau^0 \rightarrow \pi^+ + \pi^- + \pi^0$  with the subsequent decay of the  $\pi^0$ -meson into an electron pair and a  $\gamma$ -ray. The  $\tau^0$ -meson is produced in carbon in a small nuclear interaction which may be a charge exchange reaction ( $K^- + n \rightarrow \tau^0 + p$ ). The lifetime of the  $\tau^0$ -meson before decay is about  $3 \cdot 10^{-10}$  s. Other possible interpretations of the event are discussed and shown to be improbable.

### 1. — Introduction.

We have recently observed in a magnet cloud chamber at the Jungfraujoch an event of a type that has not previously been reported. The event consists of four tracks originating at a point in the gas of the cloud chamber. Two are the tracks of positive and negative electrons; the other two are tracks of fast particles and resemble a typical neutral V-event. (See Plates 1 and 2).

After considering the possible interpretations of this event we have concluded that it is most readily explained as the decay of a neutral  $\tau$ -meson with the subsequent decay of the secondary  $\pi^0$ -meson into an electron pair and a  $\gamma$ -ray. The two decay processes can be written as

$$\tau^0 \rightarrow \pi^+ + \pi^- + \pi^0,$$

and

$$\pi^0 \rightarrow e^+ + e^- + \gamma.$$

The four-pronged event is geometrically associated with a small nuclear interaction that occurs in a 2.5 cm graphite plate placed across the centre of the cloud chamber. This interaction can be interpreted most easily as a charge exchange reaction,

$$K^- + n \rightarrow \pi^0 + p,$$

though it could also be an example of double production according to the scheme

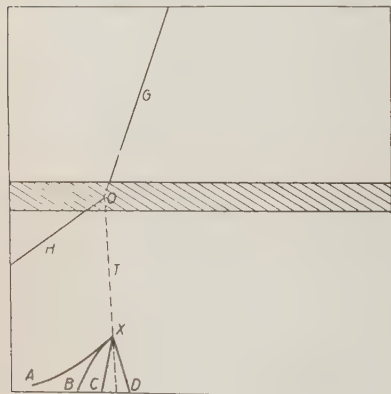
$$\pi^+ + n \rightarrow \pi^0 + \Sigma^+,$$

in which the  $\Sigma$ -particle decays inside the graphite plate into a proton and a  $\pi^0$ -meson that escapes detection.

The existence of the  $\pi^0$ -meson has frequently been suggested<sup>(1)</sup> as an explanation of some of the «anomalous» neutral V-events that have been observed<sup>(\*)</sup>. A  $\pi^0$ -decay in which only the two charged  $\pi$ -mesons are seen can never be definitely identified and, even for our event, there are other possible explanations that have to be considered. We present, in this paper, all the measurements that have been made on our event and the details of the reasoning that leads us to our interpretation.

## 2. - Measurements of the Event.

A drawing of the complete event is given in the figure and all the relevant tracks are labelled. The measurements made on these tracks are recorded in Table I and in Table II the angles between the tracks are given.



The event is most easily visualized when it is realized that the three tracks *A*, *C* and *D* are very nearly coplanar and that their plane contains the nuclear interaction (*O*) in the gra-

Fig. 1. - A drawing of the complete photograph showing all the relevant tracks. The shaded area represents the 2.5 cm graphite plate placed across the centre of the cloud chamber.

<sup>(1)</sup> A full bibliography is given by R. W. THOMPSON in an article in *Progress in Cosmic Ray Physics*, **3** (1956).

<sup>(\*)</sup> The recent phenomenological theories that attempt to systematize our knowledge of the strange particles all predict the existence of the  $\pi^0$ -meson.

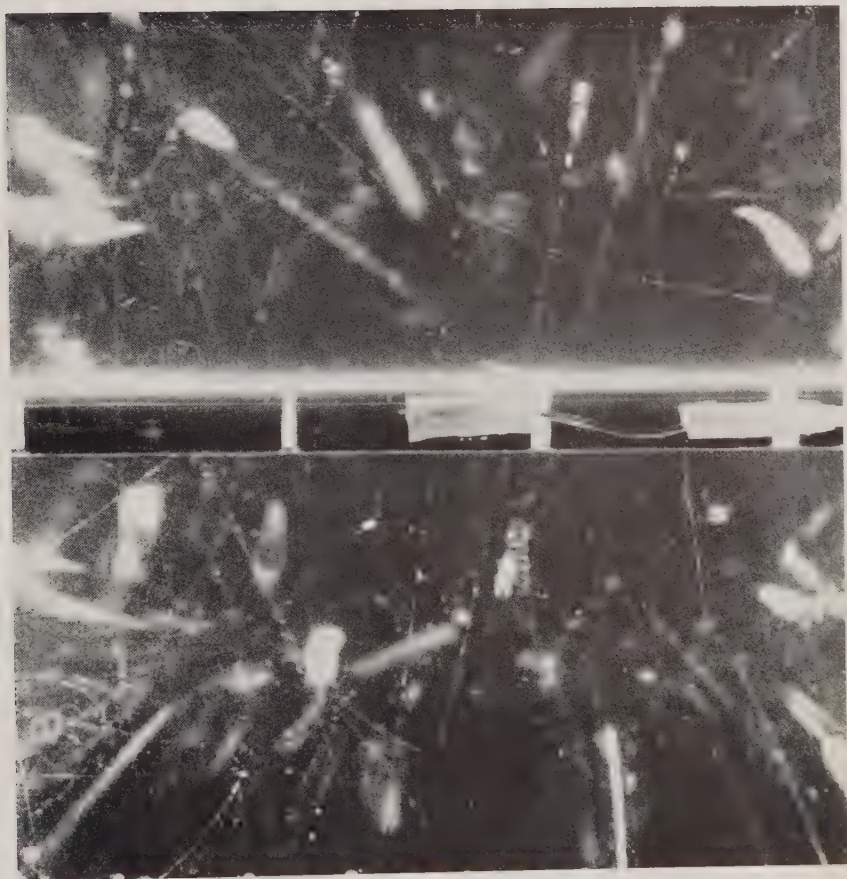


Plate 1. - A reproduction of the photograph showing the four-pronged event near to the bottom of the cloud chamber.

W. A. COOPER, H. FILTHUTH, J. A. NEWTH, G. PETRUCCI,  
R. A. SALMERON and A. ZICHICHI



Plate 2. — Enlargement showing the details of the tracks of the four-pronged event.

TABLE I. — *Measurements of the tracks in the event.*

The signs in the third column are found on the assumption that all the particles travel downwards in the chamber. For the short tracks (*A*, *B*, *C*, *D*) the error in the momentum has been derived from the noise due to ion diffusion, ignoring convective distortion. For the tracks *G* and *H* we have used the pessimistic procedure of assuming a distortion curvature that varies inversely as the square of the length of the track and corresponds to a momentum of 4 GeV/c for tracks 22 cm long. The ionization densities in the fifth column are visual estimates.

If track *H* is that of a proton, the estimated ionization corresponds to a momentum between 400 MeV/c and 700 MeV/c. The corresponding range for a K-meson is from 220 MeV/c to 370 MeV/c.

Track	Length (cm)	Sign of Charge	Momentum (MeV/c)	Ionization Density ( $I_0$ )	Mass of Particle ( $m_e$ )
<i>A</i>	5.8	+	$38 \pm 2$	$< 2$	$< 120$
<i>B</i>	4.2	—	$26 \pm 2$	$< 2$	$< 90$
<i>C</i>	4.3	?	$> 250$	$< 2$	?
<i>D</i>	4.3	?	$> 250$	$< 2$	?
<i>G</i>	18.5	+	$940^{+470}_{-240}$	$< 2$	?
<i>H</i>	12.0	+	$380^{+180}_{-90}$	2 to 4	780 to 2600

TABLE II. — *Geometry of the event.*

In (a) the plane angles between various pairs of tracks are given. In (b) the angle *A* (*CD*) is, for example, the angle between track *A* and its projection in the plane defined by *C* and *D*. The angle (*GT*) (*CD*) is the angle between the normals to the two planes.

The errors attached to the measurements have been found in two ways. First, the uncertainty in the orientation of each track was estimated from its length and position. This led to a direct estimate of the error in each angle. Second, all the measurements and calculations were made four times independently and the results compared. The errors in the table are in accord with both estimates.

(a) Angles between Tracks		(b) Coplanarity of Tracks	
Tracks	Angle (Degrees)	Tracks	Angle (Degrees)
<i>A B</i>	$23.0 \pm 2$	<i>A</i> ( <i>CD</i> )	$2.5 \pm 3$
<i>C D</i>	$25.5 \pm 1$	<i>B</i> ( <i>CD</i> )	$13.5 \pm 3$
<i>A T</i>	$56.0 \pm 2$	<i>T</i> ( <i>CD</i> )	$1.5 \pm 1$
<i>B T</i>	$37.0 \pm 2$	<i>T</i> ( <i>GH</i> )	$2.0 \pm 2$
<i>C T</i>	$13.5 \pm 2$	<i>G</i> ( <i>HT</i> )	$2.0 \pm 2$
<i>D T</i>	$12.0 \pm 2$	—	—
<i>G H</i>	$38.0 \pm 1$	( <i>GT</i> ) ( <i>CD</i> )	$45.0 \pm 3$
<i>G T</i>	$21.0 \pm 1$	—	—

Distance *OX* =  $(16.2 \pm 0.3)$  cm.



phite plate. The fourth track,  $B$ , makes an angle of  $13.5^\circ$  with this plane but, since  $B$  is the track of a low-energy electron, the vector sum of the momenta of the four particles lies very nearly in the plane of  $A$ ,  $C$  and  $D$ .

Similarly, the two tracks  $H$  and  $G$  that define the interaction in the plate lie in a plane which, within the errors of measurement, contains the apex ( $X$ ) of the four-pronged event. Thus the line  $T$ , joining  $O$  to  $X$ , is the intersection of the planes defined by  $H$ ,  $G$  and by  $A$ ,  $C$ ,  $D$ . The angle between these two planes is  $45^\circ$ .

The identification of tracks  $A$  and  $B$  as due to an electron pair is certain. The tracks  $C$  and  $D$  are very short and show no detectable curvature. Their straightness is, in itself, evidence that there is no gross convective distortion in this region of the cloud chamber. For this reason we consider that the minimum magnetic curvature that we could detect in these tracks is set by the diffusion of the ions prior to condensation<sup>(2)</sup>. The mean «noise» curvature in tracks of this length in our chamber corresponds to a momentum of 500 MeV  $c$ . In the following discussion we assume that both the particles  $C$  and  $D$  had momenta greater than 250 MeV/ $c$ .

Track  $H$  could be due either to a positive heavy meson or to a proton and, in interpreting the reaction at  $O$ , we consider both possibilities.

### 3. — Interpretation of the Event.

3.1. *General.* — In the following sections we attempt, first of all, to explain the four-pronged event in terms of known particles and processes. The three different types of process that could be responsible for it are listed below.

*a)* A neutral particle (probably a neutron) is ejected from the interaction at  $O$  and produces, itself, a nuclear interaction in the gas of the cloud chamber at  $X$ . The tracks  $A$ ,  $B$ ,  $C$ ,  $D$  are those of the charged secondary particles from the interaction. In this interpretation the electron pair  $A$ ,  $B$  results from the decay of a  $\pi^0$ -meson ( $\pi^0 \rightarrow e^+ + e^- + \gamma$ ).

*b)* A charged particle ( $C$  or  $D$ ) travelling upwards in the cloud chamber decays at  $X$  giving rise to three charged secondaries. In this interpretation the apparent association with the interaction at  $O$  must be fortuitous.

*c)* An unstable neutral particle produced at  $O$  decays spontaneously at  $X$  producing the four charged secondary particles.

The possibility of the event being a casual coincidence in space between an electron pair and a neutral V-event can be ignored since a rough calculation shows that the expected number of such coincidences in our experiment is  $\sim 10^{-5}$ .

(2) P. M. S. BLACKETT: *Suppl. Nuovo Cimento*, **11**, 264 (1954).

3'2. *A Nuclear Interaction in the Gas.* — There are strong arguments against interpretation *a*). The energy of the neutron producing the nuclear interaction would have to be at least 800 MeV and yet no charged evaporation particles are produced and there is no track due to a recoil nucleus. Interpretation as a simple collision between a neutron and a hydrogen nucleus is excluded by the requirement of charge conservation and, in a heavier nucleus, a neutron-neutron collision at 800 MeV would almost certainly produce some slow charged particles.

An additional difficulty in this interpretation arises from considering the interaction at *O*. If we assume that the particle *G* causes the interaction, that *H* is a secondary proton and that *T* is the path of a neutron with an energy of more than 800 MeV (momentum 1450 MeV/c) it is necessary to postulate additional, unseen, secondary particles to balance the energy and momentum in the interaction. If such particles were produced, the observed coplanarity of the line *T* with the tracks *G* and *H* is improbable.

Taking these arguments together we consider that interpretation *a*) is unlikely to be correct but it is not possible to assign any numerical value to the probability of seeing a nuclear interaction of this type. We have observed about 85 nuclear interactions with a visible energy greater than 800 MeV in the gas of our cloud chamber. Of these, about 25 have neutral primary particles. However, these «stars» are usually identified by the presence of slow, heavily-ionizing particles and we have no valuable information about interactions that lead to a small number of fast charged particles alone.

3'3. *Decay of a Charged Particle.* — Interpretation *b*) of the event as the decay in flight of a charged particle coming from the bottom of the cloud chamber can be excluded without difficulty. Assuming either *C* or *D* to be the unstable primary particle and the other a product of the decay, the value of  $p^*$ , the secondary momentum in the centre of mass frame of reference, is found to be  $> 400$  MeV/c. This value is much larger than that found in the decay of any known charged particle.

3'4. *Decay of a Neutral Particle.* — There remains interpretation *c*) and we list below the decay processes of known, long-lived, neutral particles that could result in a four-pronged event similar to ours.

- |     |  |
|-----|--|
| (1) | $\Lambda^0 \rightarrow n + \pi^0,$             |
| (2) | $\Lambda^0 \rightarrow p + \pi^- + \gamma,$    |
| (3) | $\theta^0 \rightarrow \pi^0 + \pi^0,$          |
| (4) | $\theta^0 \rightarrow \pi^+ + \pi^- + \gamma.$ |

In process (1) the four tracks would be those of two pairs of electrons from the decay of the  $\pi^0$ -meson. Apart from the improbability of this mode of  $\pi^0$ -decay, process (1) can be excluded as an interpretation of the event using the measurements of dynamics given in Tables I and II. If the four tracks  $A, B, C, D$  are all due to positive and negative electrons from the decay of a single particle, calculation gives the mass of the particle as greater than  $300 m_e$ . This is more than the mass of the  $\pi^0$ -meson.

In process (2) the electron pair  $A, B$  would result from the internal conversion of the  $\gamma$ -ray in the decay process. This interpretation of the event can also be completely excluded since it is easily shown that the energy of the pair  $A, B$  in the centre of mass system of the decaying particle is more than 42 MeV. This is greater than the energy released in  $\Lambda^0$ -decay.

Process (3) followed by the decay of both  $\pi^0$ -mesons into an electron pair and a  $\gamma$ -ray is a possible interpretation of the event. So, too, is process (4) where the  $\gamma$ -ray produces an electron pair by internal conversion. These two modes of  $\theta^0$ -decay are expected to arise with very different probabilities and it is valuable to estimate these probabilities.

In the decay of  $\theta^0$ -mesons the branching ratio between decay into two charged or two neutral  $\pi$ -mesons is of the order of unity <sup>(3)</sup>. The probability that both the  $\pi^0$ -mesons should decay into an electron pair and a  $\gamma$ -ray is  $\sim (1/80)^2$  <sup>(4,5)</sup>. Moreover, the tracks  $C$  and  $D$  are unlike those of a normal electron pair from  $\pi^0$ -decay. Following the suggestion of Peyrou <sup>(6)</sup> we can calculate the energy of the particles  $C$  and  $D$  in their common centre of mass system on the assumption that they are an electron pair. This quantity ( $Q_{ee}$ ) turns out to be  $> 110$  MeV. For an electron pair arising from  $\pi^0$ -decay  $Q_{ee}$  cannot be greater than the mass of the  $\pi^0$ -meson ( $135 \text{ MeV}/c^2$ ) and the probability of its lying in the range from 110 MeV to 135 MeV is only  $1/1000$ . Thus the overall probability that a  $\theta^0$ -meson should decay into two  $\pi^0$ -mesons both of which give electron pairs and that one electron pair should have a value of  $Q_{ee}$  as high as 110 MeV is

$$P_3 \sim \frac{1}{2} \cdot (1/80)^2 \cdot 1/1000 \sim 8 \cdot 10^{-8}.$$

The corresponding probability for process (4) can be estimated from the calculations of TREIMAN <sup>(7)</sup> who has considered in some detail the radiative

<sup>(3)</sup> J. OSHER and B. J. MOYER (reported by L. W. ALVAREZ): *Proc. of the Rochester Conference*, 5, 32 (1956).

<sup>(4)</sup> R. H. DALITZ: *Proc. Phys. Soc.*, A **64**, 667 (1951).

<sup>(5)</sup> N. H. KROLL and W. WADA: *Phys. Rev.*, **98**, 1355 (1955).

<sup>(6)</sup> C. PEYROU: *Proc. of the Rochester Conference*, 6, 36 (1956).

<sup>(7)</sup> S. B. TREIMAN: *Phys. Rev.*, **95**, 1360 (1954).

decay of the  $\theta^0$ -meson as a possible explanation of some of the «anomalous»  $V^0$ -events. TREIMAN calculates the probability that the radiated  $\gamma$ -ray should have an energy greater than  $E_\gamma$ . In our event  $E_\gamma = 50$  MeV and the corresponding calculated probability is  $7/1000$ . Further, the probability that the  $\gamma$ -ray should undergo internal conversion in the decay process is  $\sim 1/160$  (\*). Therefore the probability that a  $\theta^0$ -meson should decay by process (4) into four particles giving an event like ours is

$$P_4 \sim \frac{1}{2} \cdot 7/1000 \cdot 1/160 \sim 2 \cdot 10^{-5}.$$

The total number of  $\theta^0$ -mesons that have decayed in our cloud chamber during the sensitive time is about 1000 (allowing for unobserved decays into two neutral  $\pi$ -mesons). Multiplying this number by the probabilities  $P_3$  and  $P_4$  it is clear that process (3) can be neglected by comparison with (1) from which the expected number of events of our type is 0.02.

**3'5. Decay of a Neutral  $\tau$ -Meson.** — If we restrict our discussion to the decays of known particles, we find that process (4) is the most plausible interpretation of our event. However, the expected number of four-pronged events due to process (4) is very small, and there is also a difficulty in this interpretation that is discussed in § 5 below.

For these reasons it is worth considering an alternative explanation in terms of a particle whose existence has been suggested but not detected. We are led very directly to the neutral  $\tau$ -meson since the electron pair  $A, B$  could readily arise from  $\pi^0$ -decay. The process

$$(5) \quad \tau^0 \rightarrow \pi^+ + \pi^- + \pi^0 + \sim 80 \text{ MeV},$$

can, in fact, account for all the features of our event. Moreover, the probability of the  $\pi^0$ -meson decaying into an electron pair is  $1/80$  so that, if  $\tau^0$ -mesons exist and decay according to (5), one in eighty decays should give a four-pronged event.

The normal decay (5) of the  $\tau^0$ -meson would appear as a neutral  $V$ -event with an apparent  $Q$ -value less than 80 MeV. The number of such events observed is difficult to estimate accurately; from the surveys of THOMPSON<sup>(8)</sup> and of BALLAM *et al.*<sup>(9)</sup> it is likely that between 2% and 5% of all neutral  $V$ -events could be  $\tau^0$ -decays. In our experiment we have seen some 1500  $V^0$ -events; the number of  $\tau^0$ -decays is probably less than, say, 75. The expected number

(\*) There is experimental evidence that the conversion coefficient has this value in  $\pi^0$ -decay and in  $\pi^-$ -capture. The coefficient is expected to be independent of the source of the  $\gamma$ -ray at high energies. This is discussed by KROLL and WADA<sup>(5)</sup>.

(8) R. W. THOMPSON: *Report of the Pisa Conference, 1955* (to be published).

of four-pronged events similar to the one we have seen is thus, on this hypothesis, less than  $(1/80) \cdot 75 \simeq 1$ .

We should emphasize that there is no evidence that *any* anomalous  $V^0$ -events are, in fact,  $\tau^0$ -decays. The above argument only shows that the expected number of four-pronged events from  $\tau^0$ -decay could be as high as 1. It could also, of course, be zero.

In making these rough statistical estimates we have used as a basis our own observations. The observations in other similar experiments are probably 10 or 20 times more numerous. The expected numbers of events produced by the various processes we have discussed should therefore be increased by a factor of 10 or 20 if we assume that a four-pronged event like ours would have been reported wherever it was observed.

**3.6. Summary.** — From the foregoing discussion of the four-pronged event we conclude that the two processes that could best explain it are the radiative decay of the  $\theta^0$ -meson (4) and the decay of the  $\tau^0$ -meson (5).

In the following sections we consider these two interpretations of the event in more detail and ignore the other possibilities that have been discussed above. The dynamics of the interaction at  $O$  are shown to provide evidence against the interpretation as radiative  $\theta^0$ -decay.

#### 4. The Momentum and Lifetime of the Unstable Particle.

The two different interpretations of the event lead to very different results when the momentum of the neutral heavy meson is calculated. If radiative  $\theta^0$ -decay is assumed, the momentum of the  $\theta^0$ -meson can be very accurately calculated from the well-measured angles given in Table II and the energy of the electron pair  $A, B$ . The result is  $1400 \pm 40$  MeV/c. A  $\theta^0$ -meson with this momentum requires  $1.9 \cdot 10^{-10}$  s to travel the distance from  $O$  to  $X$ .

The alternative interpretation of  $\tau^0$ -decay does not lead to a unique momentum for the  $\tau^0$ -meson since the direction of the secondary  $\pi^0$ -meson cannot be deduced only from measurements of the electron pair  $A, B$ . Rather involved calculations show that the momentum of the  $\tau^0$ -meson must be between 800 MeV/c and 1400 MeV/c. The times of flight corresponding to these two momenta are  $3.3 \cdot 10^{-10}$  s and  $1.9 \cdot 10^{-10}$  s (\*).

(<sup>9</sup>) J. BALLAM, M. GRISARU and S. B. TREIMAN: *Phys. Rev.*, **101**, 1438 (1956).

(\*) If the interpretation of the event as a  $\tau^0$ -decay is correct, the lifetime provides strong evidence against the theory of Salam and Polkinghorne (<sup>10</sup>) which predicts a mean lifetime of  $10^{-19}$  s for  $\tau^0$ -decay into three  $\pi$ -mesons. For this reason, in the following discussion of production reactions we do not consider the reactions that are allowed in the theory of Salam and Polkinghorne such as  $\pi^+ + n \rightarrow \tau^0 + p$ .

(<sup>10</sup>) A. SALAM and J. C. POLKINGHORNE: *Nuovo Cimento*, **2**, 685 (1955).



In Table III the complete description of the decay is given on the assumption that it is due to a  $\tau^0$ -meson with a momentum of 930 MeV/c. This value, well inside the allowed range, is the best value found for production by the process of charge exchange.

TABLE III. — Interpretation as  $\tau^0$ -decay

If the four-pronged event is interpreted as the decay of a neutral  $\tau$ -meson of given momentum it is possible to calculate the parameters of the decay in the laboratory and centre of mass systems using only the well measured quantities (the angles between tracks and the momenta of the electrons  $A$  and  $B$ ). The table shows the results calculated when the momentum of the  $\tau^0$ -meson is taken as 930 MeV/c. The mass of the  $\tau^0$ -meson was assumed to be  $965 m_e$ .

The calculation is made easier by the experimental observation that the line of flight ( $T$ ) is coplanar with ( $CD$ ).

Quantity	Laboratory System	Centre of Mass System
Momentum of neutral $\tau$ -meson	930 (assumed)	0
Momentum of particle $C$ ( $\pi^\pm$ )	467	120
Momentum of particle $D$ ( $\pi^\pm$ )	292	61
Momentum of neutral $\pi$ -meson	196	66
Angle $T C$	+ 13.5° (measured)	+ 65°
Angle $T D$	— 12.0° (measured)	— 91°
Angle $T \pi^0$	— 14.5°	— 132°

All momenta are given in MeV/c

## 5. — The Parent Interaction.

The nuclear interaction that occurs in the graphite plate is very important for the interpretation of the decay event. It is a simple interaction and the positive particle ( $G$ ) whose momentum is only  $\sim 1$  GeV/c is apparently the primary responsible for it. The only two secondary particles for which there is evidence are the positive heavy particle  $H$  and the unstable neutral particle  $T$ . The coplanarity of the three trajectories is a striking feature of the interaction that has to be explained.

Knowing that the energy of the positive primary particle is small there are only three simple reactions in which a neutral « strange » particle can be produced without violating the rule that such particles should be produced in association (see previous footnote). These are the charge-exchange reaction





and the double production reactions

$$\begin{aligned}\pi^+ + n &\rightarrow K^0 + \Sigma^+, \\ \pi^+ + n &\rightarrow \bar{K}^0 + K^+ + n.\end{aligned}$$

We have attempted to fit the dynamics of these three processes to the measurements made on the particles  $G$ ,  $H$  and  $T$ . The results are shown in Table IV.

TABLE IV. — Possible production processes.

The table shows to what extent a number of possible production processes fit the experimental measurements made on the nuclear interaction at  $O$ . In each reaction the variables have been chosen to preserve the measured angles and to give the best fit with the measured momenta of  $G$  and  $H$ . In reactions (2) and (5) the particle  $H$  is assumed to be the proton secondary from  $\Sigma^+$ -decay.

In all the reactions except (3) and (6) we assumed that the target neutron had a Fermi energy of 20 MeV. In reaction (5) the direction of the neutron's Fermi momentum was chosen to reduce the momentum of the particle  $G$  as far as possible. In reactions (3) and (6) the target neutron was assumed to be at rest.

The last column gives, for each reaction, the probability that the line  $T$  should be as nearly coplanar with  $G$  and  $H$  as it is found to be.

Process	Momentum of Neutral Particle (MeV/c)	Momentum of Primary ( $G$ ) (MeV/c)	Momentum of Secondary ( $H$ ) (MeV/c)	Probability of Coplanarity
1) $K^+ + n \rightarrow \tau^0 + p$	930	1 000	400	35%
2) $\pi^+ + n \rightarrow \tau^0 + \Sigma^+$	800	1 200	500	5%
3) $\pi^+ + n \rightarrow \bar{\tau}^0 + K^+ + n$	800	1 850	370 (*)	5%
4) $K^+ + n \rightarrow \theta^0 + p$	1 400	1 650	700	55%
5) $\pi^+ + n \rightarrow \theta^0 + \Sigma^+$	1 400	1 600	400	10%
6) $\pi^+ + n \rightarrow \bar{\theta}^0 + K^+ + n$	1 400	2 100	370 (*)	5%
Measured Values	$\left\{ \begin{array}{l} 1\ 400 \text{ for } \theta^0 \\ 800 \text{ to } 1\ 400 \text{ for } \tau^0 \end{array} \right\} \quad 940^{+470}_{-240} (**)$			
	$380^{+180}_{-90}$			

(\*) These values could be chosen to agree with the measurements.

(\*\*) This error is discussed in the text.

In the first three rows of the table the momentum of the neutral K-meson has been restricted to the range from 800 MeV/c to 1 400 MeV/c and chosen to give the best fit with the other measurements. In the remaining three rows the momentum was fixed at 1 400 MeV/c — corresponding to the interpretation of the event as radiative  $\theta^0$ -decay.

The charge exchange reaction satisfies the dynamical conservation laws if the target neutron has a Fermi energy of about 20 MeV (a momentum of 200 MeV/c). This momentum could affect significantly the coplanarity of the three trajectories and we have calculated the probability that they should be,

by chance, as nearly coplanar as they are. The last column in Table IV shows this probability.

In the reactions leading to the production of the short-lived  $\Sigma^+$ -particle it has been assumed that track  $H$  is that of the proton arising from  $\Sigma^+$ -decay (\*). This leads to a further possible departure from coplanarity of the trajectories and the probability in the last column of Table IV is correspondingly smaller.

Concerning the three-body reaction, little need be said. In this reaction the primary momentum has to be much higher than the measured value and the probability that the observed coplanarity should arise by chance is small.

The results given in Table IV provide the evidence in favour of the event being a  $\tau^0$ -decay. It is clear that the best fit with the measurements is obtained by assuming the charge exchange reaction leading to the production of a  $\tau^0$ -meson with a momentum of about 900 MeV/c. In this case the primary has a momentum of 1 000 MeV/c and the proton secondary a momentum of 400 MeV/c, in excellent agreement with the measured values.

The three reactions that lead to a  $\theta^0$ -meson with a momentum of 1 400 MeV/c all demand a primary momentum greater than 1 600 MeV/c and assuming any more complex production reaction only increases this figure. This is significantly above the measured value of  $940^{+470}_{-240}$  MeV/c. The error in this measurement has been very pessimistically assessed; it corresponds to a maximum detectable momentum of 2.8 GeV/c for a vertical track 18.5 cm long. If we assume a maximum detectable momentum of 4 GeV/c (the measured value for tracks 22 cm long) we should quote the momentum of particle  $G$  as  $940^{+370}_{-200}$  MeV/c. The internal consistency in the measurements of the track is good and there is no evidence of distortion on neighbouring photographs.

If we consider further the reactions leading to a  $\theta^0$ -meson we see that, apart from the high primary momentum, the charge exchange reaction demands also a high momentum for particle  $H$ . On the other hand, the double production reaction (5 in Table IV) with the lowest possible value of the primary momentum (1 600 MeV/c) demands very improbable parameters for the  $\Sigma^+$ -decay if any fit is to be obtained.

It may be argued that since the  $\tau^0$ -mesons's momentum is not exactly defined there is inherently greater freedom for adjustment of the parameters of the reaction with this interpretation and a better fit with the measurements must necessarily be obtained. This is true but not of very great importance since the charge exchange reaction, for example, fits all the observations very well for any assumed momentum of the  $K^0$ -meson between 700 MeV/c and 1 100 MeV/c — including half of the range allowed by the dynamics of  $\tau^0$ -decay. When the momentum of the neutral particle is raised above about 1 200 MeV/c the difficulty of fitting the observations increases rapidly.

(\*) If  $H$  were the track of a  $\Sigma^+$ -particle, the time of flight of the particle would have to be  $\sim 10^{-9}$  s which is an order of magnitude greater than the mean lifetime.

It is this difficulty that leads us to interpret the event as an example of  $\tau^0$ -decay.

## 6. - Conclusions.

The measurements made on the four-pronged event allow its interpretation either as the radiative decay of a  $\theta^0$ -meson or as the decay of a  $\tau^0$ -meson. Either interpretation involves an element of novelty since the radiative  $\theta^0$ -decay has not been detected experimentally and the  $\tau^0$ -meson is a particle whose existence has been predicted but not established.

If the event is interpreted as a  $\theta^0$ -decay the momentum of the  $\theta^0$ -meson must be 1400 MeV/c; if it is a  $\tau^0$ -decay the momentum of the  $\tau^0$ -meson must be between 800 MeV/c and 1400 MeV/c.

The interaction that produces the neutral meson is of a very simple type and there is considerable difficulty in reconciling the measurements made on it with any process that leads to a  $K^0$ -meson with a momentum of 1400 MeV/c. This difficulty does not arise if the neutral meson has a lower momentum ( $\sim 900$  MeV/c).

For this reason the event is interpreted as an example of  $\tau^0$ -decay, the momentum of the  $\tau^0$ -meson being about 900 MeV/c and its lifetime about  $3 \cdot 10^{-10}$  s.

The production process is probably a charge exchange reaction involving a  $K^-$ -meson and a neutron but a double production reaction is not excluded.

\* \* \*

In our work at the Jungfraujoch Research Station we have received great help from the Administration and from the manager, Mr. HANS WIEDERKEHR.

Mr. S. O. LARSON has constructed a great deal of our apparatus and has helped to run it. Mlle E. JOYET has assisted in making many of the measurements reported here.

We are very grateful to Dr. B. D'ESPAGNAT and to Dr. J. PRENTKI for valuable and informative discussions.

## RIASSUNTO (\*)

Si descrive un evento a quattro rami osservato in una camera a nebbia magnetica. Lo si interpreta come il decadimento in volo di un mesone  $\tau$  neutro secondo lo schema  $\tau^0 \rightarrow \pi^+ + \pi^- + \pi^0$  col successivo decadimento del  $\pi^0$  in una coppia di elettroni e un  $\gamma$ . Il  $\tau^0$  è prodotto nel carbonio in una piccola interazione nucleare che può essere una reazione di scambio di carica ( $K^+ + n \rightarrow \tau^0 + p$ ). La vita del  $\tau^0$  prima del decadimento è di circa  $3 \cdot 10^{-10}$  s. Si discutono e si dimostra la scarsa probabilità di altre possibili interpretazioni dell'evento.

(\*) Traduzione a cura della Redazione.

## On Covariant Quantization with Application to the Scattering of Gravitating Dirac Particles.

B. E. LAURENT

*Institute of Theoretical Physics - University of Stockholm, Sweden*

(ricevuto il 9 Settembre 1956)

**Summary.** — The action method of Feynman <sup>(1)</sup> and Matthews and Salam <sup>(2)</sup> is used. In this way it seems to be easy to quantize in a generally covariant way merely using the whole invariant Lagrangian without subsidiary conditions. It is shown that such a procedure leads to the ordinary quantization in the electrodynamic case. The Lagrangian for the Dirac-field is taken from a paper by BARGMAN <sup>(3)</sup> and is developed in powers of  $\beta = \sqrt{2K}$ , where  $K$  is the Einstein gravitation constant. The same is done with the usual Lagrangian for the gravitation field, as has been proposed by GUPTA <sup>(4)</sup>. The simplest problem of two identical Dirac-particles scattered against each other without radiation corrections is solved.

### 1. — Introduction.

MATTHEWS and SALAM <sup>(2)</sup>, and recently BURTON and DE BORDE <sup>(5)</sup>, have shown how Feynman's action method may be used in calculating propagators, that is vacuum matrix elements of time-ordered field operators in the points  $x_1 \dots x_n$  <sup>(6)</sup>.

$$(1) \qquad \qquad \qquad \langle T(\varphi(1) \dots \varphi(n)) \rangle_0.$$

(<sup>1</sup>) R. P. FEYNMAN: *Rev. Mod. Phys.*, **20**, 367 (1948).

(<sup>2</sup>) P. T. MATTHEWS and A. SALAM: *Nuovo Cimento*, **2**, 120 (1955).

(<sup>3</sup>) V. BARGMAN: *Berl. Ber.*, **11**, 346 (1932).

(<sup>4</sup>) S. N. GUPTA: *Proc. Phys. Soc.*, A **65**, 161, 608 (1952).

(<sup>5</sup>) W. K. BURTON and A. H. DE BORDE: *Nuovo Cimento*, **4**, 254 (1956).

(<sup>6</sup>)  $T$  stands for the Wick ordering operator.

Their expression for (1) is the following

$$(2) \quad \left\{ \begin{array}{l} \langle T(\varphi(1) \dots \varphi(n)) \rangle_0 = N^{-1} \int \varphi(1) \dots \varphi(n) \exp [-iI[\varphi(x)]] \delta\varphi, \\ N = \int \exp [-iI[\varphi(x)]] \delta\varphi. \end{array} \right.$$

Here  $I[\varphi(x)]$  is the classical action functional of the field (or fields)  $\varphi(x)$  and the integrations are functional integrations whose definition will be given in Sect. 2 below. MATTHEWS and SALAM<sup>(2)</sup> prescribe boson fields to commute with everything in the integrands of (2) while fermion fields are completely internally anticommuting. The meaning of the latter prescription is not quite clear in every connection, but it seems none the less to be a powerful calculating tool and I will use it in the following. MATTHEWS and SALAM<sup>(2)</sup>, as well as BURTON and DE BORDE<sup>(5)</sup>, treat exclusively scalar and Dirac fields where the question of gauge transformation does not enter. One aim of the present paper is to make it probable that a correct procedure in electrodynamics is to insert the invariant action in (2) without using any subsidiary conditions, and that the expression (2) is then gauge-invariant.

Further, the same method is used for a Dirac field interacting with a gravitational field and the probability amplitude for the lowest order of gravitational scattering is evaluated.

## 2. - Variable Transformation in Functional Integrals.

A functional integral may be defined as a series of limit transitions as in the article by BURTON and DE BORDE<sup>(5)</sup>. In the following I adopt their definition with slight changes.

A propagator  $\langle T(\varphi(1) \dots \varphi(n)) \rangle_0$  is to be evaluated in the following way

1) In a region  $V$  of space-time we put a point-lattice, among the  $k$  points  $x_r$  of which are the points  $x_1 \dots x_n$  above.

2) A function  $\varphi(x)$  is defined as<sup>(7)</sup>

$$(3) \quad \varphi(x) = F \left( \sum_{j=1}^k a_j \varphi_j(x) \right),$$

where the  $\varphi_j(x)$  form a complete orthogonal set in  $V$ .  $F$  is a function such that the  $k$   $a_j$  may be determined when the  $k$   $\varphi(x_r)$  are known. (3) is only a

(7) A function of more different sums may also be used. The important thing is that the high frequency terms be abandoned.

means of getting a smooth function  $\varphi(x)$  which has given values  $q(x_r)$  in the lattice points  $x_r$ .

3)

$$(4) \quad \langle T(\varphi(1) \dots \varphi(n)) \rangle_0 = N^{-1} \int \varphi(1) \dots \varphi(n) \exp [-iI[\varphi(x)]] \delta\varphi = \\ = \lim \frac{\int \varphi(1) \dots \varphi(n) \exp [-iI[\varphi(x)]] \varepsilon d(\varphi)}{\int \exp [-iI[\varphi(x)]] \varepsilon d(\varphi)}.$$

Here  $d(\varphi)$  is an abbreviation for the product of the  $k$  differentials  $dq(x_r)$  and the integrals are  $k$ -fold going from  $-\infty$  to  $+\infty$ .  $\varepsilon$  is a function of the  $q(x_r)$ , and becomes zero for high absolute values of the  $q(x_r)$ ; it is inserted to make the integrals converge for special choices of  $I[\varphi(x)]$ . The symbol  $\lim$  means  $k \rightarrow \infty$ ;  $V \rightarrow \infty$ ;  $\varepsilon \rightarrow 1$  in that order.

It is assumed that the procedure outlined above leads to a unique result for reasonable distributions of the points in the lattice and a reasonable shape of  $V$  when  $S[\varphi(x)]$  is one of the functionals treated in the following. Further, it is assumed that the result is to a large extent independent of the choice of  $\varphi_j(x)$ ,  $F$  and  $\varepsilon$ .

If we change variables in the above integrals

$$(5) \quad \theta_s = \theta_s[\varphi(x_r)],$$

and put in the proper transformation determinant, this will leave the value of (4) unaltered.

In the limit  $k \rightarrow \infty$  (5) goes over into

$$(6) \quad \theta(s) = \theta[\varphi(x)],$$

where  $s$  may now be wholly or partly continuous and  $\theta(s)$  is functionally dependent of  $\varphi(x)$ . When in the following a transformation is written in the form (6) it is thought of as the limit of a transformation of the type (5).

If the transformation (5) is linear the transformation determinant is independent of the  $q(x_r)$  and can be cancelled in the expression (4). Suppose further that

$$(7) \quad \theta_{s_1} = \varphi(1); \theta_{s_2} = \varphi(2); \dots \theta_{s_n} = \varphi(n),$$

and that  $F$  can be changed so that  $\varphi(x)$  is transformed in a way that does not affect the form of  $I$ . Then the expression (4) is form-invariant in the transformation in question.



### 3. - Electrodynamics.

It is assumed that the following propagator will give the probability amplitude for electromagnetic scattering of electron against electron.

$$(8) \quad \langle T(\psi(1)\psi(2)\bar{\psi}(1')\bar{\psi}(2')) \rangle_0 = \\ = N^{-1} \int \psi(1)\psi(2)\bar{\psi}(1')\bar{\psi}(2') \exp[-iI_e[\psi, \bar{\psi}, A_\mu]] \delta\psi \delta\bar{\psi} \delta A_\mu,$$

with

$$(9) \quad I_e = \int d^4x \{ \mathcal{L}_D + A^\mu (\hat{g}_{\mu\nu} \square - \partial_\mu \partial_\nu) A^\nu \},$$

$$(10) \quad \mathcal{L}_D = i\bar{\psi} \hat{\gamma}^\mu (\partial_\mu - eA_\mu) \psi,$$

where  $\hat{g}_{\mu\nu}$  is the Lorentz metric (real coordinates) and  $\hat{\gamma}^\mu$  are the ordinary Dirac matrices. The  $A_\mu$  commute with everything while  $\psi$ ,  $\bar{\psi}$  is completely internally anticommuting. In this connection  $N$  means

$$(11) \quad N = \int \exp[-iI_e[\psi, \bar{\psi}, A_\mu]] \delta\psi \delta\bar{\psi} \delta A_\mu.$$

If we define a transformation of type (5) by letting  $\varphi(x)$  as well as  $F$  in (3) be changed with a gauge-transformation, while the  $\varphi_j(x)$  are kept as the same linear functions, then it becomes evident that the transformation (5) will have the following properties.

1) It becomes linear, for which reason the transformation determinant may be neglected in the transformation of (8).

2) The action  $I_e$  is form-invariant under the transformation.

3) Suppose that the points  $x_1$ , and  $x_2$ , are placed on a space-like surface in the remote past, the points  $x_1$  and  $x_2$  on a space-like surface in the remote future, and that the coupling constant (the electron charge  $e$ ) can be adiabatically switched on and off in the usual way. Then (7) will hold.

4) In the limit  $k \rightarrow \infty$  (5) becomes a gauge-transformation.

These four points show that (8) is covariant under a gauge-transformation.

Let us now consider the following transformation from the variables  $\psi$ ,  $\bar{\psi}$ ,  $A_\mu$  to the variables  $\Phi$ ,  $\bar{\Phi}$ ,  $A$ ,  $a(t)$

$$(12) \quad \psi_\alpha(x) = \exp[ie\Lambda(x)] \Phi_\alpha(x),$$

$$(13) \quad \bar{\psi}_\alpha(x) = \exp[-ie\Lambda(x)] \bar{\Phi}_\alpha(x),$$

$$(14) \quad A_\mu(x) = A'_\mu[a(t)] + \partial_\mu \Lambda(x).$$

The  $A'_\mu$  are defined with the help of (14) and some given, not gauge-invariant, relation (for instance  $\tilde{g}^{\mu\nu}\partial_\mu A'_\nu = 0$ ) which they must fulfil. They are of course determined by fewer variables than the  $A'_\mu$  themselves. The  $a(t)$  form a set of such variables, so chosen that  $A'_\mu$  are linear functions of them. The transformation (12)-(14) is not a gauge-transformation but it would have been if one had regarded  $\psi$ ,  $\bar{\psi}$ ,  $A_\mu$  and  $\Phi$ ,  $\bar{\Phi}$ ,  $A'_\mu$  respectively as the variables and  $A$  had been a given function.

The transformation

$$(15) \quad \psi_\alpha(x_r) = \exp[ie\Lambda(x_r)]\Phi_\alpha(x_r),$$

$$(16) \quad \bar{\psi}(x_r) = \exp[-ie\Lambda(x_r)]\bar{\Phi}_\alpha(x_r),$$

$$(17) \quad A_\mu(x_r) = A'_{\mu, x_r}(a_i) + D_{\mu, x_r}(\Lambda(x_s)),$$

where  $A'_{\mu, x_r}$  and  $D_{\mu, x_r}$  are linear functions, is of the type (5). Evidently it is always possible to find a transformation (15)-(17) such that the functions corresponding to  $\varphi(x)$  in (3) will be transformed according to (12)-(14) if the functions corresponding to  $F$  are changed in a suitable manner. This makes  $I_o$  in (8) independent of  $\Lambda(x_r)$ .

The transformation determinant for the transformation (15)-(17)

$$\left| \frac{\partial[\psi_\alpha(x_r), \bar{\psi}_\beta(x_s), A_\mu(x_t)]}{\partial[\Phi_\gamma(x_u), \bar{\Phi}_\delta(x_v), a_k, \Lambda(x_l)]} \right|,$$

is a constant and may therefore be neglected.

Finally,

$$\psi(1) = \Phi(1); \quad \psi(2) = \Phi(2); \quad \bar{\psi}(1') = \bar{\Phi}(1'); \quad \bar{\psi}(2') = \bar{\Phi}(2')$$

if the coupling constant is switched off on the surfaces on which are  $x_1, x_2, x'_1$  and  $x'_2$ . Hence

$$(19) \quad T(\psi(1)\psi(2)\bar{\psi}(1')\bar{\psi}(2'))_0 = N^{-1} \int \Phi(1)\Phi(2)\bar{\Phi}(1')\bar{\Phi}(2') \exp[-iI_e] \delta\Phi \delta\bar{\Phi} \delta a,$$

where  $N$  now means

$$N = \int \exp[-iI_e] \delta\Phi \delta\bar{\Phi} \delta a.$$

It has been possible to cancel  $d\Lambda(x_s)$  because everything in the integrand of (8) is independent of  $\Lambda(x_s)$ . In (19) the integration is performed over the

« real degrees of freedom » only. Now

$$(20) \quad \int \exp \left[ i \int d^4x \left( \frac{\partial A_\mu}{\partial x_\mu} \right)^2 \right] \delta A = \int \exp \left[ i \int d^4x \left( \frac{\partial A'_\mu}{\partial x_\mu} + \square A \right)^2 \right] \delta A = \\ = \text{const. independent of } a_t,$$

because  $\partial A'_\mu / \partial x_\mu$  merely shifts  $A$ 's zero-point. (20) may be used to express (19) in another form, i.e. the following

$$(21) \quad \langle T(\psi(1)\psi(2)\bar{\psi}(1')\bar{\psi}(2')) \rangle_0 = \\ = N^{-1} \int \psi(1)\psi(2)\bar{\psi}(1')\bar{\psi}(2') \exp \left[ i \int d^4x (\mathcal{L}_D + A^\mu \square A_\mu) \right] \delta \psi \delta \bar{\psi} \delta A_\mu,$$

where  $N$  now means

$$N = \int \exp \left[ -i \int d^4x (\mathcal{L}_D + A^\mu \square A_\mu) \right] \delta \psi \delta \bar{\psi} \delta A_\mu.$$

The propagator in the form (21) corresponds to the ordinary quantum electrodynamics with Fermi's state-vector condition and the Gupta-Bleuler indefinite metric. (See for instance Heitler's book <sup>(8)</sup>).

#### 4. - Gravitation.

According to BARGMAN <sup>(3)</sup> the invariant action-functional for gravitation and Dirac fields in interaction may be written

$$(22) \quad I = \int \mathcal{L} d^4x,$$

$$(23) \quad \mathcal{L} = \sqrt{g} \left\{ \frac{1}{\beta^2} R - i\psi^\dagger (\gamma^\alpha \nabla_\alpha - \mu) \psi \right\},$$

where

$$R = g^{\mu\nu} R_{\mu\nu},$$

$g^{\mu\nu}$  being the metric tensor,  $R_{\mu\nu}$  the contracted curvature tensor (the Einstein tensor) and  $g = -|g_{\mu\nu}|$ .

$\psi$  is a spinor field,

$$\varphi = \alpha \psi,$$

<sup>(8)</sup> W. HEITLER: *The Quantum Theory of Radiation*. 3-rd edition, 1954, Appendix 3, p. 406.

with  $\alpha$  having the properties

$$(24) \quad \alpha + \alpha^\dagger = 0; \quad \alpha \gamma^\mu + \gamma^{\mu\dagger} \alpha = 0.$$

$\gamma^\mu$  must satisfy the following relations

$$(25) \quad [\gamma^\mu, \gamma^\nu]_+ = 2g^{\mu\nu}.$$

The  $\nabla_\mu$  work on  $\psi$  in the following way

$$(26) \quad \nabla_\mu \psi = (\partial_\mu - I_\mu) \psi,$$

and  $I_\mu$  must satisfy

$$(27) \quad \frac{\partial \gamma_\mu}{\partial x^\nu} = \gamma^\alpha I_{\alpha\mu\nu} + I_\nu \gamma_\mu - \gamma_\mu I_\nu,$$

where  $I_{\alpha\mu\nu}$  is the usual affine connexion. (27) determines the  $I_\nu$  except for additive functions commuting with all the  $\gamma_\mu$ . In the following a special solution of (27) will be used. Finally,  $\beta = \sqrt{2K}$ , here  $K$  is the Einstein gravitation constant.

Later on it will become interesting to know how the  $\nabla_\mu$  operate from the right on  $\varphi^\dagger$ . They work in the following way

$$(28) \quad \varphi^\dagger \overleftarrow{\nabla}_\mu = \varphi^\dagger (\overleftarrow{\partial}_\mu + I_\mu),$$

where

$$\varphi^\dagger \overleftarrow{\partial}_\mu = \frac{\partial}{\partial x^\mu} \varphi^\dagger.$$

The action (22) is invariant in the case of general coordinate transformations as well as in general  $S$ -transformations. [See BARGMAN's paper <sup>(3)</sup>].

When the propagator

$$T(\psi(1)\psi(2)\bar{\psi}(1')\bar{\psi}(2'))_0$$

is to be evaluated in the gravitational case we are faced with a problem that was not so serious in the electromagnetic case: How are the integration variables to be chosen? Shall we integrate with respect to  $g_{\mu\nu}$ ,  $\mathfrak{g}_{\mu\nu} = \sqrt{g}g_{\mu\nu}$ ,  $\Gamma^\alpha_{\beta\gamma}$  or some other variables? The question is important because the relations between the different sets of variables are non-linear and one can consequently not neglect the transformation determinant when going from one set to ano-

ther<sup>(9)</sup>. The transformation determinant can of course be included in the action, which then gets a new imaginary term that is of no importance for the classical limit<sup>(10)</sup>. The above question may accordingly also be formulated thus: How is the action function to be chosen for a certain set of variables?

In the following I shall assume the classical action (22) to belong to the variables  $\mathbf{g}_{\mu\nu}$  which is of course quite arbitrary.

Hence

$$(29) \quad \langle T\{\psi(1)\psi(2)\bar{\psi}(1')\bar{\psi}(2')\} \rangle_0 = \\ = N^{-1} \int \psi(1)\psi(2)\bar{\psi}(1')\bar{\psi}(2') \exp[-iI[\psi, \bar{\psi}, \mathbf{g}_{\mu\nu}]] \delta\psi \delta\bar{\psi} \delta\mathbf{g}_{\mu\nu}.$$

Behind the integral sign the gravitation field  $\mathbf{g}_{\mu\nu} = \sqrt{g}g_{\mu\nu}$  commutes with everything, while the Dirac fields  $\psi$  and  $\bar{\psi}$  are completely internally anti-commuting as is proposed by MATTHEWS and SALAM<sup>(2)</sup>. In this connection  $N$  means

$$N = \int \exp[-iI[\psi, \bar{\psi}, \mathbf{g}_{\mu\nu}]] \delta\psi \delta\bar{\psi} \delta\mathbf{g}_{\mu\nu}.$$

In a general coordinate as well as in an  $S$ -transformation the fields  $\psi$ ,  $\bar{\psi}$ ,  $\mathbf{g}_{\mu\nu}$  are transformed in a linear way and one can show with the same kind of arguments as in the electrodynamic case that (29) is covariant in such transformations, provided that the points  $x_1$ ,  $x_2$ ,  $x_1$  and  $x_2$  are placed on space-like surfaces where the coupling constant  $\beta$  is switched off.

## 5. - Expansion of the Dirac Field Lagrangian.

The aim of the rest of this article is to evaluate (29) in the lowest order of approximation and to apply the result to the electron-electron gravitational scattering (« gravitational Møller scattering »). Therefore the Lagrangian (23) will be expanded by powers of  $\beta$ .

Before performing the expansion the Dirac part of the Lagrangian

$$\mathcal{L}_{GD} = -i\sqrt{g}\bar{\psi}(\gamma^\mu \nabla_\mu - \mu)\psi$$

<sup>(9)</sup> The question does not arise in electrodynamics because it is linear in all its aspects.

<sup>(10)</sup> This is best seen when  $\hbar$  is written out explicitly (in this paper  $\hbar = c = 1$ ). Then

$$\langle T(\varphi(1) \dots \varphi(n)) \rangle_0 = N^{-1} \int \varphi(1) \dots \varphi(n) \exp\left[-i \frac{1}{\hbar} I\right] \delta\varphi,$$

and the classical limit is reached by putting  $\hbar \rightarrow 0$  (see FEYNMAN<sup>(1)</sup>).

will be written in a more suitable form. To this end we introduce the fields  $\Phi_{\mu\nu}$ ,  $\psi^{\mu\nu}$ ,  $\theta_{\alpha\beta}$  and  $\Omega^{\alpha\beta}$  defined through the formulas

$$(30) \quad g_{\mu\nu} = \hat{g}_{\mu\nu} + \beta \Phi_{\mu\nu},$$

$$(31) \quad g^{\mu\nu} = \hat{g}^{\mu\nu} - \beta \psi^{\mu\nu},$$

$$(32) \quad \gamma_\alpha = \hat{\gamma}_\alpha + \frac{1}{2} \beta \theta_{\alpha\beta} \hat{\gamma}^\beta,$$

$$(33) \quad \gamma^\alpha = \hat{\gamma}^\alpha - \frac{1}{2} \beta \Omega^{\alpha\beta} \hat{\gamma}_\beta.$$

With help of (25) and  $g^{\mu\alpha} g_{\alpha\nu} = \delta^\mu_\nu$  we obtain the following relations between the new fields

$$(34) \quad \psi^\alpha_\beta = \Phi^\alpha_\beta - \beta \Phi^\alpha_\epsilon \psi^\epsilon_\beta \quad \text{or} \quad (\delta^\lambda_\nu + \beta \Phi^\lambda_\nu)(\delta^\alpha_\lambda - \beta \psi^\alpha_\lambda) = \delta^\alpha_\nu,$$

$$(35) \quad \theta_{\alpha\beta} = \Phi_{\alpha\beta} - \frac{1}{4} \beta \theta^\epsilon_\alpha \theta_{\beta\epsilon},$$

$$(36) \quad \Omega^{\alpha\beta} = \psi^{\alpha\beta} + \frac{1}{4} \beta \Omega^\epsilon_\alpha \Omega^{\beta\epsilon},$$

$$(37) \quad \Omega^\alpha_\beta = \psi^\alpha_\beta - \frac{1}{2} \beta \Omega^{\alpha\epsilon} \psi_{\epsilon\beta} \quad \text{or} \quad \left( \delta^\lambda_\nu + \frac{\beta}{2} \theta^\lambda_\nu \right) \left( \delta^\alpha_\lambda - \frac{\beta}{2} \Omega^\alpha_\lambda \right) = \delta^\alpha_\nu.$$

Here we have used the convention that indices of the new fields can be raised and lowered with the help of  $\hat{g}^{\mu\nu}$  and  $\hat{g}_{\mu\nu}$ : (34)-(37) give in principle three of the fields in terms of the remaining one.

The expressions (32) and (33) imply a specialization of  $\gamma^\alpha$  and  $\gamma_\alpha$  and a coupling between the coordinate transformations and the  $S$ -transformations.

Let us further introduce the fields  $\Theta_{\alpha\sigma\mu}$  and  $G_{\alpha\mu\nu}$  through

$$(38) \quad \Gamma_\mu = -\frac{\beta}{4} \hat{g}^{\alpha\sigma} \Theta_{\alpha\sigma\mu},$$

where

$$(39) \quad \hat{g}^{\alpha\sigma} = \frac{1}{2} [\hat{\gamma}^\alpha, \hat{\gamma}^\sigma],$$

$$(40) \quad G_{\alpha\mu\nu} = \frac{1}{\beta} \Gamma_{\alpha\mu\nu} = \frac{1}{2} (\Phi_{\mu\alpha,\nu} + \Phi_{\nu\alpha,\mu} - \Phi_{\mu\nu,\alpha}),$$

$\alpha = -\hat{\gamma}_4$  satisfies the relations (24). This gives  $q^+ = \bar{\psi}$ . Equation (27) gives

$$(41) \quad \hat{\gamma}^\alpha \left[ \frac{\partial \theta_{\mu\alpha}}{\partial x^\nu} - 2 \delta^\sigma_\alpha \left( \delta^\sigma_\mu - \frac{1}{2} \beta \Omega^\sigma_\alpha \right) G_{\sigma\mu\nu} + (\Theta_{\alpha\sigma\nu} - \Theta_{\sigma\alpha\nu}) \left( \delta^\sigma_\mu + \frac{1}{2} \beta \theta^\sigma_\mu \right) \right] = 0.$$

This equation is certainly satisfied if the expression between the square brackets is zero. If we insert  $G_{\alpha\mu\nu}$  from (40) in this equation we see that a possible



solution of (41) is

$$(42) \quad \Theta_{\theta\sigma\alpha} = \left( \delta_\theta^\delta - \frac{1}{2} \beta \Omega_\theta^\delta \right) \left( \delta_\sigma^\gamma - \frac{1}{2} \beta \Omega_\sigma^\gamma \right) \left( \Phi_{\alpha\delta,\gamma} + \frac{\beta}{4} 6_\gamma^\beta \theta_{\delta\beta,\alpha} \right),$$

$\mathcal{L}_{\theta D}$  is, omitting a complete divergence (see BARGMAN <sup>(3)</sup>),

$$\mathcal{L}_{\theta D} = -\frac{i}{2} \sqrt{g} \{ \varphi^\dagger (\gamma^\mu \nabla_\mu - \mu) \psi - \varphi^\dagger (\overleftarrow{\nabla}_\mu \gamma^\mu + \mu) \psi \},$$

or with (26) and (28)

$$(43) \quad \mathcal{L}_{\theta D} = -\frac{i}{2} \sqrt{g} \{ \varphi^\dagger \gamma^\mu (\partial_\mu - \Gamma_\mu) \psi - \varphi^\dagger (\overleftarrow{\partial}_\mu + \Gamma_\mu) \gamma^\mu \psi - 2\mu \varphi^\dagger \psi \}.$$

Inserting (33), and (38), (42), in (43) one gets

$$(44) \quad \left\{ \begin{array}{l} \mathcal{L}_{\theta D} = \mathcal{L}_I + \mathcal{L}_{II} + \mathcal{L}_{III}, \\ \mathcal{L}_I = -\frac{i}{2} \sqrt{g} \bar{\psi} (\hat{\gamma}^\alpha \partial_\alpha - \overleftarrow{\partial}_\alpha \hat{\gamma}^\alpha - 2\mu) \psi, \\ \mathcal{L}_{II} = \frac{i}{4} \beta \sqrt{g} \Omega_\alpha^\mu \bar{\psi} (\hat{\gamma}^\alpha \partial_\mu - \overleftarrow{\partial}_\mu \hat{\gamma}^\alpha) \psi, \\ \mathcal{L}_{III} = -\frac{i}{32} \beta^2 \sqrt{g} (\delta_\alpha^\mu - \frac{1}{2} \beta \Omega_\alpha^\mu) (\delta_\beta^\nu - \frac{1}{2} \beta \Omega_\beta^\nu) (\delta_\gamma^\rho - \frac{1}{2} \beta \Omega_\gamma^\rho) \theta_{\nu\sigma,\mu}^{\sigma} \bar{\psi} [\hat{\gamma}^\alpha, \hat{s}^{\beta\gamma}]_- \psi. \end{array} \right.$$

$[\hat{\gamma}^\alpha, \hat{s}^{\beta\gamma}]_-$ , being antisymmetric in all three indices, is a pseudovector, and we see that the interaction is a mixture of derivative tensor coupling and pseudovector coupling.

Now we want the approximation to first order in  $\beta$  of  $\mathcal{L}_{\theta D}$  expressed as a function of  $\mathbf{g}_{\mu\nu}$  instead of  $g_{\mu\nu}$ .

Let us define a function  $\chi^{\mu\nu}$  through

$$(45) \quad \mathbf{g}^{\mu\nu} = \hat{g}^{\mu\nu} - \beta \chi^{\mu\nu}.$$

Up to the first order then

$$\psi_{\mu\nu} = (\delta_\alpha^\mu \delta_\beta^\nu - \frac{1}{2} \hat{g}^{\mu\nu} \hat{g}_{\alpha\beta}) \chi^{\alpha\beta} + \dots,$$

which inserted in (44) gives, up to the first order,

$$(46) \quad \left\{ \begin{array}{l} \mathcal{L}_I = -\frac{i}{2} \left( 1 - \frac{\beta}{2} \chi_\delta^\delta \right) \bar{\psi} (\hat{\gamma}^\alpha \partial_\alpha - \overleftarrow{\partial}_\alpha \hat{\gamma}^\alpha - 2\mu) \psi + \dots, \\ \mathcal{L}_{II} = \frac{i}{4} \beta (\delta_\theta^\mu \delta_\alpha^\sigma - \frac{1}{2} \delta_\alpha^\mu \delta_\theta^\sigma) \chi_\theta^\sigma \bar{\psi} (\hat{\gamma}^\alpha \partial_\mu - \overleftarrow{\partial}_\mu \hat{\gamma}^\alpha) \psi + \dots, \\ \mathcal{L}_{III} = 0 + \dots \end{array} \right.$$

## 6. - Expansion of the Gravitation Lagrangian.

The Lagrangian of the pure gravitational field in (23) may, as is well known, be written

$$(47) \quad \mathcal{L}_g = \frac{1}{2\beta^2} \mathbf{g}^{\mu\nu} \left( -\frac{\partial \Gamma_{\mu\nu}^\alpha}{\partial x^\alpha} + \frac{\partial \Gamma_{\mu\alpha}^\nu}{\partial x^\nu} \right),$$

omitting a complete divergence (see for example TOLMAN<sup>(11)</sup>).

Putting in the expression for  $\Gamma_{\varrho\mu\nu}$  one gets

$$(48) \quad \mathcal{L}_g = -\frac{1}{2\beta} \frac{1}{\sqrt{g}} \mathbf{g}^{\mu\nu} \mathbf{g}^{\alpha\varrho} (\Phi_{\varrho\nu, \mu\alpha} - \Phi_{\mu\nu, \varrho\alpha}) - \\ - \frac{1}{4} \mathbf{g}^{\mu\nu} \psi^{\alpha\varrho}_{, \sigma} (\delta_\nu^\sigma \Phi_{\varrho\alpha, \mu} - 2\delta_\alpha^\sigma \Phi_{\varrho\nu, \mu} + \delta_\alpha^\sigma \Phi_{\mu\nu, \varrho}).$$

Expanding  $\mathcal{L}_g$  up to zeroth order and regarding it as a function of  $\mathbf{g}_{\mu\nu}$  rather than  $g_{\mu\nu}$ , one gets

$$(49) \quad \mathcal{L}_g = -\frac{1}{4} \chi^{\alpha\beta} (\delta_\alpha^\mu \delta_\beta^\nu \hat{g}^{\delta\gamma} - \delta_\beta^\nu \delta_\alpha^\gamma \hat{g}^{\delta\mu} - \delta_\alpha^\delta \delta_\beta^\mu \hat{g}^{\gamma\nu} - \frac{1}{2} \hat{g}_{\alpha\beta} \hat{g}^{\mu\nu} \hat{g}^{\gamma\delta}) \chi_{\mu\nu, \gamma\delta} + \dots$$

The minus first order term may be neglected because it is a complete derivative.

## 7. - The First Order Theory.

In this section we shall investigate the gravitation field in zeroth order of approximation interacting in first order with the Dirac field only.

The action for this case is given by (46) and (49)

$$(50) \quad \begin{cases} I_1 = \int \mathcal{L}_1 d^4x, \\ \mathcal{L}_1 = \mathcal{L}_g^{(0)} + \mathcal{L}_{gd}^{(0)} + \mathcal{L}_{gd}^{(1)}. \end{cases}$$

This action is invariant in first order in the case of the transformation

$$(51) \quad \begin{cases} \chi_{\alpha\beta} = \chi'_{\alpha\beta} + \frac{\hat{\gamma}_\alpha \hat{A}_\beta}{\partial x^\beta} + \frac{\hat{\gamma}_\beta \hat{A}_\alpha}{\partial x^\alpha} - \hat{g}_{\alpha\beta} \frac{\hat{\gamma}_\gamma \hat{A}^\gamma}{\partial x^\gamma}, \\ \psi = \left( 1 - \frac{\beta}{4} \hat{g}^{\alpha\beta} \frac{\partial \hat{A}_\alpha}{\partial x^\beta} \right) \left( \psi' + \beta \frac{\partial \psi'}{\partial x^\gamma} \hat{A}^\gamma \right), \\ \bar{\psi} = \left( \bar{\psi}' + \beta \frac{\partial \bar{\psi}'}{\partial x^\gamma} \hat{A}^\gamma \right) \left( 1 + \frac{\beta}{4} \hat{g}^{\alpha\beta} \frac{\partial \hat{A}_\alpha}{\partial x^\beta} \right). \end{cases}$$

(11) R. C. TOLMAN: *Relativity, Thermodynamics and Cosmology* (1934), § 87, p. 222.

where the  $A_\alpha$  are arbitrary functions. (51) corresponds to a first order coordinate transformation

$$(52) \quad x'^\mu = x^\mu + \beta_\alpha A^\mu; \quad A_\alpha = \hat{g}_{\alpha\mu} A'^\mu,$$

connected with an  $S$ -transformation such that (32) and (33) are always true, with  $\hat{\gamma}^\mu$  as given constant Dirac-matrices.

If one is interested in (29) only up to the first order of the interaction between the gravitation and the Dirac field, one may eliminate the non-real degrees of freedom essentially in the same way as in the electrodynamic case, (12)-(14) being replaced by (51), where the  $A_\alpha$  are now regarded as new variables. We let  $\chi'_{\alpha\beta}$  satisfy

$$(53) \quad \hat{g}^{\beta\gamma} \frac{\partial \chi'_{\alpha\beta}}{\partial A^\gamma} = 0.$$

The transformation determinant is in this case a function of  $A_\alpha$  only. If one considers (53) one gets in the same way as in electrodynamics a result corresponding to (21)

$$(54) \quad \langle T(\psi(1)\psi(2)\bar{\psi}(1')\bar{\psi}(2')) \rangle_0 = \\ = N^{-1} \int \psi(1)\psi(2)\bar{\psi}(1')\bar{\psi}(2') \exp \left[ -i \int d^4x (\mathcal{L}_D^{(0)} + \mathcal{L}_D^{(1)} + \mathcal{L}_G^{(a)}) \right] \delta\psi \delta\bar{\psi} \delta\mathbf{g}_{\mu\nu},$$

where

$$(55) \quad \mathcal{L}_G^{(a)} = -\frac{1}{4} \chi^{\alpha\beta} (\delta_\alpha^\mu \delta_\beta^\nu \hat{g}^{\delta\gamma} - \frac{1}{2} \hat{g}_{\alpha\beta} \hat{g}^{\mu\nu} \hat{g}^{\gamma\delta}) \chi_{\mu\nu, \gamma\delta},$$

and where  $N$  now means

$$N = \int \exp \left[ -i \int d^4x (\mathcal{L}_D^{(0)} + \mathcal{L}_D^{(1)} + \mathcal{L}_G^{(a)}) \right] \delta\psi \delta\bar{\psi} \delta\mathbf{g}_{\mu\nu}.$$

For the moment we are interested only in the lowest order scattering process where every electron line is either ingoing or outgoing. This makes a part of the interaction Lagrangian vanish, and we use the following action in (54)

$$(56) \quad \left\{ \begin{array}{l} I_2 = \int d^4x (\mathcal{L}_G^{(a)} + \mathcal{L}_D^{(0)} + \mathcal{L}_{\text{int}}), \\ \mathcal{L}_G^{(a)} = -\frac{1}{4} \chi_\beta^\alpha \square (\chi_\alpha^\beta - \frac{1}{2} \delta_\alpha^\beta \chi_\mu^\mu), \\ \mathcal{L}_D^{(0)} = -\frac{i}{2} \bar{\psi} (\hat{\gamma}^\alpha \hat{\partial}_\alpha - \hat{\bar{\partial}}_\alpha \hat{\gamma}^\alpha - 2\mu) \psi, \\ \mathcal{L}_{\text{int}} = \frac{i}{4} \beta \chi_\beta^\alpha \bar{\psi} \hat{\partial}_\alpha^\beta \psi, \end{array} \right.$$

where

$$(57) \quad O_{\alpha}^{\beta} = (\delta_{\alpha}^{\mu} \delta_{\nu}^{\beta} - \frac{1}{2} \delta_{\nu}^{\mu} \delta_{\alpha}^{\beta}) (\gamma^{\nu} \partial_{\mu} - \overleftarrow{\partial}_{\mu} \gamma^{\nu}) .$$

## 8. - The Power Expansion Solution.

We shall now consider only the processes connected with the following type of Feynman graph

$$\begin{array}{cc} \rangle & \backslash \\ / \text{ electron line;} & \text{ graviton line.} \end{array}$$

For this purpose we can be content with the gravitation field in zeroth approximation, interacting in first approximation with the Dirac field only. Hence we may use the results of the preceding section. The interesting term in the power expansion of (54) (see (2)) is the second order term

$$(58) \quad S'_2(1, 2, 1', 2') = -\frac{1}{2} N^{-1} \int \psi(1) \psi(2) \bar{\psi}(1') \bar{\psi}(2') \left\{ i \frac{\beta}{4} \right\}^2 \cdot \\ \cdot \iint dx dx' (\chi_r''(x) \psi(x) O_{\mu}^{\nu}(x) \psi(x) \chi_{\beta}'(x') \bar{\psi}(x') O_{\nu}^{\mu}(x') \psi(x')) \cdot \exp[-i(I_e^{(a)} - I_D^{(0)})] \delta\psi \delta\psi' \delta\chi_{\mu\nu} .$$

With the elementary propagators

$$(59) \quad S(1, 1') = \int \psi(1) \bar{\psi}(1') \exp[-iI_D^{(0)}] \delta\psi \delta\bar{\psi} ,$$

and

$$(60) \quad R_{\sigma\beta}^{\alpha\gamma}(1, 1') = \int \chi_{\sigma}^{\alpha}(1) \chi_{\beta}^{\gamma}(1') \exp[-iI_G^{(a)}] \delta\chi_{\mu\nu} ,$$

one gets according to (2)

$$(61) \quad S'(1, 2, 1', 2') = \frac{1}{2} \iint dx dx' R_{\sigma\beta}^{\alpha\gamma}(x, x') \cdot \\ \cdot \left( i \frac{\beta}{4} \right)^2 \sum_{A(12, 1'2')} S(1, x) O_{\sigma}^{\alpha}(x) S(x, 1') S(2, x') O_{\beta}^{\gamma}(x') S(x', 2') .$$

Here  $\sum_{A(12, 1'2')}$  means summation over all permutations of 1 and 2 among themselves and of 1' and 2' among themselves, where the sign is minus for odd and plus for even permutations.

Further, in the same manner as in (2)

$$(62) \quad S(1, 1') = S_F(1 - 1'),$$

$$(63) \quad R_{\beta\varrho}^{\alpha\sigma}(1, 1') = -\frac{i}{2} \cdot G_{\beta\varrho}^{\alpha\sigma}(1 - 1'),$$

where  $G_{\beta\varrho}^{\alpha\sigma}(x)$  is the Green function satisfying

$$(64) \quad \frac{1}{4}(\delta_\alpha^\kappa \delta_\lambda^\beta - \frac{1}{2} \delta_\alpha^\beta \delta_\lambda^\kappa)(-\square - i\varepsilon)G_{\beta\pi}^{\alpha\varphi}(x) = \delta_\pi^\kappa \delta_\lambda^\varphi.$$

(64) gives for the Fourier transform of  $G_{\beta\pi}^{\alpha\varphi}(x)$

$$(65) \quad G_{\beta\pi}^{\alpha\varphi}(k) = \frac{4}{(2\pi)^2} \left( \delta_\pi^\alpha \delta_\beta^\varphi - \frac{1}{2} \delta_\beta^\alpha \delta_\pi^\varphi \right) \frac{1}{k^2 - i\varepsilon}.$$

## 9. - The Momentum Representation.

On the assumption that the points 1, 2, 1' and 2' are placed on space-like surfaces where the coupling constant is switched off, one can write

$$(66) \quad S'(1, 2, 1', 2') = \langle T(\psi^{(\text{out})}(1)\psi^{(\text{out})}(2)\bar{\psi}^{(\text{in})}(1')\bar{\psi}^{(\text{in})}(2')) \rangle_0,$$

where  $\psi^{(\text{out})}$  and  $\bar{\psi}^{(\text{in})}$  are free particle operators. We expand

$$(67) \quad \left\{ \begin{aligned} \psi^{(\text{out})}(x_1) &= (2\pi)^{-\frac{3}{2}} \int d^3k \left( \frac{\mu^2}{|\mathbf{k}|^2 + \mu^2} \right)^{\frac{1}{2}} \cdot \\ &\quad \cdot \left( \sum_s u_{s+}(\mathbf{k}) \exp[ikx_1] b_{ks+}^{(\text{out})} + \sum_s u_{s-}(-\mathbf{k}) \exp[-ikx_1] b_{ks-}^{(\text{out})} \right) \\ \bar{\psi}^{(\text{in})}(x'_1) &= (2\pi)^{-\frac{3}{2}} \int d^3k \left( \frac{\mu^2}{|\mathbf{k}|^2 + \mu^2} \right)^{\frac{1}{2}} \cdot \\ &\quad \cdot \left( \sum_s \bar{b}_{ks+}^{(\text{in})} u_{s+}(\mathbf{k}) \exp[-ikx'_1] + \sum_s \bar{b}_{ks-}^{(\text{in})} u_{s-}(-\mathbf{k}) \exp[ikx'_1] \right). \end{aligned} \right.$$

Here

$$(68) \quad k_\mu = (k_1, k_2, k_3, \sqrt{|\mathbf{k}|^2 + \mu^2}),$$

and  $u_{s+}$ ,  $u_{s-}$  are the plane wave solutions to

$$(69) \quad (i\gamma^\alpha k_\alpha + \mu)u_{s+}(\mathbf{k}) = 0,$$

$$(70) \quad (i\gamma^\alpha k_\alpha - \mu)u_{s-}(-\mathbf{k}) = 0.$$

Now we use the following formulas — (71) and (72) — in (61) and (66).

For  $x'^4 > x^4$

$$(71) \quad \left( \frac{|\mathbf{k}'|^2 + \mu^2}{\mu^2} \right)^{\frac{1}{2}} \int d^3x' \bar{u}_{s+}(\mathbf{k}') \exp[-ik'x'] S_{\mathcal{P}}(x' - x) = \\ = -2\bar{u}_{s+}(\mathbf{k}') \exp[-ik'x].$$

For  $x'^4 < x^4$

$$(72) \quad \left( \frac{|\mathbf{k}'|^2 + \mu^2}{\mu^2} \right)^{\frac{1}{2}} \int d^3x S_{\mathcal{P}}(x' - x) u_{s+}(\mathbf{k}') \exp[ik'x] = -2u_{s+}(\mathbf{k}') \exp[ik'x].$$

Hence

$$(73) \quad \langle b_{k_1 s+}^{(\text{out})} b_{k_2 t+}^{(\text{out})} \bar{b}_{k_1' u+}^{(\text{in})} \bar{b}_{k_2' v+}^{(\text{in})} \rangle_0 = \\ = \frac{1}{(2\pi)^8} A \int dx dx' \int d^4k \exp[-ik(x - x')] (\delta_\beta^\alpha \delta_\sigma^\alpha - \frac{1}{2} \delta_\beta^\alpha \delta_\sigma^\alpha) \frac{1}{k^2 - i\epsilon} \cdot \\ \cdot \sum_{A(12, 1'2')} (\bar{u}_{s+}(\mathbf{k}_1) \exp[-ik_1 x] O_\beta^\alpha(x) u_{u+}(\mathbf{k}_1') \exp[ik_1' x] \cdot \\ \cdot \bar{u}_{t+}(\mathbf{k}_2) \exp[-ik_2 x'] O_\sigma^\beta(x') u_{v+}(\mathbf{k}_2') \exp[ik_2' x']),$$

where

$$(74) \quad A = i\beta^2 \frac{1}{(2\pi)^2} \left( \frac{\mu^2}{|\mathbf{k}_1|^2 + \mu^2} \cdot \frac{\mu^2}{|\mathbf{k}_2|^2 + \mu^2} \cdot \frac{\mu^2}{|\mathbf{k}_1'|^2 + \mu^2} \cdot \frac{\mu^2}{|\mathbf{k}_2'|^2 + \mu^2} \right).$$

Finally, from (73)

$$b_{k_1 s+}^{(\text{out})} b_{k_2 t+}^{(\text{out})} \bar{b}_{k_1' u+}^{(\text{in})} \bar{b}_{k_2' v+}^{(\text{in})} = A (\delta_\alpha^\alpha \delta_\lambda^\beta - \frac{1}{2} \delta_\lambda^\alpha \delta_\alpha^\beta) \sum_{A(12, 1'2')} \frac{(k_{1\beta}' + k_{1\beta})(k_{2\alpha}' - k_{2\alpha})}{(k_1' - k_1')^2} \cdot \\ \cdot \bar{u}_{s+}(\mathbf{k}_1) \gamma^\alpha u_{u+}(\mathbf{k}_1') \cdot \bar{u}_{t+}(\mathbf{k}_2) \gamma^\lambda u_{v+}(\mathbf{k}_2') \cdot \delta(k_1 + k_2 - k_1' - k_2').$$

\* \* \*

I wish to thank professor O. KLEIN, whose suggestions and encouragement have throughout been of invaluable help, fil. lic. S. DEPKEN, with whom I collaborated in the early stages of the work, and Dr. S. DESER, who kindly read the manuscript with a critical eye.

*Note added in proof.* — Prof. J. A. WHEELER kindly told me in a letter that the most natural choice of integration variables, according to a work done by Dr. C. MISNER, seems to be the 16 fields  $S_{\alpha\beta}$ , which fulfil

$$g_{\mu\nu} = S_{\mu\alpha} \gamma^{\alpha\beta} S_{\beta\nu}.$$



## RIASSUNTO (\*)

Si segue il metodo d'azione di Feynman e di Matthews e Salam. In tal modo sembra facile quantizzare in modo generalmente covariante, semplicemente utilizzando l'intero lagrangiano invariante senza imporre condizioni sussidiarie. Si dimostra che tale procedura conduce alla quantizzazione ordinaria nel caso elettrodinamico. Il lagrangiano per il campo di Dirac è preso da un lavoro di BARGMANN <sup>(3)</sup> e lo si sviluppa in potenze di  $\beta = \sqrt{2K}$ , dove  $K$  è la costante gravitazionale di Einstein. Lo stesso si fa con l'usuale lagrangiano del campo gravitazionale, come è stato proposto da GUPTA <sup>(4)</sup>. Si risolve il semplice problema di due particelle di Dirac identiche sottoposte a scattering reciproco senza correzioni radiative.

(\*) Traduzione a cura della Redazione.

## High Energy Behaviour of Renormalizable Fields. - II.

M. KONUMA and H. UMEZAWA

*Department of Physics, University of Tokyo, Japan*

(ricevuto il 10 Settembre 1956)

**Summary.** — The asymptotic forms of the many-body propagators are discussed by means of the renormalization invariance. The results show a simple relation between the many-body and one-body-propagators. We take advantage of this to discuss the peculiar features of the  $S$ -matrix when the observed value of the coupling constant is out of the normal zone.

## 1. — Introduction.

The question as to the renormalization theory, i.e. its internal consistency and predictions for the high energy phenomena, have called attention of many authors. It is assumed in the renormalization theory that the renormalized coupling constant  $g_r$  is equal to the observed one  $g_{ob}$ . When the unrenormalized coupling constant  $g$  runs over all the possible values for which the interaction Hamiltonian is hermitian, the renormalized one  $g_r$ , being a function of  $g$ , runs over a certain domain  $N(g_r)$ , which is called the normal zone <sup>(1)</sup>. Then, it is clear that  $g_{ob}$  being out of  $N(g_r)$  leads to a physically irrational result, i.e. to the appearance of a negative probability state.

In this way it is found that renormalization theory in some cases is consistent only when we introduce the cut-off momentum  $\Lambda$  which is smaller than the critical cut-off  $\lambda$ . There are some reasons which support the viewpoint that, in quantum electrodynamics,  $\lambda$  has about the value of  $m \exp[3\pi \cdot 137/2]$  ( $m$ : the electron mass) <sup>(2)</sup>. This is much larger than any of the masses of

<sup>(1)</sup> H. UMEZAWA, Y. TOMOZAWA, M. KONUMA and S. KAMEFUCHI: *Nuovo Cimento*, **3**, 772 (1956); *Prog. Theor. Phys.*, **15**, 417 (1956). Hereafter the former will be referred to as I.

<sup>(2)</sup> L. D. LANDAU, A. A. ABRIKOSOV and I. M. HALATNIKOV: *Dokl. Akad. Nauk SSSR*, **95**, 497, 733, 1177 (1954); **96**, 261 (1954); S. KAMEFUCHI and H. UMEZAWA: *Nuovo Cimento*, **3**, 1060 (1956); J. C. TAYLOR: *Proc. Roy. Soc., A* **234**, 296 (1956).

known particles. On the other hand, in the  $\pi$ -meson theory, it seems that the critical cut-off constant  $\lambda$  is equal to about the nucleon mass.

By using the method of the renormalization cut-off, the problem of the consistency of the theory was shown to be closely connected with the theoretical predictions for the high energy phenomena. There, use was made of the «effective coupling». This was defined in I to contain both of the radiative corrections for the one-body propagators and vertices in the form of the effective change of the interaction strength.

In the high energy region there appear essential differences between the renormalized propagators with  $g_{ob}$  in  $N(g_r)$  and the one with  $g_{ob}$  out of  $N(g_r)$ . It is sometimes better to discuss the predictions for the high energy phenomena than to consider negative probability states which appear in the case where  $g_{ob}$  is out of  $N(g_r)$ , because we can never observe the latter states. Hitherto the main interests have been in the one-body propagators and the vertices. However, to talk about the observations need to consider the scattering matrix elements which are derived from the many-body propagators.

Quite generally, the many-body propagators describe the various secondary interactions which are constructed out of some primary interactions. It seems probable that the strength of the secondary interactions is limited in a certain region (normal zone), because it depends on the strength of the primary interactions. Thus, to clarify the problem about the consistency of the renormalization theory, we need to investigate the many-body propagators; in particular their high energy behaviour.

To do this, we shall apply the renormalization transformation <sup>(3)</sup> to derive the functional equations for the many-body propagators. It has been recently pointed out that the renormalization transformation (or the renormalization group) is of some importance. The Sect. 2 is devoted to the derivation of the equations for the many-body propagators. They are solved in Sect. 3 to lead us to the asymptotic forms of the propagators. It is shown in Sect. 4 that they are the simple functions of the effective couplings.

## 2. Renormalization Invariance and Function Equation for the Many-Body Propagators.

We start from the following Lagrangian:

$$(1) \quad L = -\frac{1}{2}Z_3(\partial_\mu\varphi\partial_\mu\varphi + \mu^2\varphi^2) - \frac{1}{2}Z_3\delta\mu^2\varphi^2 - \\ - Z_2\bar{\psi}(\gamma_\mu\partial_\mu + m)\psi - Z_2\delta m\bar{\psi}\psi + g_rZ_1\bar{\psi}\phi\psi\varphi.$$

<sup>(3)</sup> E. C. G. STUECKELBERG and A. PETERMANN: *Helv. Phys. Acta*, **26**, 499 (1953); H. UMEZAWA and A. VISCONTI: *Nuovo Cimento*, **1**, 1079 (1955); N. N. BOGOLJUBOV and D. V. SIRKOV: *Nuovo Cimento*, **3**, 845 (1956).

Here  $q(\psi)$  is the renormalized field of spin 0 ( $\frac{1}{2}$ ) and  $Z$  factors are defined from the renormalization factors calculated by using the suitable cut-off  $\Lambda$  and by making the limit  $\Lambda \rightarrow \infty$ . The matrix  $O$  is the vertex operator. Let us apply the transformation

$$(2) \quad \begin{cases} \psi \rightarrow \alpha_2^{\frac{1}{2}} \psi' \\ q \rightarrow \alpha_3^{\frac{1}{2}} q' \\ O \rightarrow \alpha_1^{-1} O' \\ g_i \rightarrow g_{i1} \end{cases}$$

to Eq. (1). Then, we can obtain the modified Lagrangian

$$(3) \quad L' = -\frac{1}{2} Z_3 \alpha_3 (\partial_\mu \varphi \partial_\mu \varphi + \mu^2 \varphi^2) - \frac{1}{2} Z_3 \alpha_3 \delta \mu^2 \varphi^2 - \\ - Z_2 \alpha_2 \bar{\psi} (\gamma_\mu \partial_\mu + m) \psi - Z_2 \alpha_2 \delta m \bar{\psi} \psi + g_A \alpha_1^{-1} \alpha_3 \alpha_3^{\frac{1}{2}} \bar{\psi} O' \psi \varphi.$$

It is easy to derive the equation of the one-body propagators for the meson field (\*). Following the notation in I, we shall write the mass operator  $\Sigma(-k^2)$  as follows (cf. (I-6a)):

$$(4) \quad \Sigma(-k^2) = \Sigma(\mu^2) + (k^2 + \mu^2) \left( \frac{\partial \Sigma(-k^2)}{\partial k^2} \right)_{k^2 = -\mu^2}, \\ \frac{1}{Z_3} (k^2 - \mu^2) A(-k^2, g_A).$$

Then, the Lagrangian  $L'$  leads to the following equation for the one-body propagator of the meson field  $G_A(k^2, g_A)$  (cf. (I-4a), (I-5a)):

$$(5) \quad Z_3 \alpha_3 (k^2 + \mu^2) \left[ 1 + \left( \frac{\partial \Sigma(-k^2)}{\partial k^2} \right)_{k^2 = -\mu^2} \right] + \frac{1}{Z_3} A(-k^2, g_A) G_A(k^2, g_A) = 1.$$

Taking account of the definition of  $Z_3$  (I-9a):

$$(6) \quad \frac{1}{Z_3} = 1 + \frac{\partial}{\partial k^2} \Sigma(-k^2)_{k^2 = -\mu^2},$$

we obtain

$$(7) \quad G_A(k^2, g_A) = \frac{1}{\alpha_3 (k^2 + \mu^2) (1 + A(-k^2, g_A))}.$$

(\*) It is easy to extend a similar discussion to the case of spinor field.

It is apparent that the renormalized theory is obtained by taking  $\alpha_j = 1$  ( $j = 1, 2, 3$ ). On the other hand,  $\alpha_j = 1/Z_j$  leads to the unrenormalized theory. Further, when we regard  $\alpha_3^{-1}$  as  $Z^R(\Lambda^2, g_A)$  given by (I-15a) and (I-16a):

$$(8) \quad \alpha_3 = \frac{1}{Z^R(\Lambda^2, g_A)} = 1 + \frac{\hat{c}}{\hat{c}k^2} \sum_{k^2 = -\mu^2} (-k^2) + \frac{\text{Re} [\sum (\Lambda^2)] - \sum (\mu^2)}{\Lambda^2 - \mu^2} = \\ = 1 + \frac{1}{\text{Re} [A(\Lambda^2, g_A)]},$$

the  $G_A$  is just the propagator obtained by the renormalization cut-off in I:

$$(9) \quad G_A(k^2, g_A) = \frac{1 + \text{Re} [A(\Lambda^2, g_A)]}{(k^2 + \mu^2)(1 + A(k^2, g_A))}.$$

Such an  $\alpha_j$  can be regarded as the function of  $\Lambda$ . The renormalized theory corresponds to the case  $\Lambda^2 = m^2$ , and the unrenormalized one corresponds to the case  $\Lambda^2 \rightarrow \infty$ . Let us define the coupling constant  $g_{Ab}$  as follows:

$$(10) \quad g_{Ab} = g_A \alpha_1^{-1} \alpha_2 \alpha_3^{\frac{1}{2}}.$$

In Eq. (2) we have made the transformation  $g_r \rightarrow g_A$ . In this connection the two standpoints are possible. The first is to regard  $g_{Ab} = g$  (the unrenormalized coupling constant) and, therefore,  $g_A = g_r$ . This means that the contribution from the high energy part of the proper field is taken away by the cut-off procedure and, in this way, the renormalized coupling  $g_r$  shifts to be  $g_A$ . This idea is just the one used in the renormalization cut-off in I. The second is to regard  $g_A = g_r$ . In this case the renormalized quantities have nothing to do with the transformation (2) and  $g_{Ab}$  should be considered as a coupling constant, in which the effect of the proper field is partially renormalized.

We shall now take the second standpoint. As the observable quantities do not depend on the value of  $\Lambda$ , the transformation (2) is only the change of the normalization factors of the propagators, that is, the renormalization transformation. Since the observable quantities are renormalization invariant <sup>(3)</sup> in the case where  $g_A = g_r$ , we can immediately set up the functional equation for the many-body propagators.

The many-body propagator may be written as

$$g_{Ab}^n F \left( \frac{(p_i p_j)}{m^2}, \frac{(p_i p_j)}{\mu^2}, \frac{(p_i p_j)}{\Lambda^2}, g_{Ab} \right),$$

where  $p_i$  is the energy momentum of the  $i$ -th external line. The suffixes  $i$  and  $j$  run over all the external lines. The power  $n$  is the number of the ver-

tices which correspond to the external lines. Then, in general, we obtain the following equation (\*) for any  $A$  and  $A'$  ( $\pm$ ).

$$(11) \quad Z_A g_{Ab}^n F \left( \frac{(p_i p_j)}{m^2}, \frac{(p_i p_j)}{\mu^2}, \frac{(p_i p_j)}{A^2}, g_{Ab} \right) = \\ = Z_{A'} g_{A'b}^n F \left( \frac{(p_i p_j)}{m^2}, \frac{(p_i p_j)}{\mu^2}, \frac{(p_i p_j)}{A'^2}, g_{A'b} \right).$$

Here,  $Z_A$  is the factor due to the renormalization of the external lines. Taking  $A'^2 = m^2$ , we have the functional equation:

$$(12) \quad Z_A g_{Ab}^n F \left( \frac{(p_i p_j)}{m^2}, \frac{(p_i p_j)}{\mu^2}, \frac{(p_i p_j)}{A^2}, g_{Ab} \right) = \\ = g_A^n F \left( \frac{(p_i p_j)}{m^2}, \frac{(p_i p_j)}{\mu^2}, \frac{(p_i p_j)}{m^2}, g_A \right).$$

Here,  $Z_A$  and  $n$  are given as follows.

A) In the case where there are external fermion lines. When the number of the external fermion lines is  $2f$  ( $f > 0$ ) and that of the external boson lines  $b$ , we have ( $\times$ )

$$(13.A) \quad \begin{cases} Z_A = (Z_2(A^2, g_A))^f (Z_3(A^2, g_A))^{b/2} \\ n = 2f + b - 2. \end{cases}$$

B) In the case where no external fermion line exist,

$$(13.B) \quad \begin{cases} Z_A = (Z_3(A^2, g_A))^{b/2} \\ n = b. \end{cases}$$

C) An exception for Eq. (12) is given by the propagator of the meson-meson scattering, that is the case of  $f = 0$  and  $b = 4$ . In this case, Eq. (12)

(\*) The divergent contributions due to the square fermion loop inside the diagram are cancelled out by a suitable counter term, whose coupling constant depends on  $g_{Ab}$ ,  $A^2/m^2$  and  $A^2/\mu^2$ .

( ) Quite generally, we can introduce two cut-off momenta  $A_f$  and  $A_b$  which correspond to the fermion and boson fields respectively. Here we consider only the case  $A_f = A_b$ , because there is not difficulty in extending our results into the general cases ( $A_f \neq A_b$ ).

( $\times$ ) It must be noted that the  $Z$ -functions here mean the  $Z^R$ , i.e. the real part of the  $Z$ -functions in I.



must be modified as follows. As the final integration of the unrenormalized theory gives the logarithmic divergence in the meson-meson scattering, we must introduce a  $\Lambda$ -dependent constant in the functional equation in order to cancel out the divergence. We shall give the explicit form of the equation in the Sect. 3'2.

The renormalization transformation may be briefly expressed in the following way. Assuming  $z_3$  in the renormalization transformation represented by Eq. (8), we may have the particle which contains an inner part of the proper field (the radius  $\approx \Lambda^{-1}$ ) as its part. The interaction of such a particle is of the strength  $g_A$ . To change the  $\Lambda$  corresponds to the renormalization transformation. Most of the particles in an inner part of the proper field have high energy-momenta  $p^2$ . Their behaviours tell us the high energy properties of the renormalized fields on account of the renormalization invariance of the theory. Since the proper field contains only a small number of particles in its inner zone, its brief characteristics can be obtained from the perturbation calculation.

In this way we can derive the asymptotic form of the renormalized propagator independently of the perturbation calculation by using the renormalization invariance (i.e. the functional equation) with the information given by the perturbation calculation for the behaviour of the bare particles.

An example for this has been given in the quantum electrodynamics<sup>(2)</sup>. There, the asymptotic form of the photon propagator can be derived from that of the bare particle by means of the renormalization transformation. The mass operator for the latter part can be approximately calculated by the perturbation calculation. This result is independent of the perturbation approximation; indeed, it has been many times derived independently of the perturbation calculation. Anyhow, our discussions here may give us the reason why we can obtain the asymptotic behaviour of the  $S$ -matrix by means of the functional equations.

### 3. - Asymptotic Form of the Many-Body Propagators.

The asymptotic form of the one-body propagator for the meson field has been already given by A. A. ABRIKOSOV *et al.*<sup>(4)</sup> and by J. C. TAYLOR<sup>(5)</sup>. By assuming the non-singular character of the propagators at  $g_A^2 = 0$ , TAYLOR

<sup>(4)</sup> A. A. ABRIKOSOV, I. M. HALATNIKOV and A. D. GALANIN: *Dokl. Akad. Nauk SSSR*, **97**, 783 (1954).

<sup>(5)</sup> J. C. TAYLOR: *Proc. Roy. Soc., A* **234**, 296 (1956).

obtained the following relations:

$$(14) \quad \begin{cases} \frac{g_A^2}{g^2} = 1 - \frac{5}{4\pi} g_A^2 \log \frac{A^2}{m^2} = \alpha(A^2), \\ Z_2(A^2, g_A) = \{\alpha(A^2)\}^{2/5}, \\ Z_3(A^2, g_A) = \{\alpha(A^2)\}^{3/5}, \end{cases}$$

for the symmetrical  $ps$  ( $ps$ ) meson' theory.

The divergent contribution due to the square fermion loop is disregarded in Eq. (14), because they are proportional to the fourth power of  $g_A$ . Using the relations (14), we can immediately solve Eq. (12).

3.1. *The solution of Eq. (12).* — We first consider the simple case where one of the  $(p_i p_j)$ 's is extremely large. We denote this by  $(pq)$ . This is either the scalar product of the two momenta  $p$  and  $q$  or the magnitude  $p^2$  (i.e.  $p = q$ ) of the one momentum  $p$ . In this case, taking  $A^2$  quite large, it may be justified to disregard  $(p_i p_j)/A^2$  except the largest one  $(pq)/A^2$ . Then, Eqs. (14) and (12) lead to

$$(15) \quad \{\alpha(A^2)\}^s F\left(\frac{(p_i p_j)}{m^2}, \frac{(p_i p_j)}{\mu^2}, \frac{(pq)}{A^2}, \frac{g_A^2}{\alpha(A^2)}\right) = \\ = F\left(\frac{(p_i p_j)}{m^2}, \frac{(p_i p_j)}{\mu^2}, \frac{(pq)}{m^2}, g_A^2\right).$$

Here  $s$  is a certain constant depending only on  $f$  and  $b$  (cf. Eqs. (21.A) and (21.B)). Since the right hand side is independent of  $A$ , Eq. (15) can be re-written as

$$(16) \quad \{\alpha(A^2)\}^s F\left(\frac{(p_i p_j)}{m^2}, \frac{(p_i p_j)}{\mu^2}, \frac{g_A^2}{\alpha(A^2)} \log \frac{(pq)}{A^2}\right) = \\ = F\left(\frac{(p_i p_j)}{m^2}, \frac{(p_i p_j)}{\mu^2}, g_A^2 \log \frac{(pq)}{m^2}\right).$$

This can be transformed into an equation of the form

$$(17) \quad \{\alpha(A^2)\}^s F\left(\frac{(p_i p_j)}{m^2}, \frac{(p_i p_j)}{\mu^2}, \frac{\alpha(pq)}{\alpha(A^2)}\right) = F\left(\frac{(p_i p_j)}{m^2}, \frac{(p_i p_j)}{\mu^2}, \alpha(pq)\right),$$

on account of the relations

$$(18) \quad \frac{g_A^2}{\alpha(A^2)} \log \frac{(pq)}{A^2} = \frac{4\pi}{5} \left(1 - \frac{\alpha(pq)}{\alpha(A^2)}\right), \quad g_A^2 \log \frac{(pq)}{m^2} = \frac{4\pi}{5} (1 - \alpha(pq)).$$

Since the right hand side of Eq. (17) is independent of  $A$ ,  $\alpha(A^2)$  should be

cancelled out in the left hand side of Eq. (17). Thus, we find the asymptotic form of the propagators as follows:

$$(19) \quad g_{A0}^n F\left(\frac{(p_i p_j)}{m^2}, \frac{(p_i p_j)}{\mu^2}, \frac{(pq)}{\Lambda^2}, g_{A0}\right) = g_{A0}^n f\left(\frac{(p_i p_j)}{m^2}, \frac{(p_i p_j)}{\mu^2}\right) \left(\frac{\alpha(pq)}{\alpha(\Lambda^2)}\right)^s = \\ = g_{A0}^n f\left(\frac{(p_i p_j)}{m^2}, \frac{(p_i p_j)}{\mu^2}\right) \left\{1 - \frac{5}{4\pi} g_{A0}^2 \log \frac{(pq)}{\Lambda^2}\right\}^s,$$

$$(20) \quad g_A^n F\left(\frac{(p_i p_j)}{m^2}, \frac{(p_i p_j)}{\mu^2}, \frac{(pq)}{m^2}, g_A\right) = g_A^n f\left(\frac{(p_i p_j)}{m^2}, \frac{(p_i p_j)}{\mu^2}\right) \{\alpha(pq)\}^s = \\ = g_A^n f\left(\frac{(p_i p_j)}{m^2}, \frac{(p_i p_j)}{\mu^2}\right) \left\{1 - \frac{5}{4\pi} g_A^2 \log \frac{(pq)}{m^2}\right\}^s.$$

$$(21.A) \quad \text{Here} \quad s = \frac{10 - 7f - b}{10}, \quad \text{for the case (A),}$$

$$(21.B) \quad s = -\frac{b}{10}, \quad \text{for the case (B).}$$

The function  $f((p_i p_j)/m^2, (p_i p_j)/\mu^2)$  is obtained from the lowest order perturbation theory, because it does not contain any coupling constant. The remaining factors in Eqs. (19) and (20) are the contributions from all the internal corrections. Furthermore, in the case of no external fermion line, the asymptotic form mainly depends on the isolated closed loop, because no coupling constant appears in the functions  $f((p_i p_j)/m^2, (p_i p_j)/\mu^2)$ . We should keep in mind the fact that the reliability of (14) is still an open problem. Here, we have used (14) only to illustrate the way for deriving the many-body-propagators from the one body-propagators.

So far we have considered only the case where only  $(pq)/\Lambda^2$  has remained to be taken into consideration. We shall consider the general case in Sect. 3'3.

3'2. *Asymptotic form of the propagator for the meson-meson scattering.* — As was stated in the end of the Sect. 2, the functional equation must be modified for the propagator of the meson-meson scattering. Let us consider that  $g_{A0}^2 F$  corresponds to a square fermion loop, which is corrected by inserting the internal lines in all the possible ways. The counter term  $g_{A0}^2 C q^{-1}$  should be introduced to cancel out the divergence of the final integration. The remaining finite term is the renormalized one and will be denoted by  $g_A^2 G$ . For simplicity, we shall use the relations Eq. (14). Further, making use of the fact that the primitive divergence for the meson-meson scattering is logarithmic; i.e. of the asymptotic form  $g_{A0}^4 \log(pq)/\Lambda^2$ , we obtain the following functional

equation:

$$(22) \quad \{Z_3(A^2, g_A)\}^2 g_{Ab}^2 \left\{ F \left( g_{Ab}^2 \log \frac{(pq)}{A^2} \right) - C \right\} = g_A^2 G \left( g_A^2 \log \frac{(pq)}{m^2} \right).$$

It may be justified that no meson mass appears in  $G$ , because we consider the case where  $(pq) \gg m^2$  and  $m^2$  is much larger than  $\mu^2$ . The  $Z_3$  in Eq. (22) comes from the renormalization for the external lines. Applying the renormalization cut-off to the final integration, we have the condition for  $F$ :

$$(23) \quad F \left( g_{Ab}^2 \log \frac{(pq)}{A^2} \right) = 0 \quad \text{for } (pq) = A^2.$$

To solve Eq. (22), we shall rewrite it as

$$(24) \quad \{\alpha(A^2)\}^{3/5} \left\{ F \left( g_{Ab}^2 \log \frac{(pq)}{A^2} \right) - C \right\} = G \left( g_A^2 \log \frac{(pq)}{m^2} \right),$$

by using Eq. (14). As is shown in Eq. (18),  $F$  depends only on  $\alpha(pq)/\alpha(A^2)$ . In the same way the argument of  $G$  can be transformed into  $\alpha(pq)$ . Then Eq. (24) with the condition of Eq. (23) leads to

$$(25) \quad \{\alpha(A^2)\}^{3/5} F \left( \frac{\alpha(pq)}{\alpha(A^2)} \right) + G(\alpha(A^2)) = G(\alpha(pq)).$$

Taking  $\alpha(pq) = 0$  in Eq. (25), we obtain

$$-A \{\alpha(A^2)\}^{3/5} + G(\alpha(A^2)) = D.$$

Here  $A$  and  $D$  are constants independent of  $A^2$ ,  $(pq)$  and  $g_A^2$ . Substituting this into Eq. (25), we obtain

$$(26) \quad g_{Ab}^2 F \left( g_{Ab}^2 \log \frac{(pq)}{A^2} \right) = g_{Ab}^2 A \left\{ \left( \frac{\alpha(pq)}{\alpha(A^2)} \right)^{3/5} - 1 \right\} = \\ = g_{Ab}^2 A \left\{ \left( 1 - \frac{5}{4\pi} g_{Ab}^2 \log \frac{(pq)}{A^2} \right)^{3/5} - 1 \right\},$$

$$(27) \quad g_{Ab}^2 \left\{ g_{Ab}^2 \log \frac{(pq)}{m^2} - g_{Ab}^2 A \left( \frac{\alpha(pq)}{\alpha(A^2)} \right)^{3/5} - D \right\} = \\ = g_{Ab}^2 \left\{ A \left( 1 - \frac{5}{4\pi} g_{Ab}^2 \log \frac{(pq)}{m^2} \right)^{3/5} - D \right\}.$$

Here Eq. (26) is the unrenormalized solution and Eq. (27) the renormalized

one. The constant  $A$  is given by the lowest order perturbation calculation. The counter term  $g_{Ab}^2 C \varphi^4$  is obtained from Eqs. (24), (26) and (27) as

$$(28) \quad C = - \frac{D}{\{z(\Lambda^2)\}^{3.5}} - A ,$$

which leads to

$$g_{Ab}^2 C = -g_A^2 \left\{ (D + A) + \left( \frac{8}{5} D + A \right) \frac{5}{4\pi} g_A^2 \log \frac{\Lambda^2}{m^2} + O(g_A^4) \right\} .$$

When the power series for  $C$  in the perturbation calculation contains no second order term,  $D$  is determined such that

$$D = -A .$$

Up to now the Feynman graphs made up of the series of the square fermion loops have been out of consideration. They have been investigated by DYATLOV *et al.* <sup>(6)</sup>.

3.3. *The generalized functional equation.* — In the preceeding sections, we have considered the asymptotic form of the propagators on the assumption that  $(p_i p_j)/\Lambda^2$  except  $(pq)/\Lambda^2$  can be disregarded. However, it is not a difficult matter to solve Eq. (12) in the more general case:

$$(12) \quad Z_A g_{Ab}^n F \left( \frac{(p_i p_j)}{m^2}, \frac{(p_i p_j)}{\mu^2}, \frac{(p_i p_j)}{\Lambda^2}, g_{Ab} \right) = \\ = g_A^n F \left( \frac{(p_i p_j)}{m^2}, \frac{(p_i p_j)}{\mu^2}, \frac{(p_i p_j)}{m^2}, g_A \right) .$$

According to Taylor's assumption Eq. (14), this equation can be transformed into

$$(29) \quad \{ \alpha(\Lambda^2) \}^s F \left( \frac{(p_i p_j)}{m^2}, \frac{(p_i p_j)}{\mu^2}, g_{Ab}^2 \log \sum \frac{\alpha_{ij}^{(k)}(p_i p_j)}{\Lambda^2} \right) = \\ = F \left( \frac{(p_i p_j)}{m^2}, \frac{(p_i p_j)}{\mu^2}, g_A^2 \log \sum \frac{\alpha_{ij}^{(k)}(p_i p_j)}{m^2} \right) ,$$

and further, into

$$\{ \alpha(\Lambda^2) \}^s F \left( \frac{(p_i p_j)}{m^2}, \frac{(p_i p_j)}{\mu^2}, \frac{\alpha(\sum \alpha_{ij}^{(k)}(p_i p_j))}{\alpha(\Lambda^2)} \right) = F \left( \frac{(p_i p_j)}{m^2}, \frac{(p_i p_j)}{\mu^2}, \alpha(\sum \alpha_{ij}^{(k)}(p_i p_j)) \right) .$$

<sup>(6)</sup> I. T. DYATLOV and K. A. TER MARTIROSYAN: *Žu. Èkper. Teor. Fiz.*, **30**, 416 (1956). Eq. (24) in this paper is identical with their result.

This can be immediately solved as follows:

$$\begin{aligned}
 (30) \quad g_{Ab}^n F \left( \frac{(p_i p_j)}{m^2}, \frac{(p_i p_j)}{\mu^2}, \frac{(p_i p_j)}{\Lambda^2}, g_{Ab} \right) = \\
 = g_{Ab}^n \sum_{[\nu_k]} f_{[\nu_k]} \left( \frac{(p_i p_j)}{m^2}, \frac{(p_i p_j)}{\mu^2} \right) \prod_{\Sigma \nu_k = s} \left\{ \frac{\alpha(\sum a_{ij}^{(k)}(p_i p_j))}{\alpha(\Lambda^2)} \right\}^{\nu_k} \\
 = g_{Ab}^n \sum_{[\nu_k]} f_{[\nu_k]} \left( \frac{(p_i p_j)}{m^2}, \frac{(p_i p_j)}{\mu^2} \right) \prod_{\Sigma \nu_k = s} \left\{ 1 - \frac{5}{4\pi} g_{Ab}^2 \log \frac{\sum a_{ij}^{(k)}(p_i p_j)}{\Lambda^2} \right\}^{\nu_k},
 \end{aligned}$$

$$\begin{aligned}
 (31) \quad g_A^n F \left( \frac{(p_i p_j)}{m^2}, \frac{(p_i p_j)}{\mu^2}, \frac{(p_i p_j)}{m^2}, g_A \right) = \\
 = g_A^n \sum_{[\nu_k]} f_{[\nu_k]} \left( \frac{(p_i p_j)}{m^2}, \frac{(p_i p_j)}{\mu^2} \right) \prod_{\Sigma \nu_k = s} \left\{ \alpha(\sum a_{ij}^{(k)}(p_i p_j)) \right\}^{\nu_k} = \\
 = g_A^n \sum_{[\nu_k]} f_{[\nu_k]} \left( \frac{(p_i p_j)}{m^2}, \frac{(p_i p_j)}{\mu^2} \right) \prod_{\Sigma \nu_k = s} \left\{ 1 - \frac{5}{4\pi} g_A^2 \log \frac{\sum a_{ij}^{(k)}(p_i p_j)}{m^2} \right\}^{\nu_k}.
 \end{aligned}$$

Here, the symbol  $[\nu_k]$  denotes the set of powers  $\nu_k$ . The constants  $a_{ij}^{(k)}$  and  $\nu_k$  and the function  $f_{[\nu_k]}$  can be determined by comparing Eq. (30) with the lower order perturbation calculation. In particular,  $a_{ij}^{(k)}$  is fixed by the second approximation (i.e. the  $g^{n+2}$ -th order) in the perturbation calculation.

#### 4. - Discussions.

The renormalized propagators of the  $\pi$ -meson and the nucleon with high energy momenta may depend on effects due to the heavy mesons and hyperons, and therefore we should carefully take into account the latter effects in order to obtain the normal zone for the meson-nucleon interaction. If to take account of the effects of various particles and interactions could increase the critical cut-off  $\lambda$  up to that of the quantum electrodynamics, it might be possible that the remaining difficulty could be settled by means of the interactions of the second kind.

However, it seems not easy to increase  $\lambda$  by using the effects of the various interactions. We have known that, in the perturbation calculation, the various particles contribute to the function  $A(\Lambda^2, g_A)$  in Eq. (8) by the terms of the same sign (?) and, thus, decrease  $\lambda$ . Further, as was discussed in Sect. 2, the perturbation calculation might have some benefits to peep into the inner part of the proper field whose behaviour is intimately connected with the asymptotic characters.

However, for the present, we shall consider only the  $\pi$ -meson and nucleon.

(?) J. C. TAYLOR: *Proc. Camb. Phil. Soc.* **52**, 534 (1956).



As far as we assume Eq. (14),  $\lambda$  appears to be about the nucleon mass. This is the energy within the reach of the present experiments.

The high energy behaviour of the renormalized one-body propagator depends on the factor  $D_F'/D_F$  and, therefore, on  $\alpha(p^2)$  in Eq. (14). When the renormalized coupling constant  $g_A$  is out of its normal zone,  $\alpha(p^2)$  changes its sign in the high energy region. The effective coupling is given by  $g_r^2/\alpha(p^2)$ .

As we have seen from Eqs. (20) and (27), any many-body propagator depends on  $\alpha(p^2)$  or  $\alpha(pq)$  in a simple way as the one-body propagator does. Thus, it can be seen from the many-body propagators or the  $S$ -matrix element whether or not  $g_A$  lies in its normal zone. Although Eqs. (20) and (27) hold only for  $(pq) \gtrsim m^2$ , they suggest that the many-body propagators, in general, show a resonance character in the high energy region (see Eq. (20) with  $s < 0$ ). Exceptions are given by the nucleon-meson scattering ( $s > 0$ ) and the one-meson production in the  $\pi$ -meson-nucleon collision ( $s = 0$ ). It must be noted that the propagator for the latter process is independent of  $\alpha(p^2)$  or of  $\alpha(pq)$ . The situation for the solution (31) in the general case is rather complicated. However, Eq. (31) also depends only on  $\alpha(\sum x_{ij}^{(k)}(p_i p_j))$  in a simple way.

It should be noted that the energy momentum  $p^2$  in the  $S$ -matrix elements for the real processes is  $\nu^2$  or  $\mu^2$ . However, for the collision of particles with large momentum transfer, the scalar product of two energy-momentum vectors  $(pq)$  can appear to be quite large. In this way the behaviour of the  $S$ -matrix elements may be seen from the characteristics of the asymptotic form of the many-body propagators.

Finally, we note that Eq. (14) leaves room for adding the terms which are negligibly small for the small  $g_A^2$ , e.g. the  $g_A^4 \log \lambda^2/m^2$ . Improving Eq. (14), the functional equation with the improved  $Z$  functions gives us the refined result for the asymptotic form.

\* \* \*

The authors are indebted to Prof. S. TOMONAGA for his inspiring discussions. They also wish to thank Dr. Y. TOMOZAWA for his advices and encouragement.

#### RIASSUNTO (\*)

In base all'invarianza alla rinormalizzazione si discutono le forme asintotiche dei propagatori multipli. I risultati mostrano una relazione semplice fra i propagatori multipli e quelli singoli. Si prende spunto da ciò per discutere la speciale configurazione della matrice  $S$  quando il valore osservato della costante di accoppiamento cade fuori della zona normale.

(\*) Traduzione a cura della Redazione.

## A High Energy Jet in Nuclear Emulsions.

F. D. HÄNNI, C. LANG, M. TEUCHER and H. WINZELER

*Physikalisches Institut der Universität Bern (Schweiz)*

E. LOHRMANN

*Hochspannungslaboratorium Hechingen (Deutschland)*

(ricevuto il 16 Settembre 1956)

**Summary.** — In stripped emulsions Ilford G5 a nuclear interaction of the type  $20+56p$  was found. In the very dense core of this jet 6 secondary interactions were found, 4 of which are produced by singly charged primaries, the other 2 by neutral particles. The average energy of these secondary interactions is about 200 GeV. From this and from the angular distribution of the primary jet an energy of  $10^{13}$  eV is deduced. The interaction mean free path of the charged particles in the core is  $54^{+58}_{-21}$  cm.

### 1. — Description of the Event.

In a stack of 108 stripped emulsions, Ilford G-5, 600  $\mu$ m thick,  $20 \times 30$  cm, which was flown in Texas in January 1955 for 8 hours at an altitude of 29 km, a jet of type  $20-56p$  was found. The primary particle is singly charged. It forms an angle with the vertical of  $40^\circ$ .

The integral angular distribution of the shower tracks is shown in Fig. 1. 23 tracks lie in a very dense core of  $6 \cdot 10^{-3}$  half opening angle. (This is the situation 3.6 mm from the origin of the star.) The target diagram for the core tracks at this point is shown in Fig. 2.

In order to study the interactions of the high energy shower particles we scanned the core for a length of 12.4 cm, which was the total length available in the stack. Great care was taken for this procedure. In the Table I are listed all the secondary interactions found by this manner.

TABLE I.

Number	Description	Half Angle ( $^{\circ}$ )	Energy (GeV)
1	22 + 22 p	14.5	30
2	0 + 19 p	5.5	200
3	3 + 11 p	6	180
4	3 + 9 p	4.5	300
5	1 + 8 n	5.5	200
6	23 + 37 n	6.5	150

They all look like jets. Since we found one jet without heavy prongs and another one with only one grey track, we estimate the number of omitted interactions to be rather small. Two jets are produced by neutral particles, 4 by charged ones. The axes of the 2 jets which are produced by neutral particles

are exactly parallel to the axis of the core. The half angles of the 6 jets do not show very large fluctuations. The energy of 200 GeV, which can be deduced from No. 2 and No. 5 should be most reliable, because No. 5 has only one grey prong and No. 2 has no heavy prongs at all. With the exception of No. 1 all jets are consistent with this energy.

The average multiplicity is 18.

There is no significant difference between jets made by neutral and by charged particles, but it is difficult to explain such a number of neutral jets without the assumption that besides  $\pi$ -mesons, other particles, probably K-mesons are produced in the primary nucleon-nucleon collision.

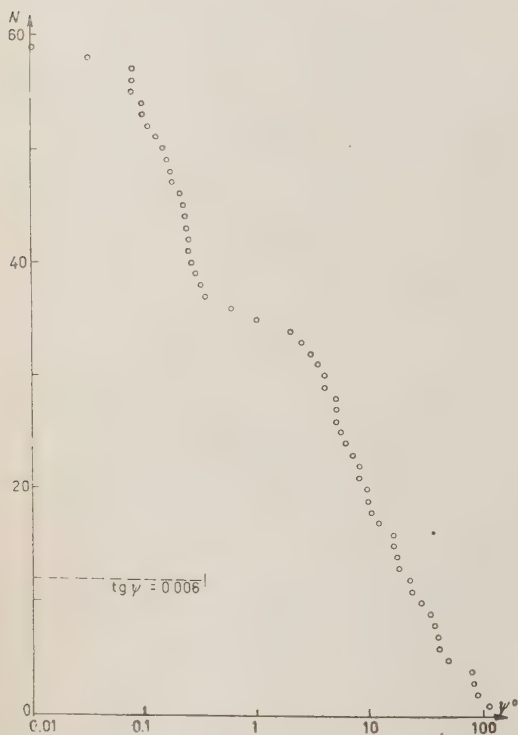


Fig. 1. Integral angular distribution in the L-system,  
 $\psi \equiv \vartheta_L$ .

The position of the secondary jets in the target diagram of the primary jet is also given in Fig. 2. For those jets which occurred in too large a distance from the primary jet it was not possible to determine the exact position with respect to the other initial core tracks. Only the projection of their position

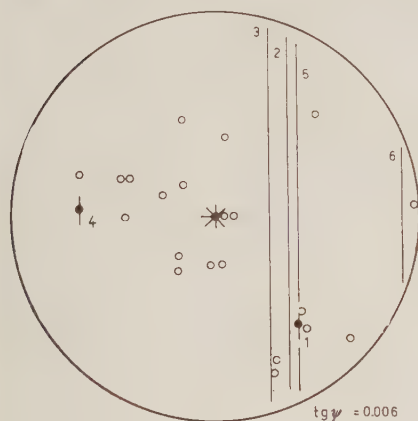


Fig. 2. - Target diagram after 3.6 mm  
 $\psi \equiv \psi_L$ .

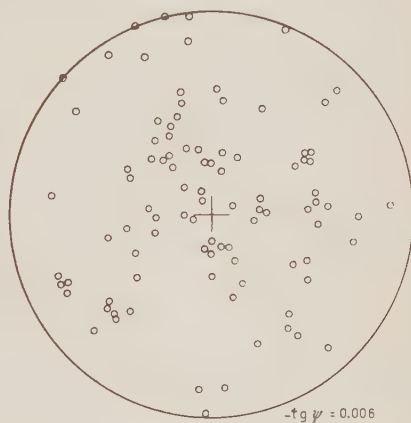


Fig. 3. - Target diagram after 46 mm  
 $\psi \equiv \psi_L$ .

could be measured, comparing one plate with the other by the help of calibration tracks. We cannot see a correlation between the energy of the secondary jets and their position in the target diagram.

The development of the soft cascade is illustrated by Fig. 3. This is the target diagram of the core at a distance of 43 mm from the primary jet. Since the dip of the event is  $30^\circ$  and the track density becomes rather high, a more detailed analysis was impossible.

In our case the development of the soft cascade begins very close to the origin of the star. On the other hand it was not possible clearly to resolve the individual tracks at a distance nearer to the jet than 3.6 mm. So we subtracted 3 tracks from the 23 core tracks to account for 1.5 electron pairs, produced by  $\gamma$ -quanta up to this distance and for the possible direct decay of  $\pi^0$ -mesons.

The total track length of the remaining 20 charged particles in the core is 217 cm. This leads to an interaction mean free path of

$$54^{+58}_{-21} \text{ cm},$$

for shower particles of about 200 GeV. The errors given are the purely statistical ones following from the Poisson distribution.

## 2. - The Energy of the Primary Jet.

From Fig. 1 and from the fact that the primary jet has 20 grey and black prongs it follows that the event cannot be treated in terms of one single nucleon-nucleon collision without assuming secondary interactions inside the same nucleus. But we shall try to identify the core as the forward cone of the first nucleon-nucleon collision and estimate the « visible » energy. This gives a lower limit for the energy of the primary jet.

If we assume all the initial 20 particles in the core, with an average energy of 200 GeV, to be  $\pi$ -mesons we have to add 10  $\pi^0$ -mesons. Still more neutral particles must be added if also K-mesons are produced, according to the theories of PAIS, NISHIJIMA and GELL-MANN <sup>(1)</sup>. Therefore we get 6000 GeV as a lower limit for the primary energy.

We ask now for the situation in the center of mass system (C-system). The angular distribution of the shower particles in the laboratory system (L-system) was transformed into the C-system for different values of  $\gamma_c$  between 60 and 300 by

$$\operatorname{tg}(\theta_c/2) = \gamma_c \operatorname{tg} \theta_L,$$

which is a good approximation to the exact formula <sup>(2)</sup>, where

$$\gamma_c = 1/\sqrt{1 - \beta_c^2}, \text{ and } \theta \text{ is the angle against the axis of the jet.}$$

Fig. 4 shows the result for  $\gamma_c = 60$ . A rather strong collimation of the particles in the forward and backward direction can be seen. This is in good agreement with the result of other authors with similar events <sup>(3-5)</sup>.

In fact we see 24 tracks in the forward cone, while the core contains only 23 tracks. This means that the core is only an inner part of the forward cone and supports the assumption that all the 20 core particles have approximately the same energy in the L-system.

Tracks with  $\theta_L > 12^\circ$  in all cases are transformed to  $\theta_c < 170^\circ$ . This shows that most of these particles are due to secondary interactions. Except for the 14 tracks, there is good symmetry. (Dotted line in Fig. 4).

<sup>(1)</sup> A. PAIS: *Physica*, **19**, 869 (1953); M. GELL-MANN and A. PAIS: *Proc. of Glasgow Conference* (1954); K. NISHIJIMA: *Progr. Theor. Phys.*, **12**, 107 (1954).

<sup>(2)</sup> W. HEISENBERG: *Kosmische Strahlung* (Berlin, 1953), p. 561.

<sup>(3)</sup> M. SCHEIN, D. M. HASKIN and R. G. GLASSER: *Phys. Rev.*, **95**, 955 (1955).

<sup>(4)</sup> E. LOHRMANN: *Zeits. f. Naturf.*, **11a**, 561 (1956).

<sup>(5)</sup> A. DEBENEDETTI, C. M. GARELLI, L. TALLONE and M. VIGONE: *Nuovo Cimento*, **4**, 1142 (1956). We thank the authors for a preprint.

The transformation for  $\gamma_c = 80$  shows already an asymmetrical shift of tracks towards the backward cone and this situation becomes even worse with higher  $\gamma$ 's (Fig. 4a). So there is no reason to assume the most probable value of the primary energy to be much different from  $10^{13}$  eV.

With this primary energy the average energy of the mesons in the C-system is 1.4 GeV. If the total number of charged and neutral  $\pi$ -mesons produced in the first nucleon-nucleon collision is 63, the total energy of the mesons in the C-system is 90 GeV. This figure has to be compared with 130 GeV which are available

for meson production in the C-system. From this we have to conclude that approximately 70% of the energy is emitted into the meson field. This result is rather interesting, because it shows clearly that a very pronounced anisotropy in the angular distribution of the mesons in the C-system can exist even in head-on collisions. This is in agreement with the Heisenberg theory of meson production<sup>(6)</sup>. The mean energy of the particles in the C-system following from the theory for  $\pi$ -mesons is 0.7 GeV. If there is an appreciable number of K-mesons produced, as could be the case in this star, the value of the mean energy would be higher (for K-mesons 2 GeV) giving a better agreement with the experimental findings.

As a test one can also apply the maximum angle<sup>(7)</sup>. In our case we use the formula

$$\sin(\vartheta_L)_{\max} = \frac{E_{L,M}}{2\gamma_c^2 Mc^2},$$

where  $E_{L,M}$  is the average energy of the mesons in the core.  $Mc^2$  their rest energy. For  $\pi$ -mesons and  $\gamma_c = 70$ , which would correspond to  $10^{13}$  eV,

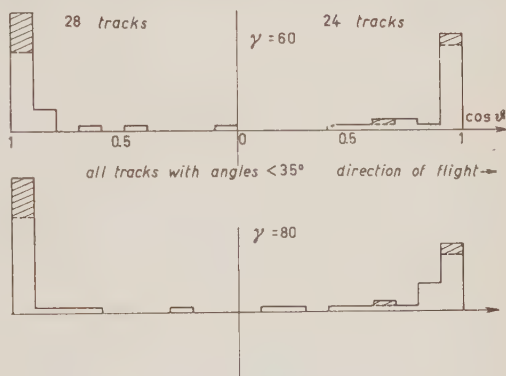


Fig. 4. - Angular distribution in the C-system. The hatched area is due to corrections for the soft cascade and for symmetry arguments (see text).

<sup>(6)</sup> W. HEISENBERG: *Zeits. f. Phys.*, **133**, 65 (1952).

<sup>(7)</sup> CH. PEYROU, B. D'ESPAGNAT and L. LEPRINCE-RINGUET: *Compt. Rend. Acad. Sci. Paris*, **228**, 1777 (1949).



we obtain  $(\vartheta_L)_{\max} = 8.2^\circ$ . Not counting the 14 tracks which are due to secondary interactions as mentioned above, there remain still 4 tracks with  $\vartheta_L > 8.2^\circ$ . But this result is not surprising, because the formula was derived under the assumption that all mesons have the same energy in the C-system.

\* \* \*

We wish to thank Professors F. G. HOUTERMANS and CH. PEYROU for stimulating discussions and Mrs. CH. B. ALBRECHT, who found the event. The participants of the Texas-stack left us their plates to investigate this event. Our special thanks are due to Professors HÄNNY, Lausanne, OCCHIALINI, Milan, and WATAGHIN, Turin. The Texas flight was organized by the Office of Naval Research and we are very grateful to Dr. A. ROBERTS. The financial means for the stack were granted by the Schweizer Nationalfonds. One of us (E.L.) thanks Prof. F. G. HOUTERMANS for the hospitality in his Institute, Prof. E. SCHOPPER for granting a leave of absence and the Deutsche Forschungsgemeinschaft for a maintenance grant.

#### RIASSUNTO (\*)

In emulsioni Ilford G5 nude è stata trovata una interazione nucleare del tipo 20+56p. Nel nocciolo assai denso di questo getto furono trovate 6 interazioni secondarie, 4 delle quali prodotte da primari a carica singola, le altre 2 da particelle neutre. L'energia media di queste interazioni secondarie è di circa 200 GeV. Da ciò e dalla distribuzione angolare del getto primario si deduce un'energia di  $10^{13}$  eV. Il cammino libero medio d'interazione delle particelle cariche nel nocciolo è  $54^{+58}_{-21}$  cm.

(\*) Traduzione a cura della Redazione.

## Atmospheric Effects on the Cosmic Ray Total Intensity at Sea Level.

F. BACHELET and A. M. CONFORTO

*Istituto di Fisica dell'Università - Roma*  
*Istituto Nazionale di Fisica Nucleare - Sezione di Roma*

(ricevuto il 19 Settembre 1956)

**Summary.** — The atmospheric effects on the total intensity of Cosmic Rays (C.R.) at sea level have been studied from an experimental point of view according to three different methods proposed by Duperier, Olbert and Dorman. One year's C.R. measurements have been analyzed with respect to the day-to-day and seasonal variation. The results are discussed in comparison with the findings of other Authors.

### 1. — Introduction.

A great deal of research has been made in the last 30 years on the influence of atmospheric factors on the cosmic ray (C.R.) intensity and particularly on the meson component at sea level<sup>(1-5)</sup>. Various ways of correlating these effects with different atmospheric variables have been attempted, as more information on the properties of mesons has become available. The most satisfactory method proved to be Duperier's, in which the meson intensity is correlated to the pressure at the ground, the height of the mean meson production level, and the temperature in the neighbourhood of the same level. The experimental values of the positive temperature coefficient, however, were found to be not very consistent in different experiments, and were usually

---

(<sup>1</sup>) L. MYSSOWSKY and L. TUWIM: *Zeits. f. Phys.*, **39**, 146 (1926).

(<sup>2</sup>) A. H. COMPTON and R. N. TURNER: *Phys. Rev.*, **52**, 799 (1937).

(<sup>3</sup>) P. M. S. BLACKETT: *Phys. Rev.*, **54**, 973 (1938).

(<sup>4</sup>) B. ROSSI: *Rev. Mod. Phys.*, **11**, 296 (1939).

(<sup>5</sup>) A. DUPERIER: *Terr. Magn. and Atm. El.*, **49**, 1 (1944).

(<sup>6</sup>) A. DUPERIER: *Proc. Phys. Soc.*, A **62**, 684 (1949).

(<sup>7</sup>) A. DUPERIER: *Journ. Atm. Terr. Phys.*, **1**, 296 (1951).

too high when compared to a theoretical estimation based on the competition between the decay and the nuclear capture of  $\pi$ -mesons.

Subsequently, several authors re-examined the problem as a whole, from a theoretical point of view, taking into account the recent data on  $\pi$  and  $\mu$ -mesons as well as the influence of new factors so far neglected, as for instance the so-called « redistribution of masses » in the troposphere.

Investigations in this line have been made by FEINBERG and DORMAN<sup>(8-10)</sup>, and OLBERT<sup>(11)</sup>, in order to give a complete treatment of all the meteorological effects on the meson intensity, and to obtain theoretical formulae for the correction of experimental data, but very few experimental checks on these formulae have been made. The atmospheric temperature effect has been studied theoretically also by MAEDA and WADA<sup>(12)</sup>.

On the other hand, TREFALL<sup>(13-16)</sup> carefully examined the available results of Duperier's correlation analysis and gave a reliable interpretation of the three coefficients involved. His work is based chiefly on the properties of the multiple correlation method itself, and on the fact that for practical reasons the chosen reference level actually never coincides with the mean meson production level.

The work of all these Authors has certainly thrown much light on the influence that meteorological factors bear on the meson intensity. However, the problem of the most reliable and practical way to be followed to correct the C.R. experimental data for purely atmospheric effects has not yet been solved. But this question is of particular importance to those who wish to study the primary C.R. variations by continuous measurements at sea level or near it.

In this paper we are primarily concerned with investigating the problem from an experimental point of view, in the particular case of the total intensity as registered in Rome. It is unnecessary to stress that, for the total intensity of C.R., the problem of clearly interpreting the influence of meteorological factors would be even more difficult. However, for the purpose of a correlation analysis, the same equations that were proposed for the meson intensity can be reasonably used for the total intensity, since at sea level the former component is by far the most important ( $\sim 80\%$ ).

---

(<sup>8</sup>) E. L. FEINBERG: *Dokl. Akad. Nauk SSSR*, **53**, 421 (1946).

(<sup>9</sup>) L. I. DORMAN: *Dokl. Akad. Nauk SSSR*, **94**, 433 (1954).

(<sup>10</sup>) L. I. DORMAN: *Dokl. Akad. Nauk SSSR*, **95**, 49 (1954).

(<sup>11</sup>) S. OLBERT: *Phys. Rev.*, **92**, 454 (1953).

(<sup>12</sup>) K. MAEDA and M. WADA: *Journ. Sci. Res. Inst. Tokyo*, **48**, 71 (1954).

(<sup>13</sup>) H. TREFALL: *Nature*, **171**, 888 (1953).

(<sup>14</sup>) H. TREFALL: *Proc. Phys. Soc.*, A **68**, 625 (1955).

(<sup>15</sup>) H. TREFALL: *Proc. Phys. Soc.*, A **68**, 893 (1955).

(<sup>16</sup>) H. TREFALL: *Proc. Phys. Soc.*, A **68**, 953 (1955).

The C.R. data in Rome were analyzed for a whole year, from April 1954 to March 1955, that is during the period of minimum solar activity. This would appear to be a particularly suitable time to study atmospheric effects, since magnetic and solar disturbances are smallest in that period.

The C.R. total intensity was measured with 12 counter telescopes in three different directions (vertical, and symmetrically inclined at  $30^\circ$  with respect to the vertical in the North-South plane). For experimental details we refer the reader to a previous paper <sup>(17)</sup>.

Atmospheric data (s.l. pressure, temperature and height of different isobaric levels) were measured at Ciampino, at a 12 km distance from the C.R. detector. Three-hourly ground pressure data were available, and two radio-sonde ascents a day (at 0200 and 1400 local time) supplied the upper atmosphere data.

## 2. - Duperier's Analysis.

2.1. *Statistical correlation method.* - According to Duperier's suggestion <sup>(6)</sup>, the multiple linear regression equation has been used

$$(1) \quad \frac{\delta F}{\bar{F}} = I_B \delta B + I_H \delta H + I_T \delta T,$$

where  $F$  is the C.R. intensity,  $B$  the barometric pressure,  $H$  and  $T$  the height and temperature of the reference isobar level, and  $\delta$  the variation of these quantities with respect to their mean value in the considered period.

The regression coefficients  $I$  have been determined by least square method, and the calculations involved have been carried out by means of FINAC, a Ferranti electronic calculating machine. Also the total and partial first- and second-order correlation coefficients (as  $r_{FB}$ ,  $r_{FB,H}$ ,  $r_{FB,HT}$  et sim.) have been computed with FINAC. The multiple correlation coefficient  $R$  and the errors  $S_F$  of regression coefficients were obtained by desk computing machines, the formula used for the latter being of the type <sup>(18)</sup>

$$(2) \quad S_{I_B} = \frac{100 S_{F,BHT}}{\bar{F}} \left\{ \frac{1 - r_{HT}^2}{(1 - r_{BH}^2 - r_{BT}^2 - r_{HT}^2 + 2r_{BH}r_{BT}r_{HT}) \sum_1^n \delta B^2} \right\}^{\frac{1}{2}},$$

$$(3) \quad S_{F,BHT} = \left\{ \frac{(1 - R^2) \sum_1^n \delta F^2}{n - 4} \right\}^{\frac{1}{2}}.$$

<sup>(17)</sup> F. BACHELET and A. M. CONFORTO: *Nuovo Cimento*, **12**, 923 (1954).

<sup>(18)</sup> B. OSTLE: *Statistics in Research* (Iowa, 1954).

The significance of  $r$  and  $R$  coefficients has been judged with the help of the Fisher  $z$ -function<sup>(19)</sup>.

A first group of correlation analyses was carried out separately on the intensities measured by the vertical telescopes and by the inclined ones. They included three different reference levels in three different periods; it resulted that both the regression and correlation coefficients were very close to one another, with a high probability level, for the three different directions in each period analysed and with each group of variables.

For this reason, in the following we refer to the mean values of the regression and correlation coefficients as obtained by the correlation of inclined and vertical C.R. intensities separately; the estimated error for each coefficient is taken as the smallest one of the separate evaluations, which obviously are not independent.

The consistency of the results for inclined and vertical directions is not surprising in view of the small inclination angles, since very little difference can be expected both in the cut-off produced by the energy losses throughout the atmosphere and in the mean meson production layer.

This agreement among different directions was verified also in the case of the multiple correlation performed according to Olbert's suggestion (see Sect. 3).

*2.2. Multiple correlation with different reference isobar levels.* — Fig. 1 shows the results of the multiple correlation analysis according to Eqn. (1) at three different reference levels (200, 100 and 50 mb). This analysis has been carried out on mean C.R. daily values (day-to-day correlation) in 3 quarterly periods as well as on mean monthly values (seasonal correlation) in one annual period. The daily values of the pressure are taken as the averages of the 8 daily readings, and those of  $H$  and  $T$  as the weighted means of 3 measurements (two of the day being considered plus the first of the two measurements relative to the next day).

The following points are worth noting:

a) There appears to be no significant difference in the multiple correlation coefficients  $R$  and in the partial coefficients  $r_{FB,HT}$ .

b) The partial correlation coefficients  $r_{FH,BT}$  do not appear to show any systematic trend in favour of the 100 mb level, which is the closest to the mean meson production level.

c) The partial coefficients  $r_{FT,BH}$  increase steeply from 200 mb to 50 mb level both in the seasonal and in the day-to-day correlations, although the

---

(19) R. A. FISHER: *Statistical Methods for Research Workers* (London, 1954).

values of  $\sum \delta T^2$  decrease correspondingly. The regression coefficients  $I'_T$  behave similarly, in good agreement with TREFALL'S considerations<sup>(15)</sup> on the

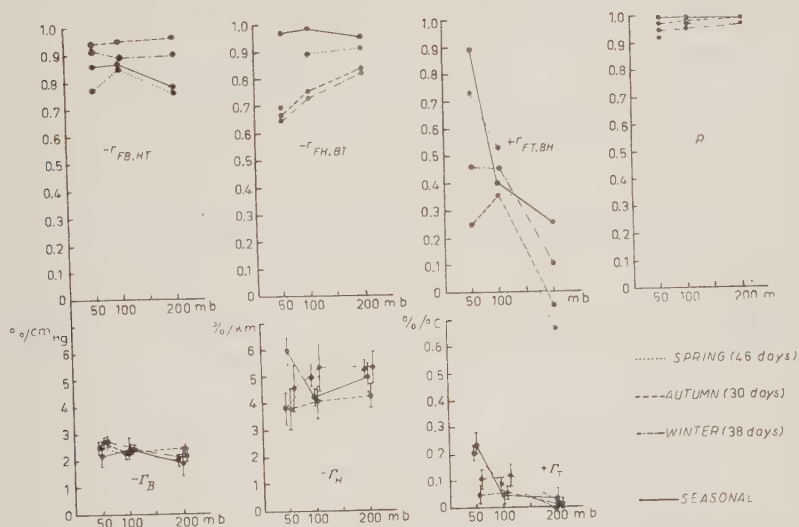


Fig. 1. Multiple correlation according to Eqn. (1) with different reference isobar levels.

influence of  $\mu$ - $\epsilon$  decay on the temperature coefficient in a multiple correlation in which the height of an isobar level different from the mean meson production level is maintained constant.

2'3. *Seasonal and day-to-day correlation with 100 mb reference level.* — Day-to-day correlations with a 100 mb reference level have been carried out for all the data by grouping the daily means in 6 two-month periods, so that within each period the variations due to instrumental causes were as small as possible. The various groups included 36, 30, 48, 31, 32, 43 days respectively.

In Fig. 2 the correlation and regression coefficients are shown, which derive from the 6 day-to-day correlations, as well as from the seasonal correlation analysis with a 100 mb reference level. Since in the fifth case we have  $r_{FB,BT} = -0.004$ , that is quite negligible, the corresponding value of  $I'_H$  was excluded from the computation of the mean values of the day-to-day regression coefficients, as given in Table I along with the seasonal coefficients. In Table II the results of multiple correlations made by different Authors are given for comparison. They were obtained from Eqn. (1) with a 100 mb reference level for the case of the total as well as the hard and soft C.R. components.



TABLE I. — *Day-to-day and seasonal correlations in Rome, according to Duperier's Eqn. (1)*

Correlation	$r_{FB,HT}$	$r_{FH,HT}$	$r_{FT,BH}$
Day-to-day in 6 two-month periods	$-0.88 \div -0.97$	$-0.62 \div -0.86$	$+0.40 \div +0.78$
Seasonal	$-0.87$	$-0.98$	$+0.40$

TABLE II. — *Record of day-to-day correlation results according to Duperier's Eqn. (1) with 100 mb isobars*

C.R. Compo- nent	Author	cm Pb	Time length for C.R. means	Ascents per time length	Station for up- atm. d.
<i>Total</i>	(a) DAWTON-ELLIOT 1953 <sup>(20)</sup>	—	24 hours	4	1
	(b) TRUMPY-TREFALL 1953 <sup>(21)</sup>	—	2 »	1	1
	(c) TRUMPY 1954 <sup>(22)</sup>	—	6 »	1	1
<i>Hard</i>	(d) DUPERIER 1949 <sup>(6)</sup>	25	24 hours	4	2
	(e) DUPERIER 1951 <sup>(7)</sup>	40	24 »	4	2
	(f) COTTON-CURTIS 1951 <sup>(23)</sup>	10+roof	24 »	2	2
	(g) DAWTON-ELLIOT 1953 <sup>(20)</sup>	10	24 »	4	1
	(h) TRUMPY-TREFALL 1953 H <sub>1</sub> <sup>(21)</sup>	10	2 »	1	1
	(i) TRUMPY-TREFALL 1953 H <sub>2</sub> <sup>(21)</sup>	22	2 »	1	1
	(j) TRUMPY 1954 <sup>(22)</sup>	15	2 »	1	1
	(k) CHASSON 1954 <sup>(24)</sup>	20	3 »	1	1
		absorbed in			
<i>Soft</i>	(l) DAWTON-ELLIOT 1953 <sup>(20)</sup>	10	24 hours	4	1
	(m) TRUMPY-TREFALL 1953 <sup>(21)</sup>	10	Obtained from coefficients (b),		
	(n) TRUMPY 1954 <sup>(22)</sup>	10	6 hours	1	1

From Fig. 2 and Tables I and II one can see that:

a) The various  $I_B$  coefficients obtained in Rome are very consistent; they also agree very closely with the values so far obtained elsewhere for the total component.

<sup>(20)</sup> D. I. DAWTON and H. ELLIOT: *Journ. Atm. Terr. Phys.*, **3**, 295 (1953).

<sup>(21)</sup> B. TRUMPY and H. TREFALL: *Physica*, **19**, 636 (1953).

<sup>(22)</sup> B. TRUMPY: *Univ. Bergen, Naturvit. rekke*, no. 3, Årbok 1954.

<sup>(23)</sup> E. S. COTTON and H. O. CURTIS: *Phys. Rev.*, **84**, 840 (1951).

<sup>(24)</sup> R. L. CHASSON: *Phys. Rev.*, **96**, 1116 (1954).

b) reference level. One year's data (April 1954 - March 1955) for the total component.

$R$	Mean	$\Gamma_B$ (%/cm Hg)	$\Gamma_H$ (%/km)	$\Gamma_T$ (%/°C)
0.942 $\div$ 0.985	Weighted	$-2.45 \pm 0.06$	$-2.87 \pm 0.18$	$+0.086 \pm 0.007$
	Arithmetic	$-2.47 \pm 0.07$	$-3.25 \pm 0.58$	$+0.089 \pm 0.008$
0.989	—	$2.44 \pm 0.46$	$-4.19 \pm 0.33$	$+0.042 \pm 0.031$

reference level, for the total, hard and soft components measured at sea level by counter telescopes.

No. of rela- cases	No. of record- ings	Atmospheric variables	$R$	$\Gamma_B$ (%/cm Hg)	$\Gamma_H$ (%/km)	$\Gamma_T$ (%/°C)
8	30	$B, H_{100}, T_{100}$	—	$-2.49 \pm 0.18$	$-3.02 \pm 0.49$	$+0.054 \pm 0.011$
3	40-60	$B, H_{100}, T_{100-200}$	0.90-0.98	$-2.57 \pm 0.09$	$-3.20 \pm 0.50$	$+0.050 \pm 0.020$
298 data		$B, H_{100}, T_{100-200}$	—	$-2.65 \pm 0.08$	$-3.68 \pm 0.41$	$+0.028 \pm 0.011$
5	9-33	$B, H_{100}, T_{100-200}$	0.88-0.99	$-1.05 \pm 0.16$	$-3.90 \pm 1.10$	$+0.123 \pm 0.024$
6	18-35	$B, H_{100}, T_{100-200}$	—	$-1.21 \pm 0.06$	$-3.48 \pm 0.45$	$+0.075 \pm 0.010$
1	45	$B, H_{100}, T_{100}$	0.84	$-1.36 \pm 0.14$	$-3.16 \pm 0.87$	$-0.023 \pm 0.027$
8	30	$B, H_{100}, T_{100}$	—	$-1.67 \pm 0.16$	$-4.00 \pm 0.43$	$+0.056 \pm 0.018$
3	40-60	$B, H_{100}, T_{100-200}$	0.90-0.98	$-1.69 \pm 0.11$	$-4.45 \pm 0.53$	$+0.036 \pm 0.021$
2	40-60	$B, H_{100}, T_{100-200}$	0.90-0.98	$-1.49 \pm 0.14$	$-3.48 \pm 0.60$	$+0.038 \pm 0.019$
298 data		$B, H_{100}, T_{100-200}$	—	$-1.65 \pm 0.05$	$-4.46 \pm 0.37$	$+0.048 \pm 0.016$
1	78	$B, H_{100}, T_{100-200}$	0.61	$-1.56 \pm 0.23$	$-3.22 \pm 0.49$	$+0.068 \pm 0.018$
8	30	$B, H_{100}, T_{100}$	—	$-4.70 \pm 0.23$	$-1.05 \pm 0.43$	$+0.021 \pm 0.020$
298 data		$B, H_{100}, T_{100-200}$	—	$-4.62 \pm 0.40$	$-0.24 \pm 2.07$	$+0.083 \pm 0.082$
		$B, H_{100}, T_{100-200}$	—	$-4.66 \pm 0.13$	$-1.38 \pm 0.80$	$+0.021 \pm 0.027$

b) The  $\Gamma_H$  day-to-day coefficients obtained in Rome appear to be significantly scattered even when the fifth case is excluded. However, because of the different meteorological conditions in different periods and of the fact that the so-called «independent» variables are often correlated, there is reason to believe that the errors as obtained for each case (Fig. 2) and used for the computation of the weighted means (Table I) are actually underestimated; therefore, we have also quoted the arithmetic means with the standard deviation calculated from the scatter of the individual determinations about the mean. In this way the discrepancy between seasonal and day-to-day correlations appears to be slighter.

c) The  $\Gamma'_T$  coefficients are quite consistent in the day-to-day correlations, and their mean value is higher than the seasonal coefficient, which however is hardly significant.

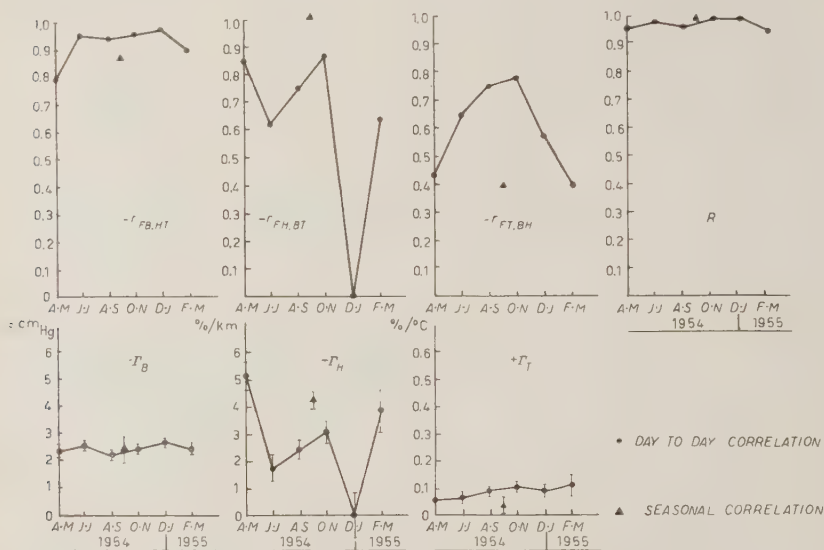


Fig. 2. — Day-to-day and seasonal correlations according to Eqn. (1) with 100 mb reference level.

2.4. *Comparison between multiple correlation and simple correlation with pressure.* — For the three-month periods the results of the multiple correlation according to Equ. (1), at a 100 mb reference level, are compared in Table III with the results of simple correlation according to the equation

$$(4) \quad \frac{\delta F}{F} = \Gamma'_R \delta B.$$

The mean square deviation, after correcting for the total barometric effect, is calculated as <sup>(18)</sup>

$$(5) \quad S'_{F,B} = \left\{ \frac{1 - R^2}{n - 2} \sum_1^n \delta F^2 \right\}^{\frac{1}{2}},$$

and is compared with  $S_{F,BHT}$  given by Eqn. (3). Both have proved to be good estimates of the actual residual mean square deviation.

While the  $\Gamma'_B$  coefficients of the multiple correlation appear to be very well reproducible (as already noted in the two-month periods), the  $\Gamma'_B$  are widely

TABLE III. — *Simple and multiple day-to-day correlation (Vertical telescopes only).*

Period	$n$ (days)	$S_F$ $\left(\frac{\sum \delta F^2}{n-1}\right)^{\frac{1}{2}}$	Simple correlation, Eqn. (4)			Multiple correlation, Eqn. (1)		
			$S'_{F.B}$	$R' =  r_{FB} $	$\Gamma'_B (\%/\text{cm}_{\text{Hg}})$	$S_{F.BHT}$	$R$	$\Gamma_B (\%/\text{cm}_{\text{Hg}})$
Spring	46	1848	1241	0.75	$-3.64 \pm 0.48$	465	0.970	$-2.30 \pm 0.23$
Summer	43	914	634	0.73	$-2.01 \pm 0.43$	297	0.950	$-2.17 \pm 0.14$
Autumn	30	2694	850	0.95	$-3.13 \pm 0.19$	553	0.981	$-2.53 \pm 0.16$
Winter	38	2333	1063	0.89	$-3.10 \pm 0.25$	722	0.955	$-2.47 \pm 0.22$

different in different cases, depending on the actual values of  $\partial H/\partial B$  and  $\partial T/\partial B$ , since they roughly include also the two temperature effects. That the simple correlation cannot account completely for the atmospheric effects can also be seen from the comparatively low values of the  $R$  coefficient, and correspondingly high values of the residual mean square deviation.

25. *Discussion on Duperier's correlation.* — The results of the correlation analysis at different reference levels do not seem to point towards a preferential discrimination of the reference level, at least for the atmospheric conditions in Rome and for the one-year data worked out. This is not surprising because, as pointed out by TREFALL<sup>(15,16)</sup>, owing to the very nature of the correlation method and to the properties of the atmospheric variables, the three terms in Eqn. (1) have not distinct physical meanings, but each of them includes the contribution of the effects which should be represented by the two other terms separately. It is obvious that the situation is even more complicated in the case of the total component: therefore, one cannot expect that for a particular level, that is the closest one to the mean production level at the energies involved, the 3 partial correlation coefficients be simultaneously maxima (this was, in fact, the line along which Duperier worked).

Nevertheless, the observation of at least the coefficient  $r_{FT,HB}$  can suggest the exclusion of the 200 mb level, for which there is never a significant correlation with the temperature. On the other hand, the choice between the other two levels was based on a practical point of view, and the 50 mb isobar has been ruled out because too many radiosonde ascents do not reach this pressure level. For these reasons the 100 mb level was chosen for further studies, which also made it possible to compare our results with those obtained by other Authors.

From Tables I and II one can see that for each C.R. component there is a general consistency among the results so far obtained by means of Duperier's correlation analysis as far as the pressure and height effects are concerned, the first being definitely greater and the second smaller for the total than for the hard component.

Conversely, the dependence on the selected component, on the absorber energy cut-off and on the opening angle of the detecting apparatuses (TREFALL<sup>(14,15)</sup>) does not seem to account completely for the spread in the values obtained for the temperature coefficients; other causes for this might be sought in the lack of precision of the temperature measurements in the upper atmosphere, and in the small number of ascents available per day, which are likely to give inaccurate estimates of the daily mean.

In order to overcome the latter difficulties, several Authors<sup>(21,22,24)</sup> have used for correlation analysis only C.R. data collected during a few hour intervals bracketing the times of morning and afternoon flights separately. In our case, however, a check in this direction, carried out at the 3 reference levels for 2 groups of three-monthly data and taking six-hour intervals, gave a negative result. In fact, the partial correlation coefficients of C.R. intensity with  $H$  and  $T$  thus obtained, did not increase, in comparison with those obtained from the daily correlation, whilst the regression coefficients remained practically unchanged and the  $R$  coefficients were smaller because of the lesser C.R. statistics.

As already noticed, there appears to be a difference between the values obtained for both  $\Gamma_H$  and  $\Gamma_T$  from the day-to-day and the seasonal correlations respectively. Although not highly significant, this difference could induce us to suspect that some particular physical feature exists in the seasonal variations of C.R. intensity and of atmospheric variables.

For instance, some influence of geomagnetic activity might become more apparent in seasonal than in day-to-day variation. However, after correction of the monthly averages with the day-to-day coefficients, the correlation of the residual seasonal variation with planetary geomagnetic indexes  $K_p$  proved to be irrelevant (see Sect. 5).

On the other hand, an apparent seasonal effect might be the result of instrumental errors in upper atmosphere temperature measurements, such as those due to radiation absorption, which in its turn varies seasonally. Such effect might be traced in the actual monthly averages of the diurnal temperature variation at the 100 mb level; but it was found to be too small to justify the smaller seasonal  $\Gamma_T$  value.

Some anomaly in correcting the seasonal C.R. intensity variation by means of day-to-day coefficients was also noticed by DAWTON and ELLIOT<sup>(20)</sup>. Therefore, apart from other unknown properties of seasonal variations, the only conclusion possible at present is that these results emphasize the importance of the role played by the atmospheric variables in the correlation method itself, as both their mean square deviations and the actual correlation existing among them widely differ from the day-to-day to the seasonal analyses.

In brief, it is possible that by increasing the statistics of the correlation cases computed for a certain detecting apparatus at different meteorological

conditions, the Duperier correlation analysis would lead to more reliable results for the mean values of the regression coefficients and for the correction of the C.R. intensity data. On the other hand, at least for the atmospheric conditions in Rome, one cannot rule out  $H$  and  $T$  variables for the sake of simplicity, because it has been established that the correction for the total barometric effect alone is not enough in any case.

### 3. - Olbert's Analysis.

Starting from the exact expression for the survival probability of  $\mu$ -mesons through the atmosphere and making some assumptions on the properties of the atmosphere at  $40^\circ$  N latitude with a view to getting some analytical simplifications, OLBERT <sup>(11)</sup> derived the following three-term regression formula for the relative changes of the  $\mu$ -meson vertical intensity:

$$(6) \quad \frac{\delta F}{F} = A_P \delta x_0 + A_H \delta H(\bar{x}_1) + A_K [\delta T(\bar{x}_2)]_{\Delta v},$$

where  $x_0$  is the barometric pressure at sea level,  $\bar{x}_1$ ,  $\bar{x}_2$  are characteristic pressure levels suitably calculated and depending upon the instrumental energy cut-off, and

$$(7) \quad \delta[T(\bar{x}_2)]_{\Delta v} = \frac{1}{x_0 - \bar{x}_2} \int_{\bar{x}_2}^{x_0} \delta T(x') dx'.$$

Theoretical values of  $A_P$ ,  $A_H$ ,  $A_K$  coefficients are shown in reference <sup>(11)</sup> as functions of the minimum residual range of the recorded mesons. In the case of the total component, the values predicted by OLBERT are not directly usable, and we have tentatively applied Eqn. (6) to get experimental coefficients through multiple correlation analysis. We used the  $\bar{x}_1$  and  $x'_2$  plots to have an indication of the suitable reference levels.

The results of this analysis for one three-month period (Spring 1954, 15 days) are shown in Table IV along with some other Author's results. We note that:

a) In our results,  $A_P$  is in complete agreement with the  $I'_B$  coefficient obtained from Eqn. (1), 100 mb reference level. If we tentatively compare our  $A_H$  and  $A_K$  coefficients with Olbert's graphs, they do not seem inconsistent with the predicted values, and the smaller value of  $A_H$  in comparison with the meson value could be accounted for considering that a part of the soft component is not produced by mesons (see also Table II). This value, however, is not very significant since the partial coefficient  $r_{FH.BT} = -0.2$ . Moreover, the correlation coefficient  $r_{HT.B}$  is particularly high, as already predicted by OLBERT, and this fact can alter the meaning of the statistical correlation.



TABLE IV. *Experimental correlations according to Olbert's method*

Author	C. R. Component	No. of recordings and time length	Ascents per time unit	Olbert's		
				$\bar{x}_1$ (mb)	$\bar{x}_2$ (mb)	$A_p$ (%/cm)
BACHELET-CONFORTO	Total	45 24 h	2	100	200	$-2.41 \pm 0.1$
WADA-KUDO <sup>(25)</sup>	Hard	50 24 h	1	100	300	$-1.94 \pm 0.2$
CHASSON <sup>(26)</sup>	Hard	79 39 h	1	100	200	$-1.76 \pm 0.2$

b) Similar considerations can be made for the results of the other Authors, such as Wada and Kudo's  $r_{FH,HT}$  and  $r_{HT,B}$  coefficients, while the huge error in Chasson's  $A_H$  coefficient shows that the situation is not any better in that case. As to the regression coefficients,  $A_p$  presents the usual reliable values, whereas  $A_H$  is insignificant in one case and unexpectedly positive in another, and Wada and Kudo's  $A_K$  coefficient is far too high when compared with Olbert's graph.

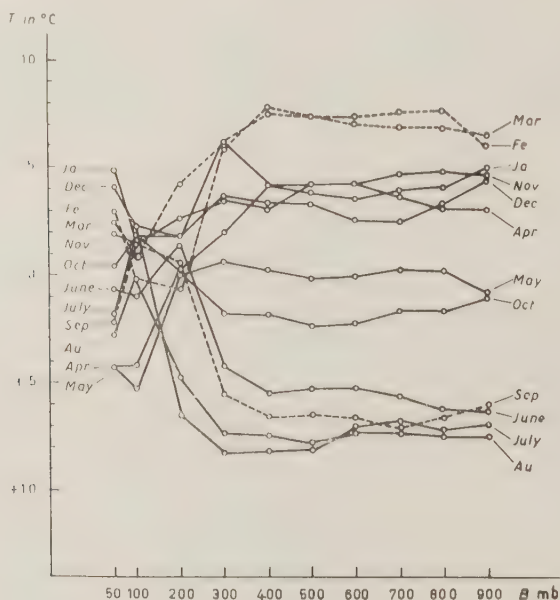


Fig. 3. — Monthly deviations,  $\delta T$ , from the annual mean value of the atmospheric temperature at different isobar levels.

<sup>(25)</sup> M. WADA and S. KUDO: *Journ. Sci. Res. Inst. Tokyo*, **48**, 245 (1954).

<sup>(26)</sup> R. L. CHASSON: *Guanajuato Meeting* (September 1955).

comparison with some results obtained from a Duperier analysis in the same periods.

Eqn. (6)					Duperier's regression Eqn. (1)			
(%/km)	$A_K$ (‰/°C)	$r_{FH.BT}$	$r_{HT.B}$	$R$	Variables	$r_{FH.BT}$	$r_{HT.B}$	$R$
$65 \pm 0.99$	$-0.190 \pm 0.041$	-0.25	+0.93	0.97	$B, H_{100}, T_{100}$	-0.89	-0.41	0.97
$56 \pm 0.81$	$-0.349 \pm 0.033$	+0.30	+0.86	0.83	$B, H_{300}, T_{100-200}$	—	—	0.84
$84 \pm 2.11$	$-0.168 \pm 0.050$	—	—	0.73	$B, H_{100}, T_{100-200}$	—	—	0.72

Although it is daring to draw any conclusion from the results of only three correlation periods, the above checks of the Olbert analysis show that the disadvantage, already pointed out by OLBERT, of a high correlation between two of the « independent » variables is quite considerable when determining experimental coefficients. On the other hand, this determination is most desirable in all cases. Therefore, if we wish to find a better regression equation, we must not only be able to take into better account the meson behaviour, but also acquire a deeper knowledge of the properties of the atmosphere and find more suitable variables.

Futhermore, great care must be taken when making assumptions on the meteorological variables. For instance, we note that the assumption made by OLBERT, that the  $\delta T$  values do not vary greatly for different pressure levels up to the  $x_2$  values, does not appear to be satisfied in our atmosphere, at least as far as the seasonal variation from 300 to 200 mb is concerned (Fig. 3). Thus, the approximation adopted on account of this supposed property can partly affect the results.

#### 4. — Dorman's Analysis.

Starting from FEINBERG's works (\*), DORMAN (9.10) developed the theory of atmospheric effects on the meson component of C.R.

As in the OLBERT investigation, the chief starting points are the continuous production and the ionization losses of  $\mu$ -mesons throughout the atmosphere. Moreover, DORMAN points out that any general assumption on a standard atmosphere should be carefully avoided.

A very complex and general analytical expression is obtained, where different terms represent different physical effects, each of which, however, involves several variables. These are substantially the pressure at the ground and the density of different isobar levels, from the top of the atmosphere down to the C.R. recorder.

In giving the results of the integrations involved, Dorman states that they

were obtained partly analytically and partly numerically. The integrals depend on the meson production function, on the relation between density and temperature at different levels, and on the instrumental energy cut-off. Ultimately, the meteorological effects are summarized in the equation

$$(8) \quad \frac{\delta F}{F} = \beta \delta x_0 + \int_0^{x_0} W(x') \delta T(x') dx',$$

where  $W(x')$  is a function called « density of the temperature coefficient » and has been plotted in a graph.

Again, we have tentatively applied Eqn. (8) to the total component. Since the contribution of the temperature variation of different atmospheric layers has been purposely kept separated in this case, we have not tried to reduce it to a simpler expression with few variables in order to use the statistical correlation method for the determination of the experimental coefficients. On the contrary, we used Eqn. (8) to correct monthly C.R. intensities, introducing the value  $I'_B$  obtained in the experimental Duperier correlation with 100 mb reference level for the pressure coefficient, and the values from Fig. 1 of reference <sup>(27)</sup> (\*) for the function  $W(x')$ .

The results are shown in Fig. 5 together with similar corrections according to other schemes, and will be discussed in the next Section.

## 5. Seasonal Variation of Atmospheric Data and C.R. Intensity.

The monthly mean values of atmospheric data in Rome from April 1954 to March 1955 are plotted in Fig. 4.

It is worth noting the shift in phase of the seasonal variation of 100 and 50 mb temperature with respect to all the deeper levels, the very close correlation of the height of 100 mb level with the Olbert temperature  $T_{Av}$  (200-900 mb), and the average height of the tropopause which is generally at  $\sim 16$  km (100 mb level) and increases in winter ( $\sim 20$  km, 50 mb level). This latter feature is not in agreement with the behaviour predicted by several Authors (see, for instance, reference <sup>(28)</sup>) for our latitude.

---

<sup>(27)</sup> L. I. DORMAN and E. L. FEINBERG: *Guanajuato Meeting* (September 1955).

(\*) In lack of any explicit indication of the assumed energy cut-off, as well as of the criteria used in calculating the function  $W(x')$ , we chose the plot shown in this more recent paper, which clearly refers to a lower instrumental cut-off in comparison with the one given in reference <sup>(10)</sup>. See also reference <sup>(12)</sup>.

<sup>(28)</sup> F. A. BERRY, E. BOLLAY and N. R. BEERS: *Handbook of Meteorology* (New York, 1945).

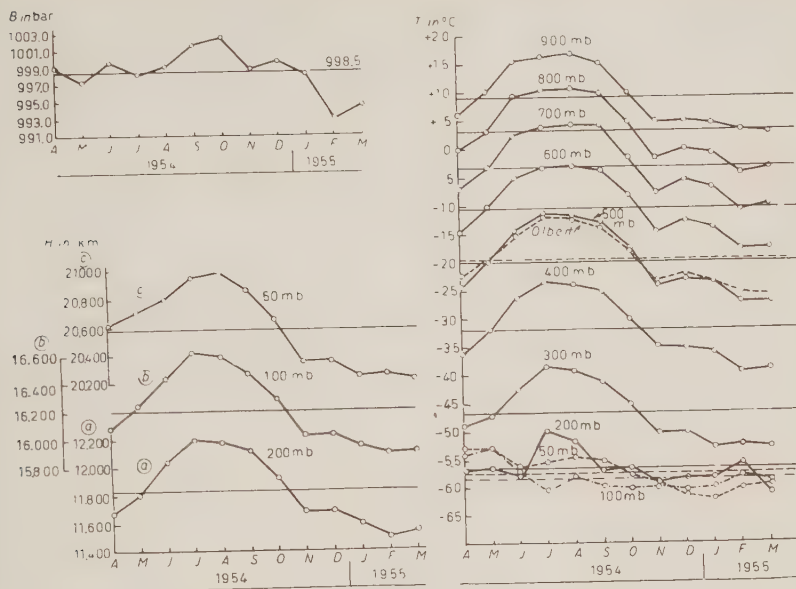


Fig. 4. - Seasonal variation of atmospheric data.

The seasonal variation of uncorrected C.R. intensity is plotted in Fig. 5 together with the curves of values corrected according to different schemes:

- DUPERIER: experimental values of the day-to-day coefficients (Table I);
- OLBERT: experimental values of the day-to-day coefficients (Table IV);
- DORMAN: experimental Duperier coefficient for  $\beta = \Gamma_B$  and Dorman theoretical value for  $W(x')$  (27).

The respective experimental mean square deviation  $S_{\text{uncorr}}$  and  $S_{\text{corr}}$  are also given.

It is evident that most of the seasonal variation disappears in all cases after allowing for meteorological effects. The residual mean square deviations corresponding to all three methods are of the same order, so that there is no indication that for the total component a certain method is to be preferred.

On the other hand, it is worth noting that in no case the residual mean square deviation is reduced to the expected statistical fluctuation. An attempt to account for that on the basis of the influence of the geomagnetic activity was not successful, since the correlation of the three corrected intensities with  $K_p$  monthly indexes, which are also plotted in Fig. 5, is not only insigni-

ficient, but also of the wrong sign (positive) to account for any geomagnetic effect.

A further correlation analysis of the recent data of the total C.R. intensity is underway in Rome, and a new apparatus is being built to record both the

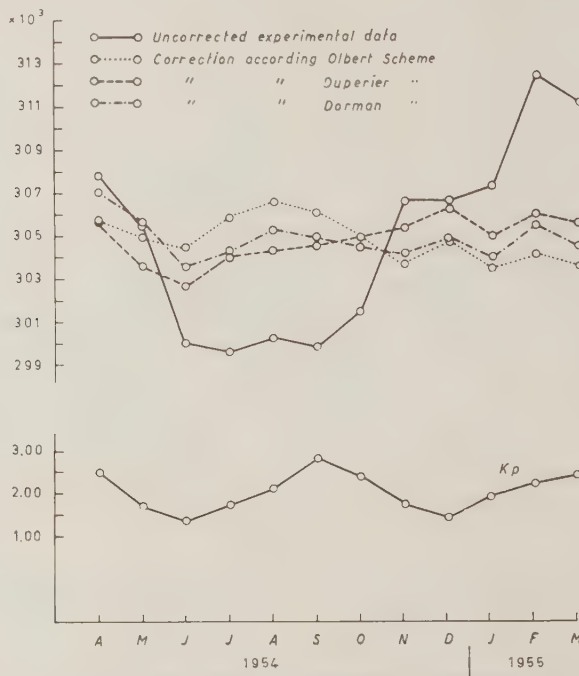


Fig. 5. - Seasonal variation of C.R. intensity and  $K_p$  geomagnetic indexes.

$$S_{\text{uncorrected}} = 664; \quad S_{\text{Superier}} = 1075; \quad S_{\text{Olbert}} = 1016; \quad S_{\text{Dorman}} = 922.$$

total and the hard component, so that more suitable data will be available to check the theoretical formulae for the meson intensity.

\* \* \*

We are deeply indebted to the Ispettorato delle Telecomunicazioni e Assistenza al Volo, Ministero della Difesa Aeronautica for supplying us with meteorological data, and to the Istituto Nazionale per le Applicazioni del Calcolo for carrying out most of the numerical calculations with the FINAC computer. Thanks are due to Miss A. FELICI, Miss A. MARCON and Mr. A. CECARELLI for the desk machine computations, and to Mr. M. CASALI for his assistance in the maintenance of the apparatus. We are very grateful to

Dr. H. ELLIOT for the helpful discussions on the subject. One of the writers (F. B.) wishes to express deep gratitude to the Fondazione F. Somaini of Como for a fellowship and Prof. P. M. S. BLACKETT for his kind hospitality at the Imperial College of Science and Technology in London.

#### RIASSUNTO

Si studiano da un punto di vista sperimentale gli effetti atmosferici sulla totale dei raggi cosmici al livello del mare secondo tre diversi metodi proposti da Duperier, Olbert e Dorman. Si analizzano le misure dei raggi cosmici per un intero anno sia riguardo alle variazioni da un giorno all'altro che alle variazioni stagionali. Si discutono i risultati confrontandoli con quelli di altri autori.



## On the Trident Cross-Section between 1 and 10 GeV.

F. A. BRISBOUT, C. DAHANAYAKE (\*), A. ENGLER (+), and D. H. PERKINS

*H. H. Wills Physical Laboratory, University of Bristol - Bristol*

(ricevuto il 19 Settembre 1956)

**Summary.** — An estimate has been made of the trident cross-section for electrons of energy between 1 and 10 GeV. Energy determinations were made by scattering measurements on each track under conditions where the effects of spurious scattering have been shown to be negligible. In a total track length of 219 cm, the estimated number of true tridents was found to be 3, as compared with 2.4 expected from theory. Even on the basis of this small number of events, there is a marked discrepancy between our results and those of previous experiments at high energies. Reasons for this discrepancy are discussed.

### Introduction.

Since the discovery of direct pair production by electrons, commonly referred to as tridents, various attempts have been made with nuclear emulsions to compare the experimental observations with theory. Recently several authors <sup>(1-3)</sup> have reported disagreement between theory and experiment at high energies. FREIER and NAUGLE were the first to claim a discrepancy with theory, by at least a factor of three, at energies around 50 GeV. This in turn led BLOCK and KING <sup>(4)</sup> to consider the various experimental factors which

---

(\*) Now at University of Ceylon, Colombo.

(+) Now at University of Rochester, N.Y.

(1) P. S. FREIER and T. E. NAUGLE: *Phys. Rev.*, **92**, 1086 (1953).

(2) M. F. KAPLON and M. KOSHIBA: *Phys. Rev.*, **97**, 193 (1955).

(3) M. KOSHIBA and M. F. KAPLON: *Phys. Rev.*, **100**, 327 (1955).

(4) A. DEBENEDETTI, C. M. GARELLI, L. TALLONE, M. VIGONE and G. WATAGHIN: *Nuovo Cimento*, **12**, 954 (1954).

(5) E. LOHRMANN: *Nuovo Cimento*, **4**, 820 (1956).

(6) M. M. BLOCK and D. T. KING: *Phys. Rev.*, **95**, 171 (1954).

could lead to an overestimation of the trident cross-section. These authors pointed out that it would be impossible to distinguish true tridents from bremsstrahlung (henceforth called B.S.) pairs converting very close to the parent electron, due to the limitations imposed by the grain size on the resolution between closely adjacent tracks recorded in emulsion. However, the number of B.S. pairs expected to fall within the resolving distance (commonly referred to as pseudo-tridents) may be computed and corrected for. This correction depends critically on the energy of the primary electron and the assumed resolving distance.

KAPLON and KOSHIBA <sup>(2,3)</sup> have refined the calculations of BLOCK and KING and, (on the basis of their own experimental data), claim that, in spite of the corrections, the trident cross-section is larger, by at least a factor of 2.5, than that expected on the basis of Bhabha's theory. BLOCK *et al.* <sup>(7)</sup> have made certain necessary modifications in the calculations of BHABHA <sup>(8)</sup>, which reduce his cross-section by about a factor two and thus bring it into agreement with RACAH's <sup>(9)</sup> results. Furthermore, BLOCK *et al.* have measured the trident cross-section at a mean energy of 400 MeV, (in the energy interval 0.1 to 10 GeV) and find agreement with RACAH's predictions. On the other hand, if KAPLON's results are correct, the discrepancy between theory and experiment would amount to about a factor of five at high energies. This discrepancy seems, at first sight, to be supported by the work of several other authors <sup>(1,5)</sup>.

So far, there is no other evidence to contradict the validity of quantum electrodynamics at high energies. Furthermore, the determination of the energy of particles in emulsions by measurement of multiple scattering along the tracks, is generally subject to systematic errors due to the effects of « spurious scattering » <sup>(10,11)</sup>. For high-energy particles, such effects may lead to serious under-estimation of the energy. Any apparent disagreement between the observations and the theoretical predictions will therefore be greatly enhanced, since lower energies correspond not only to a smaller correction for pseudo-tridents, but also to a lower predicted trident cross-section.

In view of the above uncertainties, it is by no means clear that the results of previous experiments are in fact at variance with theory. We have therefore thought it worthwhile to make an independent determination of the trident cross-section under conditions which ensure that systematic errors in determination of energy are negligible.

---

<sup>(7)</sup> M. M. BLOCK, D. T. KING and W. W. WADA: *Phys. Rev.*, **96**, 1627 (1954).

<sup>(8)</sup> H. T. BHABHA: *Proc. Roy. Soc.*, A **152**, 559 (1935).

<sup>(9)</sup> G. RACAH: *Nuovo Cimento*, **14**, 93 (1937).

<sup>(10)</sup> S. BISWAS, B. PETERS and RAMA: *Proc. Ind. Acad.*, A **41**, 154 (1955).

<sup>(11)</sup> F. A. BRISBOUT, C. DAHANAYAKE, A. ENGLER, P. H. FOWLER and P. B. JONES: *Nuovo Cimento*, **3**, 1400 (1956).

## 1. - Experimental Procedure.

In the present experiment, measurements were restricted to events in a single stack of emulsion, in which the spurious scattering had been extensively investigated<sup>(11,12)</sup>. The values of energy obtained by multiple scattering measurements along tracks of length  $\geq 1$  cm per emulsion, were shown to be virtually unaffected by spurious scattering provided that  $E \leq 10$  GeV.

The electrons investigated in the present work originated as the components of high energy pairs, found either in the cores of cosmic ray jets or by direct scanning. Particular care was taken to ensure that the  $\gamma$ -rays producing the pairs in the jet events originated directly from the decay of neutral pions, and not from bremsstrahlung of electrons generated closer to the origin. Similarly, a pair found by direct scanning was accepted only if it was clear that it originated from an isolated  $\gamma$ -ray, i.e., there were no associated electron tracks within a radial distance of about 200  $\mu\text{m}$  of the pair origin. Sixty per cent of the selected electron tracks originated in jets.

Starting at the pair origins, scattering measurements were made along all electron tracks of length greater than one cm per emulsion. If the measured scattering over the first centimeter of track length indicated an energy inside the interval 1 GeV to 10 GeV, the track was accepted. It was then followed further and continuous scattering measurements taken, until the measured energy over the last section of track fell below 1 GeV (on account of radiation loss).

Although it had already been established that the *average* level of spurious scattering in the stack employed was extremely low, further checks were made on the validity of the energy estimates obtained from scattering observations. For example, observations of the relative multiple scattering between the two electrons of a pair were compared with the values of scattering obtained from each electron track separately. In the case of pairs associated with jets, scattering measurements were also performed on the tracks of neighbouring high energy shower particles. The results obtained again indicated that with the exception of two pairs which were rejected, the effects of spurious scattering in the particular locality of the pair were unimportant.

As a result of the above checks on the contribution from spurious scattering we are confident that systematic errors in the estimation of energies by the scattering method in the energy interval considered, cannot exceed 15%; the average degree of under-estimation of energy is certainly very much less.

Scattering measurements were made by the co-ordinate method, using 500  $\mu\text{m}$  cells, the mean scattering angle  $\bar{\alpha}$  being determined on each conse-

(12) P. H. FOWLER and C. J. WADDINGTON: *Phil. Mag.*, in press.

cutive centimeter of track by noise elimination between observed values of the second differences on 500, 1000 and 1500  $\mu\text{m}$  cells. If the values of  $\bar{\alpha}$  obtained in two or more consecutive intervals of one centimeter did not differ significantly, the average value of  $\bar{\alpha}$  for the entire segment of track was taken. The average number of independent cells on each segment of track was about 12, corresponding to a statistical uncertainty in  $\bar{\alpha}$  of  $\sim 25\%$ . The skewness in the energy distribution resulting from the small number of independent cells will result in a slight error in identifying the mean energy with the reciprocal of the mean angle of scattering.

In the process of following a selected electron track from its origin, the co-ordinates were recorded of all those secondary electron pairs which originated within a distance of 25  $\mu\text{m}$  from the parent electron track, as measured in the plane of the emulsion. When a secondary pair originated within 25  $\mu\text{m}$  of *either* electron of a primary pair, its parent was assumed to be that electron closer to it in space.

The energies of all secondary pairs were determined from scattering measurements. The energy spectrum obtained indicated that an appreciable fraction of pairs of energy less than 15 MeV escaped detection. In order, therefore, to ensure a uniform detection efficiency for secondary pairs irrespective of energy, we have excluded all pairs and apparent tridents having energies below 40 MeV.

## 2. - Results.

A total of 69 electron tracks from 54 pairs with an aggregate length of 219 cm fulfilled the acceptance criteria. Fig. 1 shows the observed distribution in the projected distance  $y$ , for the S2 secondary pairs, including apparent tridents, for which the energy exceeded 40 MeV. It is seen that the distribution is strongly peaked near the origin. In our experience, provided  $y$  exceeds about 0.4  $\mu\text{m}$ , the origin of a secondary pair can be clearly resolved from the parent electron track. In two cases, where the value of  $y$  was estimated to be less than 0.4  $\mu\text{m}$ , the pair and the primary electron track were clearly resolved in depth. There remain 9 cases in which the pair origin was not resolvable from the primary track either in depth or in the plane of the emulsion.

The details of our experimental results are shown in Table I. The number of B.S. pairs and apparent tridents are indicated in columns 2 to 8 corresponding to various intervals of longitudinal distance from the origins of the parent electron pairs.

The effective mean energy, at which theory and experiment are to be com-

pared, has been determined in a manner similar to that of BLOCK *et al.* (<sup>7</sup>). The mean crosssection was computed from the relation

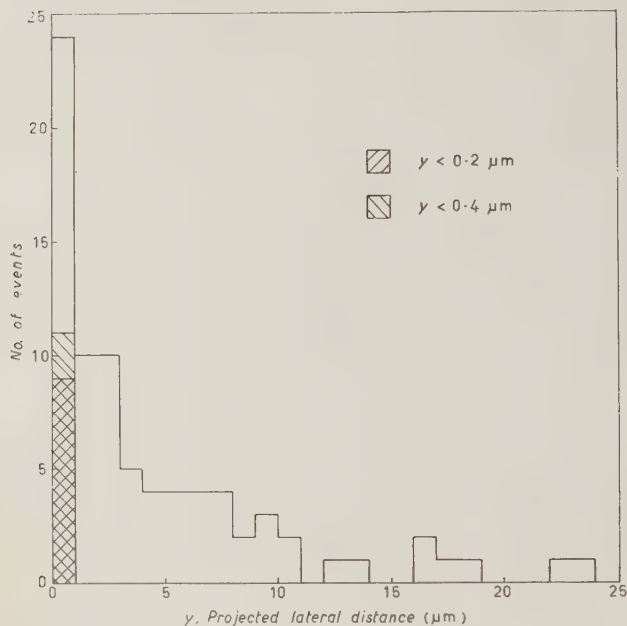


Fig. 1.

$$\sigma_{\text{mean}} = \frac{\sum \sigma_i(E_i) \cdot l_i}{\sum l_i},$$

where  $\sigma_i$  is the theoretical cross-section corresponding to the experimentally determined energy,  $E_i$ , of a particle of track-length  $l_i$ . This mean cross-section corresponds in our experimental conditions to a mean effective energy of 2.8 GeV, and a mean free path of 92 cm for trident production.

TABLE I. — Distance from origin of parent electron pair in radiation units.

	0.00 ÷ 0.05	0.05 ÷ 0.1	0.1 ÷ 0.2	0.2 ÷ 0.4	0.4 ÷ 0.8	0.8 ÷ 1.6	> 1.6	Total
Number of B. S. pairs with $y \geq 0.4 \mu\text{m}$	0	1	5	8	26	27	4	71
Number of B. S. pairs with $0.2 \leq y < 0.4 \mu\text{m}$	0	0	0	0	1	1	0	2
Number of apparent tridents, $y < 0.2 \mu\text{m}$	1	0	2	4	1	0	1	9
Number of apparent tridents, $y < 0.4 \mu\text{m}$	1	0	2	4	2	1	1	11



Alternatively the mean energy computed according to the relation

$$\left(\frac{1}{E}\right)_{\text{mean}} = \frac{\sum (1/E_i) \cdot l_i}{\sum l_i},$$

is 2.2 GeV, corresponding to an expected mean free path of 106 cm. The difference between these two values is due to the skewness in the energy determination mentioned before.

In order to derive a cross-section from the experimental observations, it is necessary to estimate the correction for pseudo-tridents. For this purpose we have used KAPLON and KOSHIBA's results (eqn. B5' of (2)), including the modifications suggested in their second paper (3). This expression was used in preference to their eqn. B6', since B5' extracts more detailed information from the observations provided that a sufficient number of B.S. pairs is available.

A rigorous expression for this correction would have to include the angular distribution of the emitted photon with respect to the scattered electron. KAPLON and KOSHIBA have assumed this distribution to be a Gaussian centred around zero. Now it is virtually certain that whatever the form of this distribution, its mode is not zero. Therefore our correction will tend to over-estimate the contribution from pseudo-tridents.

### 3. - Conclusions.

In Table II we have summarized the results of various authors together with the theoretical predictions. Since BLOCK *et al.* have shown that the original calculations of BHABHA have to be modified and are then in agreement with those of RACAH, the theoretical values according to the modified Bhabha formula (with the appropriate energy cut-off) are quoted. In column 2 we have included the number of events observed (tridents and pseudo-tridents) since the statistical error is determined by the total number of events and *not* by the number of true tridents after correction.

It is clear that the statistical weight of our results is low, so that the apparent agreement with theory, though gratifying, does not have great significance. Moreover, there is an uncertainty in the applied correction which comes mainly from our lack of knowledge of the true angular distribution of the emitted photons. Nevertheless, the difference between our results and those of the other authors who claim a serious discrepancy with theory, is significant. We suggest that this may be due to large systematic errors on their part, in the determination of energy of the parent electrons, in particular from the effects of spurious scattering.



We conclude that so far there is no reliable evidence to suggest that the trident cross-section at high energies ( $\sim 10$  GeV), is widely at variance with theoretical expectations. Moreover, since the results of PINKAU<sup>(13)</sup> have

TABLE II.

Energy (GeV)	Total No. of events observed	Estimated number of true tridents	Assumed resolving distance, in $\mu\text{m}$	Total track length (r.u.)	Number of tridents expected	Authors
1 : 10	4	3.5	0.2	15.7	0.45 : 1	KAPLON and KOSHIBA <sup>(2)</sup>
10 : 100	8	6.4	0.2	7.1	0.46 : 0.83	
8	11	6.7	0.2	20.6	1.3	KOSHIBA and KAPLON <sup>(2)</sup>
4.75	4	2.7	0.2	5.85	0.24	
100 : 1000	4	2.5	0.2	3.45	0.7 : 1.28	DEBENEDETTI <i>et al.</i> <sup>(4)</sup>
50	6	4	0.2	2	0.5	LOHRMANN <sup>(5)</sup>
0.4		11.8	0.2	500	10.2	BLOCK <i>et al.</i> <sup>(7)</sup>
2.8	9	3	0.2	75.5	2.4	Present work
	11	2.1	0.4	75.5		

The results of FRIED and NAUGLE<sup>(6)</sup> have not been included since these authors have not corrected for pseudo-tridents.

shown that the conversion length for photons at energies  $\sim 100$  GeV does not differ from the theoretical value, it appears that at present there exist no serious experimental reasons to doubt the validity of quantum electro-dynamics in this energy region.

\* \* \*

We wish to express our indebtedness to Professor C. F. POWELL for extending to us the hospitality of his laboratory.

We gratefully acknowledge the help of Mr. P. B. JONES with some of the measurements. We wish to thank Dr. R. H. DALITZ and many of our col-

<sup>(13)</sup> K. PINKAU: *Nuovo Cimento*, **3**, 1156 (1956).

leagues in the laboratory for many fruitful discussions and Mrs. M. HERMAN and Mrs. S. GATEHOUSE for scanning the plates.

C. D. wishes to thank the Government of Ceylon for a maintenance grant.

#### RIASSUNTO (\*)

Si è stimata la sezione d'urto dei tridenti prodotti da elettroni da 1 e 10 GeV. Le determinazioni dell'energia sono state effettuate per mezzo di misure di scattering su ogni traccia in condizioni in cui gli effetti dello scattering spurio risultavano trascurabili. Il numero di tridenti veri presenti in una lunghezza totale di traccia di 219 cm è risultato 3 contro i 2.4 predetti dalla teoria. Anche in base a tale piccolo numero di eventi, si ha una marcata discrepanza tra i nostri risultati e quelli di precedenti esperimenti ad alte energie. Si discutono le ragioni di tale discrepanza.

(\*) *Traduzione a cura della Redazione.*

## On the Problem of the Static Helium Film.

### I. - General Considerations and Density Distribution in the Film.

S. FRANCHETTI

*Istituto di Fisica dell'Università - Firenze*

(ricevuto il 24 Settembre 1956)

**Summary.** — The change in free energy when an amount of helium is moved from the bulk liquid to the film is analyzed and some of the terms in its expression are explicitly calculated. The dependence of the density in the film on the distance from the wall is studied, on the basis of the Van der Waals forces acting in the system. Two cases of experimental interest are numerically worked out.

#### 1. - Introduction.

The problem of the  $^4\text{He}$  film, in static conditions, is considered here in the light of a model for liquid  $^4\text{He}$  previously proposed by the Author <sup>(1)</sup>.

In this model, in agreement to London's view for He II, the superfluid is considered as formed by the atoms belonging to the fundamental state (between the individual particle states). The excited states, forming the normal fluid, are thought to fall in two classes: those having collective character and energy linearly dependent on momentum (phonons), and those having the character of individual particle motions with quadratic energy-momentum dependence, which are assimilated to Bloch waves <sup>(2)</sup>.

<sup>(1)</sup> S. FRANCHETTI: *Nuovo Cimento*, **12**, 743 (1954); **2**, 1127 (1955); *Conf. de Physique des Basses Températures*, Paris (1955), p. 124.

<sup>(2)</sup> The opposition to the introduction of the Bloch wave concept, or indeed that of individual motions, into the theory of liquid helium isotopes is not, in the opinion of the Author (and just in the case of *these* liquids), so firmly grounded as not to warrant the exploration of just the opposite attitude. This point, however, will not be discussed in detail here.

For the purposes of the present investigation it will be sufficient to treat the superfluid as a continuum extending throughout the liquid. As for the excitations, the « Bloch waves » can be treated as free moving particles with a suitable effective mass. The particle representation, on the other hand, is usual with phonons. Thus both types of excitations are represented as two Bose-Einstein gases filling the space of the liquid.

The formation of the film is attributed—in agreement with SCHIFF<sup>(3)</sup> and FRENKEL's theory—to the Van der Waals forces exerted by the wall on the atoms of the liquid.

The theory differs from the Schiff and Frenkel's one in that it takes into consideration some effects arising from the smallness of one of the geometrical dimensions of the system. These effects refer

- a) to the zero-point energy,
- b) to the « exciton gases » already mentioned.

Point a) has been considered for the first time by ATKINS<sup>(4)</sup>. Point b) is characteristic of the present treatment, and it will be seen that the « Bloch wave » contribution is the main one determining the dependence of the film on the temperature.

## 2. - The Equilibrium Equation and the Consideration of the Van der Waals Forces.

Clearly, the form of the static film is to be deduced from the condition of thermodynamical equilibrium for the system *film—bulk liquid*. To avoid useless complication, we shall assume that the external pressure is negligibly small, meaning that the work done by it contributes unimportant terms in the equilibrium equation (and not necessarily involving negligibility against atmospheric pressure). The thermodynamical function to be minimized is then the Helmholtz free energy  $F = U - TS$ .

Since the material constituting the film is retired from the bulk liquid, the procedure requires essentially to determine the *difference*  $\Delta F$  between the free energy of an amount of helium in the film and that of the same amount belonging to the bulk liquid

$$(1) \quad \Delta F = F_{\text{film}} - F_{\text{bulk}}.$$

(3) L. J. SCHIFF: *Phys. Rev.*, **59**, 839 (1941).

(4) K. R. ATKINS: *Canad. Journ. Phys.*, **32**, 347 (1954); *Paris Conf.*, p. 100. It may be mentioned here that the zero-point energy was considered for the first time in connection with the formation of the film (though from another standpoint) by A. BIJL, J. DE BOER and A. MICHELS: *Physica*, **8**, 655 (1941).

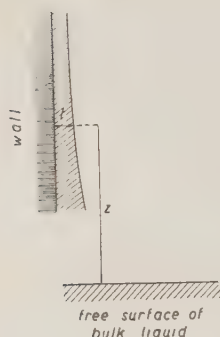


Fig. 1.

It will be convenient to refer to the free energy per  $\text{cm}^2$  of the film at a given height  $z$  above the free surface of the bulk liquid, where the thickness is  $t$  (Fig. 1).  $\Delta F$  is a function of  $z$  and  $t$  (and of course of the temperature  $T$ ).

Considering a strip 1 cm wide of the film between any two heights  $a$ ,  $b$ , the difference in free energy with respect to the bulk liquid will be  $\int_a^b \Delta F(z, t) dz$  and the condition of stability requires

$$\delta \int_a^b \Delta F(z, t) dz = 0,$$

where  $t(z)$  is our unknown. This gives immediately the equation

$$(2) \quad \frac{\partial}{\partial t} \Delta F(z, t) = 0.$$

There are four contributions to  $\Delta F$  arising from

- a) the Van der Waals forces (wall-helium and helium-helium)  $\Delta F_w$ ,
- b) the zero-point energy change  $\Delta E_0$ ,
- c) the exciton free energy change  $(\Delta F)_{\text{exc}}$ ,
- d) the gravitational energy change  $\Delta W_g$ ,

so that

$$(3) \quad \Delta F = \Delta F_w + \Delta E_0 + (\Delta F)_{\text{exc}} + \Delta W_g.$$

If  $\varrho(x, t)$  is the density in the film at a distance  $x$  from the wall, the gravity term can be written immediately as

$$(3') \quad \Delta W_g = \int_{x_0}^t \varrho(x, t) g x dx,$$

where  $x_0$  is some minimal distance from the wall (of the order of atomic dimensions). Since however the density change affects only a region small in comparison with the thickness of the film in current experiments, the above expression can be simplified in

$$(3'') \quad \Delta W_g = \varrho_0 g z t,$$

with  $\varrho_0$  the ordinary density of the liquid (under zero pressure).

To calculate  $\Delta F_w$  let us analyze the following imaginary experiment (Fig. 2). A sort of infinitesimal beaker, having infinitely thin indeformable walls, isolates in the interior of the liquid (A) an amount of liquid such that when brought on the wall it will have just the thickness  $t$  of the film.

We bring it first in B, at the surface of the liquid. There is an energy increase  $\gamma d\sigma$ : as a surface energy this can be decomposed in a potential term  $\gamma_p d\sigma$  and a dynamical one  $\gamma_d d\sigma$  (due to surface waves). Being an effect of the small He-He forces, a particularly rigorous treatment is not needed, and we shall assume that the dynamical term is  $t$ -independent. The other term can be interpreted as the potential energy with respect to the «lacking liquid». As such it can be written

$$(1) \quad \gamma_p d\sigma = - \frac{\rho_0 d\sigma}{m} \int_{x_l}^t V_{\text{He}}(x) dx.$$

Here:  $\rho_0$  is the density of the liquid ( $0.1445 \text{ g cm}^{-3}$ )<sup>(5)</sup>,  $m$  is the He atom mass ( $6.64 \cdot 10^{-24} \text{ g}$ ),  $x_l$  is some length of the order of the interatomic distance in the liquid and  $-V_{\text{He}}(x)$  is the potential energy of an He atom at a distance  $x$  from a plane beyond which there are He atoms uniformly distributed so as to give the density  $\rho_0$ . As is well known and is easily verified, if  $W(r) = -cr^{-6}$  is the potential energy between two atoms a distance  $r$  apart,  $V(x)$  is (at least as far as the distribution of attracting centers may be replaced by a continuous one) a negative third power function of  $x$  given by

$$(5) \quad V(x) = -\frac{\pi}{6} n c x^{-3} = -A x^{-3},$$

where  $n$  is the number of atoms per unit volume.

In the case of the He-He interaction here considered, we shall write

$$(6) \quad V_{\text{He}}(x) = -\frac{\pi}{6} \frac{\rho_0}{m} c_{\text{He-He}} x^{-3} = -A_{\text{He}} x^{-3}.$$

(5) We neglect the density change near the surface, which however will be considered in another connection at the end of Sect. 3.

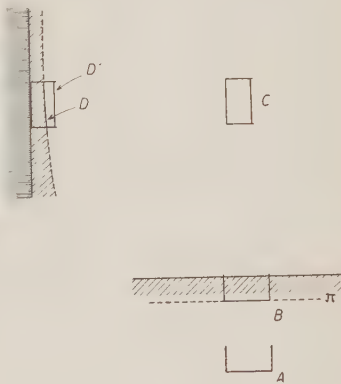


Fig. 2.



With  $c_{\text{He-He}} = 1.5 \cdot 10^{-60}$  (from currently accepted data) one finds

$$(6') \quad A_{\text{He}} = 0.17 \cdot 10^{-37} \text{ abs. un.}$$

With the aid of (6) and (6') expression (4) may be evaluated and the final result is

$$(7) \quad \gamma = \gamma_a + \frac{\varrho_0}{2m} A_{\text{He}} (x_l^{-2} - t^{-2}),$$

for the increase of energy per  $\text{cm}^2$  in going from  $A$  to  $B$ .

We then lift the beaker out of the liquid (position  $C$ ) performing a work which is the same as that just calculated, this time being done against the forces exerted by the liquid occupying the space below plane  $\pi$  in Fig. 2.

Summing up, in position  $C$  we find a free energy increase (per  $\text{cm}^2$ ) with respect to  $A$ :

$$(7') \quad \gamma_a + \frac{\varrho_0}{m} A_{\text{He}} (x_l^{-2} - t^{-2}).$$

The path  $ABC$  is imagined to be sufficiently removed from the wall so that the Van der Waals energy of the displaced liquid with respect to the wall remains everywhere at its highest value (taken to be zero).

We now allow the liquid, rested on some support, to approach the wall under the action of the Van der Waals forces, taking care, however to immobilize it, for instance by introducing in it infinitely thin rigid diaphragms normal to the lines of force. At the end (position  $D'$ ) the liquid will rest on the wall, which we suppose indeformable. Since nothing has changed within the liquid, the work performed by the forces has to be spent entirely outside the system thus giving a measure of the free energy decrease. The thickness reached in  $D'$  is of course not the final equilibrium value  $t$  and we shall write it as  $t + \Delta t'$ . The free energy change—that is the change of the Van der Waals potential energy—is therefore (per  $\text{cm}^2$ )

$$(8) \quad \frac{\varrho_0}{m} \int_{x_0}^{t + \Delta t'} V_f(x) dx,$$

where  $V_f(x)$  is the potential energy of a He atom at a distance  $x$  from the wall due to the mutual Van der Waals forces. (We label it with an  $f$  since it is just the cause of the formation of the film).

In the same approximation as before,  $V(x)$  is of the form (5) with  $n$  and  $c$  appropriate to the nature of the wall. We shall write

$$(9) \quad V_f(x) = -A_f x^{-3}.$$

Values for  $A_f$  may be deduced from the numerical data given by SCHIFF<sup>(3)</sup> or may be calculated following the indications given there, in particular on the basis of BARDEEN's paper<sup>(6)</sup>. An example of such calculation is given in the appendix.

With the aid of (9) the expression (8) can be written (taking advantage of the smallness of  $\Delta t'$ )

$$(8') \quad -\frac{\varrho_0}{2m} A_f (x_0^{-2} - t^{-2}) - \frac{\varrho_0}{m} A_f t^{-3} \Delta t'.$$

We now suppose that the liquid is allowed to compress under the action of the wall, going from situation  $D'$  to the final situation  $D$ . This brings the thickness to its true value  $t$  and is accompanied by a free energy change that requires careful consideration.

One of the effects of the compression is the *solidification* of the film's innermost layers. This is likely to involve free energy changes (at least when  $T=0$ ). However, the thickness  $t_s$  of the solidified layer, though temperature dependent, is—for any film thickness of experimental interest (say  $> 5 \cdot 10^{-7}$  cm)—practically rigorously  $t$ -independent. Thus the corresponding term contributes nothing to the fundamental equation (2). We just design it as  $E_{\text{sol}}$  and bother no longer about it.

For the main, non solidified part of the film, we have our model characterizing the liquid as an assembly distributed among quantum states. The population of the *fundamental state* (the superfluid) can give no contribution to the free energy change. Indeed, all that can happen to the superfluid (which is so to speak statistically structureless) in going from  $D'$  to  $D$  is an (adiabatic) change of a certain amount of Van der Waals potential energy into an equivalent amount of other forms of mechanical energy (internal potential and zero-point kinetic energies). As regards the *excited states*, they will be treated as a gas of excitons and will undergo free energy changes not only due to the fact of one dimension becoming very small<sup>(7)</sup>, but also because of the slight change of average specific volume, affecting such parameters as the velocity of sound or the effective mass. This is the only  $t$ -dependent contribution along  $D'D$  and its consideration will be deferred until we treat  $(\Delta F)_{\text{exc}}$ .

Summing up, we have for the change  $\Delta F_w$  due to Van der Waals forces, recalling (7') and (8')

$$(10) \quad \Delta F_w = \gamma_d + E_{\text{sol}} + \frac{\varrho_0}{2m} (2A_{\text{He}} x_l^{-2} - A_f x_0^{-2}) + \\ + \frac{\varrho_0}{2m} (A_f - 2A_{\text{He}}) t^{-2} - \frac{\varrho_0}{m} t^{-3} \Delta t'.$$

(6) J. BARDEEN: *Phys. Rev.*, **58**, 727 (1940).

(7) This effect will be dealt with in a paper to follow.

Of course, only the last two ( $t$ -dependent) terms will contribute to the equilibrium equation (2). Of these, the second is only a small correction<sup>(8)</sup>.

The effect on the zero point energy  $\Delta E_0$  and on the exciton gas  $(\Delta F)_{\text{exc}}$  mentioned in connection with eq. (3), will be considered in a forthcoming paper. However let it be noted that these effects, arising as they do, because of the *isolation* of a part of the system from the remaining, should find their place, in the ideal experiment symbolized in Fig. 2, in going from  $A$  to  $B$ , apart from a further effect, on  $(\Delta F)_{\text{exc}}$  only, in going from  $D'$  to  $D$ .

It is the evaluation of the latter effect that makes it necessary to study the density distribution in the film. This is the subject of the following section.

### 3. — The Density Distribution in the Film.

From hydrostatics we know that if a fluid with density  $\varrho(P)$  is subjected to a field of force of  $(\varrho/m)V(P)$  erg cm<sup>-3</sup> we must have

$$-\frac{\varrho}{m} \text{grad } V = \text{grad } p.$$

In our case  $V$  is the field of Van der Waals forces  $V_f(x)$ , so that

$$-\frac{\varrho}{m} \frac{dV_f}{dx} = \frac{dp}{dx},$$

whence

$$(11) \quad -\frac{1}{m} V_f = \int_0^p \frac{dp}{\varrho} + \text{const.}$$

A priori we should assume  $\varrho$  to be a function of  $x$  and  $t$ . However, as already mentioned, the region of changing density is small compared to the usual thickness of the film, (see graphs in Fig. 5), so that we may replace  $\varrho(x, t)$  by its limiting value  $\varrho(x, \infty) = \varrho(x)$ . According to our assumption of a negligible external pressure, we shall moreover assume that for  $x = t$  we have  $p = 0$  as well as  $V = 0$  (which would strictly require  $x = \infty$ ). The constant then drops from eq. (11) and we are left (recalling eq. (9)) with

$$(11') \quad \frac{A_f}{m} x^{-3} = \int_0^p \frac{dp}{\varrho} = I(\varrho).$$

(8) See values for  $\Delta t$ , which is greater than  $\Delta t'$ , at the end of Sect. 3.

To get  $\varrho(x)$  from this equation we need the function  $I(\varrho)$  both for liquid and solid He since the inner layers of the film are solidified.

Strictly speaking,  $I(\varrho)$  is not only different for the two states, but is also dependent on temperature. However this dependence is slight and the main influence of the temperature on the film comes through the strong raise of the melting point pressure with increasing temperature that causes the solid-liquid boundary to shift somewhat with varying  $T$ .

To avoid useless complication, we have computed  $I_{\text{sol}}(\varrho)$  at  $T = 0^\circ\text{K}$ , but the data of DUGDALE and SIMON<sup>(9)</sup> that were utilized show that there is practically no change for some degrees above absolute zero.  $I_{\text{liq}}(\varrho)$  was computed through an empirical relation which practically fits the data at any temperature between 0 and 3°K.

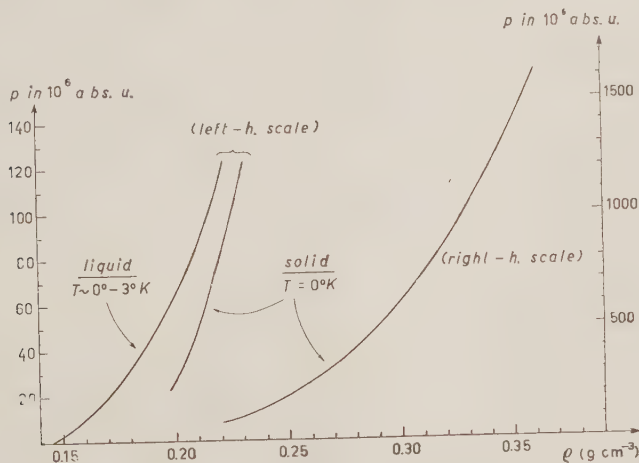


Fig. 3. - Dependence of the pressure on density in liquid and solid helium.

The relation in question was obtained by noting that in the said temperature range, the data of KEESOM<sup>(10)</sup> can be represented fairly well by the following formula for the compressibility

$$(12) \quad \chi = \frac{0.20}{p + 1.56 \cdot 10^7} \quad (\text{abs. un.}).$$

Inserting  $\chi = (1/\varrho)d\varrho/dp$ , the equation that obtains can easily be integrated,

<sup>(9)</sup> J. S. DUGDALE and F. E. SIMON: *Proc. Roy. Soc., A* **218**, 291 (1953).

<sup>(10)</sup> W. H. KEESOM: *Helium* (Amsterdam, 1942), p. 240.

with the result

$$(13) \quad \varrho = \varrho_0(1 + 6.41 \cdot 10^{-8} p)^{0.20}$$

or

$$(13') \quad p = 1.56 \cdot 10^7 \left[ \left( \frac{\varrho}{\varrho_0} \right)^5 - 1 \right].$$

With the aid of these formulae one finds

$$(14) \quad I_{\text{liq}}(\varrho) = \int_{\varrho_0}^{\varrho} \frac{dp(\varrho)}{\varrho} = 1.95 \cdot 10^7 \frac{1}{\varrho_0} \left[ \left( \frac{\varrho}{\varrho_0} \right)^4 - 1 \right].$$

No simple empirical relation could be fitted to DUGDALE and SIMON's data for solid helium, thus the integration for  $I_{\text{sol}}(\varrho)$  had to be performed numerically in this case.

Tables I and II and the graphs of Fig. 3 and 4 give the results together with the  $p(\varrho)$  curves. To obtain the density  $\varrho(x)$  at a given distance  $x$  from the wall we need simply—according to eq. (11')—to read out from the graphs for  $I(\varrho)$  the abscissa corresponding to the value of  $(A_f/m)x^{-3}$ . Use shall be made of either  $I_{\text{liq}}$  or  $I_{\text{sol}}$  according to whether the pressure turns out to be smaller or larger than  $p_m(T)$ , melting point pressure at the temperature considered <sup>(11)</sup>.

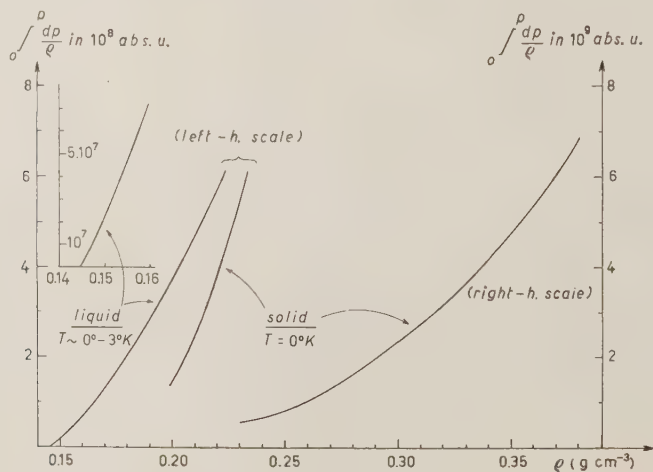


Fig. 4. — The function  $\int_{\varrho_0}^{\varrho} dp(\varrho)/\varrho = I(\varrho)$  in liquid and solid helium.

<sup>(11)</sup> In the case of the liquid, the computation may obviously be performed directly, by solving with respect to  $\varrho$  the equation that obtains eliminating  $I$  from (11') and (14).

TABLE I. -  $p$  versus  $\varrho$  in liquid and solid helium.  
( $\varrho$  in  $\text{g cm}^{-3}$ ,  $p$  in  $10^6$  abs. un.).

$\varrho$	$p_{\text{liq}}$ (0 $\div$ 3 $^{\circ}\text{K}$ )	$\varrho$	$p_{\text{sol}}$ (0 $^{\circ}\text{K}$ )	$\varrho$	$p_{\text{sol}}$ (0 $^{\circ}\text{K}$ )
0.1445	0	0.20	27.3	0.29	500
0.16	10.6	0.21	45	0.30	605
0.17	20.3	0.22	81	0.31	725
0.18	32.3	0.23	118	0.32	870
0.19	47.0	0.24	153	0.33	1025
0.20	64.6	0.25	200	0.34	1210
0.21	88.0	0.26	255	0.35	1400
0.22	117.0	0.27	320	0.36	1620
—	—	0.28	405	—	—

TABLE II. -  $I(\varrho) = \int_0^{\varrho} dp/\varrho$  in liquid and solid helium.  
 $I$  in  $10^8 \text{ erg g}^{-1}$ ,  $\varrho$  in  $\text{g cm}^{-3}$ ).

$\varrho$	$I_{\text{liq}}$ (0 $\div$ 3 $^{\circ}\text{K}$ )	$\varrho$	$I_{\text{sol}}$ (0 $^{\circ}\text{K}$ )	$\varrho$	$I_{\text{sol}}$ (0 $^{\circ}\text{K}$ )
0.1445	0	0.20	1.45	0.29	20.0
0.15	0.23	0.21	2.53	0.30	23.5
0.16	0.75	0.22	3.95	0.31	27.5
0.17	1.35	0.23	5.50	0.32	32.5
0.18	2.10	0.24	7.0	0.33	37.2
0.19	2.87	0.25	9.0	0.34	42.5
0.20	3.75	0.26	11.0	0.35	48.0
0.21	4.70	0.27	13.5	0.36	54.0
0.22	5.72	0.28	16.7	—	—

Two sorts of wall have been considered: a typical metal, i.e. copper, and a stearate layer (the latter in view of the experiments of JACKSON and collaborators <sup>(12)</sup>). A glass wall would give intermediate results (somewhat nearer to the metal). The values for the parameter  $A$  are

$$(15) \quad A_{\text{Cu}} = 5.3 \cdot 10^{-37}, \quad A_{\text{stear}} = 1.7 \cdot 10^{-37} \text{ (abs. un.)}.$$

(The first value is the same as in ref. <sup>(3)</sup> and the results should also hold for Al or Fe. For the second value see the appendix). The results are plotted in Fig. 5.



TABLE III. — *The contraction  $\Delta_l t$  of the liquid portion of the film, in Å, as a function of  $T$  (in °K).*

$T$	$\Delta_l t$ copper wall	$\Delta_l t$ stearate coated wall	$T$	$\Delta_l t$ copper wall	$\Delta_l t$ stearate coated wall
0	0.69	0.32	1.8	0.855	0.44
0.5	0.693	0.323	2.0	0.92	0.505
1.0	0.71	0.34	2.2	1.0	0.58
1.2	0.73	0.35	2.5	1.14	0.71
1.4	0.76	0.37	3.0	1.35	0.87
1.6	0.80	0.395	—	—	—

The graphs in Fig. 6 and 7 give the thickness  $t_s$  of the solid layer, the total contraction of the film  $\Delta t$  and the contraction  $\Delta_l t$  of the liquid layer (which is also given in Table III) as functions of the temperature. The latter quantities (which, as well as  $t_s$ , are independent of  $t$  for any film thickness encountered in current experiments) are defined as follows

$$(16) \quad \Delta t = \int_{x_0}^{\infty} \left( \frac{\rho(x)}{\rho_0} - 1 \right) dx - \Delta_s t,$$

$$(16') \quad \Delta_l t = \int_{t_s}^{\infty} \left( \frac{\rho(x)}{\rho_0} - 1 \right) dx - \Delta_s t.$$

The integrals appearing in these formulae represent the contraction of the film due to the attractive action of the wall <sup>(13)</sup>. The negative term  $-\Delta_s t$  is added because, with respect to the situation in the bulk liquid, there is also an *expansion* of the outer layers of

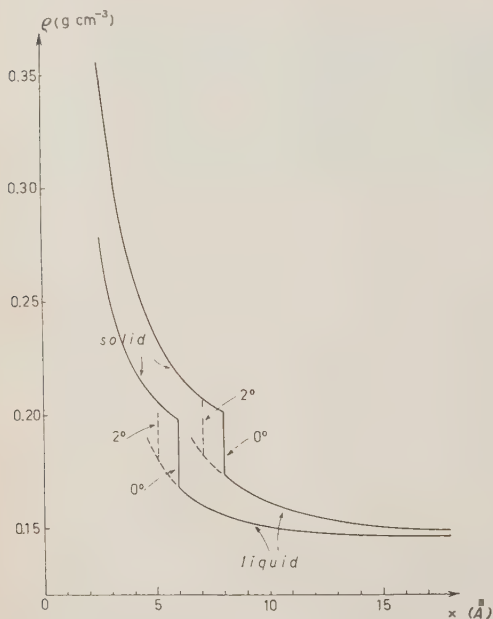


Fig. 5. — The density in the film as a function of the distance  $x$  from the wall. Upper curves: copper wall; lower curves: stearate coated wall.

the film, due to the absence of liquid beyond the free surface.

<sup>(12)</sup> In particular: A. C. HAM and L. C. JACKSON: *Phil. Mag.*, **45**, 1084 (1954).

<sup>(13)</sup> The integral in eq. (16) is just the quantity noted  $\Delta t'$  in expression (8). Of

A rigorous treatment of the latter feature—even at all feasible—would be out of proportion with the present aim which requires little more than an order of magnitude. For the purpose of a simple evaluation we shall therefore con-

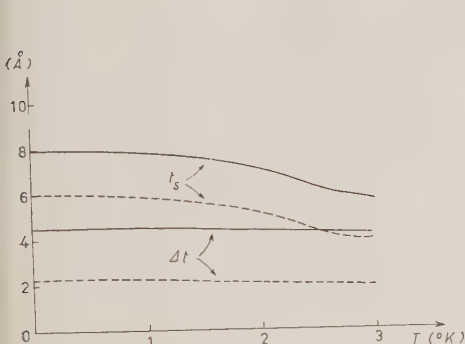


Fig. 6. — The thickness  $t_s$  of the solidified layer and the contraction  $\Delta t$  of the total thickness (i.e., the difference in thickness with respect to a layer having the same mass per  $\text{cm}^2$  and the density of the bulk liquid) as functions of the temperature. Full line: copper wall; broken line: stearate coated wall.

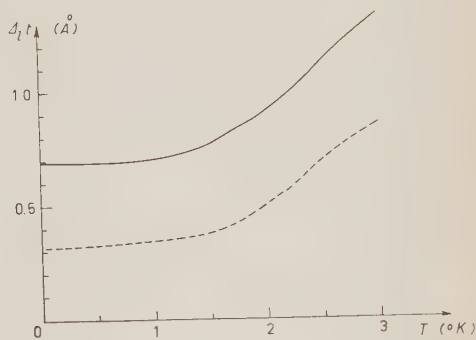


Fig. 7. — The contraction  $\Delta_l t$  of the liquid portion of the film (i.e. the difference between the thickness of the liquid layer and that of a layer having the same mass per  $\text{cm}^2$  and the density of the bulk liquid) as a function of the temperature. Full line: copper wall; broken line: stearate coated wall.

sider the effect of the lacking liquid as a negative pressure exerted on the liquid initially at density  $\varrho_0$ .

The problem then becomes exactly similar to that expressed by eq. (11) except that  $V_f(x)$  has to be replaced by  $-V_{\text{He}}(y) = A_{\text{He}} y^{-3}$  where  $y$  is the distance from the surface of the film. Since, moreover, the density changes are not large, the expression (14) for  $I_{\text{He}}(\varrho)$  can be simplified in

$$I_{\text{He}}(\varrho) = 5.4 \cdot 10^8 \left( \frac{\varrho}{\varrho_0} - 1 \right).$$

Equating to  $-(A_{\text{He}}/m)y^{-3}$  gives an expression for  $\varrho/\varrho_0 - 1$  which can imme-

the two equations (16) and (16'), it is the second that matters for the film theory, and this is fortunate, since the parameter  $x_0$  entering the first one is a somewhat uncertain quantity.

diately be integrated with the result

$$(17) \quad \Delta_s t = - \int_{x_l}^{\infty} \left( \frac{\rho}{\rho_0} - 1 \right) dx = 2.37 \cdot 10^{-24} x_l^{-2}.$$

For  $x_l$  a value  $3.2 \cdot 10^{-8}$  has been adopted (approximate interdistance of atoms in the liquid). To check this value one may compute  $(\rho_0/m) \int_{x_l}^{\infty} V_{\text{He}}(y) dy$ , that gives  $1.85 \cdot 10^{-16} x_l^{-2}$ . This should equal the surface energy if this quantity were of static origin only. In fact, with  $x_l = 3.2 \cdot 10^{-8}$  one gets  $0.18 \text{ erg cm}^{-2}$ , which is about half the surface energy at  $0^\circ \text{K}$ . This is in qualitative agreement with Atkins' finding that the static and dynamic contributions to the surface energy are of the same order of magnitude at absolute zero <sup>(14)</sup>.

We have then, inserting the above value in (17)

$$(17') \quad \Delta_s t \approx 0.23 \cdot 10^{-8} \text{ cm}.$$

From the value of  $\Delta_l t$  the average relative change of the specific volume for the liquid phase can be computed. Clearly, if  $v$  is the average specific volume for the liquid in the film and  $v_0$  that of the bulk liquid, we have

$$(18) \quad \frac{v}{v_0} = \frac{t}{t + \Delta_l t},$$

from which follows <sup>(15)</sup>

$$(18') \quad \frac{\partial v}{\partial t} = v_0 \frac{\Delta_l t}{(t + \Delta_l t)^2}.$$

These relations will be useful later.

\* \* \*

It is a pleasure for the Author to thank Prof. F. E. SIMON for having kindly pointed out the data in ref. (9) on which the calculations of Sect. 3 are based. Thanks are also due to Prof. E. FERRONI, of the Physical Chemistry Institute, Florence University, for interesting literature data about stearates.

<sup>(14)</sup> K. R. ATKINS: *Canad. Journ. Phys.*, **31**, 1165 (1953).

<sup>(15)</sup> Do not confuse  $\Delta_l t$ , a physical ( $t$ -independent) parameter, with any arbitrary variation of  $t$ .

## APPENDIX

## Van der Waals Forces between Helium and a Stearate Wall.

We consider a helium atom acted upon by a wall, that is a uniform indefinite distribution — bounded by a plane — of attracting centers, each acting according to a potential  $-er^{-6}$  (and lying sufficiently close together to be replaced by a continuous distribution).

From the simplified formula (53) of Bardeen's paper <sup>(6)</sup> one gets for  $c$

$$c = \frac{3}{2} \frac{A \cdot A_{\text{He}} \alpha \alpha_{\text{He}}}{A + A_{\text{He}}},$$

where  $A$  and  $\alpha$  are ionization potential and polarizability for the «centers of force» in question, and  $A_{\text{He}}$ ,  $\alpha_{\text{He}}$  the same quantities for He. From known data this gives

$$c = 1.57 \cdot 10^{-35} \cdot \frac{1}{A + 24.6} \alpha,$$

( $A$  in electron volt). From this and eq. (5) of the present paper we have for the constant  $A$  in the expression  $-Ax^{-3}$  for the potential energy of a He atom at a distance  $x$  from the wall

$$A = \frac{\pi}{6} 1.57 \cdot 10^{-35} \frac{1}{A + 24.6} \alpha n,$$

$n$  being the number of attracting centers per unit volume.

For the polarizability one has the formula

$$\alpha = \frac{3}{4\pi} \frac{\epsilon - 1}{\epsilon + 2} \frac{1}{n},$$

so that

$$(A.1) \quad A = 1.96 \cdot 10^{-38} \cdot \frac{A}{A + 24.6} \frac{\epsilon - 1}{\epsilon + 2}.$$

To meet the requirement of a sufficiently dense distribution of centers of force when applying this formula to a stearate «wall» one has to consider each molecule as formed by smaller units, independently polarizable. This however does not look as too heavy an assumption, considering moreover that the choice of the «submolecules» is immaterial. (Their number per unit volume disappears from (A.1)).

Since in practice we have a mono-layer with the «dipolar» part of the molecule lying *away* from helium, the effect will be more or less that of non-

polar linear-chain molecules, as for instance paraffin. From the value of  $\epsilon$  for paraffin and taking into account the increase of density, one finds a value 2.27 for  $\epsilon$  in the stearate. For  $A$  a value of about 10 eV seems appropriate for a long chain paraffin <sup>(16)</sup>. With these data formula (A.1) gives

$$(A.1') \quad A_{\text{stear}} = 1.7 \cdot 10^{-37} \text{ abs. un. ,}$$

a substantially lower value than for a metal or a glass. ( $A_{\text{Cu}} = 5.3 \cdot 10^{-37}$ , while  $A_{\text{glass}} \approx 4.3 \cdot 10^{-37}$ ) <sup>(17)</sup>. However, one must remember that all these quantities, especially when obtained from simplified formulae, are estimates rather than exact values. The graphs in Fig. 5, 6 and 7 and the data in Table III are therefore correct only to the extent that the above constants are.

<sup>(16)</sup> LANDOLT-BÖRNSTEIN: *Zahlenwerte und Funktionen*, 6<sup>a</sup> ed., Vol. I, 3, p. 36.

<sup>(17)</sup> The latter value can be obtained from eq. (A.1) introducing suitable data.

---

#### RIASSUNTO

Si analizza il cambiamento di energia libera che accompagna il trasferimento di una data quantità di elio dalla massa liquida al film. Alcuni termini dell'espressione di questa grandezza vengono calcolati esplicitamente. Si studia inoltre la dipendenza della densità nel film dalla distanza dalla parete, sulla base delle forze di Van der Waals agenti nel sistema. Vengono ricavati i risultati numerici in due casi di particolare interesse sperimentale.

## On the Decay of $^{132}\text{Cs}$ .

K. S. BHATKI, R. K. GUPTA and S. JHA

*Tata Institute of Fundamental Research - Bombay*

(ricevuto il 25 Settembre 1956)

**Summary.** — Gamma rays from 7 day  $^{132}\text{Cs}$  have been studied in a scintillation spectrometer with a large well-type NaI crystal. In addition to the 670 keV  $\gamma$ -ray, 1080 keV, 1200 keV, and 1300 keV  $\gamma$ -rays have been observed. From the sum peaks, levels in  $^{132}\text{Xe}$  at 670 keV, 1440 keV, 1960 keV and 2200 keV are inferred. From the sum peak areas, the intensities of electron capture to different levels have been estimated. A tentative decay scheme has been suggested.

### 1. - Introduction.

The isotope  $^{132}_{55}\text{Cs}$  has been reported to decay by electron capture with a half-life of 7.1 days <sup>(1-4)</sup>. It is known that a  $\gamma$ -ray of energy of 670 keV is emitted in the process <sup>(1-4)</sup>. In the process  $^{132}_{55}\text{Cs} \rightarrow ^{132}_{54}\text{Xe}$ ,  $\beta$ -decay systematics <sup>(5)</sup> predict the decay energy to be about 2 MeV, and in the process  $^{132}_{55}\text{Cs} \rightarrow ^{132}_{56}\text{Ba}$  a decay energy of about 1.2 MeV.

### 2. - The Details of the Present Studies.

The isotope  $^{132}_{55}\text{Cs}$  was obtained by the irradiation of caesium chloride with protons of about 25 MeV in the Oak Ridge cyclotron by the reaction  $^{133}_{55}\text{Cs}(\text{p}, \text{pn})^{132}_{55}\text{Cs}$ . Barium 133 that was produced by the  $(\text{p}, \text{n})$  reaction was removed

<sup>(1)</sup> M. CAMAC: *Plutonium Project CC-2409*.

<sup>(2)</sup> A. H. WAPSTRA, N. F. VERSTER and M. BOELHOUWER: *Physica*, **19**, 138 (1953).

<sup>(3)</sup> M. LANGER and G. FORD: unpublished.

<sup>(4)</sup> B. SARAF: *Phys. Rev.*, **94**, 642, (1954).

<sup>(5)</sup> K. WAY and M. WOOD: *Phys. Rev.*, **94**, 119 (1954).



from the target material by the perchlorate method. It was purified finally in an ion exchange column with Dowex 50.

The radiations were studied in a scintillation spectrometer with a Harshaw NaI(Tl) well-type crystal,  $4'' \times 4''$  in size and a Du Mont photomultiplier, model 6364. The spectra of the  $\gamma$ -rays emitted from  $^{132}\text{Cs}$ , with the source outside and inside the well of the scintillator, are shown in Fig. 1 and Fig. 2.

In Fig. 1, which shows the spectrum of the  $\gamma$ -rays with the source outside the well of the scintillator, there are peaks at 670 keV, 1080 keV, 1200 keV and 1300 keV. At the high energy end of the 670 keV peak, there is a small intensity peak at 770 keV. Corrected for the efficiency of detection, the intensities of the 1080 keV, 1200 keV and 1300 keV  $\gamma$ -rays are about 0.6%, 0.6% and 1% respectively of the intensity of the 670 keV  $\gamma$ -ray. In Fig. 2, which shows the spectrum of the  $\gamma$ -rays of  $^{132}\text{Cs}$  with the source in the well of the crystal, there are peaks at 670 keV, 1080 keV, 1440 keV and at about 1960 keV and 2200 keV. The low intensity

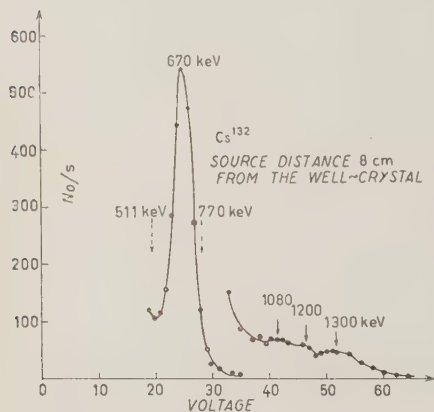


Fig. 1.

peak at 1300 keV, appearing clearly in Fig. 1, gets smeared when the source is in the well of the crystal. It has been shown by the studies of Lu *et al.* <sup>(6,7)</sup> that the peak at the high energy end of the spectrum that appears when the source is in the well of a large scintillator represents the maximum decay energy radiated in the form of  $\gamma$ -rays. This is so provided that there are no isomeric states of the daughter isotope involved in the decay process. One would thus conclude that the maximum energy radiated in the form of  $\gamma$ -rays in the decay of  $^{132}\text{Cs}$  is about

2200 keV. The intensities of the sum peaks at 1440 keV, 1960 keV and 2200 keV in comparison to the intensity of the  $\gamma$ -ray peak at 670 keV are about 1.5%, 0.4% and 0.15% respectively. These peaks continued appearing with the same relative intensities in spite of repeated chemical purifications. They decayed with the half life of about 7 days. One can, therefore, be reasonably certain that they are all due to the radiations from  $^{132}\text{Cs}$ .

<sup>(6)</sup> D. C. LU and M. L. WIEDENBECK: *Phys. Rev.*, **95**, 501 (1954).

<sup>(7)</sup> D. C. LU, W. H. KELLY and M. L. WIEDENBECK: *Phys. Rev.*, **95**, 121, 1533 (1954); **97**, 139 (1955).

Since the  $\beta$ -decay systematics predict for the process  $^{132}_{55}\text{Cs} \rightarrow ^{132}_{54}\text{Xe}$  a decay energy of about 2 MeV and our results show that it must be more than 2.2 MeV, it is reasonable to expect that  $^{132}\text{Cs}$  may decay by the emission of positrons also. The annihilation radiation of 510 keV should then show up in the spectrum in Fig. 1. There is no peak visible at this energy. It has been estimated that the annihilation radiation is not emitted with an intensity of more than about 2% of the intensity of the 670 keV  $\gamma$ -ray.

In order to explore the possibilities of the existence of  $\beta$ -emission from  $^{132}\text{Cs}$ , a source, weighing a few milligrams, was deposited on a thin mica piece, and the radiations from it were examined in a scintillation spectrometer with a stilbene crystal. Making allowance for the Compton electron due to the 670 keV  $\gamma$ -ray, the count of electrons gave an upper limit of  $\beta$ -branching at about 5%.

### 3. - The Decay Scheme of $^{132}\text{Cs}$ .

The occurrence of the sum peaks at 1440 keV, 1960 keV and 2220 keV shows that there are levels in the decay product of  $^{132}\text{Cs}$  at these energies in addition to

the one at 670 keV, and that these de-excite themselves by the emission of  $\gamma$ -rays in cascade. These levels are attributed to the decay process  $^{132}_{55}\text{Cs} \rightarrow ^{132}_{54}\text{Xe}$  because the decay energy in this process has been estimated to be about 2 MeV, and because these levels correspond, as can be seen from Fig. 3, to the levels, which arise in the decay process  $^{132}_{53}\text{I} \rightarrow ^{132}_{54}\text{Xe}$  (<sup>8</sup>). Although there is no level at about 2.2 MeV excited in the decay of  $^{132}\text{I}$ , it has been found necessary to attribute this level to  $^{132}\text{Xe}$ , because the sum peak at this energy continued appearing after repeated chemical purifications and decayed with a half-life of about 7 days. When the source is kept outside the well of the crystal, and sufficiently away from it, one observes two  $\gamma$ -ray peaks at 1080 keV and 1200 keV. It is presumed that they arise due to the de-excitation of the level at 2.2 MeV and that it is these  $\gamma$ -rays which sum up, when the source

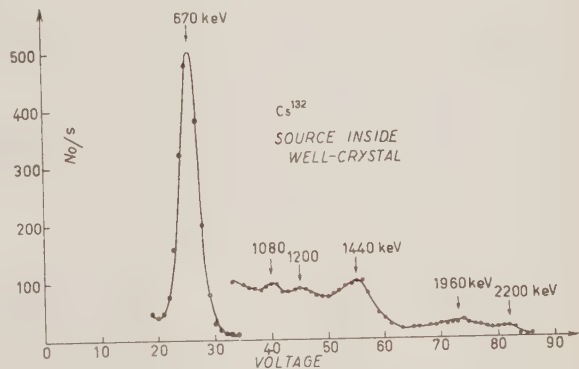


Fig. 2.

(<sup>8</sup>) H. L. FINSTON and W. BERNSTEIN: *Phys. Rev.*, **96**, 71 (1954).

is in the well of the scintillator, to give a peak at about 2200 keV. This explanation demands also the existence of a level in  $^{132}\text{Xe}$  at 1080 keV or 1200 keV, which does not arise in the decay of  $^{132}\text{I}$ . The sum peak at 1960 keV is interpreted to arise from the summing of the 1300 keV and the 670 keV  $\gamma$ -rays. This sum peak can also arise from the summing of 670 keV, 770 keV and a possible 520 keV  $\gamma$ -rays. Lastly the sum peak at 1440 keV can arise from the summing of the 670 keV and 770 keV  $\gamma$ -rays.

If the interpretation of the sum peaks given here is correct, it is possible to make an estimate of the intensities of different branches by which a state de-excites itself. One can see from Fig. 3 that the state at 1960 keV can de-excite itself by the emission of the following cascade  $\gamma$ -rays, a) 670 keV + 1300 keV; b) 670 keV + 770 keV + 520 keV. Let us suppose that the intensities of the two channels are  $n_1$  and  $n_2$  respectively in comparison to the intensity of the 670 keV  $\gamma$ -ray. The photoelectric efficiencies of the scintillator for the detection of these  $\gamma$ -rays have been estimated<sup>(9)</sup>, when the source is in the well of the scintillator, to be  $E_{1300 \text{ keV}} = 0.25$ ,  $E_{770 \text{ keV}} = 0.45$ ,  $E_{670 \text{ keV}} = 0.5$  and  $E_{520 \text{ keV}} = 0.7$ . Then the area of the sum peak at 1960 keV,  $S_{1960}$ , which represents the total number of coincidences in these two channels, is given by

$$S_{1960} = n_1 E_{1300} E_{670} + n_2 E_{520} E_{670} E_{770}.$$

One knows from the spectrum in Fig. 1 that  $n_1$  is about 1% of the intensity of the 670 keV  $\gamma$ -ray. Then one gets for the other branch an intensity  $n_2 \sim 1\%$

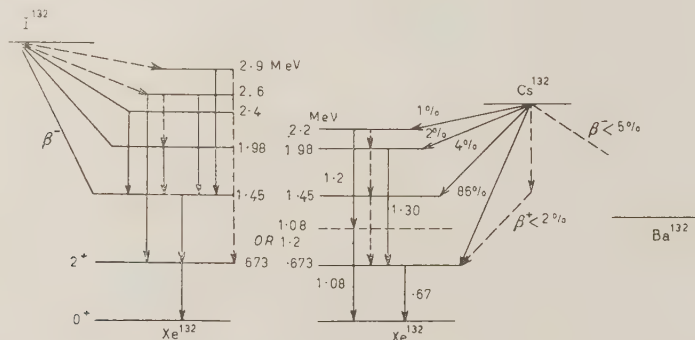


Fig. 3.

of the intensity the 670 keV  $\gamma$ -ray. Similarly, considering the area of the sum peak at 1440,  $S_{1440}$ , one gets

$$S_{1440} = n E_{670} E_{770},$$

<sup>(9)</sup> R. K. GUPTA and S. JHA: *Nuclear Physics*, **1**, 2 (1956).

where  $n$  is the intensity of the 770 keV  $\gamma$ -ray in comparison to the 670 keV  $\gamma$ -ray, with which it sums up in the well of the crystal to give a sum peak at 1440 keV. One gets for  $n$  a value of about 4%. One can similarly consider the sum peak at 2200 keV. One finds that the intensity of the possible branching 240 keV + 520 keV + 770 keV + 670 keV is about 0.5% of the intensity of the 670 keV  $\gamma$ -ray.

Considering all these together, one gets the percentages of the electron capture decay leading to the levels at 2200 keV, 1960 keV, 1440 keV and 670 keV, which have been estimated to be about 1%, 2%, 4% and 86% respectively.  $^{132}\text{Cs}$  decays by positron emission in less than 2% cases and by  $\beta^-$ -emission in less than 5% cases. On the basis of these results, the decay scheme of  $^{132}\text{Cs}$  has been given in Fig. 3.

#### 4. - Discussion.

On account of the small specific activity of the source of  $^{132}\text{Cs}$  at our disposal and rather small resolution of the spectrometer in the present studies, the intensity values given above are only approximate. The accuracy of this method of finding out the intensity of the cascade  $\gamma$ -rays depends on the accuracy with which the sum peak areas can be measured and the corrections applied for the continuous spectrum due to the summing of the photo-peak pulses and the compton hump pulses.

Although the  $\beta$ -decay systematics predict only about 2 MeV for the decay energy in the process  $^{132}_{55}\text{Cs} \rightarrow ^{132}_{54}\text{Xe}$ , it must be a little more than 2.2 MeV. In such a case, the log ft. values for the electron capture decay to the 1960 keV, 1440 keV and 670 keV levels are about 7. The first excited state of  $^{132}\text{Xe}$  at 670 keV has, presumably, the spin and parity 2-. If the electron capture decay of  $^{132}\text{Cs}$  is of the first forbidden character, the parity of  $^{132}\text{Cs}$  must be odd and may have a spin 1. It may be pointed out that in the decay of  $^{132}\text{Cs}$ , a level in  $^{132}\text{Xe}$  has been observed at 2.2 MeV, which does not appear in the decay of  $^{132}\text{I}$  and which is interpreted as decaying by the emission of cascade  $\gamma$ -rays of energies 1080 keV and 1200 keV. The state at 2.2 MeV must have a spin of low value, and this may possibly be the reason why it does not appear in the decay of  $^{132}\text{I}$ , to which spin and parity  $4^-$  have been assigned. It may be observed that the appearance of such high energy levels in the decay of  $^{132}\text{Cs}$  requires a high value for the decay energy, which then makes the decay have the first forbidden character. This requires  $^{132}\text{Cs}$  to have an odd parity, although the shell model predicts an even parity. Similar situation arises in the decay of the neighbouring isotopes  $^{130}\text{I}$  <sup>(10)</sup> and  $^{134}\text{Cs}$  <sup>(11)</sup>, which are all

<sup>(10)</sup> A. C. G. MITCHELL: *Beta and Gamma-ray Spectroscopy* (Amsterdam, 1955).

<sup>(11)</sup> R. W. KING: *Rev. Mod. Phys.*, **26**, 327 (1954).

assigned an odd parity, although for each of them the shell model predicts an even parity.

\* \* \*

Our sincere thanks are due to Dr. P. RADHAKRISHNA for his advice in the purification of the  $^{132}\text{Cs}$  source. We thank Dr. B. V. THOSAR for many helpful discussions.

#### RIASSUNTO (\*)

In uno spettrometro a scintillazione con un grande cristallo di NaI cavo si sono studiati i raggi  $\gamma$  del  $^{132}\text{Cs}$  di 7 giorni. Oltre ai raggi  $\gamma$  di 670 keV, si sono osservate radiazioni di raggi  $\gamma$  di 1080 keV, 1200 keV e 1300 keV. I picchi di somma lasciano supporre per il  $^{132}\text{Xe}$  l'esistenza di livelli a 670 keV, 1440 keV, 1960 keV e 2200 keV. In base alle aree dei picchi di somma si sono stimate le intensità delle catture elettroniche a differenti livelli. Si suggerisce un ipotetico schema di decadimento.

(\*) Traduzione a cura della Redazione.

## Confirmation de la période du Thorium-232.

E. PICCIOTTO et S. WILGAIN (\*)

*Laboratoire de Physique Nucléaire, Université Libre de Bruxelles*

(ricevuto il 27 Settembre 1956)

**Résumé.** — La période du  $^{232}\text{Th}$  est déduite de l'activité du  $^{228}\text{Th}$  mesurée par les étoiles de désintégrations successives dans les émulsions nucléaires. On trouve  $T = 1.39 \cdot 10^{10}$  ans avec une dispersion relative de  $\pm 2\%$ , en parfait accord avec la valeur de KOVARIK et ADAMS.

Les âges géologiques des minerais radioactifs mesurés d'après le rapport  $^{208}\text{Pb}$   $^{232}\text{Th}$  sont généralement plus faibles que les âges calculés d'après les rapports Pb/U. Le travail récent de WASSERBURG et HAYDEN <sup>(1)</sup> montre notamment un écart systématique qui pourrait s'expliquer par une erreur par défaut de 10 à 15% sur la valeur utilisée pour la période du Thorium qui est celle de KOVARIK et ADAMS <sup>(2)</sup>,  $T = 1.39 \cdot 10^{10}$  ans ou  $\lambda = 1.58 \cdot 10^{-18} \text{ s}^{-1}$ .

Une nouvelle détermination a été récemment effectuée pendant le cours de ce travail par LAZAR, SENFTLE et FARLEY <sup>(3)</sup>. Ces auteurs se basant sur l'activité  $\gamma$  du Th( $^{232}\text{Th}$ ) en équilibre obtiennent  $T = 1.40 \cdot 10^{10}$  ans avec une incertitude évaluée à  $\pm 5\%$ .

Lors de la mise au point d'une méthode de microdosage du Th, nous avons été amenés à vérifier la période du  $^{232}\text{Th}$  par une voie différente. Nous donnons ici les résultats en réservant à une autre publication la description des détails expérimentaux et les applications analytiques de la méthode.

La période du Thorium a été déduite de l'activité du Radiothorium en équilibre, activité mesurée par les étoiles d'x à 5 branches produites par ce nucléide dans les émulsions photographiques nucléaires.

(\*) Attachée à l'Institut Interuniversitaire des Sciences Nucléaires.

<sup>(1)</sup> G. J. WASSERBURG et R. J. HAYDEN: *Geochim. et Cosmochim. Acta*, **7**, 51 (1955).

<sup>(2)</sup> A. F. KOVARIK et N. I. ADAMS: *Phys. Rev.*, **54**, 413 (1938).

<sup>(3)</sup> N. H. LAZAR, F. E. SENFTLE et T. FARLEY: ORNL, 1975, *Progress Report*, (1956) p. 43.



Deux solutions étalons de  $\text{Th}(\text{NO}_3)_4$  ont été utilisées: l'échantillon Th I, provenant de l'Institut Océanographique de Göteborg était vieux de plus de 50 ans et pratiquement en équilibre. Th II est un échantillon provenant de l'Institut du Radium de Paris, dans lequel le Mésothorium a été séparé en 1931.

La concentration en Thorium a été mesurée par pesée de l'oxyde après calcination du nitrate. Plusieurs gravimétries ont été effectuées sur chaque solution et concordent à  $\pm 0.3\%$ . La pureté chimique du Thorium ( $> 99\%$ ) a été vérifiée par comparaison spectrophotométrique avec une solution de Thorium spectrographiquement pure, en utilisant la coloration spécifique formée avec le « Toron ».

L'activité spécifique en étoiles à 5 branches a été mesurée par la méthode de la double émulsion <sup>(4)</sup>. Des gouttes de  $2 \cdot 10^{-3}$  ml ont été déposées à l'aide d'une microseringue Agla sur des émulsions Ilford C-2 et recouvertes après séchage d'une seconde couche d'émulsion. Le volume des gouttes a été calibré par pesée. Les plaques ont été développées après des temps d'exposition variant de 4 à 27 jours. Le nombre total d'étoiles à 5 branches émises dans chaque goutte a été compté. Les conditions d'exposition et de développement ainsi que la résolution des problèmes posés par la diffusion du Thoron seront discutées ailleurs.

La constante radioactive du  $^{232}\text{Th}$  est donnée par:

$$\lambda = \frac{S_5 \cdot f(t)}{N \cdot t},$$

$$S_5 \cdot f(t) = n_{\text{RdTh}} = n_{\text{Th}} \cdot \varphi,$$

$N$  = nombre d'atomes de  $^{232}\text{Th}$  présents dans une goutte;

$t$  = temps d'exposition;

$S_5$  = nombre d'étoiles à 5 branches émises par une goutte durant le temps  $t$ ;

$f(t)$  = rapport du nombre de désintégrations du RdTh au nombre d'étoiles à 5 branches. Ce facteur a été calculé d'après les formules de FLAMENT <sup>(5)</sup> et de SENFLE, FARLEY et STIEFF <sup>(6)</sup>;

$n_{\text{RdTh}}$  et  $n_{\text{Th}}$  = nombre de désintégrations du RdTh et du Th par goutte, durant le temps  $t$ ;

$$\varphi = n_{\text{RdTh}}/n_{\text{Th}}.$$

<sup>(4)</sup> E. E. PICCIOTTO: *Compt. Rend.*, **228**, 2020 (1949).

<sup>(5)</sup> R. FLAMENT: *Bull. Centre Phys. Nucl. Univ. Bruxelles*, n. 3 (1948).

<sup>(6)</sup> F. E. SENFLE, T. A. FARLEY et L. R. STIEFF: *Geochim. et Cosmochim. Acta*, **6**, 197 (1954).

L'incertitude sur  $N$  est estimée à  $\pm 1\%$ , elle dépend des erreurs sur le titre des solutions et le volume moyen des gouttes.

Le facteur  $f(t)$ , comme on le voit clairement dans la formulation de Flament, dépend surtout de la période du Th X qui est connue à mieux que  $1\%$  près: il est pratiquement indépendant des périodes des autres membres de la famille du Thorium.

Le facteur d'équilibre  $\varphi$  vaut 1, ( $> 0.995$ ) pour la solution Th I. Pour la solution Th II, purifiée en 1931, il a été calculé égal à 0.867 (en 1954) en utilisant les équations de Bateman avec les valeurs suivantes des périodes:  $T_{\text{MsTh}} = 6.7$  ans et  $T_{\text{RdTh}} = 1.9$  an. Il faut souligner que  $\varphi$  est peu sensible aux variations de  $T_{\text{MsTh}}$  et  $T_{\text{RdTh}}$ ; un changement de  $10\%$  sur  $T_{\text{MsTh}}$  ou  $T_{\text{RdTh}}$  introduit respectivement une variation de  $1\%$  et  $0.3\%$  sur  $\varphi$ .

Les valeurs de  $\lambda$  obtenues à partir des deux solutions étalons sont données au Tableau I. Sur 30 gouttes comptées, une seule a conduit à un résultat nettement aberrant (écart à la moyenne de  $5 \times \sigma$ ) qui a été exclu du calcul de la moyenne.

TABLEAU I.

	Th par goutte en $10^{-9}$ g	Nombre de gouttes	Nombre total d'étoiles à 5 branches	$\lambda$ en $10^{-18}$ s $^{-1}$	$\sigma$ relatif expéri- mental	$\sigma$ relatif théorique
Th I	33.1	10	1298	1.60	$\pm 2\%$	$\pm 2.8\%$
Th II	29.3	19	1894	1.57	$\pm 1.5\%$	$\pm 2.3\%$

$\lambda$  = moyenne des valeurs obtenues à partir de chaque goutte, pondérée d'après les nombre d'étoiles de la goutte.

$\sigma$  expérimental = dispersion relative calculée à partir des écarts expérimentaux par rapport à la valeur moyenne de  $\lambda$ .

$\sigma$  théorique = dispersion relative théorique sur le nombre total d'étoiles comptées pour chaque échantillon.

Les dispersions expérimentales sur les moyennes sont du même ordre, et même inférieures, à la dispersion théorique due aux fluctuations statistiques du nombre de désintégrations: c'est principalement ce dernier facteur qui limite la précision de notre détermination de  $\lambda$ .

En prenant la moyenne pondérée des déterminations sur les deux solutions, on trouve

$$\lambda = (1.58 \pm 0.03) \cdot 10^{-18} \text{ s}^{-1}$$

correspondant à  $T = (1.39 \pm 0.03) \cdot 10^{10}$  ans.

Cette valeur est en parfait accord avec celle de KOVARIK et ADAMS et de LAZAR *et al.* Il semble exclu que la valeur admise pour la période du  $^{232}\text{Th}$  puisse être erronée de plus de 5 %: les différences systématiques dans les mesures d'âge mentionnées plus haut doivent être attribuées à une autre cause.

\* \* \*

Nous remercions les Dr. F. KOCZY, M. HAÏSSINSKY et G. BOUSSIÈRES pour les échantillons de Thorium âgé, le Dr. M. HUYBRECHTS pour l'interprétation statistique des résultats et le Dr. F. SEXTLE pour la communication de résultats encore inédits.

#### RIASSUNTO (\*)

Dall'attività del  $^{228}\text{Th}$  misurata per mezzo delle stelle di disintegrazioni successive nelle emulsioni nucleari si deduce il periodo del  $^{232}\text{Th}$ . Si trova  $T = 1.39 \cdot 10^{10}$  anni con una dispersione relativa di  $\pm 270$ , in perfetto accordo col valore di KOVARIK e ADAMS.

(\*) Traduzione a cura della Redazione.

## On the $Q$ -Value of the Tau-Decay.

G. L. BACCHELLA, A. BERTHELOT, M. DI CORATO, O. GOUSSU, R. LEVI SETTI,  
M. RENÉ, D. REVEL, L. SCARSI, G. TOMASINI and G. VANDERHAEGHE

*Centre de Physique Nucléaire de l'Université Libre - Bruxelles*

*Istituto di Fisica dell'Università - Genova*

*Istituto di Scienze Fisiche dell'Università - Milano*

*Istituto Nazionale di Fisica Nucleare - Sezione di Milano*

*Centre d'Etudes Nucléaires - Saclay*

(ricevuto il 23 Ottobre 1956)

**Summary.** — The  $Q$ -value of the  $\tau$ -decay has been determined in photographic emulsions, by a procedure which, using the joint information given by ranges and angles of the secondary particles, excludes the need of a given  $R$ - $E$  relation known a priori. The results obtained on a statistics of 45 events is:  $Q = (74.9 \pm 0.4)$  MeV. An empirical expression for the  $R$ - $E$  relation for  $\pi$ -mesons valid in the velocity interval  $0.27 < \beta < 0.67$  is obtained:  $\log [(E/m_{\pi}c^2) \cdot 10^3] = 1.649 + 0.566 \log R_{mm} + 0.010 (\log R_{mm})^2$ . The standard deviation on the energy derived from a given mean range by this relation is 0.5%.

### 1. - Introduction.

Previous determinations of the  $Q$  of the  $\tau$ -meson were reviewed by AMALDI at the Pisa Conference in June 1955<sup>(1)</sup>; the mean value of these results was  $Q = (75.0 \pm 0.2)$  MeV. As the author pointed out, the statistical error on the mean  $Q$  is inadequate since the values were obtained by various groups working with methods not standardised and employing different  $R$ - $E$  relations. AMALDI suggested that an error of  $\pm 1.5$  MeV should be more appropriate.

It then appeared that a new determination, aiming at overcoming the difficulties pointed out by AMALDI would be of interest. Two different lines

<sup>(1)</sup> E. AMALDI: *Pisa Conference on Elementary Particles* (June 1955), mimeographed report, p. 1.

of approach were possible to obtain a result achieving greater accuracy than the previous ones.

The first method was to determine very carefully the range-energy relation valid for pions in the energy interval concerned, either on theoretical or experimental grounds, or more generally by a combination of both. The, by normalising this range-energy relation to the stack containing the  $\tau$ 's, one can deduce the  $Q$ -value of a number of  $\tau$ 's through the measurement of the ranges of the three pions produced by the decay at rest. This is essentially the way followed by the Berkeley people, in two recently published works <sup>(2,3)</sup>.

The present work follows another line of thought. The idea was to use a method as self-consistent as possible. In fact, as will be seen in the following paragraph, by making use of much more of the information contained in the same emulsion stack (that is to say: angles of the three pions in the plane of decay, ranges of the pions, range of the  $\mu$  from the  $\pi$  decay at rest) the method needs no other external information than the ratio of the masses of  $\pi$  and  $\mu$  to give the value of  $Q$  in units equal to  $m_\pi c^2$ .

The present paper deals with its application to 47  $\tau$  decays found in a section of 40 plates of the stack K<sub>1</sub> of 120 stripped emulsions Ilford G5, 40 cm  $\times$  26 cm  $\times$  600  $\mu$ m exposed to the Berkeley Bevatron positive K beam, with momentum approximately equal to 350 MeV/c.

## 2. - Method.

The angles  $\alpha_i$  between the directions of emission of the secondaries of a  $\tau$ -meson suffering a three body decay at rest define, on the basis of conservation of momentum and energy, the repartition of energy among the three secondaries.

Defining:

$$(1) \quad \frac{p_1}{mc} / \sin \alpha_1 = \frac{p_2}{mc} / \sin \alpha_2 = \frac{p_3}{mc} / \sin \alpha_3 = \lambda,$$

and

$$(2) \quad w_i = mc^2(1 + \lambda^2 \sin^2 \alpha_i)^{\frac{1}{2}},$$

where:  $p_1, p_2, p_3$  are the momenta of the three secondaries;

$m$  the mass of the charged  $\pi$ -meson;

$w_i$  the total energy of the  $i$ -th secondary,

(2) W. H. BARKAS, H. H. HECKMAN and F. M. SMITH: *Nuovo Cimento*, **4**, 50 (1956).

(3) R. P. HADDOCK: *Nuovo Cimento*, **4**, 240 (1956).

the equation of conservation of energy can be written:

$$(3) \quad Q + 3mc^2 = mc^2[(1 + \lambda^2 \sin^2 \alpha_1)^{\frac{1}{2}} + (1 + \lambda^2 \sin^2 \alpha_2)^{\frac{1}{2}} + (1 + \lambda^2 \sin^2 \alpha_3)^{\frac{1}{2}}].$$

From this equation  $\lambda$  and hence  $w_i$  can be determined for a given value of  $Q$ . Each  $\tau$  gives in this way three points on a range-energy relation for a given choice of  $Q$ , and a sufficient number of points will define the form of the curve. We can so construct a family of curves each corresponding to a given  $Q$ -value. The existence in the stack of a calibration point, with known range and energy, will define uniquely the curve valid for the stack and the  $Q$ -value of the  $\tau$  decay.

The choice of the correct curve can be made by successive approximations. If the a priori  $Q$ -value chosen is sufficiently close to the true value, the following method can be used.

If  $E_i$  is the kinetic energy of the  $i$ -th secondary obtained from the  $Q$ -value chosen, it can easily be shown that a variation of  $Q$  to  $(Q + \Delta Q)$  will cause a variation of  $E_i$  to  $(E_i + \Delta E_i)$  such that:

$$(4) \quad \frac{\Delta E_i}{E_i} = \frac{\Delta Q}{Q} (1 + \varepsilon).$$

The coefficient  $\varepsilon$  depends on the particular  $\tau$  and on the energy of the secondary under consideration. In all the cases considered in our experiment however this coefficient is less than 0.06. If we consider variations in  $Q$  of the order of 1% we can then neglect  $\varepsilon$ , committing thereby an error on the energy of less than 0.1%. In the limits of validity of this approximation, if  $\Delta E_0$  be the difference between the energy given by the calibration point and the energy corresponding to the same range on the  $R$ - $E$  curve defined by the chosen  $Q$ , equation (4) gives:

$$(5) \quad Q^* = Q \left( 1 + \frac{\Delta E_0}{E_0} \right).$$

Thus, translating the  $R$ - $E$  curve along the axis of energy by the ratio  $(\Delta E_0/E_0)$ , we obtain the best estimate of the relation valid for the stack.

### 3. — Measurements.

The principles of the measurement of a  $\tau$  decay are well known: we shall therefore detail here only some of the precautions applied.

Since the true initial mean thickness of the emulsions was unknown, we



determined it by the method of the  $\alpha$ -particles of  $\text{ThC}'$  <sup>(4)</sup>; the mean value obtained on a group of 11 plates, out of the 40 used, was  $(580 \pm 10) \mu\text{m}$ . The mean value of the distortion vector of the second order, determined over the whole section of stack employed, was  $20 \mu\text{m}$  (with maximum value of  $40 \mu\text{m}$  in a few cases) and the individual vectors were found to be oriented at random. The first order distortion has not been determined but it may be assumed <sup>(5)</sup> to be oriented in a manner similar to that of the second order and to be of the same order of magnitude.

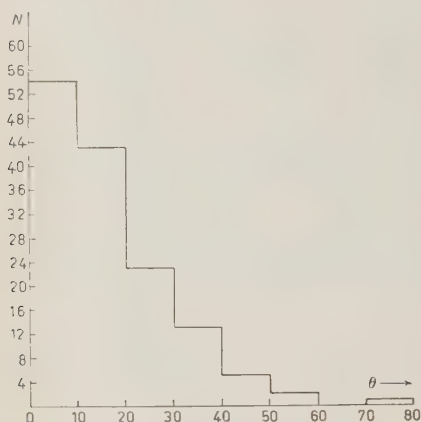


Fig. 1. — Distribution in angle of dip at emission of the 141  $\tau$ -meson secondaries from  $\tau$  decay.

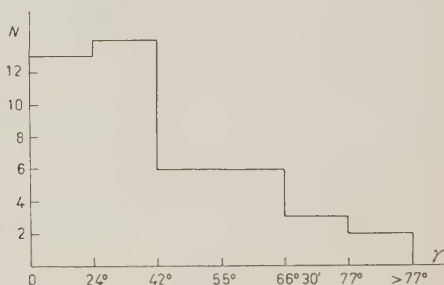


Fig. 2. — Distribution of the angle between the plane of decay and the plane of the plate.

In the choice of the events to be measured, a compromise was struck between the necessity of having a convenient statistics and that of choosing events in which all three tracks have a small inclination to the plane of the emulsion (to minimize the effect of distortion and uncertainty in the thickness of the emulsions on the measurement both of angles and ranges). The choice of events with at least two secondaries dipping at an angle of less than  $30^\circ$  led to the selection of 42, out of 166  $\tau$  decays, found in the laboratories of Bruxelles, Genoa, Milan and Saclay; to these were added 5 events, out of a total of 44, kindly lent by the emulsion group of Padua. Fig. 1 shows the distribution of the angles  $\theta_i$  of inclination to the plane of the plate at emission of the branches of the  $\tau$ 's measured. Fig. 2 shows the distribution of the angles  $\gamma$  between the plane of disintegration and the plane of the emulsion; it is clear that our selection of  $\tau$ 's is not unbiased with regard to angles

<sup>(4)</sup> L. VIGNERON: *Thèse, Université de Paris*, cap. II (1952).

<sup>(5)</sup> G-STACK COLLABORATION: *Nuovo Cimento*, **2**, 1063 (1955).

so that care must be taken not to use it in any compilation relative to a search for polarization or analysis of the kinds proposed by DALITZ and FABRI <sup>(6,7)</sup>.

Care was taken to assure that the four separate groups making the measurements worked in identical conditions. The micrometer scales used in calibration of the measuring screws were calibrated against each other; the methods of measurements of ranges and angles, and the methods of determination of the initial thickness of the emulsions, of the distortion and stopping power, were identical for all the groups.

The measurement of range were made by subdividing the track into cells of variable length corresponding for each case to the scattering of the particle and adding up the chords obtained in this way. The length of the measuring cells has been selected in such a way that the sagitta of the tracks with respect to the chords was not more than 3% of the chords.

An other cause of systematic errors in measurement of range is the fact that the original thickness of emulsion is not exactly known, since the calibration with  $\text{ThC}''$   $\alpha$ -particles was not made in all plates. Assuming the errors of the original thickness of the emulsions to be 5%, the percentage error of range is  $(\sin^2 \theta)$  5%. The mean value of this error is 1%, in three cases is more than 3% and in one case is as high as 5%.

Non systematic causes of fluctuations are straggling and errors arising from 1) distortion, 2) fluctuation of the thickness of the individual emulsion sheets around the mean value of the stack, 3) indetermination on the points of entrance and exit of the track in each plate. The principal fluctuation is that due to straggling: following the calculation of BARKAS *et al.*, for the energies of  $\tau$  secondaries this is comprised between 2.8% and 4%.

The non systematic errors due to the 3 causes above mentioned lead to a total mean error of less than 0.3% (see G-stack publication <sup>(5)</sup>).

The angles in the plane of the emulsion were measured by a goniometer accurate to 1', using a cell ( $10 \div 35 \mu\text{m}$ ) chosen to minimize the errors of scattering and noise. The resultant error was of the order of  $10' \div 20'$ . The thermal drift of the microscope (Koristka MS2 and Leitz Ortholux) and the finite focal depth of the objective, rendered necessary, in the determination of the angles of dip by reconstruction of the track based on the measurement of  $5 \div 10$  grains, the height of each grain above the glass being measured repeatedly. The optimum cell for measurement of dip angle varied from 50 to  $150 \mu\text{m}$  depending on the energy of the secondary and the error on the angle lay between  $20'$  and  $40'$ .

(6) R. H. DALITZ: *Phil. Mag.*, **44**, 1068 (1953); *Phys. Rev.*, **94**, 1046 (1954).

(7) E. FABRI: *Nuovo Cimento*, **11**, 479 (1954).

Both ranges and angles were corrected for the second order distortion: in the evaluation of the error, the uncorrected first order distortion was taken into account, the magnitude being deduced from the value of the second order vector.

#### 4. - Experimental Results.

In a  $\tau$  event, measured the angles  $\varphi_i$  in the plane of the emulsion and the dip angles  $\theta_i$ , the best estimate  $\alpha_i^*$  of the angles between the secondaries is obtained adjusting, by the method of maximum likelihood the six measured angles to obtain coplanarity, a procedure which can be carried out only if the decay can be considered coplanar within the limits of the experimental error. As a criterion of coplanarity we have employed the volume  $\Delta$  of the

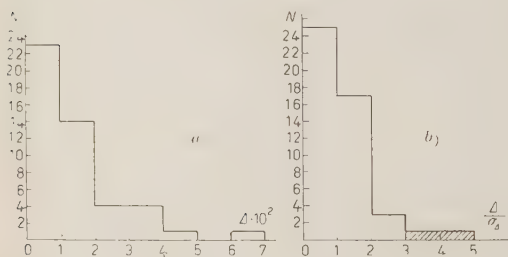


Fig. 3. Analysis of coplanarity for the 47  $\tau$ -events.

with  $\Delta/\sigma_\Delta > 3$ . The imposition of coplanarity of these two events would involve a variation of the measured angles by more than three times the experimental error, and they have therefore been excluded from the statistics. The method used for adjusting to coplanarity is described in Appendix I.

The experimental data obtained on the 47  $\tau$ 's measured are given in Table I. In our stack the only available calibration point for the choice of the correct  $R$ - $E$  relation was that given by the range of the  $\mu$ -meson from the  $\pi \rightarrow \mu + \nu$  decay. The mean value obtained for this range on a total of 300 events was:  $R_\mu = (598 \pm 1.4) \mu\text{m}$  (see Appendix II).

Taking as the ratio of the masses  $m_\pi/m_\mu = 1.321$  <sup>(8)</sup> (\*), the energy at

<sup>(8)</sup> W. H. BARKAS, W. BIRNBAUM and F. M. SMITH: *Phys. Rev.* **101**, 778, (1956).

(\*) BARKAS, BIRNBAUM and SMITH <sup>(8)</sup> report  $m_{\pi^+}/m_{\pi^-} = (0.998 \pm 0.002)$ . In what follows we take this ratio equal to one. For the mass of the charged pion we assumed the value  $(273.0 \pm 0.3) m_e$  average between the value  $(273.3 \pm 0.2) m_e$  obtained for the  $\pi^+$  <sup>(8)</sup> and  $(272.8 \pm 0.3) m_e$  <sup>(8)</sup> and  $(272.7 \pm 0.3) m_e$  <sup>(9)</sup> obtained for the  $\pi^-$ .

<sup>(9)</sup> K. M. CROWE and R. H. PHILIPS: *Phys. Rev.*, **96**, 470 (1954).

emission of the  $\mu$ -meson is:

$$E_{\mu} = \frac{mc^2}{2} \left( 1 - \frac{m_{\mu}}{m_{\pi}} \right)^2 = 0.0295 mc^2,$$

and the equivalent range and energy of a  $\pi$ -meson of same velocity will be:

$$R_0 = 0.790 \text{ mm}, \quad E_0 = 0.039 mc^2.$$

Of three trial values chosen for the  $Q$ : 0.530; 0.540; 0.550  $mc^2$ , the value 0.540  $mc^2$  ( $= 75.1 \text{ MeV}$ ) gave values of energy of the secondaries such that

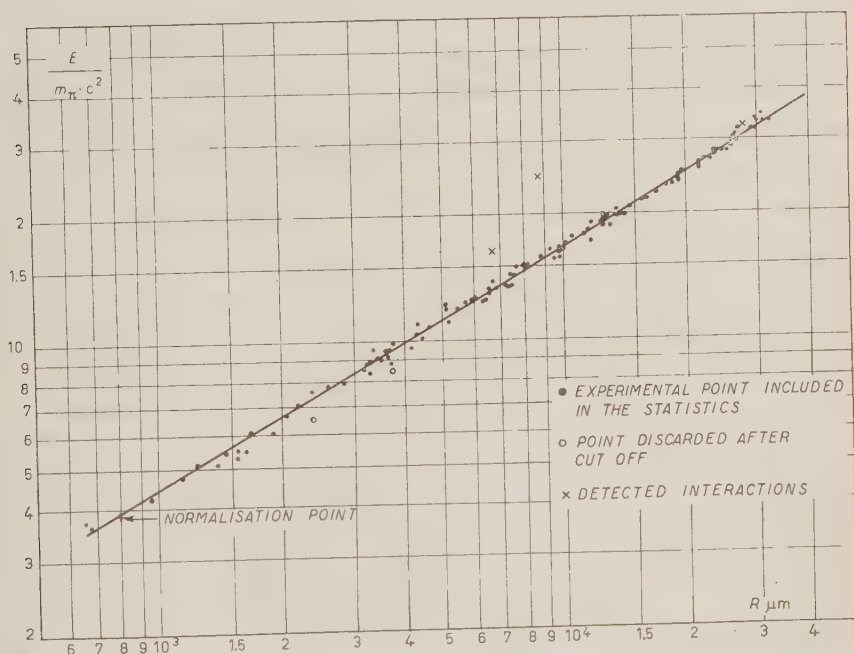


Fig. 4. — Curve of best fit of experimental points. Kinetic energies calculated assuming  $Q = 540 \cdot 10^{-3} m_{\pi} \cdot c^2$ .

the  $R$ - $E$  relation so defined passed closest to the calibration point. These values are given in Fig. 4 in double logarithmic scale. The corresponding range-energy relation was approximated to a polynomial of the second order:

$$(6) \quad y = \alpha + \beta x + \gamma x^2,$$

where:

$$y = \log \left( \frac{E}{mc^2} \cdot 10^3 \right) \quad \text{and} \quad x = \log R_{\text{mm}}.$$

TABLE I.

Event	$A$	$\Delta/\sigma_A$	$\gamma$	Branch	No. of plates	Sign	$\alpha_i^*$	Energy ( $Q = 537 \cdot 10^3 \text{ mc}^2$ )	Range (mm)	Energy from $R\text{-}E$ Relation ( $10^{-3} \text{ m.e.}^2$ )	Notes
$Bx_2$	0.02153	1.64	$8^\circ 41'$	1	(3)	+	$142^\circ 45'$	$98.9 \pm 1.9$	$3.786 \pm 0.01$	95.44	
				2	(11)	---	$95^\circ 55'$	$249.1 \pm 4.1$	$19.533 \pm 0.43$	249.19	
				3	(4)	+	$121^\circ 20'$	$189.0 \pm 1.5$	$12.466 \pm 0.28$	191.23	
$Bx_3$	0.01469	1.16	$21^\circ 52'$	1	(7)	—	$126^\circ 37'$	$166.7 \pm 2.3$	$10.038 \pm 0.23$	168.34	
				2	(2)	+	$96^\circ 42'$	$246.1 \pm 2.5$	$19.286 \pm 0.42$	247.88	
				3	(2)	+	$136^\circ 41'$	$124.2 \pm 2.4$	$5.764 \pm 0.14$	121.78	
$Bx_4$	0.01962	1.77	$36^\circ 08'$	1	(15)	+	$64^\circ 51'$	$302.6 \pm 1.3$	$26.258 \pm 0.55$	297.00	
				2	(1)	+	$154^\circ 26'$	$76.4 \pm 3.5$	$2.365 \pm 0.06$	72.78	
				3	(8)	—	$140^\circ 43'$	$158.0 \pm 4.0$	$9.803 \pm 0.23$	166.08	
$Bx_7$	0.00652	0.56	$65^\circ 12'$	1	—	—	$60^\circ 25'$	—	—	—	Goes out of stack
				2	(5)	+	$154^\circ 33'$	$83.5 \pm 4.3$	$3.767 \pm 0.09$	95.14	
				3	(3)	+	$145^\circ 02'$	$144.5 \pm 5.5$	$6.855 \pm 0.16$	134.54	
$Bx_9$	0.00860	0.63	$37^\circ 12'$	1	—	+	$110^\circ 25'$	—	—	—	Goes out of stack
				2	(1)	+	$152^\circ 04'$	$61.0 \pm 4.3$	$1.669 \pm 0.05$	59.62	Suffers interaction
				3	(3)	—	$97^\circ 31'$	$250.1 \pm 2.8$	$> 8.77$	—	in flight
$Bx_{14}$	0.01766	1.39	$20^\circ 42'$	1	(12)	—	$99^\circ 44'$	$238.6 \pm 2.4$	$18.550 \pm 0.12$	241.69	
				2	(6)	+	$126^\circ 14'$	$165.1 \pm 2.9$	$9.821 \pm 0.23$	166.21	
				3	(3)	+	$134^\circ 02'$	$133.3 \pm 2.9$	$6.526 \pm 0.15$	130.90	
$Bx_{18}$	0.0141	0.12	$37^\circ 50'$	1	(3)	+	$148^\circ 52'$	$88.2 \pm 4.8$	$3.721 \pm 0.09$	94.49	
				2	(8)	—	$135^\circ 24'$	$165.6 \pm 4.3$	$9.345 \pm 0.22$	161.43	
				3	(16)	+	$75^\circ 44'$	$283.2 \pm 6.0$	$24.848 \pm 0.53$	287.42	

$\text{Bx}_{23}$	$0.003912$	$2.75$	$23.13$	$3$	$(12)$	$+$	$120^\circ 05'$	$188.7 \pm 2.7$	$13.043 \pm 0.29$	$196.94$	
				1	(2)	+	$165^\circ 38'$	$51.3 \pm 6.7$	$1.222 \pm 0.03$	49.93	Goes out of stack.
				2	—	—	$41^\circ 05'$	$322.0 \pm 3.5$	—	—	Suffers inelastic scattering.
				3	—	—	$153^\circ 17'$	$163.7 \pm 5.3$	$> 6.57$	—	
$\text{Bx}_{24}$	$0.01123$	$1.40$	$69.18'$								
				1	(1)	+	$165^\circ 55'$	$37.4 \pm 3.8$	$0.652 \pm 0.02$	35.00	
				2	(12)	+	$48^\circ 30'$	$312.0 \pm 3.0$	$26.700 \pm 0.58$	299.71	
				3	(5)	—	$145^\circ 35'$	$187.6 \pm 4.9$	$12.458 \pm 0.28$	191.11	
$\text{Bx}_{25}$	$0.00228$	$0.24$	$16.09'$								
				1	(2)	—	$134^\circ 38'$	$134.7 \pm 1.6$	$7.426 \pm 0.27$	140.78	Goes out of stack.
				2	—	+	$94^\circ 37'$	$250.7 \pm 1.0$	—	—	
				3	(3)	+	$130^\circ 45'$	$151.6 \pm 1.6$	$7.997 \pm 0.29$	147.04	
$\text{Ge}_1$	$0.0159$	$1.10$	$21.39'$								
				1	—	+	$151^\circ 6'$	$317.4 \pm 6$	—	—	Goes out of stack.
				2	(3)	+	$155^\circ 10'$	$95.3 \pm 4.5$	$3.717 \pm 0.16$	93.81	
				3	(5)	—	$53^\circ 44'$	$124.3 \pm 6.7$	$6.337 \pm 0.29$	128.27	
$\text{Ge}_2$	$0.02462$	$1.87$	$25.45'$								
				1	(11)	+	$52^\circ 43'$	$317.4 \pm 1.2$	$29.87 \pm 1.1$	324.21	
				2	(6)	—	$157^\circ 47'$	$79.8 \pm 3.9$	$2.84 \pm 0.2$	80.59	
				3	(3)	+	$149^\circ 30'$	$139.8 \pm 4.5$	$6.72 \pm 0.26$	132.72	
$\text{Ge}_7$	$0.00349$	$0.37$	$65.41'$								
				1	(4)	+	$156^\circ 45'$	$120.2 \pm 2.8$	$5.475 \pm 0.25$	118.13	
				2	(2)	—	$160^\circ 12'$	$89.8 \pm 2.5$	$3.511 \pm 0.13$	91.01	
				3	(15)	+	$43^\circ 3'$	$327.0 \pm 0.7$	$31.07 \pm 1.2$	330.59	
$\text{Ge}_8$	$0.01849$	$1.96$	$3.11'$								
				1	(4)	—	$122^\circ 3'$	$172.4 \pm 1.5$	$10.12 \pm 0.36$	168.96	
				2	(7)	+	$122^\circ 2'$	$172.5 \pm 1.4$	$11.66 \pm 0.54$	183.90	
				3	(3)	+	$115^\circ 55'$	$192.1 \pm 1.3$	$11.778 \pm 0.41$	184.93	
$\text{Ge}_9$	$0.0112$	$0.836$	$28.5'$								
				1	(2)	+	$91^\circ 10'$	$258.4 \pm 1$	$21.7 \pm 0.9$	266.92	
				2	(2)	—	$137^\circ 9'$	$127.1 \pm 2.2$	$6.041 \pm 0.22$	124.68	
				3	(6)	+	$131^\circ 41'$	$151.5 \pm 2.3$	$8.150 \pm 0.37$	148.66	
$\text{Ge}_{11}$	$0.00711$	$0.465$	$12.36'$								



TABLE I (continued).

Event	$\Delta$	$\Delta/\sigma_\Delta$	$\gamma$	Branch	No. of plates	Sign	$\alpha_i^*$	Energy ( $Q = 537 \cdot 10^{-8} \text{ mc}^2$ )	Range (mm)	Energy from $R$ - $E$ Relation ( $10^{-3} \text{ m}_\pi c^2$ )	Notes
$\text{Mi}_1$	0.00804	0.795	$31^\circ 7'$	1 2 3	(1) (6) (17)	+ + —	$164^\circ 23'$ $111^\circ 50'$ $83^\circ 47'$	$22.5 \pm 2$ $241.5 \pm 8$ $273.0 \pm 6.9$	$0.260 \pm 0.03$ $18.79 \pm 0.7$ $22.34 \pm 1$	21.53 244.67 271.66	
$\text{Mi}_2$	0.02438	2.34	$49^\circ 27'$	1 2 3	(7) (4) (3)	+ + +	$139^\circ 49'$ $153^\circ 55'$ $66^\circ 16'$	$158.8 \pm 3.9$ $77.9 \pm 2.9$ $300.3 \pm 1.6$	$8.82 \pm 0.45$ $2.600 \pm 0.17$ $26.276 \pm 0.9$	155.75 76.63 299.85	
$\text{Mi}_3$	0.00213	0.49	$89^\circ 42'$	1 2 3	(12) (7) (2)	+ + —	$46^\circ 58'$ $151^\circ 5'$ $161^\circ 57'$	$320.8 \pm 1.5$ $151.3 \pm 5.9$ $64.9 \pm 4.6$	$29.030 \pm 1.45$ $7.660 \pm 0.41$ $2.39 \pm 0.13$	318.62 143.33 73.04	
$\text{Mi}_4$	0.0197	1.34924	$27^\circ 38'$	1 2 3	(18) (5) (3)	— + +	$92^\circ 56'$ $129^\circ 48'$ $137^\circ 16'$	$254.3 \pm 1.1$ $158.0 \pm 2.3$ $124.7 \pm 3.4$	$19.82 \pm 1$ $9.565 \pm 0.3$ —	252.7 156.7 —	Goes out of stack.
$\text{Mi}_{13}$	0.00339	0.53	$24^\circ 49'$	1 2 3	(11) (3) (1)	— + +	$27^\circ 57'$ $162^\circ 52'$ $169^\circ 11'$	$333.2 \pm 1.1$ $143.2 \pm 5.3$ $60.6 \pm 4.2$	$31.37 \pm 1.1$ $7.54 \pm 0.31$ $1.885 \pm 0.07$	334.06 142.01 63.84	
$\text{Mi}_{26}$	0.01886	1.93	$66^\circ 21'$	1 2 3	(2) (3) (18)	+ + —	$160^\circ 49'$ $123^\circ 15'$ $75^\circ 56'$	$36.5 \pm 1.7$ $216.9 \pm 4.2$ $283.6 \pm 2.7$	$0.675 \pm 0.055$ $15.70 \pm 0.56$ $25.49 \pm 1.1$	36.05 219.59 294.33	
$\text{Mi}_{26}$	0.006338	1.87	$83^\circ 15'$	1 2 3	(7) (2) (2)	— + +	$34^\circ 18'$ $165^\circ 49'$ $159^\circ 53'$	$331.6 \pm 1.7$ $70.6 \pm 8.7$ $134.8 \pm 7.9$	$30.115 \pm 1.1$ $2.190 \pm 0.12$ $7.32 \pm 0.28$	325.84 69.42 139.56	

$M_{34}$	0.00398	12 13	3	+	155° 46'	66.6 ± 1.4	2.051 ± 0.10	60.3 ± 0.3
			1	(3)	+	283.6 ± 1.7	24.20 ± 0.85	285.2
			2	(7)	+	200.5 ± 1.4	12.56 ± 0.51	192.1
$Mi_{34}$	0.01620	1 50'	3	(1)	—	52.9 ± 1.6	1.547 ± 0.06	57.11
			1	(3)	+		19.52 ± 0.72	248.9
			2	(13)	+		23.67 ± 0.95	279.0
$Mi_{57}$	0.0637	3.90	3	(1)	+		0.460 ± 0.02	28.8
			1	(3)	+			$\Delta/\sigma_A > 3$ Non coplanar
			2	(13)	+			Not included
			3	(1)	+			in the statistics
			1	(3)	+			
			2	(3)	+			
$Mi_{61}$	0.0296	1.88	24 45'	3	(4)	—		
			1	(3)	+	99° 33'	242.4 ± 1.2	18.36 ± 0.64
			2	(3)	+	115° 24'	206.8 ± 1.5	13.59 ± 0.48
			3	(4)	—	145° 3'	87.9 ± 1.5	3.25 ± 0.19
			1	(3)	+	160° 4'	110.9 ± 5.3	5.21 ± 0.22
			2	(3)	+	161° 40'	95.1 ± 4.9	3.61 ± 0.16
$Mi_{62}$	0.00999	1.52	55 14'	3	(7)	—	38° 16'	(27.82)
			1	(2)	+	155° 40'	96.1 ± 5.2	4.195 ± 0.17
			2	(7)	+	52° 12'	319 ± 1.2	27.38 ± 0.93
			3	(6)	+	152° 8'	122 ± 5.3	5.13 ± 0.29
			1	(4)	+	134° 47'	195.8 ± 2	12.55 ± 0.44
			2	(6)	+	63° 48'	298.9 ± 0.9	26.55 ± 0.71
$Mi_{65}$	0.01216	0.91	2 52'	3	(1)	+	161° 25'	0.947 ± 0.04
			1	(2)	+			14.48 ± 0.43
			2	(5)	—			28.35 ± 0.79
$Mi_{66}$	0.03794	4.12	10 20'	3	(1)	+		0.234 ± 0.012
			1	(1)	+	156° 40'	47.4 ± 3.8	1.125 ± 0.045
			2	(5)	—	117° 40'	218.7 ± 1.9	16.190 ± 0.597
			3	(8)	—	85° 40'	270.9 ± 1.5	23.250 ± 0.830
			1	(1)	+			47.64
			2	(5)	—			223.05
$Na_4$	0.00424	0.47	11	3	(8)	—		276.3

Suffers  
inelastic  
scattering $\Delta/\sigma_A > 3$  Non  
coplanar  
Not included  
in the statistics

TABLE I (continued).

Event	$A$	$A/\sigma_A$	$\gamma$	Branch	No. of plates	Sign	$\alpha_i^*$	Energy ( $Q = 537 \cdot 10^{-3} \text{ mc}^2$ )	Range (mm)	Energy from $E-E$ Relation ( $10^{-3} \text{ m.e.}^2$ )	Notes
$S_{a_6}$	0.00268	0.03	$38^\circ 10'$	1		—	$151^\circ 18'$	$66.3 \pm 1.6$	—	—	Goes out of stack.
				2	(6)	+	$90^\circ 23'$	$262.4 \pm 1.9$	$21.726 \pm 0.902$	265.4	
				3	(17)	+	$118^\circ 19'$	$208.4 \pm 2.3$	$14.680 \pm 1.1$	210.4	
$S_{a_9}$	0.00203	0.09	$57^\circ 21'$	1	(15)	+	$49^\circ 57'$	$321.2 \pm 0.9$	$29.133 \pm 1.2$	316.0	
				2	(3)	+	$157^\circ 17'$	$90.7 \pm 3.0$	$3.439 \pm 0.17$	90.2	
				3	(7)	—	$152^\circ 46'$	$125.1 \pm 3.2$	$6.442 \pm 0.43$	129.9	
$S_{a_{11}}$	0.00356	0.32	$27^\circ$	1	(3)	+	$76^\circ 04'$	$285.0 \pm 0.6$	$23.680 \pm 0.83$	279.3	
				2	(2)	+	$156^\circ 49'$	$52.2 \pm 1.4$	$1.375 \pm 0.077$	53.4	
				3	(7)	—	$127^\circ 07'$	$199.8 \pm 1.4$	$12.794 \pm 0.56$	194.1	
$S_{a_{13}}$	0.00079	0.07	$65^\circ$	1	(6)	+	$146^\circ 11'$	$111.2 \pm 3.9$	$4.372 \pm 0.43$	103.73	Goes out of stack.
				2		—	$71^\circ 07'$	$295.4 \pm 1.5$	—	—	
				3	(5)	+	$142^\circ 42'$	$130.4 \pm 3.9$	$6.550 \pm 0.33$	131.2	
$S_{a_{19}}$	0.01047	1.05	$47^\circ$	1	(12)	—	$103^\circ 31'$	$240.4 \pm 1.9$	$19.420 \pm 0.68$	248.4	
				2	(4)	+	$102^\circ 54'$	$241.7 \pm 1.9$	$18.925 \pm 0.66$	245.9	
				3	(2)	+	$153^\circ 35'$	$54.9 \pm 1.1$	$1.632 \pm 0.06$	58.87	
$S_{a_{22}}$	0.00647	0.40	$44^\circ 10'$	1	(4)	—	$142^\circ 57'$	$96.0 \pm 1.7$	$3.374 \pm 0.14$	89.31	Goes out of stack.
				2	(7)	+	$116^\circ 33'$	$201.6 \pm 2.8$	$14.205 \pm 0.57$	206.5	
				3		+	$100^\circ 30'$	$239.4 \pm 2.2$	—	—	
$S_{a_{23}}$	0.00647	0.81	$75^\circ 50'$	1	(2)	+	$161^\circ 08'$	$118.4 \pm 6.1$	$5.148 \pm 0.23$	114.05	
				2	(4)	+	$164^\circ 11'$	$85.5 \pm 5.4$	$3.174 \pm 0.23$	86.22	
				3	(10)	—	$34^\circ 41'$	$333.1 \pm 1.1$	$32.640 \pm 1.14$	338.1	



The constants  $\alpha$ ,  $\beta$  and  $\gamma$ , determined by the method of least squares were:

$$\alpha = 1.651 \pm 0.004$$

$$\beta = 0.566 \pm 0.011$$

$$\gamma = 0.010 \pm 0.006$$

thus indicating a slight concavity of the curve in the direction of positive  $y$ . The number of points finally used in the calculation of the regression curve

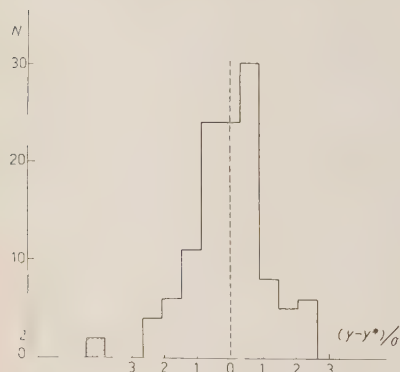


Fig. 5. - Dispersion of the 118 experimental points around the line of best fit.

was 115 since of the 135 branches corresponding to the 45  $\tau$ 's used, 14 could not be followed to their end in the stack, 3 suffered visible interaction in flight, two lay more than three times the experimental error off the mean line of regression (see Fig. 5) and one lay isolated in a region of energy far below the calibration point ( $\tau$ - $\text{Mi}_1$  - branch 1).

The  $Q$ -value obtained from the difference in energy  $\Delta E_0$  of the calibration point and that given by the curve of regression for the corresponding range  $R_0$  is:

$$Q = (0.537 \pm 0.003) \text{ mc}^2$$

$$= (71.9 \pm 0.4) \text{ MeV.}$$

The error given is the one resulting from the composition of the errors on the constants of the relation (6) and the error on the mean range of the  $\mu$ -meson from the  $\pi$  decay.

The mass of the  $\tau$ -meson is then

$$M_\tau = (3.537 \pm 0.003) \text{ mc}^2$$

$$= (965.6 \pm 1.3) \text{ m}_e$$

taking account of the incertainty in the  $\pi$ -meson mass when expressed in electron masses.

The range-energy relation for  $\pi$ -mesons valid for our stack in the velocity

interval  $0.27 < \beta < 0.67$ , results:

$$(7) \quad \log \left( \frac{E}{mc^2} 10^3 \right) = 1.649 + 0.566 \log R_{\text{mm}} + 0.010 (\log R_{\text{mm}})^2.$$

The standard deviation on the energy derived from a given mean range by this relation is 0.5%.

TABLE II.

Residual Range for $\pi$ -mesons (mm)	Kinetic energy $E/mc^2 \cdot 10^3$ Present <sup>(1)</sup> experiment	Kinetic energy $E/mc^2 \cdot 10^3$ BARKAS <sup>(2)</sup> (1956)	$\frac{E_1 - E_2}{E_1} \cdot 10^2$	Kinetic energy $E/mc^2 \cdot 10^3$ BARONI <sup>(3)</sup> (1954)	$\frac{E_1 - E_3}{E_1} \cdot 10^2$
0.924	42.62	42.63	0.0	42.4	+ 0.5
1.364	53.15	53.29	— 0.3	52.4	+ 1.3
1.875	63.72	63.95	— 0.4	63.1	+ 0.5
2.457	74.39	74.61	— 0.3	74.1	+ 0.5
3.103	85.07	85.27	— 0.2	84.8	+ 0.5
3.812	95.79	95.93	— 0.1	95.3	+ 0.5
4.582	106.55	106.58	0.0	106.0	+ 0.5
6.289	128.05	127.90	+ 0.1	127.4	+ 0.5
10.324	171.05	170.53	+ 0.3	169.6	+ 0.8
12.622	192.50	191.85	+ 0.3	191.1	+ 0.8
15.088	214.8	213.17	+ 0.8	213.0	+ 0.8
20.489	256.2	255.8	+ 0.2	257.7	— 0.6
26.447	298.1	298.4	— 0.1	300.6	— 0.8
29.613	318.8	319.8	— 0.3	322.1	— 1.2
32.895	339.4	341.1	— 0.2	343.6	— 1.2
36.285	359.9	362.4	— 0.7	366.5	— 1.8
39.778	380.2	383.7	— 0.9	388.0	— 2.1
		Experimental values from BARKAS <i>et al.</i> <sup>(4)</sup> U.C.R.L. 3254	$\frac{E_1 - E_4}{E_1} \cdot 10^2$		
15.115	214.15	213.43	+ 0.3		
36.350	360.47	362.84	— 0.65		
Normalisation point 0.790	39.00	39.00		39.00	

<sup>(1)</sup> Present experiment:  $R$ - $E$  relation:

$$\log \left( \frac{E}{m\pi c^2} 10^{+3} \right) = 1.649 + 0.566 \log R_{\text{mm}} + 0.010 (\log R_{\text{mm}})^2.$$

<sup>(2)</sup> W. H. BARKAS: *Preliminary calculations R-E curve for protons in G5 emulsion of density 3.815 g/cm<sup>3</sup>* (April 9, 1956; private communication).

<sup>(3)</sup> G. BARONI, C. CASTAGNOLI, G. CORTINI, C. FRANZINETTI and A. MANFREDINI: BS9 (1951).

<sup>(4)</sup> W. H. BARKAS, P. H. BARRET, P. CUER, H. H. HECKMAN, F. M. SMITH and H. K. TITCHO: *University of California Radiation Laboratory Report. No UCRL 3254* (1956); *Phys. Rev.*, **102**, 583 (1956).



A variation of  $\pm 0.003$  (one standard deviation) of the ratio  $m_\pi/m_\mu$  from the accepted value 1.321 (\*) corresponds to a variation of  $\pm 0.8\%$  on the  $Q$  and the values of energy derived from relation (7).

In Table III the result of the present experiment is given together with the values obtained in previous determinations.

In Table II the  $R$ - $E$  relations calculated by BARKAS<sup>(10)</sup>, by BARONI *et al.*<sup>(11)</sup> and the two experimental points of BARKAS *et al.*<sup>(12)</sup> are compared on the basis of a common normalization to the range of the  $\mu$ -meson from  $\pi$ -decay,  $R_\mu = 598 \mu\text{m}$ . We note that our relation differs from that of BARKAS by less than  $0.9\%$  over the whole velocity range concerned, whereas it differs by more than  $1\%$  from that of BARONI *et al.* for  $\beta > 0.6$ .

## 5. - Discussion.

5.1. *Internal consistency.* - As a test of the internal consistency of our data and of the suitability of the line of regression, we may now calculate the

$Q$ -value from the sum of the kinetic energies of the  $\pi$  secondaries of the complete  $\tau$ 's using the  $R$ - $E$  relation which we have established. It is clear that the value obtained is not an independent determination of  $Q$ . Using the 32 complete events, we get the same values as before (\*):

$$Q = 74.9 \left\{ \begin{array}{l} \pm 0.2_{\text{(statistical)}} \\ \pm 0.35_{\text{(due to } R-E \text{ incl.)}} \end{array} \right. \text{ MeV.}$$

The first error quoted is the one resulting from the finite number of  $\tau$ 's

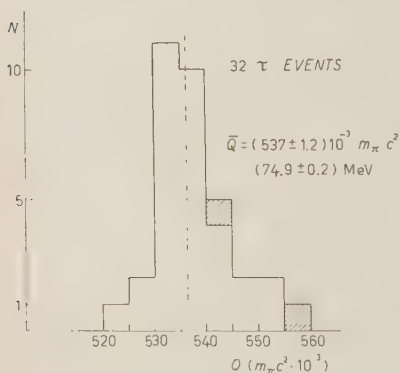


Fig. 6.

<sup>(10)</sup> W. H. BARKAS: private communication (April 1956).

<sup>(11)</sup> G. BARONI, C. CASTAGNOLI, G. CORTINI, C. FRANZINETTI and A. MANFREDINI, B.S. 9 (1954).

<sup>(12)</sup> W. H. BARKAS, P. H. BARRET, P. CUER, H. H. HECKMAN, F. M. SMITH and H. K. TICHO: *Phys. Rev.*, **102**, 583 (1956).

(\*) A preliminary report on the present work was given at the 1956 Rochester Conference. Due to the insufficient statistics available at that time only a linear line of regression was calculated. The corresponding  $Q$ -value obtained was then 76.4 MeV, while the  $Q$ -value obtained from the sum of the kinetic energies of the three secondaries of the complete  $\tau$ 's was 75.4 MeV. This inconsistency was removed when a larger statistics became available, justifying the use of a quadratic line of regression.

and from the  $Q$  distribution (as shown by Fig. 6) and the second one comes from the 0.5% uncertainty of the range-energy relation as quoted in the preceding paragraph.

5.2. *Test for anomalies.* — There are three physical sources of error in the  $Q$  determination:

- a) Undetected interactions of the  $\pi$  secondaries.
- b) Decay in flight of a  $\tau$  near the end of its range.
- c) Radiative decay.

In our analysis the effect of any of these three cases can be considered as eliminated, unless it was so small as to lie within the statistical or experimental fluctuations.

a) Ranges lying outside three times the statistical fluctuation were not taken into account in the construction of the regression curve (see Sect. 4).

b) A decay in flight can in principle be detected either by lack of coplanarity, presence of a residual momentum in the balance of the momenta of the three secondaries or an incompatibility in the sum of the kinetic energies of the three  $\pi$ 's with the mean  $Q$  distribution. Of the three, the first test is the less sensitive due both to the large errors in angle measurements which can give a spurious lack of coplanarity and to the fact that the extent to which the coplanarity is disturbed depends on the orientation at decay of the direction of flight of the  $\tau$  to the plane of decay. This orientation is extremely difficult to determine due to the high scattering of the track in the last few microns. Of the other two tests, the presence of a residual momentum is the most sensitive, the distribution due to experimental errors being such as to permit the recognition of a residual momentum of 7 MeV/c or more (Fig. 7); this corresponds to a change in  $Q$  of 0.05 MeV not detectable in our  $Q$  distribution (Fig. 6). The two events excluded from the analysis due to the impossibility of bringing them into coplanarity fall on the curve of Fig. 7 at the limit of distribution and therefore might represent decays in flight.

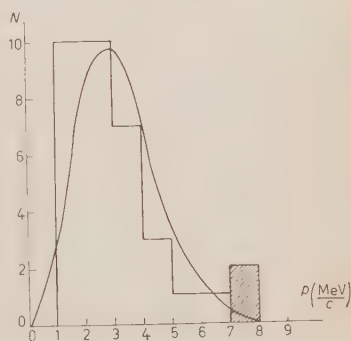


Fig. 7. - Distribution of residual momentum.

c) There is some evidence of presence among  $\tau$  decays of emission of a  $\gamma$  together with the three  $\pi$  secondaries (<sup>13</sup>). To detect such a case once again the test of coplanarity is not efficient, since the efficiency depends on the direction of emission of the  $\gamma$ . Due to the low associated momentum of a  $\gamma$  the residual momentum is less indicative than the total visible energy; the 7 MeV c minimum of residual momentum detectable with our experimental distribution corresponds directly to 7 MeV in the total visible energy, quantity easily discernable in the histogram of Fig. 6. We can therefore be sure that any radiative decay existing in the selected group of events, was associated with  $\gamma$  emitted with energy less than 2 MeV.

It is clear from a glance at the three Figs. 5-6-7 and from the above considerations that a single  $\tau$  can be defined either as radiative or as having taken place in flight only on the basis of a sufficient statistics on normal  $\tau$ 's and then only if the effect is sufficiently large as to lie well outside the normal distribution.

5'3. *Comparison with other determinations.* — In Table III are summarized together with ours, the results of AMALDI's analysis (<sup>1</sup>) and of the measurements of W. H. BARKAS, H. H. HECKMAN and F. M. SMITH (<sup>2</sup>), and R. P. HADDOCK (<sup>3</sup>).

In this table there is a distinction between the total error and the error involving only statistical and experimental terms since the Berkeley workers have not in their evaluation of the error introduced any term taking account of the possibility of an indetermination coming from the range-energy

TABLE III.

Reference	Number of events	Q-value	Error (statistical and experimental)	Error (total (*))
E. AMALDI ( <sup>1</sup> )	54	75.0	0.2	(1.5)
W. H. BARKAS, H. H. HECKMAN and F. M. SMITH ( <sup>2</sup> )	27	75.08	0.2	
R. P. HADDOCK ( <sup>3</sup> ) . . . .	67	75.13	0.18	
Present experiment . . . .	45	74.9		0.4

(\*) i. e. including uncertainty in  $R$ - $E$  relation.

(<sup>13</sup>) R. R. DANIEL and Y. PAL: *Proc. Ind. Acad. Sci.*, **40**, 115 (1954).

curve used. Such an error, which is probably very small may not be completely negligible. This may occur from the fact that in one case <sup>(3)</sup>, this range-energy relation was not verified experimentally, in the energy-range of the decay products of the  $\tau$ -meson, and in the other case <sup>(2)</sup> depended on a theoretical interpolation between three experimental points.

As can be seen from the table the agreement is very satisfactory.

5.1. *Final remarks.* — The procedure adopted here for the determination of the  $Q$  should be free from systematic errors apart the possible inexactitude of the ratio  $m_{\pi}/m_{\mu}$ . Two objections may be raised to the manner of execution:

a) The use of a single point of calibration for the R-E curve (that of the  $\mu$  from the  $\pi \rightarrow \mu$  decay), not lying in a region of energy close to that of the majority of the  $\pi$ -secondaries.

b) The limited statistics which reduced the precision of the determination of the regression curve.

In both points we were limited by the material we had. No other calibration point was available, and the  $\tau$ 's measured represented all the suitable events found in the section of the stack at our disposal.

The agreement of our result with results obtained by quite different methods strengthens our feeling that no significant systematic error may arise from these points and that they cannot produce effect else than those which have been included in the quoted error.

\* \* \*

For the exposure of the stack we are deeply indebted to the staff of the Berkeley Bevatron and in particular we wish to express our gratitude to Prof. LOFGREN. We also thank the Bristol team who took care of the processing of the stack.

## APPENDIX I

### Adjustment of the Angles between the Secondaries.

The condition of coplanarity of the three secondaries of the  $\tau$  decay is expressed by the relation:

$$(1) \quad \Delta = \begin{vmatrix} \cos \theta_1 \cos \varphi_1 & \cos \theta_1 \sin \varphi_1 & \sin \theta_1 \\ \cos \theta_2 \cos \varphi_2 & \cos \theta_2 \sin \varphi_2 & \sin \theta_2 \\ \cos \theta_3 \cos \varphi_3 & \cos \theta_3 \sin \varphi_3 & \sin \theta_3 \end{vmatrix} = 0.$$

This condition is not satisfied, due to the presence of experimental errors in the measurement of the angles. The experimental data are therefore adjusted to satisfy the relation (1) by the method of least squares, minimising the expression:

$$(2) \quad \sum_{i=1}^3 \frac{(q_i - q_i^*)^2}{\sigma_{q_i}^2} + \sum_{i=1}^3 \frac{(\theta_i - \theta_i^*)^2}{\sigma_{\theta_i}^2},$$

where  $q_i^*$  and  $\theta_i^*$  represent the angles satisfying relation (1);  $q_i$  and  $\theta_i$  represent the experimental data and  $\sigma_{q_i}$  and  $\sigma_{\theta_i}$  the experimental errors on  $q_i$  and  $\theta_i$ .

The solutions obtained are represented by the system of equation:

$$\frac{q_i^* - q_i}{\sigma_{q_i}} = -\frac{\Delta}{\sigma_A^2} s_i, \quad \frac{\theta_i^* - \theta_i}{\sigma_{\theta_i}} = -\frac{\Delta}{\sigma_A^2} s_{(i+3)},$$

where  $\left\{ \begin{array}{l} \Delta \text{ is the value of determinant (1) for the set of no adjusted values } q_i \text{ and } \theta_i, \\ s_{i(i=1,2,3)} = \frac{\partial \Delta}{\partial q_i}; \quad s_{(i+1)(i=1,2,3)} = \frac{\partial \Delta}{\partial \theta_i}; \quad \sigma_A^2 = (\sum s_i^2)^{-1}. \end{array} \right.$

The experimental errors on  $q_i$  and  $\theta_i$  have been applied to  $q_i^*$  and  $\theta_i^*$ .

## APPENDIX II

### Calibration of the Range of the $\mu$ -Meson from the $\pi \rightarrow \mu + \nu$ Decay.

The calibration was made on 300  $\mu$ -mesons each contained within a single emulsion and therefore it was necessary to apply a correction to the mean range to take into account the resultant bias towards shorter ranges due to the effects of scattering and straggling. The calculation of this correction was reduced to that for straight line by accepting for measurement only those tracks for which the line joining the end point to the point of origin lay within the central 400  $\mu$ m of the emulsion at a dip angle less than  $20^\circ$ . Under these conditions the correction for geometric loss to the mean range was of the order of  $0.1\%$ ; a variation of  $5\%$  of the value of the mean thickness of the emulsions causes a variation of  $0.5\%$  on the mean range. The ranges were measured by aligning the tracks roughly along the X-axis of the microscope and taking readings of the  $x$ ,  $y$  and  $z$  coordinates at various points along the track, chosen in such a way as to reduce the effect of smoothing while keeping as low as possible the number of measurements and therefore the total experimental error. The track was subdivided in this way in 5-10 segments according to the number of large single scatterings. The reproducibility of the

results was controlled by repetition of the measurements by independent observers. The screws controlling the movements of the measuring microscopes

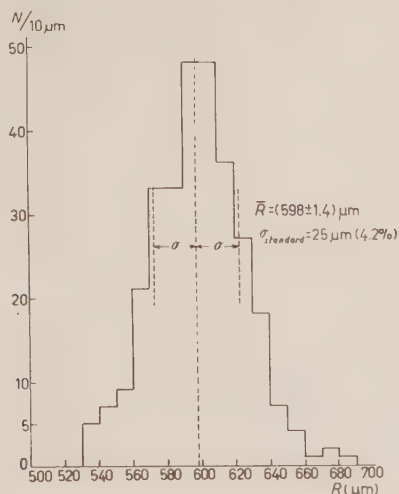


Fig. 8. — Range distribution of 300  $\mu$ -mesons from  $\pi \rightarrow \mu + \nu$  decay.

were controlled in each laboratory and normalized to a single precision micrometer scale of Leitz.

The mean range on the 300 events resulted  $(598 \pm 1.4) \mu\text{m}$  (experimental straggling: 4.2%). The distribution of individual ranges is given in Fig. 8.

#### RIASSUNTO (\*)

Il valore del  $Q$  del decadimento  $\tau$  è stato determinato nelle emulsioni nucleari con un procedimento che, sfruttando contemporaneamente gli elementi forniti dai range e dagli angoli delle particelle secondarie rende inutile la preventiva conoscenza di una data relazione  $R$ - $E$ . Il risultato ottenuto elaborando una statistica di 45 eventi è:  $Q = (74.9 \pm 0.4) \text{ MeV}$ . Si ottiene un'espressione empirica per la relazione  $R$ - $E$  per i mesoni  $\pi$  valida nell'intervallo di velocità  $0.27 < \beta < 0.67$ :  $\log [(E^3 m_\pi) \cdot 10^3] = 1.649 + 0.566 \log R_{\text{mm}} + 0.010 (\log R_{\text{mm}})^2$ . L'errore standard in cui, usando questa relazione, si incorre nel calcolare l'energia a partire da un range medio dato è del 0.5%.

(\*) Traduzione a cura della Redazione.



## Millimicrosecond Time Analyzer.

C. COTTINI and E. GATTI

CISE - Milano

(ricevuto il 19 Settembre 1956)

**Summary.** — A millimicrosecond time analyzer is described. For artificial pulses of 0.1 V minimum amplitude and some  $\mu\text{s}$  width, the resolving power is about  $5 \cdot 10^{-11}$  s. The instrument works on frequency conversion of two high frequency sinusoidal damped waves ballistically excited by the input pulses.

### 1. - General Description.

A millimicrosecond time analyzer based on a new principle mentioned in a previous preliminary note is described. The note will serve as an introduction (1).

The block scheme of the system is given in Fig. 1. The output pulses of a photomultiplier excite ballistically two resonant circuits, one tuned to 20 MHz, the other to 20.2 MHz. Output signals of the two resonant circuits are mixed in a ring diode modulator whose 200 kHz output has a phase linearly related to the time interval between the two pulses that excite the two resonant circuits. The phase is measured with a discriminator having a threshold near zero and gives an output pulse when its input 200 kHz signal crosses the zero voltage the first time. This pulse blocks (in the time/height converter) a linear voltage rise which is started every time two pulses are given by the photomultiplier within a time interval of  $2 \cdot 10^{-8}$  s.

The height so obtained is a measure of the time interval between the two events. By means of the frequency conversion, the method magnifies the time to be evaluated by a factor of 100.

The C coincidence, having a  $2 \cdot 10^{-8}$  s resolving time, selects couples of pulses that are not separated in time by more than half period of the 20 MHz oscillation. In fact a pulse in the 20 MHz channel or another separated by  $50 \cdot 10^{-9}$  s

(1) C. COTTINI, E. GATTI and G. GIANNELLI: *Nuovo Cimento*, **4**, 156 (1956).



Suppose the exciting pulse is very short in comparison with the damping time. After a short time, only the two following terms corresponding to the complex poles  $-\sigma_r \pm j\omega_r$  of the oscillating circuit will be present in the inverse transform of 1:

$$i(-\sigma_r \pm j\omega_r) \frac{1}{1 + (-\sigma_r \pm j\omega_r)} \exp[-(\sigma_r \mp j\omega_r)t],$$

i.e., a damped sinusoidal oscillation having (a constant value apart) a phase equal to the argument of  $i(-\sigma_r + j\omega_r)$  and with a good approximation (being  $\sigma_r \ll \omega_r$ ) to the argument of  $i(j\omega_r)$ .

If  $i(p)$  is normalized so that  $\int_0^\infty i(t) dt = 1$ , it can be written:

$$i(p) = 1 - p \int_0^\infty ti(t) dt + \frac{p^2}{2} \int_0^\infty t^2 i(t) dt + \dots$$

If, further, the period corresponding to the resonant angular frequency of the oscillating circuit is large respecting the pulse width of  $i(t)$  it may be concluded that  $\arg i(j\omega_r) = \omega_r \int_0^\infty ti(t) dt$ .

i.e. the phase of the excited damped oscillation is proportional to the position of the centre of gravity of the phototube output pulse. The time position of the centre of gravity of the electron pulse at the collector of the phototube is the quantity that defines the time position of the event in the instrument. The standard deviation of the position of centre of gravity of  $N$  photoelectrons emitted by the photocathode following a scintillation decaying according to  $\exp[-t/\tau]$  is  $\tau/\sqrt{N}$ . The standard deviation is supposed to be the same for the output pulse of the phototube provided small size scintillators are used in contact with small regions of the photocathode <sup>(3)</sup>.

It is noted that the time definition  $\tau/\sqrt{N}$  is inferior to  $\tau/N$  standard deviation relative to the emission of the first photoelectron, but the method allows definition of the time <sup>(1,4)</sup> at which the event occurs, independently from the height of the pulse, whereas the other methods which, to define such time, use the current pulse from the first photoelectron, have to be supplemented by a device sensitive to the pulse height <sup>(5)</sup>. In fact the time in which the electronic tube is cut off depends on whether or not current pulses due to further photoelectrons superimpose each other. Obviously the probability of such pile up depends on the number of photoelectrons totally emitted i.e. on the scintillation amplitude.

The described instrument can be modified to work on the basis of these

<sup>(3)</sup> R. V. SMITH: *Nucleonics*, **14**, 55 (April 1956).

<sup>(4)</sup> P. WEINZIERL: *Rev. Scient. Instr.*, **27**, 226 (1956).

<sup>(5)</sup> I. D. LEWIS and F. H. WELLS: *Millimicrosecond Pulse Techniques* (London, 1954), p. 253.



The damped sinusoidal oscillation of the first resonant circuit is amplified by a tuned stage. The response of the two cascaded circuits to a pulse excitation is given in Fig. 3a. This wave form is fed to an amplitude limiting

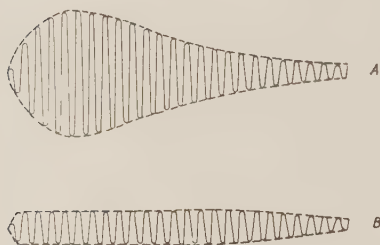


Fig. 3. - a) Response of two cascaded resonant circuits to impulsive excitation. b) Output waveform of the limiter stage.

stage using a 6BN6 tube with a low  $Q$  tuned anodic load. The output wave form of the limiter stage is given in Fig. 3b.

Absolute care should be taken to shield the input and output of the limiter stage from each other. As the phases of a capacitively or a magnetically induced signal differ from the phase of a signal transmitted through the electronic coupling in 6BN6 tube, and as the latter is of constant amplitude whereas those induced are dependent on the input amplitude, the output phase would not be determined by the input signal alone, but also by its amplitude.

The next stage serves to feed a  $120\ \Omega$  characteristic impedance coaxial cable of a few meters, which in turn transmits the signal to the modulator circuit to which, by a similar cable, is transmitted the output signal of the other channel.

The other amplifying stage, directly connected to the output of the photo-multiplier, carries, through a coaxial cable, a signal to the slow coincidence proportional to the scintillation. This signal eventually serves also to select, by means of a pulse analyzer, definite signal heights in one or in the other channel of the time analyzer.

#### 4. - Modulator Circuit and Detector of the First Passage through Zero of the Signal Produced by Modulation.

The scheme is given in Fig. 4. Transformers were wound on toroidal nuclei of ferroxcube IVb. Diodes were balanced at 1 V according to steady measurements of forward and backward resistance. Careful symmetry was given to the circuit so that the diode ring could not be unbalanced by parasitic capacities. 20 and 20.2 MHz signals of 0.2 V rms were present at the output to the ratio of 1:20 with respect to the 200 kHz modulation product. A simple  $RC$  time constant further reduced the high frequency signal to negligible percentage.

The 200 kHz signal of about 0.3 V rms was applied to a millidiscriminator with 1.5 mV threshold <sup>(6)</sup>.

The rise time of the output pulse of the millidiscriminator depends to a

<sup>(6)</sup> S. BARABASCHI, C. COTTINI and E. GATTI: *Nuovo Cimento*, **2**, 1042 (1955).

certain extent on the zero-crossing velocity of the input signal and for this reason, the modulator has been fed by the constant amplitude wave trains obtained by the above mentioned limiter stages.

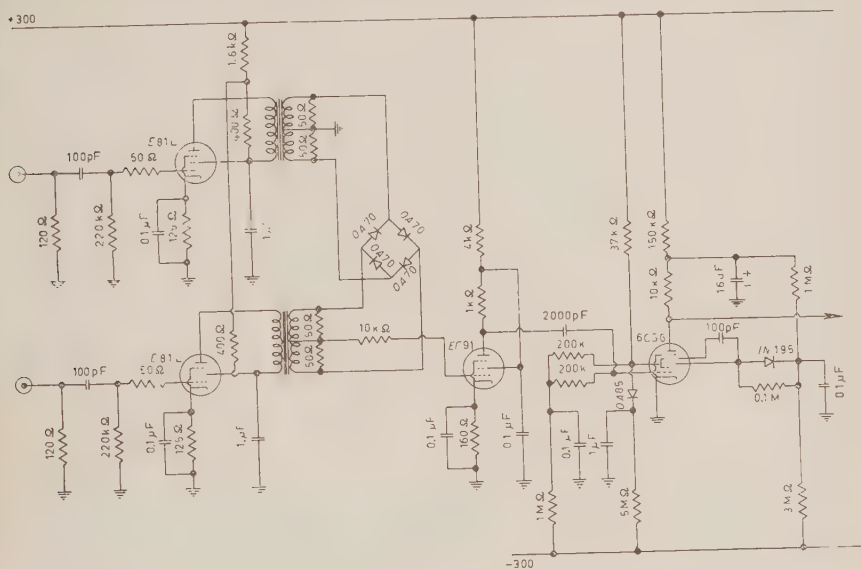


Fig. 4. - Modulator circuit and millidiscriminator.

## 5. - Experimental Results.

The linearity and calibration have been determined by a single 3  $\mu$ ms artificial pulse applied to both inputs of the instrument. The amplitude of the signal of the analyzer output has been plotted against different lengths of coaxial cables inserted between the modulator and one or the other channel (Fig. 5).

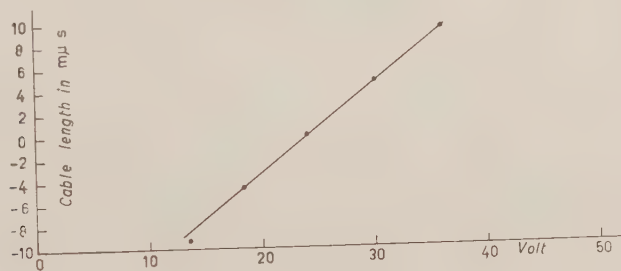


Fig. 5. - Calibration curve.



It was ascertained that all coincidences due to artificial pulses fall into an amplitude channel corresponding to  $5 \cdot 10^{-11}$  s time interval. It was also ascertained that the variation of the input pulse height up to a factor of 10 did not alter the calibration points by more than  $10^{-10}$  s.

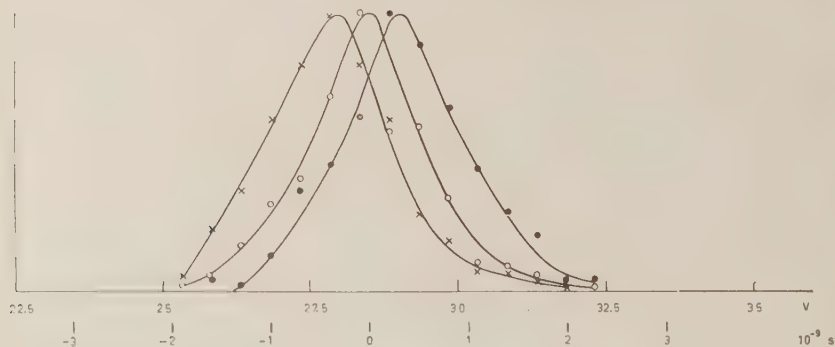


Fig. 6. Calibration with  $\gamma$ -rays time of flight.

Two plastic cylindrical phosphors of 16 mm diameter and 8 mm length were successively mounted on the phototubes, and the output pulses due to the  $\gamma$  coincidences coming from positrons emitted by a  $^{22}\text{Na}$  source were amplitude analyzed. This analysis was done for 3 different positions of the  $^{22}\text{Na}$  source, at 5 cm intervals, in line with the two scintillators (Fig. 6).

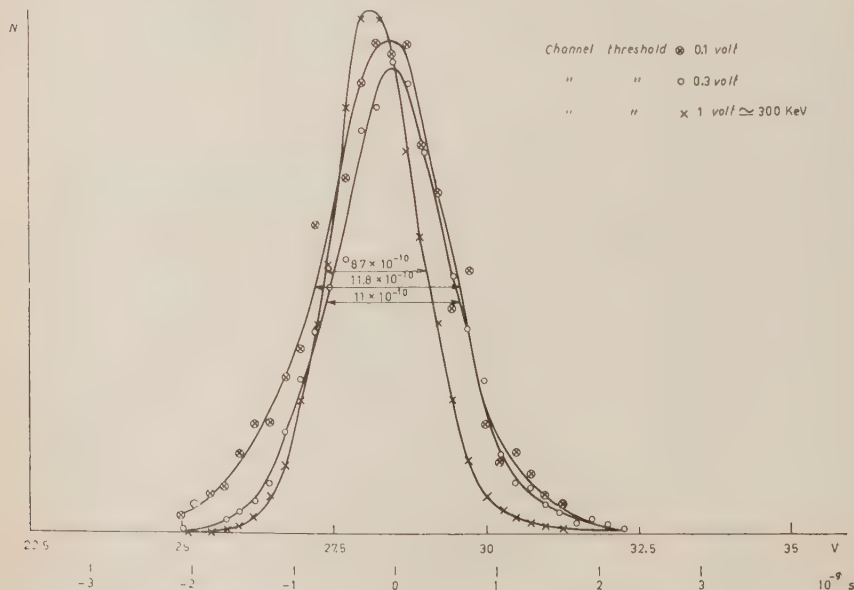


Fig. 7. — Line width as a function of threshold of accepted pulses.

The line width is due mainly to the standard deviation of the center of gravity of the photoelectrons following the scintillation. This is confirmed by curves of Fig. 7 in which, for identical position of the  $^{22}\text{Na}$  source, the threshold of the minimum pulses accepted is varied.

If, referring to threshold of 0.1 V, we suppose that an average energy of 200 keV is released by the  $\gamma$ -rays in the scintillators and consequently an average of 100 photoelectrons emitted, and if the scintillation time of the plastic scintillators is supposed to be  $3 \cdot 10^{-9}$  then the standard deviation of the center of gravity of the photoelectronic pulse is  $3 \cdot 10^{-10}$  s, which combined with a standard deviation of  $2 \cdot 10^{-10}$  due to different transit times of photoelectrons emitted in different points of the photocathode (within a 16 mm circle centred in the photocathode) and with another standard deviation of  $0.5 \cdot 10^{-10}$  due to the geometric extension of the source and scintillators, gives an overall standard deviation of  $3.64 \cdot 10^{-10}$ .

The standard deviation of the time difference between pulse centres of gravity in the two channels is  $\sqrt{2} \cdot 3.64 \cdot 10^{-10}$  s =  $5.12 \cdot 10^{-10}$  s, which finally corresponds to a line width of  $12 \cdot 10^{-10}$  s calculated at half amplitude of the resolution curve in good agreement with the experimental value.

## 6. - Conclusions.

The instrument described seems to solve quite simply the problems of the measurement with high resolution of time intervals between nuclear events: the instrument requires small pulses of 0.1 V on 20 pF and presents a resolution of  $5 \cdot 10^{-11}$  for artificial pulses of some m $\mu$ s width.

The resolution appears to be practically limited only by the behaviour of scintillators and phototubes and the experience obtained in constructing this instrument leads us to believe that, working with higher frequency, it will not be very difficult to achieve much higher resolving power for artificial pulses.

## RIASSUNTO

Si descrive un analizzatore di ritardi nel campo dei millimicrosecondi. Per impulsi artificiali di almeno 0.1 V di ampiezza e di durata di alcuni millimicrosecondi il potere risolutivo è di circa  $5 \cdot 10^{-11}$  s. Per impulsi derivanti da raggi  $\gamma$  di 0.5 MeV rivelati da scintillatori plastici e fototubi il potere risolutivo è di  $5 \cdot 10^{-10}$  s, senza operare una selezione di ampiezza degli impulsi in uscita dai fototubi. Lo strumento è basato sulla conversione di frequenza di due treni d'onda ad alta frequenza provocati dall'eccitazione balistica di due circuiti oscillanti da parte degli impulsi in considerazione.

## A Cosmic-Ray Gas Čerenkov Counter with Adjustable Velocity Threshold.

R. J. HANSON (\*) and D. C. MOORE (+)

*University of Nebraska - Lincoln, Nebraska*

(ricevuto il 20 Settembre 1956)

**Summary.** — Measurements of performance have been made on a gas Čerenkov counter with  $\text{CO}_2$  at a pressure of 13.1 atm as the dielectric radiator. The corresponding index of refraction is 1.00569. Cosmic-ray  $\mu$ -mesons with velocities greater than that of light in the gas were counted with an efficiency of  $(86 \pm 2)\%$ . Tests indicate that the efficiency for counting  $\mu$ -mesons with velocities less than that of light in the gas is less than 3%.

### 1. — Introduction.

BALZANELLI and ASCOLI <sup>(1)</sup> and BARCLAY and JELLEY <sup>(2)</sup> have demonstrated the feasibility of designing a Čerenkov counter with gaseous dielectric for counting single high energy charged cosmic rays. In the work of Barclay and Jelley, counts due to Čerenkov radiation in air at atmospheric pressure were detected for about 15% of the  $\mu$ -mesons traversing the telescope.

This paper describes a gas Čerenkov counter which has been constructed and tested at the University of Nebraska. An index of refraction,  $n$ , much greater than that of air at atmospheric pressure, was obtained by using  $\text{CO}_2$  at high pressure as the dielectric radiator. The corresponding velocity threshold of counting,  $c/n$ , where  $c$  is the velocity of light in a vacuum, is much lower than that obtained with air at atmospheric pressure <sup>(1-2)</sup>. This fact facilitates

(\*) Now at Grinnell College, Grinnell, Iowa, U.S.A.

(+) Now at Schlumberger Well Surveying Corporation, Ridgefield, Connecticut, U.S.A.

<sup>(1)</sup> A. ASCOLI BALZANELLI and R. ASCOLI: *Nuovo Cimento*, **11**, 562 (1954).

<sup>(2)</sup> F. R. BARCLAY and J. V. JELLEY: *Nuovo Cimento*, **2**, 27 (1955).

range measurements of the  $\mu$ -mesons so that a direct determination of counting efficiency can be made. The velocity threshold is easily adjustable since the index of refraction can be changed by varying the pressure.

## 2. - Description of Equipment.

Fig. 1 shows the Čerenkov counter, and the auxiliary counters and absorber which were used to test its performance. Scintillation counters, *A* and *B*, define the solid angle of acceptance. The area-solid angle product is  $\sim 2.2 \text{ cm}^2 \text{ sr}$ .

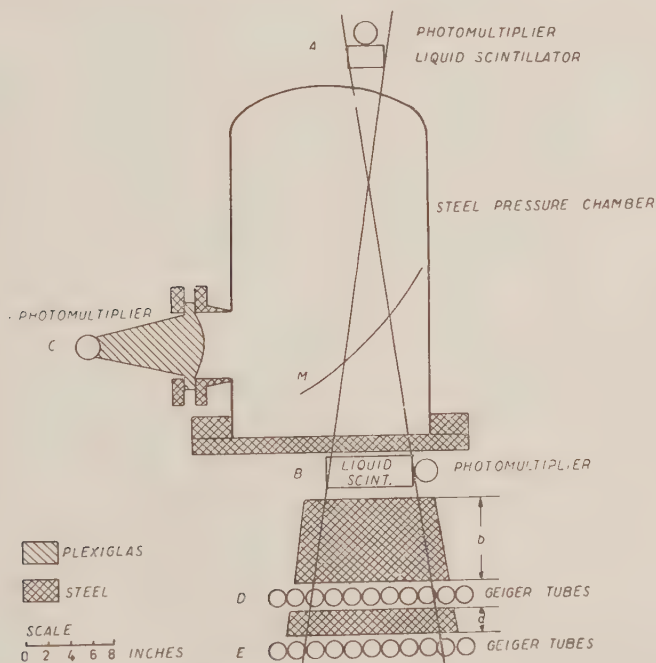


Fig. 1. - Arrangement used for testing gas Čerenkov counter. The radiating gas is enclosed in the pressure chamber. *M* is a spherical mirror which reflects the Čerenkov photons through the side port.

All particles which pass through *A* and *B* with a velocity greater than  $c/n$  produce Čerenkov radiation in the gas enclosed in the pressure chamber. *M* is a spherical mirror which reflects the Čerenkov photons through the side port. A Plexiglas lens and light pipe aid in converging the light on the cathode of the photomultiplier, *C*. The phototube was not placed within the solid angle of the counter since relatively slow particles could produce enough Čerenkov photons in the glass envelope to make the efficiency for counting

such particles appreciable. Counts could also result from the secondary electrons produced in the glass envelope or in the cathode itself by slow incident particles. The front-aluminized surface of the mirror was not overcoated because of the possibility of production of Čerenkov and fluorescent radiation by slow particles.

Counters  $D$  and  $E$ , and the steel absorber are used for range measurements of the particles passing through the pressure chamber. The thicknesses  $b$  and  $d$  are adjustable in one-half inch steps. Mirror  $M$  rests on a two inch thick steel plate not shown in Fig. 1. This plate and the chamber base plate shown in Fig. 1 introduce  $3\frac{1}{2}$  inches of steel absorber between the gas and counter  $B$ .

In the spectral range from  $4000 \text{ \AA}$  to  $5500 \text{ \AA}$ , a singly charged particle with a velocity,  $v$ , greater than  $c/n$  produces approximately  $300 (1 - 1/n^2\beta^2)$  Čerenkov photons per centimeter, where  $\beta = v/c$ . For an index of 1.005 ( $\text{CO}_2$  at about 12 atm) the maximum number of photons is about 3 per centimeter. Since the average path length in the chamber is about 50 cm, the number of emitted photons ranges from 0 for  $\beta = 0.995$  to 150 for  $\beta = 1$ . The number of photons which actually reach photomultiplier  $C$  is smaller because of the losses in the optical system. Since the photocathode efficiency is of the order of  $10\%$ , it can be seen that if the counter is to have high efficiency, events in which only one electron is emitted from the photocathode of  $C$  must be counted. An AFIF 17 stage tube<sup>(3)</sup> is used. It can be operated at gains greater than  $10^9$  with dark current corresponding to only several thousand electrons per second leaving the photocathode. Many of the dark current pulses, presumably resulting from one electron leaving the photocathode, are greater than two volts for a load consisting of a terminated  $125 \Omega$  line. To practically eliminate dark current counts, triple coincidences among  $A$ ,  $B$ , and  $C$  are obtained using a coincidence circuit with resolving time of  $2 \cdot 10^{-8}$  s.

The choice of gas depends upon the desired index of refraction. High index vapors at atmospheric pressure and room temperature have indices  $\sim 1.0015$  corresponding to a velocity threshold of  $0.9985c$ . If higher indices are desired, the pressure must be higher than one atmosphere. High index vapors would then not be suitable since in general they liquefy at about room temperature and atmospheric pressure. Lower index gases such as  $\text{CO}_2$ ,  $\text{N}_2$ , or  $\text{A}$  can provide very high indices if a chamber capable of withstanding the corresponding pressure is used.

Table I gives indices of a number of gases under different conditions. Except where a direct measurement is indicated, the index at pressures higher than one atmosphere is found assuming  $(n - 1)$  proportional to density<sup>(4)</sup>. The values at 14 atm ( $\sim 200$  psi) are given since standard boiler techniques and fittings can be used for constructing a chamber capable of withstanding such a pressure. An index as high as 1.014 can be obtained with moderate pressure

(3) Produced at the *Abteilung für industrielle Forschung (AFIF) des Institutes für technische Physik der E. T. H.*, Zurich, 7, Switzerland, under the direction of Dr. N. SCHAEFFLI.

(4) For values of  $n$  nearly one, as in the case of gases, the theoretical Lorentz-Lorenz Law,  $(n - 1)[(n + 1)/(n^2 + 2)] = K\rho$  is well approximated by  $(n - 1) = K_1\rho$ , where  $K$  and  $K_1$  are constants for the material considered and  $\rho$  is the density of the material.

if Freon 13 B1 is used <sup>(5)</sup>. For somewhat lower indices CO<sub>2</sub> is a reasonable choice.

TABLE I.

Gas	$n$ 1 atm abs.	ref.	$n$ (*) at pt. of liquefaction	$n$ (**) at 14 atm, 25 °C
Helium	1.000036    0 °C	( <sup>1</sup> )	crit. temp. — 267.9 °C	1.00046
Argon	1.000281    0 °C	( <sup>1</sup> )	crit. temp. — 122 °C	1.00360
Nitrogen	1.000296-    0 °C 1.000298	( <sup>1</sup> )	crit. temp. — 147.1 °C	1.00381
Carbon dioxide	1.000415    25 °C	( <sup>2</sup> )	1.0264 25 °C, 63.5 atm	1.0060
Ethane	1.000706    25 °C	( <sup>2</sup> )	1.0263 20 °C, 37.3 atm	1.0099
Propane	1.001005    25 °C	( <sup>2</sup> )	1.0090 22 °C, 9 atm	—
Ethyl ether	1.001521-    0 °C 1.001544	( <sup>1</sup> )	1.00136 34.6 °C, 1 atm	—
Freon 13B1	1.000864    42 °C	( <sup>3</sup> )	1.0153 42 °C, 14.4 atm	1.0153

(<sup>1</sup>) *Handbook of Chemistry and Physics*, 37th edition (Chemical Rubber Publishing Company), p. 2685. Measurements with sodium D light.

(<sup>2</sup>) *Proc. Roy. Soc., London*, A 156, 151 (1936). Measurements at 4359 Å.

(<sup>3</sup>) Measurement by Professor C. E. BENNETT, University of Maine at 4947 Å.

(\*) ( $n - 1$ ) assumed proportional to density except for Freon 13B1 which was measured directly (ref. (<sup>3</sup>)). For He, A, and N<sub>2</sub> the value of index is limited only by the pressure the system can withstand.

(\*\*) ( $n - 1$ ) assumed proportional to density except for Freon 13B1 measured at 14.4 atm and 42 °C, and CO<sub>2</sub> the value of which was taken from a curve of measurements by BENNETT at 32 °C.

### 3. — Means of Testing the Efficiency of the Counter.

Since  $\mu$ -mesons possess a rather definite range-energy relationship they are well suited for efficiency measurements. A  $\mu$ -meson with sufficient energy to produce Čerenkov radiation in a gas, will penetrate an amount of absorber which will stop nearly all sea-level cosmic radiation other than  $\mu$ -mesons.

(<sup>5</sup>) Produced by E. I. Du Pont de Nemours and Co., Inc., Wilmington, Delaware.



For most of the tests several trays of Geiger tubes placed around counters A and B provided anti-coincidence pulses to discriminate against particles associated with showers. The shower protection tubes were all in parallel and are referred to as S.

The two most important tests are:

1) Efficiency of Čerenkov counter for  $\mu$ -mesons with  $v > c/n$ .

Thickness  $b$  is such that a  $\mu$ -meson reaching tray D after passing through A and B would have possessed sufficient velocity to have produced Čerenkov radiation in the chamber. Coincidence rates ABCD-S and ABD-S are recorded simultaneously. The ratio of the ABCD-S rate to that of ABD-S yields the efficiency of the Čerenkov counter.

2) Efficiency of Čerenkov counter for  $\mu$ -mesons with  $v < c/n$ .

Absorber thickness  $b$  is 0. Thickness  $d$  is such that the amount of absorber between the gas and tray E is less than the amount which would just stop a  $\mu$ -meson with  $v = c/n$ . The ratio of the ABCD-E-S rate to that of ABD-E-S yields the efficiency, providing that the number of particles, other than  $\mu$ -mesons, reaching D is negligible.

Ideally, the ABCD-E-S rate for  $\mu$ -mesons in test 2) should be zero. The test was intended to be a measure of fluorescence produced in the gas by the passage of charged particles.

#### 4. - Results.

All the tests which are reported were made with  $\text{CO}_2$  at 13.1 atm and 26 °C. The corresponding value of  $n$  is 1.00569 at 4047 Å. An 0.89 GeV  $\mu$ -meson possesses a velocity  $v_0 = c/n$ . The range of such a particle is 73 cm of steel.

For test 1) there were 85 cm of steel absorber between the gas and counter tray D. In order to reach tray D, a  $\mu$ -meson must possess an energy of at least 1.06 GeV while passing through the gas. The following is a summary of results of test 1) for a total of 65.2 h:

ABCD-S	« trouble »	ABD-S	ABD-S rate	efficiency
$2425 \pm 49$	25	$2799 \pm 53$	$(0.716 \pm 0.014)/\text{min}$	$(85.7 \pm 1.7)\%$

The statistical errors quoted are standard deviations. « Trouble » counts were recorded whenever an ABCD-S count was not accompanied by a simultaneous ABD-S count. The coincidence circuit arrangement consisted of two fast ( $2 \cdot 10^{-8}$  s) circuits yielding ABC and AB pulses which were fed to slower circuits yielding the ABCD-S and ABD-S counts. The trouble counts were a result of difficulty in adjusting the discriminators between the fast and slow circuits such that the ABD-S counter would never fail to operate if there were an ABCD-S count. For the calculation of efficiency, the trouble counts were subtracted from the ABCD-S counts. The error in the efficiency was obtained

by assuming the same relative error in the efficiency as in the number of [(ABC'D-S)-trouble] counts. For reasons to be discussed, there were two inches of lead absorber inside the chamber near the top for all trials of test 1) reported here. Since the lead was above the radiating gas it was not included in the 85 cm of absorber.

For test 2) absorber thickness  $b$  was zero. Thickness  $d$  was such that there were 49 cm of steel absorber between the gas and counter tray E. In preliminary work the efficiency could be reduced from 15-20% to 7-10% by using the shower protection Geiger tubes around A and B. In later work, two inches of lead were placed inside the chamber near the top. This was done in an attempt to reduce the effect due to very energetic cosmic-ray electrons which could reach tray D, or to knock-on electrons produced by slow  $\mu$ -mesons in the roof of the chamber and in scintillation counter A above it. To cause trouble, the knock-on electrons need only to possess sufficient energy (4.3 MeV) to produce Čerenkov radiation, since the slow meson could discharge a counter in tray D. With lead inside the chamber, the following results were obtained for a 116.3 h test.

ABC'D-E-S	ABD-E-S	« trouble »	ABC'D-E-S rate	ABD-E-S rate	efficiency
$63 \pm 8$	$1531 \pm 38$	1	$(0.54 \pm 0.07)/h$	$(13.2 \pm 0.3)/h$	$(4.1 \pm 0.5)\%$

These results combined with a total of 135.2 h of other tests under the same circumstances except for changes in the arrangement and number of shower protection tubes yielded a value of  $(4.1 \pm 0.3)\%$ . Under the same conditions, except for no shower protection, an efficiency of  $(8.8 \pm 1.1)\%$  was obtained.

With the lead removed and with shower protection tubes around both A and B the efficiency was  $(7.1 \pm 1.0)\%$ . The ABD-E-S rate was  $(14.5 \pm 0.5)/h$  compared with  $(13.2 \pm 0.3)/h$  for the lead inside the chamber.

Short tests with lead or steel absorber above counter A yielded  $(2.7 \pm 0.7)\%$  using 2 inches of lead and  $(3.8 \pm 0.8)\%$  using  $4\frac{1}{2}$  inches of steel. The ABD-E-S rates were respectively  $(12.6 \pm 0.5)/h$  and  $(12.8 \pm 0.5)/h$ . The fact that the efficiency was at least as high with the lead inside the chamber as above it suggests that knock-on electrons produced in scintillation counter A and in the roof of the chamber do not affect the results appreciably.

Slightly lower efficiencies were obtained by connecting trays D and E in parallel and placing both of them below absorber thickness  $d$ . Then the ABC'D-E-S rate was compared with that of AB'D-E-S. Values of the efficiency were  $(2.4 \pm 0.4)\%$  with the lead inside the chamber, and  $(2.9 \pm 0.4)\%$  with lead above the chamber. The ABC'D-E-S rate was  $\sim 10/\text{day}$ , whereas the number of particles traversing the telescope which the anti-coincidence circuit must eliminate was greater than 1000/day. It is reasonable to expect, therefore, that a slight increase in anti-coincidence efficiency would lower the rate. For most of the work, tray D had been used in coincidence with AB to eliminate chance coincidences in the circuit not including C. However, tests in which a delay was introduced in channel A or B indicated that the accidental rate was practically negligible. For example, with a  $6.8 \cdot 10^{-8}$  s delay in channel A there were no ABC'D-E-S counts, and 3 AB'D-E-S counts in 45.5 h.

To make sure that the small number of counts in the Čerenkov counter

in test 2) were actually the result of light being produced in the gas, tests were made with the chamber evacuated. In a 14.2 h test with 70 cm of steel above D there were 654 ABD-S counts and no ABCD-S counts. In a 17 h test with tray D above the steel absorber there were 1108 ABD-S counts and no ABCD-S counts.

## 5. - Conclusions.

On the basis of the tests made, it is concluded that for an index of 1.00569 the counter has an efficiency of  $(86 \pm 2)\%$  for counting  $\mu$ -mesons of energy  $> 1.06$  GeV, i.e., which are capable of penetrating 85 cm of steel absorber. A  $\mu$ -meson energy of 0.89 GeV is necessary to produce Čerenkov photons at 1017 Å. A 0.89 GeV  $\mu$ -meson will penetrate, on the average, 73 cm of steel.

In tests designed to measure the efficiency for counting  $\mu$ -mesons unable to penetrate 49 cm of steel, values were reduced from about 7% to 2% or 3% by placing lead or steel absorber above the gas. This indicates that high energy electrons incident on the equipment were producing counts when the absorber was not in place. Further tests would be necessary to determine the cause of the remaining 2% to 3%. Incident electrons not eliminated by the absorber above the gas, or knock-ons produced in the absorber by slow  $\mu$ -mesons could be significant. Calculations based on the proton spectrum given by WILLIAMS<sup>(6)</sup> indicate that there may be 2 or 3 fast protons per day capable of producing Čerenkov radiation. Since it is likely that a fast proton would stop in the absorber as a result of nuclear interactions, an ABD-E-S count would be recorded and would be interpreted to be due to a meson with  $v < c/n$ . Thus, protons could perhaps account for an efficiency of 1% or more in test 2). It is possible that the entire 2% to 3% is due to electrons and protons, and that  $\mu$ -mesons with  $v < c/n$  are not detected.

There have been no indications from the tests which have been made that fluorescence produced by the charged particles in the gas is significant.

\* \* \*

We wish to thank the National Science Foundation and the Nebraska University Research Council for financial assistance. We also wish to thank Professor C. E. BENNETT of the University of Maine for his cooperation in providing measurements of indices of refraction.

---

(<sup>6</sup>) R. W. WILLIAMS: *Phys. Rev.*, **98**, 1393 (1955).

## RIASSUNTO (\*)

Si sono eseguite misure di rendimento su un contatore Čerenkov a gas riempito di CO<sub>2</sub> alla pressione di 13.1 atm come radiatore dielettrico. L'indice di rifrazione corrispondente è 1.00569. Si sono contati i mesoni  $\mu$  dei raggi cosmici con velocità nel gas maggiori di quelle della luce, con un rendimento di  $(86 \pm 2)\%$ . Le prove eseguite indicano che il rendimento nel contare i mesoni  $\mu$  con velocità inferiori a quella della luce è minore del 3%.

---

(\*) Traduzione a cura della Redazione.

## Analisi fotometrica delle tracce nelle emulsioni nucleari.

### I. — Dispositivo sperimentale.

M. DELLA CORTE

*Istituto di Fisica dell'Università - Arcetri (Firenze)*

(ricevuto il 24 Settembre 1956)

**Riassunto.** — Si descrive un apparecchio per l'analisi fotometrica delle tracce in emulsioni nucleari. L'apparecchio particolarmente adatto al rilievo del profilo fotometrico trasversale è di costruzione piuttosto semplice e permette di operare con precisione del 2-3% pur mantenendo una velocità di lavoro di circa 500  $\mu\text{m}$  di traccia per ora.

La necessità di rendere più oggettive le misure di alcune grandezze caratteristiche delle tracce di particelle ionizzanti in emulsioni nucleari ha condotto all'applicazione di metodi fotometrici che si sono rivelati utilissimi sia nella determinazione della massa di particelle di carica unitaria sia nello studio dei nuclei pesanti.

Fra i metodi di analisi fotometrica <sup>(1)</sup> adottati nei diversi laboratori, la misura della larghezza media della traccia ottenuta dal profilo fotometrico trasversale si presta particolarmente bene allo studio dei nuclei pesanti e può sostituire il conteggio dei raggi  $\delta$ . Tale misura, fra l'altro, ha il vantaggio di essere praticamente insensibile all'effetto di diffusione degli strati di emulsione sovrastanti alla traccia, e non richiede altra correzione che quella relativa all'inclinazione sul piano dell'emulsione.

Il profilo trasversale della traccia si ottiene, come è noto, registrando il flusso luminoso che attraversa una fenditura molto sottile e parallela all'immagine della traccia quando questa si sposta perpendicolarmente alla sua direzione.

<sup>(1)</sup> L. VAN ROSSUM: *Suppl. Nuovo Cimento*, **2**, 212 (1954).

L'apparecchio descritto in questa nota presenta rispetto ad altri dello stesso tipo una maggior semplicità costruttiva, permette di operare rapidamente con una precisione soddisfacente e può facilmente essere adattato ad altri metodi di analisi fotometrica.

Lo schema generale dell'apparecchio è indicato in Fig. 1.

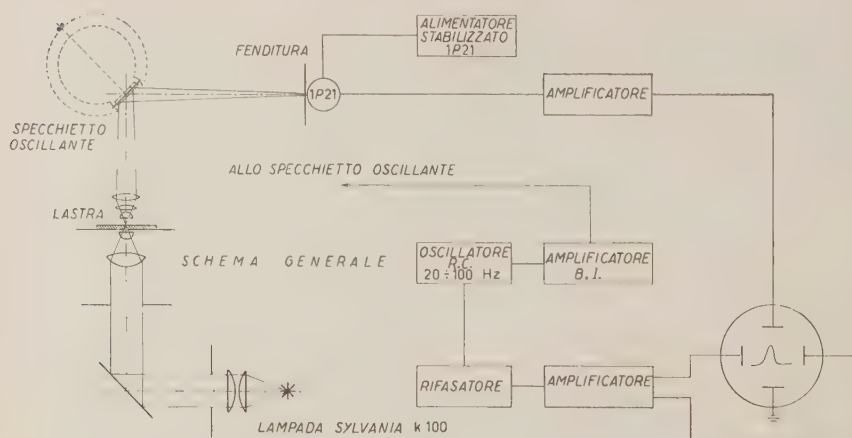


Fig. 1.

Un microscopio Koristka, modello Standard (\*) porta in luogo dell'oculare uno specchietto alluminato inclinato di  $45^\circ$  sull'asse ottico.

Questo specchietto è solidale con la bobina mobile di uno strumento di misura per c.c. Un filo di vetro di qualche decimo di millimetro è fissato alla bobina parallelamente all'indice dello strumento e all'altro estremo può scorrere fra altri due fili ad esso perpendicolari fissati al magnete. Quando la bobina ruota, il filo subisce una flessione e la reazione elastica aumenta la costante di richiamo conferendo al sistema un periodo proprio di oscillazione abbastanza piccolo ed una certa stabilità alle vibrazioni meccaniche.

Quando lo strumento è attraversato da una corrente alternata sinusoidale lo specchietto oscilla e l'immagine della traccia, che si forma in un piano sul quale si trova una fenditura ed a questa parallela, si sposta pure con moto sinusoidale.

Dietro la fenditura si trova un fotomoltiplicatore 1P21 il cui segnale di uscita, opportunamente amplificato, è inviato alle placche  $y$  di un oscillografo catodico.

Un oscillatore a resistenza-capacità pilota sia l'amplificatore con uscita a bassa impedenza che alimenta il sistema dello specchietto oscillante, sia un secondo amplificatore la cui uscita ad alta impedenza è collegata alle placche  $x$  dell'oscillografo.

(\*) L'apparecchio può esser montato su qualsiasi microscopio senza richiedere alcuna modifica.



Fra l'oscillatore e quest'ultimo amplificatore è inserito uno stadio rifasatore in modo che il moto del pennello catodico sull'asse  $x$  possa essere portato in fase con l'oscillazione meccanica dello specchietto.

Gli schemi elettrici dell'oscillatore, rifasatore e degli amplificatori sono riportati in Fig. 2.

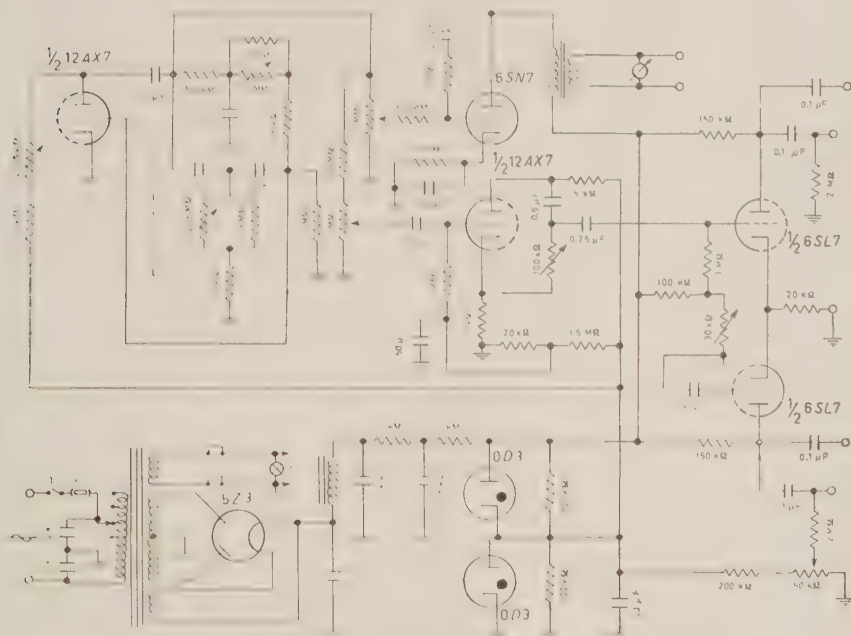


Fig. 2.

Se l'oscillazione meccanica dello specchietto e lo spostamento  $x$  del pennello catodico sono privi di armoniche e in fase, sullo schermo dell'oscillografo compare il profilo fotometrico trasversale della traccia privo di deformazioni.

La fenditura da noi usata ha una larghezza di 0.03 mm e la sua lunghezza può essere variata fra 1 mm e 5 mm. Essa è montata su un supporto solidalmente con un oculare e può essere intercambiata rapidamente con quest'ultimo spostando lateralmente l'insieme. Un tratto di riferimento sul crocifilo dell'oculare corrisponde esattamente alla posizione occupata dalla fenditura.

La lastra viene orientata in modo che la traccia risulti approssimativamente parallela alla fenditura. Questo allineamento, che deve essere il più accurato possibile, viene perfezionato ruotando di qualche grado il sistema fenditura-oculare intorno all'asse ottico. In conseguenza di questa ultima rotazione, la direzione di oscillazione dell'immagine non risulta più perpendicolare a quella della traccia e della fenditura ed è quindi necessario correggere la misura della larghezza dividendo per il coseno dell'angolo di rotazione.



Il tavolino porta oggetti è spostabile micrometricamente in una direzione parallela alla fenditura in modo da poter ottenere rapidamente il profilo trasversale di porzioni successive alla traccia.

L'illuminazione è del tipo convenzionale con una sorgente puntiforme ad alta intensità costituita da una lampada ad arco concentrato Sylvania K 100 alimentata in corrente continua 15.4 V 6.25 A con filtro assorbitore per eliminare l'infrarosso. La messa a punto del sistema di illuminazione deve essere accuratamente verificata con una certa frequenza.

Il sistema fenditura-oculare è montato sullo stativo di un microscopio e può essere spostato verticalmente, cioè nella direzione dell'oscillazione dell'immagine, con movimento micrometrico. Ciò permette, oltre ad un rapido centraggio del profilo, anche la misura diretta dell'ingrandimento « elettromeccanico » cioè del rapporto fra la distanza di due punti sull'oscillogramma e quella fra i corrispondenti punti sul piano della fenditura. È possibile inoltre operare una verifica diretta della costanza di tale ingrandimento nei diversi punti dell'oscillogramma.

L'ingrandimento totale (ingr. ottico  $\times$  ingr. elettromeccanico) può facilmente raggiungere un valore intorno a 20-30 000 in modo che la determinazione della larghezza può essere agevolmente effettuata con un errore di lettura che non supera il 2 o 3%.

La possibilità di ruotare e spostare micrometricamente la fenditura riduce moltissimo il tempo necessario all'aggiustamento che è quello che più incide sulla velocità di lavoro dell'apparecchio.

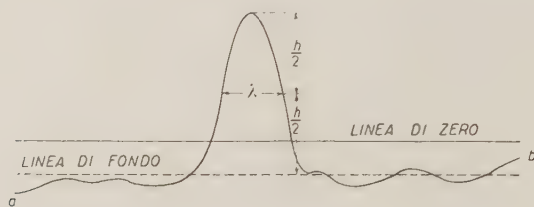


Fig. 3.

I profili si presentano come in Fig. 3. Aumentando l'ampiezza di oscillazione dello specchio si può fare in modo che nei punti estremi *a* e *b* la traccia, compresi gli eventuali  $\delta$ , si trovi tutta fuori della fenditura così che la quota del profilo in questi punti dipenda unicamente dal « fondo » di granuli sparsi dell'emulsione.

La parallela alla linea ottenuta in assenza di segnale (linea di 0) ad una quota media fra quella dei punti *a* e *b* è la « linea di fondo » ed è rispetto a questa che si considera la semi altezza del profilo per la misura della larghezza  $\lambda$ . Questo criterio è giustificato nell'ipotesi di una distribuzione casuale dei granuli di fondo e tien conto di eventuali disuniformità di illuminazione o di assorbimento nell'emulsione.

L'altezza del profilo è molto sensibile alla messa a fuoco ed è conveniente fare questa operazione osservando il profilo e considerando a fuoco il segmento di traccia quando l'altezza del profilo è massima.

Se la traccia da misurare non è parallela al piano dell'emulsione non tutti i suoi punti sono contemporaneamente a fuoco ed il profilo risulta più largo di quanto dovrebbe essere. La correzione da apportare è stata dedotta dalla misura della larghezza del profilo di una traccia parallela all'emulsione in funzione della messa a fuoco. Da questi dati e tenendo conto dell'effetto di « affastellamento » dovuto alla contrazione dell'emulsione si deduce che la correzione da apportare è lineare e raggiunge l'8% per inclinazioni del 20%. Per inclinazioni maggiori tale correzione perde di significato e la misura non è possibile.

La velocità di lavoro del nostro apparecchio è di circa 500  $\mu\text{m}$  all'ora con celle consecutive di 11  $\mu\text{m}$  escluso il tempo per l'aggiustamento iniziale. Un tempo circa uguale è richiesto per le misure sui profili e per i semplici calcoli delle larghezze.

Questo apparecchio è stato realizzato con i fondi messi a nostra disposizione dall'I.N.F.N. - Sezione di Roma.

#### SUMMARY

A simple apparatus for the photometric analysis of the tracks in nuclear emulsions is described. The optically magnified image of a portion of a track is formed on the plane of a slit and parallel to it, after having been reflected by an alluminated (movable) mirror. This mirror is fastened to the moving coil of a d.c. instrument, suitably modified to respond to  $50 \div 100$  Hz a.c. When a.c. is supplied to the coil the image is accordingly displaced sinusoidally in the direction normal to the slit. The variable luminous flux through the slit modulates the output current of a 1P21 Photomultiplier. This current is duly amplified and displayed on the  $y$  axis of a cathode ray oscillograph, whose  $x$ -axis is swept by an a.c. of the same frequency and suitable phase. The photometric profile thus appears on the screen without appreciable deformation. The total magnification is about 20 to 30 thousand times. The working speed is 500  $\mu\text{m}$  of track every hour; the precision of the width measurements is about  $2 \div 3\%$ .

# LETTERE ALLA REDAZIONE

(La responsabilità scientifica degli scritti inseriti in questa rubrica è completamente lasciata dalla Direzione del periodico ai singoli autori)

## A Semi-Empirical Formula for $\alpha$ -Disintegration Energy in the Region of Rare-Earth Nuclides.

M. K. RAMA SWAMY (\*)

Department of Physics, The Johns Hopkins University - Baltimore, Maryland, U.S.A.

(ricevuto il 18 Luglio 1956)

Recently PAL VARSHNI <sup>(1)</sup> has proposed a semi-empirical formula for  $\alpha$ -emitters beyond  $N = 132$  relating the  $\alpha$ -disintegration energy with the neutron and proton numbers. In the course of some studies on the  $\alpha$ -activity of lighter nuclei, the author has arrived at an empirical formula for  $\alpha$ -emitters in the rare-earth region. It is the following

$$E_{\alpha} = 0.36Z - 1.19(N - 82)^{\frac{1}{2}} - 17.89,$$

for  $N > 82$ ,  $Z < 82$

where  $E_{\alpha}$  =  $\alpha$ -disintegration energy

$Z$  = proton number

$N$  = neutron number.

In Table I are reproduced data given by RASMUSSEN, THOMPSON and GHIORSO <sup>(2)</sup>. The penultimate column

lists the  $\alpha$ -disintegration energies as obtained by using the author's formula. The last column contains the difference  $I_{13}$  between the observed and calculated values of the disintegration energies. The average percentage error is  $\pm 5.32$  and hence the agreement between observed values and those calculated by the new formula can be considered quite satisfactory.

As an extension of the above formula beyond rare earths, we calculate the  $\alpha$ -disintegration energy for  $^{178}_{74}\text{W}$ . We obtain  $E_{\alpha} = 3.16$  MeV, whereas the observed value <sup>(3)</sup> is about 3.15 MeV. One may, therefore, expect that the new empirical formula would prove very helpful in predicting  $\alpha$ -disintegration energies in cases where no experimental observations have been made.

\* \* \*

The author is grateful to Prof. L. MANDANSKY for his keen interest in the work.

(\*) On leave from University of Mysore, India.

<sup>(1)</sup> Y. PAL VARSHNI: *Nuovo Cimento*, **3**, 1148 (1956).

<sup>(2)</sup> J. O. RASMUSSEN, S. G. THOMPSON and A. GHIORSO: *Phys. Rev.*, **89**, 33 (1953).

<sup>(3)</sup> W. PORSCHEN and W. RIEZLER: *Zeits. f. Naturf.*, **8a**, 502 (1953).

TABLE I.

	Nuclide	<i>N</i>	(1)	(2)	$\Delta_{12}$ Difference between (1) and (2) (MeV)	(3)	$\Delta_{13}$ Difference between (1) and (3) (MeV)
			$E_{\alpha}$ (experimental) (MeV)	$E_{\alpha}$ (Calc. from semi-empirical mass formula) (MeV)		$E_{\alpha}$ (Calc. from author's formula) (MeV)	
1	<sup>147</sup> Sm	85	<b>2.26</b>	0.08	2.18	<b>2.37</b>	— 0.11
2	<sup>147</sup> Eu	84	<b>2.98</b>	0.73	2.25	<b>3.11</b>	+ 0.13
3	<sup>148</sup> Gd	84	<b>3.27</b>	1.19	2.08	<b>3.47</b>	— 0.20
4	<sup>149</sup> Gd	85	<b>3.10</b>	1.01	2.10	<b>3.09</b>	+ 0.01
5	<sup>150</sup> Gd	86	<b>2.80</b>	0.87	1.90	<b>2.77</b>	+ 0.03
6	<sup>149</sup> Tb	84	<b>4.08</b>	1.60	2.48	<b>3.83</b>	+ 0.25
7	<sup>151</sup> Tb	(86)	<b>3.56</b>	1.28	2.28	<b>3.13</b>	+ 0.43
8	<sup>150</sup> Dy	(84)	<b>4.35</b>	2.05	2.30	<b>4.19</b>	+ 0.16
9	<sup>151</sup> Dy	(85)	<b>4.20</b>	1.87	2.33	<b>3.81</b>	+ 0.39
10	<sup>152</sup> Dy	(86)	<b>3.73</b>	1.73	2.00	<b>3.49</b>	+ 0.24
11	<sup>147</sup> Pm	86	<b>1.56</b> (*) (calc.)	— 0.59	2.15	<b>1.69</b>	— 0.13
12	<sup>147</sup> Nd	87	<b>1.04</b> (*) (calc.)	— 1.28	2.32	<b>1.05</b>	— 0.01
13	<sup>144</sup> Nd	84	<b>1.9</b> (**)	— 0.68	2.58	<b>2.03</b>	— 0.13
14	<sup>148</sup> Sm	86	< <b>2.1</b>	0.07	< 2.2	<b>2.05</b>	< 0.02
15	<sup>146</sup> Sm	84	> <b>2.4</b>	+ 0.28	> 2.1	<b>2.75</b>	> — 0.35

(\*) Calculated from closed decay cycle by RASMUSSEN, THOMPSON and GHIORSO: *Phys. Rev.*, **89**, 33 (1953).

(\*\*) W. PORSCHE and A. RIEZLER: *Zeits. f. Naturf.*, **11a**, 143 (1956).

Interactions faibles directes bosons-leptons et désintégrations des mésons  $K$ .

B. D'ESPAGNAT et J. PRENTKI

CERN - Genève

(ricevuto il 13 Agosto 1956)

Il est bien connu que la complexité de phénomènes de désintégration des hyperons et des mésons lourds rend très délicat le choix entre les divers types d'interactions faibles élémentaires. Différentes possibilités ont été envisagées telles que: interaction universelle de Fermi, interaction universelle de Yukawa (interaction fermions-bosons du type  $\bar{\psi}\psi\varphi\varphi$ ) ou encore un mélange des deux; chacun de ces types d'interaction est d'ailleurs susceptible *à priori* de prendre différentes formes. Dans ces conditions il semble indiqué de procéder par élimination c'est-à-dire de trouver des arguments qui par comparaison avec l'expérience, permettent de rejeter certains couplages.

La présente lettre a pour but de présenter un argument de cette sorte, applicable aux interactions du type de Yukawa. Cet argument est basé d'une part sur les abondance relatives des  $K_{\mu 2}$ ,  $K_{\pi 2}$ ,  $K_{\pi 3}$ ,  $K_{\mu 3}$  et  $K_{e 3}$  qui expérimentalement sont de l'ordre 60:25:7.5:3:5 respectivement <sup>(1)</sup> et d'autre part sur la remarque suivante: les graphes représentant les désintégrations  $K_{\mu 3}$  et  $K_{e 3}$  sont, dans l'hypothèse considérée, néces-

sairement représentés par la Fig. 1, dont la caractéristique essentielle est que le méson  $K$  virtuel qui y figure est de

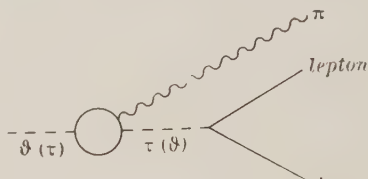


Fig. 1

parité opposée à celle du méson initial. [On peut en effet montrer que les graphes pour lesquels ces parités seraient les mêmes donnent une contribution nulle]. En liaison avec ceci il convient d'observer que l'effet bien connu des couplages du type gradient, consistant à défavoriser la production d'électrons par rapport à celle de muons dans le rapport du carré des masses, subsiste intégralement lorsque le méson lourd qui se désintègre en leptons est non pas réel mais virtuel.

Comme exemple d'application de ces remarques, considérons les hypothèses selon lesquelles 1)  $\theta$  et  $\tau$  appartiennent aux classes  $(0^+)$  et  $(0^-)$  respectivement,

<sup>(1)</sup> S. GOLDBABER: *Conférence de Rochester* (1956), sous presse.

2)  $\mu$  et  $e$  interagissent de la même manière avec les mésons  $K$ , 3)  $\mu$ ,  $e$ ,  $\nu$  ont la même parité intrinsèque <sup>(2)</sup>.

Bien entendu la proportion des  $\theta$  et des  $\tau$  à la production est à priori inconnue: toutefois on ne saurait évidemment avoir  $Nb. \theta \ll Nb. \tau$  vue l'abondance des  $K_{\pi 2}$ . Restent les cas  $Nb. \theta \approx Nb. \tau$  et  $Nb. \theta \gg Nb. \tau$ .

### 1. $Nb. \theta \approx Nb. \tau$ .

Cette hypothèse implique nécessairement que les  $\tau$  créés doivent se désintégrer de préférence en  $K_{\mu 2}$  et contribuer appréciablement à ce mode. L'absence de  $K_{e 2}$  observés implique alors un couplage  $\tau$ -leptons du type  $\gamma_{57'\mu}$ . Trois cas sont alors à considérer:

a)  $\theta$  non couplé aux leptons;

b) couplage  $\theta$ -leptons du type  $\gamma_{\mu}$  (vectoriel).

Ces deux hypothèses sont s'après les remarques du début incompatibles avec l'expérience car, ce qui est facile à voir, elles entraînent  $Nb. K_{e 3} \ll Nb. K_{\mu 3}$ :

c) Couplage  $\theta$ -leptons du type 1 (scalaire).

Pour que néanmoins  $Nb. K_{\mu 2} \gg$

$Nb. K_{e 2}$ , il faut que  $\theta^+$  se désintègre beaucoup plus souvent en  $K_{\pi 2}$  qu'en  $K_{\mu 2}$ : mais alors la réaction

$$(1) \quad \tau \rightarrow \pi + \theta \rightarrow \pi + \mu(e) + \nu$$

serait beaucoup moins fréquente que

$$(2) \quad \tau \rightarrow \pi + \theta \rightarrow \pi + \pi + \pi.$$

Ceci est d'autant plus vrai que la réaction (2) peut s'effectuer aussi par l'in-

termédiaire d'un  $\theta^0$  dont l'élément de matrice de désintégration en  $2\pi$  est plus grand que celui du  $\theta^+$  qui seul figure dans (1). De cette manière apparaît au moins un facteur  $10^{-3}$ . Les  $K_{\mu 3}$  et  $K_{e 3}$  seraient donc dus essentiellement à  $\theta \rightarrow \pi + \tau \rightarrow K_{\mu 3}$ ,  $K_{e 3}$  et d'après la remarque du début  $K_{\mu 3}$  serait beaucoup plus fréquent que  $K_{e 3}$ .

Ainsi l'hypothèse  $Nb. \theta \approx Nb. \tau$  n'est pas compatible avec le schéma d'interactions étudié ici.

### 2. $Nb. \theta \gg Nb. \tau$ .

Dans cette hypothèse les  $K_{\mu 2}$  proviennent nécessairement en majeure partie des  $\theta$ . L'absence de  $K_{e 2}$  implique dès lors un couplage  $\theta$ -leptons du type  $\gamma_{\mu}$ . Trois cas sont de nouveau à considérer:

a)  $\tau$  non couplé aux leptons;

b) couplage  $\tau$ -leptons du type  $\gamma_{57'\mu}$ .

Ces hypothèses sont à rejeter pour la même raison que les hypothèses 1 a, b: elles conduisent nécessairement à

$$Nb. K_{\mu 3} \gg Nb. K_{e 3};$$

c) couplage  $\tau$ -leptons du type  $\gamma_5$ .

Cette hypothèse est la plus favorable: en fait elle n'implique pas de contradiction rédhibitoire avec les résultats expérimentaux concernant les mésons  $K$  chargés pourvu bien entendu que soit convenablement choisi le rapport des constantes de couplage. Notons seulement, pour la suite, que tous les  $K_{\mu 3}$  et  $K_{e 3}$  proviennent des  $\theta$ : en effet la probabilité de  $\tau \rightarrow K_{\pi 3}$  est beaucoup plus grande que celles de  $\tau \rightarrow K_{\mu 3}$ ,  $K_{e 3}$  pour les mêmes raisons que dans le cas 1c, alors que déjà les  $\tau$  sont rares par hypothèse. Une difficulté cependant se présente qui concerne l'explication des  $\theta^0$  anormaux non interprétable en terme de  $K_{\pi 3}^0$  (partie supérieure du spectre pour laquelle l'interprétation  $\pi^{\pm} + \mu^{\mp}(e) + \nu$  semble la plus vraisemblable).

<sup>(2)</sup> On pourrait, moyennant des modifications convenables, s'affranchir de l'hypothèse 3) qui est introduite ici pour des raisons de simplicité. Les résultats essentiels n'en seraient pas changés.



En effet

$$(4) \quad \theta^+ \rightarrow \tau^+ + \pi^0 \rightarrow K_{\mu 3}^+, K_{e3}^+$$

et

$$(5) \quad \theta^0 \rightarrow \tau^+ + \pi^- \rightarrow \begin{cases} \mu^+ + \nu + \pi^- \\ e^+ + \nu + \pi^- \end{cases}$$

ont certainement ici des probabilités de transition du même ordre de grandeur; or la première peut être estimée: elle est approximativement 1/10 de l'inverse de la vie moyenne du  $\theta^+$  soit environ  $10^7$ , c'est-à-dire  $10^{-3}$  fois la probabilité de la transition  $\theta^0 \rightarrow 2\pi$ . Ainsi le nombre des  $V^0$  anormaux provenant des  $\theta^0$  serait très faible. De même  $\tau^0 \rightarrow \pi^+ + \pi^- + \theta^+ \rightarrow \pi^+ + \mu^+ + \nu$  est nécessairement plus rare que

$$(6) \quad \begin{array}{ccc} \tau^0 & \rightarrow & \pi^+ + \theta^+ \\ & \rightarrow & \pi^0 + \theta^0 \end{array} \rightarrow 3\pi$$

par un facteur d'environ 100 (même argument que dans 1c) ce qui, vu la rareté supposée des  $\tau$ , conduit également à une proportion très faible ( $\approx 10^{-3}$ ) des phénomènes  $\tau^0 \rightarrow K_{\mu 3}^0; K_{e3}^0$  par rapport aux  $\theta^0$  normaux. Cette hypothèse conduit donc à un nombre de  $V^0$  anormaux non interprétable en terme de  $K_{\pi 3}^0$  nettement trop faible par rapport au nombre des

$\theta^0$  normaux ou autrement dit à un rapport Nb.  $(K_{\mu 3}^0 + K_{e3}^0)/\text{Nb. } K_{\pi 3}^0$  dont la valeur est incompatible avec ce que l'on peut déduire du spectre observé <sup>(3)</sup>.

On ne peut naturellement exclure la possibilité qu'une autre explication se fasse jour <sup>(4)</sup> pour la majorité des  $V^0$  anormaux qui ne peuvent être des  $\tau^0$ . Dans ce cas les couplages  $\gamma_5$  (pour  $\tau$ ) et  $\gamma_\mu$  (pour  $\theta$ ) seraient les seuls acceptables et la théorie aurait les conséquences suivantes: la grande majorité des  $\tau$  donneraient  $3\pi$ ; le méson  $\theta$  serait responsable des modes de désintégration  $K_{\pi 2}; K_{\mu 2}; K_{\mu 3}$  et  $K_{e3}$ ; évidemment aucune raison n'existerait pour l'égalité des vies moyennes des  $\theta$  et  $\tau$  chargés; concernant les  $V^0$  anormaux on devrait observer des  $K_{\pi 3}^0$  de vie moyenne  $\approx 10^{-8}$  s, un  $K_{e3}^0$  et un  $K_{\mu 3}$  fréquents de  $\sim 10^{-8}$  s et des  $K_{e3}$  et  $K_{\mu 3}$  rares de  $10^{-10}$  s.

Néanmoins de la discussion précédente résulte qu'à l'heure actuelle il semble très difficile d'interpréter toutes les désintégrations des mésons K à l'aide d'interactions de Yukawa si du moins on suppose que les électrons et les muons subissent les mêmes interactions.

<sup>(3)</sup> J. BALLAM, M. GRESARU et S. B. TRETMAN: *Phys. Rev.*, **101**, 1438 (1956).

<sup>(4)</sup> Cfr. M. GELL-MANN and A. PAIS: *Phys. Rev.*, **97**, 1387 (1955).

## On the Basic Formulation of Classical and Quantum Theories.

I. FUJIWARA

*Department of Physics, University of Osaka Prefecture - Sakai, Japan*

(ricevuto il 17 Settembre 1956)

The behavior of any physical system is determined by a Lagrange equation of motion in classical mechanics and by a Schrödinger equation in quantum mechanics respectively. At present these two types of dynamical principles stand independently as rigid postulates for which any disputes have ended for ever. But I want now to point out the possibility of basing them on a single system of fundamental postulates and thus of bringing to light an intimate interrelationship among them.

Historically classical mechanics evolved into quantum theory with the introduction the of quantum of action. The development of this theory culminated in the abstraction of the mathematical framework of the Hilbert space, which is the best suited for formulating the probabilistic features of fundamental facts of microscopic observation. The first step to the reexamination of basic physical principles must be the analysis of the Hilbert space, which is sufficiently abstract in mathematical sense and nevertheless makes a concrete correspondence with real physical situations in atomic level. Contrary to the hitherto accepted belief that the Hilbert space furnishes merely an empty framework for the description of quantum phenomena, it will be shown in the followings that it implies so much as is sufficient to yield the dynamical specification of macroscopic as well as microscopic phenomena combined with the presence of the quantum of action.

A microscopic entity which can be localized by observation at a space-time point  $(q, t)$  is considered. Let the eigenvectors in Hilbert space  $|q, t\rangle$  or  $\langle q, t|$  correspond to the above event of localization. Here we specialize to one space dimension. On these eigenvectors are imposed the conditions of orthogonality and normalization

$$(1) \quad \langle q'', t | q', t \rangle = \delta(q'' - q'),$$

and that of completeness

$$(2) \quad \int |q, t\rangle \langle q, t| dq = 1.$$

The physical implications of these formal conditions are also evident. The inner product of these eigenvectors is then interpreted as the probability amplitude con-

neeting a pair of events of localization at two different space-time points. The conditions (1) and (2) turn out to be the unitary condition for the transformation function:

$$(3) \quad \int \langle q'', t' | q, t \rangle dq \langle q, t | q', t' \rangle = \delta(q'' - q').$$

To this we must add a formal condition

$$(4) \quad \langle q_A, t_A | q_B, t_B \rangle = [\langle q_B, t_B | q_A, t_A \rangle]^*,$$

where the asterisk denotes the complex conjugate. In order to satisfy the conditions (3) and (4) the transformation function must be of the form

$$(5) \quad \langle q_B, t_B | q_A, t_A \rangle = [iU(q_B, t_B; q_A, t_A)]^{\frac{1}{2}} \exp [2\pi i W(q_B, t_B; q_A, t_A)],$$

where  $U(q_B, t_B; q_A, t_A)$  and  $W(q_B, t_B; q_A, t_A)$  are real functions which change signs for the interchange of space-time points  $(q_B, t_B)$  and  $(q_A, t_A)$  and are connected with each other by

$$(6) \quad U(q_B, t_B; q_A, t_A) = \pm \partial^2 W(q_B, t_B; q_A, t_A) / \partial q_B \partial q_A.$$

To fix the sign in (6) we must invoke a further condition

$$(7) \quad \langle q_B, t_B | q_A, t_A \rangle = \int \langle q_B, t_B | q, t \rangle dq \langle q, t | q_A, t_A \rangle,$$

given by formal application of (2). But this does not mean that any function of a pair of space-time points conforms automatically to the recurrence condition (7). The recurrence requirement is quite restrictive, for it demands not only the positive sign in (6) but also that the addition rule

$$(8) \quad W(q_B, t_B; q_A, t_A) = W(q_B, t_B; x, t) + W(x, t; q_A, t_A),$$

must be satisfied for any value of  $t$  at a special point  $x$  defined by

$$(9) \quad \frac{\partial}{\partial x} \{W(q_B, t_B; x, t) + W(x, t; q_A, t_A)\} = 0.$$

We thus get a quantum path  $x(t)$  connecting given space-time points  $(q_A, t_A)$  and  $(q_B, t_B)$ , along which the addition rule (8) holds always true. In the limit of  $(x, t)$  approaching  $(q_B, t_B)$ , (8) reduces to

$$(10) \quad \frac{d}{dt} W(x, t; q_A, t_A) = \lim_{t \rightarrow t_B} \frac{1}{t - t_B} W(q_B, t_B; x, t) = \mathcal{L}[\dot{x}(t), x(t), t].$$

We term  $\mathcal{L}(\dot{x}, x, t)$  as quantum Lagrange function and (10) is integrated to give

$$(11) \quad W(q_B, t_B; q_A, t_A) = \int_{t_A}^{t_B} \mathcal{L}[\dot{x}(t), x(t), t] dt.$$

At the same time (9) turns into

$$(12) \quad \frac{\partial \mathcal{L}}{\partial q} - \frac{d}{dt} \left( \frac{\partial \mathcal{L}}{\partial \dot{q}} \right) = 0,$$

which gives the equation of motion of an imaginary mass point along the quantum path. This can also be derived from the variation principle

$$(13) \quad \delta \int_{t_A}^{t_B} \mathcal{L}(\dot{q}(t), q(t), t) dt = 0,$$

with  $\delta q(t_B) = \delta q(t_A) = 0$ .

The above considerations do not exhaust what is implied by the conditions (3) and (7). The further analysis will be successful only when the restrictions imposed on  $U(q_B, t_B; q_A, t_A)$  and  $W(q_B, t_B; q_A, t_A)$  are all translated into the language of  $\mathcal{L}(\dot{q}, q, t)$ . For example the unitary condition (3) is absorbed in the differential equations

$$(14) \quad \left\{ \begin{array}{l} 2 \frac{\partial^2 \mathcal{L}}{\partial \dot{q}^2} \frac{\partial^4 \mathcal{L}}{\partial \dot{q}^4} - 3 \left( \frac{\partial^3 \mathcal{L}}{\partial \dot{q}^3} \right)^2 = 0, \\ \text{and} \\ \frac{\partial^3}{\partial \dot{q}^3} \left\{ \left( \frac{\partial \mathcal{L}}{\partial q} - \frac{\partial^2 \mathcal{L}}{\partial q \partial \dot{q}} \dot{q} \right) \frac{\partial^2 \mathcal{L}}{\partial \dot{q}^2} \right\} = 0. \end{array} \right.$$

A similar treatment is also possible for the recurrence condition (7) and this is now under investigation. That is all that can be said about the Hilbert space without the introduction of the quantum of action.

In the condition (7) we see a characteristic feature of the probabilistic description of quantum phenomena. The probability amplitude  $\langle q_B, t_B | q_A, t_A \rangle$  is composed of  $\langle q_B, t_B | q, t \rangle$  and  $\langle q, t | q_A, t_A \rangle$ , but the product must be integrated over all possible values of  $q$ . In the macroscopic level the situation is quite different. The point  $x$  where the localization occurs at any time  $t$  is uniquely determined by events of localization at two space-time points  $(q_A, t_A)$  and  $(q_B, t_B)$ . In order to incorporate this classical determinism into the framework of the abstract Hilbert space we set the postulate that there exists a certain universal constant  $\varkappa$  yet unknown and very small in e.g.s. units and in addition to this that in the limit  $\varkappa \rightarrow 0$  all the contribution in the integral (7) vanishes except from a very narrow range around a particular point  $x$ . Now the transformation function involves the constant  $\varkappa$  and we can expand  $W(q_B, t_B; q_A, t_A)$  in an ascending power series in  $\varkappa$ . Only when the exponential factor of the integrand in (7)

$$\exp [2\pi i \{ W(q_B, t_B; q, t) + W(q, t; q_A, t_A) \}],$$

oscillates more and more rapidly with diminishing  $\varkappa$ , the required cancellation occurs. We thus see that the power series in  $\varkappa$  must begin with the term  $\varkappa^n$  with any finite

positive integer  $n$ . Introducing a new constant  $h = \kappa^n$  we can set

$$(15) \quad W(q_B, t_B; q_A, t_A) = \frac{1}{h} \{S(q_B, t_B; q_A, t_A) + T(q_B, t_B; q_A, t_A)\},$$

where  $S$  is independent of  $h$  and  $T$  subsumes all terms of higher order than the first. The classical point  $x$  which contributes most strongly to the integral (7) is defined, as is easily seen, by

$$(16) \quad \frac{\partial}{\partial x} \{S(q_B, t_B; x, t) + S(x, t; q_A, t_A)\} = 0,$$

and equating the phases in both sides of (7) we get the addition rule

$$(17) \quad S(q_B, t_B; q_A, t_A) = S(q_B, t_B; x, t) + S(x, t; q_A, t_A).$$

These are of completely the same form as (8) and (9). In terms of

$$(18) \quad L[\dot{x}(t), x(t), t] = \lim_{t \rightarrow t_B} \frac{1}{t_B - t} S(q_B, t_B; x, t),$$

the equation for the classical path (16) is transformed into

$$(19) \quad \frac{\partial L}{\partial q} - \frac{d}{dt} \left( \frac{\partial L}{\partial \dot{q}} \right) = 0$$

and the addition rule (17) into

$$(20) \quad S(q_B, t_B; q_A, t_A) = \int_{t_A}^{t_B} L[\dot{x}(t), x(t), t] dt.$$

As (19) furnishes the classical equation of motion, we can identify  $L(\dot{q}, q, t)$  with the classical Lagrange function itself, so that  $S(q_B, t_B; q_A, t_A)$  must be Hamilton's first principal function or the classical action function. Moreover (15) shows that the constant  $h$  is of the physical dimension of action. We term this as the quantum of action. But at present there is no need for specifying its actual magnitude. This is the whole story of classical mechanics.

In the limit  $t \rightarrow t_B$  (15) reduces to

$$(21) \quad \mathcal{L}(\dot{q}, q, t) = \frac{1}{h} \{L(\dot{q}, q, t) + M(\dot{q}, q, t)\}.$$

Thus if the classical Lagrange function  $L(\dot{q}, q, t)$  is given, the differential equations such as (14) determine the additional term  $M(\dot{q}, q, t)$  and accordingly the quantum Lagrange function  $\mathcal{L}(\dot{q}, q, t)$  itself. Then we can find the quantum path with the aid of (12), and (11) determines  $W(q_B, t_B; q_A, t_A)$ . Finally (5) and (6) complete the computation of the probability amplitude  $\langle q_B, t_B | q_A, t_A \rangle$ . The way has thus been paved leading from the classical Lagrange function directly to the quantum mechanical transformation function. We had better term this procedure as the classicalization of the general mathematical framework of the Hilbert space through the mediation of the classical Lagrange function embodying the classical model of the physical system under consideration rather than as the quantization of the classical dynamical system specified by a given  $L(\dot{q}, q, t)$ .

The usual formulation of quantum mechanics is based on the fundamental postulate that as to the dynamical description of the same physical system the generator of the canonical transformation in classical mechanics and the generating operator of the unitary transformation in quantum mechanics have identical functional constitution. In order to be able to decide the question whether the present point of view is completely equivalent to the time-honored postulate of quantum mechanics we must make a more elaborate discussion of the conditions imposed on the quantum Lagrange function  $\mathcal{L}$ . If such conditions are sufficiently restrictive to permit a unique determination of  $\mathcal{L}$  for any given  $L$  except for trivial additional terms, the situation is rather simple. But if this is not actually the case, there arises an interesting problem of searching a further principle that helps us to arrive at the Schrödinger equation. At any rate it is now clear that the dynamical principle of quantum mechanics is a composite of several formal conditions in the Hilbert space and the requirement of the transition to the macroscopic determinism combined with the existence of the quantum of action. This is nothing but a definite postulation of the correspondence principle, without which any formulation of basic physical principles can not claim to be complete.

The origin of the present thinking is Dirac's remarks on the action principle <sup>(1)</sup> and especially Feynman's over-all-space-time version of quantum mechanics <sup>(2)</sup>. One can easily see that many ideas are taken from these preceding investigations, for which I want to express sincere thanks. But the most characteristic difference lies in the fundamental attitude toward the unification of basic physical principles. It is intended here to minimize the number of fundamental postulates and especially to eliminate a special principle termed as dynamical from any mode of description of natural phenomena.

Now I want to make only one comment on Feynman's recipe for the construction of the transformation function

$$22) \quad K(q_B, t_B; q_A, t_A) = \int \exp [2\pi i S/h] d(\text{paths}) .$$

This was based essentially on the observation that the transformation function might sufficiently be approximated by  $(1/4) \exp [2\pi i S(q_B, t_B; q_A, t_A)/h]$  in the limit  $t_B \rightarrow t_A$ . The question is whether one can find a good reason sufficient to assure the vanishing of  $T(q_B, t_B; q_A, t_A)$  in (15) in the limit  $t_B \rightarrow t_A$  without relying upon the Schrödinger equation. Moreover the mathematical definition of integral over all possible paths is rather obscure and so we have to reinterpret it as straightforward iteration of (7) regarded simply as the composition rule but not as the recurrence requirement. Then I am afraid that one would be surprised to find that the final result of (22) could not actually furnish the original form  $(1/4) \exp [2\pi i S/h]$  in the limit  $t_B \rightarrow t_A$  except for the trivial cases of free particle and harmonic oscillator. At any rate the neglect of the recurrence requirement (7) is fatal and at this point my solution is as follows. The classical Lagrange function may be set rather arbitrarily. But the quantum Lagrange function is subject to severe restrictions. The gap is bridged over by the additional term  $M(\dot{q}, q, t)$  in (21) with the intervention of the quantum of action  $h$ .

<sup>(1)</sup> P. A. M. DIRAC: *Phys. Zeits. Sowjetunion*, **3**, 64 (1933); *Rev. Mod. Phys.*, **17**, 195 (1945); *The Principles of Quantum Mechanics* (Oxford, 1947), third edition.

<sup>(2)</sup> R. P. FEYNMAN: *Rev. Mod. Phys.*, **20**, 367 (1948).



Tracce  $\alpha$  in emulsioni nucleari esposte in aria ad alto contenuto di radon.

G. ALIVERTI e A. DE MAIO

*Istituto Superiore Navale - Napoli*

G. LOVERA e R. PERILLI-FEDELI

*Istituto di Fisica dell'Università - Modena**Istituto Nazionale di Fisica Nucleare - Sezione di Torino*

(ricevuto il 18 Settembre 1956)

Di recente, sono stati resi noti da DEUTSCH<sup>(1)</sup> i risultati di uno studio sulle tracce di particelle  $\alpha$ , dovute a radioattività naturale, presenti alla superficie delle emulsioni nucleari, indipendentemente da una specifica esposizione a sorgenti radioattive. Le lastre Ilford, del tipo C<sub>2</sub> «purificate», spesse 200  $\mu\text{m}$ , sono state conservate per 116 giorni, a emulsioni affacciate, fuori dell'imballaggio, in ambiente secco a 4 °C. Delle tracce  $\alpha$  in esse osservate, aventi un estremo almeno alla superficie dell'emulsione, l'85% è attribuito dall'A. al Rn presente nella sottile intercapedine d'aria (circa 0.1 mm) separante le emulsioni affacciate, ed ai successori RaA e RaC'; ed il 15% restante all'attività di polveri, depositate alla superficie, con ancorati atomi di radionuclidi a vita lunga, ed all'attività propria dell'emulsione (tracce  $\alpha$  provenienti dall'interno delle medesime: queste ultime, secondo un lavoro precedente<sup>(2)</sup>, contribuirebbero per il 10%

circa dell'effetto totale). Non sono state osservate stelle a due rami, dovute a coppie di tracce  $\alpha$  del RaA e RaC'.

Risultati in parte analoghi ed in parte discordanti sono stati da noi ottenuti nelle osservazioni delle tracce di particelle  $\alpha$  in emulsioni nucleari (Ilford C<sub>2</sub> ordinarie, 2.5 cm  $\times$  7.5 cm, spessore 100  $\mu\text{m}$ ), esposte in aria arricchita di Rn. Precisamente, in un ambiente chiuso, del volume di 11 litri, contenente  $\frac{2}{3}$  di litro circa di acqua proveniente da sorgenti radioattive dell'Isola d'Ischia (e dalla quale, mediante un'appropriata agitazione, grande parte dell'emanazione era stata liberata nell'aria dell'ambiente stesso), è stata introdotta, immediatamente dopo queste operazioni preliminari eseguite rapidamente, una coppia di lastre (A, B), delle quali la B con la superficie dell'emulsione rivolta verso l'acqua, e la A in senso opposto; le lastre sono rimaste 2 ore nella camera.

Le lastre A e B, dopo sviluppo, sono state esplorate al microscopio, per campi discreti situati ai vertici di un reticolato (con maglia di 1 mm per la lastra A, e di 2 mm per la lastra B). Entro ciascun campo individuato da una quadrettatura

(<sup>1</sup>) S. DEUTSCH: *Nuovo Cimento*, **3**, 1166 (1956).

(<sup>2</sup>) S. DEUTSCH e E. C. DODD: *Nuovo Cimento*, **10**, 858 (1953).

del micrometro oculare, si sono contate le tracce di particelle  $\alpha$  aventi un estremo, almeno, alla superficie dell'emulsione, e le coppie di tracce uscenti da uno stesso punto situato pure alla superficie dell'emulsione stessa. I risultati dei conteggi sono contenuti nella tabella I. Una lastra testimonio, non esposta all'aria arricchita di Rn, ha presentato, in superficie, una densità di 11.1 tracce per  $\text{mm}^2$ .

TABELLA I.

lastra	A	B
area totale esplorata ( $\text{mm}^2$ ) . .	38.25	8.91
n. totale tracce singole . . . .	4935	1871
n. tracce singole per $\text{mm}^2$ . . .	129.0	210.0
n. totale coppie	87	43
n. coppie		
n. tracce singole	0.018	0.023

Per identificare gli atomi emettitori delle particelle  $\alpha$ , sono state eseguite misure di lunghezza sia di tracce isolate, sia delle tracce di tutte le coppie; per le tracce inclinate rispetto al piano dell'emulsione, sono state misurate le due proiezioni, rispettivamente parallela e ortogonale a questo piano, e per la seconda si è tenuto conto del fattore di contrazione dell'emulsione.

Precisamente, nella lastra A si è misurata la lunghezza di 504 tracce singole (con percorso residuo superiore a  $5 \mu\text{m}$ ), senza alcuna discriminazione per l'inclinazione: in Fig. 1 è riportato l'istogramma delle lunghezze, raggruppate in intervalli di  $5 \mu\text{m}$ . La Fig. 2 è invece l'istogramma delle lunghezze di tutte le coppie osservate nelle lastre A e B.

Il diagramma di Fig. 1 presenta una notevole somiglianza con quello di Deutsch (l.c. (1), Fig. 1); in particolare vi si notano i massimi: tra 25 e  $30 \mu\text{m}$

(RaA) prevalente, e tra 35 e  $40 \mu\text{m}$  (RaC'), di altezza un po' minore. Effettivamente, le condizioni di esposizione



Fig. 1.

delle lastre A e B si avvicinano, fisicamente, a quelle delle lastre di Deutsch: in quanto nel nostro caso all'inizio della esposizione nella camera non erano presenti apprezzabilmente i depositi attivi

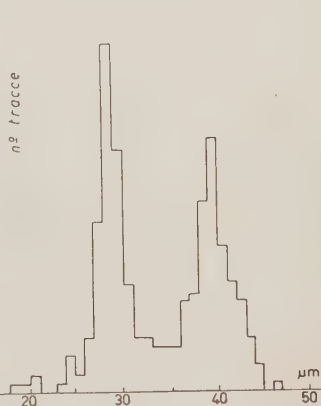


Fig. 2.

del Rn (che poi soltanto alla fine delle due ore di esposizione, hanno potute avvicinarsi all'equilibrio col Rn), e

analogamente, nel caso di Deutsch, nello stretto interstizio tra le emulsioni delle due lastre circolerebbero alcuni atomi di Rn, dai quali sporadicamente, di tanto in tanto, si originerebbero atomi dei nuclidi successori a vita breve, in media secondo il ritmo delle rispettive disintegrazioni radioattive.

Anche la parte dell'istogramma verso le lunghezze minori, dovuta a tracce che hanno esaurito solo in parte il loro cammino nella emulsione, è simile nei due casi, benché nella disposizione di Deutsch il Rn fosse contenuto in uno strato sottile tra le emulsioni affacciate, mentre nella disposizione nostra lo spazio libero antistante alle emulsioni era enormemente più esteso, anzi con spessore uguale (in direzione ortogonale alle lastre) al percorso massimo, nell'aria, delle particelle  $\alpha$  dei radionuclidi interessati. Bisogna notare, a questo riguardo, che nel caso di Deutsch, il 10% circa delle tracce  $\alpha$  che attraversano la superficie ha origine nella disintegrazione di atomi radioattivi contenuti nell'interno dell'emulsione: ora, questo 10% dà ragione, evidentemente, di una buona parte dell'effetto di fondo nell'istogramma, ed in particolare della parte verso le lunghezze minori; d'altro canto, lo spessore dell'emulsione usato in quelle esperienze (200  $\mu$ m) è largamente superiore al massimo percorso delle tracce  $\alpha$  della radioattività naturale nell'emulsione stessa, sicché per l'effetto di fondo si riproducono, sia pure per motivi differenti, condizioni analoghe a quelle delle nostre lastre.

Una netta differenza tra i nostri risultati e quelli di Deutsch è costituita dall'osservazione, nelle nostre lastre, di coppie di tracce con origine in comune, mentre il Deutsch non ne ha riscontrate nelle sue osservazioni.

Dall'istogramma di Fig. 2 appare chiaramente che le lunghezze delle tracce delle coppie si raggruppano intorno ai valori relativi al  $RaA$  e  $RaC'$ : anche lo spoglio dei valori inerenti alle singole coppie conferma che si tratta, in generale, di coppie di tracce dovute l'una a  $RaA$  e l'altra a  $RaC'$ . (Questo fatto e la circostanza che la frequenza delle coppie, come risulta sia dalla tabella I sia da altre lastre sulle quali non si è qui riferito, stia in rapporto pressoché costante con quello delle tracce singole, indipendentemente dalla densità di queste per  $mm^2$ , porta ad escludere che si tratti di coincidenze casuali, almeno in misura apprezzabile). Il fatto che la frequenza delle coppie possa essere minore di quanto prevedibile, non infirma il risultato, data la possibilità, per un atomo radioattivo che si trovi alla superficie dell'emulsione, di staccarsene per rinculo nella emissione di una particella  $\alpha$  verso l'interno dell'emulsione stessa.

La presenza di coppie trova del resto riscontro in risultati di osservazioni<sup>(3)</sup> precedenti, eseguite con altro procedimento di raccolta della radioattività atmosferica.

(<sup>3</sup>) G. ALIVERTI, A. DE MAIO, G. LOVERA, e R. PERILLI-FEDELI: *Nuovo Cimento*, **12**, 270, (1954).

## Dimensionality of Charge Space.

D. C. PEASLEE (\*)

*Radiation Laboratory University of California - Berkeley, Cal.*

(ricevuto il 18 Settembre 1956)

There is no dearth of experimental evidence to indicate that real space-time is a four-dimensional manifold. At present there is much less certainty in attributing dimensions to the charge space of heavy particles, and it may be worth while to review various hypotheses and the meager experimental evidence in this regard. The Clebsch-Gordon coefficients for  $I$ -spin that appear in the  $\pi$ -N (nucleon) scattering resonance imply at least a two-dimensional space for unitary transformations<sup>(1)</sup>, which are conveniently represented in the usual terms of rotations in a three-dimensional space.

The apparent symmetry between  $\Xi$  and N can be emphasized to the maximum extent by regarding the charge displacement number  $a = q - I_z$  of heavy particles as the third component of another vector  $\mathbf{A}$  in charge space<sup>(2)</sup>. If  $\mathbf{A}$  is to be independent of  $\mathbf{I}$ , there must be added an independent pair of co-ordinates for the unitary transformations

corresponding to rotations of  $\mathbf{A}$ , implying a charge space of at least four dimensions<sup>(3)</sup>, which might perhaps be extended to five dimensions. The four-dimensional scheme in its primary form specifically neglects the  $\Xi$ , N mass difference and assumes complete symmetry between these particles, whose four varieties comprise the elements of a vector in four-dimensional charge space. The  $\Lambda$  is a charge scalar and may in this approximation have the same mass as  $\Xi$ , N. From this four-scalar and four-vector one can construct a five-vector.

A recent proposal<sup>(4)</sup> for writing  $q = I_z + a + b$  invites recasting in terms of charge vectors by putting  $a = A_z$  and  $b = B_z$ , where  $\mathbf{B}$  is a third independent vector in charge space<sup>(5)</sup>. This appears as the simplest way of introducing the additional complexity needed; it requires another pair of independent co-ordinates

(\*) Permanent address: Purdue University, Lafayette, Indiana.

(1) E.g., B. L. VAN DER WAERDEN: *Gruppentheoretische Methode* (Berlin, 1932).

(2) F. D'IMBIO: *Nuovo Cimento*, **3**, 595 (1956); D. C. PEASLEE: in press.

(3) A. PAIS: *Proc. Nat. Acad. Sci. U.S.*, **40**, 484 (1954); A. SALAM and J. C. POLKINGHORNE: *Nuovo Cimento*, **2**, 685 (1955).

(4) R. G. SACHS and S. B. TREIMAN: *Nuovo Cimento*, **2**, 1331 (1955).

(5) The introduction of three independent vectors in charge space has been independently suggested by O. HARA and Y. FUJII (private communication).

for the associated unitary transformations and raises the minimum dimensionality of charge space to six. There is in principle no end to this process: one can postulate additional charge vectors  $\mathbf{C}, \mathbf{D}, \dots$ ; for  $n$  such independent vectors the minimum dimensionality of charge space is  $2n$ , and there will be  $(n-1)$  distinct hierarchies of strange particles.

To illustrate simply how each independent spin vector requires the addition of two more dimensions, consider the Dirac equation in  $2n$  dimensions. Let

$$(1) \quad \gamma_A \gamma_B + \gamma_B \gamma_A = 2\delta_{AB} \quad A, B = 1 \dots 2n$$

be matrices for linearizing a quadratic form in  $2n$  dimensions. Adjoin to this a two-dimensional space with associated Pauli spin operators  $\sigma_x, \sigma_y, \sigma_z$  and corresponding  $2 \times 2$  unit matrix 1. Then define

$$(2) \quad \begin{cases} \Gamma_A = 1 \gamma_A, & A = 1 \dots 2n-1 \\ \Gamma_n, \Gamma_{n+1}, \Gamma_{n+2} = \sigma_x \gamma_n, \sigma_y \gamma_n, \sigma_z \gamma_n \end{cases}$$

so that

$$(3) \quad \Gamma_A \Gamma_B + \Gamma_B \Gamma_A = 2\delta_{AB}, \\ A, B = 1 \dots 2n+2.$$

The  $\Gamma_A$  are the Dirac matrices for  $2n+2$  dimensions; for  $n=1$  this procedure corresponds to the  $\mathbf{p}, \boldsymbol{\sigma}$  formulation of the usual Dirac equation. The customary arguments for the four- and six-dimen-

sional<sup>(6)</sup> cases can be repeated to show that all irreducible representations of Eq. (3) are equivalent to Eq. (2). Thus each increase of dimensionality by two units allows the introduction of an independent spin vector  $\boldsymbol{\sigma}$ ; in each such spin space higher spin values follow by vectorial addition of a sufficient number of basic spins  $\frac{1}{2}$ .

The same procedure illustrates how spaces of  $2n+1$  dimensions also allow at most  $n$  independent spin vectors. For by defining  $\gamma_{2n+1} = \gamma_1 \gamma_2 \dots \gamma_{2n}$ , we can write Eq. (1) for  $A, B = 1 \dots 2n+1$  without introducing a new Pauli spin  $\boldsymbol{\sigma}$ . The number of independent spin vectors accordingly increases only with the even-dimensional spaces.

Experimental evidence on the dimensionality of charge space becomes increasingly tenuous with increasing  $n$ . The four-dimensional scheme cannot readily account for the  $\Xi, N$  mass difference but has a number of formal attractions and is accessible to further experimental study<sup>(2)</sup>. The possibility of some five-dimensional charge symmetry is not yet ruled out, but would require the  $\Lambda$  and  $N$  to have identical spins and parities. The six-dimensional hypothesis<sup>(4)</sup> would require increased statistics on anomalous V-decays for verification.

\* \* \*

This work was performed under the auspices of the U.S. Atomic Energy Commission.

(6) D. C. PEASLEE: *Phys. Rev.*, **84**, 373 (1951).

## On the Vanishing of the Interaction Hamiltonian (\*).

J. M. COOK

*Argonne National Laboratory - Lemont, Illinois*

(ricevuto il 23 Settembre 1956)

Assertions of LANDAU, POMERANČUK, and others <sup>(1)</sup> that point interaction in quantum field theory produces no physical interaction, can be derived from the following simpler considerations.

Assume that two quantized fields have a Fock representation <sup>(2)</sup> with states corresponding to elements of the Hilbert spaces  $\mathfrak{F}_1$  and  $\mathfrak{F}_2$  respectively. Couple them by a non-local interaction of range  $\Lambda^{-1}$ , with corresponding interaction Hamiltonian  $H_\Lambda$ . We show that if  $\lim_{\Lambda \rightarrow \infty} H_\Lambda = H_\infty$  exists in any sense <sup>(3)</sup>, then it commutes with an irreducible set of operators and therefore is merely a constant multiple of the identity,  $H_\infty = cI$ .

The system consisting of both fields has states represented by elements of the tensor product  $\mathfrak{F}_1 \otimes \mathfrak{F}_2$  <sup>(4)</sup>.  $H_\Lambda$  is an operator on  $\mathfrak{F}_1 \otimes \mathfrak{F}_2$  given by the

symbolic integral

$$\int_{(\sigma, \sigma)} f_\Lambda(\mathbf{x}_1, \mathbf{x}_2) H(\mathbf{x}_1, \mathbf{x}_2) d\mathbf{x}_1 d\mathbf{x}_2.$$

where:  $\mathbf{x}_1$  and  $\mathbf{x}_2$  vary separately over the same space-like surface  $\sigma$  (i.e.,  $(\mathbf{x}_1, \mathbf{x}_2)$  varies over the cartesian product  $(\sigma, \sigma)$ ); the form factor  $f_\Lambda$  is zero when  $|\mathbf{x}_1 - \mathbf{x}_2| > \Lambda^{-1}$ ; and  $H(\mathbf{x}_1, \mathbf{x}_2)$  is an improper operator which represents the contribution of the coupling of the fields at the point  $(\mathbf{x}_1, \mathbf{x}_2)$  to the total energy. (E.g., in the electromagnetic case

$$H(\mathbf{x}_1, \mathbf{x}_2) = \sum_{\kappa=0}^3 A_\kappa(\mathbf{x}_1) \otimes j_\kappa(\mathbf{x}_2).$$

Such point-wise defined operators, let  $G(\mathbf{x}_1, \mathbf{x}_2)$  stand for the general case, must be multiplied by a numerical function, say  $g(\mathbf{x}_1, \mathbf{x}_2)$ , and the product integrated in order to obtain a proper operator

$$G(g) = \int_{(\sigma, \sigma)} g(\mathbf{x}_1, \mathbf{x}_2) G(\mathbf{x}_1, \mathbf{x}_2) d\mathbf{x}_1 d\mathbf{x}_2.$$

The symbolic expression

$$\begin{aligned} [H(\mathbf{x}_1, \mathbf{x}_2), G(\mathbf{x}'_1, \mathbf{x}'_2)] = \\ = \delta(\mathbf{x}_1 - \mathbf{x}'_1, \mathbf{x}_2 - \mathbf{x}'_2), \end{aligned}$$

(\*) Work performed under the auspices of the U. S. Atomic Energy Commission.

(1) I. POMERANČUK: *Nuovo Cimento*, **3**, 1186 (1956).

(2) V. FOCK: *Zeits. f. Phys.*, **75**, 622 (1932).

(3) L. D. LANDAU, A. A. ABRIKOSOV and I. M. HALATNIKOV: *Suppl. Nuovo Cimento*, **3**, 80 (1956).

(4) F. J. MURRAY and J. VON NEUMANN: *Ann. Math.*, **37**, 116 (1936). Especially Ch. II, pp. 127-138.



implies that  $[H(f), G(g)] = 0$  when the set of points on which  $f$  is non-zero is disjoint from the set on which  $g$  is non-zero. In particular, if  $g_\varepsilon$  has the property that  $g_\varepsilon(\mathbf{x}_1, \mathbf{x}_2) = 0$  when  $|\mathbf{x}_1 - \mathbf{x}_2| \leq \varepsilon$ , and if  $G(g_\varepsilon)$  represents an observable, then  $[H_A, G(g_\varepsilon)] = 0$  when  $A^{-1} < \varepsilon$ ; so  $[H_\infty, G(g_\varepsilon)] = 0$ .

Let  $u_1(\mathbf{x})$  and  $u_2(\mathbf{x})$  be any two functions square-integrable over  $\sigma$ , and define  $g_\varepsilon(\mathbf{x}_1, \mathbf{x}_2)$  on  $(\sigma, \sigma)$  by

$$g_\varepsilon(\mathbf{x}_1, \mathbf{x}_2) = \begin{cases} u_1(\mathbf{x}_1)u_2(\mathbf{x}_2) & \text{if } |\mathbf{x}_1 - \mathbf{x}_2| > \varepsilon, \\ 0 & \text{if } |\mathbf{x}_1 - \mathbf{x}_2| \leq \varepsilon; \end{cases}$$

and now impose on  $G$  the restriction that it represents a product of observables of the two uncoupled fields, so  $G(g_0) = G(u_1 u_2) = G_1(u_1) \otimes G_2(u_2)$  for some  $G_1$  and  $G_2$ . Then, as above,  $[H_\infty, G(g_\varepsilon)] = 0$  for  $\varepsilon > 0$ . But  $g_\varepsilon \rightarrow g_0$  and  $G(g_\varepsilon) \rightarrow G(g_0)$  as  $\varepsilon \rightarrow 0$ , so  $[H_\infty, G_1(u_1) \otimes G_2(u_2)] = 0$ .

The set of all such  $G_1(u_1)$  is irreducible on  $\mathfrak{F}_1$ , as is that of all such  $G_2(u_2)$  on  $\mathfrak{F}_2$ : Therefore the set of all  $G_1(u_1) \otimes G_2(u_2)$  is irreducible on  $\mathfrak{F}_1 \otimes \mathfrak{F}_2$  and so  $H_\infty$ , which commutes with every element of this irreducible set, must be a constant times

the identity. Hence it can have no effect on the behaviour of the system.

This result is based essentially on the fact that the subset of  $(\sigma, \sigma)$  consisting of all  $(\mathbf{x}_1, \mathbf{x}_2)$  with  $\mathbf{x}_1 = \mathbf{x}_2$ , is a subset of Lebesgue measure zero. When the interaction Hamiltonian is written

$$H_{\text{int}} = \int_{\sigma} H_{\text{int}}(\mathbf{x}) d\mathbf{x},$$

the integral appears to have been taken over a set of positive measure, namely, all of  $\sigma$ . The notation conceals the fact that  $H_{\text{int}}(\mathbf{x}) = H(\mathbf{x}, \mathbf{x})$ , where operators relating to  $\mathbf{x}_1$  in  $H(\mathbf{x}_1, \mathbf{x}_2)$  operate on one space,  $\mathfrak{F}_1$ , while those relating to  $\mathbf{x}_2$  operate on another,  $\mathfrak{F}_2$ .

The above considerations arose during an attempt, sponsored by the National Science Foundation, to give a completely rigorous treatment of the point interaction. This rigorization does not seem worth pursuing since, as the preceding formal treatment shows, the point interaction Hamiltonian apparently does not exist as a legitimate operator on Hilbert space.

## Nuclear Isomeric Shift on Spectral Lines. (\*)

R. WEINER

*Physical Institute of the Academy of the Roumanian People's Republic - Bucharest*

(ricevuto il 25 Settembre 1956)

According to the nuclear shell model, the states of odd nuclei are described by the states of odd (« optical ») nucleons (a proton for odd-even nuclei, a neutron for even odd nuclei). Hence it follows directly that for nuclei with an « optical » proton the nuclear electric density and consequently the electric field in which atomic electrons move will depend on the energy state of the nucleus. This should be more easily shown experimentally with nuclear isomers which possess metastable states (where the shell theory has given good results).

We shall deal therefore with the isomeric nuclei in the fourth shell and in particular with  $^{115}_{49}\text{In}$  III and we shall prove that the above electron-proton interaction should give place to a spectral line shift within the reach of interferential spectroscopy. This shift presents theoretical interest and if it is confirmed, it might lay, together with the hyperfine structure effect (the nuclear spin depends also on the energy state of the nucleus) the basis for a new experimental method for research and spectral analysis of nuclear isomerism.

The nuclear electric density is:

$$\varrho = e \sum_{i=1}^{i=Z} \Psi_i^* \Psi_i.$$

where  $Z$  is the nuclear charge and  $\Psi_i$  the nucleon wave function in the  $i$ -th state.

From the linearity of Poisson's equation it follows that the difference  $\varphi_m - \varphi_f$  where  $\varphi_m$  is the electric nuclear potential for the metastable state and  $\varphi_f$  the same potential for the fundamental state, depends only on the difference of the respective densities  $\varrho$ , that is on:

$$\varrho_m - \varrho_f = e(\Psi_m^* \Psi_m - \Psi_f^* \Psi_f),$$

where  $\Psi_m$  and  $\Psi_f$  are the wave functions of the optical proton in the metastable and the fundamental states, respectively.

The first approximation of the perturbation method gives us the following

---

(\*) Details will appear in *Studii si Cercetări de Fizică*, 7, n. 4 (1956).

spectral term shift due to nuclear isomerism:

$$\Delta E = -e \int (\varphi_m - \varphi_f) |\psi_e|^2 d\tau,$$

where  $\psi_e$  is the wave function of the optical electron (we limit ourselves to atoms with a single optical electron) and the integration is to be carried out over the whole space.

For an  $s$ -electron, we make use for  $|\psi_e|^2$  of Racah's expression <sup>(1)</sup>:

$$|\psi_e|^2 = \frac{2(1+\gamma)\psi_e^2(0)}{F^2(2\gamma+1)} \left(\frac{2Z}{a_0}\right)^{2\gamma-2} r^{2\gamma-2},$$

with  $\gamma = \sqrt{1 - \alpha^2 Z^2}$ , where  $\alpha$  is the fine structure constant,  $a_0$  the radius of the first Bohr orbit, and  $\psi_e(0)$  the value of the non-relativistic wave function in the origin. This value has been calculated for fundamental electronic state from the empirical data of the hyperfine structure spectrum of In III <sup>(2)</sup>. We obtained

$$\psi_e^2(0) = 1.3 \cdot 10^{26} \text{ cm}^{-3}.$$

As to  $\varphi_m - \varphi_f$ , we have:

$$\varphi_m - \varphi_f = \int \frac{\varrho_m - \varrho_f}{|\mathbf{r} - \mathbf{r}'|} d\mathbf{r}' = e \int \frac{\psi_m^* \psi_m - \psi_f^* \psi_f}{|\mathbf{r} - \mathbf{r}'|} d\mathbf{r}'.$$

For  $\psi$  we use the oscillator wave functions. The radial component of these functions is:

$$R_{n_r, l} = r_0^{-(2l+3)/4} \left( \frac{2}{n_r! 2^{2n_r} \Gamma(n_r + l + \frac{3}{2})} \right)^{\frac{1}{2}} r^{-(l+1)} \exp \left[ \frac{1}{2} \left( \frac{r}{r_0} \right)^2 \right] \left( \frac{1}{r} \frac{d}{dr} \right)^{n_r} \cdot \exp \left[ - \left( \frac{r}{r_0} \right)^2 \right] r^{2n_r + l + 1}$$

with:

$$n_r = \frac{n - l}{2},$$

$n$  being the principal quantum number related to the oscillator energy  $E$  and frequency  $\omega/2\pi$  by

$$E = \hbar \omega (n + \frac{3}{2}),$$

$l$  is the azimuthal quantum number and

$$r_0 = \sqrt{\frac{\hbar}{\mu \omega}},$$

where  $\mu$  is the nucleon mass.

<sup>(1)</sup> G. RACAH, *Nature*, **129**, 723 «1932».

<sup>(2)</sup> F. PASCHEN and J. L. CAMPBELL: *Ann. d. Phys.*, **31**, 29 «1938».

In the fourth shell the interesting states are  $1g_{\frac{7}{2}}$  and  $2p_{\frac{3}{2}}$ . (For In,  $1g_{\frac{7}{2}}$  is the fundamental state; it is obvious that the absolute magnitude of the effect differs from one element to another by the value of  $\psi_e$  only.

To determine  $\omega$  we identify the nuclear radius  $R$ , calculated from the formula:

$$R = R_0 A^{\frac{1}{3}},$$

where  $R_0 = 1.2 \cdot 10^{-13}$  cm and  $A$  is the mass number, with the convenient root of the equation

$$\frac{d^2 q_t}{dr^2} = 0,$$

$q_t$  being here the total nuclear density (including the neutrons). The result is

$$r_0 \approx 2.5 \cdot 10^{-13} \text{ cm}.$$

After calculating  $q_m - q_f$  and carrying out the integration, we obtain finally:

$$\Delta E \approx -5 \cdot 10^{-2} \text{ cm}^{-1}.$$

An analogous but much smaller effect is to be expected from the even-odd nuclei, due to electron-neutron interaction. Preliminary calculations for Hg, in which the empirical value of the electron-neutron interaction potential was used, led us to an effect which is by two orders of magnitude smaller than the above one, and thus at the limit of optical measurability. Nevertheless, a more accurate calculation is needed without using the empirical interaction potential, because this potential concerns the interaction bound electron-free neutron, whereas the isomeric shift is due to bound electron-bound neutron interaction. We are studying at present this problem.

## Role of Continued Excitation in the Potential Inversion of the Joshi Effect.

S. R. MOHANTY, L. V. KANNAN and S. VISVANATHAN

*Physico-Chemical Laboratories, Banaras Hindu University, India*

(ricevuto il 26 Settembre 1956)

The exciting potential  $V$  is one of the chief determinants of the sign and the magnitude of the Joshi effect  $\pm \Delta i$  <sup>(1,2)</sup>. MOHANTY <sup>(3)</sup> has shown that the sign reversal of the effect,  $+\Delta i \rightleftharpoons -\Delta i$  at the first inversion potential  $V_i^I > V_m$  the threshold potential of the self-maintained discharge and the subsequent change  $+\Delta i \rightleftharpoons +\Delta i$  at  $V_i^II \gg V_m$ , is significant for the mechanism of the phenomenon. Furthermore,  $+\Delta i$  in fresh tubes also inverts <sup>(4)</sup> under continued discharge (aging) at constant  $V$  in the range  $V_m - V_i^I$ . The present communication describes a typical set of results on the role of aging in the potential inversion of the effect.

A freshly prepared and chemically cleaned discharge tube, a glass cylinder (inner diameter, 4.9 mm; outer diameter, 6.6 mm) provided with external (platinum) ring electrodes 3.0 cm apart, con-

tained pure oxygen at 25 mm<sub>Hg</sub> (29 °C) pressure. Mercury vapour from the pumps and the manometers was avoided by making use of tin, gold and liquid-air traps. The tube was excited at different (2-4.5 kV, rms)  $V$  of 50 Hz frequency and  $\pm \Delta i$  was measured on a galvanometer-crystal (1N34, Sylvania) assembly

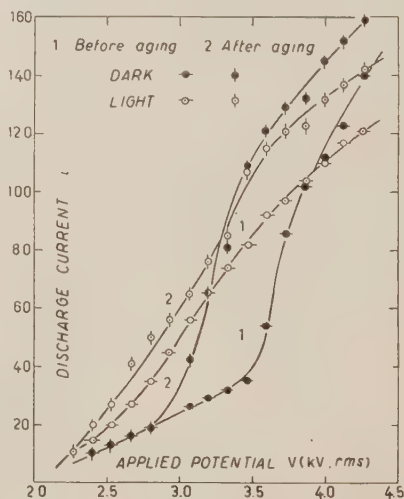


Fig. 1. — Potential-current characteristics, in dark and under light, before and after ageing.

<sup>(1)</sup> S. S. JOSHI: *Proc. Ind. Sci. Congr.*, Presidential Address, Chemistry Section (1943).

<sup>(2)</sup> S. R. MOHANTY, K. R. K. RAO and T. R. BHAT: *Nuovo Cimento*, **4**, 1463 (1956).

<sup>(3)</sup> S. R. MOHANTY: *Journ. Chem. Phys.*, **23**, 1533 (1955).

<sup>(4)</sup> S. R. MOHANTY: *Zeits. f. Phys. Chem. (Neue Folge)*, **4**, 233 (1955).

with light (3700-7800 Å) from a 300 W 200 V incandescent tungsten filament lamp. It was next subjected to continuous discharge for three hours at 4.3 kV and  $\pm \Delta i$  redetermined over the above  $V$ -range. The results are shown graphically in Figs. 1 and 2.

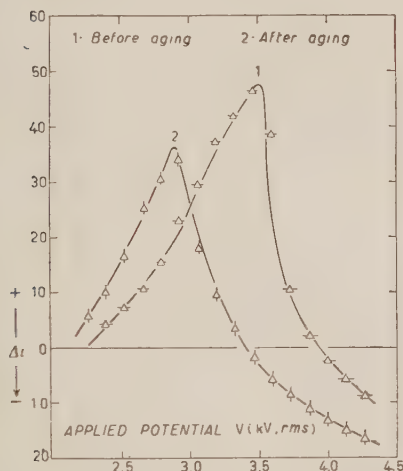


Fig. 2. — Shift in the potentials for maximum positive Joshi effect and inversion due to ageing.

It is seen from Fig. 1 that whereas in dark there is a well defined  $V_m$  characterized by a sudden increase in the current  $i$ , under light the discharge passes more or less smoothly from the non-self- to

the self-maintained one, resulting in the observed monotonous increase in  $i$  with the applied  $V$ . This fact is of importance for theories of the mechanism of the gas discharge<sup>(5)</sup> and the influence thereon of external irradiation<sup>(6)</sup>. Furthermore, in agreement with the earlier findings of MOHANTY<sup>(7)</sup>,  $V_m$  is diminished due to ageing, viz. from 3.52 to 2.92 kV, and since  $i$  is a  $f(V - V_m)$ , the discharge current  $i$  is augmented.

On theoretical considerations, MOHANTY<sup>(2,8)</sup> has identified the potential  $V_{+\Delta i \max}$  for maximum  $+\Delta i$  (cf. Fig. 2) with  $V_m$ . Experimental evidence for the validity of this deduction is furnished by the results of the present investigations;  $V_{+\Delta i \max}$  is 3.52 kV before and 2.91 kV after ageing. The inversion potential  $V_i$  and the  $V$ -range for the occurrence of  $+\Delta i$  are diminished due to ageing, the former from 3.93 to 3.42 kV.

\*\*\*

(Grateful thanks of the authors are due to Professor S. S. JOSHI for his kind interest in the work.

(<sup>5</sup>) S. R. MOHANTY: *Journ. Chem. Phys.*, **22**, 2095 (1954).

(<sup>6</sup>) S. R. MOHANTY: *Zeits. f. Phys.*, **140**, 370 (1955).

(<sup>7</sup>) S. R. MOHANTY: *Journ. Chim. Phys.*, **52**, 815 (1955).

(<sup>8</sup>) S. R. MOHANTY: *Journ. Sci. Res. Banaras Hindu Univ.*, **6**(1), 58 (1955-56).



Radiations from  $^{66}\text{Ge}$  and  $^{67}\text{Ge}$ .

R. A. RICCI (\*) and R. VAN LIESHOUT

*Instituut voor Kernfysisch Onderzoek - Amsterdam, The Netherlands*

(ricevuto il 28 Settembre 1956)

H. H. HOPKINS produced  $^{66}\text{Ge}$  and  $^{67}\text{Ge}$  for the first time in spallation reactions <sup>(1)</sup>. These isotopes decay into  $^{66}\text{Ga}$  and  $^{67}\text{Ga}$  by positron emission with a period of  $\sim 2.5$  h and 21 min respectively. The decay of  $^{67}\text{Ge}$  was investigated by ATEN *et al.* <sup>(2)</sup>, who reported a half life of 19 min, a complex positron spectrum with a branch of maximum energy  $\sim 2.9$  MeV and a  $\gamma$ -ray of  $(170 \pm 10)$  keV. CHAPMAN *et al.* <sup>(3)</sup> recently observed levels in  $^{67}\text{Ga}$ , which are not in agreement with the 170 keV  $\gamma$ -ray found by Aten.

In order to clarify this question and to have more information on these decays, we have investigated the  $^{66}\text{Ge}$  and  $^{67}\text{Ge}$  isotopes produced from chemically pure Zn irradiated by about 52 MeV  $\alpha$ -particles in the cyclotron.

$^{67}\text{Ge}$  was produced during a bombarding time of 5 to 10 min (corresponding to a flux of 0.1 to 0.3  $\mu\text{ah}$ ) and

for  $^{66}\text{Ge}$  a bombarding time up to 1 h (i.e. up to  $\sim 2 \mu\text{ah}$ ) was used.

The Ge fraction was distilled off and counted in standard geometry with single channel analysers connected with  $\gamma$ -scintillation counters and, in some cases, with a kicksorter of the Hutchinson-Scarrott type. The results are shown in Table I. The relative intensities are only approximate.

TABLE I

$E_\gamma$ (keV)	Half life	Nuc- lide	Rel. $\gamma$ -Intensity
$\sim 360$	$2 \div 4$ h	$^{66}\text{Ge}?$	—
$186 \pm 4$	$(160 \pm 10)$ min	$^{66}\text{Ge}$	$\sim 0.5$
$182 \pm 4$	long	$^{67}\text{Ga}$	—
$170 \pm 3$	$(21 \pm 1)$ min	$^{67}\text{Ge}$	$> 60\%$ of the $\beta^+$ -disin- tegrations of $^{67}\text{Ge}$
$114 \pm 2$	$(145 \pm 5)$ min	$^{66}\text{Ge}$	$\sim 0.5$
$92 \pm 2$	long	$^{67}\text{Ga}$	—
$70 \pm 1$	$(145 \pm 5)$ min	$^{66}\text{Ge}$	$\sim 0.2$
$45 \pm 1$	$(150 \pm 5)$ min	$^{66}\text{Ge}$	1

(\*) On leave from the «Istituto di Fisica Sperimentale del Politecnico di Torino», Italy.

<sup>(1)</sup> H. H. HOPKINS JR.: *Phys. Rev.*, **77**, 717 (1950); H. H. HOPKINS JR. and B. B. CUNNINGHAM: *Phys. Rev.*, **73**, 1406 (1948).

<sup>(2)</sup> A. H. W. ATEN JR., T. DE VRIES-HAMERLING and L. LINDNER: *Physica*, **19**, 1046 (1953); A. H. W. ATEN JR.: *Physica*, **22**, 288 (1956).

<sup>(3)</sup> R. A. CHAPMAN, J. B. MARION and J. C. SLATTERY: *Bull. Am. Phys. Soc.*, **1**, No. 2, 95, No. 3 (1953).

From this table the following considerations can be drawn:

$^{67}\text{Ge}$  - Only one strong  $\gamma$ -ray

decaying with a half life of  $21 \pm 1$  min was found and its energy was  $(170 \pm 3)$  keV. The presence of weak  $\gamma$ -rays in the region of 300 to 1000 keV cannot be excluded, but they may be assigned to  $^{66}\text{Ge}$  and  $^{66}\text{Ga}$ , which are present in our sources and have weak  $\gamma$ -rays in this region.

The methods of production and separation used enable us to exclude the presence in the source of an appreciable quantity of  $^{70}\text{Ga}$  which is known to decay with a  $\gamma$ -ray of  $(174 \pm 5)$  keV (0.3%) and a half life of 21 min. Therefore, the 170 keV  $\gamma$ -ray can be assigned to  $^{67}\text{Ge}$  with the highest probability.

-  $^{66}\text{Ge}$  - The peaks found in our  $\gamma$ -ray spectrum have energies of  $(114 \pm 2)$ ,  $(70 \pm 1)$  and  $(45 \pm 1)$  keV. These  $\gamma$ -rays decay all with a half life of  $\sim 2.5$  h; therefore, they are assigned to  $^{66}\text{Ge}$ . A peak with energy of about 186 keV has been observed and after preliminary computations, we believe that it should be assigned to  $^{66}\text{Ge}$  owing to its half life ( $\sim 2.5$  h) and its strong intensity relative to the 92 keV  $\gamma$ -ray of  $^{67}\text{Ga}$  which grows from the decay of  $^{67}\text{Ge}$ . In fact the 182 keV  $\gamma$ -ray, which is also present in the decay of  $^{67}\text{Ga}$ , is known to be 43% of the 92 keV  $\gamma$ -ray; therefore the 186 keV  $\gamma$ -ray observed is probably due to  $^{66}\text{Ge}$ .

The annihilation peak has also been

observed and followed in its decay; it shows components of 20 min and 2.5 h in different proportions depending on the duration of the bombardment. A peak at about 360 keV with a half life of  $2 \div 4$  h seems to be due to  $^{66}\text{Ge}$ , but more conclusive experiments are necessary to clarify this question.

More detailed descriptions of this investigation and more conclusive considerations will be submitted for publication in *Nuclear Physics*.

\* \* \*

Thanks are due to Miss M. GROEN for performing the chemical separations and to the group Philips of the cyclotron for the bombardments.

The interest of Prof. Dr. P. C. GUGELOT, Prof. Dr. A. H. W. ATEN jr. and of Prof. Dr. A. H. WAPSTRA is gratefully acknowledged. One of the authors (R.A.R.) wishes to thank the « Politecnico di Torino » for a grant and Prof. E. PERUCCA for his interest in the work. He also expresses his gratitude for the hospitality at the « Instituut voor Kernfysisch Onderzoek ».

This work was performed as part of the research program of the « Stichting voor Fundamenteel Onderzoek der Materie F.O.M. » which is financially supported by the « Nederlandse Organisatie voor Zuiver Wetenschappelijk Onderzoek Z.W.O. ».

Elastic Scattering of  $\alpha$ -Particles.

S. W. MAC-DOWELL and J. J. GIAMBIAGI

*Centro Brasileiro de Pesquisas Físicas - Rio de Janeiro, Brasil*

(ricevuto il 1° Ottobre 1956)

Porter's explanation <sup>(1)</sup> of the elastic scattering of  $\alpha$ -particles is based upon a nuclear model in which the protons are more concentrated close to the center than the neutrons, as suggested by JOHNSON and TELLER <sup>(2)</sup>. Indeed the distortion of the Coulomb orbits due to the distribution of protons in the nucleus may be neglected if the  $\alpha$ -particles do not penetrate deeply into this distribution. The nuclear absorption would be due to the presence of the external neutron layer.

If we assume a uniform distribution of protons in a sphere of radius  $R = 1.2 \cdot 10^{-13} A^{\frac{1}{3}}$  cm, then the  $\alpha$ -particles with 22 MeV energy colliding with nuclei of  $^{108}\text{Ag}$  can penetrate only slightly into the charged sphere. However, at higher energies, such a 48 MeV <sup>(3)</sup>, the  $\alpha$ -particles may penetrate deeply into this sphere and are able to overcome the Coulomb barrier. Therefore we must expect essential deviations from the pure hyperbolic paths. Thus, at these energies, we cannot use the Coulomb potential as in Porter's work. However when the potential for a uniformly charged sphere is used to calculate the classical trajectories, we get into a serious difficulty as the scattering angle has a maximum value in complete disagreement with the experimental results.

The scattering angle, as given by Hamilton-Jacobi theory, is:

$$(1) \quad \theta = \omega + 2 \cos^{-1} \left[ \left( 1 + \frac{\alpha}{2} \operatorname{ctg}^2 \frac{\omega}{2} \right) \sin \frac{\omega}{2} \right] - \cos^{-1} \left\{ \frac{\frac{\alpha}{2} \operatorname{ctg}^2 \frac{\omega}{2} - \left( \frac{1}{\alpha} - \frac{3}{2} \right)}{\left[ \frac{\alpha}{2} \operatorname{ctg}^2 \frac{\omega}{2} + \left( \frac{1}{\alpha} - \frac{3}{2} \right)^2 \right]^{\frac{1}{2}}} \right\},$$

where  $\alpha = ZZ'e^2/RE$  and  $\omega$  is the corresponding scattering angle in a pure Coulomb field. In Fig. 1,  $\theta$  is plotted against  $\omega$  and it is shown that  $\theta_{\max}$  is about  $42^\circ$ ; experimental data give a finite scattering cross-section until far beyond this angle. In

<sup>(1)</sup> C. E. PORTER: *Phys. Rev.*, **99**, 1400 (1955).

<sup>(2)</sup> M. H. JOHNSON and E. TELLER: *Phys. Rev.*, **93**, 357 (1954).

<sup>(3)</sup> R. E. ELLIS and L. SCHECTER: *Phys. Rev.*, **101**, 636 (1956).

order to avoid this difficulty, it should be necessary to take a much smaller radius for the distribution of protons than is indicated in any other experiments.

On the other hand, when we try to improve Porter's calculation of the hyperbolic orbits in a pure Coulomb field, we are led again to unsatisfactory results. We have assumed a uniform distribution of matter in a sphere of radius  $R = R_{Ag} + R_{\alpha} =$

$= 8.4 \cdot 10^{-13}$  cm; therefore, the ratio

$$\frac{\sigma}{\sigma_C} = \exp \left( - \int \frac{\rho ds}{\epsilon_0 l_0} \right),$$

becomes

$$(2) \quad \frac{\sigma}{\sigma_C} = \exp \left[ - \frac{s}{l_0} \right],$$

and we used for  $s$  an approximate formula

$$(3) \quad s = \frac{1}{3}(v_M + 2v_m)T,$$

where  $T$  is the time spent by the  $\alpha$ -particles inside the sphere,  $v_m$  is the velocity at its nearest position from the center, and  $v_M$  is that at the entrance into the nucleus. (This formula would be exact if  $v = v_m + \text{const} \times t^2$ , which is a reasonably good approximation). Hamilton-Jacobi theory gives for  $T$ :

$$(4) \quad T = \left( \frac{m}{2E} \right)^{\frac{1}{2}} \frac{ZZ'e^2}{E} \left\{ \left( A^2 - \csc^2 \frac{\omega}{2} \right)^{\frac{1}{2}} + \ln \left( \left| A + \left( A^2 - \csc^2 \frac{\omega}{2} \right)^{\frac{1}{2}} \right| \sin \frac{\omega}{2} \right) \right\},$$

where

$$A = \frac{2RE}{ZZ'e^2} \quad (5)$$

Fig. 2 shows the experimental values of  $\sigma/\sigma_C$  plotted against  $s$  varying either

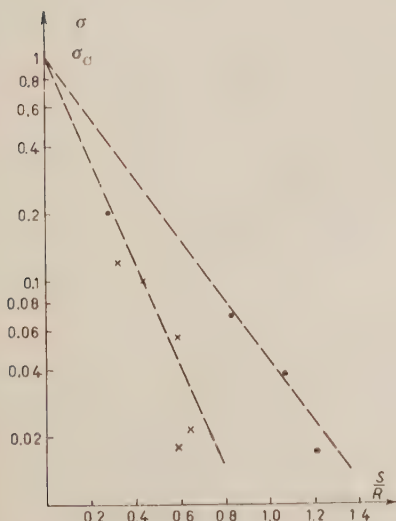


Fig. 2. -- Plot of differential elastic scattering cross-section divided by the Coulomb cross-section of  $\alpha$ -particles by  $^{108}\text{Ag}$ , versus the  $\alpha$ -particle path inside a uniform distribution of matter divided by the total radius of the distribution:

$$R = R_{Ag} + R_{\alpha} = 8.4 \cdot 10^{-13} \text{ cm}$$

are data for constant scattering angle  $\sim 61^\circ$   
are data for constant energy  $E = 22 \text{ MeV}$ .

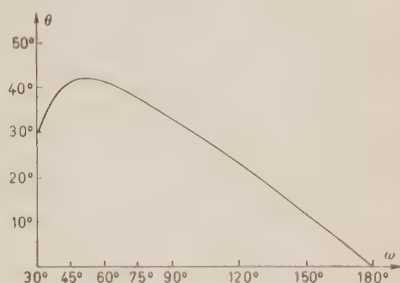


Fig. 1. -- Theoretical scattering angle of 48 MeV  $\alpha$ -particles by  $^{108}\text{Ag}$ . The curve shows the scattering angle for a uniform distribution of charge with radius of  $1.2 \cdot 10^{-13} \text{ cm}$ , as a function of the Coulomb scattering angle.

the energy <sup>(4)</sup> or the scattering angle <sup>(5)</sup>. According to (2), both curves should be coincident straight lines. Moreover, it can be shown that, at constant energy,  $\int \varrho \, ds$  exhibits a maximum at a certain angle whatever the distribution of matter is, provided  $\varrho$  is a decreasing function of  $r$ . At this angle,  $\sigma/\sigma_c$  has a minimum. With a uniform distribution, this minimum occurs at an angle where a decreasing behaviour has been observed experimentally.

\* \* \*

The authors are indebted to Prof. J. TIOMNO for useful discussions on the subject.

---

<sup>(4)</sup> N. S. WALL, J. R. REES and K. W. FORD: *Phys. Rev.*, **97**, 726 (1955).

<sup>(5)</sup> G. W. FARWELL and H. E. WEGNER: *Phys. Rev.*, **95**, 1212 (1954).

On the Spin and Parity of the First Excited State of  $^{19}\text{O}$ .

R. V. POPIĆ

*Institute of Nuclear Sciences «Boris Kidrič» - Vinča, Belgrade*

(ricevuto il 4 Ottobre 1956)

The theoretical attempt done <sup>(1)</sup> to predict energies, spins and parities of the levels of  $^{19}\text{O}$  did not succeed completely, because the three nucleon configuration is a rather complicated theoretical problem. It seems that the nuclear models we know today are not consistent enough to reproduce the experimental state of affairs of this situation.

Even a so refined work as that of ELLIOTT and FLOWERS gives a too low value (0.5 MeV) for the excitation energy of the  $\frac{1}{2}^+$  state of  $^{19}\text{O}$  which experimentally is found <sup>(2)</sup> to be 1.468 MeV above the ground state, and is unable to account for the excited state at  $94 \pm 8$  keV <sup>(3)</sup>.

We shall now try to derive spin and parity of this excited state by using the angular distribution <sup>(3)</sup> of the stripping reaction  $^{18}\text{O}(d, p)^{19}\text{O}$ . The Tobocman's theory of stripping <sup>(4)</sup>, which in

spite of some deficiencies seems to be the most consistent one, will be here applied. Because the energy of the incoming deuteron beam is 0.8 MeV, the Coulomb effect has to be taken into account, while effects due to the interactions of the deuterons and the protons with the target nucleus will be neglected. As it can be seen from Fig. 1, the last effects should be considered in order to

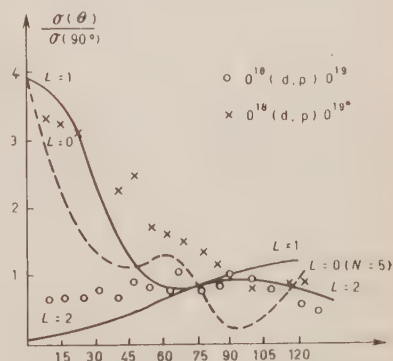


Fig. 1. — Experimental and theoretical angular distributions for the reactions  $^{18}\text{O}(d, p)^{19}\text{O}$  and  $^{18}\text{O}(d, p)^{19}\text{O}^*$ . Energy of deuterons 0.8 MeV. The theoretical angular distribution for  $L=0$  has been reduced by a factor 5. The denoted  $L$  is the orbital quantum number of the captured neutron.

<sup>(1)</sup> J. P. ELLIOTT and B. H. FLOWERS: *Proc. Roy. Soc., A* **229**, 536 (1955).

<sup>(2)</sup> T. F. STRATTON, J. M. BLAIR, K. F. FARMULARO and R. V. STUART: *Phys. Rev.*, **98**, 629 (1955).

<sup>(3)</sup> K. AHN Lund: *Ark. f. Fys.*, **10**, 425 (1956).

<sup>(4)</sup> W. TOBOCMAN: *Phys. Rev.*, **94**, 1655 (1954); W. TOBOCMAN and M. H. KALOS: *Phys. Rev.*, **97**, 132 (1955).



improve the agreement between the theoretical results and the experimental data, but for our purpose this better fit is not needed.

The data for the  $^{18}\text{O}(\text{d}, \text{p})^{19}\text{O}$  reaction confirm the known result that the ground state of  $^{19}\text{O}$  is a  $\frac{5}{2}^{+}$  state. As far as the excited state is concerned, the experimental data show clearly the trend of a  $L = 1$  curve, so that there are the two possibilities for the spin of the excited state, i.e. either  $\frac{1}{2}^{-}$  or  $\frac{3}{2}^{-}$ .

From the theoretical point of view, we have two possibilities to obtain in  $^{19}\text{O}$  an odd parity excited state: either from a breakup of the  $^{19}\text{O}$  double closed shell or from an excitation of one of the

outer nucleons up to the  $f$ -shell <sup>(5)</sup>. We believe that the later alternative cannot possibly work with such a low excitation energy of the level, and therefore we are lead to suggest the spin  $\frac{1}{2}^{-}$  for the level of  $^{19}\text{O}$  found at  $94 \pm 8$  keV. This choice would, of course, imply an excitation of a  $p$ -nucleon of the  $^{19}\text{O}$  core to the nearest even shell.

\* \* \*

I wish to thank Dr. E. CLEMENTEL and Dr. B. H. FLOWERS for some useful discussions concerning this problem.

---

<sup>(5)</sup> M. G. REDLICH: *Phys. Rev.*, **99**, 1427 (1955).

Study of a Low-intensity Component in the  $\beta$ -ray Spectrum of  $^{214}_{83}\text{Bi}$  (RaC).

G. R. BISHOP and F. DEMICHELI

*École Normale Supérieure - Laboratoire de Physique, Paris*  
*Istituto di Fisica Sperimentale del Politecnico - Torino*

(ricevuto il 10 Ottobre 1956)

The  $\beta$ -ray spectrum in the transition  $^{214}_{83}\text{Bi}$  (RaC)  $\rightarrow$   $^{214}_{84}\text{Po}$  (RaC') has recently been examined by absorption and coincidence techniques <sup>(1)</sup>.

This work demonstrated the existence of a ground state transition (end point 3.17 MeV), and of a transition (end point 2.56 MeV) to the first excited state (0.606 MeV) of  $^{214}_{84}\text{Po}$ , among others.

Subsequently the angular correlation between the 2.56 MeV  $\beta$ -ray, and the 0.606 MeV  $\gamma$ -ray was measured <sup>(2)</sup>, and indicated a forbidden  $\beta$ -ray transition.

However further examination <sup>(3)</sup> of the  $\beta$ -spectrum with a magnetic spectrograph, showed no trace of the 2.56 MeV  $\beta$ -ray. Since the intensity of this ray, as found by the analysis of absorption curves, is quite small (6%), its detection with a magnetic spectrograph is difficult.

We have therefore conducted a search for the 2.56 MeV  $\beta$ -ray, using a proportional scintillation counter.

This counter consisted of a cylinder of plastic phosphor (\*), measuring 4 cm  $\times$  4 cm, with a central conical hole, (1.5 cm deep, 1 cm minimum diameter at the entrance, 1.4 cm maximum diameter at the bottom) into which the  $\beta$ -rays were collimated with aluminium stops. The response of the crystal to  $\beta$ -rays was calibrated with internal conversion electrons (0.661 MeV) of a source of  $^{137}_{55}\text{Cs}$ , and the  $\beta$ -spectrum (end point 1.71 MeV) of  $^{32}_{15}\text{P}$ . A resolution of 15% was obtained for the internal conversion electrons of  $^{137}_{55}\text{Cs}$ .

With the same geometry we then measured the differential spectrum of  $\beta$ -rays of a source of  $^{214}_{83}\text{Bi}$  in equilibrium, and we found a curve (Fig. 1a) showing definite breaks at energies corresponding to 3.2 MeV, 2.6 MeV and 1.7 MeV.

This experimental curve demonstrates conclusively the existence of the 2.56 MeV

<sup>(1)</sup> R. A. RICCI and G. TRIVERO: *Nuovo Cimento*, **2**, 745 (1955); A. WAPSTRA: private communication.

<sup>(2)</sup> F. DEMICHELI and L. A. RADICATI *Nuovo Cimento*, **3**, 152 (1956).

<sup>(3)</sup> H. DANIEL and R. NIERHAUS *Zeits. f. Natur.*, **11**, 3, 212 (1956).

(\*) Polystyrene with terphenyl and tetraphenyl butadiene.

$\beta$ -ray, because of the definite change of slope of this plot at an energy of 2.6 MeV.

We then measured coincidences between the  $\beta$ -rays and the 0.606 MeV  $\gamma$ -ray as a function of the pulse height in the  $\beta$ -ray counter. We obtained a

\*\*\*

We would like to thank Prof. Y. ROCARD for extending to us the facilities of the Laboratoire de Physique of the École Normale Supérieure, where the

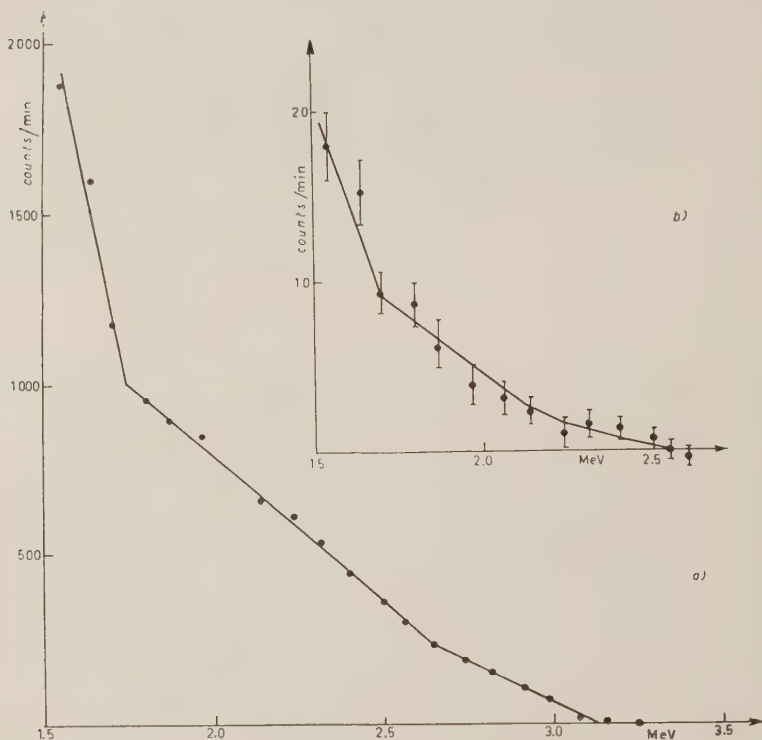


Fig. 1. — *a*) Differential  $\beta$ -spectrum, versus  $\beta$ -particle energy; *b*) Coincidence  $\beta$ - $\gamma$ , versus  $\beta$ -particle energy.

curve (Fig. 1*b*) showing a sharp break at an energy of 1.7 MeV, and the coincidence spectrum then fell off to zero at 2.6 MeV.

We thus have demonstrated the existence of a 2.56 MeV  $\beta$ -ray, using a method very different from those previously employed.

research has been carried out and Prof. H. HALBAN for his interest in this work. One of the authors (F.D.) wishes to thank the Consiglio Nazionale delle Ricerche for a grant making possible her displacement from the Politecnico to the École Normale, and Prof. E. PERUCCA for his interest.

## Metodi funzionali nelle teorie dei campi.

R. CIRELLI

*Istituto Nazionale di Fisica Nucleare - Sezione di Milano*

M. PUSTERLA

*Istituto di Fisica dell'Università - Pavia  
Istituto Nazionale di Fisica Nucleare - Sezione di Milano*

(ricevuto l'11 Ottobre 1956)

Nell'ordinaria meccanica quantistica, il propagatore di un sistema è una funzione delle coordinate connesse con lo stato iniziale e finale <sup>(1)</sup>:

$$K(q', t | q_0', t_0) = \langle q', t | q_0', t_0 \rangle .$$

Passando ad una teoria di campo il propagatore diviene un funzionale delle variabili  $\psi$  in quanto dipende, sia all'istante  $t_0$  che all'istante  $t$ , dagli autovalori di  $\psi(\mathbf{x})$  in ogni punto dello spazio:

$$K[\psi_t(\mathbf{x}), t; \psi_0(\mathbf{x}), t_0] = \langle \psi'_t(\mathbf{x}_1), \psi'_t(\mathbf{x}_2) \dots | \psi'_0(\mathbf{x}_1), \psi'_0(\mathbf{x}_2) \dots \rangle .$$

Nel caso di un campo bosonico scalare neutro tale propagatore può essere ottenuto formalmente da un'analisi del campo in oscillatori:

$$(\square - \mu^2)\psi(x, y, z, t') = 0 ,$$

assumiamo come base di sviluppo la successione orto-normale

$$2\sqrt{2}V^{-\frac{1}{2}} \sin\left(\frac{\pi n_x}{L}x\right) \sin\left(\frac{\pi n_y}{L}y\right) \sin\left(\frac{\pi n_z}{L}z\right) ,$$

si ha:

$$\psi(x, y, z, t') = 2\sqrt{2}V^{-\frac{1}{2}} \sum_{(n)} q(t') \sin\left(\frac{\pi n_x}{L}x\right) \sin\left(\frac{\pi n_y}{L}y\right) \sin\left(\frac{\pi n_z}{L}z\right) .$$

$$\ddot{q}_{(n)} + \omega_{(n)}^2 q_{(n)} = 0 , \quad \omega_{(n)} = c \left( \frac{\mathbf{n}^2 \pi^2}{L^2} + \mu^2 \right)^{\frac{1}{2}} ,$$

<sup>(1)</sup> R. P. FEYNMAN: *Rev. Mod. Phys.*, **20**, 367 (1948). W. PAULI: *Ausgewählte Kapitel aus der Feldquantisierung* (Zürich, 1951), p. 139.

con le condizioni al contorno:

$$q_{0(n)} = 2\sqrt{2}V^{-\frac{1}{2}} \int_V dV \psi_0(x, y, z) \sin\left(\frac{\pi n_x}{L} x\right) \sin\left(\frac{\pi n_y}{L} y\right) \sin\left(\frac{\pi n_z}{L} z\right),$$

$$q_{l(n)} = 2\sqrt{2}V^{-\frac{1}{2}} \int_V dV \psi_l(x, y, z) \sin\left(\frac{\pi n_x}{L} x\right) \sin\left(\frac{\pi n_y}{L} y\right) \sin\left(\frac{\pi n_z}{L} z\right).$$

Dall'espressione della funzione di Green di un oscillatore otteniamo

$$\begin{aligned} [\psi'_t][\psi'_0] &= \langle q'_{1t}, q'_{2t} \dots | q'_{1t_0}, q'_{2t_0} \dots \rangle = \\ &= \prod_{(n)} \left( \frac{\omega_{(n)}}{2\pi\hbar i \sin \omega_{(n)}(t-t_0)} \right)^{\frac{1}{2}} \exp \left[ \frac{i}{\hbar} \omega_{(n)} \left( \frac{q_{0(n)}^2 + q_{l(n)}^2}{2} \cotg \omega_{(n)}(t-t_0) - \right. \right. \\ &\quad \left. \left. - q_{0(n)} q_{l(n)} \operatorname{cosec} \omega_{(n)}(t-t_0) \right) \right]. \end{aligned}$$

### Metodo parametrico per il calcolo del propagatore di un campo scalare.

Allo scopo di constatare la possibilità di estensione alle teorie di campo del metodo parametrico di Davison <sup>(2)</sup> per il calcolo dei propagatori, mostriamo come per un campo bosonico libero il funzionale di Green computato con detto metodo è il medesimo di quello ottenuto da un'analisi in oscillatori.

Si sviluppi la  $\dot{\psi}(x, y, z, t')$  sulla base quadridimensionale

$$\lambda_{n_t} \sin\left(\frac{\pi n_x}{L} x\right) \sin\left(\frac{\pi n_y}{L} y\right) \sin\left(\frac{\pi n_z}{L} z\right) \cos\left(\frac{\pi n_t}{t} t'\right),$$

ove

$$\lambda_{n_t} = \begin{cases} 4t^{-\frac{1}{2}}V^{-\frac{1}{2}}, & \text{per } n_t \neq 0, \\ 2\sqrt{2}t^{-\frac{1}{2}}V^{-\frac{1}{2}}, & \text{per } n_t = 0, \end{cases}$$

$$\begin{aligned} \dot{\psi}(x, y, z, t') &= 4t^{-\frac{1}{2}}V^{-\frac{1}{2}}\sqrt{\hbar 2\pi} \sum_{\substack{(n, n_t) \\ n_t \neq 0}} a_{(n, n_t)} \sin\left(\frac{\pi n_x}{L} x\right) \sin\left(\frac{\pi n_y}{L} y\right) \sin\left(\frac{\pi n_z}{L} z\right) \cos\left(\frac{\pi n_t}{t} t'\right) + \\ &+ 2\sqrt{2}t^{-\frac{1}{2}}V^{-\frac{1}{2}}\sqrt{\hbar 2\pi} \sum_{\substack{(n) \\ n_t = 0}} a_{(n, 0)} \sin\left(\frac{\pi n_x}{L} x\right) \sin\left(\frac{\pi n_y}{L} y\right) \sin\left(\frac{\pi n_z}{L} z\right). \end{aligned}$$

Integrando si ottiene

$$\begin{aligned} \psi(x, y, z, t') &= 4t^{-\frac{1}{2}}V^{-\frac{1}{2}}\sqrt{\hbar 2\pi} \sum_{\substack{(n, n_t) \\ n_t \neq 0}} \frac{t}{n_t \tau} a_{(n, n_t)} \sin\left(\frac{\pi n_x}{L} x\right) \sin\left(\frac{\pi n_y}{L} y\right) \sin\left(\frac{\pi n_z}{L} z\right) \sin\left(\frac{\pi n_t}{t} t'\right) + \\ &+ 2\sqrt{2}t^{-\frac{1}{2}}V^{-\frac{1}{2}}\sqrt{\hbar 2\pi} \sum_{\substack{(n) \\ n_t = 0}} a_{(n, 0)} t' \sin\left(\frac{\pi n_x}{L} x\right) \sin\left(\frac{\pi n_y}{L} y\right) \sin\left(\frac{\pi n_z}{L} z\right) + \psi_0(x, y, z, t_0). \end{aligned}$$

(2) B. DAVISON: *Proc. Roy. Soc.*, **225** A, 252 «1954».

$$\begin{aligned} \frac{\partial}{\partial x} \psi(x, y, z, t') = \\ - 4l^{\frac{1}{2}} V^{-\frac{1}{2}} \sqrt{\hbar 2\pi} \sum_{\substack{(n, n_t) \\ n_t \neq 0}} \frac{t}{n_t \pi} a_{(n, n_t)} \frac{n_t \pi}{L} \cos\left(\frac{\pi n_x}{L} x\right) \sin\left(\frac{\pi n_y}{L} y\right) \sin\left(\frac{\pi n_z}{L} z\right) \sin\left(\frac{\pi n_t}{t} t'\right) - \\ - 2 \sqrt{2} l^{\frac{1}{2}} V^{-\frac{1}{2}} \sqrt{\hbar 2\pi} \sum_{\substack{(n) \\ n_t = 0}} t' \frac{n_t \pi}{L} a_{(n, 0)} \cos\left(\frac{\pi n_x}{L} x\right) \sin\left(\frac{\pi n_y}{L} y\right) \sin\left(\frac{\pi n_z}{L} z\right) + \frac{\partial \psi_0}{\partial x}. \end{aligned}$$

Il funzionale

$$\frac{i}{\hbar} I = \frac{i}{\hbar} \int_0^t dt' \int dV \frac{1}{2} [\dot{\psi}^2 - c^2 (\nabla \psi)^2 - c^2 \mu^2 \psi^2],$$

mediante la sostituzione degli sviluppi delle  $\psi$ ,  $\dot{\psi}$ ,  $\nabla \psi$  sopra riportati, si trasforma in una funzione delle infinite variabili  $a_{(n, n_t)}$ :

$$\begin{aligned} \frac{i}{\hbar} I = \frac{1}{2} \frac{i}{\hbar} 2\pi \hbar \left[ \sum_{\substack{(n, n_t) \\ n_t \neq 0}} a_{(n, n_t)}^2 + \sum_{\substack{(n) \\ n_t = 0}} a_{(n, 0)}^2 \right] - \frac{1}{2} \frac{i}{\hbar} c^2 \left\{ 2\pi \hbar \sum_{\substack{(n, n_t) \\ n_t \neq 0}} \frac{t^2}{n_t^2 \pi^2} \frac{\pi^2}{L^2} n^2 a_{(n, n_t)}^2 + \right. \\ + 2\pi \hbar \frac{t^3}{3} \sum_{\substack{(n) \\ n_t = 0}} \frac{\pi^2}{L^2} n^2 a_{(n, 0)}^2 + t \int_V (\nabla \psi_0)^2 dV + 4\sqrt{2}\pi \hbar \sum_{\substack{(n, n_t) \\ n_t \neq 0}} a_{(n, 0)} a_{(n, n_t)} \frac{-t^2}{n_t^2 \pi^2} (-1)^{n_t} \frac{\pi^2}{L^2} n^2 + \\ + 8t^{\frac{1}{2}} V^{-\frac{1}{2}} (2\pi \hbar)^{\frac{1}{2}} \sum_{\substack{(n, n_t) \\ n_t \neq 0}} \frac{t^2}{n_t^2 \pi^2} [1 - (-1)^{n_t}] a_{(n, n_t)} \left[ \frac{\pi n_x}{L} \int_V \frac{\partial \psi_0}{\partial x} \cos \frac{\pi n_x}{L} x \cdot \sin \frac{\pi n_y}{L} y \cdot \sin \frac{\pi n_z}{L} z dV + \dots \right] + \\ + 2\sqrt{2} t^{\frac{1}{2}} V^{-\frac{1}{2}} (2\pi \hbar)^{\frac{1}{2}} t^2 \sum_{\substack{(n, n_t) \\ n_t = 0}} a_{(n, 0)} \left[ \frac{\pi n_x}{L} \int_V \frac{\partial \psi_0}{\partial x} \cos \frac{\pi n_x}{L} x \cdot \sin \frac{\pi n_y}{L} y \cdot \sin \frac{\pi n_z}{L} z dV + \dots \right] - \\ \left. \frac{1}{2} \frac{i}{\hbar} c^2 \mu^2 \left\{ 2\pi \hbar \sum_{\substack{(n, n_t) \\ n_t \neq 0}} \frac{t^2}{n_t^2 \pi^2} a_{(n, n_t)}^2 + 2\pi \hbar \frac{t^3}{3} \sum_{\substack{(n) \\ n_t = 0}} a_{(n, 0)}^2 + t \int_V \psi_0^2 dV - \right. \right. \\ - 4\sqrt{2}\pi \hbar \sum_{\substack{(n, n_t) \\ n_t \neq 0}} a_{(n, n_t)} a_{(n, 0)} \frac{t^2}{n_t^2 \pi^2} (-1)^{n_t} + \\ + 8t^{\frac{1}{2}} V^{-\frac{1}{2}} (h 2\pi)^{\frac{1}{2}} \sum_{\substack{(n, n_t) \\ n_t \neq 0}} a_{(n, n_t)} \frac{t^2}{n_t^2 \pi^2} [1 - (-1)^{n_t}] \int_V \psi_0 \sin \frac{\pi n_x}{L} x \cdot \sin \frac{\pi n_y}{L} y \cdot \sin \frac{\pi n_z}{L} z dV + \\ \left. \left. - 2t^{\frac{1}{2}} V^{-\frac{1}{2}} (h 2\pi)^{\frac{1}{2}} \sum_{\substack{(n) \\ n_t = 0}} t^2 a_{(n, 0)} \int_V \psi_0 \sin \frac{\pi n_x}{L} x \cdot \sin \frac{\pi n_y}{L} y \cdot \sin \frac{\pi n_z}{L} z dV \right\} \right]. \end{aligned}$$

Pertanto il calcolo dell'integrale di Feynman viene ricondotto ad una integrazione infinitamente multipla sulle  $a_{(n, n_t)}$ .



Ricordando le formule

$$\begin{aligned} \int_{-\infty}^{\infty} \exp [i(\alpha x^2 + \beta x)] dx &= \left(\frac{i\pi}{\alpha}\right)^{\frac{1}{2}} \exp \left[-\frac{i\beta^2}{4\alpha}\right], \\ \prod_{n=1}^{\infty} \left(1 - \frac{z^2}{n^2}\right) &= \frac{\sin \pi z}{\pi z}, \\ \sum_{n=1}^{\infty} \frac{1}{n^2(n^2 - z^2)} &= \frac{1}{z^2} \left(\frac{1}{2z^2} - \frac{\pi}{2z} \cotg \pi z - \frac{\pi^2}{6}\right), \\ \sum_{n=1}^{\infty} \frac{(1)^n}{n^2(n^2 - z^2)} &= \frac{1}{z^2} \left(\frac{1}{2z^2} - \frac{\pi}{2z} \operatorname{cosec} \pi z + \frac{\pi^2}{12}\right), \end{aligned}$$

e tenuto presente che

$$a_{(n,0)} = t^{-\frac{1}{2}} (\hbar 2\pi)^{-\frac{1}{2}} (q_{t(n)} - q_{0(n)}),$$

si valuta l'integrale

$$\left[ \prod_{(n)} \left(\frac{1}{2\pi i \hbar t}\right)^{\frac{1}{2}} \int_{-\infty}^{\infty} \frac{da}{\sqrt{-i}} \dots \int_{-\infty}^{\infty} \frac{da_{(n,p)}}{\sqrt{-i}} \dots \exp \left[\frac{i}{\hbar} I\right] \right],$$

e si ottiene la seguente espressione

$$K[\psi_t(\mathbf{x}), t; \psi_0(\mathbf{x}), t_0] =$$

$$\prod_{(n)} \left(\frac{1}{2\pi i \hbar t}\right)^{\frac{1}{2}} \left(\frac{\omega_{(n)} t}{\sin \omega_{(n)} t}\right)^{\frac{1}{2}} \exp \left[\frac{i}{\hbar} \omega_{(n)} \left(\frac{q_{t(n)}^2 + q_{0(n)}^2}{2} \cotg \omega_{(n)} t - q_{0(n)} q_{t(n)} \operatorname{cosec} \omega_{(n)} t\right)\right].$$

ove le  $q$  sono le ampiezze dello sviluppo in serie di  $\psi(x, y, z, t')$  sulla base

$$2\sqrt{2} V^{-\frac{1}{2}} \sin \left(\frac{\pi n_x}{L} x\right) \sin \left(\frac{\pi n_y}{L} y\right) \sin \left(\frac{\pi n_z}{L} z\right).$$

N. B. - 1) Si vorrebbe a tal punto segnalare l'utilità che il suaccennato metodo funzionale potrebbe offrire allo scopo di calcolare il propagatore di campi in interazione; la difficoltà maggiore, lo si prevede facilmente, sta nel riuscire a calcolare l'integrale parametrizzato del problema in questione.

2) Il metodo sopra usato è stato utilizzato da P. T. MATTHEWS e A. SALAM (3) per calcolare il propagatore di una o più particelle attraverso il formalismo della teoria dei campi. Riteniamo però, al contrario di P. T. MATTHEWS e A. SALAM, il metodo di FEYNMAN essenzialmente inapplicabile a campi fermionici; inoltre i risultati da essi ottenuti non ci sembrano esenti da incongruenze matematiche (per esempio la base di sviluppo non è completa) (4).

\*\*\*

Ringraziamo il prof. P. CALDIROLA per il suo interessamento e gli amici A. LOINGER e P. BOCCHIERI per le utili discussioni sull'argomento.

(3) P. T. MATTHEWS and A. SALAM: *Nuovo Cimento*, **12**, 563 (1954).

(4) P. BOCCHIERI, A. LOINGER and G. M. PROSPERI: *Nuovo Cimento*, **3**, 832 (1956).

## Dispersion Relations for Decay Processes.

E. CORINALDESI

*Department of Natural Philosophy - The University of Glasgow*

(ricevuto il 13 Ottobre 1956)

The purpose of this note is to show that the amplitudes for decay processes satisfy dispersion relations analogous to those of scattering. This is true of any reaction in which a particle disappears and at least three other particles are produced.

The formalism is almost identical with that devised by POLKINGHORNE <sup>(1)</sup> to deal with reactions in which the initial state consists of a nucleon and  $n_i$  mesons and the final state of a nucleon and  $n_f$  mesons.

We shall illustrate the method by applying it to the decay of the  $\tau$ -meson into three  $\pi$ 's. Let  $\Phi_\alpha$  ( $\alpha = 1, 2, 3$ ) be the hermitian operator for the  $\pi$ -meson field obeying the equation  $(\square - \mu^2)\Phi_\alpha = -j_\alpha$  and  $\Phi_k$  ( $k = 1, 2$ ) that for the charged  $\tau$ -meson field obeying a similar equation  $(\square - M^2)\Phi_k = -J_k$ . The Feynman and causal transition amplitudes are

$$\begin{aligned} \left[ \begin{array}{c} F_{\alpha\beta\gamma,k}(k_i, p) \\ M_{\alpha\beta\gamma,k}(k_i, p) \end{array} \right] &= i \sum_{k_1\alpha, k_2\beta, k_3\gamma} P \int_{-\infty}^{\infty} d^4x_1 d^4x_2 d^4x_3 d^4y \exp[-i(k_1x_1 + k_2x_2 + k_3x_3 - py)] \cdot \\ &\cdot \left\{ \begin{array}{l} \langle 0 | j_\alpha(x_1) j_\beta(x_2) j_\gamma(x_3) J_k(y) | 0 \rangle \left[ \begin{array}{c} \eta(x_1 - x_2) \eta(x_2 - x_3) \eta(x_3 - y) \\ \eta(x_1 - x_2) \eta(x_2 - x_3) \eta(x_3 - y) \end{array} \right] + \\ + \langle 0 | j_\alpha(x_1) j_\beta(x_2) J_k(y) j_\gamma(x_3) | 0 \rangle \left[ \begin{array}{c} \eta(x_1 - x_2) \eta(x_2 - y) \eta(y - x_3) \\ -\eta(x_1 - x_2) \eta(x_2 - y) \eta(x_3 - y) \end{array} \right] + \\ + \langle 0 | j_\alpha(x_1) J_k(y) j_\beta(x_2) j_\gamma(x_3) | 0 \rangle \left[ \begin{array}{c} \eta(x_1 - y) \eta(y - x_2) \eta(x_2 - x_3) \\ \eta(x_1 - y) \eta(x_2 - y) \eta(x_3 - x_2) \end{array} \right] + \\ + \langle 0 | J_k(y) j_\alpha(x_1) j_\beta(x_2) j_\gamma(x_3) | 0 \rangle \left[ \begin{array}{c} \eta(y - x_1) \eta(x_1 - x_2) \eta(x_2 - x_3) \\ -\eta(x_1 - y) \eta(x_2 - x_1) \eta(x_3 - x_2) \end{array} \right] \end{array} \right\}. \end{aligned}$$

where the upper lines in the square brackets refer to  $F$  and the lower lines to  $M$ . [The step-function  $\eta(x)$  is equal to one for  $x_0 > 0$  and to zero for  $x_0 < 0$ .]

<sup>(1)</sup> J. C. POLKINGHORNE: *Nuovo Cimento*, **4**, 216 (1956), where references to the literature on dispersion relations can be found.

The dispersion relations are established in a special frame where the energies of the  $\pi$ -mesons are all equal,  $k_{10} = k_{20} = k_{30} = \omega/3$  and therefore  $p_0 = \omega$ ,  $|\mathbf{k}_1| = |\mathbf{k}_2| = |\mathbf{k}_3| = \frac{1}{3}\sqrt{\omega^2 - 9\mu^2}$ ,  $|\mathbf{p}| = \sqrt{\omega^2 - M^2}$ .

Employing a system of axes with  $z$  in the direction of  $\mathbf{p}$ , a decay process is completely characterized by  $\omega$  and by the angles  $\varphi_1, \varphi_2, \varphi_3$  between the  $x$ -axis and the projections  $\mathbf{k}_1^\perp, \mathbf{k}_2^\perp, \mathbf{k}_3^\perp$  of the meson momenta on the  $(xy)$ -plane. The Lorentz transformation along the  $z$ -axis with  $a_{33} = \omega/M$ ,  $a_{34} = -a_{43} = (i\sqrt{\omega^2 - M^2})/M$ ,  $a_{44} = \omega/M$  brings the  $\tau$ -meson to rest and leaves the angles  $\varphi_1, \varphi_2, \varphi_3$  invariant. Moreover, if  $\mathbf{k}_{i,z} = \frac{1}{3}\sqrt{\omega^2 - 9\mu^2} \cos \vartheta_i$ ,  $|\mathbf{k}_i^\perp| = \frac{1}{3}\sqrt{\omega^2 - 9\mu^2} \sin \vartheta_i$  in the special frame, then in the laboratory frame  $|\mathbf{k}_i^\perp|' = \frac{1}{3}\sqrt{\omega^2 - 9\mu^2} \sin \vartheta_i$ ,  $k_{i,z}' = \omega/3M \cdot (\sqrt{\omega^2 - 9\mu^2} \cos \vartheta_i - \sqrt{\omega^2 - M^2})$ . This suggests a procedure for analysing the experimental data, to be elaborated in a forthcoming paper.

The following properties can be proved as in Polkinghorne's paper.

i) In the special frame the causal amplitude  $M(\omega)$  is the Fourier transform of a function  $M'(\tau)$  which vanishes for  $\tau < 0$ . In fact, for  $\omega \rightarrow \infty$  the exponent

$i(\sum_{i=1}^3 k_i x_i - p y)$  in  $M(\omega)$  tends to  $i(\omega/3) \sum_{i=1}^3 [(x_{i0} - y_0) - \mathbf{n}_i \cdot (\mathbf{x}_i - \mathbf{y})] = iA\omega$  with  $A > 0$ . By interchanging the  $\omega$  and the  $x_i, y$  integrations in

$$M'(\tau) = \frac{1}{2\pi} \int d\omega M(\omega) \exp[-i\omega\tau],$$

the assertion is easily verified, since for  $\tau < 0$  the integration path can be completed with a semicircle in the upper half of the complex  $\omega$ -plane.

ii) The dispersion relation

$$M(\omega) = \frac{1}{i\pi} P \int_{-\infty}^{\infty} \frac{M(\omega')}{\omega' - \omega} d\omega',$$

is then satisfied by the causal amplitude:

$$\text{iii)} \quad F(\omega; \varphi_1, \varphi_2, \varphi_3) = M(\omega; \varphi_1, \varphi_2, \varphi_3), \quad \text{for } \omega > 0;$$

$$\text{iv)} \quad M(-\omega; \varphi_1, \varphi_2, \varphi_3) = M^*(\omega; \varphi_1, \varphi_2, \varphi_3),$$

v) If  $M$  and  $F$  are represented as the sum of a dispersive and an absorptive part,  $M = D + i\mathcal{A}$  and  $F = D + iA$ , then  $A(\omega) = \mathcal{A}(\omega) = 0$  for  $\omega > 0$ , and  $A(\omega) = -\mathcal{A}(\omega)$  for  $\omega < 0$ .

vi) The range of values  $0 < \omega < M$  is non-physical. In this range  $M(\omega)$  is better represented as a sum over intermediate states. It is easy to see that only the second and third term.

$$\sum_{\alpha_i} \dots \langle 0 | j_\alpha | \alpha_1 \rangle \langle \alpha_1 | j_\beta | \alpha_2 \rangle \langle \alpha_2 | j_k | \alpha_3 \rangle \langle \alpha_3 | j_\gamma | 0 \rangle,$$

and

$$\sum_{\alpha_i} \dots \langle 0 | j_x | \alpha_1 \rangle \langle \alpha_1 | J_k | \alpha_2 \rangle \langle \alpha_2 | j_\beta | \alpha_3 \rangle \langle \alpha_3 | j_\gamma | 0 \rangle \dots$$

may give a contribution and this only for  $3\mu < \omega < M$ . By making a suitable « Ansatz » for the matrix elements  $\langle \alpha | j_\alpha | \beta \rangle$ ,  $\langle \alpha | J_k | \beta \rangle$  it should be possible to derive from the dispersion relations much valuable information about the  $\pi$ - $\tau$ -meson interaction.

\* \* \*

I am especially indebted to Dr. R. J. BLIN-STOYLE of the Clarendon Laboratory, Oxford, for taking an interest in some early attempts to deal with this problem.

## Application of Feynman's New Variational Procedure to the Calculation of the Ground State Energy of Excitons.

H. HAKEN

*Institut für theoretische Physik der Universität - Erlangen, Deutschland*

(ricevuto il 13 Ottobre 1956)

FEYNMAN <sup>(1)</sup> has recently determined the energy and the effective mass of slow electrons in a polar crystal (« polarons ») by means of a new variational procedure, which is based on the use of his path integrals. We have extended his procedure in a way to calculate the ground state energy of excitons (electron-hole pairs) in a polar crystal. Treating the exciton as a two particle system and using the effective mass approximation, the Hamiltonian of an exciton interacting with lattice vibrations (optical branch only) is given by

$$(1) \quad H = H_0 + \sum b_{\mathbf{w}}^{\dagger} b_{\mathbf{w}} + \sum (H_{\mathbf{w}} b_{\mathbf{w}} + H_{\mathbf{w}}^* b_{\mathbf{w}}^{\dagger}),$$

with

$$H_0 = -(1/2M)A_{\mathbf{R}} - (1/2M')A_{\mathbf{Y}} + W_0(y), \quad \hbar = \omega = 1,$$

where  $M$ ,  $M'$  are the total and the reduced masses respectively,  $W_0(y)$  is the interaction potential between electron and hole in the lattice at rest,  $\mathbf{R}$  the coordinate of the centre of gravity,  $\mathbf{Y}$  the relative coordinate,  $\mathbf{w}$  the wave vectors.  $H_{\mathbf{w}}$  is given by  $(\gamma/w) (\exp[i\mathbf{w}\mu_2\mathbf{y}] - \exp[-i\mathbf{w}\mu_1\mathbf{y}]) \exp[i\mathbf{w}\mathbf{R}]$  with  $\mu_i = m_i/M$  where  $m_i$  is the mass of a single particle.

In performing the calculations it turned out to be convenient first to transcribe the formulation of FEYNMAN into the notation of conventional quantum theory <sup>(2)</sup>. Thus instead of FEYNMAN's trial actions,  $S_1$ , we have to use trial Hamiltonians,  $H_1$ : We have considered the following trial Hamiltonians:

$$(2) \quad H_1 = -(1/2M)A_{\mathbf{R}} + \kappa R^2 - (1/2M')A_{\mathbf{Y}} + W(y),$$

<sup>(1)</sup> R. P. FEYNMAN: *Phys. Rev.*, **97**, 660 (1955).

<sup>(2)</sup> A report on this transcription in the case of polarons has been given at the authors' lecture held at Theoretisch-Physikalische Arbeitstagung Oberwolfach, April 1956.

with

$$(2a) \quad W(y) = -d/y$$

or

$$(2b) \quad W(y) = dy^2$$

and using FEYNMAN'S concept of an auxiliary particle with coordinate  $\mathbf{Z}$ :

$$(3) \quad H_1 = -(\tilde{\omega}^3/8c)A_{\mathbf{Z}} - \frac{1}{2}\tilde{\omega} + (2c/\tilde{\omega})(\mathbf{R} - \mathbf{Z})^2 - (1/2M) \frac{1}{R} - (1/2M')A_{\mathbf{Y}} + W(y).$$

$d$ ,  $z$ ,  $c$  and  $\tilde{\omega}$  are considered as variational parameters. The choice of these Hamiltonians seems to be well adapted to the case of small exciton orbitals in which case the exciton is accompanied by a single polarization cloud.

With the trial Hamiltonian (2) we have to evaluate the following expression for the energy:

$$(4) \quad \langle \varphi_0^* H_0 \varphi_0 | \sum_w \sum_n \frac{q_0^* H_w \varphi_n}{1 - E_n - E_0} \rangle$$

where  $E_n$  and  $\varphi_n$  are the eigenvalues and eigenstates belonging to  $H_1$ . If  $W(y)$  is chosen identical with  $W_0(y)$  and  $z = 0$ , we arrive at the formula given by usual second order perturbation theory, using  $H_0 + \sum b_w^+ b_w$  as unperturbed Hamiltonian and the last terms in (1) as perturbation. If case (2a) and  $z = 0$  is chosen and if we retain only the first member from the sum over  $n$  in (4),  $n = 0$ , we get the result previously obtained by H. J. G. MEYER<sup>(3)</sup>. Finally using (2b) and retaining the first member of the sum, we get the expression of DYKMAN and PEKAR<sup>(4)</sup>. We have been interested in performing the summation over  $n$  and  $w$ , especially in the case  $z = 0$  which is of more interest, as here the translational invariance of the problem is conserved. Using (2b), the summation may be condensed into a single rather simple integral, whereas in case (2a) we have been forced to make approximations.

Finally we have evaluated the energy arising from (3) which is given by

$$\begin{aligned} & \langle \varphi_0^* (H_1 + W_0(y) - W_1(y)) \varphi_0 \rangle - \\ & - \sum_w \sum_n \frac{|\langle \varphi_0^* H_w \varphi_n \rangle|^2}{E_n + 1 - E_0} - (2c/\tilde{\omega}) \langle \varphi_0^* R^2 \varphi_0 \rangle + 2c \sum_n \frac{|\langle \varphi_0^* \mathbf{R} \varphi_n \rangle|^2}{E_n - \tilde{\omega} - E_0}. \end{aligned}$$

Again, if  $W(y)$  is an oscillator potential we obtain for the first sum a rather simple integral, whereas using a Coulomb potential approximations have been necessary. All the other expressions, however, were obtained in an explicit form.

If the orbital radius of the exciton is large, we get approximately the same effective interaction potential which has been already communicated by the author<sup>(5)</sup>, but no change of the effective masses is obtained. To improve this result the use of two auxiliary particles seems desirable. The evaluation of the corresponding expressions is now being performed.

<sup>(3)</sup> H. J. G. MEYER: *Physica*, **22**, 109 (1956).

<sup>(4)</sup> I. M. DYKMAN and S. J. PEKAR: *Dokl. Akad. USSR*, **83**, 825 (1952).

<sup>(5)</sup> H. HAKEN: *Nuovo Cimento*, **3**, 1230 (1956).



## An Apparatus for Continuous Isotopic Analysis of Hydrogen-Deuterium Mixtures.

M. SILVESTRI and N. ADORNI

*Laboratori CISE - Milano*

(ricevuto il 22 Ottobre 1956)

An apparatus for the isotopic analysis of hydrogen-deuterium mixtures by means of thermal conductivity is now in operation in our laboratory.

A detailed account of the apparatus, shown in the accompanying picture (Fig. 1), was published elsewhere as soon as the experimental phase was ter-

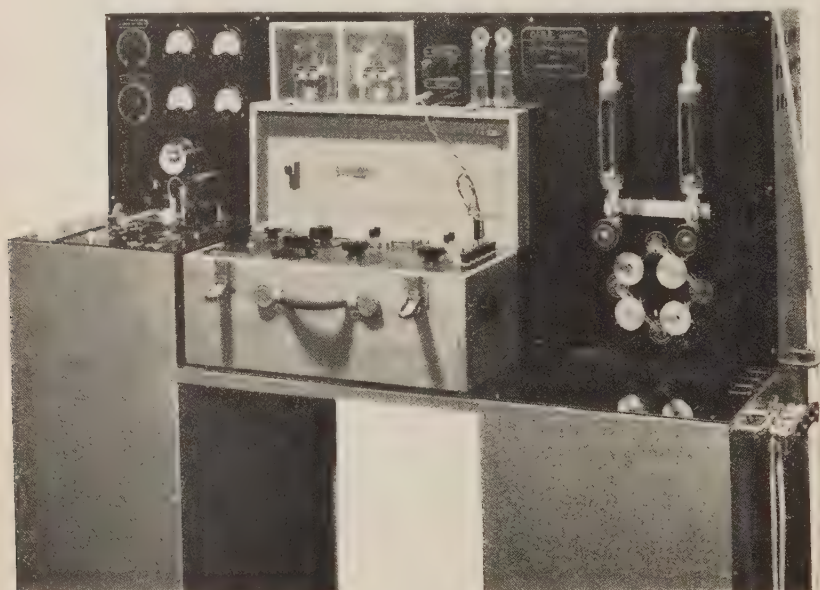


Fig. 1. - A picture of the apparatus.

minated and construction just begun <sup>(1)</sup>.

In the definitive version, a few devices were introduced, in order to obtain greater simplicity and safety; moreover, a refrigerator of 120 kcal/h, instead of tap water, is used for thermostating the sensitive element.

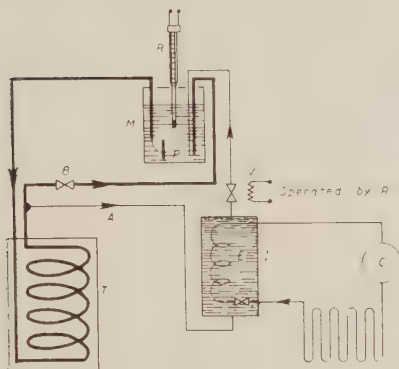


Fig. 2. — Diagram of the arrangement for thermostating the sensitive element.

The thermostating diagram is shown in Fig. 2. Water is still the thermostating fluid; it is pumped, by means of a small centrifugal pump *P* from the tank *M*, to the thermostat *T*, in which the element is located, and then back again, through the pressure drop *B*. A fraction of the total flow is taken away through the small duct *A* and sent to the tank *I*, in which the evaporator of the refrigerator is located. Temperature in *I* is kept between 6° and 12 °C, by means of a thermoswitch. From the tank *I*, through the electromagnetic valve *V*, the water enters *M* again. The electromagnetic valve *V* is operated by a mercury thermoregulator *R*, placed in *M*; and controls the flow rate of cold water through *A*, so that the water bath in *M* is kept at a temperature of  $15 \pm 0.1$  °C.

Calibration of the new apparatus was repeated up to a concentration of 5%  $[D]/([D] + [H])$  by a set described elsewhere in this issue of *Nuovo Cimento* <sup>(2)</sup>.

Hydrogen before exchange with deuterated water was used as reference gas; hydrogen after exchange as deuterated gas.

Details of calibration are the same as in the preceding calibration <sup>(2)</sup>.

Experimental results are drawn in Fig. 3; they are consistent with the

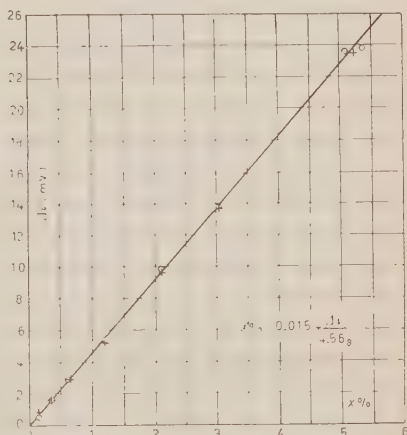


Fig. 3. — Calibration graph. (Measurements are marked with *O*, when unknown gas is flowing in one side of the sensitive element, and with *+*, when unknown gas is flowing in the other side).

equation:  $Av = 4.568(X - 0.015)$  mV up to  $X = 5$ , where  $X = [D] \cdot 100/([D] + [H])$ . The proportionality constant is  $\frac{1}{2}\%$  lower in respect to that of the preceding calibration; the cause of this is very probably a slight difference in the voltage input, because the electrical circuit was completely remade.

Accuracy is better than

$$1 \cdot 10^{-4} [D]/([D] + [H]).$$

<sup>(1)</sup> M. SILVESTRI and N. ADORNI: *Rev. Sci. Instr.*, **27**, 388 (1956).

<sup>(2)</sup> M. SILVESTRI and N. ADORNI: *Nuovo Cimento*, to appear.

in the concentration range from zero to 3 per cent, provided that

1) Deviation in voltage input  $\leq \pm 5$  mV;

2) deviation in temperature of the thermostat  $< \pm 0.4$  °C;

3) deviation in gas flow rate  $\leq 2\%$ .

Moreover, variations of atmospheric pressure of  $\pm 7$  mm<sub>Hg</sub> are without any appreciable effect on the signal.

In regard to sensitivity to the gas flow rate, it must be remembered that

the measurement is carried out in two steps: in the first, the reference gas is sent to one side of the sensitive element and the unknown gas to the other; in the second step, the reference gas is sent to both sides of the sensitive element. The signal  $\Delta v$  is the difference between readings of the potentiometer in these conditions. No appreciable difference in  $\Delta v$  results, even if the flow rate is increased or decreased by a factor of two in respect to the flow rate of 50 cm<sup>3</sup>/min used by us in calibration, provided the constancy of the flow rate between the first and the second run is better than two per cent.

# On the Higher Limit for the Mass of an Assembly of Particles.

G. BUSSETTI

*Istituto di Fisica dell'Università - Torino*  
*Istituto Nazionale di Fisica Nucleare - Sezione di Torino*

(ricevuto il 27 Ottobre 1956)

1. If the natural distribution of the chemical elements is studied with the methods of statistical thermodynamics, admitting that the elements formation has happened in conditions near to the thermodynamical equilibrium, several laws of conservation are used, and among these the total energy conservation law <sup>(1,2)</sup>:

$$(1) \quad \sum_{Z, A} n_{ZAs} E_{ZAs} \left( 1 + \frac{\varphi}{c^2} \right) + \left( 1 + \frac{\varphi}{c^2} \right) \sum_s [N_s h\nu_s + n_{e-s} E_{e-s} + \dots + n_{\nu s} E_{\nu s}] = E,$$

where  $n_{ZAs}$ ,  $N_s$ ,  $N_{e-s}$ , ...,  $n_{\nu s}$  are the numbers per  $\text{cm}^3$  of nuclei ( $Z, A$ ), photons, electrons, ..., antineutrinos having momenta between  $p_s$  and  $p_s + dp_s$ ;  $\varphi$  is the external gravitational potential and  $E_{ZAs} = m_{ZAs} c^2$ . (In <sup>(1)</sup> the interaction energy is neglected).

It is known <sup>(2)</sup> that solving the above problem one finds that an agreement with the observational data can be obtained only admitting initial densities  $\rho \gtrsim 10^{13} \text{ g cm}^{-3}$ .

2. - We assume that the potential is approximately constant in the volume occupied by the particles in the initial state. Since the first member of (1) cannot be negative, we must have  $1 + (\varphi/c^2) \geq 0$ , thereafter, being  $\varphi < 0$ , we obtain:

$$(2) \quad |\varphi| \leq c^2.$$

Formula (2) gives a higher limit for the absolute value of the gravitational potential of an assembly of particles.

The order of magnitude of  $|\varphi|$  for a spherical mass  $m$  of radius  $R$  and mean

<sup>(1)</sup> G. WATAGHIN: *Suppl. Nuovo Cimento*, **9**, 241 (1949).

<sup>(2)</sup> G. BUSSETTI: *Nuovo Cimento*, **12**, 769 (1954).

density  $\varrho$ , is:

$$(3) \quad |\varphi| \simeq G \frac{m}{R} = G \frac{4}{3} \pi R^2 \varrho,$$

where  $G$  is the gravitational constant. Supposing  $\varrho \simeq 10^{13} \text{ g cm}^{-3}$ , from (2) and (3) we get  $R \lesssim 10^7 \text{ cm}$ ; therefore the mass has order of magnitude:

$$(4) \quad m \lesssim 2.7 \cdot 10^{35} \text{ g}.$$

This higher limit is in agreement with the astrophysical data on the stellar masses.

3. — The conservation law (1) is valid in the domain of special relativity. If we want a more general formula, in agreement with general relativity, we must substitute (1) with an equation of the kind (3):

$$(5) \quad \int \left( 1 + \frac{2\chi}{c^2} \right)^{\frac{1}{2}} (T_4^4 + t_4^4) dV = \text{const.}$$

where the mixed tensors  $T_4^4$  and  $t_4^4$  depend on the spatial distribution, of matter and energy's,  $dV$  is the tridimensional volume element,  $\chi$  is the scalar potential related to the metric tensor by:  $g_{44} = -1 - (2\chi/c^2)$ .

Owing to the reality of the first member of (5), we must have  $1 + (2\chi/c^2) \geq 0$ .

In our case, since we are concerned with gravitational forces only, one has clearly  $\chi < 0$  and it follows:

$$(6) \quad |\chi| \leq \frac{1}{2} c^2.$$

Apart from the factor  $\frac{1}{2}$ , formula (6) is formally analogous to formula (2). We are going now to apply the results to a homogeneous sphere. In the interior near the surface  $\chi$  is nearly equal to the classical newtonian potentials. Therefore the order of magnitude of  $|\chi|$  is the same that we found before for  $|\varphi|$  and is again given by (3). Hence the higher limit of the mass of an assembly of particles subjected to gravitational forces has still the order of magnitude shown by (4).

In conclusion, as far concerns our problem, the theory of general relativity does not change substantially the results which we already derived from considerations of special relativity. \*

(\*) C. MÖLLER: *The theory of Relativity* (Oxford, 1952), p. 339.

## Angular Correlations Between Decay Planes of $\tau^+$ -Mesons and their Production Geometry

T. REGGE

*University of Rochester - New York (\*)*

(ricevuto il 27 Ottobre 1956)

If  $\tau^+$ -mesons are produced by the reaction:

$$P + P \rightarrow P + \Lambda_0 + \tau^+,$$

the question arises whether or not it is possible to detect any correlation between the decay plane of the  $\tau^+$ -meson and its production angles. It would be also interesting to know if any conclusions can be drawn on the value of the spin of the meson from any experimental data on the subject.

In this paper such a correlation is shortly discussed assuming that the meson has spin  $1 \pm$ ,  $2 \pm$  and the  $\Lambda_0$  has the same spin and parity of the nucleon.

We label here the initial spin and orbital momentum in the CM system of the protons with  $S$  and  $L$  respectively. Clearly  $S + L$  is always even. In the final state if the energy of the incident protons is just above threshold we can restrict ourselves to  $S$  states only.

If  $S_{\tau^+}$ ,  $S_P$ ,  $S_{\Lambda_0}$  are the spins of the final particles only the transitions included in the following table are allowed:

	$S$	$L$	$ L + S  = J$	$ S_{\Lambda_0} + S_P $
$S_{\tau^+} = 1 +$	0	0	0 +	1
	0	2	2 +	1
$S_{\tau^+} = 1 -$	1	1	0 -	1
	1	1	1 -	0
	1	1	1 -	1
	1	1	2 -	1
$S_{\tau^+} = 2 +$	0	2	2 +	0
	0	2	2 +	1
$S_{\tau^+} = 2 -$	1	1	2 -	0
	1	1	2 -	1
	1	1	1 -	1
	1	3	2 -	0
	1	3	2 -	1
	1	3	3 -	1

(\*) Now at the Istituto di Fisica dell'Università di Torino (Italy).



We are going now to construct the transition matrix  $M$  for these four cases.

$S_{\pi^+} = 1+$ : The three spin states of the  $\pi^+$ -meson form a pseudovector  $\xi$  and  $M$  is known to be a scalar constructed out of this pseudovector and out of the hermitian conjugate of the initial singlet state  $\zeta^\dagger$ , the initial relative momentum of the protons in their CM system:  $\mathbf{k} = (k)\chi$  and the final  $\Lambda_0$ -P triplet wave function  $\theta$  (a pseudovector). In agreement with the table there are only two such invariants and the general form of  $M$  is:

$$M = A(\xi\theta)\zeta^\dagger + B(\xi\chi)(\theta\chi)\zeta^\dagger.$$

In this formula  $A$  and  $B$  are some constants, functions of the energy. Both initial particles are supposed to be unpolarized. The deduced density matrix  $\varrho_f$  for the outgoing meson,  $\varrho_f = M\varrho_i M^\dagger$  with  $\varrho_i = \frac{1}{4}$  is moreover averaged on the spins of the final proton and  $\Lambda_0$  particle. The result is:

$$\varrho_f = \frac{1}{4}[|A|^2 \cdot (\xi\xi^\dagger) + (|B|^2 + 2|A||B|\cos\varphi_{AB}) \cdot (\xi\chi)(\xi^\dagger\chi)];$$

$$A^*B + B^*A = 2|A||B|\cos\varphi_{AB}.$$

If  $|B| + 2|A|\cos\varphi_{AB} = 0$  the obtained density is a multiple of the unity matrix  $(\xi\xi^\dagger)$  and it represents therefore a totally depolarized beam.

$S_{\pi^+} = 1-$ . In quite similar fashion we construct here the matrix  $M$ :

$$M = A \cdot \theta(\chi \wedge \xi; \zeta^\dagger) + B(\theta\chi)(\xi\zeta^\dagger) + C(\chi\xi)(\theta\zeta^\dagger) + D(\theta\xi)(\chi\zeta^\dagger),$$

$\xi$  is here a vector,  $\theta$  (scalar) is the final singlet wave function,  $\zeta^\dagger$  (pseudovector) is the hermitian conjugate of the initial triplet wave function. The corresponding density  $\varrho_f$  has the form:

$$\varrho_f = R_1(\xi\xi^\dagger) + R_2(\xi\chi)(\xi^\dagger\chi).$$

Where  $R_1, R_2$  depend on  $A, B, C, D$ . With a suitable choice of these constants it is possible to have  $R_2 = 0$  and therefore to produce an isotropic distribution of spins and no correlation. On the other hand if  $R_1 = 0$  a simple relation exists between the correlated ( $P_C$ ) and the uncorrelated ( $P_U$ ) decay probability:

$$P_C = 3 \cos^2 \theta_n P_U,$$

where  $\theta_n$  is the angle between the normal  $\mathbf{N}$  of the decay plane and  $\chi$ . To show it we point out that in our case the decay matrix  $T$  has the form:

$$T = (\mathbf{N}\xi^\dagger) \cdot \Omega(\cos \theta).$$

In this formula  $\mathbf{N}$  is the normal vector to the decay plane.  $\Omega$  is an odd function of  $\cos \theta = (\mathbf{p}, \mathbf{p}')/|p||p'|$  in Fabri's conventions <sup>(1)</sup>.

$P_C$  and  $P_U$  are then proportional to  $T\varrho_f T^\dagger (R_1 = 0)$  and  $T\varrho_f T^\dagger (R_2 = 0)$  respectively.

<sup>(1)</sup> E. FABRI: *Nuovo Cimento*, **11**, 479 (1954).

The proportionality factor is the same for both. Relation (1) then follows immediately. Averaging  $P_C$  on all directions we obtain  $P_U$ : Similar formulas can be found for any value of  $S_\tau$  but they are not so simple.

$S_{\tau^+} = 2+$ . In this case it is convenient to arrange the spin states of the meson into a symmetrical traceless second order tensor  $\xi_{\mu\nu}$ . The matrix  $M$  is given by

$$M = \sum_{\mu, \nu} [A(\xi_{\mu\nu}\chi_\mu\chi_\nu) \cdot \theta\zeta^\dagger + B(\xi_{\mu\nu}\chi_\mu(\chi \wedge \theta)_\nu)\zeta^\dagger],$$

and  $\varrho_f$  by

$$\varrho_f = \sum_{\mu\nu\lambda\varrho} [|A|^2 - |B|^2] \cdot (\xi_{\mu\nu}\chi_\mu\chi_\nu)(\xi_{\lambda\varrho}^\dagger\chi_\lambda\chi_\varrho) + |B|^2 \cdot (\xi_{\mu\nu}\chi_\mu\xi_{\lambda\nu}^\dagger\chi_\lambda\chi_\varrho).$$

Clearly it is not possible to obtain, under any choice of  $A$  and  $B$ , a completely depolarized beam of mesons. A more direct way of obtaining the same result is to write the law of conservation of the components of the angular momentum along  $\chi$ :

$$S_\chi + L_\chi = S_{\tau, \chi} + S_{\Lambda, \chi} + S_{P, \chi}.$$

In the initial state we have obviously  $L_\chi = 0$ ,  $S_\chi = 0$  (singlet state), moreover the sum  $S_{\Lambda, \chi} + S_{P, \chi}$  can never exceed 1 in absolute value. Hence  $S_{\tau, \chi}$  is also limited to the set  $\pm 1, 0$  out of the whole set  $\pm 2, \pm 1, 0$ . Such a limitation implies a polarization of the outgoing  $\tau^+$ -meson, since an unpolarized particle would be found with equal probability in all spin states.

$S_{\tau^+} = 2-$ . This case is more complicated than the others and we outline the essential features only. Our table shows that under our assumptions the matrix  $M$  has six terms. The deduced density has the form:

$$\varrho_f = \sum_{\mu\nu\lambda\varrho} [S_0(\xi_{\mu\nu}\xi_{\mu\nu}^\dagger) + S_1(\xi_{\mu\nu}\chi_\mu\chi_\nu)(\xi_{\lambda\varrho}^\dagger\chi_\lambda\chi_\varrho) + S_2(\xi_{\mu\nu}\chi_\nu\xi_{\mu\lambda}^\dagger\chi_\lambda)],$$

and it can be made isotropic with a suitable choice of the constants in  $M$ .

We conclude that if no correlation is observed there is no reason to believe that the  $\tau^+$ -meson has spin 0. The only value which could be excluded, if the contribution of  $P$  waves will be proved to be small in the final state, is  $S_{\tau^+} = 2+$ . To obtain any conclusion the correlation experiment should be performed therefore not far from the threshold.

\* \* \*

The author wishes to thank Dr. R. E. MARSHAK for his warm help and kind encouragement. This work was partly supported by a Fulbright Travel Grant.

Further Measurements on  $n, p$  Reactions at 14 MeV.

## I - Magnesium, Silicon, Calcium, Zinc, Zirconium.

C. BADONI, L. COLLI and U. FACCHINI

*Laboratori CISE - Milano*

(ricevuto il 12 Novembre 1956)

With the same technique described in a former paper <sup>(1)</sup>, employing a coincidence between a proportional counter and a scintillation counter, we measured the energy spectra of protons emitted

by the three elements silicon, calcium and zirconium in their natural isotopic mixture under bombardment of 14.5 MeV neutrons.

In this new group of measurements, the technique of proton detection was improved by reducing the background and extending the counting to lower energy protons, bringing the lower limit of the proton spectra to 3 MeV.

Furthermore, a good calibration of the energy scale of the scintillation counter was made: the energy scale is now given with an error of a few percentage points.

In view of these changes in the experimental conditions, we have made new measurements of the proton spectra of zinc and magnesium, which we are reporting in this paper.

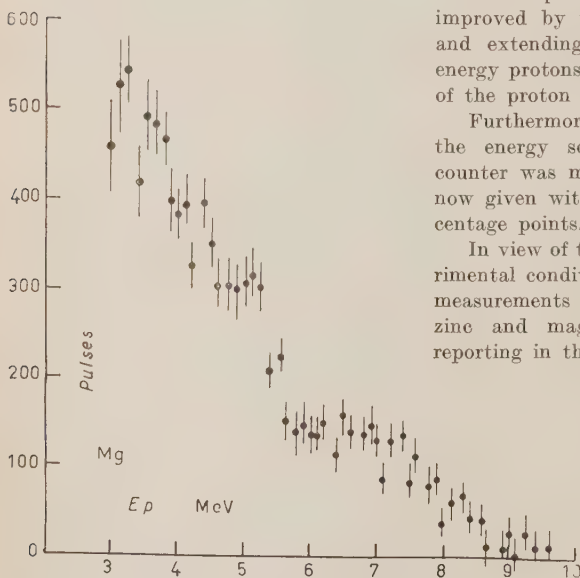


Fig. 1. - Proton spectrum of  $n, p$  reaction on magnesium. Ordinates are number of protons versus proton energy. On each point is indicated the statistical error.

(1) L. COLLI and U. FACCHINI: *Nuovo Cimento*, **4**, 671 (1956).

Figs. 1-5 show proton spectra, with the background subtracted, for the elements studied: magnesium, silicon, calcium, zinc and zirconium.

results and considering the abundance of these two isotopes in the natural mixture, the contribution of proton from  $^{25}\text{Mg}$  was found to be only of a small

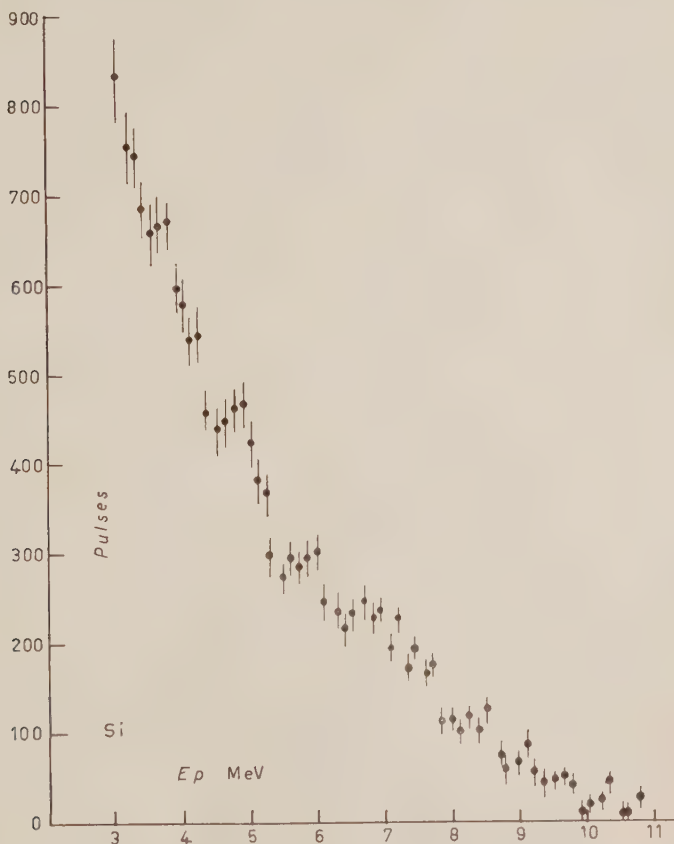


Fig. 2. - Proton spectrum of n, p reaction on silicon.

### Magnesium.

The value of the cross-section of the reaction  $\text{Mg}(n, p)\text{Na}$  was measured for the two isotopes  $^{24}\text{Mg}$  and  $^{25}\text{Mg}$  by PAUL and CLARKE <sup>(2)</sup>. On the basis of these

percentage, and so can be completely disregarded. The cross section value of  $^{26}\text{Mg}$  (11% of the isotope mixture) is not known.

However the shape of the proton spectrum, which ends at 9.5 MeV, is in agreement with the maximum energy expected for the  $^{24}\text{Mg}(n, p)^{24}\text{Na}$  reaction which has the value of the reaction energy  $Q = -4.7$  MeV.

<sup>(2)</sup> E. B. PAUL and R. L. CLARKE: *Canad. Journ. Phys.*, **31**, 267 (1953).

The spectrum shows a rather irregular shape. A sharp drop is clearly visible at 5 MeV, followed by a large hump between 6 and 8.5 MeV.

section value of the  $^{28}\text{Si}(n, p)^{28}\text{Al}$  reaction is given by Paul and Clarke.

Of the other two isotopes  $^{29}\text{Si}$  and  $^{30}\text{Si}$  only the cross section value of the

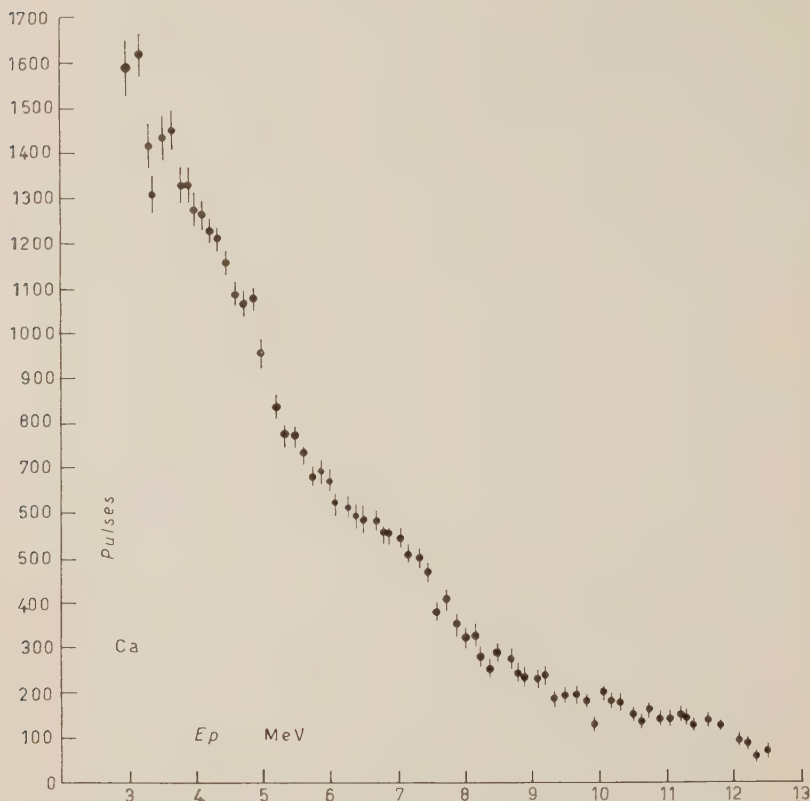


Fig. 3. — Proton spectrum of n, p reaction on calcium.

For magnesium a possible contribution of protons from the action n, np can be excluded because none of the three isotopes can give protons of energy higher than 3 MeV.

#### Silicon.

$^{28}\text{Si}$  is the most abundant isotope in the natural mixture (92.37%); the cross

first is known and is found to be half the value as that of  $^{28}\text{Si}$ . The proton contribution from  $^{29}\text{Si}$  is therefore very small. Nothing is known about  $^{30}\text{Si}$ , but taking into account its small concentration it is probable that its contribution is not important. The  $Q$  value for the reaction  $^{28}\text{Si}(n, p)^{28}\text{Al}$  is  $-3.9$  MeV.

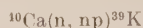
The spectrum shows a descent with small deviations, which do not stand clearly out of experimental errors.

In this case too no contributions from the n, np reaction are expected in the energy range studied.

### Calcium.

No measurement is known of the cross section value of calcium. If protons are attributed to  $^{40}\text{Ca}$  having a concentration of 96.92%, the  $Q$  value of

Protons from the reaction



are possibly emitted at energies under 6.3 MeV.

### Zinc.

Measurements of the n, p reactions for the two isotopes  $^{64}\text{Zn}$  and  $^{66}\text{Zn}$  have

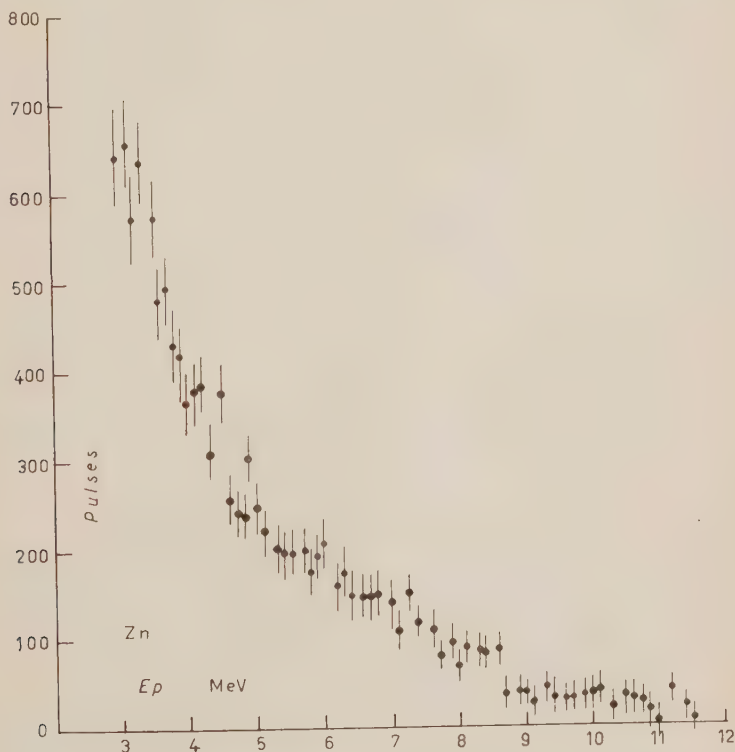


Fig. 4. — Proton spectrum of n, p reaction on zinc.

the reaction is  $-0.5$  MeV. The spectrum shape is characterized by a rather exponential descent, on which can be seen a bump around 7 MeV.

been taken by Paul and Clarke. These isotopes have the abundance of 48.9 and 27.8%. Nothing is known about the others ( $^{67}\text{Zn}$  4.1%,  $^{68}\text{Zn}$  18.6% and



$^{72}\text{Zn}$  0.6%). According to Paul and Clarke's results, protons are mainly due to  $^{64}\text{Zn}$ . The  $Q$  value for the reactions  $^{64}\text{Zn}(n, p)^{64}\text{Cu}$  is  $-0.96$  MeV. For the same nucleus the  $n, np$  reaction can give only protons at energies under 6 MeV.

$Q$  value for the reaction  $^{90}\text{Zr}(n, p)^{90}\text{Y}$  is  $-1.4$  MeV. The spectrum shows a slope less steep than for the others.

The curve is affected by greater experimental errors than the other curves, due to the fact that the statistics that

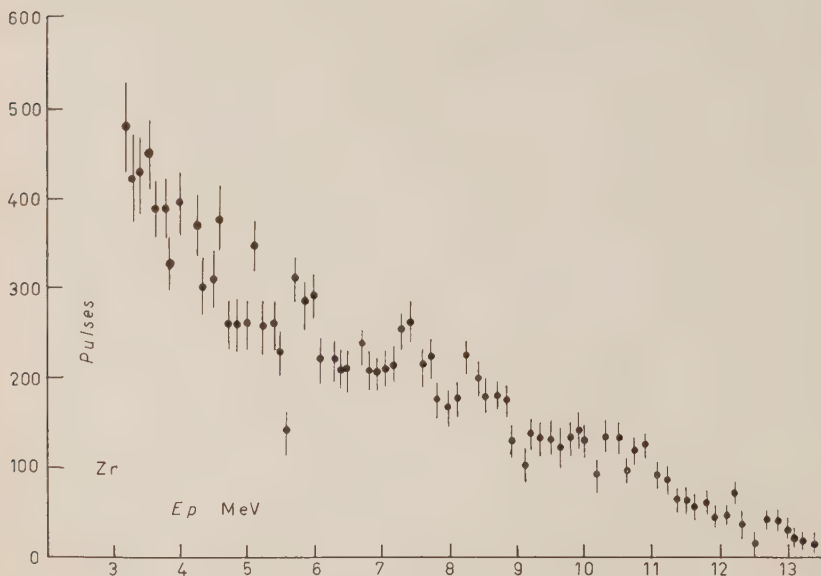


Fig. 5. — Proton spectrum of  $n, p$  reaction on zirconium.

### Zirconium.

Cross-section values are known for the isotopes  $^{90}\text{Zr}$  and  $^{91}\text{Zr}$ , which have respectively a concentration of 48% and 17% in natural zirconium. No measurements have been done on other isotopes  $^{91}\text{Zr}$  (11%),  $^{92}\text{Zr}$  (22%) and  $^{96}\text{Zr}$  (1.5%). As the cross-section of  $^{90}\text{Zr}$  has a value 24 times that of  $^{91}\text{Zr}$  (according to Paul and Clarke) it is perhaps responsible for most of the emitted protons. The

may be obtained in this case are not adequate.

The  $n, np$  reaction of  $^{90}\text{Zr}$  does not give protons above 3 MeV.

\* \* \*

We sincerely thank Professor B. FERRETTI for his very interesting discussions throughout the work. We thank also Mr. T. ROSSINI for his constant help in the measurements.

## Errors in Constant-Sagitta Scattering Measurements in Nuclear Emulsions.

A. J. HERZ, R. M. MAY and N. SOLNTSEFF

*The F.B.S. Falkiner Nuclear Research and Adolph Bassar Computing Laboratories,  
School of Physics (\*), The University of Sydney - Sydney, N.S.W. Australia*

(ricevuto il 18 Novembre 1956)

In recent work on  $K^-$ -particles coming to rest in nuclear emulsion <sup>(1)</sup>, we found that the distribution of the scattering parameters, obtained from constant-sagitta scattering measurements, was wider than predicted by the estimation formulae derived by D'ESPAGNAT <sup>(2)</sup> on the basis of Molière's theory. Similar observations have been reported by other workers <sup>(3)</sup>. In order to see whether this excess spread can be reasonably attributed to errors of observation and instrumental errors which are not of the random-fluctuation (« noise ») type, and which are therefore not eliminated by the statistical treatment, we arranged for repeated constant-sagitta range-scattering measurements to be made of a selected K-particle track. The track was chosen because it lay entirely in one sheet of emulsion. Five members of our team of scanners took part, and the

track was measured fifty times on the same microscope (a Cooke M4003).

The expressions used in our work are

i) for the mean second difference  $D_s$ , corrected for random noise:

$$(1) \quad D_s^2 = \frac{2}{\pi} \cdot \frac{12}{11} \left( \frac{2}{3} D_i^2 + D_i D_{i+1} \right),$$

where  $D_i$  is the  $i$ -th second difference and the bar denotes the arithmetic mean value;

ii) for the random noise  $\varepsilon$  in the second differences:

$$(2) \quad \varepsilon^2 = \frac{2}{\pi} \cdot \frac{12}{11} \left( \frac{1}{4} \overline{D_i^2} - \overline{D_i D_{i+1}} \right),$$

iii) for the estimated *theoretical* standard deviation  $\sigma_{th}$  of the estimates  $D_s$  with respect to the population mean  $\overline{D_s}$

$$(3) \quad \sigma_{th}^2 = \frac{\overline{D_s}^2}{2n} \left( 2 \cdot 10 + 0.31 \frac{\overline{\varepsilon}^2}{\overline{D_s}^2} + 0.18 \frac{\overline{\varepsilon}^4}{\overline{D_s}^4} \right),$$

(\*) Also supported by the Nuclear Research Foundation within the University of Sydney.

<sup>(1)</sup> E. P. GEORGE, A. J. HERZ, J. H. NOON and N. SOLNTSEFF: *Nuovo Cimento*, **3**, 94 (1956).

<sup>(2)</sup> B. D'ESPAGNAT: *Journ. de Phys. et Rad.*, **13**, 74 (1952).

<sup>(3)</sup> M. DI CORATO, D. HIRSCHBERG and B. LOCATELLI: *Suppl. Nuovo Cimento*, **12**, 380 (1954).

where  $n$  is the number of values of  $D_i$  used. These expressions are equivalent to those of D'ESPAGNAT (2); they have been modified to take account of the fact that we are here dealing with angles between chords.

If the same track is measured repeatedly with the same mechanical set-up, then the fluctuations in the values of  $D_s$  which are normally caused by track-to-track variations in the true scattering will not occur. On the other hand, as there will still be random noise due to reading errors, setting errors and the like, the value of  $D_s$  found will vary from measurement to measurement, and theoretically one expects the standard deviation of the distribution of the  $D_s$  to be given by the last two terms of (3). As can be seen by substituting the experimental values of  $\bar{D}_s$  and  $\bar{\epsilon}$  given below into (3), this standard deviation is quite small, of the order of 1%. If the spread of the experimental distribution of the  $D_s$  is greater than this, the cause must be sources of error which do not appear in the form of random noise.

We can define the total standard deviation of the  $D_s$ ,  $\sigma_{\text{tot}}$ , by

$$(2) \quad \sigma_{\text{tot}}^2 = \sigma_{\text{th}}^2 + \sigma'^2,$$

where  $\sigma'$  is the contribution of the non-random sources of error which are present when the same track is measured repeatedly, and which are not taken into account by the noise-elimination procedures.

For the case of repeated measurements on the same track we have already seen that  $\sigma_{\text{th}}$  is very small; we can conclude that  $\sigma_{\text{tot}}$  in that case will be very nearly equal to  $\sigma'$  if  $\sigma'$  is at all appreciable.

In the experiment we used the constant-sagitta range-scattering scheme of Biswas, George and Peters (4), and the number of cells  $n$  was 100.

The length of track involved was therefore 11.2 mm. During the measurement the track had to be reorientated once in forty cases, twice in eight cases and three times in two, making the average number of reorientations 1.25 per measurement.

The total standard deviation  $\sigma_{\text{tot}}$  was calculated from

$$(5) \quad \sigma_{\text{tot}}^2 = \frac{1}{N-1} \sum_{k=1}^N (D_{sk} - \bar{D}_s)^2,$$

where  $N$  is the number of track measurements made. Two methods for the elimination of large-angle scatters were tried: the conventional one of rejecting all values of  $D_i$  greater than  $\pm 4|\bar{D}_i|$  and the one proposed by RITSON (5) in which values of  $D_i$  greater than  $\pm 4|\bar{D}_i|$  are replaced by  $\pm 4\bar{D}_i$ . We found that  $\sigma_{\text{tot}}$  is 7.8% for the total-rejection method, and 5.2% for the « shaving-off » method of Ritson. The reason for this is easily seen if one remembers that large values of  $|D_i|$  strongly affect  $|\bar{D}_i|$  and that the exact position of the cut-off is subject to statistical fluctuations. Shaving off is thus the preferable of the two methods, but it must be remembered that the scattering constant for this method is slightly different from that applicable to the total-cut-off method.

In Table I we give the results of our measurements.  $\bar{D}_s$  is the arithmetic mean of the  $D_s$ , and the standard error in it is equal to  $\sigma_{\text{tot}}/\sqrt{N}$ . We note that the data on  $\bar{D}_s$  provide some evidence for systematic variations from observer to observer, but, on the whole, the individual means for all but one of the scanners are reasonably consistent with the overall mean.

Using (3) and (4) and the data given in Table I we can now calculate the experimental value of  $\sigma'$ , the excess standard deviation not due to random noise. We find that  $\sigma'$  is about 5.1% — very nearly equal to  $\sigma_{\text{tot}}$ . This can be compared with the experimental data

(4) S. BISWAS, E. C. GEORGE and B. PETERS: *Proc. Ind. Acad. Sci.*, A 38, 418 (1953).

TABLE I.

Observer	$N$ (*)	$\overline{D}_s$ ( $\mu\text{m}$ )	$\overline{\varepsilon}$ ( $\mu\text{m}$ )	$\sigma_{\text{tot}}$ ( $\mu\text{m}$ )	$\sigma_{\text{tot}}/\overline{D}_s$ (%)
A	11	$1.34 \pm 0.009$	0.51	0.03	2.2
B	11	$1.38 \pm 0.015$	0.41	0.05	3.6
C	10	$1.37 \pm 0.025$	0.52	0.08	5.8
D	10	$1.26 \pm 0.016$	0.51	0.05	4.0
E	8	$1.38 \pm 0.018$	0.30	0.05	3.6
A + B + C + E	40	$1.37 \pm 0.009$	—	0.056	4.1
All	50	$1.35 \pm 0.01$	0.46	0.07	5.2

(\*)  $N$  is the number of values of  $D_s$  obtained.

obtained from our  $K^-$  experiment <sup>(1)</sup> where the conditions of measurement were similar, and where we found that the spread of the  $D_s$  values of the  $K^-$ -particles was 20% greater than expected from (3). We find that combining  $\sigma_{\text{th}}$  from (3) with the value of  $\sigma'$  from this experiment raises the expected standard deviation for the measurement of a large number of tracks (100 cells each) from 10.4% to 11.6%: an increase of 11.5%. This is quite satisfactorily in agreement with experiment, for emulsion distortion is certain to have introduced some additional variations.

We conclude that errors not accounted for by the Molière theory can make an appreciable contribution to the total error in scattering measurements. The elimination of large-angle scatters is one of the sources of fluctuations, and its importance can be reduced by employing the shaving-off method of Ritson <sup>(5)</sup>. The magnitude of the additional spread will, of course, depend on the experimental conditions and on the observer, and other workers <sup>(3)</sup> have found increases of up to 60% in the course of calibrating constant-sagitta schemes for  $\pi$ -mesons and protons. The fact that some of our scanners were able to get quite low values for  $\sigma'$  (see Table I) shows that the Molière theory is sub-

stantially correct when non-random sources of error are unimportant.

It is important to emphasize in connection with the present work that we are *not* dealing here with fluctuations in the scattering characteristic which occur if a number of different tracks are measured. These fluctuations which have been discussed recently by HUYBRECHTS <sup>(6)</sup> do not enter into our results which were obtained by repeated measurements on the same track. Similarly, the fluctuations we find cannot be caused by the spurious scattering described by BISWAS *et al.* <sup>(7)</sup>, for, apart from being very small in magnitude, spurious scattering is a fixed quantity for any one track.

\* \* \*

We would like to express our gratitude to Dr. B. A. CHARTRES with whom we had many helpful discussions. Thanks are due to our team of scanners who did the experimental work. One of us (N.S.) is indebted to the Research Committee of the University of Sydney for a Research Studentship, and we all would like to thank Professor H. MESSEL for making provision for the excellent facilities we enjoy in this laboratory.

<sup>(6)</sup> M. HUYBRECHTS: *Supplemento al Vol. IV, Nuovo Cimento, Report of Pisa Conference, Sezione C.*

<sup>(7)</sup> S. BISWAS, B. PETERS and RAMA: *Proc. Ind. Acad. Sci., A* **41**, 154 (1955).

<sup>(5)</sup> D. M. RITSON: Communication CERN-B33 of C.E.R.N. Bureau of Standards (1954).

R. CAMPBELL - *Théorie générale de l'équation de Mathieu et de quelques autres équations différentielles de la mécanique*. (Collection d'ouvrages de mathématiques à l'usage des physiciens, publiée sous la direction de G. Darmon et A. Lichnerowicz; Ed. Masson et Cie, Paris, 1955).

Si tratta di un interessante volume sull'equazione di Mathieu, avente un carattere assai diverso da quello delle opere già esistenti sullo stesso argomento. L'Autore non si limita ad esporre, nei suoi vari aspetti, la teoria dell'equazione e delle funzioni di Mathieu, ma cerca soprattutto di porre bene in evidenza quali siano le difficoltà insite nella teoria stessa e quale sia la intima ragione del successo dei metodi usati per superarle. Un esame così approfondito di tali metodi lo porta naturalmente a mettere in rilievo che essi sono applicabili anche ad altre classiche equazioni differenziali lineari della Fisica matematica, cosicchè il volume tratta non soltanto dell'equazione di Mathieu propriamente detta:

$$(1) \quad y'' + (p - 2q \cos 2x)y = 0,$$

e della corrispondente equazione modificata:

$$(1') \quad y'' + (p - 2q \cosh 2x)y = 0,$$

ma altresì della cosiddetta equazione di

Mathieu associata:

$$(2) \quad y'' - 2v \operatorname{tg} x \cdot y' + (a + k^2 \sin^2 x)y = 0,$$

dell'equazione di Whittaker:

$$(3) \quad y'' + (\theta_0 + 2\theta_1 \cos 2x + 2\theta_2 \cos 4x)y = 0,$$

e dell'equazione di Lamé:

$$(4) \quad y'' - [n(n+1)k^2 \sin^2 x + h]y = 0,$$

ove figura la funzione ellittica di Jacobi  $\operatorname{sn} x$ . L'Autore si preoccupa anche di mostrare che, nella teoria delle equazioni differenziali sopra considerate, molte questioni sono ancora da chiarire; perciò il libro, oltre che apparire assai utile per le applicazioni, fornirà certamente lo spunto per nuove ricerche.

L'opera si inizia con una « Introduzione » ove sono rammentati i problemi di Fisica matematica che hanno condotto all'equazione di Mathieu. Seguono tre « Parti » costituite complessivamente da dieci Capitoli. Alla fine vi è una « Bibliografia ». Ogni Capitolo è seguito da tabelle ove sono raccolte le formule incontrate nel Capitolo stesso.

La « Parte I » è dedicata alle funzioni di Mathieu, cioè a quelle soluzioni della (1) che sono periodiche col periodo  $2\pi$ . Esse possono esistere soltanto se il parametro  $p$  è una opportuna funzione  $p = p(q)$  dell'altro parametro  $q$ ; questa funzione definisce nel piano  $(p, q)$  le cosiddette linee caratteristiche. Nel



Cap. I viene dato il metodo di Ince per ricavare gli sviluppi trigonometrici delle funzioni di Mathieu ed in pari tempo l'equazione delle linee caratteristiche; vengono anche studiate, da un analogo punto di vista, le equazioni (1'), (2), (3), (4) e si accenna al vecchio metodo di Mathieu, che determinò le funzioni portanti il suo nome attraverso sviluppi in serie di potenze del parametro  $q$ . Nel Cap. II sono studiati gli sviluppi delle funzioni di Mathieu (e analoghe) in serie di funzioni di Bessel; notevole è l'indagine sulla « correlazione » esistente fra questi sviluppi e quelli del Cap. I. Il Cap. III tratta delle equazioni integrali soddisfatte dalle funzioni in istudio; sono descritti numerosi metodi per ricavarle e ne sono fatte varie applicazioni. Nel Cap. IV sono studiate le questioni di carattere asintotico che si presentano per le funzioni di Mathieu (e analoghe).

La « Parte II » tratta delle *funzioni di Mathieu di seconda specie*, cioè del secondo integrale (non periodico) della (1) nel caso che  $p, q$  abbiano valori caratteristici. Tali funzioni possono essere date sotto forme diverse, a seconda del metodo seguito per determinarle; nel Cap. V è esposto il metodo di Whittaker, nel Cap. VI quello di Mac Lachlan. Quando è possibile, questi metodi sono anche applicati alle altre equazioni (2), (3), (4).

Nella « Parte III » è esposta la teoria generale dell'equazione di Mathieu; si suppone pertanto che  $p, q$  siano qualunque (non necessariamente caratteristici). Dopo un breve richiamo della teoria di Floquet sulle equazioni differenziali lineari a coefficienti periodici, si studiano nel Cap. VII le soluzioni stabili e nel Cap. VIII quelle instabili. Il Cap. IX tratta dei problemi asintotici per un integrale qualsiasi della (1); nel Cap. X la stessa (1) viene trasformata in altre a coefficienti razionali, le cui soluzioni sono studiate nel campo complesso. Anche in questi ultimi quattro Capitoli molte questioni sono considerate per le equazioni (2), (3), (4).

Tutto il volume è redatto con stile chiaro e preciso ed ogni problema vi è illustrato in modo originale e suggestivo.

Purtroppo il testo contiene un gran numero di errori di stampa ed un « errata et addenda » posto all'inizio non arriva ad indicarli tutti.

A. GHIZZETTI

*Reports on Progress in Physics* - Volume XIII, 1955; a cura di A. C. STICKLAND - Ed. The Physical Society, London; pagg. 477.

I lavori scientifici sugli argomenti di maggiore attualità vengono pubblicati al giorno d'oggi con un ritmo tale da rendere difficile seguire l'intera produzione mondiale anche su un solo argomento. Le pubblicazioni periodiche di aggiornamento, come questi Reports, sono perciò preziosissime ed, in alcuni casi, assolutamente indispensabili. Gli argomenti di questo volume sono scelti, come sempre, tra quelli di maggiore attualità e taluni di essi sono collegati da evidenti nessi di analogia. Sei articoli riuniti insieme alla fine del volume sotto il titolo di « Rassegna sulla teoria dei campi » hanno lo scopo di riassumere le idee fondamentali ed i risultati della teoria delle particelle elementari, in termini comprensibili dai fisici non specializzati. Questi articoli sono dovuti a R. E. PEIERLS, A. SALAM, P. T. MATTHEWS e G. FELDMAN e riferiscono il contenuto di una serie di lezioni tenute presso l'Università di Birmingham in occasione di una riunione della Physical Society (dicembre 1954).

Vi è una introduzione generale, una breve esposizione della teoria, un capitolo sulle interazioni delle particelle, con particolare riguardo a quelle tra elettroni e fotoni, ed uno dedicato alle proprietà del mesone  $\pi$  in cui si ricerca un accordo tra le conclusioni teoriche ed i risultati sperimentali, che si sono rapidamente accumulati dall'entrata in funzione del



sincrociclotrone di Berkeley. Su questi risultati sperimentali si sofferma la parte quinta in una breve rassegna. La sesta conclude con osservazioni riassuntive sui limiti classici dei campi e sulle proprietà dei mesoni pesanti recentemente scoperti.

Le conferenze di questo gruppo, per la loro stessa natura, non sono molto estese: possono servire ottimamente per chi voglia formarsi una idea generale dei problemi o aggiornarsi sul loro sviluppo senza approfondirlo. Un trattamento più dettagliato e più strettamente teorico sul medesimo argomento si trova in questo stesso volume nell'articolo di J. C. GUNN, sulla teoria della radiazione, che ha il programma di considerare le interazioni fondamentali tra particelle cariche e campo elettromagnetico. L'Autore afferma che la teoria della radiazione ha raggiunto ormai uno stato di grande completezza e che la precisione con la quale è possibile calcolare un qualsiasi processo è limitata soltanto dalla fatica dei calcoli.

Altri tre articoli del volume riguardano aspetti diversi delle interazioni tra radiazioni e materia. B. T. PRICE studia la ionizzazione prodotta da particelle relativistiche; in questo campo la teoria, già sviluppata da tempo, trova oggi dettagliata conferma nei risultati sperimentali. L'energia perduta, per unità di lunghezza del percorso da una particella carica è, a velocità relativamente bassa, inversamente proporzionale al quadrato della velocità stessa, mentre per velocità relativistiche cresce con legge logaritmica fino a raggiungere un limite di saturazione previsto da Swann e studiato da Fermi già nel 1939. Dopo un riassunto della teoria l'articolo contiene un'analisi dettagliata dei risultati sperimentali, ottenuti mediante i vari dispositivi, con rivelatori gassosi o condensati.

G. H. KINCHIN e R. S. PEASE si occupano invece dello spostamento di atomi nei solidi per effetto di radiazioni, cioè di uno degli aspetti del così detto « radiation damage ». Questo argomento

è oggi di grande attualità e presenta notevolissimo interesse pratico. Iniziata con lo studio delle alterazioni nelle proprietà dei materiali causate dagli enormi flussi di neutroni a cui venivano esposti nei reattori, questa indagine ha dimostrato di poter fornire dei dati preziosi per lo studio della fisica dei solidi ed ha anche permesso di ottenere in alcuni casi, notevoli miglioramenti nelle proprietà tecnologiche dei materiali.

L'articolo svolge un'ampia e dettagliata analisi dei problemi e dei risultati, prevalentemente dal punto di vista sperimentale, sulle principali conseguenze del bombardamento con particelle cariche pesanti e con neutroni; degli effetti dei raggi  $\gamma$  e degli elettroni si tratta solo brevemente perchè queste radiazioni non producono in grande quantità spostamenti di atomi. Per la stessa ragione, mentre sono esaminati gli effetti su metalli, leghe, semiconduttori, composti covalenti e cristalli ionici, rimangono esclusi quelli prodotti dalle radiazioni sugli alti polimeri, che pure presentano aspetti di grande interesse pratico, perchè causati prevalentemente da eccitazione elettronica e ionizzazione.

Problemi di questo tipo, cioè quelli riguardanti le collisioni elettroniche sulle molecole di un gas poliatomico, sono invece trattati nel lavoro di J. D. CRAGGS e C. A. McDOWELL. Questo articolo contiene un'ampia rassegna di tecniche e risultati sperimentali, posti in relazione con la teoria.

La misura di intensi campi magnetici interessa oggi più che mai, se non altro per quanto riguarda gli acceleratori di particelle: d'altra parte nuove tecniche sono state sviluppate in tempi recenti, in particolare quelle basate sulla risonanza paramagnetica, nucleare ed elettronica.

Nell'articolo di J. L. SYMONDS questi ed altri metodi, come quelli basati sulla variazione di resistenza elettrica del bismuto in campo magnetico, sull'effetto Hall, ecc. vengono brevemente descritti

e criticamente analizzati, onde stabilirne i limiti di applicabilità, i pregi ed i difetti; segue una ampia bibliografia, classificata per metodo.

Sul fenomeno della risonanza paramagnetica verte l'articolo di K. D. BOWERS e J. OWEN che, facendo seguito ad un lavoro su analogo argomento apparso due anni fa in questa serie, raccoglie, dopo una introduzione teorica, i dati sperimentali esistenti sulla risonanza paramagnetica dei solidi cristallini contenenti ioni dei gruppi di transizione. Le estese tabelle numeriche che raccolgono la maggior parte delle informazioni sono accompagnate da citazioni degli articoli originali.

Due lavori di orientamento prevalentemente teorico riguardano rispettivamente la magnetostrizione e l'elettrostrizione. Il primo, ad opera di E. W. LEE si occupa principalmente della magnetostrizione lineare e passa in rassegna i vari tentativi per calcolare le costanti magnetostrittive a partire dalle forze interatomiche. Viene anche considerata l'interazione tra magnetostrizione e sforzi che dà origine ad ulteriore anisotropia. Magnetostrizione di volume ed effetto di forma sono pure esaminati.

L'articolo di H. F. KAY sulla elettrostrizione è più breve e meno strettamente teorico, ma in compenso offre un quadro generale del fenomeno, sia nei cristalli che nei materiali ceramici, descrivendone le modalità ed i fondamenti, distinti da quelli della piezoelettricità. Per quanto riguarda le applicazioni pratiche l'Autore fa riferimento alla letteratura.

Diremo finalmente dello scritto di E. AMBLER e R. P. HUDSON il cui titolo, «Magnetic Cooling» non rende piena giustizia al contenuto, che si estende in un campo più vasto, ma sempre legato alla tecnica delle temperature prossime allo zero assoluto. Infatti, dopo avere esposto teoria e risultati sperimentali sulla demagnetizzazione adiabatica di sali paramagnetici, gli Autori passano alla misura delle bassis-

sime temperature, per la quale si fa uso ancora degli stessi sali. Uscendo poi dal campo applicativo, si occupano dello studio delle proprietà dei sali paramagnetici a bassissima temperatura, le quali, di per se stesse, presentano grande interesse. Le proprietà di altre sostanze, come i metalli e l'elio, non sono per altro trascurate, come pure alcuni problemi termici, isolamento e contatto termico, che in questo tipo di esperienze, assumono straordinaria importanza e mettono in giuoco fenomeni che in condizioni usuali sono trascurabili.

Le ultime pagine poi sono dedicate alle idee più ardite nel campo del raffreddamento magnetico, come ad esempio la demagnetizzazione nucleare, mediante la quale dovrebbe esser possibile raggiungere la temperatura di  $10^{-6}$  °K, ma per cui si incontrano ancora gravi difficoltà sperimentali.

Concludendo, mentre alcuni degli articoli di questo volume mettono a punto in modo completo ed esauriente gli argomenti trattati, altri hanno piuttosto un carattere didattico ed introduttivo, tutti però condividono i pregi della attualità della materia e della cura con cui essa è esposta; la maggior parte degli articoli è corredata da vasta ed aggiornata documentazione bibliografica, preziosa per chi voglia approfondire lo studio.

Può essere interessante ricordare che, oltre al volume completo, sono in vendita presso la Physical Society dei fascicoli contenenti i singoli articoli separati.

F. A. LEVI

W. PRAGER and P. G. HODGE jr. - *Theorie idealplastischer Körper*, pp. VII + 274, Springer, Wien, 1954.

Che cosa intende per corpo plastico ideale? È facile chiarirlo.

Il diagramma cartesiano dell'andamento delle deformazioni subite da un

corpò sotto l'azione di una tensione esterna ha un aspetto ben noto. Partendo da piccoli valori della tensione, vale all'inizio la legge di Hooke, mentre per valori superiori ad una tensione determinata, si instaurano deformazioni permanenti.

Una schematizzazione della situazione, che permette la trattazione matematica anche delle zone in cui non vale più la legge di Hooke, è costituita dal corpo plastico ideale. Esso è definito come il corpo che segue la legge di Hooke fino a un valore determinato della tensione applicata; quando questo valore è sorpassato, il corpo fluisce plasticamente. La curva deformazione-tensione è in tal caso parallela all'asse delle tensioni.

La schematizzazione non è affatto astratta, poichè in pratica si può riuscire a rappresentare una curva deformazione-tensione assegnata, pensandola come una combinazione di un certo numero di curve dello stesso tipo, relative a corpi plastici ideali.

L'opera riveste quindi un carattere essenzialmente applicativo ed anzi essa è espressamente dedicata dagli Autori allo studente ed al laureato in ingegneria.

La trattazione impone, in alcuni punti, l'uso di metodi di calcolo non usuali. In questi casi gli Autori hanno inserito paragrafi in cui, a partire dalle nozioni di analisi che vengono impartite nei corsi universitari, sviluppano le teorie matematiche che sono alla base di tali metodi di calcolo.

Il carattere didattico e di informazione su casi di interesse pratico è accentuato dalla presenza di numerosi esercizi al termine di ogni capitolo.

Il presente volume è la traduzione in lingua tedesca, ad opera di F. Chmelka, di un libro americano comparso nel 1951.

Per instradare il lettore ad una esatta comprensione della letteratura specializzata anglo-americana, evitando di far sorgere incertezze sul significato corrispondente di parole tedesche ed inglesi,

il traduttore ha posto in fondo al libro un breve vocabolario tecnico tedesco-inglese.

G. CORTELESSA

*Techniques Générales du Laboratoire de Physique*, vol. I (II édition) a cura di J. Surugue; pp. 671, figg. 69, Centre National de la Recherche Scientifique - Paris, 1955. Frs. 2400.

In confronto con la prima edizione del 1947, questa seconda presenta diversi ampliamenti ed aggiornamenti nei vari capitoli che trattano le diverse tecniche, e l'aggiunta inoltre di un capitolo sulla tecnica dei circuiti elettrici e dei tubi elettronici. I dieci capitoli che formano questo primo volume della seconda edizione trattano i seguenti argomenti: Cap. I (62 pag.): Principi generali della costruzione di apparecchi scientifici; II (16 pp.): Principali operazioni sulla lavorazione del vetro in laboratorio; III (42 pp.): Tecnica del vuoto; IV (91 pp.): Realizzazione e misura di alte temperature; V (65 pp.): Tecniche generali di laboratorio di ottica; VI (78 pp.): Sorgenti di luce e filtri; VII (32 pp.): Cellule fotoelettriche; VIII (52 pp.): Registrazione; IX (57 pp.): Regolazione e raddrizzamento di tensioni e correnti; X (133 pp.): Tecnica dei circuiti elettrici e dei tubi a vuoto.

Alla fine del volume esiste un indice analitico piuttosto dettagliato.

Il lodevole scopo che si è prefisso l'A. nella stesura del libro è di fornire ai tecnici dei laboratori scientifici ed industriali una guida che possa permettere di farsi una conoscenza generale di tutte le tecniche in uso corrente in laboratori diversi, sufficiente per rendersi conto delle possibilità da esse presentate, e che possa servire come introduzione allo studio di opere specializzate. Tale scopo può dirsi in linea di

massima raggiunto; il volume però non è esente da difetti che, giustificabili in una prima edizione, lo sono meno in una seconda. Il principale di essi è la disuniformità di livello nella trattazione dei vari argomenti. Mentre alcuni capitoli, per es. il X, richiedono che il lettore abbia già almeno una superficiale conoscenza dell'argomento, ed una preparazione matematica superiore a quella normale di un tecnico di laboratorio, altri capitoli, per es. il II, presentano una trattazione puramente descrittiva di dettagli della tecnica trattata, di per sé non molto utili, senza illustrare in maniera un po' costruttiva le questioni basilari sulle quali tale tecnica viene a svilupparsi.

Questo difetto, che infirma una netta caratterizzazione del volume, è evidentemente imputabile al fatto che i vari capitoli sono opera di AA. diversi; un lavoro di revisione più accurato avrebbe però portato ad una maggiore omogeneità nel livello della trattazione. Anche una maggiore estensione delle tabelle riportanti le caratteristiche dei materiali o degli strumenti più comuni, tabelle in qualche capitolo eccessivamente succinte o addirittura mancanti, sarebbe stato di utile complemento all'opera.

M. CHIOZZOTTO

M. SUZUKI - *Structure of a group and the structure of its lattice of subgroups*, (Ergebnisse der Mathematik und ihrer Grenzgebiete, Neue Folge, Heft 10, Springer Verlag, Berlin-Göttingen-Heidelberg, 1956) pag. VIII + 96.

Negli ultimi vent'anni, a seguito del costituirsi della teoria dei reticoli a ramo autonomo dell'algebra, hanno acquistato molto interesse le ricerche concernenti il reticolo costituito dai sottogruppi di un gruppo. Notevoli passi innanzi in questo

campo sono stati compiuti, specie ad opera di studiosi giapponesi, americani e italiani, di modo che si è venuta a costituire una mole abbastanza cospicua di risultati, alcuni dei quali alquanto interessanti e riposti. Ma, sino ad ora mancava un'esposizione organica di tutta la materia: una parte di questa poteva trovarsi nell'ottimo trattato di Teoria dei gruppi di KURO, ma per tutto il resto era necessario ricorrere alle memorie originali dei vari autori, adottanti spesso notazioni e terminologie diverse, con conseguente aggravio di lavoro per il lettore. Si sentiva l'esigenza di una trattazione sistematica e completa: essa ci è ora fornita dal volumetto di M. SUZUKI, il giovane matematico giapponese che ha apportato a questo campo, nelle sue due ormai classiche memorie del 1951, contributi della massima importanza.

Il volume consta di quattro capitoli. Il primo di essi è dedicato allo studio di categorie di gruppi caratterizzate da qualche particolare proprietà del reticolo dei sottogruppi. Segnaliamo, a tal riguardo, il teorema di ORE asserente che il reticolo dei sottogruppi di un gruppo  $G$  è distributivo quando e solo quando ogni sottoinsieme finito di elementi di  $G$  genera un sottogruppo ciclico, i bei risultati delle complesse ricerche di K. IWASAWA, A. W. JONES, N. ITO e S. SATO, in cui sono caratterizzati i gruppi per cui il reticolo dei sottogruppi è modulare, sottomodulare o sopramodulare, i teoremi di P. HALL e del nostro ZACHER sui gruppi per cui il reticolo dei sottogruppi è complementato e relativamente complementato.

Il secondo capitolo concerne lo studio delle proiettività tra gruppi, cioè degli isomorfismi intercorrenti tra i reticoli dei sottogruppi di due gruppi non isomorfi. L'esistenza di proiettività tra gruppi non isomorfi fu per la prima volta messa in luce da A. ROTTLANDER mentre a BAER si devono i principali risultati sulle proiettività tra gruppi abeliani, e allo stesso SUZUKI quelli sulle

proiettività tra gruppi qualunque. Notevole a tal riguardo il fatto che le proprietà di un gruppo finito di essere semplice, perfetto o risolubile si conservano per effetto di una proiettività. In questo capitolo figurano anche vari risultati di SUZUKI pubblicati qui per la prima volta: ad es. quelli sulle immagini dei sottogruppi normali in una proiettività e quelli sulle autoproiettività.

Il terzo capitolo riguarda gli automorfismi tra i reticoli dei sottogruppi di due gruppi. Quest'ordine di problemi fu posto da P. M. WHITMAN, mentre i principali risultati sono dovuti allo stesso SUZUKI, ed a vari autori italiani. Anche qui sono esposti alcuni risultati nuovi di SUZUKI.

Infine, l'ultimo capitolo concerne l'esistenza di isomorfismi duali tra i reticoli dei sottogruppi di due gruppi. In generale un gruppo non ha un duale, cioè il duale del reticolo dei sottogruppi di un

gruppo non è isomorfo al reticolo dei sottogruppi di nessun gruppo. BAER ha determinato i gruppi abeliani che hanno un duale, mentre i gruppi speciali e i gruppi risolubili che ammettono un duale sono stati indicati da SUZUKI.

L'Autore indica qua e là anche varie questioni non ancora risolte. Il volume, scritto con la chiarezza e la concisione proprie dell'autore, è chiuso da un'accurata ed esauriente bibliografia. Esso può interessare non soltanto gli specialisti, ma anche, in qualche misura, cultori di altri rami di matematica e studiosi di fisica, viste le sempre più copiose applicazioni che la teoria dei gruppi ha nei vari campi delle scienze fisico-matematiche.

Sento il dovere di ringraziare vivamente l'Autore per avere ben valorizzato, nella sua esposizione, il contributo dei ricercatori italiani.

G. ZAPPA



IL NUOVO CIMENTO

INDICI

DEL VOLUME IV - SERIE X

1956

PRINTED IN ITALY





# INDICE SISTEMATICO

## PER NUMERI SUCCESSIVI DEL PERIODICO

N. 1 - 1° LUGLIO 1956

H. A. BETHE and J. HAMILTON - Anti-Proton Annihilation . . . . .	pag. 1
P. BUDINI and L. TAFFARA - On the Energy Loss and Specific Ionization of a Relativistic Particle in a Polarizable Medium (I) . . . . .	" 23
M. M. BLOCK, E. M. HARTH, M. E. BLEVINS and G. G. SLAUGHTER - Observation of Electron Secondaries from $V^0$ Decays . . . . .	" 46
H. H. HECKMAN, F. M. SMITH and W. H. BARKAS - Mass and Spin-Parity Character of the $\tau$ -Meson . . . . .	" 51
A. BRACCI and C. COCEVA - The Diffusion Parameters of Thermal Neutrons in Water . . . . .	" 59
P. HILLMAN, G. H. STAFFORD and C. WHITEHEAD - A New Method of Measuring Asymmetries in Neutron Polarization Experiments. . . . .	" 67
T. TATI - An Attempt in the Theory of Elementary Particles . . . . .	" 75
R. K. GUPTA and S. JHA - On the Electron Capture Decay Energy of $^{153}_{64}\text{Gd}$ . . . . .	" 88
F. DEMICHELIS and R. A. RICCI - $\beta$ - $\gamma$ Angular Correlation of $^{208}_{81}\text{Tl}(\text{ThC}'')$ . . . . .	" 96
E. L. LOMON - A Soluble Model of Meson-Nucleon S-State Scattering . . . . .	" 106
A. ASCOLI, E. GERMAGNOLI and L. MONGINI - On Intermetallic Diffusion in Gold-Lead System . . . . .	" 123

### *Lettere alla Redazione:*

B. CHINAGLIA, F. DEMICHELIS e R. A. RICCI - Tempo di decadimento del $\text{ZnS}(\text{Ag})$ e preparazione di ricevitori a $\text{ZnS}(\text{Ag})$ . . . . .	" 134
SHIH-HUI HSIEH - On the Photodisintegration of the Deuteron and p-p Scattering . . . . .	" 138
K. YAMAZAKI - On the Field Theory in Functional Form . . . . .	" 141
D. AMATI and B. VITALE - Some Considerations on the Charge-Exchange Scattering of Antinucleons on Nucleons . . . . .	" 145
R. ASCOLI e G. BUSSETTI - Sulla polarizzazione della Bremsstrahlung . . . . .	" 147
R. CIRELLI e M. PUSTERLA - Estensione del metodo parametrico di Davison al caso di potenziali cinetici. . . . .	" 150
A. WATAGHIN - On the Anelasticity of Cosmic Ray Jets . . . . .	" 154
C. COTTINI, E. GATTI and G. GIANNELLI - High Resolution Millimicrosecond Time Interval Measurements Based Upon Frequency Conversion . . . . .	" 156
P. H. FOWLER and K. H. HANSEN - Two Examples of Mesonic Decay of Hyperfragments . . . . .	" 158
J. P. ELLIOTT and T. H. R. SKYRME - Effect of Centre-of-Mass Motion on Nuclear Moments. . . . .	" 164

R. PAPPALARDO — Su una nuova equazione relativistica dell'elettrone proposta da Zaitsev . . . . .	pag. 166
A. STANGHELLINI — Determination of the $p$ -Wave Coupling Constant $f^2$ of Pion-Nucleon Scattering from Analysis of the $\alpha_{31}$ Phase-Shift. . . . .	» 168
D. AMATI and B. VITALE — On the Pion Annihilation of Nucleon-Antiproton Pairs . . . . .	» 171

*Documenti e Informazioni:*

Simboli e unità U.I.P.P.A. . . . .	» 172
------------------------------------	-------

<i>Libri ricevuti e Recensioni</i> . . . . .	» 185
--	-------

N. 2 - 1° AGOSTO 1956

R. ASCOLI and G. BUSSETTI — On the Study of the Bremsstrahlung by Bloch and Nordsieck's Method. . . . .	pag. 189
R. GATTO — Angular Correlation Methods for Determining the Spins of the Hyperons . . . . .	» 197
F. KORTEI — On Some Solutions of Gürsey's Conformal-Invariant Spinor Wave Equation . . . . .	» 210
J. C. POLKINGHORNE — General Dispersion Relations . . . . .	» 216
D. J. CANDLIN — On Sums over Trajectories for Systems with Fermi Statistics . . . . .	» 231
R. P. HADDOCK — Analysis of one Hundred Bevatron $\pi^+$ Particles . . . . .	» 240
W. K. BURTON and A. H. DE BORDE — Functional Integration in Quantum Field Theory. . . . .	» 254
P. SEN — Renormalized Dirac-Maxwell Equations . . . . .	» 270
P. AMIRAJU and L. M. LEDERMAN — A Diffusion Chamber Study of Very Slow Mesons - IV. Absorption of Pions in Light Nuclei . . . . .	» 283
A. BISI, L. ZAPPA and E. ZIMMER — Orbital Electron Capture in $^{179}\text{Ta}$ . . . . .	» 307
W. E. FRAHN — On the Nucleon-Nucleus Interaction . . . . .	» 313
M. BENEVENTANO, G. BERNARDINI, D. CARLSON-LEE, G. STOPPINI and L. TAU — Differential Cross-Sections for Photoproduction of Positive Pions in Hydrogen . . . . .	» 323
M. KOSHIBA — The Application of Charge Independence to the Nuclear Capture of Negative K-Mesons . . . . .	» 357
A. MARTIN — Meson Nucleon $S$ Scattering and Crossing Theorem . . . . .	» 369
W. A. COOPER, H. FILTHUTH, J. A. NEWTH and R. A. SALMERON — Further Measurements on Charged V-Events . . . . .	» 390
L. PAOLONI — Coulomb Repulsion Integrals ( $pp pp$ ) and Bonding Power of an Atom in a given Valence State. . . . .	» 410
F. FERRERO, A. O. HANSON, R. MALVANO and C. TRIBUNO — Fast Photoneutrons from Bismuth . . . . .	» 418
J. M. BLATT — Pair Correlations in Dilute Gases at Low Temperatures . . . . .	» 430
J. M. BLATT — The Second Virial Coefficient Near Absolute Zero . . . . .	» 466
A. MINGUZZI — Non Linear Effects in the Vacuum Polarization . . . . .	» 476
M. FERENTZ and S. RABOY — On the Consequences of the Possible Existence of the Hyperdeuteron. . . . .	» 487

*Note Tecniche:*

P. BASSI, A. LORIA, J. A. MEYER, P. MITTNER and I. SCOTONI — On n-Pentane Bubble Chambers . . . . .	pag. 491
---	----------

*Lettere alla Redazione:*

S. BHATTACHARYA — On Certain Hydrodynamical Considerations of an Imperfect Fluid in a General Relativistic Field . . . . .	» 501
G. POIANI and G. SALVATORI — On the Positive Excess at Low Energies and at Sea Level . . . . .	» 503
<i>Libri ricevuti e Recensioni</i> . . . . .	» 505

N. 3 - 1° SETTEMBRE 1956

M. DEMEUR, A. HULEUX et G. VANDERHAEGHE — Désintégrations des noyaux légers de l'émulsion nucléaire par des mésons $\pi^-$ lents . . . . .	pag. 509
R. GATTO — About the Possible Annihilation Mode of a Nucleon-Antinucleon System into a K-K Pair . . . . .	» 526
Y. TAKAHASHI — Theory of Multiple Boson Production . . . . .	» 531
D. M. BRINK and G. R. SATCHLER — Holes and Particles in Shell Models . . . . .	» 549
G. R. BURBIDGE and F. HOYLE — Matter and Anti-Matter . . . . .	» 558
G. H. DERRICK — On the Existence of a Bound Nucleon- $\Lambda^0$ State . . . . .	» 565
J. I. HORVÁTH — Contribution to Stephenson-Kilmister's Unified Theory of Gravitation and Electromagnetism . . . . .	» 571
J. I. HORVÁTH — Contributions to the Unified Theory of Physical Fields . . . . .	» 577
C. C. GROSJEAN — On a New Approximate One-Velocity Theory of Multiple Scattering in Infinite Homogeneous Media . . . . .	» 582
A. KIND and L. JESS — On the Real Part of the Complex Potential Well of the Nucleus . . . . .	» 595
D. KESSLER and P. KESSLER — On the Validity of the Williams-Weizsäcker Method and the Problem of the Nuclear Interactions of Relativistic $\mu$ -mesons . . . . .	» 601
Y. EISENBERG, E. LOMON and S. ROSENDORFF — An Analysis of the Spin and Parity of the $\tau$ -Meson . . . . .	» 610
N. N. BISWAS, L. CECCARELLI-FABBRICHESI, M. CECCARELLI, K. GOTTSTEIN, N. C. VARSHNEYA and P. WALOSCHKE — Decay Modes and Mean Life of Scattered $K^0$ -Mesons . . . . .	» 631

*Note Tecniche:*

S. KAFTAL, R. SOMIGLIANA e S. TERRANI — Sull'impiego dei radioisotopi per la determinazione dell'usura di utensili da taglio . . . . .	» 637
B. STILLER and F. I. LOUCKES, Jr. — Semi-Automatic Recorder for Filar Micrometer Eyepiece and Its Application to Track Measurement . . . . .	» 642

*Lettere alla Redazione:*

W. WOLTER and M. MIESOWICZ - Ionization at the Origin of an Electron Pair of Very High Energy . . . . .	pag.	648
S. NARANAN, P. V. RAMANAMURTY, A. B. SAHAR, SIDDHESHWAR LAL and A. SUBRAMANIAN - Unusual Cosmic Ray Events Observed in a Multiplate Cloud Chamber. . . . .	"	651
S. SORIANO - Perturbazione dei livelli energetici di una particella in una buca di potenziale sferoidale . . . . .	"	657
A. O. BARUT - Anisotropy of Cosmic Rays due to Galactic Rotation . . . . .	"	661
W. THIRRING - Depolarization of Stopped Particles. . . . .	"	666
W. CZYŻ and J. SAWICKI - Polarization of Nucleons from Photonicuclear Reactions . . . . .	"	668
U. HABER-SCHAIM - A Test for the «Median Angle» Method . . . . .	"	669
L. COLLI and U. FACCHINI - Measurement of the Energy Spectrum of Protons from (n, p) Reactions on Mg and Zn with 14 MeV Neutrons . . . . .	"	671
S. T. BUTLER, J. M. BLATT and M. R. SCHAFROTH - Nature of the $\lambda$ -Transition in Liquid Helium . . . . .	"	674
J. M. BLATT, S. T. BUTLER and M. R. SCHAFROTH - Superfluidity of Liquid Helium . . . . .	"	676

## N. 4 - 1° OTTOBRE 1956

F. PORRECA - Experimental Decay Law of the Diffracted Light Remaining in the Liquids at the Stopping of the Ultrasonic Waves. . . . .	pag.	679
P. GOSAR - Multiple Small Angle Scattering of Waves by an Inhomogeneous Medium . . . . .	"	688
N. SEEMAN and R. G. GLASSER - Analysis of an Electron Shower Associated with a Very Energetic He Nucleus . . . . .	"	703
T. TAMURA - On the Collective Description of Nuclear Surface Oscillation . . . . .	"	713
S. HIROKAWA, H. KOMORI and S. OGAWA - On the Anomalous Magnetic Moment of $\mu$ -Mesons . . . . .	"	736
M. CRESTI, W. D. B. GREENING, L. GUERRIERO, A. LORIA and G. ZAGO - Inelasticity in Collisions between Pions and Lead Nuclei. . . . .	"	747
A. BISI, S. TERRANI and L. ZAPPA - An Investigation of the First Rotational Level of $^{119}\text{Tm}$ . . . . .	"	758
A. BISI, E. GERMAGNOLI and L. ZAPPA - A Coincidence Arrangement for the Detection of Low Energy Quanta . . . . .	"	764
S. I. HUSAIN - Conservation Laws and other Identities in Bonnor's Unified Field Theory. . . . .	"	768
G. H. A. COLE - On the Dynamics of a Non-Uniform Electrically Conducting Fluid . . . . .	"	779
M. R. SCHAFROTH and J. M. BLATT - Phenomenological Equations for Superconductors . . . . .	"	786
R. GIACCONI, A. LOVATI, A. MURA and C. SUCCI - High Energy Nuclear Interactions in Lead by Cosmic Rays Protons at 3500 m . . . . .	"	826
R. W. BIRGE, D. H. PERKINS, J. R. PETERSON, D. H. STORK and M. N. WHITEHEAD - Decay Characteristics and Masses of Positive K-Mesons Produced by the Bevatron . . . . .	"	834

J. OREAR — Evaluation of the Scattering Lengths in Pion-Nucleon Scattering	pag.	856
W. SCHMIDT and K. BAUMANN — Quantentheorie der Felder als Distributionstheorie . . . . .	»	860
G. THURO et M. PAIĆ — Étude de la dissolution des grains d'argent des plaques nucléaires épaisses dans le fixateur . . . . .	»	887
B. BERTOTTI — On Gravitational Motion. . . . .	»	898
R. S. MISHRA — Basic Principles of Unified Field Theory . . . . .	»	907
C. D'ANDLAU, R. ARMENTEROS, A. ASTIER, H. C. DESTAEBLER, B. P. GRÉGORY, L. LEPRINCE-RINGUET, F. MULLER, C. PEYROU and J. H. TINLOT — A $V^0$ Decay with an Electron Secondary . . . . .	»	917

*Note Tecniche:*

J. E. PLAINEVAUX — Étude des déformations d'une lame de suspension élastique. . . . .	»	922
---	---	-----

*Lettere alla Redazione:*

N. C. BARFORD and G. T. REYNOLDS — Graphical Determination of the Path of a Scattered Particle . . . . .	»	929
G. T. REYNOLDS — Laboratory Energy Distribution of $\Lambda^0$ Particles . . .	»	933
E. CLEMENTEL and C. VILLI — On a New Nucleon-Nucleon Potential . .	»	935
C. MARCHI, E. PEDRETTI and S. STANTIC — Interaction and Decay of $K^+$ Mesons in Flight . . . . .	»	940
B. HAHN — A Carbon Dioxide-Hexane Gas Bubble Chamber . . . . .	»	944
A. ASCOLI, M. ASDENTE and E. GERMAGNOLI — On the Ratio between $\gamma$ - and $\alpha$ -Activities in $^{210}\text{Po}$ . . . . .	»	946
F. BRISBOUT, M. W. FRIEDLANDER and P. IREDALE — Mesonic Decay in Flight of Triton Hyperfragment . . . . .	»	948
B. FERRETTI — On the Conservation of the Nucleons . . . . .	»	951
P. E. ARGAN and A. GIGLI — On the Bubbles Formation in Supersaturated Gas-Liquid Solutions . . . . .	»	953
B. LÜTHI and J. L. OLSEN — A New Effect in the Magnetoresistance of Aluminium. . . . .	»	957

N. 5 - 1° NOVEMBRE 1956

F. T. ADLER and D. BARONCINI — Approximations for Linear Betatron Oscillations . . . . .	pag.	959
W. KRÓLIKOWSKI and J. RZEWUSKI — One-Time Formulation of the Relativistic Two-Body Problem. Separation of Angular Variables . . . .	»	975
I. E. MCCARTHY — Analytical Solution of the Covariant Meson Nucleon Integral Equation . . . . .	»	991
A. CARRELLI and A. DE VITO — Dynamic Determination of Viscosity . .	»	1009
H. EKSTEIN — Scattering in Field Theory . . . . .	»	1017
N. BRENE, K. H. HANSEN, J. E. HOOPER and M. SCHARFF — Remarks on the Analysis of $\tau$ -Meson Experiments . . . . .	»	1059



M. HAÏSSINSKY et A. M. MANGEOT - Actions chimiques des ultrasons sur l'eau et les solutions aqueuses . . . . .	pag. 1086
L. MEZZETTI and J. W. KEUFFEL - On the Mean Life Time of K-Mesons Produced by the Cosmic Radiation . . . . .	" 1096
E. MINARDI - Sulla teoria bilocale dell'elettrone . . . . .	" 1127
J. E. PLAINEVAUX - Mouvement de tangage d'une suspension élémentaire sur lames élastiques . . . . .	" 1133
A. DEBENEDETTI, C. M. GARELLI, L. TALLONE and M. VIGONE - A High Energy Nuclear Interaction . . . . .	" 1142
A. DEBENEDETTI, C. M. GARELLI, L. TALLONE and M. VIGONE - A Study on Electromagnetic Showers in Nuclear Emulsions . . . . .	" 1151
B. CHINAGLIA and F. DEMICHELIS - Magnetic and Scintillation Spectrometers; the case of the $\gamma$ -Rays of $^{228}_{90}\text{Th}$ and its Decay Products . . .	" 1160

#### *Note Tecniche:*

E. AMALDI, C. CASTAGNOLI and C. FRANZINETTI - An Electronic Scanner for Nuclear Emulsions . . . . .	" 1165
P. FAVERO e G. GRIFONE - Spettrografo a microonde con modulazione ausiliaria . . . . .	" 1174

#### *Lettere alla Redazione:*

G. BECK - Phenomenological Theory of Conductivity. . . . .	" 1190
T. THIEZ - Über Eine Approximation der Thomas-Fermi Funktion . . .	" 1192
J. CRUSSARD, V. FOUCHÉ, J. HENNESSY, G. KAYAS, L. LEPRINCE-RINGUET, D. MORELLET and F. RENARD - Addendum to « K-Mesons in Emulsions Exposed to a 6.2 GeV Proton Beam » . . . . .	" 1195
F. ANDERSON, D. KEEFE, A. KERNAN and J. LOSTY - A Probable Example of the Reaction $K^+ + {}^{12}_6\text{C} \rightarrow K^+ + 3{}^4_2\text{He}$ . . . . .	" 1198
N. N. BISWAS, L. CECCARELLI-FABBRICHESI, M. CECCARELLI, K. GOTTSTEIN, N. C. VARSHNEYA and P. WALOSCHIEK - Further Evidence of ${}^{12}\text{C}$ Tripartition Induced by $K^+$ -Mesons. . . . .	" 1201
J. IWADARE, S. OTSUKI, R. TAMAGAKI and W. WATARI - Pion Theory of Nuclear Forces and n-p Polarization. . . . .	" 1204
F. CLEMENTEL and C. VILLI - On the Scattering of High Energy Electrons by Protons . . . . .	" 1207
W. KRÓLIKOWSKI and J. RZEWUSKI - A New Proof of the One-Time Equation in the Theory of Bound States. . . . .	" 1212
R. L. BRAHMACHARY - A Generalization of Reissner-Nordström Solution - I	" 1216
E. MINARDI - On the Resonance Nucleon-Nucleus Scattering . . . . .	" 1219
G. MORPURGO - The Angular Distributions in the Hyperon Decays - II	" 1222

<i>Libri ricevuti e Recensioni</i> . . . . .	" 1227
--	--------

## N. 6 - 1° DICEMBRE 1956

J. RAYSKI - Bilocal Field Theories and their Experimental Tests - I . . .	pag. 1231
M. HAMAGUCHI - On the Hydrodynamical Model in Multiple Production of Mesons . . . . .	» 1242
P. W. HIGGS - Vacuum Expectation Values as Sums Over Histories . . .	» 1262
R. GATTO - Coherence Effects in the Lee-Yang Parity Doublets Theory of Strange Particles . . . . .	» 1274
W. R. WEBBER - New Determination of the Intensities of Primary Cosmic Ray Alpha Particles and Li, Be, B Nuclei at $\lambda = 41.5^\circ$ Using a Čerenkov Detector . . . . .	» 1285
F. COESTER - Rotational States of Spheroidal Nuclei . . . . .	» 1307
R. OEHME - Causality and Dispersion Relations for the Scattering of Mesons by Fixed Nucleons . . . . .	» 1316
J. T. JONES jr. and J. M. KELLER - Binding Energies of the Light Hyperfragments . . . . .	» 1329
H. MESSEL - On the Solutions of the Fluctuation Problem in Cascade Showers . . . . .	» 1339
E. VAN DER SPUY - Investigation of the States of an Electron in a Proposed Electromagnetic Field . . . . .	» 1349
M. SIMONETTA, G. FAVINI, S. CARRÀ and V. PIERPAROLI - Electronic Spectra of Mono-, Di- and Tri-Azines of the Naphtalene Series - I. Benzotriazine and its Derivatives . . . . .	» 1364
E. CORINALDESI - Dispersion Relations for Photoproduction of Mesons . .	» 1384
L. FONDA and I. REINA - Nucleon Recoil in the Pion-Nucleon Scattering . .	» 1399
S. YOSHIDA - Anisotropy of Cosmic Rays During the Cosmic-Ray Storms . .	» 1410
W. A. COOPER, H. FILTHUTH, J. A. NEWTH, G. PETRUCCI, R. A. SALMERON and A. ZICHICHI - A Probable Example of the Production and Decay of a Neutral Tau-Meson . . . . .	» 1433
B. E. LAURENT - On Covariant Quantization with Application to the Scattering of Gravitating Dirac Particles . . . . .	» 1445
M. KONUMA and H. UMEZAWA - High Energy Behaviour of Renormalizable Fields - II . . . . .	» 1461
F. D. HÄNNI, C. LANG, M. TEUCHER and H. WINZELER - A High Energy Jet in Nuclear Emulsions . . . . .	» 1473
F. BACHELET and A. M. CONFORTO - Atmospheric Effects on the Cosmic Ray Total Intensity at Sea Level . . . . .	» 1479
F. A. BRISBOUT, C. DAHANAYAKE, A. ENGLER and D. H. PERKINS - On the Trident Cross-Section between 1 and 10 GeV . . . . .	» 1496
S. FRANCHETTI - On the Problem of the Static Helium Film. - I. General Considerations and Density Distribution in the Film . . . . .	» 1504
K. S. BHATKI, R. K. GUPTA and S. JHA - On the Decay of $^{132}\text{Cs}$ . . . . .	» 1519
E. PICCIOTTO et S. WILGAIN - Confirmation de la période du Thorium-232 . .	» 1525
G. L. BACHELLA, A. BERTHELOT, M. DI CORATO, O. GOUSSU, R. LEVI SETTI, M. RENÉ, D. REVEL, L. SCARSI, G. TOMASINI and G. VANDERHAEGHE - On the $Q$ -Value of the Tau-Decay . . . . .	» 1529

*Note Tecniche:*

C. COTTINI and E. GATTI -- Millimicrosecond Time Analyzer . . . . .	pag. 1550
R. J. HANSON and D. C. MOORE -- A Cosmic-Ray Gas Čerenkov Counter with Adjustable Velocity . . . . .	" 1558
M. DELLA CORTE -- Analisi fotometrica delle tracce nelle emulsioni nucleari. - I. Dispositivo sperimentale . . . . .	" 1565

*Lettere alla Redazione:*

M. K. RAMA SWAMY -- A Semi-Empirical Formula for $\alpha$ -Disintegration Energy in the Region of Rare-Earth Nuclides . . . . .	" 1570
B. D'ESPAGNANT and J. PRENTKI -- Interactions faibles directes bosons- leptons et désintégrations des méson K . . . . .	" 1572
I. FUJIWARA -- On the Basic Formulation of Classical and Quantum Theories . . . . .	" 1575
G. ALIVERTI, A. DE MAIO, G. LOVERA e R. PERILLI-FEDELÌ -- Tracce $\alpha$ in emulsioni nucleari esposte in aria ad alto contenuto di radon . . . . .	" 1580
D. C. PEASLEE -- Dimensionality of Charge Space . . . . .	" 1583
J. M. COOK -- On the Vanishing of the Interaction Hamiltonian . . . . .	" 1585
R. WEINER -- Nuclear Isomeric Shift on Spectral Lines . . . . .	" 1587
S. R. MOHANTY, L. V. KANNAN and S. VISVANATHAN -- Role of Continued Excitation in the Potential Inversion of the Joshi Effect . . . . .	" 1590
R. A. RICCI and R. VAN LIESHOUT -- Radiations from $^{66}\text{Ge}$ and $^{67}\text{Ge}$ . . . . .	" 1592
S. W. MAC-DOWELL and J. J. GIANBIAGI -- Elastic Scattering of $\alpha$ -Particles . . . . .	" 1594
R. V. POPIĆ -- On the Spin and Parity of the First Excited State of $^{19}\text{O}$ . . . . .	" 1597
G. R. BISHOP and F. DEMICHELIS -- Study of a Low Intensity Component in the $\beta$ -Ray Spectrum of $^{214}_{83}\text{Bi}(\text{RaC})$ . . . . .	" 1599
R. CIRELLI e M. PUSTERLA -- Metodi funzionali nelle teorie dei campi . . . . .	" 1601
E. CORINALDESI -- Dispersion Relations for Decay Processes . . . . .	" 1605
H. HAKEN -- Application of Feynman's New Variational Procedure to the Calculation of the Ground State Energy of Excitons . . . . .	" 1608
M. SILVESTRI and N. ADORNI -- An Apparatus for Continuous Isotopic Analysis of Hydrogen Deuterium Mixtures . . . . .	" 1610
G. BUSSETTI -- On the Higher Limit for the Mass of an Assembly of Particles . . . . .	" 1613
T. REGGE -- Angular Correlations between Decay Planes of $\tau^+$ -Mesons and their Production Geometry . . . . .	" 1615
G. BADONI, L. COLLI and U. FACCHINI -- Further Measurements on $\mu, p$ Reactions at 14 MeV - I. Magnesium, Silicon, Calcium, Zinc, Zirconium . . . . .	" 1618
A. J. HERZ, R. M. MAY and N. SOLNSTEIFF -- Errors in Constant-Sagitta Scattering Measurements in Nuclear Emulsions . . . . .	" 1623

<i>Libri ricevuti e Recensioni</i> . . . . .	" 1626
--	--------

<i>Indici del Volume IV, Serie X, 1956</i> . . . . .	" 1633
--	--------

# INDICE PER AUTORI

Le sigle L. N.T. e N.d.L., si riferiscono rispettivamente alle *Lettere alla Redazione*, alle *Note Tecniche*, e alle *Note di Laboratorio*.

ADLER F. T. and D. BARONCINI - Approximations for Linear Betatron Oscillations . . . . .	pag. 959
ADORNI N. (vedi SILVESTRI M.) (L.) . . . . .	» 1610
ALIVERTI, G., A. DE MAIO, G. LOVERA e R. PERILLI-FEDEL - Tracce $\alpha$ in emulsioni nucleari esposte in aria ad alto contenuto di radon (L.) . .	» 1580
AMALDI E., C. CASTAGNOLI and C. FRANZINETTI - An Electronic Scanner for Nuclear Emulsions (N.T.) . . . . .	» 1165
AMATI D. and B. VITALE - Some Considerations on the Charge-Exchange Scattering of Antinucleons on Nucleons (L.) . . . . .	» 145
AMMIRAJU P. and L. M. LEDERMAN - A Diffusion Chamber Study of Very Slow Mesons. - IV. Absorption of Pions in Light Nuclei . . . . .	» 283
ANDERSON F., D. KEELER, A. KERNAN and J. LOSTY - A Probable Example of the Reaction $K^+ + {}^{12}_6C \rightarrow K^+ + {}^3_2He$ (L.) . . . . .	» 1198
ARGAN P. E. and A. GIULI - On the Bubbles Formation in Supersaturated Gas-Liquid Solutions (L.) . . . . .	» 953
ARMENTEROS R. (vedi D'ANDLAU C.) . . . . .	» 917
ASCOLI A., M. ASDENTE and E. GERMAGNOLI - On the Ratio between $\gamma$ and $\alpha$ Activities of ${}^{210}Po$ (L.) . . . . .	» 946
ASCOLI R. e G. BUSSETTI - Sulla polarizzazione della Bremsstrahlung (L.)	» 147
ASCOLI R. and G. BUSSETTI - On the Study of the Bremsstrahlung by Bloch and Nordsieck's Method. . . . .	» 189
ASCOLI A., E. GERMAGNOLI and L. MONGINI - On Intermetallic Diffusion in Gold-Lead System . . . . .	» 123
ASDENTE M. (vedi ASCOLI A.) (L.) . . . . .	» 946
ASTIER A. (vedi D'ANDLAU C.) . . . . .	» 917
BACCHIELLA L., A. BERTHELOT, M. DI CORATO, O. GOUSSU, R. LEVI SETTI, M. RENÉ, D. REVEL, L. SCARSI, G. TOMASINI and G. VANDERHAEGHE - On the Q-Value of the $\tau$ -Decay . . . . .	» 1529
BACHELET F. and A. M. CONFORTO - Atmospheric Effects on the Cosmic Ray Total Intensity at Sea Level . . . . .	» 1479
BADONI C., L. COLLI and U. FACCHINI - Further Measurements on n,p Reactions at 14 MeV - I. Magnesium, Silicon, Calcium, Zinc, Zirconium (L.)	» 1618
BARFORD N. C. and T. REYNOLDS - Graphical Determination of the Path of a Scattered Particle (L.) . . . . .	» 929
BARKAS W. H. (vedi HECKMAN H. H.) . . . . .	» 51
BARONCINI D. (vedi ADLER F. T.) . . . . .	» 959
BARUT A. O. - Anisotropy of Cosmic Rays due to Galactic Rotation (L.)	» 661
BASSI P., A. LORIA, J. A. MEYER, P. MITTNER and I. SCOTONI - On n-Pentane Bubble Chambers (N.T.) . . . . .	» 491
BAUMANN K. (vedi SCHMIDT W.) . . . . .	» 860
BECK G. - Phenomenological Theory of Conductivity (L.) . . . . .	» 1190

BENEVENTANO M., G. BERNARDINI, D. CARLSON-LEE, G. STOPPINI and L. TAU - Differential Cross-Sections for Photoproduction of Positive Pions in Hydrogen . . . . .	pag. 323
BERNARDINI G. (vedi BENEVENTANO M.) . . . . .	» 323
BERTHELOT A. (vedi BACCHELLA L.) . . . . .	» 1529
BERTOTTI B. - On Gravitational Motion. . . . .	» 898
BETHE H. A. and J. HAMILTON - Anti-Proton Annihilation . . . . .	» 1
BHATKI K. S., R. K. GUPTA and S. JHA - On the Decay of Caesium-132 . . . . .	» 1519
BHATTACHARYA S. - On Certain Hydrodynamical Considerations of an Imperfect Fluid in a General Relativistic Field (L.) . . . . .	» 501
BIRGE R. W., D. H. PERKINS, J. R. PETERSON, D. H. STORK and M. N. WHI- TEHEAD - Decay Characteristics and Masses of Positive K-Mesons Pro- duced by the Bevatron . . . . .	» 834
BISHOP G. R. and F. DEMICHELIS - Study of a Low-Intensity Component in the $\beta$ -Ray Spectrum of $^{214}_{88}\text{Bi}(\text{RaC})$ (L.) . . . . .	» 1599
BISI A., E. GERMAGNOJI and L. ZAPPA - A Coincidence Arrangement for the Detection of Low Energy Quanta . . . . .	» 764
BISI A., S. TERRANI and L. ZAPPA - An Investigation of the First Rotational Level of $^{169}\text{Tm}$ . . . . .	» 758
BISI A., L. ZAPPA and E. ZIMMER - Orbital Electron Capture in $^{179}\text{Ta}$ . . . . .	» 307
BISWAS N. N., L. CECCARELLI-FABBRICHESI, M. CECCARELLI, K. GOTT- STEIN, N. C. VARSHNEYA and P. WALOSCHEK - Decay Modes and Mean Life of Scattered $K^+$ -Mesons. . . . .	» 631
BISWAS N. N., L. CECCARELLI-FABBRICHESI, M. CECCARELLI, K. GOTT- STEIN, N. C. VARSHNEYA and P. WALOSCHEK - Further Evidence of $^{12}\text{C}$ Tripartition Induced by $K^+$ -Mesons (L.) . . . . .	» 1201
BLATT J. M. - Pair Correlations in Dilute Gases at Low Temperatures . . . . .	» 430
BLATT J. M. (vedi BUTLER S. T.) (L.) . . . . .	» 674
BLATT J. M., S. T. BUTLER and M. R. SCHAFROTH - Superfluidity of Liquid Helium (L.) . . . . .	» 676
BLATT J. M. (vedi SCHAFROTH M. R.) . . . . .	» 786
BLEVINS M. E. (vedi BLOCK M. M.) . . . . .	» 46
BLOCK M. M., E. M. HARTH, M. E. BLEVINS and G. G. SLAUGHTER - Ob- servation of Electron Secondaries from $V^0$ Decays . . . . .	» 46
BRACCI A. and C. COCEVA - The Diffusion Parameters of Thermal Neutrons in Water . . . . .	» 59
BRAHMACHARY R. L. - A Generalization of Reissner-Nordström Solution. I (L.) . . . . .	» 1216
BRENE N., K. H. HANSEN, J. E. HOOPER and M. SCHARFF - Remarks on the Analysis of $\tau$ -Meson Experiments . . . . .	» 1059
BRINK D. M. and G. R. SATCHLER - Holes and Particles in Shell Models . . . . .	» 549
BRISBOUT F., M. W. FRIEDLANDER and P. IREDALE - Mesonic Decay in Flight of a Triton Hyperfragment (L.) . . . . .	» 948
BRISBOUT F. A., C. DAHANAYAKE, A. ENGLER and R. D. PERKINS - On the Trident Cross-Section between 1 and 10 GeV . . . . .	» 1496
BUDINI P. and L. TAFFARA - On the Energy Loss and Specific Ionization of a Relativistic Particle in a Polarizable Medium. I . . . . .	» 23
BURBRIDGE G. R. and F. HOYLE - Matter and Anti-Matter . . . . .	» 558
BURTON W. K. and A. H. DE BORDE - Functional Integration in Quantum Field Theory. . . . .	» 254
BUSSETTI G. (vedi ASCOLI R.) (L.) . . . . .	» 147

BUSSETTI G. (vedi ASCOLI R.) . . . . .	pag. 189
BUSSETTI G. — On the Higher Limit for the Mass of an Assembly of Particles (L.) . . . . .	» 1613
BUTLER S. T., J. M. BLATT and M. R. SCHAFFROTH — Nature of the $\lambda$ -Transition in Liquid Helium (L.) . . . . .	» 674
BUTLER S. T. (vedi BLATT J. M.) (L.) . . . . .	» 676
CANDLIN D. J. — On Sums over Trajectories for Systems with Fermi Statistics . . . . .	» 231
CARLSON-LEE D. (vedi BENEVENTANO M.) . . . . .	» 323
CARRÀ S. (vedi SIMONETTA M.) . . . . .	» 1364
CARRELLI A. and A. DE VITO — Dynamic Determination of Viscosity . . . . .	» 1009
CASTAGNOLI C. (vedi AMALDI E.) (N. T.) . . . . .	» 1165
CECCARELLI M. (vedi BISWAS N. N.) . . . . .	» 631
CECCARELLI M. (vedi BISWAS N. N.) (L.) . . . . .	» 1201
CECCARELLI-FABBRICHESI L. (vedi BISWAS N. N.) . . . . .	» 631
CECCARELLI-FABBRICHESI L. (vedi BISWAS N. N.) (L.) . . . . .	» 1201
CHINAGLIA B. and F. DEMICHELI — Magnetic and Scintillation Spectrometers for the $\gamma$ -rays of $^{228}_{90}\text{Th}$ and its Decay Products . . . . .	» 1160
CHINAGLIA B., F. DEMICHELI and R. A. RICCI — Tempo di decadimento del $\text{ZnS(Ag)}$ e preparazione di ricevitori a $\text{ZnS(Ag)}$ (L.) . . . . .	» 134
CIRELLI R. e M. PUSTERLA — Estensione del metodo parametrico di Davison al caso di potenziali cinetici (L.) . . . . .	» 150
CIRELLI R. e M. PUSTERLA — Metodi funzionali nelle teorie dei campi (L.) . . . . .	» 1601
CLEMENTEL E. and C. VILLI — On a New Nucleon-Nucleon Potential (L.) . . . . .	» 935
CLEMENTEL E. and C. VILLI — On the Scattering of High Energy Electrons by Protons (L.) . . . . .	» 1207
COCEVA C. (vedi BRACCI A.) . . . . .	» 59
COESTER F. — Rotational States of Spheroidal Nuclei. . . . .	» 1307
COLE G. H. A. — On the Dynamics of a Non-Uniform Electrically Conducting Fluid . . . . .	» 779
COLLI L. and U. FACCHINI — Measurement of the Energy Spectrum of Protons from (n, p) Reactions on Mg and Zn with 14 MeV Neutrons (L.) . . . . .	» 671
COLLI L. (vedi BADONI C.) (L.) . . . . .	» 1618
CONFORTO A. M. (vedi BACHELET F.) . . . . .	» 1479
COOK J. M. — On the Vanishing of the Interaction Hamiltonian (L.) . . . . .	» 1585
COOPER W. A., H. FILTHUTH, J. A. NEWTH and R. A. SALMERON — Further Measurements on Charged V-Events . . . . .	» 390
COOPER W. A., H. FILTHUTH, J. A. NEWTH, G. PETRUCCI, R. A. SALMERON and A. ZICHICH — A Probable Example of the Production and Decay of a Neutral Tau-Meson . . . . .	» 1433
CORINALDESI E. — Dispersion Relations for Photoproduction of Mesons . . . . .	» 1384
CORINALDESI E. — Dispersion Relations for Decay Processes (L.) . . . . .	» 1605
COTTINI C., E. GATTI and G. GIANNELLI — High Resolution Millimicrosecond Time Interval Measurements Based Upon Frequency Conversion (L.) . . . . .	» 156
COTTINI C. and E. GATTI — Millimicrosecond Time Analyzer (N. T.) . . . . .	» 1550
CRESTI M., W. D. B. GREENING, L. GUERRIERO, A. LORIA and G. ZAGO — Inelasticity in Collisions between Pions and Lead Nuclei. . . . .	» 747
CRUSSARD J., V. FOUCHÉ, J. HENNESSY, G. KAYAS, L. LEPRINCE-RINGUET, D. MORELLET and F. RENARD — Addendum to K-Mesons in Emulsions Exposed to a 6.2 GeV Proton Beam (L.) . . . . .	» 1195



CZYŻ W. and J. SAWICKI — Polarization of Nucleons from Photonnuclear Reactions (L.) . . . . .	pag. 668
DAHANAYAKE C. (vedi BRISBOUT F. A.) . . . . .	" 1496
D'ANDLAI C., R. ARMENTEROS, A. ASTIER, H. C. DESTAEBLER, B. P. GRÉGORY, L. LEPRINCE-RINGUET, F. MULLER, C. PEYROU and J. H. TINLOT — A $V^0$ Decay with an Electron Secondary . . . . .	" 917
DEBENEDETTI A., C. M. GARELLI, L. TALLONE and M. VIGONE — A High Energy Nuclear Interaction . . . . .	" 1142
DEBENEDETTI A., C. M. GARELLI, L. TALLONE and M. VIGONE — A Study on Electromagnetic Showers in Nuclear Emulsions . . . . .	" 1151
DE BORDE A. H. (vedi BURTON W. K.) . . . . .	" 254
DELLA CORTE M. — Analisi fotometrica delle tracce nelle emulsioni nucleari (N. T.) . . . . .	" 1565
DE MAIO A. (vedi ALIVERTI G.) (L.) . . . . .	" 1580
DEMETRIU M., A. HULEUX and G. VANDERHAEGHE — Désintégrations des noyaux légers de l'émulsion nucléaire par des mésons $\pi^-$ lents . . . . .	" 509
DEMICHELIIS F. (vedi CHINAGLIA B.) (L.) . . . . .	" 134
DEMICHELIIS F. (vedi CHINAGLIA B.) . . . . .	" 1160
DEMICHELIIS F. and R. A. RICCI — $\beta$ - $\gamma$ Angular Correlation of $^{208}\text{Pb}(\text{Th})''$ . . . . .	" 96
DEMICHELIIS F. (vedi BISHOP G. R.) (L.) . . . . .	" 1599
DERRICK G. H. — On the Existence of a Bound Nucleon $V^0$ State . . . . .	" 565
D'ESPAGNAT B. et J. PRENTEK — Interactions faibles bosons-leptons et désintégration des mésons K (L.) . . . . .	" 1572
DESTAEBLER H. C. (vedi D'ANDLAI C.) . . . . .	" 917
DE VITO A. (vedi CARRELLI A.) . . . . .	" 1009
DI CORATO M. (vedi BACCHELLA L.) . . . . .	" 1529
EKSTEIN H. — Scattering in Field Theory . . . . .	" 1017
ELLIOTT J. P. and T. H. R. SKYRME — Effect of Centre-of-Mass Motion on Nuclear Moments (L.) . . . . .	" 164
EISENBERG Y., E. LOMON and S. ROSENDORFF — An Analysis of the Spin and Parity of the $\tau$ -Meson . . . . .	" 610
ENGLER A. (vedi BRISBOUT F. A.) . . . . .	" 1496
FACCHINI U. (vedi COLLI L.) (L.) . . . . .	" 671
FACCHINI U. (vedi BADONI C.) (L.) . . . . .	" 1618
FAVERO P. e G. GRIFONE — Spettrografo a microonde con modulazione ausiliaria (N. T.) . . . . .	" 1174
FAVINI G. (vedi SIMONETTA M.) . . . . .	" 1364
FERENTZ M. and S. RABOY — On the Consequences of the Possible Existence of the Hyperdeuteron . . . . .	" 487
FERRERO F., A. O. HANSON, R. MALVANO and C. TRIBUNO — Fast Photoneutrons from Bismuth . . . . .	" 418
FERRETTI B. — On the Conservation of the Nucleons (L.) . . . . .	" 951
FILTHUTH H. (vedi COOPER W. A.) . . . . .	" 390
FILTHUTH H. (vedi COOPER W. A.) . . . . .	" 1433
FONDA L. and I. REINA — Nucleon Recoil in the Pion-Nucleon Scattering . . . . .	" 1399
FOUCHÉ V. (vedi CRUSSARD J.) (L.) . . . . .	" 1195
FOWLER P. H. and K. H. HANSEN — Two Examples of Mesonic Decay of Hyperfragments (L.) . . . . .	" 158
FRAHN W. E. — On the Nucleon-Nucleus Interaction . . . . .	" 313
FRANCHETTI S. — On the Problem of the Static Helium Film. — I. General Considerations and Density Distribution in the Film . . . . .	" 1504

FRANZINETTI C. (vedi AMALDI E.) (N.T.) . . . . .	pag. 1165
FRIEDLANDER M. W. (vedi BRISBOUT F.) (L.) . . . . .	» 948
FUJIIWARA I. - On the Basic Formulation of Classical and Quantum Theories . . . . .	» 1575
GARELLI C. M. (vedi DEBENEDETTI A.) . . . . .	» 1142
GARELLI C. M. (vedi DEBENEDETTI A.) . . . . .	» 1151
GATTI E. (vedi COTTINI C.) (N.T.) . . . . .	» 1550
GATTI E. (vedi COTTINI C.) (L.) . . . . .	» 156
GATTO R. Angular Correlation Methods for Determining the Spins of the Hyperons . . . . .	» 197
GATTO R. - About the Possible Annihilation Mode of a Nucleon-Antinucleon System into a K-K Pair . . . . .	» 526
GATTO R. - Coherence Effects in the Lee-Yang Parity Doublets Theory of Strange Particles . . . . .	» 1274
GERMAGNOLI E. (vedi ASCOLI A.) . . . . .	» 123
GERMAGNOLI E. (vedi ASCOLI A.) (L.) . . . . .	» 946
GERMAGNOLI E. (vedi BISI A.) . . . . .	» 764
GIACCONI R., A. LOVATI, A. MURA and C. SUCCI - High Energy Nuclear Interactions in Lead by Cosmic Rays Protons at 3500 m . . . . .	» 826
GIANBIAGI J. J. (vedi MACDOWELL S. W.) (L.) . . . . .	» 1594
GIANNELLI G. (vedi COTTINI C.) (L.) . . . . .	» 156
GIGLI A. (vedi ARGAN P. E.) (L.) . . . . .	» 953
GLASSER R. G. (vedi SEEMAN N.) . . . . .	» 703
GOSAR P. - Multiple Small Angle Scattering of Waves by an Inhomogeneous Medium . . . . .	» 688
GOTTSTEIN K. (vedi BISWAS N. N.) . . . . .	» 631
GREENING W. D. B. (vedi CRESTI M.) . . . . .	» 747
GOTTSTEIN K. (vedi BISWAS N. N.) (L.) . . . . .	» 1201
GOUSSU O. (vedi BACCHELLA L.) . . . . .	» 1529
GRÉGORY B. P. (vedi D'ANDLAU C.) . . . . .	» 917
GRIFONE G. (vedi FAVERO P.) (N.T.) . . . . .	» 1174
GROSJEAN C. C. - On a New Approximate One-Velocity Theory of Multiple Scattering in Infinite Homogeneous Media . . . . .	» 582
GUERRIERO L. (vedi CRESTI M.) . . . . .	» 747
GUPTA R. K. and S. JHA - On the Electron Capture Decay Energy of $^{153}_{64}\text{Gd}$ . . . . .	» 88
GUPTA R. K. (vedi BHATKI K. S.) . . . . .	» 1519
HABER-SCHAIM U. - A Test for the « Median Angle » Method (L.) . . . . .	» 669
HADDOCK R. P. - Analysis of one Hundred Bevatron $\tau^+$ Particles . . . . .	» 240
HAHN B. - Carbon Dioxide Hexane Gas Bubble Chamber (L.) . . . . .	» 944
HAÏSSINSKY M. et A. M. MANGEOT - Actions chimiques des ultra-sons sur l'eau et les solutions aqueuses . . . . .	» 1086
HAKEN H. - Application of Feynman's New Variational Procedure to the Calculation of the Ground State Energy of Excitons (L.) . . . . .	» 1608
HAMAGUCHI M. - On the Hydrodynamical Model in Multiple Production of Mesons . . . . .	» 1242
HAMILTON J. (vedi BETHE H. A.) . . . . .	» 1
HÄNNI F. D., C. LANG, M. TEUCHER and H. WINZELER - A High Energy Jet in Nuclear Emulsions . . . . .	» 1473
HANSEN K. H. (vedi FOWLER P. H.) (L.) . . . . .	» 158
HANSEN K. H. (vedi BRENE N.) . . . . .	» 1059
HANSON A. O. (vedi FERRERO F.) . . . . .	» 418

HANSON R. J. and D. C. MOORE - A Cosmic-Ray Gas Čerenkov Counter with Adjustable Velocity (N. T.) . . . . .	pag. 1558
HARTH E. M. (vedi BLOCK M. M.) . . . . .	" 46
HECKMAN H. H., F. M. SMITH and W. H. BARKAS - Mass and Spin-Parity Character of the $\tau$ -Meson . . . . .	" 51
HENNESSY J. (vedi CRUSSARD J.) (L.) . . . . .	" 1195
HERZ A. J., R. M. MAY and N. SOLNSTEFF - Errors in Constant-Sagitta Scattering Measurements in Nuclear Emulsions (L.) . . . . .	" 1623
HIGGS P. W. - Vacuum Expectation Values as Sums Over Histories . . . . .	" 1262
HILLMAN P., G. H. STAFFORD and C. WHITEHEAD - A New Method of Measuring Asymmetries in Neutron Polarization Experiments. . . . .	" 67
HIROKAWA S., H. KOMORI and S. OGAWA - On the Anomalous Magnetic Moment of $\mu$ -Mesons . . . . .	" 736
HOOPER J. E. (vedi BRENE N.) . . . . .	" 1059
HORVÁTH J. I. - Contribution to Stephenson-Kilmister's Unified Theory of Gravitation and Electromagnetism. . . . .	" 571
HORVÁTH J. I. - Contributions to the Unified Theory of Physical Fields . . . . .	" 577
HOYLE F. (vedi BURBIDGE G. R.) . . . . .	" 558
HULEUX A. (vedi DEMEUR M.) . . . . .	" 509
HUSAIN S. I. - Conservation Laws and other Identities in Bonnor's Unified Field Theory. . . . .	" 768
IREDALE P. (vedi BRISBOUT F.) (L.) . . . . .	" 948
IWADARE J., S. OTSUKI, R. TAMAGAKI and W. WATARI - Pion Theory of Nuclear Forces and n-p Polarization (L.) . . . . .	" 1204
JESS L. (vedi KIND A.) . . . . .	" 595
JHA S. (vedi GUPTA R. K.) . . . . .	" 88
JHA S. (vedi BHATKI K. S.) . . . . .	" 1519
JONES J. T. jr. and J. M. KELLER - Binding Energies of the Light Hyperfragments . . . . .	" 1329
KAFTAL S., R. SOMIGLIANA e S. TERRANI - Sull'impiego dei radioisotopi per la determinazione dell'usura di utensili da taglio (N. T.) . . . . .	" 637
KANNAN L. V. (vedi MOHANTY S. R.) (L.) . . . . .	" 1590
KAYAS G. (vedi CRUSSARD J.) (L.) . . . . .	" 1195
KEEFE D. (vedi ANDERSON F.) (L.) . . . . .	" 1198
KELLER J. M. (vedi JONES J. T.) . . . . .	" 1329
KERNAN A. (vedi ANDERSON F.) (L.) . . . . .	" 1198
KESSLER D. and P. KESSLER - On the Validity of the Williams-Weizsäcker Method and the Problem of the Nuclear Interactions of Relativistic $\mu$ -Mesons . . . . .	" 601
KESSLER P. (vedi KESSLER D.) . . . . .	" 601
KEUFFEL J. W. (vedi MEZZETTI L.) . . . . .	" 1096
KIND A. and L. JESS - On the Real Part of the Complex Potential Well of the Nucleus . . . . .	" 595
KOMORI H. (vedi HIROKAWA S.) . . . . .	" 736
KONUMA M. and H. UMEZAWA - High Energy Behaviour of Renormalizable Fields. II . . . . .	" 1461
KORTEF F. - On Some Solutions of Gursey's Conformal-Invariant Spinor Wave Equation . . . . .	" 210
KOSHIBA M. - The Application of Charge Independence to the Nuclear Capture of Negative K-Mesons . . . . .	" 357

KRÓLIKOWSKI W. and J. RZEWUSKI - One-Time Formulation of the Relativistic Two-Body Problem Separation of Angular Variables . . . . .	pag. 975
KRÓLIKOWSKI W. and J. RZEWUSKI - A New Proof of the One-Time Equation in the Theory of Bound States (L.) . . . . .	" 1212
LANG C. (vedi HÄNNI F. D.) . . . . .	" 1473
LAURENT B. E. - On Covariant Quantization with Application to Scattering of Gravitating Dirac Particles. . . . .	" 1445
LEDERMAN L. M. (vedi AMMIRAJU P.) . . . . .	" 283
LEPRINCE-RINGUET L. (vedi D'ANDLAU C.) . . . . .	" 917
LEPRINCE-RINGUET L. (vedi CRUSSARD J.) (L.) . . . . .	" 1195
LEVI SETTI R. (vedi BACCHELLA L.) . . . . .	" 1529
LOMON E. (vedi EISENBERG Y.) . . . . .	" 610
LOMON E. L. - A Soluble Model of Meson-Nucleon <i>S</i> -State Scattering . . . . .	" 106
LORIA A. (vedi BASSI P.) (N. T.) . . . . .	" 491
LORIA A. (vedi CRESTI M.) . . . . .	" 747
LOSTY J. (vedi ANDERSON F.) (L.) . . . . .	" 1198
LOUCKES F. I. jr. (vedi STILLER R.) (N. T.) . . . . .	" 642
LOVATI A. (vedi GIACCONI R.) . . . . .	" 826
LOVERA G. (vedi ALIVERTI G.) (L.) . . . . .	" 1580
LUTHI B. and J. L. OLSEN - A New Effect in the Magnetoresistance of Aluminium (L.) . . . . .	" 957
MACDOWELL S. W. and J. J. GIANBIAGI - Elastic Scattering of $\alpha$ -Particles (L.) . . . . .	" 1594
MALVANO R. (vedi FERRERO F.) . . . . .	" 418
MARCHI C., E. PEDRETTI and S. STANTIC - Interaction and Decay of $K^+$ Mesons in Flight (L.) . . . . .	" 940
MANGEOT A. M. (vedi HAÏSSINSKY M.) . . . . .	" 1086
MARTIN A. - Meson Nucleon <i>S</i> Scattering and Crossing Theorem . . . . .	" 369
MAY R. M. (vedi HERZ A. J.) (L.) . . . . .	" 1623
MCCARTHY I. E. - Analytical Solution of the Covariant Meson Nucleon Integral Equation . . . . .	" 991
MESSEL H. - On the Solution of the Fluctuation Problem in Cascade Showers . . . . .	" 1339
MEYER J. A. (vedi BASSI P.) (N. T.) . . . . .	" 491
MEZZETTI L. and J. W. KEUFFEL - On the Mean Lifetime of <i>K</i> -Mesons Produced by the Cosmic Radiations . . . . .	" 1096
MIEŚOWICZ M. (vedi WOLTER W.) (L.) . . . . .	" 648
MINARDI E. - Sulla teoria bilocale dell'elettrone . . . . .	" 1127
MINARDI E. - On the Resonance Nucleon-Nucleus Scattering (L.) . . . . .	" 1219
MINGUZZI A. - Non Linear Effect in the Vacuum Polarization . . . . .	" 476
MISHKA R. S. - Basic Principles of Unified Field Theory . . . . .	" 907
MITTNER P. (vedi BASSI P.) (N. T.) . . . . .	" 491
MOHANTY S. R., L. V. KANNAN and S. VISVANATHAN - Role of Continued Excitation in the Potential Inversion of the Joshi Effect (L.) . . . . .	" 1590
MONGINI L. (vedi ASCOLI A.) . . . . .	" 123
MOORE D. C. (vedi HANSON R. J.) (N. T.) . . . . .	" 1558
MORELLET D. (vedi CRUSSARD J.) (L.) . . . . .	" 1195
MORPURGO G. - The Angular Distributions in the Hyperon Decays. - II (L.) . . . . .	" 1222
MULLER F. (vedi D'ANDLAU C.) . . . . .	" 917
MURA A. (vedi GIACCONI R.) . . . . .	" 826

NARANAN S., P. V. RAMANAMURTY, A. B. SAHAR, SIDDHESHWAR LAL and A. SUBRAMANIAN — Unusual Cosmic Ray Events Observed in a Multiple Cloud Chamber (L.) . . . . .	pag. 651
NEWTH J. A. (vedi COOPER W. A.) . . . . .	» 390
NEWTH J. A. (vedi COOPER W. A.) . . . . .	» 1443
OEHRM R. Causality and Dispersion Relations for the Scattering of Mesons by Fixed Nucleons . . . . .	» 1316
OGAWA S. (vedi HIROKAWA S.) . . . . .	» 736
OREAR J. — Evaluation of the Scattering Lengths in Pion-Nucleon Scattering . . . . .	» 856
OTSUKI S. (vedi IWADARE J.) (L.) . . . . .	» 1204
PAIĆ M. (vedi THURO G.) . . . . .	» 887
PAOLONI L. Coulomb Repulsion Integrals ( $pp pp$ ) and Bonding Power of an Atom in a given Valence State . . . . .	» 410
PAPPALARDO R. Su una nuova equazione relativistica dell'elettrone pro- posta da Zaitsev (L.) . . . . .	» 166
PEASLEE D. C. — Dimensionality of Charge Space (L.) . . . . .	» 1583
PEDRETTI E. (vedi MARCHI C.) (L.) . . . . .	» 940
PERILLI-FEDEL R. (vedi ALIVERTI G.) (L.) . . . . .	» 1580
PERKINS D. H. (vedi BIRGE R. W.) . . . . .	» 834
PERKINS R. D. (vedi BRISBOUT F. A.) . . . . .	» 1496
PETERSON J. R. (vedi BIRGE R. W.) . . . . .	» 834
PETRUCCI R. A. (vedi COOPER W. A.) . . . . .	» 1433
PEYROU C. (vedi D'ANDLAU C.) . . . . .	» 917
PICCIOTTO E. et S. WILGAIN — Confirmation de la période du Thorium-232 . . . . .	» 1525
PIERPAOLI V. (vedi SIMONETTA M.) . . . . .	» 1364
PLAINEVAUX J. E. Étude des déformations d'une lame de suspension élastique (N. T.) . . . . .	» 922
PLAINEVAUX J. E. Mouvement de tangage d'une suspension élémentaire sur lames élastiques . . . . .	» 1133
POIANI G. and G. SALVATORI — On the Positive Excess at Low Energies and Sea Level (L.) . . . . .	» 503
POLKINGHORNE J. C. — General Dispersion Relations . . . . .	» 216
POPIC R. V. — On the Spin and Parity of the First Excited State of $^{19}\text{O}$ (L.) . . . . .	» 1597
PORRICA F. Experimental Decay Law of the Diffracted Light Remaining in the Liquids at the Stopping of the Ultrasonic Waves . . . . .	» 679
PRENTKI J. (vedi D'ESPAGNAT B.) (L.) . . . . .	» 1572
PUSTERLA M. (vedi CIRELLI R.) (L.) . . . . .	» 150
PUSTERLA M. (vedi CIRELLI R.) (L.) . . . . .	» 1601
RABOY S. (vedi FERENTZ M.) . . . . .	» 487
RAMANAMURTY P. V. (vedi NARANAN S.) (L.) . . . . .	» 651
RAMA SWAMY M. K. A Semi-Empirical Formula for $\alpha$ -Disintegration Energy in the Region of Rare-Earth Nuclides (L.) . . . . .	» 1570
RAYSKI J. — Bilocal Field Theories and their Experimental Tests . . . . .	» 1231
REGGE T. — Angular Correlations between Decay Planes of $\tau^+$ -Mesons and their Production Geometry (L.) . . . . .	» 1615
REINA I. (vedi FONDA L.) . . . . .	» 1399
RENARD F. (vedi CRUSSARD J.) (L.) . . . . .	» 1195
RENÉ M. (vedi BACCHELLA L.) . . . . .	» 1529
REVEL D. (vedi BACCHELLA L.) . . . . .	» 1529
REYNOLD T. (vedi BARFORD N. C.) (L.) . . . . .	» 929



REYNOLDS G. T. - Laboratory Energy Distribution of $A^0$ Particles (L.) . . . . .	pag. 933
RICCI R. A. (vedi CHINAGLIA B.) (L.) . . . . .	» 134
RICCI R. A. (vedi DEMICHELIS F.) . . . . .	» 96
RICCI R. A. and R. VAN LIESHOUT - Radiations from $^{66}\text{Ge}$ and $^{67}\text{Ge}$ (L.) . . . . .	» 1592
ROSENDORFF S. (vedi EISENBERG Y.) . . . . .	» 610
RZEWUSKI J. (vedi KRÓLIKOWSKI W.) . . . . .	» 975
RZEWUSKI J. (vedi KRÓLIKOWSKI W.) (L.) . . . . .	» 1212
SAHIAR A. B. (vedi NARANAN S.) (L.) . . . . .	» 651
SALMERON R. A. (vedi COOPER W. A.) . . . . .	» 390
SALMERON R. A. (vedi COOPER W. A.) . . . . .	» 1433
SALVATORI G. (vedi POJANI G.) (L.) . . . . .	» 503
SATCHLER G. R. (vedi BRINK D. M.) . . . . .	» 549
SAWICKI J. (vedi Czyż W.) (L.) . . . . .	» 668
SCARSI L. (vedi BACCHELLA L.) . . . . .	» 1529
SCHAFROTH M. R. and J. M. BLATT - Phenomenological Equations for Superconductors . . . . .	» 786
SCHAFROTH M. R. (vedi BLATT J. M.) (L.) . . . . .	» 676
SCHAFROTH M. R. (vedi BUTLER S. T.) (L.) . . . . .	» 674
SCHMIDT W. and K. BAUMANN - Quantentheorie der Felder als Distributionstheorie . . . . .	» 860
SCHARFF M. (vedi BRENE N.) . . . . .	» 1059
SCOTONI I. (vedi BASSI P.) (N. T.) . . . . .	» 491
SEEMAN N. and R. G. GLASSER - Analysis of an Electron Shower Associated with a Very Energetic He Nucleus . . . . .	» 703
SEN P. - Renormalized Dirac-Maxwell Equations . . . . .	» 270
SHIH-HUI-HSIEH - On the Photodisintegration of the Deuteron and p-p Scattering (L.) . . . . .	» 138
SIDDHESHWAR LAL (vedi NARANAN S.) (L.) . . . . .	» 651
SILVESTRI M. and N. ADORNI - An Apparatus for Continuous Isotopic Analysis of Hydrogen-Deuterium Mixtures (L.) . . . . .	» 1610
Simboli e unità U.I.P.P.A. (D. I.) . . . . .	» 172
SIMONETTA M., G. FAVINI, S. C'ARRÀ and V. PIERPAOLI - Electronic Spectra of Mono-, Di- and Tri-Azines of the Naphtalene Series. - I. Benzotriazine and its Derivatives . . . . .	» 1364
SKYRME T. H. R. (vedi ELLIOTT J. P.) (L.) . . . . .	» 164
SLAUGHTER G. G. (vedi BLOCK M. M.) . . . . .	» 46
SMITH F. M. (vedi HECKMAN H. H.) . . . . .	» 51
SOLNSTEFF N. (vedi HERZ A. J.) (L.) . . . . .	» 1623
SOMIGLIANA R. (vedi KAFTAL S.) (N. T.) . . . . .	» 637
SORIANO S. - Perturbazione dei livelli energetici di una particella in una buca di potenziale sferoidale (L.) . . . . .	» 657
STAFFORD G. H. (vedi HILLMAN P.) . . . . .	» 67
STANGHELLINI A. - Determination of the $p$ -Wave Coupling Constant $f^2$ of Pion-Nucleon Scattering from Analysis of the $\alpha_{31}$ Phase-Shift (L.) . . . . .	» 168
STANTIC S. (vedi MARCHI C.) (L.) . . . . .	» 940
STILLER R. and F. I. LOUCKES jr. - Semi-Automatic Recorder for Filar Micrometer Eyepiece and Its Application to Track Measurement (N.T.) . . . . .	» 642
STOPPINI G. (vedi BENEVENTANO M.) . . . . .	» 323
STORK D. H. (vedi BIRGE R. W.) . . . . .	» 834
SUBRAMANIAN A. (vedi NARANAN S.) (L.) . . . . .	» 651



SUCCI C. (vedi GIACCONI R.) . . . . .	pag.	826
TAFFARA L. (vedi BUDINI P.) . . . . .	"	23
TAKAHASHI Y. — Theory of Multiple Boson Production . . . . .	"	531
TALLONE L. (vedi DEBENEDETTI A.) . . . . .	"	1142
TALLONE L. (vedi DEBENEDETTI A.) . . . . .	"	1151
TAMAGAKI R. (vedi IWADARE J.) (L.) . . . . .	"	1204
TAMURA T. — On the Collective Description of Nuclear Surface Oscillation . . . . .	"	713
TATI T. — An Attempt in the Theory of Elementary Particles . . . . .	"	75
TAU L. (vedi BENEVENTANO M.) . . . . .	"	323
TERRANI S. (vedi BISI A.) . . . . .	"	758
TERRANI S. (vedi KAFTAL S.) (N. T.) . . . . .	"	637
TEUCHER M. (vedi HÄNNI F. D.) . . . . .	"	1473
THIRRING W. — Depolarization of Stopped Particles (L.) . . . . .	"	666
THURO G. et M. PAIĆ — Étude de la dissolution des grains d'argent des plaques nucléaires épaisses dans le fixateur . . . . .	"	887
TIETZ T. — Über Eine Approximation der Thomas-Fermi Funktion (L.) . . . . .	"	1192
TINLOT J. H. (vedi D'ANDLAU C.) . . . . .	"	917
TOMASINI G. (vedi BACCHELLA L.) . . . . .	"	1529
TRIBUNO C. (vedi FERRERO F.) . . . . .	"	418
UMEZAWA H. (vedi KONUMA M.) . . . . .	"	1461
VANDERHAEGHE G. (vedi DEMEUX M.) . . . . .	"	509
VANDERHAEGHE G. (vedi BACCHELLA L.) . . . . .	"	1529
VAN DER SPUY E. — Investigation of the States of an Electron in a Proposed Electromagnetic Field. . . . .	"	1349
VAN LIESHOUT R. (vedi RICCI R. A.) (L.) . . . . .	"	1592
VARSHNEYA N. C. (vedi BISWAS N. N.) . . . . .	"	631
VARSHNEYA N. C. (vedi BISWAS N. N.) (L.) . . . . .	"	1201
VIGONE M. (vedi DEBENEDETTI A.) . . . . .	"	1142
VIGONE M. (vedi DEBENEDETTI A.) . . . . .	"	1151
VILLI C. (vedi CLEMENTEL E.) (L.) . . . . .	"	935
VILLI C. (vedi CLEMENTEL E.) (L.) . . . . .	"	1207
VISVANATHAN S. (vedi MOHANTY S. R.) (L.) . . . . .	"	1590
VITALE B. (vedi AMATI D.) . . . . .	"	171
VITALE B. (vedi AMATI D.) (L.) . . . . .	"	145
WALOSCHEK P. (vedi BISWAS N. N.) . . . . .	"	631
WALOSCHEK P. (vedi BISWAS N. N.) (L.) . . . . .	"	1201
WATAGHIN A. — On the Anelasticity of Cosmic Ray Jets (L.) . . . . .	"	154
WATARI W. (vedi IWADARE J.) (L.) . . . . .	"	1204
WEBBER W. R. — New Determination of the Intensities of Primary Cosmic Ray $\alpha$ -Particles and Li, Be, B Nuclei at $\lambda = 41.5^\circ$ Using a Čerenkov Detector. . . . .	"	1285
WEINER R. — Nuclear Isomeric Shift on Spectral Lines (L.) . . . . .	"	1587
WHITEHEAD M. N. (vedi BIRGE R. W.) . . . . .	"	834
WHITEHEAD C. (vedi HILLMAN P.) . . . . .	"	67
WILGAIN S. (vedi PICCIOTTO E.) . . . . .	"	1525
WINZELER H. (vedi HÄNNI F. D.) . . . . .	"	1473
WOLTER W. and M. MIĘSOWICZ — Ionization at the Origin of an Electron Pair of Very High Energy (L.) . . . . .	"	648
YAMAZAKI K. — On the Field Theory in Functional Form (L.) . . . . .	"	141
YOSHIDA S. — Anisotropy of Cosmic Rays During the Cosmic-Ray Storms . . . . .	"	1410

ZAGO G. (vedi CRESTI M.) . . . . .	pag.	747
ZAPPA L. (vedi BISI A.) . . . . .	"	307
ZAPPA L. (vedi BISI A.) . . . . .	"	758
ZAPPA L. (vedi BISI A.) . . . . .	"	764
ZICHICHI A. (vedi COOPER W. A.) . . . . .	"	1433
ZIMMER E. (vedi BISI A.) . . . . .	"	307

## INDICE ANALITICO PER MATERIE

### APPARATI E STRUMENTI E TECNICA SPERIMENTALE

Analisi fotometrica delle tracce nelle emulsioni nucleari, <i>M. Della Corte</i>	pag.	1565
Apparatus for Continuous Isotopic Analysis of Hydrogen-Deuterium Mixtures (L.), <i>M. Silvestri e N. Adorni</i> . . . . .	"	1610
Approximations for Linear Betatron Oscillations, <i>F. T. Adler and D. Baroncini</i> . . . . .	"	959
Bubble Formation in Supersaturated Gas-Liquid Solutions (L.), <i>P. E. Argan and A. Gigli</i> . . . . .	"	953
Carbon Dioxide Hexane Gas Bubble Chamber (L.), <i>B. Hahn</i> . . . .	"	944
Coincidence Arrangement for the Detection of Low Energy Quanta, <i>A. Bisi, E. Germagnoli and L. Zappa</i> . . . . .	"	764
Cosmic-Ray Gas Čerenkov Counter with Adjustable Velocity (N.T.), <i>R. J. Hanson and D. C. Moore</i> . . . . .	"	1558
Electronic Scanner for Nuclear Emulsions (N.T.), <i>E. Amaldi, C. Castagnoli and C. Franzinetti</i> . . . . .	"	1165
Errors in Constant-Sagitta Scattering Measurements in Nuclear Emulsions (L.), <i>A. J. Herz, R. M. May and N. Solnsteff</i> . . . . .	"	1623
Étude de la dissolution des grains d'argent des plaques nucléaires épaisses dans le fixateur, <i>G. Thuro et M. Paic</i> . . . . .	"	887
Étude des déformations d'une lame de suspension élastique (N.T.), <i>J. E. Plainevaux</i> . . . . .	"	922
Graphical Determination of the Path of a Scattered Particle (L.), <i>N. C. Barford and T. Reynolds</i> . . . . .	"	929
High Resolution Millimicrosecond Time Interval Measurements Based Upon Frequency Conversion (L.), <i>C. Cottini, E. Gatti and G. Giannelli</i>	"	156
Impiego dei radioisotopi per la determinazione dell'usura di utensili da taglio (N.T.), <i>S. Kaftal, R. Somigliana e S. Terrani</i> . . . . .	"	637
Magnetic and Scintillation Spectrometers for the $\gamma$ -Rays of $^{228}_{90}\text{Th}$ and its Decay Products, <i>B. Chinaglia and F. Demichelis</i> . . . . .	"	1160
Millimicrosecond Time Analyser (N.T.), <i>C. Cottini and E. Gatti</i> . . .	"	1150
Mouvement de tangage d'une suspension élémentaire sur lames élastiques, <i>J. E. Plainevaux</i> . . . . .	"	1133
New Method of Measuring Asymmetries in Neutron Polarization Experiments, <i>P. Hillman, G. H. Stafford and C. Whitehead</i> . . . . .	"	67
n-Pentane Bubble Chambers (N.T.), <i>P. Bassi, A. Loria, J. A. Meyer, P. Mittner and I. Scotoni</i> . . . . .	"	491

Semi-Automatic Recorder for Filar Micrometer Eyepiece and its Application to Track Measurement (N.T.), <i>R. Stiller</i> and <i>F. I. Louckes</i>	pag. 642
Spettrografo a microonde con modulazione ausiliaria (N.T.), <i>P. Favero</i> e <i>G. Grifone</i>	» 1174
Tempo di decadimento del $\text{ZnS}(\text{Ag})$ e preparazione di ricevitori a $\text{ZnS}(\text{Ag})$ , (L.), <i>B. Chinaglia</i> , <i>F. Demichelis</i> and <i>R. A. Ricci</i>	» 134
Test for the « Median Angle » Method (L.), <i>U. Haber-Schaim</i>	» 669
Tracce $\alpha$ in emulsioni nucleari esposte in aria ad alto contenuto di radon (L.), <i>G. Aliverti</i> , <i>A. De Maio</i> , <i>G. Lovera</i> e <i>R. Perilli-Fedeli</i>	» 1580

## COSMICA (RADIAZIONE)

Analysis of an Electron Shower Associated with a Very Energetic He Nucleus, <i>N. Seeman</i> and <i>R. G. Glasser</i>	» 703
Anisotropy of Cosmic Rays due to Galactic Rotation (L.), <i>A. O. Barut</i>	» 661
Anisotropy of Cosmic Rays During the Cosmic-Ray Storms, <i>S. Yoshida</i>	» 1410
Atmospheric Effects on the Cosmic Ray Total Intensity at Sea Level, <i>F. Bachelet</i> and <i>A. M. Conforto</i>	» 1479
Determination of the Intensities of Primary Cosmic Ray $\alpha$ -Particles and Li, Be, B Nuclei at $\lambda=41.5^\circ$ Using a Čerenkov Detector, <i>W. R. Webber</i>	» 1285
High Energy Jet in Nuclear Emulsions, <i>F. D. Hänni</i> , <i>C. Lang</i> , <i>M. Teucher</i> and <i>H. Winzeler</i>	» 1473
High Energy Nuclear Interactions in Lead by Cosmic Rays Protons at 3500 m, <i>R. Giacconi</i> , <i>A. Lovati</i> , <i>A. Mura</i> and <i>C. Succi</i>	» 826
Positive Excess at Low Energies and at Sea Level (L.), <i>G. Poiani</i> and <i>G. Salvatori</i>	» 503
Solution of the Fluctuation Problem in Cascade Showers, <i>H. Messel</i>	» 1339
Study on Electromagnetic Showers in Nuclear Emulsions, <i>A. Debedetti</i> , <i>C. M. Garelli</i> , <i>L. Tallone</i> and <i>M. Vigone</i>	» 1151
Trident Cross-Section Between 1 and 10 GeV, <i>F. A. Brisbout</i> , <i>C. Dahanayake</i> , <i>A. Engler</i> and <i>R. D. Perkins</i>	» 1496
Unusual Cosmic Ray Events Observed in a Multiple Cloud Chamber (L.), <i>S. Naranan</i> , <i>P. V. Ramanamurty</i> , <i>A. B. Sahiar</i> , <i>Shiddheshwar Lal</i> and <i>A. Subramanian</i>	» 651

## ELETTRODINAMICA E TEORIA DEI CAMPI

Analytical Solution of the Covariant Meson Nucleon Integral Equation, <i>I. E. McCarthy</i>	» 991
Attempt in the Theory of Elementary Particles, <i>T. Tati</i>	» 75
Basic Formulation of Classical and Quantum Theories (L.), <i>I. Fujiwara</i>	» 1575
Bilocal Field Theories and their Experimental Tests, <i>J. Rayski</i>	» 1231
Causality and Dispersion Relations for the Scattering of Mesons by Fixed Nucleons, <i>R. Oehme</i>	» 1316
Charge-Exchange Scattering of Antinucleons on Nucleons (L.), <i>D. Amati</i> and <i>B. Vitale</i>	» 145
Conservation of the Nucleons (L.), <i>B. Ferretti</i>	» 951

Covariant Quantization with Application to Scattering of Gravitating Dirac Particles, <i>B. E. Laurent</i> . . . . .	pag. 1445
Determination of the p-Wave Coupling Constant $f^2$ of Pion-Nucleon Scattering from Analysis of the $\alpha_{31}$ Phase-Shift (L.), <i>A. Stanghellini</i> . . . . .	» 168
Dimensionality of Charge Space (L.), <i>D. C. Peaslee</i> . . . . .	» 1583
Dispersion Relations for Decay Processes (L.), <i>E. Corinaldesi</i> . . . . .	» 1605
Dispersion Relations for Photoproduction of Mesons, <i>E. Corinaldesi</i> . . . . .	» 1384
Estensione del metodo parametrico di Davison al caso di potenziali cinetici (L.), <i>R. Cirelli e M. Pusterla</i> . . . . .	» 150
Field Theory in Functional Form (L.), <i>K. Yamazaki</i> . . . . .	» 141
Functional Integration in Quantum Field Theory, <i>W. K. Burton and A. H. De Borde</i> . . . . .	» 254
General Dispersion Relations, <i>J. C. Polkinghorne</i> . . . . .	» 216
High Energy Behaviour of Renormalizable Fields - II, <i>M. Konuma and H. Umezawa</i> . . . . .	» 1461
Higher Limit for the Mass of an Assembly of Particles (L.), <i>G. Bussetti</i> . . . . .	» 1613
Meson Nucleon $S$ Scattering and Crossing Theorem, <i>A. Martin</i> . . . . .	» 369
Metodi funzionali nelle teorie dei campi (L.), <i>R. Cirelli e M. Pusterla</i> . . . . .	» 1601
New Proof of the One-Time Equation in the Theory of Bound States (L.), <i>W. Królikowski and J. Rzewuski</i> . . . . .	» 1212
Non Linear Effect in the Vacuum Polarization, <i>A. Minguzzi</i> . . . . .	» 476
One-Time Formulation of the Relativistic Two-Body Problem Separation of Angular Variables, <i>W. Królikowski and J. Rzewuski</i> . . . . .	» 975
Polarizzazione della Bremsstrahlung (L.), <i>R. Ascoli e G. Bussetti</i> . . . . .	» 147
Quantentheorie der Felder als Distributionstheorie, <i>W. Schmidt and K. Baumann</i> . . . . .	» 860
Renormalized Dirac-Maxwell Equations, <i>P. Sen</i> . . . . .	» 270
Scattering in Field Theory, <i>H. Ekstein</i> . . . . .	» 1017
Scattering of High Energy Electrons by Protons (L.), <i>E. Clementel and C. Villi</i> . . . . .	» 1207
Soluble Model of Meson-Nucleon $S$ -State Scattering, <i>E. L. Lomon</i> . . . . .	» 106
Some Solutions of Gürsey's Conformal-Invariant Spinor Wave Equation, <i>F. Kortel</i> . . . . .	» 210
Sums over Trajectories for Systems with Fermi Statistics, <i>D. J. Candlin</i> . . . . .	» 231
States of an Electron in a Proposed Electromagnetic Field, <i>E. Van der Spuy</i> . . . . .	» 1349
Study of the Bremsstrahlung by Bloch and Nordsieck's Method, <i>R. Ascoli and G. Bussetti</i> . . . . .	» 189
Teoria bilocale dell'elettrone, <i>E. Minardi</i> . . . . .	» 1127
Theory of Multiple Boson Production, <i>Y. Takahashi</i> . . . . .	» 531
Vacuum Expectation Values as Sums Over Histories, <i>P. W. Higgs</i> . . . . .	» 1262
Vanishing of the Interaction Hamiltonian (L.), <i>J. M. Cook</i> . . . . .	» 1585

## LIQUIDI E SOLIDI

Application of Feynman's New Variational Procedure to the Calculation of the Ground State Energy of Excitons (L.), <i>H. Haken</i> . . . . .	» 1608
Dynamic Determination of Viscosity, <i>A. Carrelli and A. De Vito</i> . . . . .	» 1009
Intermetallic Diffusion in Gold-Lead System, <i>A. Ascoli, E. Germagnoli and L. Mongini</i> . . . . .	» 123

Nature of the $\lambda$ -Transition in Liquid Helium (L.), <i>S. T. Butler, J. M. Blatt and M. R. Schafroth</i> . . . . .	pag. 674
New Effect in the Magnetoresistance of Aluminium (L.), <i>B. Luthi and J. L. Olsen</i> . . . . .	» 957
Pair Correlations in Dilute Gases at Low Temperatures, <i>J. M. Blatt</i> . . . . .	» 430
Phenomenological Equations for Superconductors, <i>M. R. Schafroth and J. M. Blatt</i> . . . . .	» 786
Problem of the Static Helium Film (I), <i>S. Franchetti</i> . . . . .	» 1504
Superfluidity of Liquid Helium (L.), <i>J. M. Blatt, S. T. Butler and M. R. Schafroth</i> . . . . .	» 676

MESONI ( $\pi$  e  $\mu$ )

Anomalous Magnetic Moment of $\mu$ -Mesons, <i>S. Hirokawa, H. Komori and S. Ogawa</i> . . . . .	» 736
Désintégrations des noyaux légers de l'émulsion nucléaire par des mésons $\pi^-$ lents, <i>M. Demeur, A. Huleux et G. Vanderhaeghe</i> . . . . .	» 509
Differential Cross-Sections for Photoproduction of Positive Pions in Hydrogen, <i>M. Beneventano, G. Bernardini, D. Carlson-Lee, G. Stoppini and L. Tau</i> . . . . .	» 323
Diffusion Chamber Study of Very Slow Mesons. - IV. Absorption of Pions in Light Nuclei, <i>P. Ammiraju and L. M. Lederman</i> . . . . .	» 283
Evaluation of the Scattering Lengths in Pion-Nucleon Scattering, <i>J. Orear</i> . . . . .	» 856
Inelasticity in Collisions between Pions and Lead Nuclei, <i>M. Cresti, W. D. B. Greening, L. Guerriero, A. Loria and G. Zago</i> . . . . .	» 747
Nucleon Recoil in the Pion-Nucleon Scattering, <i>L. Fonda and I. Reina</i> . . . . .	» 1399
Validity of the Williams-Weizsäcker Method and the Problem of the Nuclear Interactions of Relativistic $\mu$ -Mesons, <i>D. Kessler and P. Kessler</i> . . . . .	» 601

## MESONI PESANTI E IPERONI

Analysis of $\tau$ -Meson Experiments, <i>N. Brene, K. H. Hansen, J. E. Hooper and M. Scharff</i> . . . . .	» 1059
Analysis of one Hundred Bevatron $\tau^+$ Particles, <i>R. P. Haddock</i> . . . . .	» 240
Analysis of the Spin and Parity of the $\tau$ -Meson, <i>Y. Eisenberg, E. Lomon and S. Rosendorff</i> . . . . .	» 610
Angular Correlation between Decay Planes of $\tau^+$ -Mesons and their Production Geometry (L.), <i>T. Regge</i> . . . . .	» 1615
Angular Correlation Methods for Determining the Spins of the Hyperons, <i>R. Gallo</i> . . . . .	» 197
Angular Distributions in the Hyperon Decay - II (L.), <i>G. Morpurgo</i> . . . . .	» 1222
Application of Charge Independence to the Nuclear Capture of Negative K-Mesons, <i>M. Koshiba</i> . . . . .	» 357
Binding Energies of the Light Hyperfragments, <i>J. T. Jones, jr. and J. M. Keller</i> . . . . .	» 1329
Coherence Effects in the Lee-Yang Parity Doublets Theory of Strange Particles, <i>R. Gallo</i> . . . . .	» 1274



Consequences of the Possible Existence of the Hyperdeuteron, <i>M. Ferentz</i> and <i>S. Raboy</i> . . . . .	pag. 487
Decay Characteristics and Masses of Positive K-Mesons Produced by the Bevatron, <i>R. W. Birge, D. H. Perkins, J. R. Peterson, D. H.</i> <i>Stork</i> and <i>M. N. Whitehead</i> . . . . .	» 834
Decay Modes and Mean Life of Scattered K-Mesons, <i>N. N. Biswas,</i> <i>L. Ceccarelli-Fabbrichesi, M. Ceccarelli, K. Gottstein, N. C. Varshneya</i> and <i>P. Waloschek</i> . . . . .	» 631
$V^0$ Decay with an Electron Secondary, <i>C. D'Andlau, R. Armenteros, A.</i> <i>Astier, H. C. DeStaebler, B. P. Grégory</i> and <i>J. H. Tinlot</i> . . . . .	» 917
Depolarization of Stopped Particles (L.), <i>W. Thirring</i> . . . . .	» 666
Example of the Production and Decay of a Neutral Tau-Meson, <i>W. A.</i> <i>Cooper, H. Filthuth, J. A. Newth, G. Petrucci, R. A. Salmeron</i> and <i>A. Zichichi</i> . . . . .	» 1433
Examples of Mesonic Decay of Hyperfragments (L.), <i>P. H. Fowler</i> and <i>K. H. Hansen</i> . . . . .	» 158
Existence of a Bound Nucleon $V^0$ State, <i>G. H. Derrick</i> . . . . .	» 565
Interaction and Decay of $K^+$ -Mesons in Flight (L.), <i>C. Marchi, E. Pe-</i> <i>dretti</i> and <i>S. Stantié</i> . . . . .	» 940
Interactions faibles directed bosons-leptons et désintégration des mé- sons K (L.), <i>B. d'Espagnat</i> et <i>J. Prentki</i> . . . . .	» 1572
Laboratory Energy Distribution of $\Lambda^0$ Particles (L.), <i>G. T. Reynolds</i> . . . . .	» 933
Mass and Spin-Parity Character of the $\tau$ -Meson, <i>H. H. Heckman, F. M.</i> <i>Smith</i> and <i>W. H. Barkas</i> . . . . .	» 51
Mean Lifetime of K-Mesons Produced by the Cosmic Radiations <i>L.</i> <i>Mezzetti</i> and <i>J. W. Keuffel</i> . . . . .	» 1096
Measurements on Charged V-Events, <i>W. A. Cooper, H. Filthuth, J. A.</i> <i>Newth</i> and <i>R. A. Salmeron</i> . . . . .	» 390
Mesonic Decay in Flight of a Triton Hyperfragment (L.), <i>F. Brisbout,</i> <i>M. W. Friedlander</i> and <i>P. Iredale</i> . . . . .	» 948
K-Mesons in Emulsions Exposed to a 6.2 GeV Proton Beam (L.), <i>J.</i> <i>Crussard, V. Fouché, J. Hennessy, G. Kayas, L. Leprince-Ringuet,</i> <i>D. Morellet</i> and <i>F. Renard</i> . . . . .	» 1195
Observation of Electron Secondaries from $V^0$ Decays, <i>M. M. Block,</i> <i>E. M. Harth, M. E. Blevins</i> and <i>G. G. Slaughter</i> . . . . .	» 46
Possible Annihilation Mode of a Nucleon-Antinucleon System into a K-K Pair, <i>R. Gatto</i> . . . . .	» 526
$Q$ -Value of the Tau-Decay, <i>L. Bacchella, A. Berthelot, M. di Corato,</i> <i>O. Goussu, R. Levi Setti, M. René, D. Revel, L. Scarsi, G. Tomasini</i> and <i>G. Vanderhaeghe</i> . . . . .	» 1529
$^{12}C$ Tripartition Induced by $K^+$ -Mesons (L.), <i>N. N. Biswas, L. Ceccarelli-</i> <i>Fabbrichesi, M. Ceccarelli, K. Gottstein, N. C. Varshneya</i> and <i>P.</i> <i>Waloschek</i> . . . . .	» 1201

# MOLECULE

Coulomb Repulsion Integrals ( $pp/pp$ ) and Bonding Power of an Atom in a given Valence State, <i>L. Paoloni</i> . . . . .	» 410
Electronic Spectra of Mono-, Di- and Tri-Azines of the Naphtalene Series. - I. Benzotriazine and its Derivatives, <i>M. Simonetta, G. Favini,</i> <i>S. Carrà</i> and <i>V. Pierpaoli</i> . . . . .	» 1364



## NUCLEI (FISICA NUCLEARE)

Anti-Proton Annihilation, <i>H. A. Bethe and J. Hamilton</i> . . . . .	pag. 1
Collective Description of Nuclear Surface Oscillation, <i>T. Tamura</i> . . . . .	» 713
Diffusion Parameters of Thermal Neutrons in Water, <i>A. Bracci and C. Coceva</i> . . . . .	» 59
Effect of Centre of Mass Motion on Nuclear Moments (L.), <i>J. P. Elliott and T. H. R. Skyrme</i> . . . . .	» 164
Elastic Scattering of $\alpha$ -Particles (L.), <i>S. W. MacDowell and J. J. Gianbiagi</i> . . . . .	» 1594
Electron Capture Decay Energy of $^{153}_{64}\text{Gd}$ , <i>R. K. Gupta and S. Iha</i> . . . . .	» 88
Example of the Reaction $\text{K} + ^{12}_6\text{C} \rightarrow \text{K}^+ + 3\frac{4}{2}\text{He}$ (L.), <i>F. Anderson, D. Keefe, A. Kernan and J. Losty</i> . . . . .	» 1198
Fast Photoneutrons from Bismuth, <i>F. Ferrero, A. O. Hanson, R. Malvano and C. Tribuno</i> . . . . .	» 418
High Energy Nuclear Interaction, <i>A. Debenedetti, C. M. Garelli, L. Tallone and M. Vigone</i> . . . . .	» 1142
Holes and Particles in Shell Models, <i>D. M. Brink and G. R. Satchler</i> . . . . .	» 549
Investigation of the First Rotational Level of $^{169}\text{Tm}$ , <i>A. Bisi, S. Ter-rani and L. Zappa</i> . . . . .	» 758
Matter and Anti-Matter, <i>G. R. Burbidge and F. Hoyle</i> . . . . .	» 558
Measurement of the Energy Spectrum of Protons from (n, p) Reactions on Mg and Zn with 14 MeV Neutrons (L.), <i>L. Colli and U. Facchini</i> . . . . .	» 671
Measurements on n, p Reactions at 14 MeV - Magnesium, Silicon, Calcium, Zinc, Zirconium (L.), <i>C. Badoni, L. Colli and U. Facchini</i> . . . . .	» 1618
New Nucleon-Nucleon Potential (L.), <i>E. Clementel and O. Villi</i> . . . . .	» 935
Nuclear Isomeric Shift on Spectral Lines, (L.), <i>R. Weiner</i> . . . . .	» 1587
Nucleon-Nucleus Interaction, <i>W. E. Frahn</i> . . . . .	» 313
Orbital Electron Capture in $^{179}\text{Ta}$ , <i>A. Bisi, L. Zappa and E. Zimmer</i> . . . . .	» 307
Perturbazione dei livelli energetici di una particella in una buca di po-tenziale sferoidale (L.), <i>S. Soriano</i> . . . . .	» 657
Photodisintegration of the Deuteron and p-p Scattering (L.), <i>Shih-Hui-Hsieh</i> . . . . .	» 138
Pion Theory of Nuclear Forces and n-p Polarization (L.), <i>J. Iwadare, S. Otsuki, R. Tamagaki and W. Watari</i> . . . . .	» 1204
Polarization of Nucleons from Photonuclear Reactions (L.), <i>W. Cziř and J. Sawicki</i> . . . . .	» 668
Rotational States of Spheroidal Nuclei, <i>F. Coester</i> . . . . .	» 1307
Real Part of the Complex Potential Well of the Nucleus, <i>A. Kind and L. Jess</i> . . . . .	» 595
Resonance Nucleon-Nucleus Scattering (L.), <i>E. Minardi</i> . . . . .	» 1219
Spin and Parity of the First Excited State of $^{19}\text{O}$ (L.), <i>R. V. Popić</i> . . . . .	» 1597

## ONDE ELETTROMAGNETICHE

Dynamics of a Non-Uniform Electrically Conducting Fluid, <i>G. H. A. Cole</i> . . . . .	» 779
Phenomenological Theory of Conductivity (L.), <i>G. Beck</i> . . . . .	» 1190

## QUANTISTICA (MECCANICA)

Approximation der Thomas-Fermi Funktion (L.), <i>T. Tietz</i> . . . . .	pag. 1192
Nuova equazione relativistica dell'eletttrone proposta da Zaitsev (L.), <i>R. Pappalardo</i> . . . . .	» 166

## RADIOATTIVITÀ

$\beta$ - $\gamma$ Angular Correlation of $^{208}_{81}\text{Tl}$ ( $\text{ThC}''$ ), <i>F. Demichelis</i> and <i>R. A. Ricci</i> »	96
Decay of Caesium-132, <i>K. S. Bhatki</i> , <i>R. K. Gupta</i> and <i>S. Iha</i> . . . . .	» 1519
Low-Intensity Component in the $\beta$ -Ray Spectrum of $^{214}_{83}\text{Bi}$ ( $\text{RaC}$ ), <i>G. R. Bishop</i> and <i>F. Demichelis</i> (L.) . . . . .	» 1599
Période du Thorium-232, <i>E. Picciotto</i> et <i>S. Wilgain</i> . . . . .	» 1525
Radiations from $^{66}\text{Ge}$ and $^{67}\text{Ge}$ , <i>R. A. Ricci</i> and <i>R. Van Lieshout</i> (L.)	» 1592
Ratio between $\gamma$ and $\alpha$ Activities of $^{210}\text{Po}$ (L.), <i>A. Ascoli</i> , <i>M. Asdente</i> and <i>E. Germagnoli</i> . . . . .	» 946
Semi-Empirical Formula for L-Disintegration Energy in the Region of Rare-Earth Nuclides (L.), <i>M. K. Rama Swamy</i> . . . . .	» 1570
Tracce $\alpha$ in emulsioni nucleari esposte in aria ad alto contenuto di radon (L.), <i>G. Aliverti</i> , <i>A. De Maio</i> , <i>G. Lovera</i> e <i>R. Perilli-Fedeli</i> »	1580

## RELATIVITÀ GENERALE

Conservation Laws and other Identities in Bonnor's Unified Field Theory, <i>S. I. Husain</i> . . . . .	» 768
Generalization of Reissner-Nordström Solution (I) (L.), <i>R. L. Brahma- chary</i> . . . . .	» 1216
Gravitational Motion, <i>B. Bertotti</i> . . . . .	» 898
Hydrodynamical Considerations of an Imperfect Fluid in a General Relativistic Field (L.), <i>S. Bhattacharya</i> . . . . .	» 501
Stephenson-Kilmister's Unified Theory of Gravitation and Electro- magnetism, <i>J. I. Horváth</i> . . . . .	» 571
Unified Theory of Physical Fields, <i>J. I. Horváth</i> . . . . .	» 577
Unified Field Theory, <i>R. S. Mishra</i> . . . . .	» 907

## SCATTERING MULTIPLO E IONIZZAZIONE

Energy Loss and Specific Ionization of a Relativistic Particle in a Polarizable Medium (I), <i>P. Budini</i> and <i>L. Taffara</i> . . . . .	» 23
Multiple Small Angle Scattering of Waves by an Inhomogeneous Medium, <i>P. Gosar</i> . . . . .	» 688
Ionization at the Origin of an Electron Pair of Very High Energy (L.), <i>W. Wolter</i> and <i>M. Mięsowicz</i> . . . . .	» 648
New Approximate One-Velocity Theory of Multiple Scattering in In- finite Homogeneous Media, <i>C. C. Grosjean</i> . . . . .	» 582

## ULTRASUONI

Actions chimiques des ultra-sons sur l'eau et les solutions aqueuses, <i>M. Haïssinsky et A. M. Mangeot</i> . . . . .	pag. 1086
Experimental Decay Law of the Diffracted Light Remaining in the Liquids at the Stopping of the Ultrasonic Waves, <i>F. Porreca</i> . . . . .	» 679

## INDICE DELLE RECENSIONI

<i>L. BIEBERBACH - Analytische Fortsetzung</i> . . . . .	pag. 185
<i>Niels Bohr and the development of Physics</i> (Essay dedicated to Niels Bohr on the occasion of his seventieth birthday) . . . . .	» 185
<i>K. BECHERT and C. GERTHSEN - Atomphysik</i> . . . . .	» 186
<i>G. OBERDORFER - Die Maßsysteme in Physik und Technik</i> . . . . .	» 186
<i>R. SRPOULL - Modern Physics. A Textbook for Engineers</i> . . . . .	» 187
<i>U. STILLE - Messen und Rechnen in der Physik</i> . . . . .	» 187
<i>O. BLACKWOOD and W. KELLY - General Physics</i> . . . . .	» 505
<i>EVANGELISTA TORRICELLI - De Infinitis Spiralibus</i> . . . . .	» 505
<i>O. F. MOSSOTTI - Scritti. Vol. II, t. II (Nuova teoria degli Strumenti ottici)</i> . . . . .	» 506
<i>G. PETIAU - La théorie des fonctions de Bessel exposée en vue de ses applications à la Physique Mathématique</i> . . . . .	» 506
<i>L. HEFFTER - Begründung der Funktionentheorie auf alten un neuen Wegen</i> . . . . .	» 507
<i>S. S. SCHWEBER, H. A. BETHE and F. DE HOFFMAN - Fields, Vol. I:</i> <i>H. A. BETHE and F. DE HOFFMAN: Mesons, Vol. II</i> . . . . .	» 1227
<i>K. PRZIBRAM - Irradiation Colors and Luminiscence</i> . . . . .	» 1228
<i>R. OLDENBURGER editor - Frequency Response</i> . . . . .	» 1229
<i>R. CAMPBELL - Théorie générale de l'équation de Mathieu et de quelques autres différentielles de la mécanique</i> . . . . .	» 1626
<i>Reports on Progress in Physics, vol. XIII, a cura di A. C. STICKLAND</i> . . . . .	» 1627
<i>W. PRAGER und P. G. HODGE Jr. - Theorie idealplastischer Körper</i> . . . . .	» 1629
<i>Techniques Générales du Laboratoire de Physique, vol. I (II édition) a cura di J. SURUGUE</i> . . . . .	» 1630
<i>M. SUZUKI - Structure of a Group and the Structure of its Lattice of Subgroups</i> . . . . .	» 1631

---

Fine del Volume IV, Serie X, 1956

---

PROPRIETÀ LETTERARIA RISERVATA

---

Direttore responsabile: G. POLVANI

Tipografia Compositori • Bologna

Questo fascicolo è stato licenziato dai torchi il 30-XI-1956

